August 2003 • NREL/SR-500-33196

Subcontractor Report

Alternative Design Study Report: WindPACT Advanced Wind Turbine Drive Train Designs Study

November 1, 2000 – February 28, 2002

R. Poore and T. Lettenmaier
Global Energy Concepts, LLC
Kirkland, Washington

National Renewable Energy Laboratory

1617 Cole Boulevard
Golden, Colorado 80401-3393

NREL is a U.S. Department of Energy Laboratory
Operated by Midwest Research Institute • Battelle • Bechtel

Contract No. DE-AC36-99-GO10337

August 2003 • NREL/SR-500-33196

Alternative Design Study Report: WindPACT Advanced Wind Turbine Drive Train Designs Study

November 1, 2000 – February 28, 2002

R. Poore and T. Lettenmaier
Global Energy Concepts, LLC
Kirkland, Washington

NREL Technical Monitor: A. Laxson

Prepared under Subcontract No. YAM-1-30209-01

National Renewable Energy Laboratory

1617 Cole Boulevard
Golden, Colorado 80401-3393

NREL is a U.S. Department of Energy Laboratory
Operated by Midwest Research Institute • Battelle • Bechtel

Contract No. DE-AC36-99-GO10337

NOTICE

Available electronically at http://www.osti.gov/bridge

Available for a processing fee to U.S. Department of Energy
and its contractors, in paper, from:

U.S. Department of Energy
Office of Scientific and Technical Information
P.O. Box 62
Oak Ridge, TN 37831-0062
phone: 865.576.8401
fax: 865.576.5728
email: reports@adonis.osti.gov

Available for sale to the public, in paper, from:

U.S. Department of Commerce
National Technical Information Service
5285 Port Royal Road
Springfield, VA 22161
phone: 800.553.6847
fax: 703.605.6900
email: orders@ntis.fedworld.gov
online ordering: http://www.ntis.gov/ordering.htm

Printed on paper containing at least 50% wastepaper, including 20% postconsumer waste

Table of Contents

Appendices

List of Figures

List of Tables

1. Executive Summary

1.1 Introduction

This report presents the Phase I results of the National Renewable Energy Laboratory's (NREL) WindPACT (Wind Partnership for Advanced Component Technologies) Advanced Wind Turbine Drive Train Designs Study. Global Energy Concepts, LLC (GEC) performed this work under a subcontract with NREL (subcontract number YAM-1-30209-01 entitled "WindPACT Advanced Wind Turbines Drive Train Designs").

The purpose of the WindPACT project is to identify technology improvements that will enable the cost of energy (COE) from wind turbines to be reduced. Other parts of the WindPACT project have examined blade and logistics scaling, balance-of-station costs, and rotor design. This study was designed to investigate innovative drive train designs.

The GEC subcontract is organized into three phases:

- **Phase I—Preliminary Design Studies:** The objective of this phase was to assess and identify, from an initial roster of candidates, one or more of the most attractive drive train candidates.

- **Phase II—Detailed Design Studies and Proof-of-Concept Fabrication:** The objective of this phase is to perform detailed design and proof-of-concept fabrication of the most attractive drive train configuration.

- **Phase III—Proof-of-Concept Test and Characterization:** The objective of this phase is to test and characterize the proof-of-concept prototype.

During Phase I of the study, preliminary or conceptual drive train designs were developed for nine different 1.5-MW drive train configurations, the COE was estimated for each design, and these results were scaled to estimate the COE of 750-kW and 3-MW versions for each design. This report documents the results of the Phase I effort, and contains technical descriptions and economic analysis results for several 1.5-MW wind turbine drive train designs, including the gearbox, electrical generator, power electronics, and grid interface systems. During Phase II of the study, a detailed design will be developed for one design selected from Phase I. During Phase III, the selected design will be built and tested. Future reports will cover the results of Phases II and III.

1.2 Project Team and Participants

GEC teamed with following consulting companies, individual consultants, and manufacturing companies during Phase I of the study:

- Powertrain Engineers, Inc. (PEI)—mechanical and structural design
- OEM Development Corporation (OEM)—electrical systems investigation
- Dr. William Erdman—power electronics (PE) system design, estimation, and modeling
- McCleer Power, Inc.—permanent magnet (PM) generator modeling and analysis
- Clipper Windpower, LLC—multigenerator control systems investigation
- DeWolf Engineering—transformer estimates
- Phil Forde and Associates, LLC—hydraulic system design and estimates

- Kaman Electromagnetics Development Center—PM generator design and estimates
- Milwaukee Gear Corporation—gearbox cost estimates
- The Timken Company—bearing design and estimates
- Siemens Energy and Automation—generator and PE estimates
- Loher Drive Systems—generator and PE estimates
- Rockwell Medium Drives Division—PE estimates.

Details about the roles of the participants are given in Section 2.

1.3 Approach

Before the study began, NREL specified nine drive train configurations in the subcontract scope of work. Extensive estimates existed for one of these designs (the baseline) because they had been recently completed as part of the *WindPACT Turbine Rotor Design Study* (Malcolm and Hansen 2002). The rotor study estimates were made for a primary assessment size of 1.5 MW with secondary assessment sizes of 750 kW and 3.0 MW. For consistency with the rotor study, these assessment sizes were chosen when this drive train study began. To investigate the specified drive drain designs at these assessment sizes during Phase I of the study, the following approach was taken:

1. **Specifications:** The operational and environmental requirements were defined.
2. **Loads analysis:** ADAMS™ (MSC Software Corporation, Ann Arbor, Michigan) computer modeling of the complete turbine was used to estimate the drive train loads.
3. **Conceptual drive train designs and COE estimates:** Designs (1.5-MW) were developed and COE estimates made for each of the nine configurations. Pro/E (Parametric Technology Corporation, Needham, Massachusetts) computer solid models were created for each mechanical and structural design and component costs were estimated by participating manufacturing companies.
4. **Selection of concepts for preliminary design:** Based on the COE estimates, the six most promising configurations were selected for further, more detailed preliminary design estimates.
5. **Preliminary designs and COE estimates:** Designs for the six selected configurations were developed in further detail. The initial Pro/E models for each were modified and more detail added. One-line diagrams were drawn for each electrical system. Detailed estimates were made for the components with the highest cost, especially the gearbox, the generator, and the power electronic systems. Detailed estimates of component efficiencies, operation and maintenance costs, and component costs were made and used to estimate the COE for each design.
6. **Scaling of results to 750 kW and 3.0 MW:** Component cost and COE estimates were made for 750-kW and 3.0-MW versions of the six 1.5-MW designs.
7. **Selection of preferred design:** NREL and the study team selected the configuration to be built and tested during Phases II and III.

1.4 Generator and Power Electronic Technologies

A significant result of the study was the development of a cost-effective 1.5-MW PM generator and PE system design for the three drive trains using low- or medium-speed generators. These are the direct drive, single PM, and multi-PM drive trains, which either eliminate the gearbox or reduce its size by limiting it to a single stage. This generator and PE system is a significant departure from the traditional generator-PE system used in the baseline design.

The baseline design uses a high-speed (1200-rpm synchronous speed) doubly fed generator and power electronic system, similar to the designs used in several existing turbines. The doubly fed system has the significant benefit that the PE system is partially rated for approximately 33% of the generator power, and therefore the combined generator and PE cost for this system is quite low compared to most alternatives. This system requires the use of a wound-rotor induction generator. Full-rated power electronics are necessary for squirrel-cage induction or synchronous generators.

Low- or medium-speed induction generators are not practical because induction generator magnetizing current increases with pole count. PM generators were found to have the highest efficiency and lowest cost for these applications. A full-rated PE system is necessary for PM generators, however, and this PE system can be a significant portion of the entire drive train cost. Several PE designs were investigated in detail for this application. A design using passive rectification and line-commutated silicon controlled rectifiers (SCR) was selected because of its low relative cost and high efficiency.

The following subsections describe the doubly fed generator-PE system, the WindPACT PM generator design, and the SCR-SCR PE system chosen for use with this PM generator.

1.4.1 Doubly Fed Induction Generator and PE System

The electrical diagram for the doubly fed generator-PE system used in the baseline design is shown in Figure 1-1. This system uses a wound-rotor induction generator and an insulated gate bipolar transistor (IGBT)-based, pulse width modulated (PWM) converter system that provides variable-frequency power to the generator rotor through slip rings. Most of the generator power is directly transferred from the generator stator to the grid, bypassing the power electronics. Consequently, the rating of the power electronics is only 33% of the generator power.

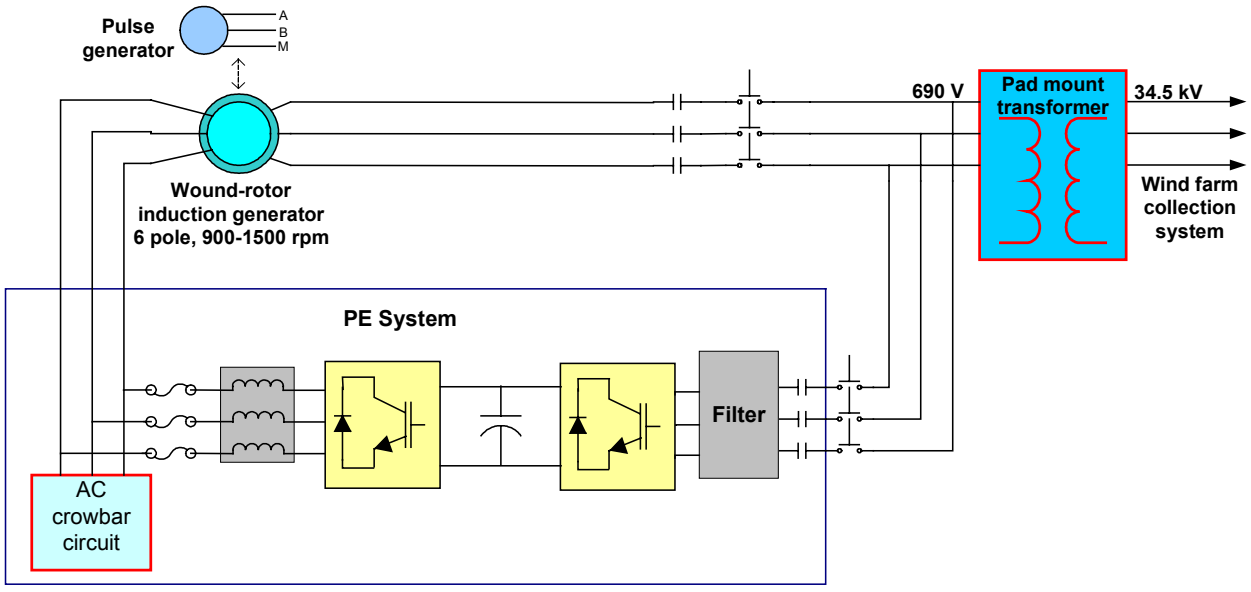

Figure 1-1. Doubly fed induction generator PE and electrical system (baseline)

1.4.2 PM Generator Design

Kaman developed the radial field, liquid cooled, salient pole stator, PM synchronous generator design shown in Figure 1-2 for this study. This design, scaled for speed and diameter, was chosen for all drive trains requiring low- or medium-speed generators. The design uses surface-mounted Neodymium Iron Boron (NeFeB) magnets in the rotor and form-wound coils around each stator lamination tooth. The diameter-to-length aspect ratio is high to minimize the active magnetic material content. Several different generator designs were considered before this design was chosen. Electrical rotor excitation, air cooling, axial field, and interleaved stator winding constructions were all considered. Estimates showed the selected design to have high efficiency and low cost relative to the other options.

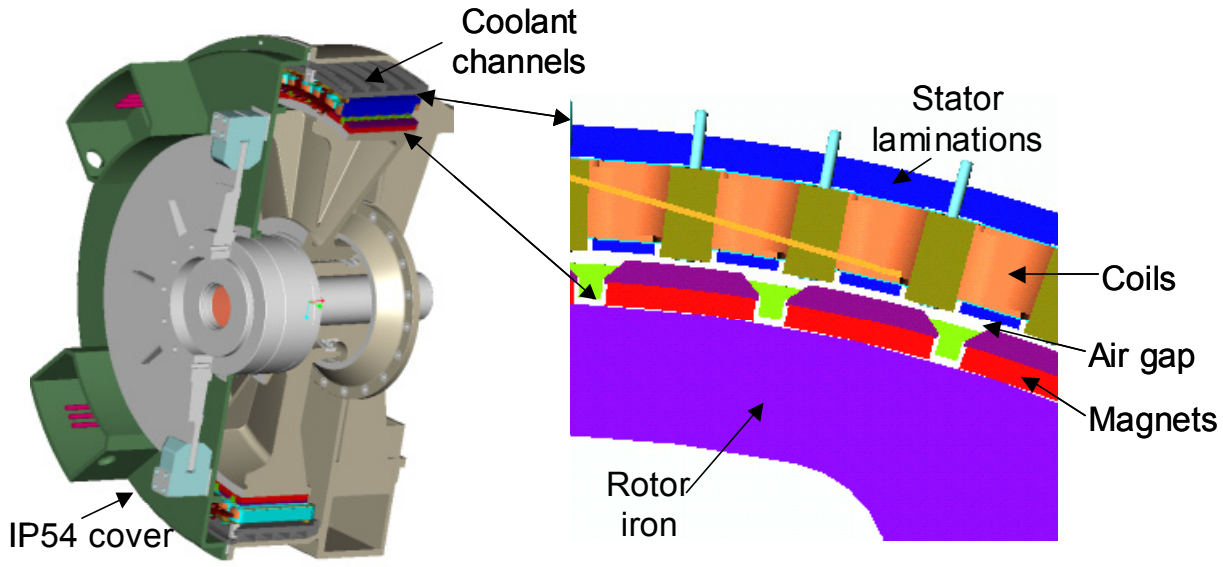

Figure 1-2. PM generator design

1.4.3 Power Electronic System for PM Generators

The electrical system shown in Figure 1-3 was developed for use with the WindPACT PM generators. This system passively rectifies the generator output to create a direct current (DC) bus, and uses a line-commutated, SCR inverter to convert to alternating current (AC) line voltage. This system has the disadvantage that the generator must have lower stator inductance and therefore be larger and more expensive than generators used with alternative PE systems that do not use passive rectification. The relatively low cost of the PE system, however, makes up for the increased generator cost. This PE system also has the disadvantages of poor power quality and a noncontrolled power factor. These deficiencies are corrected in the wind farm collection system. Alternating pad mount transformer configurations and the filtering provided by transformer and line reactances are used to improve the power quality. The power factor is corrected at the wind turbine and controlled at the wind farm substation with a separate volt ampere reactive (VAR) control system.

Several other PE systems were considered, and a detailed economic comparison was made on a COE basis among the three most favorable systems before this design was chosen. The other two PE systems used (1) traditional, back-to-back IGBT, PWM converters similar to the baseline PE design, and (2) passive diode rectification of the generator feeding a line-side, IGBT PWM converter. The estimates showed both of these systems to have higher component costs, which resulted in a higher COE when evaluated as part of an entire wind farm system.

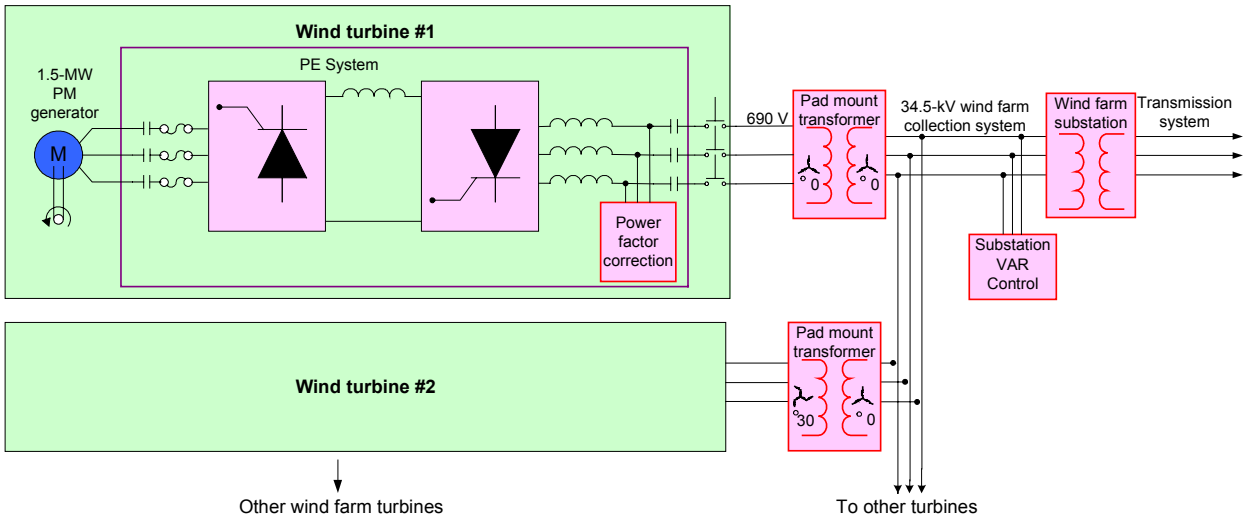

Figure 1-3. Power conversion and electrical system used for WindPACT PM generators

1.5 WindPACT Drive Train Designs

The final WindPACT drive train designs for all nine of the investigated configurations are illustrated together in Figure 1-4. Each design was evaluated at the conceptual level. The conceptual estimates showed that three of the configurations, the Klatt, Heller-De Julio (HDJ), and Henderson drive trains, had a comparable or higher COE than the baseline system and significant improvements were not anticipated. These drive train designs were not evaluated further during the study. More detailed designs and estimates were made for the remaining six configurations, and each design is described in the subsections that follow.

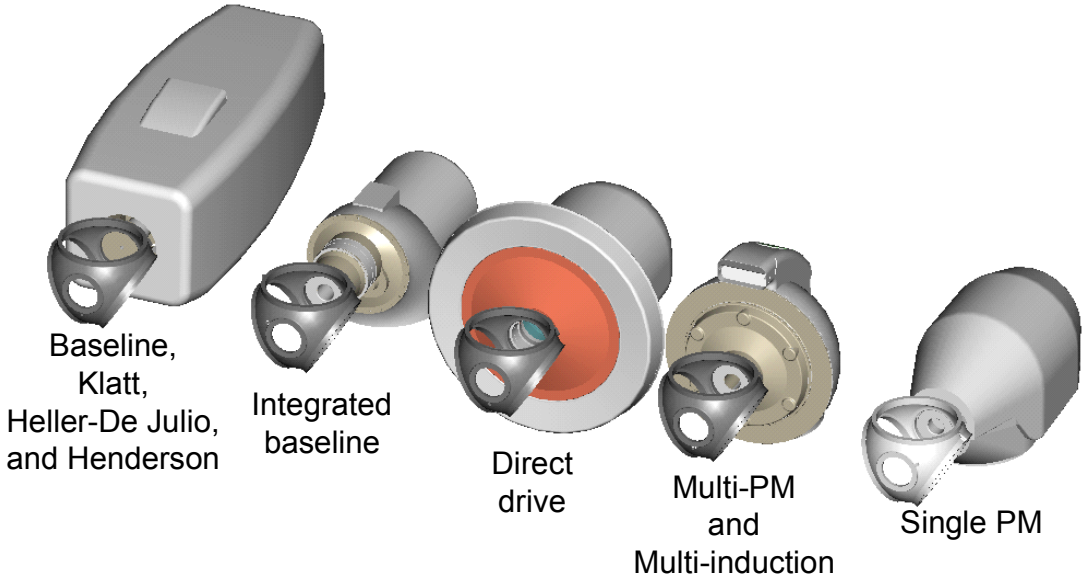

Figure 1-4. WindPACT drive train designs

1.5.1 Baseline Drive Train

The baseline drive train design is a modular bedplate design that uses a three-stage gearbox to drive a doubly fed generator and PE system. This design is similar to the 1.5-MW variable-speed turbine designs currently produced by GE Wind in the United States and several turbine manufacturers in Europe. The baseline design estimates served as a reference point for the comparative evaluation of all the other drive train designs investigated during the study. Figure 1-5 presents a system diagram for the baseline system.

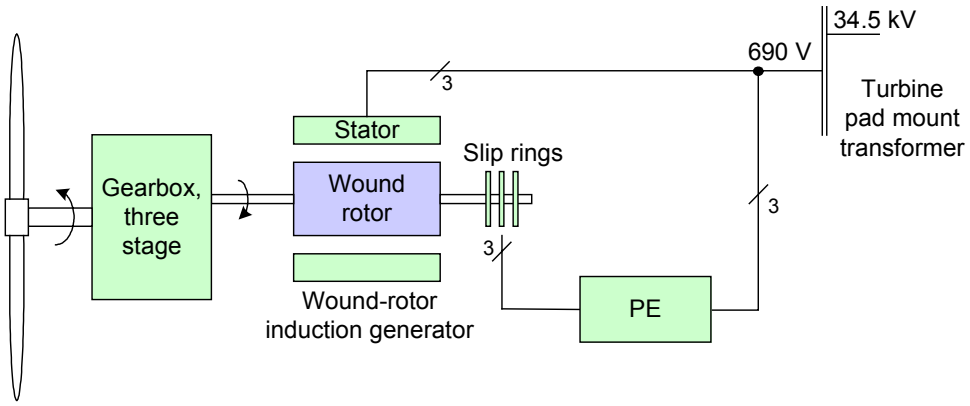

Figure 1-5. Baseline 1.5-MW system diagram

1.5.2 Integrated Baseline Drive Train

The integrated baseline design is an integrated version of the baseline drive train, using a stressed-skin structural nacelle to eliminate the bedplate. This design combines the integrated construction of the single-stage gearbox used in the single PM drive train with a conventional, secondary two-stage gear train and face-mounted generator. A short-coupled mainshaft is supported by tapered roller bearings, which in turn are supported by a housing that is common with the gearbox. A tubular, stressed-skin nacelle supports the gearbox housing. Because the electrical design of this drive train is identical to that of the baseline drive train, the system diagram for this drive train is the same as that of the baseline drive train (shown in Figure 1-5).

The integrated baseline was investigated to provide a direct comparison between a bedplate and an integrated design. The COE estimates for the integrated design are approximately 5% lower than the bedplate-designed baseline, as shown in Table 1-1, primarily because lower component costs result from the more efficient use of material. The integrated design, however, has the disadvantage of using custom components that may not be available from multiple sources. Most of the other designs investigated for this study, including the single PM, direct drive, multi-PM, and multi-induction drive trains, are also integrated designs chosen to save material costs.

1.5.3 Single PM Drive Train

The single PM drive train is an integrated design with a 190-rpm, 72-pole, permanent magnet generator driven by a gearbox with a ratio of approximately 9:1. The generator, gearbox, mainshaft, and mainshaft bearing all are integrated within a common housing. The common generator-gearbox housing is supported by a tubular bedplate structure. The tower-top assemblies are enclosed with a nonstructural fiberglass nacelle cover. The PM generator and PE system described in Sections 1.4.2 and 1.4.3 are used. Figure 1-6 is the system diagram for the single PM drive train.

The COE estimate for the single PM design is 13% lower than the baseline, as shown in Table 1-1, because of lower component costs and higher energy production. The higher energy production results primarily from the high efficiency of the generator and PE system; the lower component costs result from the benefits of integration and elimination of gearbox stages. The generator and PE system costs are comparable to the baseline. The single PM design has the lowest COE estimate of all the drive train designs investigated, and this design will be built and tested during Phases II and III of this project.

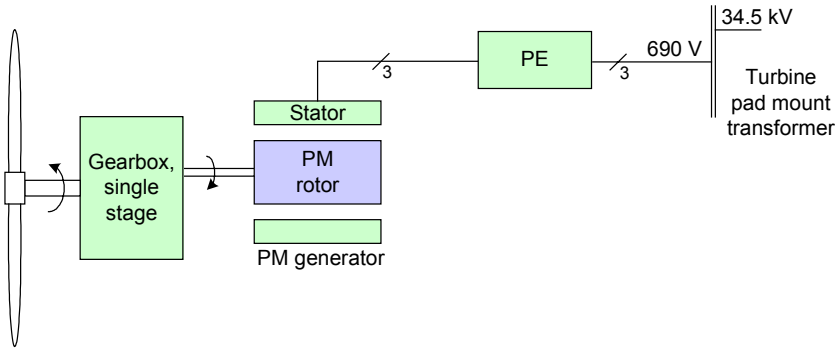

Figure 1-6. Single PM 1.5-MW generator system diagram

1.5.4 Direct Drive Drive Train

The direct drive drive train uses a 96-pole, 4.0-m diameter, PM generator that is directly driven by the turbine rotor. The generator diameter is limited to 4.0 m because larger generators are difficult to transport, even though a larger diameter generator would cost less. The PM generator and the PE system described in Sections 1.4.2 and 1.4.3 are used. Figure 1-7 is the system diagram for the direct drive design.

The COE estimate for the direct drive design is 6% higher than the baseline, as shown in Table 1-1. The high COE results from drive train component costs that are 30% higher than the baseline, because of the high cost of the generator. The higher component costs offset the benefits of higher energy production, which results from eliminating the gearbox losses, and reduced maintenance costs, which accrue from eliminating the gearbox.

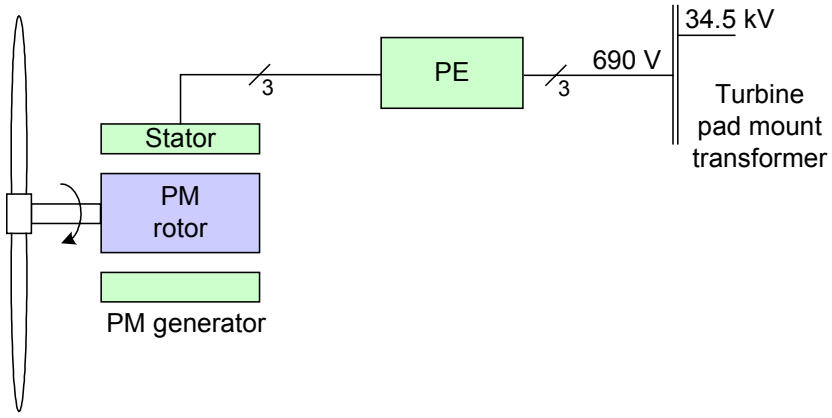

Figure 1-7. Direct drive 1.5-MW system diagram

1.5.5 Multi-PM Drive Train

Six 325-rpm, 250-kW permanent magnet generators are driven by pinions from a common bullgear, which is driven by the turbine rotor through a close-coupled mainshaft. The diameter of the entire system is 3.5 m. The generators, gearbox, mainshaft, and mainshaft bearings are all integrated within a common housing. The PM generator and the PE system described in Sections 1.4.2 and 1.4.3 are used, with the exception that six smaller passive rectifiers are used in the PE system, one for each generator interface. Figure 1-8 is the system diagram for the multi-PM drive train.

The multi-PM component costs depend heavily on the diameter of the system and the number of generators. A wide range of diameters and generator number combinations were analyzed before the minimum cost system was chosen with six generators and a 3.5-m diameter. Increasing the system diameter decreases the cost of the generator's active magnetics because the generator diameter increases and the gear ratio, and therefore generator speed, increases as well. Larger diameters, however, increase the structure and gearbox costs. Increasing the number of generators allows a larger bullgear for a given diameter system, and also decreases the mesh torque of the individual generator pinions.

The COE estimate for the multi-PM design is 11% lower than that of the baseline, as shown in Table 1-1, primarily because of lower component costs and higher energy production. The higher energy production results primarily from the high efficiency of the generator and PE system, and the lower component costs result from the benefits of integration and the efficient use of materials in the multiple-output gearbox. The generator and PE system costs are comparable to those of the baseline.

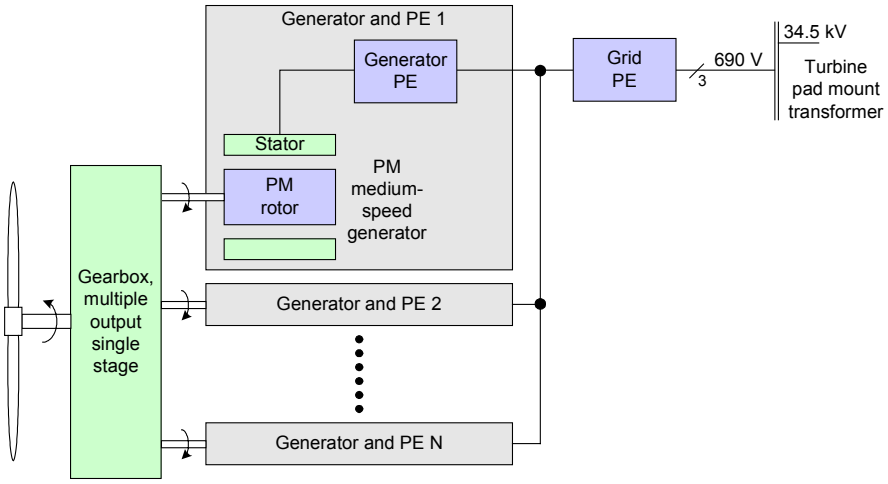

Figure 1-8. Multi-PM 1.5-MW generator system diagram

1.5.6 Multi-Induction Drive Train

In this design, eight 188-kW, 1800-rpm induction generators are driven by multiple outputs from a common gearbox. The diameter of the entire system is 2.5 m. The mechanical design is similar to the multi-PM drive train design described in Section 1.5.5. The same short-coupled mainshaft with bearings integrated into a common housing with the gearbox is used. Like the multi-PM design, the gearbox has a single, large-diameter bullgear that drives multiple pinions. In the case of the multi-induction design, however, the pinions drive multiple secondary, parallel-axis gear stages, which are integrated into the same housing as the first stage. Each gearbox output drives a generator. The generators are electrically connected directly to the grid through the pad mount transformer. Variable-speed power electronics are not used, so the design operates at constant speed. Like the multi-PM system, multi-induction component

costs are highly dependent on the system diameter and number of generators. The eight-generator, 2.5-m diameter system was selected after a wide range of generator number and system diameter combinations were analyzed. Figure 1-9 is the system diagram for this design.

The COE estimate for the multi-induction design is 9% lower than that for the baseline, as shown in Table 1-1. The multi-induction drive train component costs are 34% lower than the baseline, as a result of the benefits of integration, the efficient use of material in the multiple-output gearbox, and the elimination of the PE system. The cost of the multiple generators is lower than the baseline because readily available squirrel-cage generators are used. However, the energy production for this design is 4% less than the baseline because it operates at constant speed.

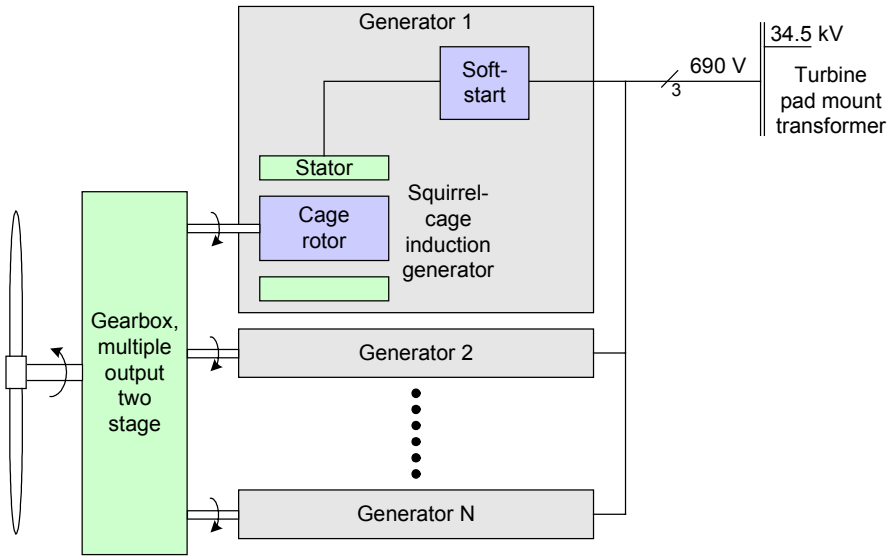

Figure 1-9. Multi-induction 1.5-MW generator system diagram

1.5.7 Klatt Drive Train

The Klatt drive train is a modification of the baseline drive train with the generator and electrical system replaced with the Klatt integrated generator and PE system. The mechanical and structural design is identical to the baseline design. Only the generator and the electrical system are modified. The Klatt generator was invented and patented by Fred Klatt of Engineering Devices, Inc., (EDI) in Bedford, Massachusetts. This system uses a wound-rotor induction generator modified with a high-frequency rotating transformer and an integrated power electronic system. Figure 1-10 is a system diagram for the Klatt drive train.

The Klatt design was investigated at the conceptual level early in the study. The initial estimates, presented in Table 1-1, show the COE of the Klatt design to be about 1% higher than the baseline because of higher combined generator and PE system costs. Other other component and maintenance costs, along with energy production, are equal to the baseline. More detailed preliminary design estimates were not made for this design because significant improvements to the initial estimates were not anticipated.

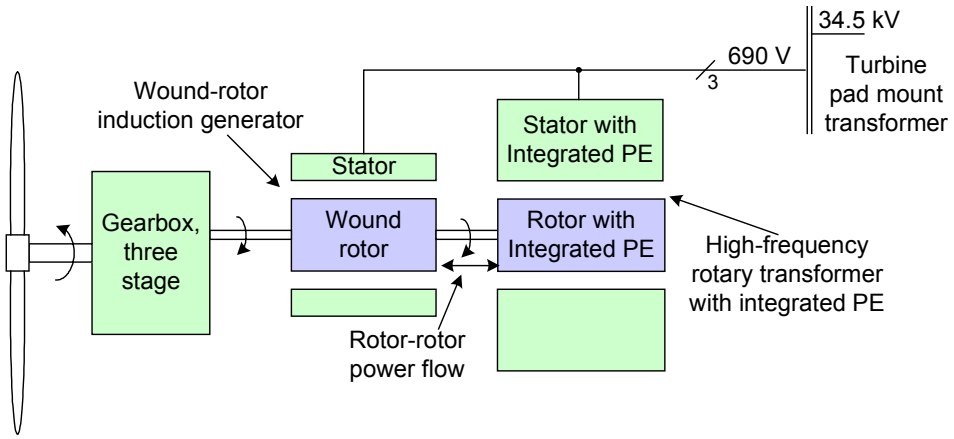

Figure 1-10. Klatt 1.5-MW generator system diagram

1.5.8 Heller-De Julio Drive Train

The HDJ drive train is a modification of the baseline drive train with the generator and power electronic system replaced with the HDJ generator. The mechanical and structural designs are identical to the baseline. Only the generator and electrical system are modified. The HDJ generator is a wound-rotor induction machine whose rotor circuit is modified to achieve a passive, variable-slip characteristic, eliminating the need for a PE system. This generator is connected directly to the grid through a pad mount transformer. The HDJ generator does not provide variable-speed operation below rated speed, but does provide torque-dependent variable compliance above rated speed to reduce gearbox torque transients during wind gusts. The HDJ generator is covered by two patents held by the Heller-De Julio Corporation of Concord, California (Wallace et al. 1999; Wallace et al. 2000). Figure 1-11 is a system diagram for the HDJ drive train.

The HDJ design was investigated at the conceptual level early in the study. The initial estimates, presented in Table 1-1, show the COE of the HDJ design to be about 3% higher than the baseline. The drive train component costs are lower for this design because the PE system is eliminated, but the lack of variable-speed operation below rated speed significantly reduces the energy production relative to the baseline. More detailed preliminary design estimates were not made for this design because significant improvements to the initial estimates were not anticipated.

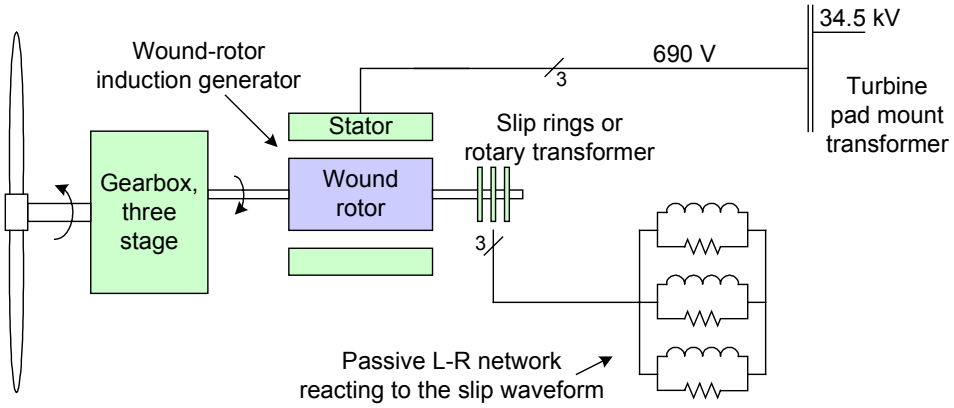

Figure 1-11. HDJ 1.5-MW generator system diagram

1.5.9 Henderson Drive Train

The Henderson drive train is a modification of the baseline drive train, using a hydraulic torque-limiting system to replace the baseline variable-speed power electronics. The baseline gearbox, generator, and PE system is replaced with the proprietary Henderson torque-limiting gearbox and a fixed-speed, grid-connected squirrel-cage induction generator. The system provides torque limiting to reduce gearbox loads without requiring a variable-speed PE system. Although the Henderson design does provide desirable torque limiting, the technique does not capture the additional energy associated with variable-speed operation. The Henderson system is covered by a U.S. patent held by Geoff Henderson, Christchurch, New Zealand (Henderson 1992). Figure 1-12 is a system diagram for the Henderson drive train.

The Henderson design was investigated at the conceptual level early in the study. The initial estimates, presented in Table 1-1, show the COE of the Henderson design to be about 1% higher than the baseline. The drive train component costs are lower for this design because the PE system is eliminated, but the lack of variable-speed operation below rated speed significantly reduces the energy production relative to the baseline. More detailed preliminary design estimates were not made for this design because further improvements to the initial estimates were not anticipated.

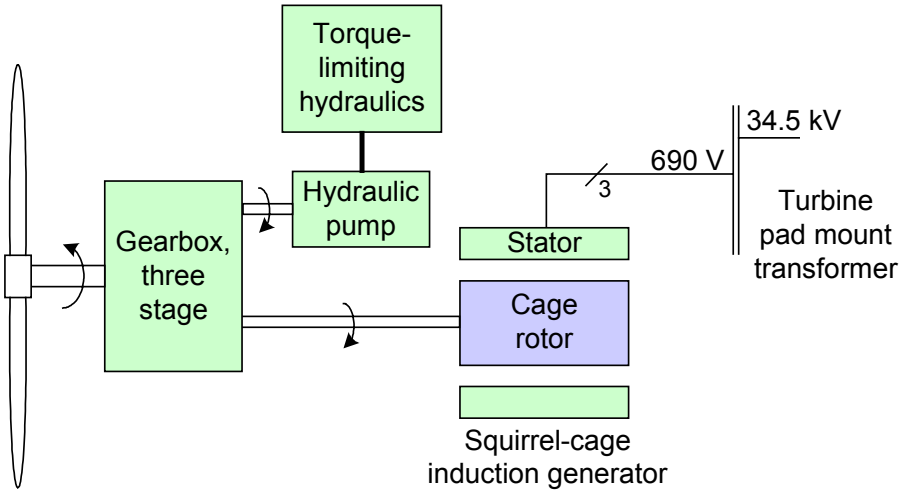

Figure 1-12. Henderson 1.5-MW torque-limiting gearbox system diagram

1.6 Summary of Cost of Energy Estimates

Table 1-1 summarizes the drive train component cost estimates, net annual energy production estimates, operations & maintenance (O&M) and levelized replacement cost (LRC) estimates, and the resulting COE for each of the candidate drive trains. The COE estimates are lower than those commonly being realized in practice because, to be constant with other WindPACT studies, a relatively low fixed charge rate was used, a turbine manufacturer overhead and profit markup was not added to the turbine rotor cost, and the balance-of-station costs were kept low. Because each of these factors was applied consistently to all estimates, however, these COE numbers still correctly state the relative merits of each drive train design.

The COE estimate for three of the drive train designs—the single PM, multi-PM, and multi-induction—are substantially lower than the baseline COE. The single PM COE estimate is the lowest, at 87% of the baseline. The multi-induction drive train has the lowest drive train component cost, but this design also has a lower energy capture because of its constant-speed operation, offsetting some of the benefits in the COE estimate. The direct drive, Klatt, HDJ, and Henderson designs all have higher COE estimates than the baseline. This is caused by higher component costs for the direct drive and Klatt designs, and by lower energy production, primarily because of constant-speed operation, for the HDJ and Henderson designs. The integrated baseline design has a COE estimate that is approximately 5% lower than the baseline estimate, resulting from a lower drive train component cost resulting from the benefits of integration. Based on these results and other factors, the single PM configuration was selected for detailed design and testing during Phases II and III of this project.

Table 1-1. Summary of Results (all costs in 2000 U.S. dollars, $)

	Baseline	Integrated Baseline	Direct Drive	Single PM	Multi-PM	Multi-induction	Klatt	Heller-De Julio	Henderson
Transmission system	155,000	120,000	NA	90,000	58,000	80,000	155,000	166,000	178,000
Support structure	34,000	21,000	55,000	20,000	19,000	11,000	34,000	34,000	34,000
External cooling system	2,400	3,000	3,400	4,400	5,300	4,500	2,400	2,400	2,400
Brake	1,400	1,300	12,400	3,200	5,600	2,800	1,400	1,400	1,400
Coupling	2,400	2,100	NA	NA	NA	1,800	2,400	2,400	6,000
Nacelle cover	17,000	9,000	14,000	8,200	7,000	13,100	17,000	17,000	17,000
Generator	60,000	60,000	304,000	54,000	78,000	40,000	60,000	77,000	42,000
Power electronics	62,000	62,000	53,000	53,000	53,000	17,000	74,000	6,000	17,000
Substation VAR control	NA	NA	12,000	12,000	12,000	12,000	NA	12,000	12,000
Transformer	23,000	23,000	26,000	26,000	26,000	23,000	23,000	23,000	23,000
Cable	18,000	18,000	16,000	16,000	16,000	18,000	18,000	18,000	18,000
Switchgear	12,000	12,000	10,000	10,000	13,000	22,000	12,000	12,000	12,000
Other subsystems	25,000	25,000	25,000	25,000	25,000	25,000	25,000	25,000	25,000
Drive train assembly and test	8,000	4,900	9,400	5,500	7,900	10,200	8,000	8,000	8,000
Drive train component cost total	**420,000**	**361,000**	**540,000**	**327,000**	**325,000**	**279,000**	**433,000**	**404,000**	**396,000**
Percentage of baseline drive train cost	**100**	**86**	**129**	**78**	**77**	**66**	**103**	**96**	**94**
Annual net energy production (AEP; in kilowatt-hours)	**4.841E+06**	**4.841E+06**	**4.990E+06**	**5.001E+06**	**4.978E+06**	**4.658E+06**	**4.841E+06**	**4.637E+06**	**4.668E+06**
Percentage of baseline AEP	**100**	**100**	**103**	**103**	**103**	**96**	**100**	**96**	**96**
Replacement costs—LRC ($/yr)	**5100**	**5100**	**5600**	**4800**	**4500**	**4700**	**5100**	**5100**	**5100**
O&M ($/yr)	**24600**	**23500**	**23700**	**21200**	**23400**	**22900**	**24600**	**24600**	**24600**
O&M ($/kWh)	**0.0051**	**0.0049**	**0.0047**	**0.0042**	**0.0047**	**0.0049**	**0.0051**	**0.0053**	**0.0053**
COE ($/kWh)	**0.0358**	**0.0339**	**0.0378**	**0.0313**	**0.0317**	**0.0325**	**0.0361**	**0.0368**	**0.0363**
Percentage of baseline COE	**100**	**95**	**106**	**87**	**89**	**91**	**101**	**103**	**101**

1.7 Summary of Scaling Estimates to 750 kW and 3.0 MW

In Figure 1-13, the drive train estimates for each design at 750 kW, 1.5 MW, and 3 MW are shown together in terms of the drive train COE. The COE for the drive train is the portion of the turbine COE attributed to the drive train capital cost. A constant hub height of 84 m is used for all sizes to eliminate the effects of height differences on wind speed in the COE calculations. All designs except the direct drive show a decreasing drive train COE from 750 kW to 1.5 MW and an approximately level COE from 1.5 MW to 3 MW. The direct drive is an exception, increasing in COE as turbine size increases. This result for the direct drive is caused by limiting the diameter of the direct drive generators to 4.0 m, a practical limit for transportation purposes. These generators have an optimum diameter that is larger than 4.0 m.

The results shown in Figure 1-13 do not necessarily reflect the COE trends when scaling an entire wind turbine system. As turbine sizes increase, the costs of rotors and other elements of the system may rise more rapidly than the energy production for the system. The most cost-effective wind turbine size for a given wind energy project will most probably depend on site-specific wind resources, transportation logistics, and construction and erection issues.

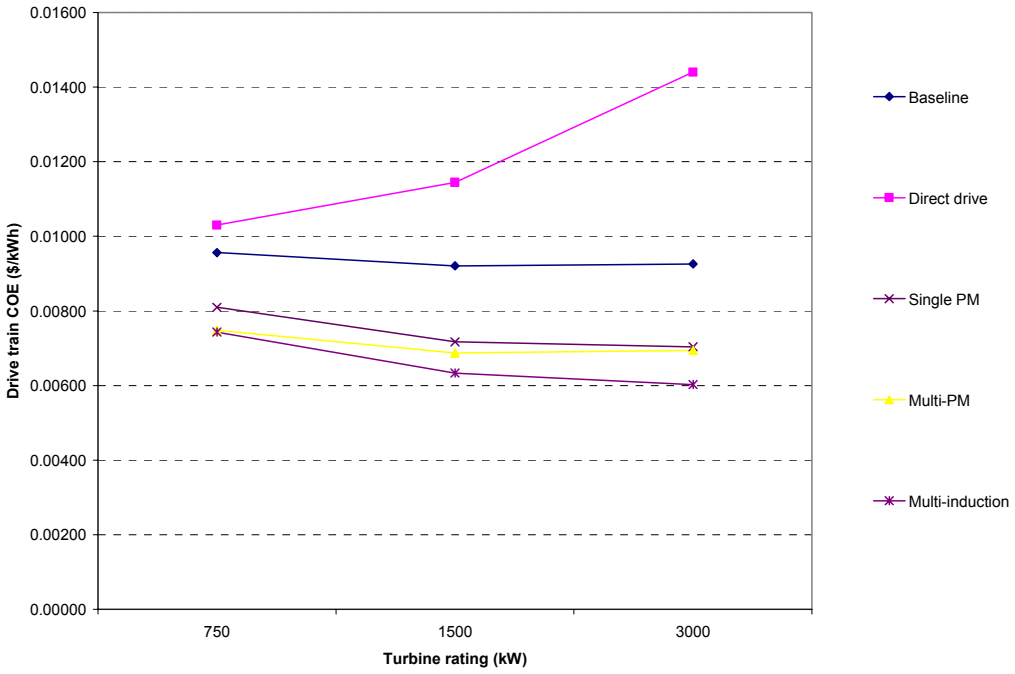

Figure 1-13. Drive train COE scaling for 84-m hub height

2. Introduction

Robert Poore led the GEC study team as the principal investigator, and Terry Lettenmaier served as the project engineer and assistant principal investigator. In this capacity, Lettenmaier contributed heavily to the technical aspects of the study. He also coordinated the activities of the study participants and supervised the lower tier subcontracts with industrial participants. Other contributing GEC staff members included Tim McCoy, Eli Reich, and Mark Young.

GEC was supported by a number of consultants with expertise in the wind industry. In addition, companies that have expertise and product offerings in the technical areas of interest participated in the study. The participants and their roles are summarized in the sections that follow.

2.1 Participating Consultants

The following consulting companies or individual consultants participated in the study.

- PEI of Pewaukee, Wisconsin, designed the drive train mechanical systems, including the gearbox, bearings, lubrication, torque coupling, and structural support subsystems. Ed Hahlbeck, the principal at PEI, led this work. PEI performed several point designs of one-, two-, and three-stage gearboxes. For the active magnetics of the permanent magnet generators, PEI analyzed and designed the rotor and stator support structures.

- OEM of Boston, Massachusetts, supported the electrical system aspects of the study including the generator, power electronics, and electrical interfaces to the balance of the utility system. Jamie Chapman, the principal of OEM, led this work.

- William Erdman of Brentwood, California, performed many of the detailed performance modeling and economic analyses of the power electronic systems used to convert the variable-frequency, variable-voltage electrical power output to standardized, utility-grade electric power. Erdman also analyzed reduced-cost techniques for coupling the processed generator power from a number of wind turbines to the wind farm substation while satisfying the prevailing electrical power quality standard, Institute of Electrical and Electronics Engineers (IEEE) 519.

- McCleer Power, Inc., of Jackson, Michigan, performed design calculations that independently verified design and performance aspects of the permanent magnet generators. Pat McCleer, the principal, developed scaling relationships that enabled extension of one 1.5-MW, medium-speed permanent magnet generator analysis to the other drive train generators at all power ratings.

- Clipper Windpower, LLC, of Goleta, California, investigated control methods for the multi-induction drive train. As part of this investigation, a 2.5-kW bench-scale unit was built and tested. Geoff Deane was the principal investigator for this work.

- DeWolf Engineering of Tracy, California, conducted a survey of pad mount transformer manufacturers. Mark DeWolf, the principal, also worked in cooperation with William Erdman to estimate reactor and transformer costs for the various power electronic system estimates.

- Phil Forde and Associates, LLC, of Tacoma, Washington, performed hydraulic system design estimates where needed. Phil Forde, the principal, performed this work.

2.2 Participating Manufacturing Companies

The following design and product system companies made significant contributions to the study. All were invited to participate because of their expertise and product offerings in the technical areas of interest. Some had significant wind industry experience; others had technologies that could be incorporated advantageously into the drive train systems.

- Kaman Aerospace Corporation, Electromagnetics Development Center, Hudson, Massachusetts. Kaman is a manufacturer of PM motors and generators. Peter Mongeau and Victor Donescu were the principal contributors. Kaman performed a concept study of various PM generators early in the study and later developed a detailed design for a 1.5-MW, medium-speed PM generator from which all other PM generator estimates were scaled.

- Milwaukee Gear Corporation, Milwaukee, Wisconsin, is a gearbox manufacturer. The company worked in cooperation with PEI to estimate production gearbox costs for PEI's designs.

- The Timken Company, Canton, Ohio, is a manufacturer of bearings for a number of industries. Timkin estimated mainshaft bearing designs and costs in coordination with PEI.

- Siemens Energy and Automation, Alpharetta, Georgia, and Nuremberg and Berlin, Germany. At its facilities in Nuremberg, Siemens is a major manufacturer of the wound-rotor and squirrel-cage induction machines that are used in wind turbine drive trains. Siemens also produces the PE systems required to process the rotor power. In addition, at the company's facilities in Berlin, Siemens develops and manufactures PM synchronous generators used in wind turbines and in ship propulsion. The principal Siemens interface was Richard Admill of Alpharetta. Hermann Conraths (Nuremberg) served as the focus for the Siemens activities in Europe, as well as for the European wind markets. Martin Kaufhold served as the focal point for the development of the PM machines. Other members of the study team visited the Siemens development and manufacturing facilities in all three locations during the course of the study.

- Loher Drive Systems, Roswell, Georgia, and Ruhstorf, Germany. Loher is a major producer of both wound-rotor induction machines as well as the more conventional squirrel-cage induction machines. Joachim Zwick (Ruhstorf) and Mark Watson (Roswell) were the principal contributors. Through its partnership with SEG of Germany and through its in-house expertise, Loher also contributed in the area of the PE systems required to process the rotor power of the wound-rotor induction machines. During the course of the study, project participants visited the Loher manufacturing and development facilities.

- Rockwell Medium Drives Division, Cambridge, Ontario. This business unit of Rockwell manufactures variable-speed drives that have rated capacities in the range from 1 MW to 10 MW. Other divisions of Rockwell manufacture drives with smaller ratings. Greg Obermeyer is the business development manager for Rockwell.

2.3 Drive Train Configurations Investigated

The following drive train designs were investigated during the study:

1. **Baseline:** A modular, bedplate design that uses a three-stage gearbox driving a wound-rotor induction generator, the rotor power of which is processed and coupled to the utility grid by a PE system with a rating about one-third that of the generator.

2. **Integrated baseline:** An integrated version of the baseline drive train that uses a stressed-skin structural nacelle to eliminate the bedplate.

3. **Direct drive:** A wind turbine mainshaft directly drives a single, low-speed, high-torque, PM synchronous generator. All of the generator's electrical output is processed and coupled to the utility grid by a full-rated PE system.

4. **Single PM:** A single-stage gearbox drives a single, medium-speed, medium-torque, PM synchronous generator. All of the generator's electrical output is processed and coupled to the utility grid by a full-rated PE system.

5. **Multi-PM:** A single-stage gearbox with multiple output shafts that drive a number of medium-speed, medium-torque, PM synchronous generators. All electrical output from the generators is processed, combined, and coupled to the utility grid by PE systems.

6. **Multi-induction:** A two-stage gearbox with multiple output shafts that drive a number of squirrel-cage induction generators. The electrical output from the generators is interfaced to the utility grid without a variable-speed PE system.

7. **Klatt:** A three-stage gearbox drives a modified wound-rotor induction generator. The generator's rotor power is processed and coupled to the utility grid by a second, high-frequency rotor-stator and PE system.

8. **Heller-De Julio:** A three-stage gearbox drives a modified wound-rotor induction generator. The generator's rotor windings are connected or coupled to a passive inductor-resistor combination that provides variable compliance without using PE.

9. **Henderson:** A three-stage gearbox with a hydraulic torque-limiting system that is integrated with the third stage. The hydraulic system drives a squirrel-cage induction generator, and the generator's electrical output is interfaced to the utility grid without a variable-speed PE system.

Detailed descriptions of these drive trains are given in Sections 5 through 13, which are devoted to their analysis.

2.4 Assessment Sizes

A 1.5-MW power rating was chosen for all drive train designs developed for the WindPACT drive train study. These 1.5-MW estimates made up the bulk of the effort for the study. The completed 1.5-MW estimates were then scaled to two additional turbine sizes, 750 kW and 3 MW, to provide approximate estimates for those sizes.

2.5 Project Approach

The NREL subcontract specified the approach taken during Phase I, which is summarized below.

1. **Select configurations and assessment sizes:** The nine drive train configurations described in Section 2.3 were specified as part of the subcontract statement of work for the project. The 1.5-MW primary assessment size and the 750-kW and 3000-kW scaling sizes were chosen with the consensus of NREL and the study team. These sizes are consistent with the assessment sizes used for the WindPACT rotor study (Malcolm and Hansen 2002). In addition, they are common sizes for existing, state-of-the-art turbines being manufactured in the United States and Europe.

2. **Develop drive train specifications:** Early in the project, a specification that defined specific operational and environmental requirements for the drive trains, along with an associated baseline turbine, was developed. The specification was developed to be consistent with the assumptions made for the WindPACT rotor study (Malcolm and Hansen 2002) and with specifications for existing, state-of-the-art turbines being manufactured in the United States and Europe.

3. **Conduct loads analysis:** Once the specification was complete, the project team used a computer model of the specified turbine, initially developed for the WindPACT rotor study (Malcolm and Hansen 2002), to calculate drive train loads.

4. **Develop conceptual drive train designs:** Initial conceptual designs were developed for each of the nine 1.5-MW drive train configurations described in Section 2.3. The objective was to develop practical designs with the lowest possible COE. This was a cooperative effort primarily involving GEC, PEI, and OEM, with input from the remaining study participants. Computer solid models were developed to visualize the designs and estimate material content.

5. **Estimate COE:** Component cost and efficiency estimates were developed for each of the conceptual drive train designs. These estimates were used to calculate the COE for an entire turbine system using each drive train design.

6. **Select concepts for preliminary design:** NREL staff and the study team reviewed the nine conceptual designs and associated economic results. Configurations 1 through 6 described in Section 2.3 were selected for further, more detailed preliminary design. Further work was discontinued on configurations 7 through 9, the Klatt, HDJ, and Henderson drive trains. The COE estimates for these three configurations were comparable or higher than the baseline system and significant improvements were not anticipated.

7. **Prepare preliminary design and economic estimates:** Preliminary 1.5-MW designs were developed for the six selected configurations. This work expanded on the conceptual design estimates already performed, with further Pro/E modeling and the development of detailed generator and power electronic designs. Detailed COE estimates were completed for each design.

8. **Scale estimates to 750 kW and 3 MW:** The 1.5-MW preliminary design results for the six configurations were scaled to estimate component costs, efficiency, and COE for equivalent 750 kW and 3 MW designs.

9. **Select the preferred design:** After reviewing the preliminary design and scaling results, the GEC team and NREL selected the preferred configuration for the detailed design and fabrication that will take place during Phase II of the project.

2.6 Report Organization

The remainder of this report is broken into the sections summarized below.

Section 3 summarizes the specifications and loads that all the drive trains evaluated were required to meet and gives a more detailed description of the turbine characteristics assumed for the analysis.

Section 4 presents design and analysis methods and information that is common for two or more of the configurations examined. The study's approach to estimate the cost of energy and to design certain

components are presented. In addition, this section contains technical descriptions of generators and PE systems that are common on multiple configurations.

Sections 5 through 13 contain the analysis results for each configuration examined. Each section addresses a single configuration and includes a system description along with the results of the analysis. Any unique analysis methods used for the configuration are also covered in these sections.

Section 14 summarizes the results presented in Sections 5 through 13 to allow a convenient comparison of the COE for each configuration studied.

Section 15 is a list of the abbreviations used in this report, and Section 16 contains references. Appendices A through M contain supporting and background information.

3. Specifications and Assumptions

This section summarizes the specifications of the baseline turbine and the drive train design loads and specifications.

3.1 Turbine Characteristics

3.1.1 Background

GEC recently completed the *WindPACT Turbine Rotor Design Study* (Malcolm and Hansen 2002). For this rotor study, a baseline turbine design was developed that included a detailed blade design and approximate designs for other structural components. Cost estimates were made for all components, for the drive train, and for other nonstructural components.

The rotor study baseline design was developed using ADAMS™ dynamic analysis software. Design loads were produced per International Electrotechnical Commission (IEC; 1998) standards for an initial design, and the loads were applied to the structural and drive train design. If the design was inadequate for the loads, the design was modified and the simulations were rerun until the design converged to a configuration that could withstand the loads.

The baseline turbine design produced for the rotor study is also the baseline design for this study. Section 3.1.2 summarizes this turbine configuration. Considerably more detail describing the design and development process of this turbine design can be found in the rotor study final report (Malcolm and Hansen 2002).

3.1.2 Specifications

The baseline turbine design is based on the specifications NREL provided for the overall WindPACT project. The NREL statement of work included the following baseline configuration specifications:

- Three blades
- Upwind
- Full-span, variable-pitch control
- Rigid hub
- Blade flapwise natural frequency between 1.5 and 2.5 per revolution
- Blade edgewise natural frequency greater than 1.5 times flapwise natural frequency
- Rotor solidity between 2% and 5%
- Variable-speed operation with maximum power coefficient = 0.50
- Maximum tip speed <= 85 m/s
- Air density = 1.225 kg/m^3
- Turbine hub height = 1.3 times rotor diameter (later modified to 1.2)
- Annual mean wind speed at 10 m = 5.8 m/s
- Rayleigh distribution of wind speed
- Vertical wind shear power exponent = 0.143
- Rated wind speed = 1.5 times annual average at hub height
- Cut-out wind speed = 3.5 times annual average at hub height
- Dynamically soft-soft tower, natural frequency between 0.5 and 0.75 per revolution (later modified to soft-stiff, natural frequency between 1 and 3 per revolution)
- Yaw rate less than 1 degree per second.

These characteristics were used to develop the baseline wind turbine design. In addition to these specifications, other assumptions were made about the architecture and operation of the turbine:

- Independent blade pitch for redundancy, mechanical parking brake only
- Stand-alone automatic operation, including start-up and shutdown (this does not include fault resets or maintenance)
- Start-up accomplished through blade pitch control
- Normal shutdown accomplished through blade pitch control only
- Emergency shutdown accomplished through blade pitch control only.

Table 3-1 summarizes the specifications for the baseline turbine at three power ratings.

Table 3-1. Baseline Wind Turbine Specifications

Rating, kW	750	1500	3000
Rotor diameter, m	50	70	99
Design tip-speed ratio	7.0	7.0	7.0
Rated wind speed, m/s	11.5	11.5	11.5
Minimum operating rpm (n_1)	8.0	5.7	4.1
Rated rpm	28.6	20.5	14.5
Maximum operating rpm (n_2 = 1.07*rated)	30.6	21.9	15.5
PE system trip rpm (= 1.14*rated)	32.6	23.4	16.5
Safety system activation rpm (n_a = 1.2*n_2)	36.7	26.3	18.6
Maximum overspeed design rpm (n_{max} = 1.3*n_2)	39.8	28.5	20.2
Hub height, m	60	84	119
Hub height V_{ave}, m/s (for production estimates)	7.5	7.9	8.3
Cut-in wind speed, m/s	3.0	3.0	3.0
Cut-out wind speed, m/s	26.3	27.6	29.0

3.2 Drive Train Specifications and Design Criteria

A general specification was developed to guide the design process for all the alternative drive train design concepts investigated. Appendix A contains this specification (GEC document N60001). The objective of this document was to specify the operational requirements and environmental operating envelope common to all the alternative drive trains. These specifications were based on the combined experience of the principal project team members.

3.3 Drive Train Loads Specification

A loads specification was developed for the baseline 1.5-MW wind turbine. This loads specification, GEC document N60003, can be found in Appendix B. The loads used in the specification were based on the results of ADAMS™ modeling of the baseline turbine performed during the rotor study (Malcolm and Hansen 2002). The loads included peak loads from the IEC-specified extreme and turbulent wind cases as well as fatigue loads from the turbulent wind cases. The load cases considered are detailed in the specification. The load points included the shaft/hub interface, the yaw bearing, and a gearbox torque/speed histogram. Additional discussion of the approach used to develop the loads is presented in Section 4.3.

4. Common Design, Analysis, and Costing Methods

4.1 Overview

This section describes the economic assessment methods; the component design, analysis, and cost methods; and results that are applicable to more than one drive train design. This information is applicable to the different drive train designs described in Sections 5 through 13. In cases where the component design and/or cost information is not common but is specific to a single drive train design, that information is included in the section that describes that particular drive train and is not duplicated in this section.

This section first describes the method used to assess the COE and each of its economic components. Next are the assumptions, methods, and computational tools used to model and describe the drive train loads and control systems. This is followed by a description of the design and costing approaches used for the gearbox and mechanical components of the drive train. A review of the generator types considered in the study is followed by a detailed discussion of the PM generators examined in the study. This section closes with a description of the PE and electrical systems, their technical characteristics, and their economics.

4.2 Cost of Energy Analysis

Economic comparisons of the different drive train designs were made using COE estimates for entire wind turbine systems using each drive train design. Two fundamental assumptions were made for all the economic estimates:

- The turbine systems, including the drive train design, were assessed as mature designs, manufactured with large volumes giving 200–1000 MW per year of installed capacity.
- The turbine systems included an entire 50- to 100-MW wind farm.

The COE values for the wind turbine system were calculated from the expression:

$$COE = \frac{ICC * FCR + O\&M + LRC}{AEP}$$

In this equation, the symbols stand for the following economic and energy parameters:

ICC	Initial capital cost (dollars)
FCR	Fixed charge rate (percentage/year)
O&M	Operations and maintenance costs (dollars/year)
LRC	Levelized replacement cost (dollars/year)
AEP	Annual net energy production (kilowatt-hours/year)

The resulting units for COE are dollars per kilowatt-hour. This method of calculating wind turbine COE is described in Cohen et al. (1989). Further discussion of this method relative to alternate assessment methods can be found in Short et al. (1995).

The methods used in this study to determine each term in the COE equation are described in the subsections that follow.

4.2.1 Initial Capital Cost

The ICC is the sum of the wind turbine system cost and the balance-of-station cost. For the calculations made in this study, the balance-of-station costs and all turbine system costs not directly affected by the drive train design were made with estimates from the WindPACT rotor study (Malcolm and Hansen 2002) as described in Section 3. Drive train component costs were estimated in detail for each design as described elsewhere in this report.

The turbine manufacturer's overhead and profit were included in the ICC. This was estimated with a 30% markup of all turbine components except the tower and rotor. Towers would normally be purchased directly by the wind farm developer and therefore not marked up by the turbine manufacturer. Rotors would typically be marked up by the turbine manufacturer; however, because a markup was not included in the WindPACT Rotor study, it was not included in these estimates for consistency with those results.

4.2.2 Fixed Charge Rate

The FCR is the amount of revenue per dollar of ICC needed to pay the carrying charges for the investment. It includes return on debt, return on equity, taxes, depreciation, and insurance. The choice of FCR rate significantly affects the calculated COE. A detailed description of the FCR and the methods used to estimate it can be found in Short et al. (1995).

NREL specified an FCR of 10.6% at the beginning of the WindPACT studies, and this percentage was used for all COE estimates presented in this report for consistency with the other WindPACT studies. However, NREL estimates of the FCR have increased since the WindPACT studies began. Current (as of the end of 2002) NREL estimates of the FCR are approximately 11.8%, which would result in higher COE estimates.

4.2.3 Annual Operations and Maintenance Cost

This is the annual cost for operating and maintaining the wind turbine system and balance of station. These costs were estimated in detail for each drive train and turbine system as part of the study.

The O&M costs for the baseline architecture were derived using several approaches, in addition to the experience of the participants. These approaches included a survey of the cost experience of a number of wind farm operators, a review of the data available in U.S. and European computer databases, and a review of past studies funded by the U.S. Department of Energy (DOE) and by the Electric Power Research Institute (EPRI). These data were used to construct a bottoms-up O&M model. The model identified the major wind turbine and wind farm subsystem components.

To calculate unscheduled maintenance, each component was assigned a failure rate, a mean time to repair, and an estimate of the associated parts and labor costs. The failure rates and replacement costs used in the model represent blended estimates between rare major catastrophic failures and more frequent minor damage or subsystem component replacement. These parameters were fed into a Weibull statistical model (Vachon 2002) to calculate the total number of failures for each component over the life of a 67-unit wind farm. An average annual failure rate per wind turbine was calculated from the total number of failures. The sum of these average yearly costs makes up the unscheduled maintenance cost projections reported in this document.

Some of these data were also used in projections of the scheduled (preventive) maintenance costs. The costs for annual and semiannual scheduled maintenance visits were calculated by assuming a maintenance crew size, the maintenance time required per wind turbine subsystem, and the associated parts and labor

costs. For the baseline drive train, this amounts to a two-person crew performing two 8-hour days of scheduled maintenance twice a year.

The costs of the operations staff were based on a three-person complement: a person for administration and inventory control, one on-call person for night and weekend coverage, and a supervisor.

To develop the O&M costs for the other drive trains, the baseline model was adjusted to reflect the additional configuration. Specific details are given in the sections that describe the results for each drive train design.

4.2.4 Levelized Replacement Cost

The LRC distributes the costs for major overhauls and replacements over the life of the wind turbine. As part of the study, these costs were estimated in detail along with the O&M estimates.

4.2.5 Annual Net Energy Production

AEP is calculated as the gross annual energy production (GAEP; defined to be at the output of the wind turbine generator and its associated PE system, see Section 4.2.6) times the availability of the turbine, minus the losses encountered as the power flows from the wind turbine to the delivery point, the output of the wind farm substation. An availability of 95% and a loss fraction of 7% were used for all estimates in the study.

4.2.6 Gross Annual Energy Production

For a given wind turbine with its associated PE system, the GAEP is the total electrical energy delivered at the output of the wind turbine-PE system. This is the electrical energy per year that the the wind turbine-PE system delivers to the pad mount transformer.

Numerical calculation of the GAEP value for a given wind turbine system requires the wind speed frequency distribution and the wind turbine power curve. Both are functions of the wind speed.

The wind speed frequency distribution gives the number of hours per year that the wind speed value lies within defined wind speed intervals or bins. Typically the bin size is 0.5 m/s or 1.0 m/s. For example, using a bin size of 1.0 m/s, wind speeds in the range 9.5 m/s to 10.5 m/s may be expected to occur for 250 hours out of the 8760 hours per year. Similarly, the turbine power curve may be partitioned into the same wind speed bins. For example, the power value characterizing the wind speed 10 m/s may be used. For the 1.5-MW baseline wind turbine, this value might be 950 kW. The product of these two values yields the value of the annual energy produced for wind speeds within this interval: (250 hours) * (0.95 MW) = 237.5 MWh. When this process is repeated for every wind speed bin and the resultant values summed, the value that results is the GAEP.

The wind speed frequency distribution used for this study is a Rayleigh distribution with a 5.8 m/s annual average wind speed at 10 m. An assumed 0.14 shear exponent was used to extrapolate the 10-m wind speed to the hub height of the turbine. This wind speed model was applied uniformly to all the drive train architectures.

The wind turbine power curves were calculated for this study using a performance coefficient (Cp) versus tip-speed ratio (TSR) model of the aerodynamic rotor developed for the WindPACT rotor study (Malcolm and Hansen 2002) and efficiency estimates made for each drive train design. The drive train efficiency estimates are based on individual efficiency versus load curves developed for each drive train component.

4.3 Modeling and Analysis of Mechanical Loads

The loads used in the study are based on ADAMS™ modeling of the baseline turbine done at GEC. ADAMS™ is a proprietary, general-purpose, commercially available package for computing the effects of the loads applied to a defined structure. The program is available from MSC Software of Santa Ana, California (formerly MDI, Inc., of Ann Arbor, Michigan). The program AeroDyn generates the required aerodynamic inputs for ADAMS™. All modeling was performed with ADAMS™ version 11.0 and AeroDyn version 12. The loads used to design the drive trains are based on a number of simulations of the ADAMS™ models. The details of the load cases and data processing for the baseline system can be found in the load specification in Appendix B. Further modeling and analysis was conducted on the single PM drive train loads as used with the SCR-based PE system torque control. These load data were found to be approximately equal to the baseline loads data and therefore were not included in this report. The bullets that follow furnish more information on the ADAMS™ model used in the analysis.

- **Aerodynamic modeling:** The aerodynamic model used in AeroDyn is the basic induction factor method with a skewed wake correction. Dynamic stall is modeled with the Beddoes model. Tip loss is accounted for with the Prandtl model. The inputs to the aerodynamic model are blade geometry (chord and twist versus radial station) along with lift and drag coefficients.

- **Structural modeling:** The ADAMS™ structural model is made up of three primary elements: parts, beams, and joints. Parts are entities that have mass and inertial properties but no flexibility. Parts are connected to one another via either beams or joints. Beams are flexible members with no mass that can connect two parts. Joints are connections between parts that allow some combination of rigid body translations, rotations, or both.

- **Blades:** The blade is modeled as a series of 15 parts connected by 14 beams. The part masses and beam stiffnesses have been calculated for the blade design described in Malcolm and Hansen (2002). Aerodynamic forces are applied to all the parts except the most inboard part. These forces are applied at the aerodynamic center of the part, estimated to be at the 25% chord location.

- **Hub:** The hub is modeled with four parts (a central hub and three pitch bearing parts). The hub part is connected to the pitch bearing parts via revolute joints for blade pitch motion.

- **Drive train:** The drive train is modeled as a beam connected to an inertia. The beam has a torsional stiffness selected to match the equivalent effect of the shafting and gearing. No gearing is modeled, and all motions and loads are in the low-speed frame of reference. The inertia representing the generator is scaled by the square of the gear ratio to represent an equivalent inertia in the low-speed frame of reference. The drive train is connected to a bedplate part through a revolute joint representing the main bearing. The bedplate has a representative mass and inertia, but is not flexible. The bedplate is connected to the tower through a revolute joint that represents the yaw bearing.

- **Tower:** The tower is modeled with a series of parts and beams. The part masses and beam stiffnesses have been calculated for a generic tower design.

4.4 Modeling and Analysis of the Pitch and Power Control Systems

The pitch and control systems were included in the ADAMS™ model developed at GEC. The details of this modeling are described in the following subsections.

4.4.1 Control System

The control model of the 1.5-MW baseline turbine is a simple approximation of the common approach to variable-speed control. The generator torque and rotor speed control are essentially independent. The generator torque control is assumed to have infinite bandwidth and is an instantaneous lookup table from rotor rpm to generator torque. The rotor speed control is a proportional integral derivative (PID) loop on rpm, with the output of the controller being a demanded blade pitch angle.

In addition to modeling the baseline variable-speed turbine, a turbine with a SCR PE system was modeled. For this PE system, the bandwidth of the generator torque control is an order of magnitude less than that of the baseline. A modification to the generator torque control was incorporated in the ADAMS™ model to reflect this.

The details of the control models used for the analysis are described in the subsections that follow.

4.4.2 Rotor Speed Control

The blade pitch is used to control rotor speed with a set point at the nominal, rated rpm (20.5). Below rated power, the blade pitch position is held at a mechanical limit and does not vary. Above rated power, the blades pitch collectively to keep the rotor at the rated rpm. The simulation uses a PID control algorithm to apply the gains to the rpm error and compute a demanded pitch setting, which is fed to an actuator algorithm. Figure 4-1 is a block diagram of the rotor speed control, and the associated constants are listed in Table 4-1.

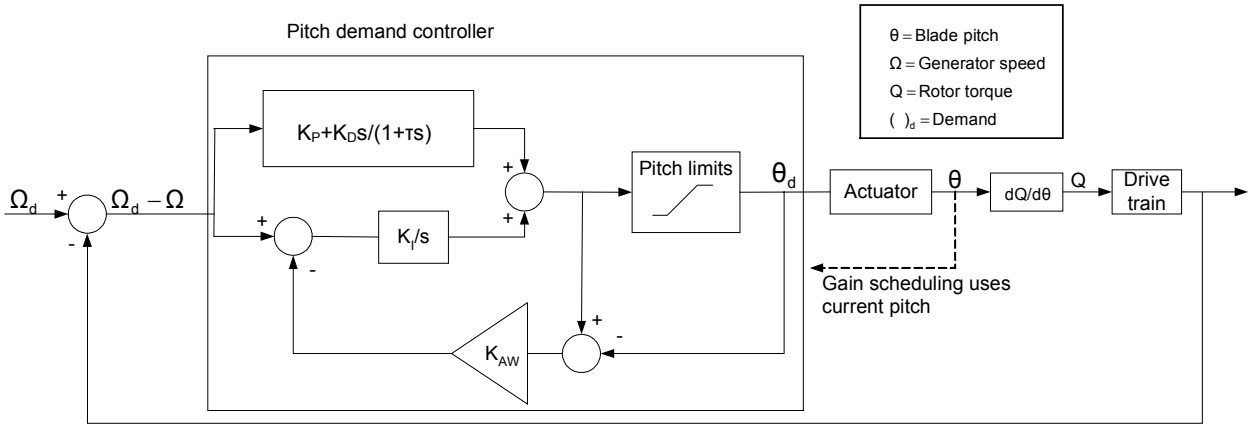

Figure 4-1. Rotor speed control block diagram

Table 4-1. Rotor Speed Control Constants

Item	Value
Proportional gain (K_p)	5.8 deg/rpm
Integral gain (K_i)	2.5 deg/rpm
Derivative gain (K_d)	-0.036 deg/(rpm/s)
τ	0.02
Anti-windup (K_{aw})	0.30 rpm/deg

4.4.3 Blade Pitch Control

The pitch actuator is simulated with another PID loop that computes blade pitching torque from pitch error. The pitching torque is applied to the simulated mechanical system that calculates blade pitch states and other turbine states from the equations of motion in ADAMS™. Table 4-2 lists the selected PID gains that provide a near critically damped response with a -3dB roll off at approximately 2 Hz (6P for nominal rpm).

Table 4-2. Pitch Actuator Control Constants

Item	Value
Proportional gain (K_p)	97.7 kNm/deg
Integral gain (K_i)	523 kNm/deg
Derivative gain (K_d)	7.1 kNm/(deg/s)

4.4.4 Generator Torque Control

The simulation of generator torque control for the baseline system is based on a torque-speed curve from a lookup table. The torque increases parabolically from the cut-in rpm to the rated rpm after which the torque rises only very slowly with rpm. This slight rise gives better damping than a flat line. The net effect is that below rated power the aerodynamic torque is balanced with the generator torque in such a way that the turbine operates at a constant TSR. Above rated power, wind gusts are absorbed in rotor speed increases until the pitch system can catch up and slow the rotor down by reducing the aerodynamic power input. The torque-speed curve is shown in Figure 4-2. Note that both torque and speed are in the low-speed shaft frame of reference.

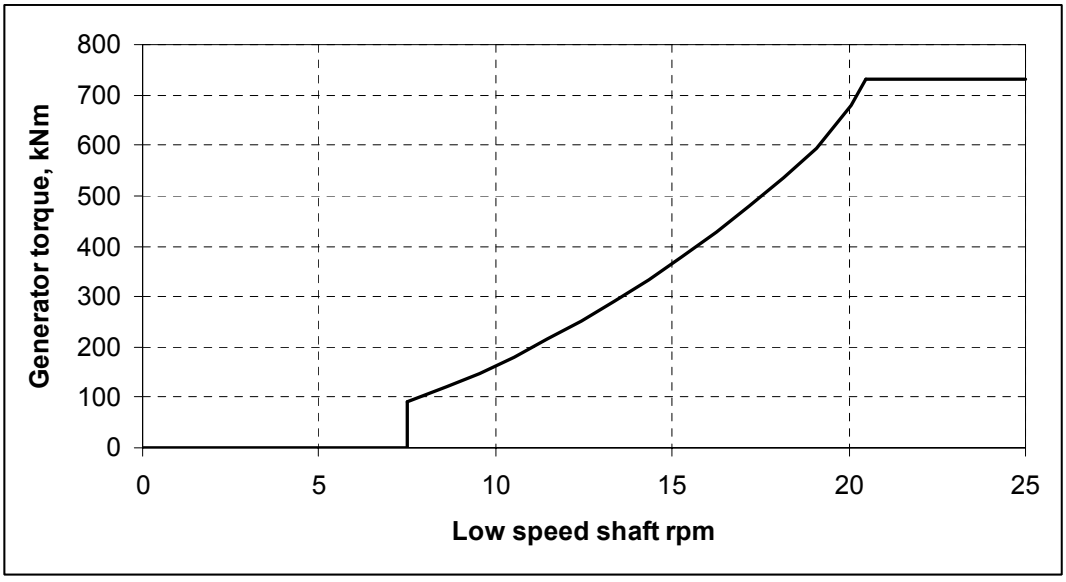

Figure 4-2. Generator torque-speed curve

Some of the evaluated configurations used PE systems that are based on SCRs and/or diodes rather than the baseline's IGBTs. In the control modeling of these systems, the response of the generator and the PE system are based on a diode-rectified PM generator with a DC link to an SCR-based grid converter. Figure 4-3 depicts this system, and the associated constants are listed in Table 4-3. The generator current

(torque) is the integral of the voltage difference between the generator and the grid converter across the DC link inductance. The DC link inductance is assumed to be the dominant element in the response time of the current to changes in voltage. The generator voltage is assumed to be a linear function of rpm. The DC link voltage provided by the grid converter is varied to keep the current, and hence the torque, at the level demanded by the torque-speed curve, as previously described for the baseline system.

Voltage demand is fed to the grid converter from a compensator that is a feedback loop on current error. The SCR-based PE system has a bandwidth of approximately 300 Hz, limiting its ability to react to rapid changes in voltage demand. The PID gains are calculated to provide optimum response given the bandwidth of the grid converter.

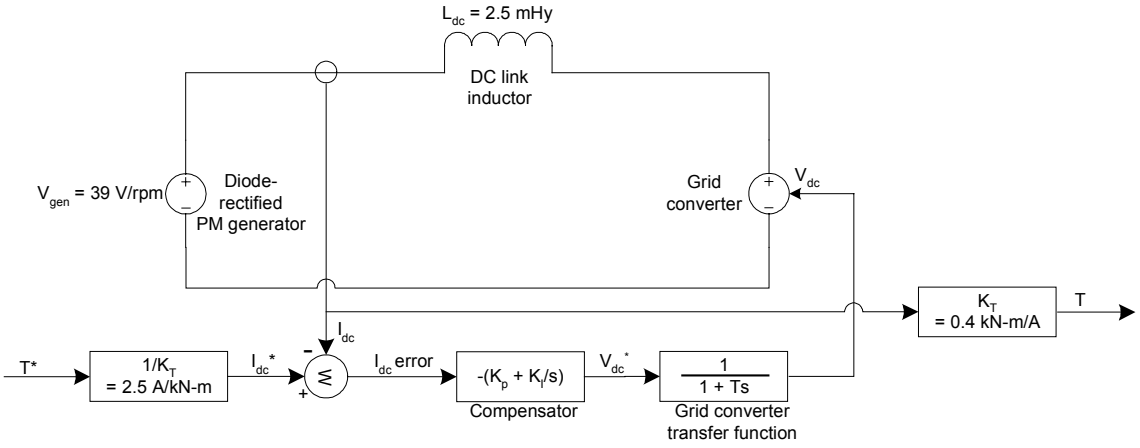

Figure 4-3. Generator/PE system control block diagram for SCR-SCR PE system

Table 4-3. Generator System and Control Constants for SCR-SCR PE System

Item	Value
K_p	0.67 V/A
K_I	15.0 V/A
K_T	2.5 A/kNm
T	2.8 ms

4.5 Design of the Gearbox and Mechanical Components

4.5.1 Introduction

For each of the alternative designs studied, the following objectives and constraints were considered:

- Economics, lowest weight, volume, and cost of gearing that meets life requirements of the gearbox at the loads specified.
- Design constraints as defined in specification AGMA/AWEA (American Gear Manufacturers Association/American Wind Energy Association) 921-A97, "Recommended Practices for Design and Specification of Gearboxes for Wind Turbine Generator Systems" (AGMA/AWEA 1997).
- Noise characteristics, not exceeding current industry practice.

4.5.2 Loads

Loads were developed as described in Section 3.3 and are provided in Appendix B. For gear design purposes, the number of cycles at a specified level is the parameter of primary interest. The data provided in Table 9-2 of Appendix B were put in terms of cycles using the following equation:

$$Cycles = rpm \cdot 60 \cdot hours\_lifetime$$

Bins of torque 10 kNm through 130 kNm were eliminated because they have 0 h. An average rpm was derived as follows:

$$Rpm\_avg = \frac{Total\_cycles}{Total\_hours * 60}$$

4.5.3 Gear Geometry, Design for Cost

It is PEI's experience that designing for minimum volume, while satisfying other design criteria, results in optimization of cost. This is because the gear specifications used are common to industrial gear vendors, meaning that cost will most closely correlate to gear size. The procedure used to design gear sets for minimum volume is found in ANSI/AGMA (1992).

4.5.4 Gear Geometry, Design Constraints

For preliminary gear design, the constraint of gear face aspect ratio was set to 1.0, as recommended in AGMA design guidelines. The minimum number of teeth is also defined as a constraint and was set to 21. This prevents excessive undercut and results in designs that are more resistant to scuffing. The high-speed or intermediate gear elements in multistage designs are based on helical gear teeth, with adequate tooth overlaps to prevent noise. Helical gearing is used also in the single-stage gearbox applications, with the expectation that this will eliminate the need to isolate the transmission and tower structure for noise control purposes.

4.5.5 Gear Material Properties

Gear rating and cost estimates in the study are based on ANSI/AGMA (2001) C95 grade 2 materials. This specification is widely used for high-performance applications in industrial service. It specifies quality attributes for internal soundness, level of cleanliness, hardenability, grain size, and other attributes.

Specific alloy selection is dependent on gear section sizes. Most of the gear elements have tooth pitch larger than 6 modular (4 diametrical pitch), which requires alloys of sufficient hardenability to ensure proper core properties. Alloys such as A1S1 4320, A1S1 9310, and DIN 17CrNiMo6 are used for the larger tooth sizes. Gears of lesser tooth size and smaller section sizes can be made of lower alloy, lower cost grades such as A1S1 8620H.

4.5.6 Gear Heat Treatments

External gear rating is based on carburized and hardened gear teeth processed to meet the requirements of the ANSI/AGMA (2001) specification for C95 grade 2. This specification defines properties of the case and core structure, as well as the hardness and quality control of these properties.

Internal (ring) gears are often made of through-hardened materials. The ratings of the gears define the hardness levels required. In the study's cost analysis, ring gear surface hardness treatments are not used unless required by the gear rating.

4.5.7 Other Gearbox Design Elements

Bearings and shafts are rated per ANSI/AGMA (1997). The gear derating factor *km* is selected based on experience and design guides for wind turbine drives. A more refined analytical model will be used in the detailed design of the gearbox selected for detailed design and testing.

4.5.8 Design Approach for the Mechanical Components

Mechanical components include general structures such as bedplates, generator adaptors, couplings, and similar items that, together with the gearbox, make up the mechanical driveline. For this study, the geometry and section sizes are guided by design experience and, in some cases, by manufacturing rules such as minimum castable wall thickness. As a validity check, structural weights were checked against weights published by several manufacturers.

Complex components not currently used in production turbines were stress analyzed using finite element analysis (FEA) at a level of detail sufficient to ensure, with reasonable certainty, that detailed designs were feasible without a large error in weight and cost of the component.

After developing the gearbox design, the support structure was developed to provide support from the tower top to the hub flange face. The hub interface to the mainshaft and its dimension to the rotor center line were fixed. The rotor hub center line to tower axis was made as short as possible, but not less than required for tower clearance. General guidelines for tower-top diameters and rotor to tower centers were taken from the GEC rotor study (Malcolm and Hansen 2002). This process produced a preliminary layout of the drive train.

From a preliminary layout, the driveline was developed as a solid model using Pro/E software from Parametric Technologies. Whenever practical, the overall dimensions were made parametric to allow resizing with minimal effort. Parametric studies were used to determine least-cost configurations. The parametric studies varied from configuration to configuration and are explained in greater detail in the alternate design sections of this report.

4.5.9 Structural Materials

With the exception of bedplates, structural components are based on cast ductile iron, grade DIN GGG-40.3 (DIN, 1997), which is approximately equal to ASTM 60-40-18 (ASTM, 1993). This is a special grade that has good cold weather impact properties and meets regulatory requirements of Germanischer Lloyd (Germanisher Lloyd 1999) for structural service in wind turbines.

Bedplate designs are based on steel weldments. A preliminary design analysis, based on FEA, was done on a limited basis to validate the general design.

4.6 Costing of the Gearbox and Mechanical Components

This section describes the empirical and computer-based cost modeling systems used to estimate the costs of gearing, bearings, castings, and other components and subsystems.

The Pro/E solid model for each drive train design was the basis of many of the cost estimates. The Pro/E software was used to estimate the material masses of each component. This information was then used to estimate the component costs based on a cost-per-unit-mass approach.

4.6.1 Baseline Gearbox Costs

The gears and other machined details of the baseline configuration and the single PM configuration were estimated with the computer-aided process planning software called OPTAPLAN at Milwaukee Gear and were based on piece-part drawings from the Pro/E models. The OPTAPLAN software processes the part to a rules-based system, producing a detailed manufacturing plan that considers actual metal removal and machine tool capabilities. The resultant plan is near optimal for manufacturing time and cost. Material costs and purchased part costs for the baseline were obtained from vendors, based on the detail drawings.

Combining the Milwaukee Gear and supplier quotations provided a complete bill of materials (BOM) for the baseline gearbox. The costed BOM of the baseline drive was compared to known market prices for similarly sized and configured wind turbine gearboxes. This comparison showed that a 25% markup in the BOM prices was appropriate.

4.6.2 Gear Costs

For gears not quoted by Milwaukee Gear, a mass-based equation, developed from the Milwaukee Gear quotes, was used to estimate cost. Table 4-4 summarizes the Milwaukee Gear data. The selling prices include a markup of 33%, recommended by Milwaukee Gear, to represent market prices for unassembled gear parts.

Table 4-4. Summary Data for Gear Estimates

Item Name	Mass, kg	Cost, $	Selling Price, $
Bullgear	969	4,398.66	5,864.88
Planet	219	1,553.10	2,070.80
Ring gear	1,124	5,300.00	7,066.67
Planet	321	2,748.75	3,665.00
Sun gear	115	1,098.00	1,464.00
Intermediate gear	347	2,102.06	2,802.75
Intermediate pinion	218	1,455.28	1,940.37
Output pinion	113	653.52	871.36

Figure 4-4 is a graphical representation of Table 4-4 and shows a linear curve fit. The equation in Figure 4-4 is the equation used for gears not quoted by Milwaukee Gear.

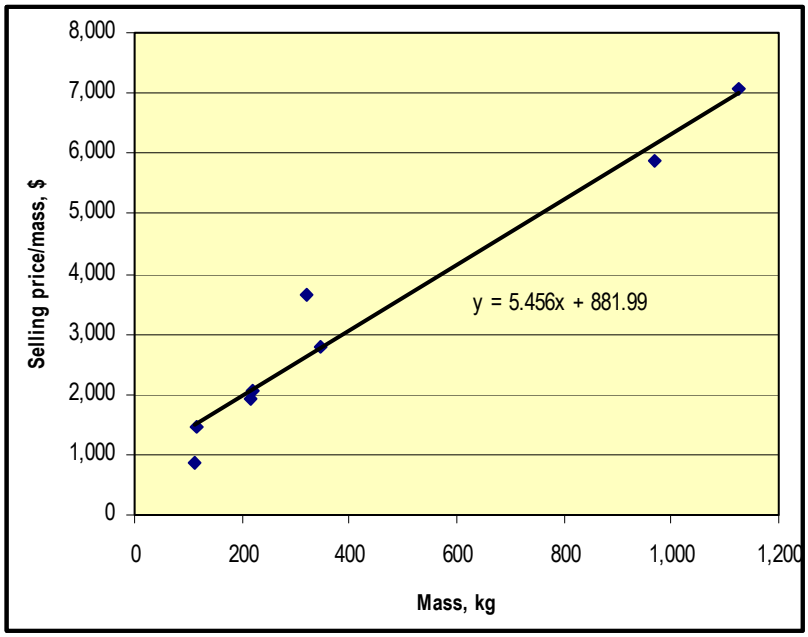

Figure 4-4. Gear cost data

4.6.3 Casting Costs

Castings for the WindPACT designs are either of ductile iron, DIN grade GGG40.3 (DIN 1997), or gray iron per SAE grade 2500 to 3500 (SAE 1993). Casting costs were estimated on a cost-per-pound basis using costs available from low-cost suppliers typically used by the wind industry. Castings show a strong correlation of mass to cost. Tables 4-5 and 4-6 summarize quoted costs for large castings for ductile iron and grey iron, respectively. Prices include freight to the central Midwest. Figure 4-5 presents a graph of these data.

Table 4-5. Quoted Costs of Large Ductile Iron Castings

Item Name	Mass, kg	$	$/kg
Carrier	2,976	3,417	1.15
Housing	5,375	7,896	1.47
Mainshaft	1,995	2,212	1.11
Generator ring cast	3,742	4,131	1.10
Milwaukee Gear housing	3,371	4,288	1.27
Generator hub	67	80	1.19
Main housing	3,480	4,465	1.28
Housing cover	1,252	1,366	1.09
Forward housing	2,140	2,345	1.10

Table 4-6. Quoted Costs of Large Gray Iron Castings

Item Name	Mass, kg	$	$/kg
Carrier	2,976	2,643	0.89
Housing	5,375	6,498	1.21
Mainshaft	1,995	1,694	0.85
Generator ring cast	3,742	3,158	0.84
Milwaukee Gear housing	3,371	3,411	1.01
Generator hub	67	63	0.93
Main housing	3,480	3,560	1.02
Housing cover	1,252	1,040	0.83
Forward housing	2,140	1,789	0.84

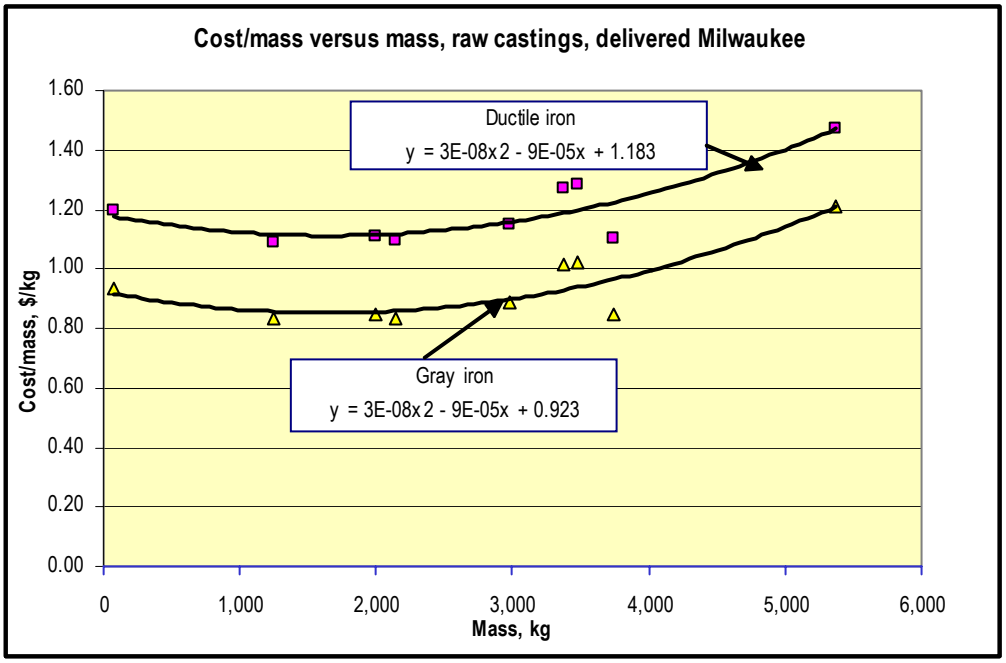

Figure 4-5. Curve fits of iron versus mass

The following cost equations are based on Figure 4-5:

$$\begin{aligned} Ductile\,iron &= R\_{DI} = 2.6\cdot10^{-8}\cdot M^2 - 8.57\cdot10^{-5}\cdot M + 1.18305 \\ Grey\,iron &= R\_{GI} = 2.6\cdot10^{-8}\cdot M^2 - 8.57\cdot10^{-5}\cdot M + .92305 \end{aligned} \quad (\$/kg)$$

These equations were used to estimate the costs of castings for this study.

4.6.4 Machining Costs

To obtain machining cost estimates, PEI completed the detailed design of several components sufficient for quotation and submitted them to two suppliers for quotation. These suppliers were familiar with machining large wind turbine parts. Table 4-7 summarizes the information obtained, and Figure 4-6 presents a graph of the summary data.

The machining costs of various components were estimated using the data presented in Figure 4-6.

Table 4-7. Summary of Machining Costs

	Machining				
	Mass, kg	Vendor 1, $ ea	Vendor 2, $ ea	Selected	$/kg
Generator hub	67	560	179	179	2.67
Generator spindle	1,207	1,530		1,530	1.27
Housing cover	1,252	1,845	2,552	1,845	1.47
Mainshaft	1,995	1,950	2,680	1,950	0.98
Forward housing	2,140	3,080	4,444	3,080	1.44
Rear housing	2,459	1,890	NA	1,890	0.77
Main housing	3,480	1,840	NA	1,840	0.53
Single-stage housing	4,253	2,025	NA	2,025	0.48
Housing assembly	4,732	3,420	6,258	3,420	0.72

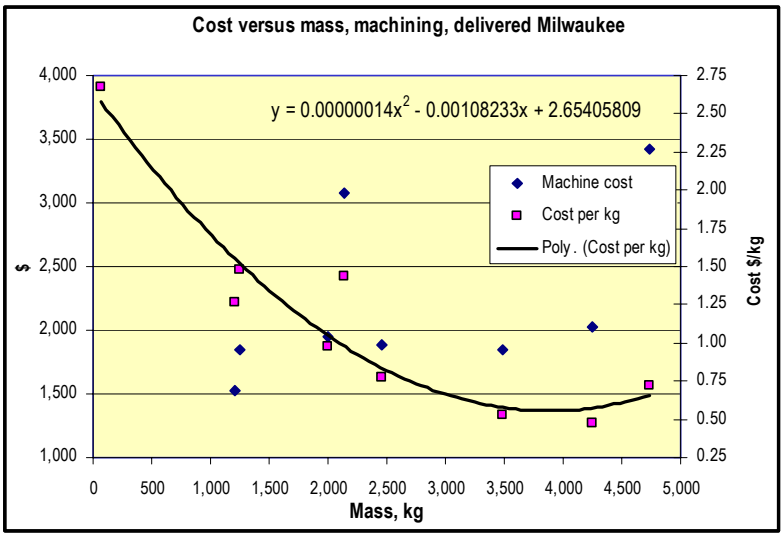

Figure 4-6. Machining cost versus mass

4.6.5 Bearing Cost

Bearing costs are estimated based on a curve fit of data taken from quoted costs for the baseline design. Based on required dynamic capacity, the data listed in Table 4-8 were used in a regression analysis.

Table 4-8. Quoted Bearing Data

Item Number	Mass	ID Inside Diameter	OD Outside Diameter	Length	Cost	Dynamic Capacity	Cost/Mass
	kg	mm	mm	mm	$	kN	$/kg
NJ330	31.2	150	320	65	506	38.2	16.22
NU315	3.3	75	160	37	41	12.1	12.28
24148	80.7	240	400	160	927	106.8	11.48
23228	17.7	140	250	88	198	37.3	11.19
NU1076	71.2	380	560	82	1,094	59.6	15.36
22248	8.1	240	440	120	94	98.9	11.57
23156	83.5	280	460	146	958	119.2	11.48

To determine dynamic capacity, the relationship between load, speed, and life was used. A first-order estimate of this is:

$$P_{dynamic} = (6*rpm\_pinion)\text{^}0.3*((wt\text{^}2+(wt*0.48)\text{^}2)\text{^}0.5)/2 \text{ (N)}$$

where wt = tooth load (N) = torque ÷ pitch radius.

In this equation, the constant 6 represents a life factor, ≈ 200,000 h, and 0.48 ≈ a ratio of tooth load to separating force, and 0.3 is the bearing fatigue life exponent.

Curve fitting the data in Table 4-8 provides the plots and curve fits shown in Figure 4-7. These relationships were used to compute mass and cost from dynamic capacity.

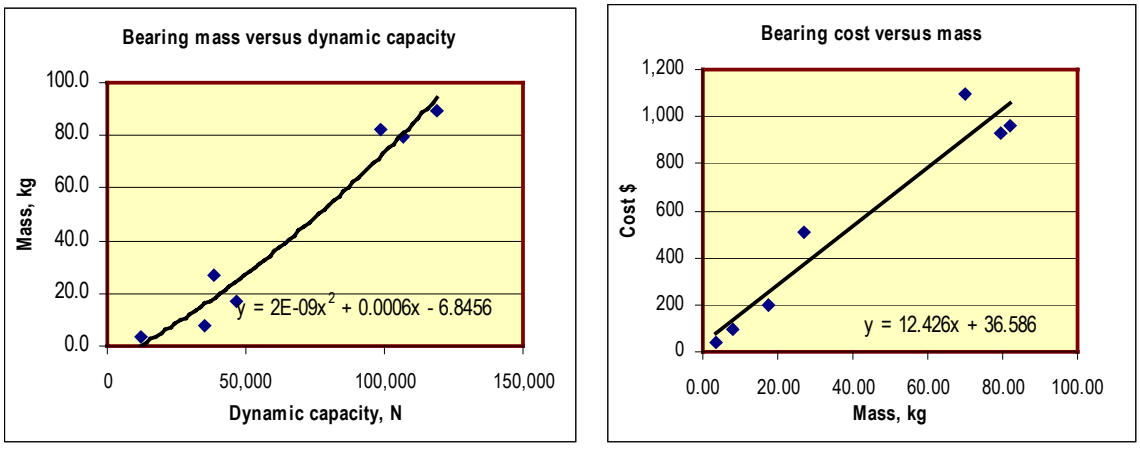

Figure 4-7. Bearing mass versus dynamic capacity and cost versus mass

The cost and mass data from Table 4-8 are also shown in Figure 4-8. Because bearing cost/mass is nearly constant, in some cases, for simplification, bearing cost was calculated with the average cost of $14.81/kg (figure price plus 12% for shipping).

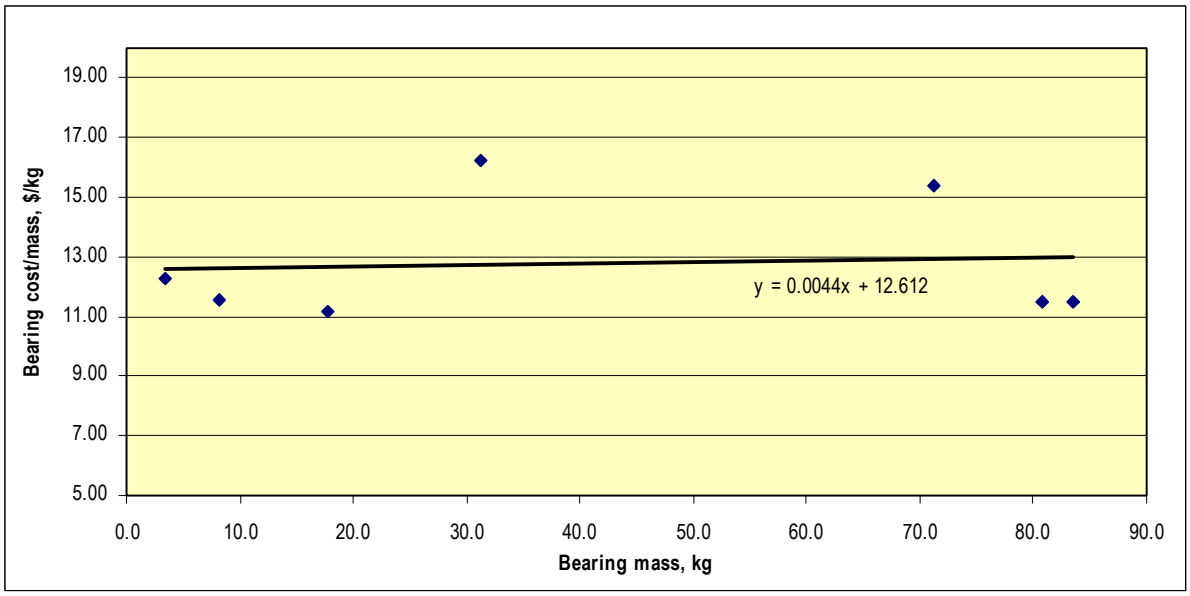

Figure 4-8. Bearing cost/mass versus bearing mass

4.6.6 Costs of Gearbox Assembly and Test

Assembly consists of a fixed base time, to which time is added for each gear stage and for each of the gear elements within a stage. All the studied components have mass that requires mechanical hoisting; therefore, no time distinction was made for differences in component mass.

The size of these machines dictates a minimum two-person crew. For this study, a fully burdened two-person crew rate of $125/h was used.

Table 4-9 gives an example of assembly and test estimates.

Table 4-9. Example Gear Assembly and Test Estimates

	Baseline		Medium Speed	Multigenerator
Stage	1	2	1	1
Gears/stage	5	2	7	7
Hours per gear	3	3	3	3
Stage assembly, total hours	15	12	21	21
Variable, total	27		21	21
Base time	15		15	15
Test	6		6	6
Total hours	48		42	42
Crew rate, $	125		125	125
Total, $	6,000		5,250	5,250

4.6.7 Coupling Costs

Couplings are used to connect rotating shafts without imposing moments on the connected components. Couplings exhibit a strong cost correlation with torque capacity. For generator connections, all based on 1,800 rpm, the correlation is also consistent with nominal power rating. From vendor catalogs (KTR Corporation 2003) and using $7.72/kg for costs, the information in Table 4-10 was developed.

This information was then used to develop the relationship in Figure 4-9, where coupling cost is related to rating. This relationship was used to cost couplings.

Table 4-10. Summary of Coupling Data

Couplings, Ka = 1.5, rpm = 1,800				
kW Rating	Torque, Nm	Weight, kg	$/kg	Projected $
750	5,966	132	7.72	1,022.00
1,000	7,954	200	7.72	1,540.00
1,500	11,931	269	7.72	2,079.00
2,000	15,908	404	7.72	3,115.00
3,000	23,862	506	7.72	3,906.00

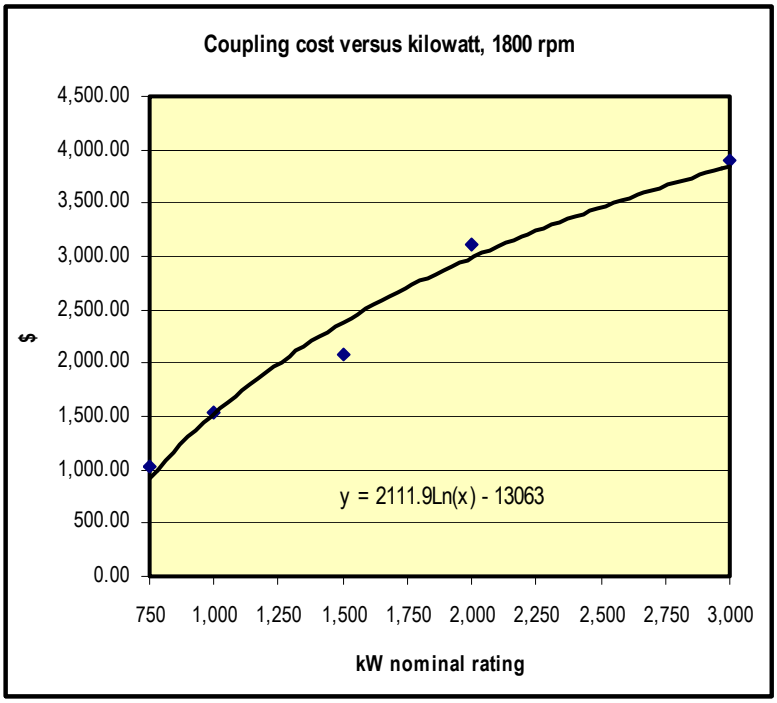

Figure 4-9. Relationship of coupling cost to turbine rating

4.6.8 Requirements and Cost of the Braking System

The turbine design, described in Section 3.1, uses independent blade pitch control, which provides a redundant system to slow the rotor during overspeed events. The mechanical brake systems were designed with sufficient torque capacity to hold the rotor in a parked position during maintenance operations, but not with the heat capacity to slow down the rotor from rated or higher speeds. This parking brake was designed to accommodate the rated torque of the turbine, calculated based on turbine operation at rated speed. In the case of the 1.5-MW machine, with a nominal speed of 20.5 rpm:

$$Q_{required} = \frac{1500kW}{20.5rpm} \bullet 7120 = 521{,}000Nm$$

The actual torque capacity of a system depends on the number of calipers n, the brake disc diameter d (m), the brake force F (Newton), the ratio between the rotor shaft and the brake disc shaft R, and the number of brake systems N:

$$Q_{brake} = (F \bullet (d - .06) \bullet R \bullet n) \bullet N$$

Sizing is done to achieve $Q_{brake} \geq Q_{required}$

Table 4-11, from a spreadsheet, depicts the results of such an analysis. The cells in green (below the heavy dashed line) have adequate capacity; those in yellow (above the heavy dashed line) do not. Cost, based on various combinations of disc size and number of calipers, is shown.

Table 4-11. Brake Analysis

Nominal torque (Nm) = 521,000
Gearbox ratio = 15.84
Design margin = 1.15

Brake worksheet

No calipers/disc =	1	1	2	1
No discs =	6	4	2	2
Brake force, N =	40,000	40,000	40,000	88,000

	Rated brake force, N			
	8,000	40,000	88,000	160,000
Caliper mass, kg	17.5	78.3	169.5	306.3
Caliper cost, $	$210	$940	$2,034	$3,676

Disk dia, mm	Brake system torque capacity			
300	396,689	264,459	264,459	290,905
400	561,976	374,650	374,650	412,115
500	727,263	484,842	484,842	533,326
550	809,906	539,937	539,937	593,931
600	892,550	595,033	595,033	654,536

	Disc			
Disc dia, mm	400	600	800	1,200
Disc mass, kg	10.1	17.9	28.0	33.9
Disc cost, $	$45	$81	$126	$153

Selected disc size =	400	550	550	500
Torque per caliper =	5,913	8,522	8,522	16,835
System cost =	$8,542	$6,199	$4,369	$4,572

Caliper cost, $/kg	$12.00
Disc cost, $/kg	$4.50

The lowest cost combination, considering physical limitations of brake disc size, was determined from worksheets similar to the one shown in Table 4-11, which were developed for each design.

4.6.9 Requirements and Cost of the Gearbox Cooling System

For gearboxes, the heat load for auxiliary cooling can be computed as follows:

$$kW_{cooler} = kW \cdot loss\% - (A_{rad} + A_{conv})$$

where:

kW = Nominal full load rating

$Loss\%$ = Percent of inefficiency / 100

A_{rad} = Radiation capacity of gearbox, kW

A_{conv} = Convection to surroundings, gearbox, kW

and

A_{rad} = 7 watts per / m^2 / per Δ°C

A_{conv} = 25 watts per / m^2 /per Δ°C

Example: for a 1500-kW machine with 3% loss, 10m^2 area, and ΔC = 30:

$$kW_{cooling} = 1500 \cdot .03 - (.007 \cdot 10 \cdot 30 + .025 \cdot 10 \cdot 30)$$

$$kW_{cooling} = 35.3kW$$

The cooling system ratings and weights summarized in Table 4-12 were based on available sizes from catalog data (HYDAC International 2002).

Table 4-12. Summary Data, Oil Coolers

Cooling, Gearbox Oil		
kW	**Mass, kg**	**Liters/minute**
13.4	66.7	401
24.6	103.0	1003
33.5	163.3	1003
44.7	183.7	1003
59.6	215.5	1003

The cooling system mass versus kilowatt capacity information listed in Table 4-12 is curve fitted to give the following equation, which is used to size the system. The corresponding curve is shown in Figure 4-10.

$$M_{cool} = -.0418 \cdot kW^2 + 6.374 \cdot kW - 15.387 \quad \text{(kg.)}$$

From vendor estimates, the approximate cost per mass rate is $20.00/kg. Applying this rate to the equation above gives the following equation, which can be directly used to estimate cooling system costs:

$$Cost_{cool\_gears} = -.837\text{kW}^2 + 127.46\ \text{kW} - 307.74\ (\$)$$

The curve for this cost equation is shown in Figure 4-10. Using this equation to estimate cost for our 1.5-MW example:

$$Cost_{cool\_gears} = -.837 \cdot 35.3^2 + 127.46 \cdot 35.3 - 307.74 = \$3{,}148$$

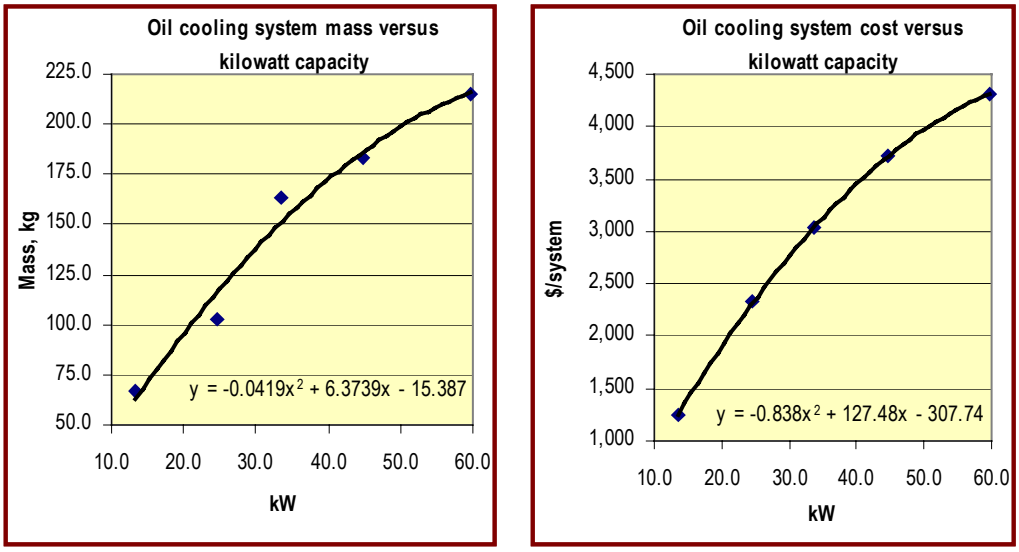

Figure 4-10. Curve fit of costing data, oil coolers

4.6.10 Requirements and Cost of the Generator Liquid Cooling System

For generators, the heat load is based on generator efficiency at rated power. No allowance is made for convective cooling.

$$kW_{cooler\_gen} = kW_{rated} \cdot loss\%$$

As an example for a 1.5-MW machine with a generator efficiency of 97.5%, we calculate the heat load:

$$kW_{cooler\_gen} = kW_{rated} \cdot loss\%$$
$$kW_{cooler\_gen} = 1{,}500 \cdot .025 = 37.5\,kW$$

Based on available sizes from catalog data (HYDAC International 2002), the system ratings and mass are summarized in Table 4-13.

Table 4-13. Summary Data, Generator Fluid Coolers

Cooling, Generator Fluid		
kW	**Mass, kg**	**Liters/minute**
13.43	53.3	106
24.62	82.4	265
33.57	130.6	265
44.76	147.0	265
59.68	172.4	265

From vendor catalogs, the cooling system mass versus kilowatt capacity is curve fitted in Figure 4-11 (left).

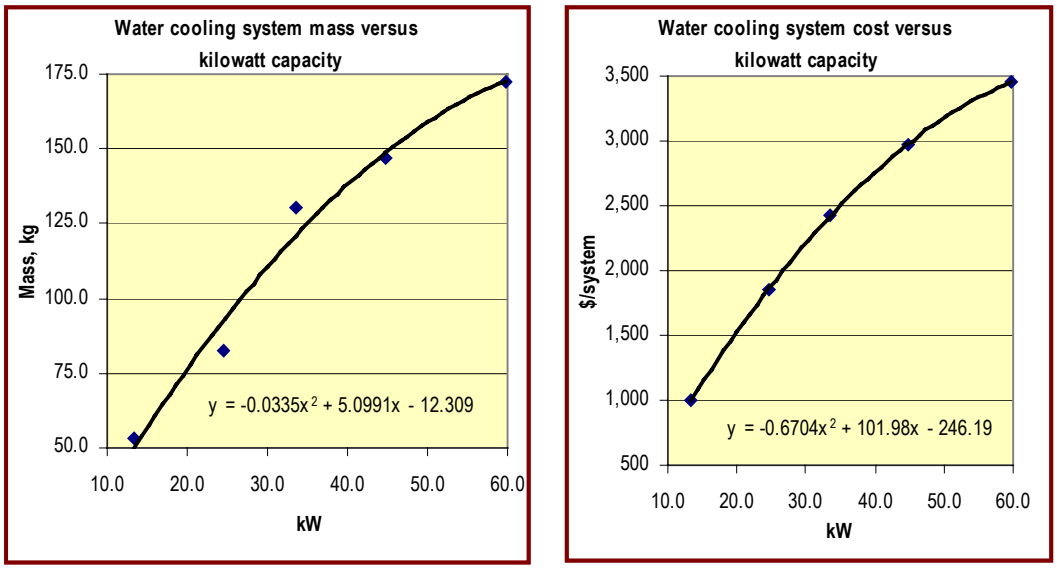

Figure 4-11. Generator cooling system mass and cost versus kilowatt capacity

The following curve fit equation, determined from Figure 4-11 (left), is used to size the system:

$$M_{cool\_gens} = -.0334\text{kW}^2 + 5.099\ \text{kW} - 12.309\ \text{(kg)}$$

From vendor estimates, the approximate cost per unit mass is $20.00/kg. Applying this to the above equation provides the cost estimate equation:

$$Cost_{cool\_gens} = -.6698HP^2 + 101.98\ \text{kW} - 246.19$$

The curve for this cost equation is shown in Figure 4-11 (right). Using this equation to estimate cost for the above example:

$$Cost_{cool\_gen} = -.6698 \cdot 37.5^2 + 101.98 \cdot 37.5 - 246.19 = \$2{,}636$$

4.6.11 Cost of the Nacelle Enclosure

The nacelle enclosure is the fiberglass enclosure required to protect the machinery from the outdoors. Some of the designs investigated for this study use structural, cylindrical steel nacelles. In those cases the structural portion of the nacelle, not constructed of fiberglass, is costed as part of the "support structure" costs and not the "nacelle cover" costs.

The nacelle cover fiberglass was assumed to have a density of 1690 kg/m^3 and cost was calculated at $11.45/kg plus $.45/kg for freight, based on industry experience. Nacelle enclosure weights were calculated for the various designs and the cost estimated with the above rates per unit mass. An additional cost for hardware was added to cover the cost of fasteners, hinges, louvers, access covers, decals, and similar details. Unless noted otherwise, the standard hardware add-on cost was $1,287, based on estimated hardware costs for the baseline drive train design. Table 4-14 gives an example of a nacelle cover estimate.

Table 4-14. Example of Nacelle Cover Estimate

Nacelle Cost Data		
Based on estimate of length, height, width, meters		
Length =	4	m
Width =	2.7	m
Height =	2.7	m
Wall thickness=	0.0127	
Volume wall material =	0.6652	m^3
Mass wall material =	1124	kg
Cost/m^3 =	19350	$/$m^3$
Density =	1690	kg/m^3
Cost/ kg =	11.45	$/kg
Cost	12,872	$
Freight rate =	0.45	$/kg
Freight cost =	506	$
Additional cost for hardware =	1,287	$
Total Cost	14,666	$

4.6.12 Drive Train Assembly and Test

Estimates were made for the turbine manufacturer's final assembly and testing costs for each type of drive train. These estimates were based on a burdened labor rate of $125/h for a two-person crew. The size of the assembled components in the drive train sizes investigated dictates a minimum two-person crew. For the baseline drive train, the approximate labor hours required were determined from informal discussions with turbine manufacturers that produce similar designs. For the other designs, estimates relative to the baseline labor hours were made based on expert judgment, taking into account the complexity and assembly steps anticipated for each design.

In the case of the multi-PM and multi-induction drive train designs, the final assembly estimates for the drive train include assembly of the integrated gearbox components. The gear designs for these drive trains are quite simple but include a single, very large bullgear, and assembly of these components by the turbine manufacturer was assumed to be more practical than assembly by a gear manufacturer. Gear assembly costs for all other drive trains are included in the gearbox cost estimates.

4.7 Induction Generators

Cost and performance estimates for conventional squirrel-cage induction generators that are available as standard products were supplied by generator manufacturers participating in the study. The following subsections give additional details about how the generator performance and cost data were developed.

4.7.1 Conventional Induction Generators

The baseline and integrated baseline generators use a wound-rotor induction generator. The multi-induction and Henderson drive trains use squirrel-cage induction generators. These generator types are widely used in existing wind turbines and are available from a number of manufacturers. Two induction generator manufacturers participated directly in the study and provided performance and cost estimates of existing generators compatible with those drive train designs. These manufacturers are Loher Drive Systems and Siemens Energy and Automation. In addition, Heller-De Julio, also a study participant, is a distributor for Teco Motor Company, another induction generator manufacturer, and provided selling prices and some performance data for comparable Teco generators.

The various sizes, types, and characteristics of squirrel-cage induction generators are described further in the sections dealing with their application. These include Section 5.3.2.1 for the baseline drive train system, Section 10.3.2.1 for the multi-induction drive train, and Section 13.3.2.1 for the Henderson variation.

4.7.2 Variations of Conventional Induction Generators

The Klatt and HDJ drive trains both use nonstandard variations of conventional wound-rotor induction generators. Each of these generators can be built as modifications to standard production wound-rotor generators. Cost estimates for these generators were based on information provided by the developers of these variations, EDI and the Heller-De Julio Corporation. The information described the modifications that would be required to the standard generators. EDI and Heller-De Julio Corporation also supplied generator performance and efficiency estimates. The modifications and characteristics of the Klatt-EDI generator are described in Section 11.2.2; while those for the HDJ variation are described in Section 12.2.2.

4.8 Permanent Magnet Generators

4.8.1 Overview

PM synchronous generators are used in the single PM, multi-PM, and direct drive drive trains. For this class of generators, detailed design and performance analyses were carried out by the Electromagnetics Development Center, a division of Kaman Aerospace Corporation (Kaman), located in Hudson, Massachusetts. The center's assessment of the PM machines began with initial conceptual design estimates of PM synchronous machines for the three drive train configurations. The initial estimates utilized rules of thumb reflecting experience that Kaman had gained through the design, test, and manufacture of a number of comparably sized PM machines. These results, when analyzed by GEC in combination with other initial drive train component estimates, indicated that all three PM generator drive trains are viable configurations. However, the single PM and multi-PM designs appeared to be more attractive on an entire turbine COE basis than the direct drive design. As a consequence, the direct drive configuration was not investigated during further, more detailed PM generator design efforts.

Following the initial survey estimates, Kaman continued developing a preliminary generator design for the 1.5-MW single PM drive train. This 2.3-m diameter generator was designed to be driven by a single-stage gearbox to achieve a rated speed of 164 rpm, the optimum diameter and speed determined during the initial conceptual designs. This design uses a radial-field, salient-stator pole construction with surface-mounted NeFeB rotor magnets. This design was chosen as the most economically and technically attractive based on a conceptual assessment of several different generator design and construction alternatives. Kaman completed this comparative scoping assessment early in the study. Kaman developed a SolidWorks solid model that included all components of the active magnetic design. Generator performance was estimated with proprietary spreadsheet models, along with FEA programs. Kaman developed a BOM and associated piece-part drawings for all major active magnetic components including magnets, retainers, coils, and stator laminations. Component costs were estimated with vendor quotes. Using these data, a complete cost model was developed to estimate the equivalent selling price of the active magnetic components of the generator.

PEI carried out the design of the mechanical and structural elements of the generator, including the rotor iron, bearings, and housing. Using models for those components imported from the Kaman SolidWorks model, PEI developed a Pro/E model for the entire generator, including the active magnetic components. PEI estimated the costs of all structural and mechanical components as described in Section 4.6.

Two versions of the 1.5-MW PM generator were designed, one optimized for use with an IGBT-based, active-rectified PE system and the other optimized for a passive-, diode- or SCR-rectified PE system. The passive-rectified version was ultimately chosen. This followed from the results of a combined economic and technical assessment of the combined PE and generator systems, as described in Section 4.10.

The active magnetic designs for the other PM generator power ratings, speeds, and diameters were derived using a unit-pole scaling technique that McCleer Power developed for this study. This scaling method is described in Section 4.8.6. The unit-pole scaling method is specific to the Kaman salient stator-pole design. The unit pole refers to a single segment of the stator and rotor that can be employed in all the PM machines considered in this study. The unit-pole design combines the stator coil, the laminated stator magnetic steel stack, the rotor magnets, and the associated mechanical hardware into a single module. Using the unit-pole module design from Kaman's 1.5-MW single PM generator, PEI was able to develop Pro/E models for the other PM generators.

4.8.2 Permanent Magnet Generator Design and Construction

A complete description of Kaman's PE generator design is included in Appendix E. Figure 4-12 illustrates the configuration of the active magnetics. This shows a segment of the stator and rotor that consists of several poles. Each stator pole is made up of a single, multiturn coil wound around a single stator tooth. The electrical connections are made in groups of three stator poles for the three phases. Each rotor pole consists of a single NeFeB magnet attached to the rotor. There are two rotor poles for each group of three stator poles.

Figure 4-13 shows an expanded view of a single stator and single rotor pole. The stator winding is a form-wound, racetrack coil using rectangular cross-section copper conductors. A plastic retainer is used to hold the winding in place on the stator tooth. Each PM is covered by a rotor pole cap constructed of powdered iron magnetic material, which is held in place by a nonmagnetic, pole cap retainer.

The complete generator is illustrated in Figure 4-14. This illustration shows the bearing and housing designs for the single PM drive train. These designs change for the different drive trains but the general design approaches are similar. A cold plate ring surrounds the stator laminations and is sealed by two sets of O-rings to the housing. The liquid coolant flows between this stator ring and the housing. IP54 environmental protection (IEC 2001) is provided by a sealed cover protecting the face of the generator.

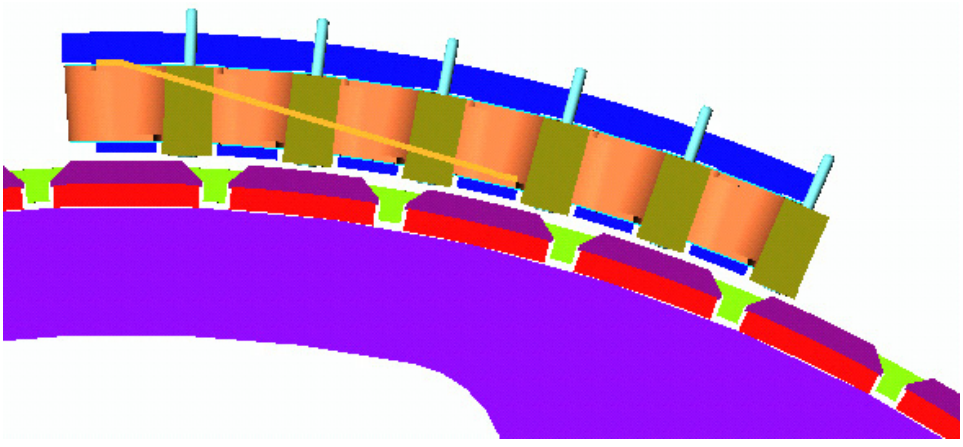

Figure 4-12. Multiple-pole segment of salient-pole PM generator

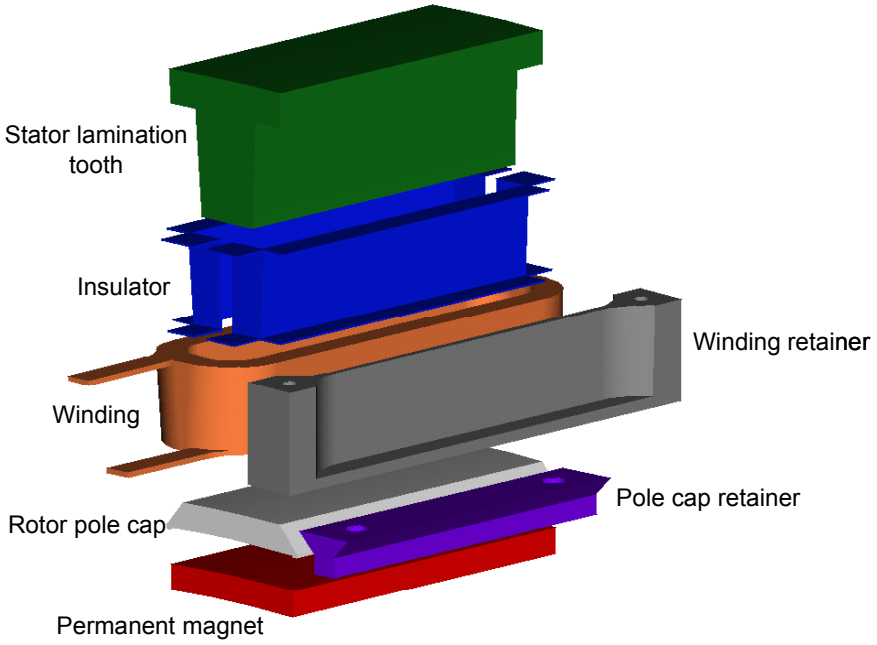

Figure 4-13. Single stator and rotor poles

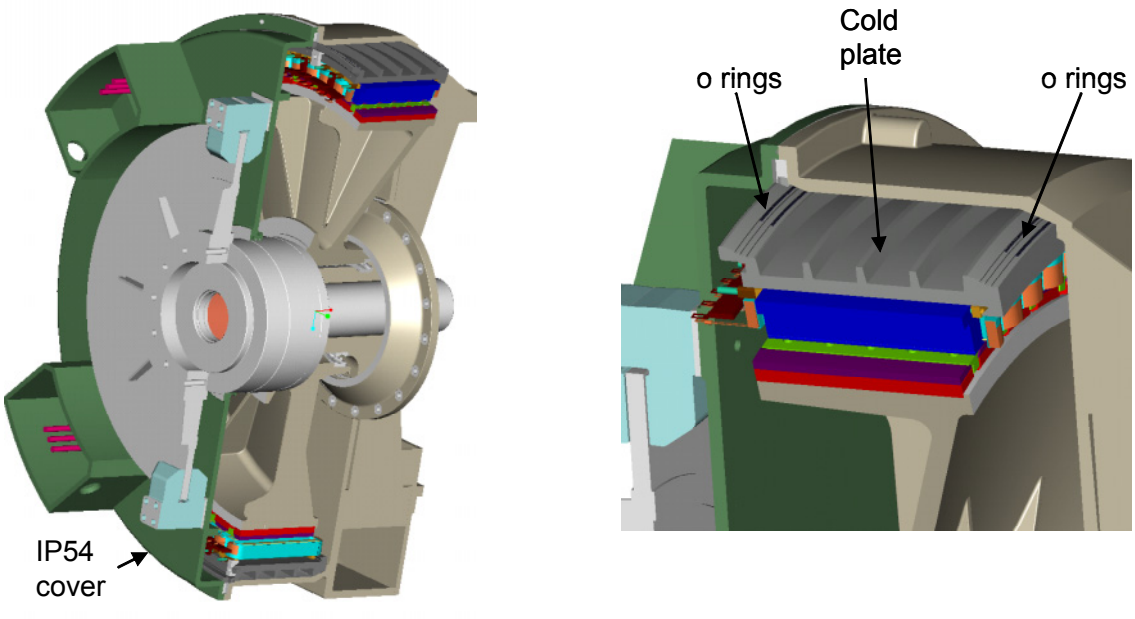

Figure 4-14. Complete generator assembly

4.8.3 Generator Reactance and Optimization for Active and Passive Rectification

Both active- and passive-rectified PE systems were considered for the interface to the (variable-speed) PM generators. The specific PE systems considered are described in Section 4.9.3. The active-rectified system uses an IGBT voltage-source inverter for the generator interface; the passive-rectified systems use either diode or SCR rectifiers. The active-rectified system allows direct, rapid control of the generator current, allowing operation at a high air-gap power factor with the generator currents in phase with the generator electromagnetic field (EMF) voltage.

The passive-rectified systems inherently operate with the generator fundamental current in phase with the terminal voltage. When the synchronous reactance of the generator is low, the terminal power factor and the air-gap power factor are nearly the same and approach unity. However, PM generators typically have a significant synchronous reactance, which decreases the air-gap power factor. This increases the operating current and limits the power output from the passive-rectified systems. These effects are described in Dubois (2000) and Grauers (1996a).

Figure 4.-15 shows a simplified per-phase equivalent circuit along with phaser diagrams for generator operation with passive and active rectification. E represents the EMF voltage. The leftmost phaser diagram shows active-rectified operation with the generator current in phase with the generator EMF voltage. This is the operating mode that gives the lowest generator current for a given power. The generator output power is proportional to the product of the EMF and the fundamental component of current in phase with the EMF.

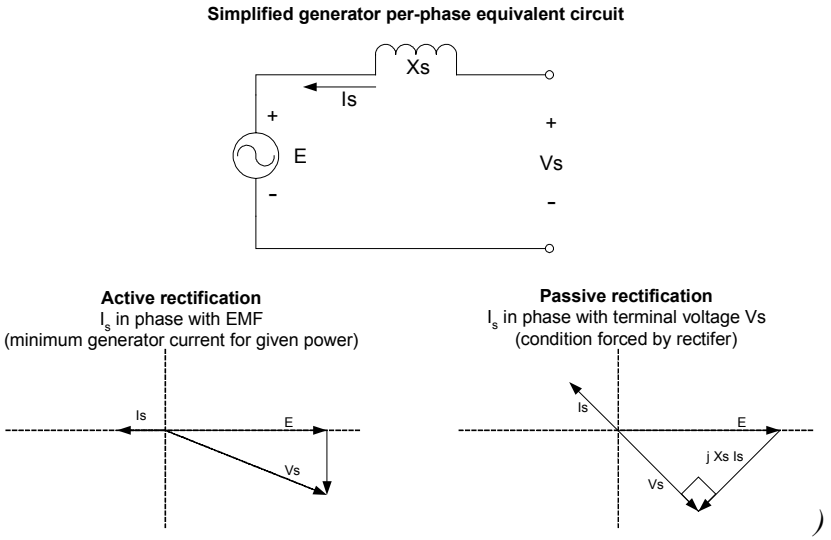

Figure 4-15. Generator voltages and currents for active- and passive-rectified PE systems

As indicated by the right phaser diagram, for the same real power, the passive-rectified system has higher current because the voltage across X_s, the synchronous reactance of the generator, causes the generator current to be out of phase with the EMF voltage. The higher current results in higher losses in the generator and a higher voltage across the (internal) synchronous reactance relative to the active-rectified case. As the output power of the generator is increased in the passive-rectified system, the total current increases faster than the power because the phase angle between EMF and current increases. As the current drawn by the load from the generator increases further, the generator-delivered power reaches a maximum and then decreases. The maximum power of the generator is therefore limited by the synchronous reactance of the generator when passive rectification is used.

To take into account the different operation of the active- and passive-rectified systems, Kaman developed two variations of its generator design, one optimized for active rectification and the other optimized for passive rectification. The passive-rectified version was designed with a lower synchronous reactance, necessary to provide a rated power output of 1.5 MW.

4.8.4 PM Generator Design and Cost

Table 4-15 lists the dimensions and electrical parameters for both optimizations of the Kaman generators. Kaman made these estimates using finite element analysis of the generator. More complete details are included in Appendix E. To decrease the reactance, the passive-rectified generator has a 25% longer stack length than the active-rectified generator. In addition, to decrease the reactance further, thicker magnets are used. As a result, the reactance of this generator is 57% less than that of the active-rectified generator. The passive-rectified generator also has a lower winding resistance, and as a result has lower losses and higher efficiency than the active-rectified generator, in spite of higher operating currents.

Table 4-15. Kaman Generator Designs

	Active-Rectified	Passive-Rectified
Rated speed, rpm	164	164
Stator outside diameter, m	2.3	2.3
Stack length, m	0.20	0.25
Number of stator poles	84	84
Number of rotor poles	56	56
Frequency at 164 rpm, Hz	76	76
Peak EMF phase voltage at 164 rpm	600	600
Phase inductance, μHy	662	288
Phase reactance at 164 rpm, ohms	0.317	0.138
Per unit reactance	0.88	0.38
Phase resistance, ohms	12.3	5.72
Full load efficiency, %	95.9	97.3
Selling price with warranty reserves, $	38,000	54,000

The estimated selling prices of the assembled active magnetics for the two Kaman generators are $38,000 and $54,000 for the passive-rectified and active-rectified generators, respectively. Rotor iron, bearings, stator cold plate ring, housing, IP54 cover, and cooling systems are estimated as part of the mechanical design of each drive train and are not included in the active magnetics estimates. These estimates include a 10% reserve for warranties that is not included in Kaman's estimates in Appendix E.

Figure 4-16 gives the approximate cost breakdown for the generator construction. The magnets have the highest cost, followed by the coils and laminations. The labor category in this estimate is for final assembly only. Coils, magnets, stator laminations, and other components are all purchased as prefabricated items.

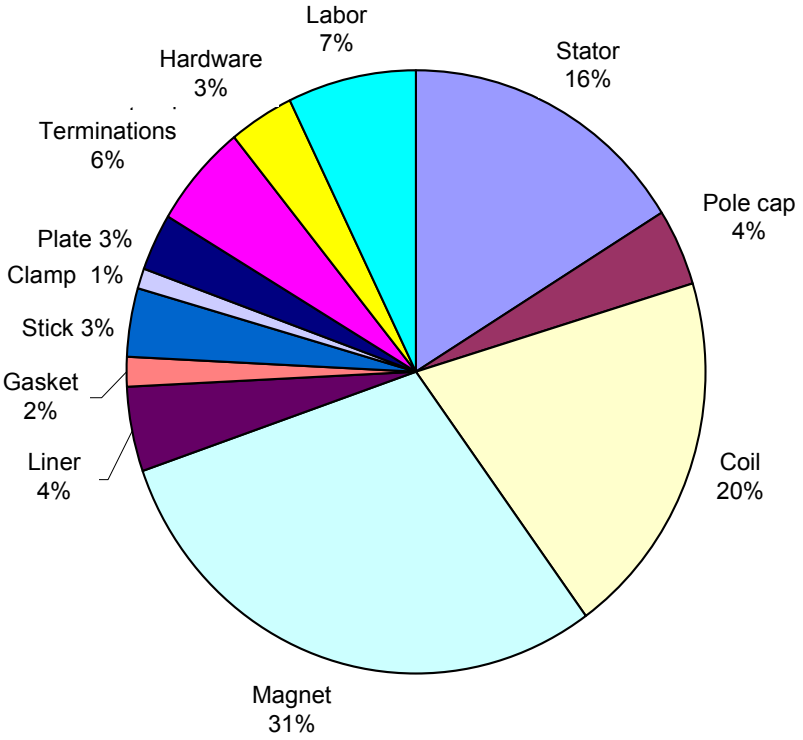

Figure 4-16. Generator cost breakdown (warranty not included)

4.8.5 Alternatives to the Selected PM Generator Design

A conceptual assessment of several different medium- and low-speed, synchronous generator configurations was made early in the study, before the specific unit-pole, radial-flux design described previously was selected. Kaman did this work with input from other sources, and Kaman's report describing the conceptual assessment is included in Appendix K. Some of the alternatives considered, along with the reasons that they were not selected, are described below:

- **Electrically excited generators:** PM generators can be built with a smaller pole pitch than electrically excited generators. As a consequence, the thickness and mass of the stator and rotor back iron can be reduced. PM generators also have increased efficiency because resistive electrical losses in the rotor are eliminated. As magnet costs have decreased in recent history, PM generators have become more cost effective for low- and medium-speed wind turbine applications. These trade-offs are described in Grauers (1996a, 1996b) and also in the Kaman report in Appendix K (pp. K-40–K-43).

- **Axial-flux generators:** Axial-flux generators were initially considered but not chosen because they have a smaller effective air-gap area for any given outside diameter of the generator. This effect is described in the Kaman report in Appendix K (p.p K-20–K-29).

- **Air-cooled generators:** Air-cooling was not chosen because the generator would need to be larger and require more active material to achieve the same performance as the selected liquid-cooled generator. Higher generator cost is expected because of the additional material. Kaman's report in Appendix K includes an analysis comparing liquid- and air-cooling of the selected generator (pp. K-93–K-99).

- **Generators using interleaved stator windings:** The selected design uses a salient pole stator construction rather than the more typical interleaved, distributed winding used in most generators. The salient pole construction is simple, using both inexpensive coils and minimizing the assembly labor. The disadvantage of this construction is an EMF voltage having increased harmonics that increase losses to some extent. The salient pole design also lends itself to easier field repair than designs using interleaved stator windings.

4.8.6 Scaling to Other PM Generator Speeds, Ratings, and Diameters

An initial approximate scaling method, provided by Kaman, was used early in the study to estimate generator size and cost for different variations of the drive train design. This method, described in Kaman's report (Appendix K), assumed a constant air-gap shear stress and did not take end turn or synchronous reactance effects into account. Generator mass and cost were assumed to be proportional to air-gap surface area. With a constant air-gap shear stress, generator torque is proportional to the product of air-gap surface area and generator radius. For a given power rating and speed, the air-gap surface area and therefore the required stack length decreases in inverse proportion to the generator radius. Large-diameter, pancake-type generators are favored. For a given generator power, the required generator torque is inversely proportional to speed, so the required generator surface area changes in inverse proportion to speed, favoring higher speed generators.

The general scaling trends estimated by this simple method are valid. However, this approach does not take into account the effect of end turns, which penalize short stack lengths. It also does not take into account the synchronous reactance requirements associated with diode rectification. For these reasons a more accurate unit-pole scaling method was developed and used for preliminary design estimates of the various drive trains presented in this report.

4.8.6.1 Unit-Pole Scaling Method

Pat McCleer of McCleer Power developed techniques for scaling the Kaman unit-pole design to other generator diameters and power ratings. Using as a starting point the base 1.5-MW, 164 rpm, 3.2-m generator, the techniques and equations developed were used to estimate the cost, size, and performance of other radial-flux, unit-pole PM generators. The method used to scale the passive-rectifier optimized machine is described here.

Each unit pole consists of a pair of rotor poles and three stator poles. The unit-pole scaling method assumes that the pole pitch, and therefore arc length, is kept constant regardless of generator diameter. Different numbers of the same unit-pole design, with axial stack length scaled as necessary but all other dimensions fixed, are used for all generators. The effects of required changes in curvature on the unit-pole design are neglected. The number of pole pairs is high enough for the scaled generator diameters considered in the study so that integral numbers of pole pairs gave the approximate diameters desired.

This scaling method was used to scale the base generator design, developed for the 1.5-MW single PM generator driven by a single-stage gearbox, to generators for the 1.5-MW direct drive and multi-PM drive trains. The techniques were also applied to the 750-kW and 3.0-MW versions of each drive train. The method is expected to have accurate results if the scaled generators have similar air-gap velocities, in which case the electrical operating frequencies are similar. From this it follows that similar performance can be expected. In cases where the air-gap velocities are different, the method is expected to give approximate results adequate to estimate costs.

The air-gap velocities for each of the configurations considered are shown in Figure 4-17. All three sizes of the single PM and multi-PM generators have similar air-gap velocities. The direct drive generator has a

lower air-gap velocity, about 25% of the base generator. For this reason the scaling to the direct drive generator designs is not expected to be as accurate as the results for the other generators.

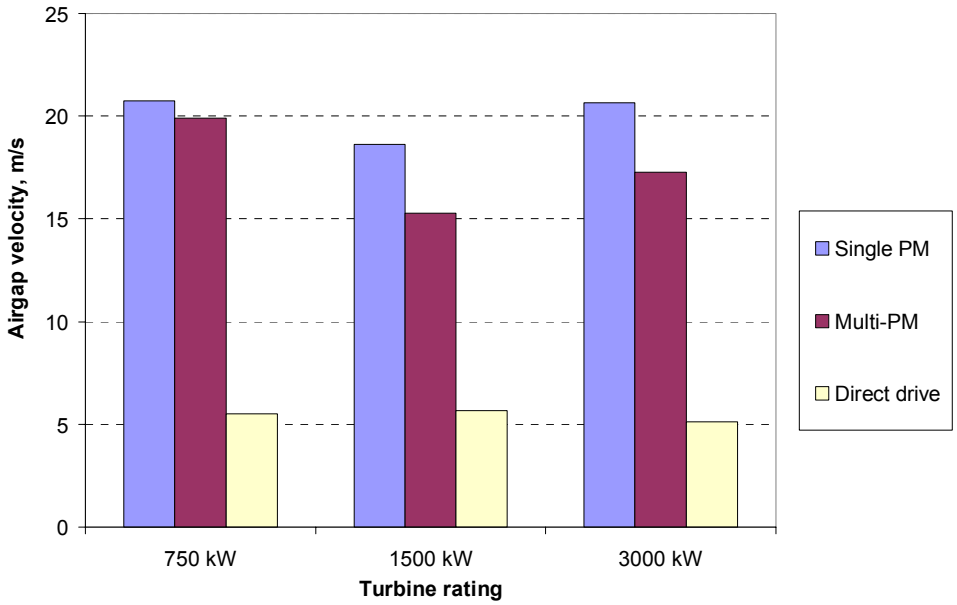

Figure 4-17. Air-gap velocities for WindPACT PM generators

The scaling equations are described below for the passive-rectified generators.

4.8.6.2 Scaling of Generator Stack Length

McCleer Power supplied the scaling relationships to determine the unit-pole electrical parameters for the scaled generator, which are given in Table 4-16. The parameters scale by stack length and operating frequency.

Table 4-16. Scaling of Unit-Pole Electrical Parameters

Parameter	Scaled Generator	Base Generator	Scaling Relationship
Stator phase resistance	R_s	R_{so}	$\frac{R_s}{R_{so}} = \left(m_e + m_s \frac{L}{L_o} \right)$
Stator phase reactance	X_s	X_{so}	$\frac{X_s}{X_{so}} = \frac{L}{L_o} * \frac{f_e}{f_{eo}}$
EMF voltage	E_{mq}	E_{mqo}	$\frac{E_{mq}}{E_{mqo}} = \frac{L}{L_o} * \frac{f_e}{f_{eo}}$
Hysteresis core loss	H_{loss}	H_{losso}	$\frac{H_{loss}}{H_{losso}} = \frac{L}{L_o} * \frac{f_e}{f_{eo}}$
Eddy current core loss	E_{loss}	E_{losso}	$\frac{E_{loss}}{E_{losso}} = \frac{L}{L_o} * \frac{f_e^2}{f_{eo}^2}$

For the scaled generator, the number of rotor pole pairs is determined by the constant pole pitch and the air-gap diameter. The electrical frequency is determined by the speed of the scaled generator as follows:

$$f_e = \frac{RPM}{60} \cdot \frac{n_p}{2} \qquad f_e = \text{electrical frequency, } n_p = \text{number of rotor poles}$$

The following equation gives the stack length of the scaled generator having equal per-unit reactance to the base generator:

$$L = L_o \frac{Z_{su} + \sqrt{Z_{su}^2 + \frac{8 m_e R_u P_{ro} f_e^2}{P_r f_{eo}^2}}}{\frac{2 P_{ro} f_e^2}{P_r f_{eo}^2}}$$

The quantities defined in Table 4-17 are used in the calculation, along with the normalized impedance Z_{su} and resistance R_u, calculated as follows:

$$Z_{su} = 2 m_s R_u + \frac{3}{\pi} \frac{f_e}{f_{eo}} X_u \qquad R_u = \frac{R_{so}}{2 R_{so} + 6 f_{eo} L_{so}}$$

R_u and the normalized reactance X_u, calculated with the equation below, are necessary to calculate Z_{su}.

$$X_u = \frac{\pi \ f_{eo} L_{so}}{R_{so} + 3 f_{eo} L_{so}}$$

With equal per-unit reactance, equivalent performance can be expected with a passive-rectified PE system, as described in Dubois (2000) and Grauers (1996a). Parameters used to scale the generators are shown in Tables 4-17 and 4-18.

Table 4-17. Base Generator Parameters

L_o	Stack length	250 mm
L_{so}	Per-phase inductance	288 μHy
R_{so}	Per-phase resistance	5.72 Ω
f_{eo}	Rated operating frequency	76.5 Hz
m_e	Fraction of R_{so} resulting from end turns	0.3
m_s	Fraction of R_{so} resulting from slot copper	0.7
$n_{po}/2$	Number of rotor pole pairs	28
P_{ro}	Machine power per rotor pole pair	53.6 kW

Table 4-18. Scaled Generator Parameters

L	Stack length
$n_p/2$	Number of rotor pole pairs
P_r	Machine power per rotor pole pair
f_e	Frequency, rated speed

With the scaled generator air-gap diameter and stack length known, the air-gap area of the scaled machine can be calculated. The generator cost is then calculated using the estimated air-gap area. The curve in Figure 4-18, provided by Kaman, gives the estimated active magnetics costs per air-gap area as a function of stack length. This curve takes into account the increased end turn material and other fixed costs associated with the active magnetic construction that penalize generators with shorter stack lengths.

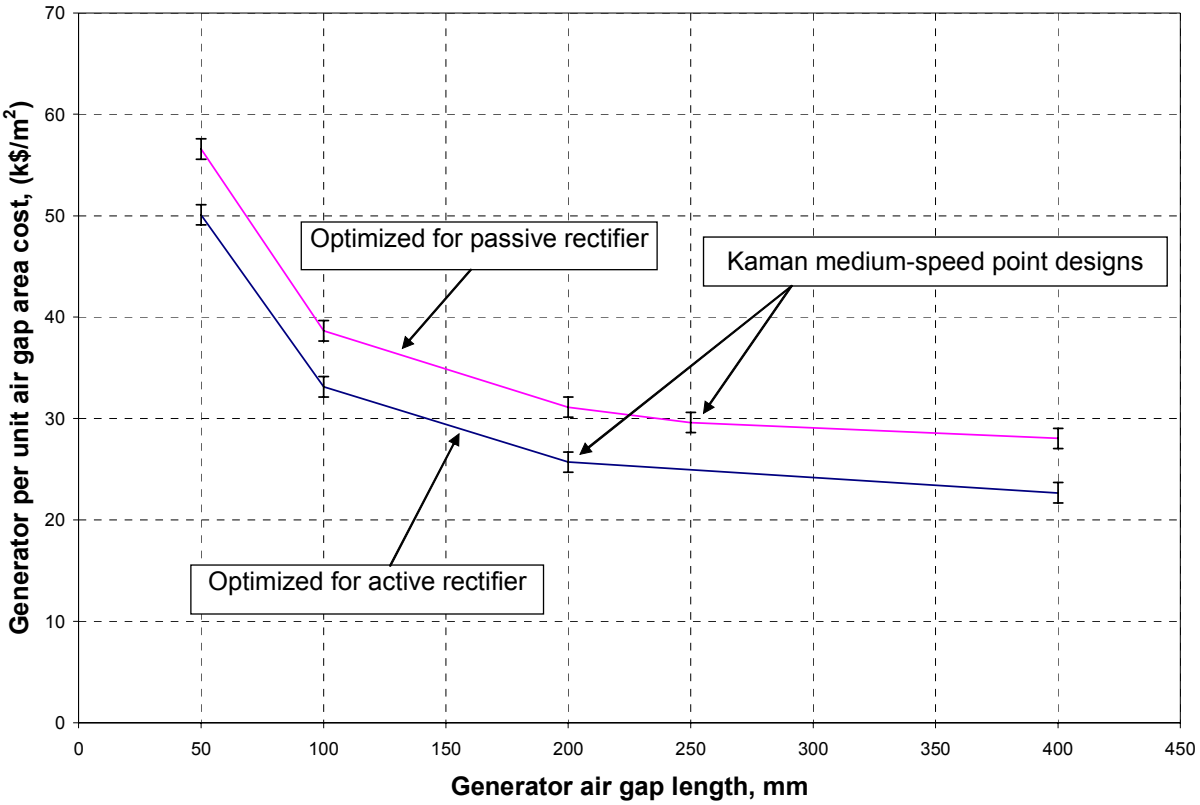

Figure 4-18. Cost scaling for WindPACT PM generators

4.8.6.3 Scaling of Generator Efficiency

Generator efficiency can be calculated using an equivalent circuit model for a single unit-pole segment. Each unit pole corresponds to a group of three stator coils, one for each three-phase connection. The base generator has 28 pole pairs, or 28 unit poles. Each generator phase has the parallel-series coil connections shown in Figure 4-19, with each phase having four series and seven parallel connections. Each connected coil represents a single phase of one unit-pole segment.

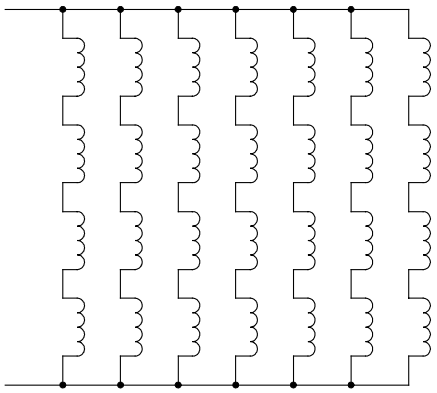

Figure 4-19. Base generator coil connections for one phase

Each unit pole can be electrically modeled with the equivalent per-phase circuit shown in Figure 4-20. Resistor R_c represents the core losses in the generator in this model. The parallel-series stator coil connections shown in Figure 4-19 for the base generator determine the pole-pair equivalent circuit quantities. The equivalent circuit for each unit pole in the base generator has 1/4 of the generator EMF and terminal voltages, 1/7 of the generator phase current, and 7/4 of the generator inductance. The circuit delivers 1/28 of the generator power and has 1/28 of the generator core losses. Using the base generator parameters shown in Table 4-17, the unit-pole quantities can be calculated. These unit-pole quantities can then be used with the equivalent circuit model shown in Figure 4-20.

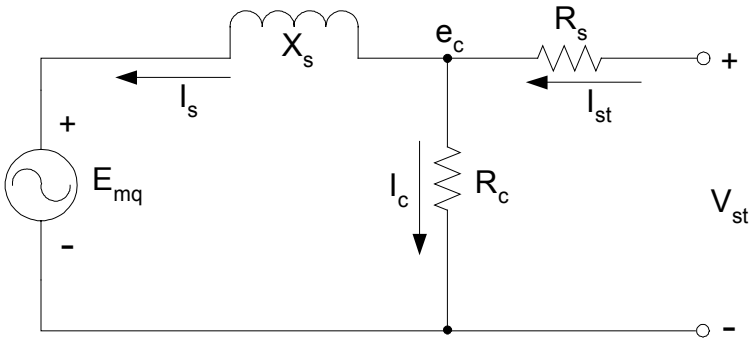

Figure 4-20. Generator unit-pole equivalent circuit model

Using the scaled unit-pole parameters calculated per Table 4-16 and the unit-pole-equivalent circuit model shown in Figure 4-20, all currents, voltages, and losses can be calculated for the unit pole of the scaled machine under all operating conditions. The currents and voltages for the entire scaled generator depend on the specific parallel-series coil connections used, but this information is not necessary to calculate the efficiency because the power output of each unit pole is dependent only on the number of pole pairs and the total generator power.

Figure 4-21 is a phaser diagram showing the relationships between the unit-pole voltages and currents. The detailed calculations are provided for the different scaled generators in spreadsheet format in Appendix G. These calculations were used to calculate estimated efficiency curves for the different scaled generators. For the purpose of these calculations, a base-machine eddy-current loss of 5.4 kW and a hysteresis loss of 2.3 kW were assumed.

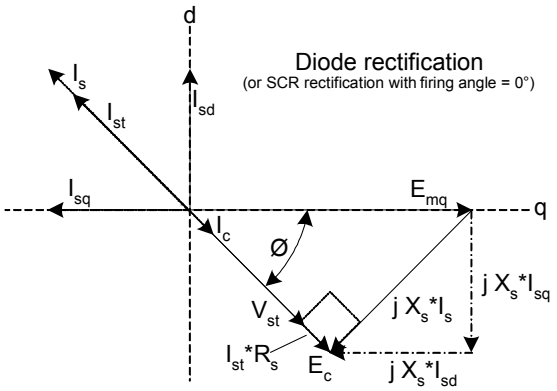

Figure 4-21. Voltages and currents for equivalent circuit model

4.9 Power Electronics and Electrical Systems

All PE cost estimates used for the final results of the study were made by William Erdman, who developed detailed bottoms-up designs, along with cost estimates for each design. Erdman used this method because many of the PE systems considered for the study are not available as standard products from existing manufacturers. The cost estimates were based on these designs for each PE system, with the principal components priced from manufacturers' quotes. Manufacturing volumes of 150–600 PE systems a year were assumed. The costs of labor for assembly and test, fixed factory overhead and other indirect costs, gross margin, and profit were then added to the component costs to develop the selling price of the PE system from a hypothetical manufacturer. All of the designs and cost estimates are included in Appendix F.

The PE selling price estimate is dependent on the choice of a gross margin for the hypothetical manufacturer. Estimates were made for 30%, 40%, and 50% gross margins. Typical gross margins are believed to be between 30% and 40%. To verify this, independent selling price estimates for the baseline drive train PE system were obtained from two manufacturers participating in the study, Loher Drive Systems and Siemens Energy and Automation. These selling prices agreed closely with the selling price estimated with the cost model using a 40% gross margin. For this reason, a 40% gross margin was used for all PE estimates in the study.

Cost estimates for the electrical switchgear and other electrical systems are based on one-line electrical diagrams and associated BOMs developed by Bouillon Integrated Systems with input from GEC, Erdman, and OEM. Switchgear component costs were estimated by Bouillon and Erdman based on vendor quotations.

4.9.1 Power Electronic Systems for Doubly Fed Induction Generators

The 1.5-MW PE system used for a doubly fed induction generator is described in Section 5.3.2 (for the baseline drive train electrical system). Detailed estimates for this PE system are included in Appendix F. The electrical diagram for this system, repeated in Section 5.3.2, is shown in Figure 4-22. This system, with minor variations, is used in several existing turbine designs. A bidirectional, IGBT-based, PWM voltage-source converter system is used to provide variable frequency power to the rotor of the doubly fed generator through slip rings. A DC voltage bus with large capacitors acts as a voltage source to link two inverters, one connected to the grid and one to the generator rotor.

The significant advantage of this system over most alternatives is the partial rating of the PE system relative to the generator rating. Typically the rating of the PE system is 33% of the generator rating for the variable-speed range required for wind turbine applications. The partial PE rating is possible because most of the generator power is directly transferred from the generator stator to the grid, bypassing the power electronics. This PE system is limited to use with doubly fed generators. Full-rated power electronics are necessary for squirrel-cage induction or synchronous generators.

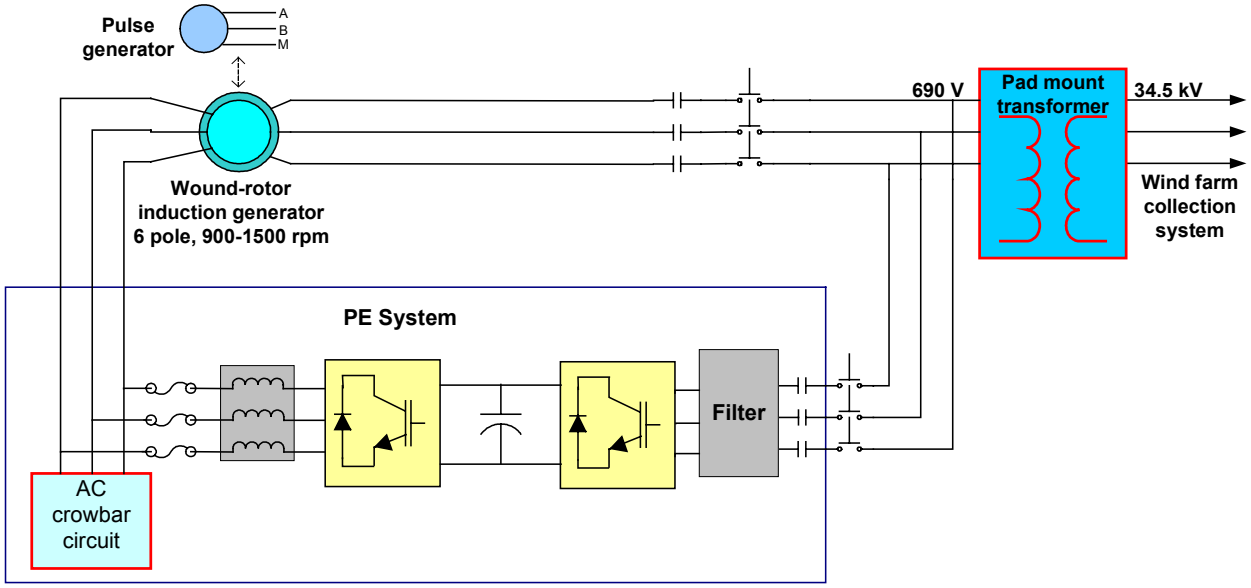

Figure 4-22. Doubly fed induction generator PE and electrical system (baseline)

4.9.2 Variations of the Doubly Fed System

Several possible variations to the baseline doubly fed system shown in Figure 4-22 were considered during the study. Some of these alternatives may offer some cost savings to the baseline drive train. However, because significant reductions were not anticipated, these systems were not investigated in detail.

- **Reduced speed range system:** The rating of the doubly fed PE system is dependent on the variable-speed range, so the PE system rating and cost could be lowered by reducing the speed range of the turbine. The reduction in speed range lessens the energy capture of the turbine by operating the rotor more hours per year further from the optimum TSR. The minimum speed of the WindPACT baseline turbine, which has a rated speed of 20.5 rpm, is 12.3 rpm. This minimum speed is approximately the same as that used on existing turbines. Rough estimates show that this minimum speed is near an optimum in the PE cost versus energy capture trade-off.

- **Subsynchronous system:** A reduced-cost, doubly fed PE system could be built by replacing the grid-side PWM converter with a diode bridge and always running the generator below synchronous speed. In this case power flow is always *into* the rotor. A number of variations using this principle are possible. The efficiency of this system will be lower because power circulates through the PE system, rotor, and out through the stator during subsynchronous operation.

- **Alternate semiconductor switch technologies:** A higher voltage system could be built with gate controlled thyristor (GCT) or other semiconductor switch technologies. These switches have advantages for systems with voltages higher than 690 V. A medium-voltage generator and PE system, advantageous because the currents are reduced, is possible with GCTs. Medium-voltage PE systems may be especially advantageous for systems larger than 1.5 MW. GCTs and similar technology switches are slower, however, so the switching frequency must be reduced from the approximately 3 kHz used in IGBT converters to 500 Hz or less. The reduced switching frequency increases the filter costs necessary to maintain power quality.

- **Reduced input filtering:** The input filter necessary to eliminate the switching frequency component of input current is costly. This filter is designed to limit PE system current harmonics to IEEE 519 standards (IEEE 1992). If IEEE 519 standards are imposed at the wind farm substation rather than at each wind turbine, there is potential to decrease the filter size in the PE system. The turbine pad mount transformer reactance and other parasitics in the wind farm system could provide some of the filtering.

4.9.3 Power Electronic Systems for PM Synchronous Generators

Compared to the doubly fed induction generator used for the baseline drive train, PM synchronous generators have a disadvantage in that the PE system must convert 100% of the generator power. As described previously, the doubly fed system requires that only about 33% of the generator power be converted by the PE system. The requirement for a higher PE rating gives a significant economic disadvantage to the use of PM generators. Because PM generators are advantageous for other reasons, low-cost PE systems to be used with PM generators were a focus of the study. Three different PE designs were investigated that are compatible with permanent magnet generators. These three PE systems are described in the following subsections.

4.9.3.1 IGBT-IGBT Power Electronics System

Figure 4-23 shows the IGBT-IGBT PE system. Two IGBT, voltage-source converters are interconnected by a DC bus. One converter provides the variable frequency and voltage necessary to control the generator output power. The other converter provides grid current control to supply 60 Hz, three-phase output power at a commanded power factor. This PE architecture can provide high-bandwidth torque control of either induction or synchronous generators with the appropriate control algorithm. A shaft-position encoder or some type of generator rotor position sensor is usually necessary for this system, although more complicated control algorithms that do not require rotor position sensing are possible. The detailed operation of this architecture is described in Richardson, et al. (1992) and Jones and Smith (1993 for induction generators and Grauers (1996a) for synchronous PM generators.

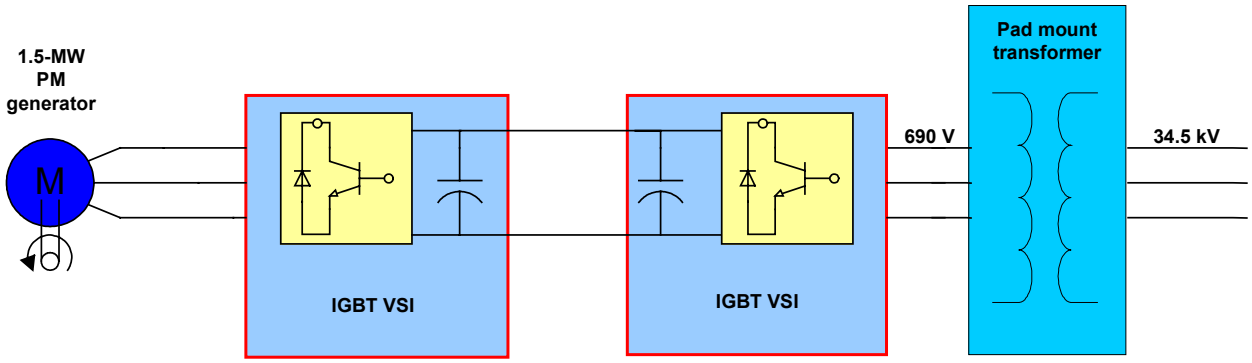

Figure 4-23. IGBT-IGBT PE system

Detailed estimates of the WindPACT 1.5-MW IGBT-IGBT system including schematics and BOMs are included in Appendix F. Two parallel 750-kW converters are used because IGBTs in large enough ratings to build a single 1.5-MW converter are not available. The system is designed for a 690-V generator output at rated speed and a 690-V grid connection. The DC bus voltage is fixed at 1100 V for all operating conditions. The grid-side converter is designed for power factor control that may be commanded from 0.95 lagging to 0.95 leading. The cost of this PE system is not dependent on the generator speed range. The 1.5-MW WindPACT estimates assume a minimum turbine speed of 5.7 rpm (rated speed is 20.5 rpm). Calculations of voltages, currents, and efficiency for this system operating with a medium-speed, 1.5-MW PM generator are included in Appendix G.

4.9.3.2 Diode-IGBT Power Electronics System

The diode-IGBT PE system is shown in Figure 4-24. The PM generator output is passively rectified by a diode bridge and filtered by an inductor and capacitor to create a variable-voltage DC bus. The DC bus voltage changes with generator speed and output power. The DC bus is converted to standardized grid frequency AC power by an IGBT, PWM voltage-source inverter. The inverter provides grid current control to supply 60-Hz three-phase output power at any commanded power factor, leading or lagging.

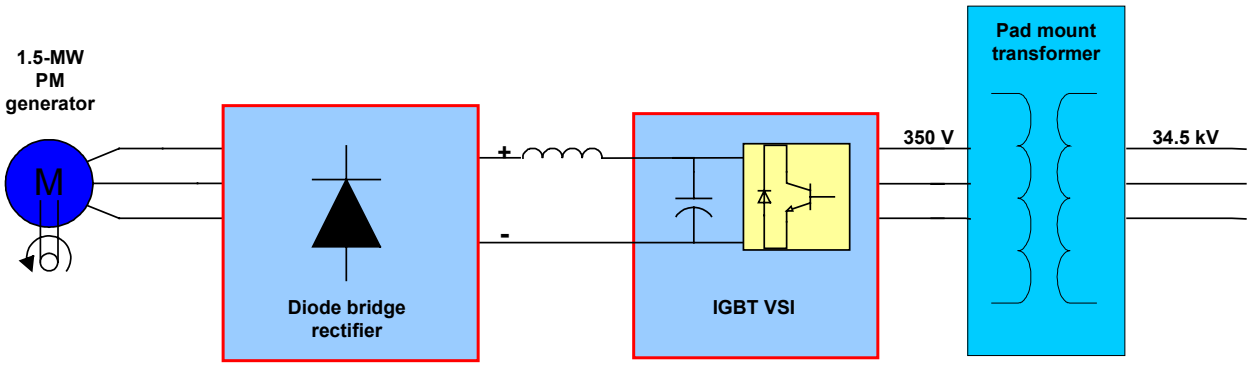

Figure 4-24. Diode-IGBT PE system

This PE system can only be used with a synchronous generator (PM or wound field), where excitation is provided either by the PMs or the DC field current. It is not compatible with induction generators because the diode rectifier is not able to supply the necessary magnetization component of current in quadrature with the generator voltage. The operation of this PE system is described and compared to the IGBT-IGBT system in Dubois (2000) and Grauers (1996a). The diode-IGBT system is lower in cost than the IGBT-IGBT system because the generator IGBT converter is replaced by a diode rectifier that costs much less. Several disadvantages to this system, however, make it less favorable than it appears at first glance:

- **Low grid voltage:** The DC bus voltage changes with generator speed. For proper operation, the voltage-source inverter requires the DC bus voltage to always be higher than the peak of the AC line voltage. Because the lowest generator output voltage (and hence the lowest DC bus voltage) occurs at minimum generator speed, this operating requirement determines the turns ratio of the pad mount transformer and thus the maximum AC voltage that the transformer presents to the grid inverter. In concert with the peak voltage capabilities of the IGBT switches and the minimum achievable pulse width for the PWM inverter, this requirement also determines the generator speed range, the corresponding range of the DC bus voltage, and the range of pulse widths for the grid PWM inverter.

This limitation is inherent for all voltage source inverters and is required to keep the parallel, freewheeling diodes from continuously conducting and distorting the peaks of the delivered current waveform. To meet this limitation, the grid-side voltage from the pad mount transformer must be reduced for the diode-IGBT system relative to the IGBT-IGBT system. This is a significant disadvantage because at rated output, the input current is significantly higher and the corresponding average PWM duty cycle is reduced. This increases component current ratings and associated losses.

- **Limited speed range:** The minimum generator speed determines the minimum DC bus voltage for the diode-IGBT system and therefore the ratio of pad mount turns as described above. System cost increases as the minimum generator speed and transformed grid voltage are decreased. On the other hand, decreasing the minimum speed increases the turbine energy production by operating the rotor at an optimum TSR at lower wind speeds. The optimum minimum speed is a compromise. For this reason and for the electronic system reason discussed above, a 2:1 ratio of rated to minimum speed was chosen for the WindPACT study.

- **Generator reactance effects:** Diode rectification of the generator output does not allow the direct control of the generator power factor that is possible with the IGBT-IGBT system. This increases the generator current and decreases the generator voltage. This effect can be counteracted to some extent by designing the generator for use with the diode-IGBT system with a higher turns ratio and reduced reactance. These effects are described in detail in Section 4.8.3.

Detailed estimates of the 1.5-MW diode-IGBT system, including schematics and BOMs, are included in Appendix F. Two parallel 750-kW IGBT converters are used. This reflects limitations on the current handling capacity of IGBT switches that are available now. The system is designed for an 1100-V DC bus at rated generator speed and load and a grid voltage of 350 V as presented by the pad mount transformer. The grid voltage is determined by the minimum DC bus voltage at the minimum turbine speed of 10.2 rpm (rated speed is 20.5 rpm). The grid-side converter is designed to operate with commanded power factors ranging from 0.95 lagging to 0.95 leading. Appendix G contains calculations of voltages, currents, and efficiency for this system operating with a medium-speed PM generator.

Variation of Diode-IGBT System Using Boost Converter. To eliminate problems associated with reduced DC bus voltage at low generator speeds, a boost converter can be added at the rectifier output to produce a fixed DC bus voltage. This system is described in Dubois (2000). The obvious disadvantage is the additional expense and complexity of the added boost converter. This added module was not investigated in detail for the study because with the added costs of the boost converter, the anticipated system cost was not expected to be significantly lower than that of the IGBT-IGBT system.

4.9.3.3 SCR-SCR Power Electronics System

Figure 4-25 illustrates the SCR-SCR PE system. The PM generator output is passively rectified by an SCR bridge and filtered by a DC link reactor (energy storage inductor) to create a variable-voltage DC bus. Under normal operating conditions, the generator-side SCRs are phased fully on to operate as diode rectifiers. As described previously for the diode-IGBT system, then, the DC bus voltage changes with generator speed and output power. The generator SCRs are phased back only when the DC bus would otherwise exceed a predetermined voltage limit.

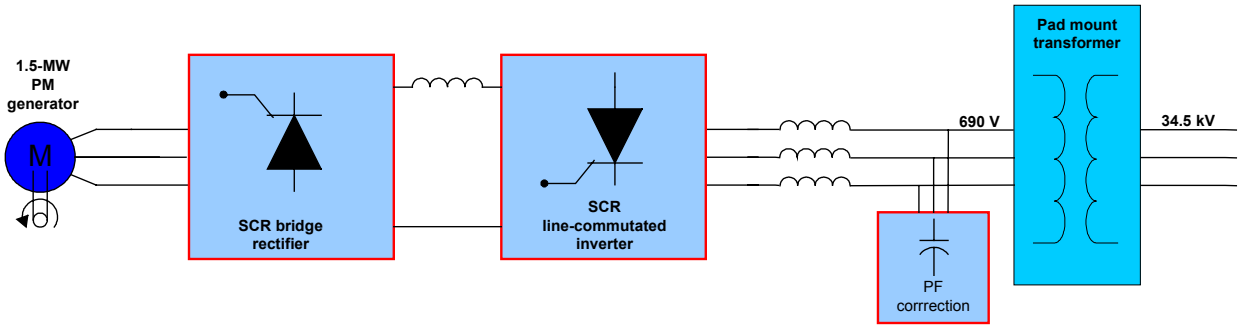

Figure 4-25. SCR-SCR PE system

The DC bus power is converted to AC grid power by an SCR line-commutated inverter that switches in synchronism with the grid frequency. If the DC link reactor is large, the grid current for this system has the classical six-pulse waveform with square steps shown in Figure 4-26. The system is operated with the maximum DC bus voltage always limited to less than the peak grid voltage. The firing angle of the grid-converter SCRs controls the DC link current and generator torque. The bandwidth of the torque control is limited by the time delay between discrete firing pulses of the SCRs, but is sufficient to mitigate gearbox torque transients (see Section 4.4).

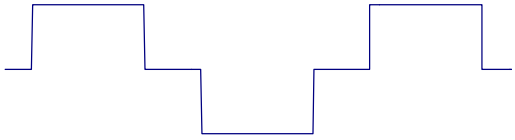

Figure 4-26. SCR-SCR six-pulse current wave forms

The line-commutated converter always operates at a lagging power factor and must therefore be compensated with an independent source of reactive power. The power factor of the converter is approximately equal to the ratio of the DC bus voltage to the peak AC grid voltage. Power factor correction capacitors are included as part of the system to supply the necessary reactive power. Four sets of switched capacitors are used to regulate power factor of the entire system to approximately 0.95 lagging. A wind farm VAR control system, described in Section 4.11.3, is used to further adjust the power factor of the entire wind farm. The AC reactors, connected between the power factor capacitors and the line-commutated inverter, supply the line reactance necessary for proper SCR commutation in the inverter.

The cost of the SCR-SCR system is not dependent on the generator speed range, so a low cut-in speed can be used. The line-commutated inverter operates at a very low power factor when the generator speed is low, but this is compensated by the correction capacitors. Because the generator power is low at low operating speeds, the reactive power consumed by the line-commutated inverter is less at low operating speeds than at rated speed, in spite of the low power factor.

The SCR-SCR PE system, like the diode-IGBT system, is compatible only with synchronous generators and cannot be used with induction generators. This system (or variations of it) has been used for many years in industrial applications. Operating theory is described in Mohan et al. (1995). It has been proposed for wind turbine applications several times (Dubois 2000; Krishnan and Rim 1989; Chan and Spooner 1998). A 1.5-MW wind turbine prototype has been built and tested in Italy (Avolio et al. 1998). The

system is low in cost and has the benefit of using SCRs that are rugged, reliable, and available at high voltage and current ratings. There are several disadvantages to this PE system, however, which necessitate the addition of other electrical system elements. These disadvantages and the effects on the remainder of the electrical system are as follows:

- **Generator reactance effects:** The SCR-SCR system, like the diode-IGBT system, passively rectifies the generator output. Passive rectification does not allow the direct control of the generator current phase angles, which increases the generator current and decreases the generator output voltage relative to operation with the diode-IGBT system. Increased generator size and some decreased generator efficiency are consequences. These effects are described in detail in Section 4.8.3.

- **Grid current harmonics:** The grid current for a single six-pulse, SCR-SCR inverter is shown in Figure 4-26. The harmonics of this current waveform far exceed the IEEE 519 standard for power quality (IEEE 1992). A harmonic filtering system is necessary to meet the standard. A proposed method of using the wind farm electrical system to filter these harmonics is described in Section 4.9.3.4.

- **Power factor correction and VAR control:** The SCR line-commutated inverter consumes reactive power and cannot be used for wind farm VAR control. Additional electrical system components are necessary for this function. Power factor correction capacitors, which are included in the cost estimates for the SCR-SCR PE system, along with the separate wind farm VAR control system, which are described in Section 4.11.3, are necessary.

Appendix F contains detailed cost estimates of the 1.5-MW SCR-SCR system, including schematics and BOMs. Calculations of voltages, currents, and efficiency for this system operating with a medium-speed PM generator are included in Appendix G. The system is designed for an 800-V DC bus at rated generator speed and load, and a grid voltage of 690 V from the pad mount transformer. Power factor is corrected to 0.95 lagging at the pad mount transformer connection. The SCR-SCR PE system can be operated over a wide speed range. The 1.5-MW estimates assume a cut-in turbine speed of 5.7 rpm (rated speed is 20.5 rpm).

4.9.3.4 SCR-SCR Distributed Filtering Wind Farm System

As described in Section 4.9.3.3, compared to the IGBT-IGBT and diode-IGBT systems, the SCR-SCR PE system has the disadvantages of excessive harmonic currents and the lack of VAR control capability. To correct these problems and minimize the added costs, the wind farm system shown in Figure 4-27 was analyzed in detail. The operation of this system is described in Erdman et al. (2002), which is included in Appendix H. This system provides power at the wind farm substation that meets IEEE 519 power quality standards (IEEE 1992) and provides 0.95 leading to 0.95 lagging VAR control. This distributed filtering technique uses the winding configuration of the pad mount transformers together with inductances in the wind farm power collection system to minimize the cost of the wind turbine and substation filtering requirements. This means that although power quality at the individual turbines does not meet the IEEE 519 standard, the power quality at the point of common connection (the output of the substation transformer) will meet the standard. Turbines in the wind farm can operate in the presence of the substandard power quality, because even though the collection system current is distorted, the collection system voltage is not significantly distorted. The voltage distortion is low because collection system impedances are relatively low compared to the wind farm output power. The design of this system is based on:

- **Phase multiplication using pad mount transformers:** Two different pad mount transformer configurations are used alternately throughout the wind farm to reduce the lower order current harmonics by phase multiplying the turbine output. Figure 4-28 shows the transformer configurations and ideal current waveforms. Half of the transformers are wye-wye with zero phase shift and the other half are zig-zag with a 30°phase shift. The sum of the currents from pairs of these create a 12-pulse current waveform that has the 5th and 7th harmonics cancelled. The zig-zag transformer has the same phase shift as a wye-delta transformer but has the advantage of a neutral connection for grounding purposes. The current waveforms shown in Figure 4-28 have square transitions to show this effect clearly. In a real system, the waveforms are rounded and appear even more sinusoidal because of filtering from the various distributed system impedances.

- **Filtering with wind plant impedances:** The parasitic inductances and capacitances in the wind farm collection system all provide some filtering of the current harmonics. Transformer reactances have the largest effect but line impedances are also beneficial. This is particularly true in wind farms that have significant collection system lengths from the pad mount transformers to the substation.

- **Power factor correction capacitors as filters:** Power factor correction capacitors in combination with AC reactors (inductors) in the PE system supply harmonic filtering.

- **Substation IGBT VAR control and harmonic correction:** Stepped or continuous 0.95 lagging to 0.95 leading VAR control is added at the substation. VAR control includes both IGBT controllers capable of continuous control and switched capacitors. The IGBT controllers are also capable of delivering harmonic current cancellation to eliminate any remaining current harmonics at the substation.

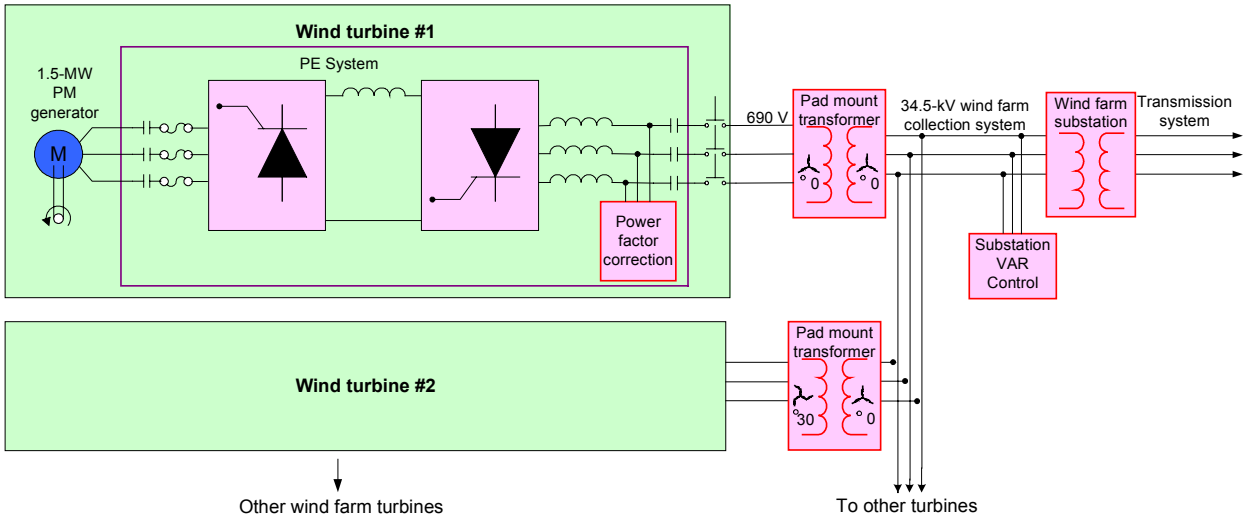

Figure 4-27. Wind farm system using SCR-SCR PE

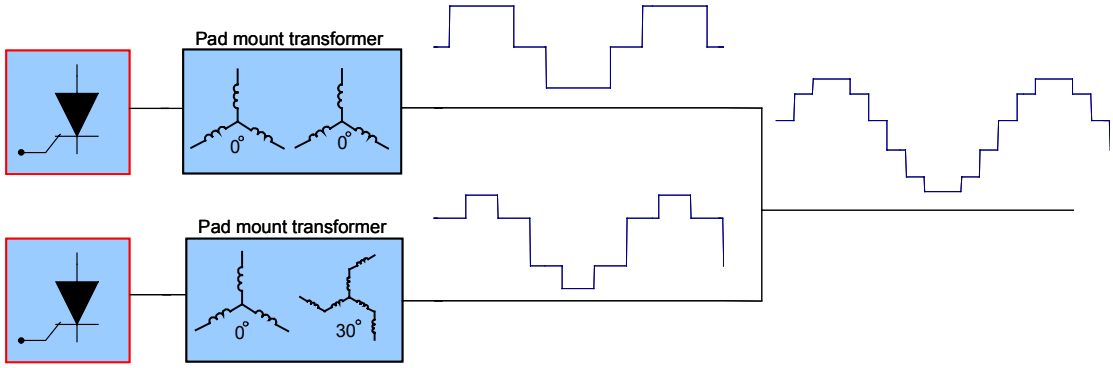

Figure 4-28. Ideal 12-pulse current wave forms

4.9.3.5 Variations of the Wind Farm System

A number of variations of this wind farm system are possible. These variations are described in Erdman et al. (2002; included in Appendix H). Some of the variations considered are described below:

- **Twenty-four-pulse system:** It is possible to use a 24-pulse system giving additional cancellation of low-order harmonics, by placing throughout the wind farm groups of four pad mount transformer configurations with transformers that have -15°, 0°, +15°, and +30° phase shifts. The added costs of the two additional transformer types are not expected to be significant based on the estimates described in Section 4.11.2. However, the filtering of the 12-pulse system in combination with harmonic cancellation provided by the distributed parasitics and the substation VAR control appears to be sufficient.

- **Single turbine, 12-pulse system:** There are a number of ways to design a single turbine that has a 12-pulse output, but all the methods require the generator output to be split into two parallel paths, then combined with phase shifting transformers. These systems have the advantage that they could be used for single turbine applications, but at the penalty of increased component cost.

- **Power factor correction (34.5 kV):** The power factor correction for each turbine can be moved from the 690-V PE system to the medium-voltage side of each pad mount transformer. This eliminates the need for the AC reactor in the PE system because the pad mount transformer reactance provides this function. Because the transformer reactance is higher than that of the AC reactor, this system offers more effective filtering. The power factor correction system must be designed for 34.5 kV, however, and the additional cost of the associated switchgear makes this approach less cost effective. For wind farms with 13.2-kV collection systems, this approach may be more cost effective.

4.10 Cost and Efficiency Comparisons of PE Options for PM Generators

The three PE systems were compared on a turbine COE basis. As described below, the choice of PE system affects several aspects of the turbine economic evaluation:

- The diode-IGBT and SCR-SCR systems require a higher cost version of the generator, optimized for passive rectification, than the version used for the IGBT-IGBT system.
- Each PE system has a different efficiency, changing turbine energy production.
- The generators operate with different efficiency for each PE system, changing turbine energy production.

- The diode-IGBT system has a reduced speed range and higher cut-in speed than the other two systems, which reduces the turbine energy production relative to the other two systems.

The COE comparison was made by evaluating component costs, efficiency, and energy production as described in the following paragraphs.

4.10.1 Component Cost Comparison

Table 4-19 lists the component costs for the single PM drive train for the three different PE systems. Estimates for the SCR-SCR PE system assume the wind farm system described in Section 4.9.3.4. Components that have changing costs dependent on the selected PE system are described below, along with the method used to estimate these costs:

Table 4-19. Component Cost Comparison for Single PM Drive Train with Different PE Systems

Component	SCR-SCR, $	Diode-IGBT, $	IGBT-IGBT, $
Transmission system	**90,000**	**90,000**	**90,000**
Gearbox components	84,000	84,000	84,000
Mainshaft	Included	Included	Included
Generator iron components	6,000	6,000	6,000
Mainshaft bearings	Included	Included	Included
Support structure (integrated nacelle)	**20,000**	**20,000**	**20,000**
External gearbox and generator (cooling system)	**4,400**	**4,400**	**4,400**
Brake system with hydraulics	**3,200**	**3,200**	**3,200**
Coupling (generator to gearbox)	**NA**	**NA**	**NA**
Nacelle cover	**8,200**	**8,200**	**8,200**
Generator active magnetics	**54,000**	**54,000**	**39,000**
Power Electronics	**53,000**	**91,000**	**121,000**
0.95–0.95 substation VAR control	**12,000**	**NA**	**NA**
Transformer	**26,000**	**23,000**	**23,000**
Cable	**16,000**	**21,000**	**18,000**
Switchgear	**10,000**	**15,000**	**13,000**
Other subsystems	**25,000**	**25,000**	**25,000**
Drive train assembly and test	**5,500**	**5,500**	**5,500**
Total	**327,000**	**360,000**	**370,000**

- **Generator:** For the same power rating, the passively rectified PM generator designed for the SCR-SCR and diode-IGBT systems is larger than the generator designed for use with the actively rectified IGBT-IGBT system. As described in Section 4.8.3, this is because a lower per-unit synchronous reactance is required. Estimates made by Kaman for the two generators are described in Section 4.8.4.

- **Cable:** Cable requirements are different for each system because the electrical currents are different. Estimates for each system are described in Section 4.11.1.

- **PE system:** Cost estimates from Appendix F for each PE system were used, with 40% gross margin assumed for the PE manufacturer. This is consistent with the cost model used to estimate the baseline power electronics.

- **Switchgear:** One-line diagrams for each electrical system are included in Appendix I, along with a BOM that itemizes the switchgear estimates for each.

- **Transformers:** The IGBT-IGBT systems use the same pad mount transformer used for the baseline design. Estimates for that transformer are described in Sections 5.3.2.3 and 4.11.2. The diode-IGBT transformer is the same as the IGBT-IGBT transformer but has a 350-V input rather than a 690-V input. The cost of this transformer was assumed to be the same as that of the IGBT-IGBT transformer.

  The SCR-SCR system uses two different transformer types alternately positioned through the wind farm, as described in Section 4.9.3.4. The average cost of these transformers is assumed to be 15% higher than the baseline transformer because (1) half of the transformers require a nonstandard zig-zag winding, estimated to increase individual transformer cost by approximately 6% based on the quotations described in Section 4.11.2; (2) increased harmonic currents in the SCR-SCR transformers increase cooling requirements; and (3) production volumes for each transformer type will be 50% of the baseline production volumes.

- **VAR control system:** Substation VAR control costs are added for the SCR-SCR PE system, but not for the IGBT-IGBT and diode-IGBT systems because these PE systems are intrinsically capable of providing VAR control for the wind farm. The VAR control system is described in Section 4.11.3 and detailed cost estimates are included in Appendix F.

4.10.2 Efficiency Comparison

The power electronics and generator efficiencies for the three systems are compared in Figure 4-29. These curves are based on the calculations included in spreadsheet format in Appendix G. The baseline doubly fed system efficiencies are included for comparison.

The PE system efficiency for the SCR-SCR system is higher than for the other two systems because losses are limited to the lower SCR conduction losses and the resistive losses in the DC reactor. Both the IGBT-IGBT and diode-IGBT PE system losses are dominated by switching losses in the IGBTs along with input filter losses. The switching losses in the diode-IGBT system are higher than might be expected because of the low modulation index and the resulting higher average currents for the IGBT converter, which are necessary because the AC grid voltage is lower for this system than for the other two.

The baseline PE system efficiency is represented as [(generator output-PE losses)/generator output]. The effective efficiency of this system is relatively high under rated conditions because only a fraction (nominally 1/3) of the total generator output power is converted by the PE system. The efficiency of the baseline power electronics is less than the other systems at lower powers because of the circulation of magnetization current through the converter.

The PE-generator efficiency of the diode-IGBT and the SCR-SCR generator systems are similar except at the lowest input powers, where the diode-IGBT generator efficiency is lower because the generator cut-in speed is higher. The efficiency of the IGBT-IGBT generator is lower than that of the other two because this generator, optimized for the IGBT conversion, is smaller and has a higher winding resistance. A higher efficiency generator could be used with the IGBT-IGBT system, but with the penalty of increased

component cost. All the PM generators have higher efficiency than the baseline doubly fed induction generators.

The combined PE and generator efficiency comparison shows that the SCR-SCR system has the highest efficiency, and that the IGBT-IGBT has the lowest efficiency.

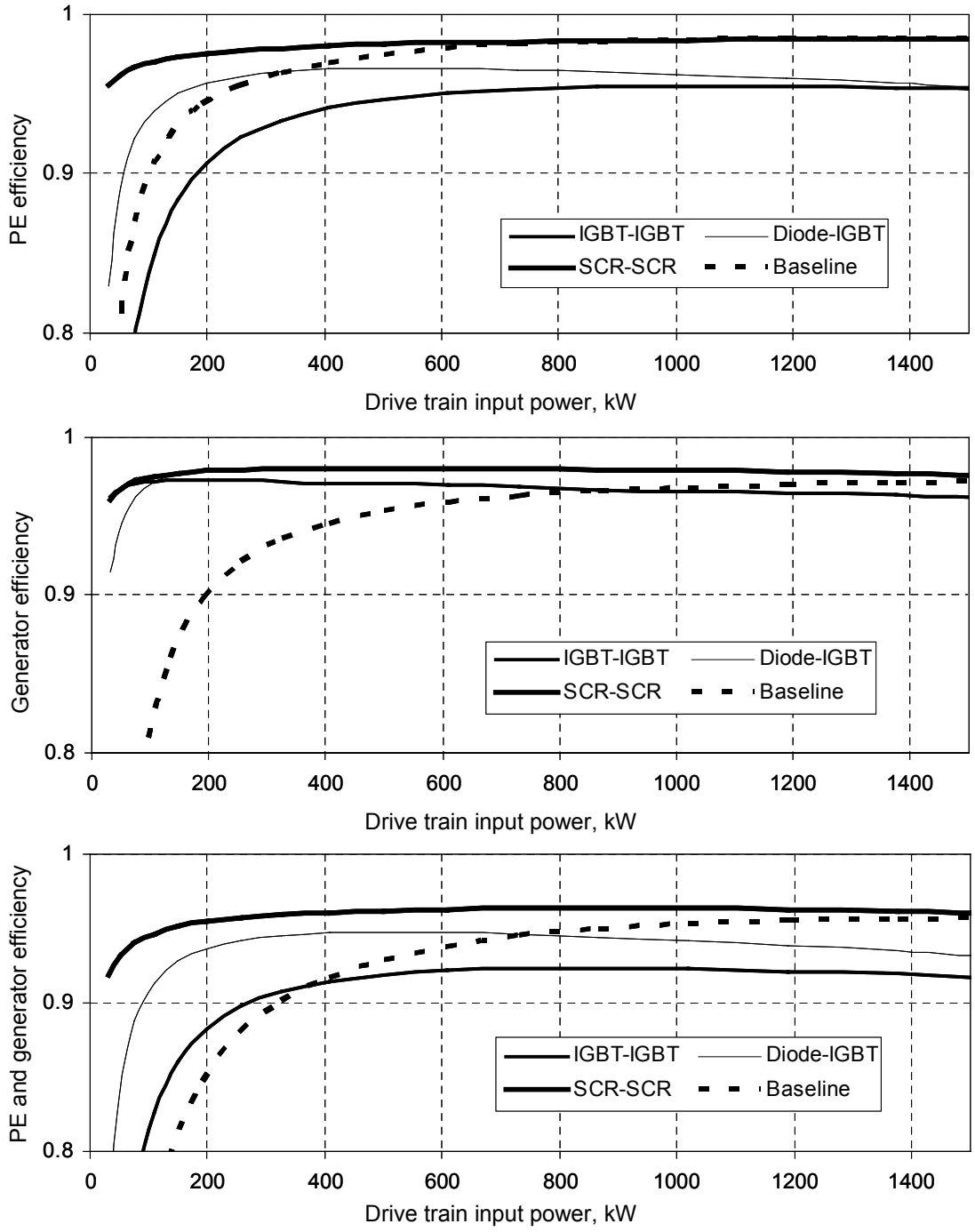

Figure 4-29. Comparison of generator efficiencies for different PE systems

4.10.3 Cost of Energy Comparison

Table 4-20 compares the COE of the 1.5-MW, single PM generator drive train using the three different PE systems. The COE is approximately 4% lower with the SCR-SCR system than with the diode-IGBT system, and 7% lower than with the IGBT-IGBT PE system. The SCR-SCR system has a lower COE because of the combination of higher efficiency and lower component costs. Note that O&M costs have been assumed constant for all systems in this analysis. It is likely that the O&M costs of the SCR-SCR system are lower than those of the other systems because of is lower component costs and expected higher reliability.

Table 4-20. Turbine COE Comparison for Single PM Drive Train with Different PE Systems

	SCR-SCR	Diode-IGBT	IGBT-IGBT
Capital Costs			
Turbine	**876,236**	**923,158**	**936,514**
Rotor	**248,000**	**248,000**	**248,000**
Drive train and nacelle	**327,358**	**360,006**	**370,280**
Yaw drive and bearing	**16,000**	**16,000**	**16,000**
Control, safety system	**7,000**	**7,000**	**7,000**
Tower	**184,000**	**184,000**	**184,000**
Turbine manufacturer's overhead and profit (30%, tower, rotor, & tranformer excepted)	**93,878**	**108,152**	**111,234**
Balance of station	**358,000**	**358,000**	**358,000**
Initial capital cost (ICC)	**1,234,236**	**1,281,158**	**1,294,514**
AEP			
Ideal annual energy output, kWh	5,660,000	5,590,000	5,506,000
Availability, fraction	0.95	0.95	0.95
Losses, fraction	0.07	0.07	0.07
Net AEP, kWh	**5,000,610**	**4,938,765**	**4,864,551**
As percentage of SCR-SCR	100.0	98.8	97.3
Replacement costs, LRC, $/yr	**4,792**	**4,792**	**4,792**
FCR, fraction/yr	**0.106**	**0.106**	**0.106**
O&M, $/kWh	**0.0042**	**0.0043**	**0.0044**
COE = O&M + ((FCRxICC)+LRC)/AEP	**0.0313**	**0.0326**	**0.0334**
As percentage of SCR-SCR	100.0	104.5	107.0

4.11 Costs of Other Electrical Subsystems and Components

4.11.1 Cable Costs

For each electrical system investigated, cable costs were calculated based on the estimated per-length material costs listed in Table 4-21 and estimates of the currents for each electrical system. The necessary cables for each configuration were determined from the one-line diagrams in Appendix I. Each 500-kcmil conductor is limited to 430 amps and each 4-in. conduit is limited to four 500-kcmil conductors per National Electric Code (National Fire Protection Association [NFPA] 2002) requirements.

The cable costs are summarized in Table 4-22 along with the number and length of each conductor type. An 84-m tower was assumed, with a junction between the rigid and the flexible windup cable at 90% of the way up the tower. The windup cable was assumed to be 15 m long, and the pad mount transformer to tower base cable was assumed to be 10 m long. In terms of cable costs, some of the advantages and disadvantages of the different electrical systems are:

- The baseline and multi-induction systems do not need an auxiliary 690-V power cable up the tower because 690 V goes to the generators.

- The diode-IGBT system has a lower input voltage and therefore higher input currents and higher transformer-to-tower base cable costs.

- Both the diode-IGBT and SCR-SCR systems were estimated with the DC bus cabled down the tower, which requires fewer conductors.

The SCR-SCR system has the lowest cable costs, approximately $1,800 less than the baseline costs, primarily because of savings associated with bringing DC power down the tower. The diode-IGBT system has the highest costs, approximately $3,300 more than the baseline costs, primarily because of the low-voltage, high-current input.

Table 4-21. Cable, Support, and Conduit Material Costs

Item	Cost/Meter, $
1-kV, 500-kcmil stranded conduit cable	11.80
2-kV, 500-kcmil stranded conduit cable	13.77
Vertical supports for cables up tower	32.80
4-conductor 6-AWG (American wire gauge) cable—auxiliary up tower	6.56
500-kcmil extra-flexible windup cable	19.68
4-in. RGS (Rigid galvanized steel) conduit—transformer to tower base	55.76

Sources: Bouillon Integrated Systems and William Erdman

Table 4-22. Cable Cost Summary

	Baseline	PM IGBT-IGBT	PM Diode-IGBT	PM SCR-SCR	Multi-Induction
500-kcmil, 2-kV conductors up tower			10		
500-kcmil, 1-kV conductors up tower	12	12		10	12
Length rigid cable up tower	75 m	75 m	75 m	75 m	75 m
Cost of conductors up tower, $	10,627	10,627	10,332	8,856	10,627
Number 500 kcmil windup conductors	12	12	10	10	12
Length windup cable	15 m	15 m	15 m	15 m	15 m
Cost, windup cable, $	3,542	3,542	2,952	2,952	3,542
Length 6-AWG aux cable up tower	NA	90 m	90 m	90 m	NA
Cost, auxiliary cable up tower, $	NA	590	590	590	NA
Length from transformer to tower base	10 m	10 m	10 m	10 m	10 m
500-kcmil, 1-kV conduit, transformer to tower base	12	12	24	12	12
Cost, conductors, transformer to tower base, $	1,417	1,417	2,834	1,417	1,417
Number of conduits, transformer to tower base	4	4	8	4	4
Cost, conduit from transformer to tower base, $	2,230	2,230	4,461	2,230	2,230
Total cost, $	**17,817**	**18,407**	**21,169**	**16,046**	**17,817**

4.11.2 Pad Mount Transformers

Wind turbine pad mount transformers are similar to transformers used in numerous other applications and are built by a number of manufacturers. Mark DeWolf of DeWolf Engineering surveyed four transformer manufacturers or distributors for price quotations and other information about turbine pad mount transformer costs. Table 4-23 summarizes the results. All quotations are for 1500-kVA oil-filled transformers and are based on volumes of 150–600 units per year. The wye-wye and wye-delta transformers are standard designs used for many applications other than wind turbines. The zig-zag or 12-pulse designs are custom designs that would be necessary for phase multiplication of the SCR PE system.

Manufacturers #2 and #4 could supply quotes only for the standard product and do not build custom designs. Manufacturers #1 and #3 were able to provide either the standard or custom designs, although Manufacturer #3 gave only the custom design quotes for this study. The zig-zag or 12-pulse custom designs appear to increase the transformer prices only slightly relative to the standard configurations. The winding voltage and conductor material have a greater impact on price.

Most manufacturers classify transformers with copper windings as high-efficiency transformers. These transformers would typically be used in a wind farm application. Aluminum windings are used in standard-efficiency transformers and those prices were quoted for comparison. The aluminum windings decrease the transformer price by about 15%. Manufacturer #2 also quoted a transformer built with an amorphous steel (Metglas or equivalent) core. This transformer has a much higher efficiency. Until recently, the cost of the amorphous steel core was prohibitive, but the price has recently begun to decrease. The high-side transformer voltage has a significant impact on transformer cost. The price of transformers built for 34.5-kV operation is approximately 30% higher than the price of those built for 13.2 kV.

All transformer prices in Table 4-23 are for 1500-kVA ratings. Transformer prices are approximately proportional to the kVA rating for small changes in rating. The actual ratings used for each drive train design depend on these considerations:

- The lowest power factor at which the drive train will operate
- The derating necessary for additional transformer heating caused by harmonic currents.

All drive train designs estimated for this study have a minimum power factor of 0.95. In the baseline and other designs using PE systems with IGBT voltage-source inverters, the turbine converters may be used for active VAR control. For these systems, the 0.95–0.95 VAR control range determines the minimum power factor. The power factor of the SCR-SCR line-commutated inverter PE system is compensated to 0.95 lagging with power factor correction capacitors included in the PE system estimates. The same is true for the multi-induction and Henderson drive trains that use line-connected, squirrel-cage induction generators.

Table 4-23. 1500-kVA Pad Mount Transformer Quotes*

Connection	Winding Material	Voltage, kV (High Side)	Manufacturer or Distributor, $ #1	#2	#3	#4
Low voltage, delta High voltage, wye grounded	Copper	13.2	15,755	17,250		
		34.5	20,650			
	Aluminum	13.2	13,600	15,700		11,744
		34.5	18,470			
	Copper with Amorphous Core	13.2		22,600		
		34.5				
Low voltage, wye High voltage, wye grounded	Copper	13.2	15,755	17,250		
		34.5	20,650			
	Aluminum	13.2	13,600	15,700		11,618
		34.5	18,470			
	Copper with Amorphous Core	13.2		22,600		
		34.5				
Low Voltage, zig-zig ± 7.5°) High voltage, wye grounded	Copper	13.2	17,291			
		34.5	21,950		22,000	
	Aluminum	13.2	14,960			
		34.5	19,735		19,500	
Low voltage—wye and delta dual windings (12-pulse connection) High voltage—wye grounded	Copper	13.2	17,915			
		34.5	21,970		23,320	
	Aluminum	13.2	15,500			
		34.5	19,625		20,570	
Low voltage—wye High voltage—zig-zag (± 7.5°)	Copper	13.2	16,940			
		34.5	21,600			
	Aluminum	13.2	14,660			
		34.5	19,430			

*All quotes for 1500-kVA transformers, 690-V low-voltage side, oil-filled, dead-front, radial-feed, 65˚C rise, factory.

4.11.3 VAR Control System

All drive train systems were evaluated with continuous VAR control capable of providing 0.95 lagging to 0.95 leading power factor at the output of the wind farm substation. For drive trains that use variable-speed electronics with a grid-connected, PWM voltage-source inverter (VSI), the inverter is capable of supplying this VAR control. No additional systems are required.

In cases where a PWM VSI is not used, a dedicated VAR control system is necessary to provide power factor correction. In these cases, capacitive power factor correction is added at each turbine to correct power factor to 0.95 lagging. Estimates for this power factor correction, when used, are included in the PE system category. A dedicated VAR control system is then added at the wind farm substation. This VAR control system is capable of supplying sufficient reactive power to correct the wind farm power factor from 0.95 lagging to 0.95 leading, as commanded by a substation control system.

A 66-MVAR reactive power control system sized for use in a 100-MW wind farm is shown in Figure 4-30. Four banks of switched capacitors are used in parallel with an IGBT-based static VAR controller. The 4.5-MVAR, 9.0-MVAR, 15.0-MVAR, and 30.0-MVAR three-phase capacitor banks can be switched in and out as necessary to give VAR control in 4.5-MVAR increments. A 5.0-MVAR, IGBT-based static VAR controller provides continuous control to compensate for the incremental switching of the capacitor banks. This controller uses the same PWM VSI architecture used for the grid-side converter in the baseline variable-speed PE system. The static VAR controller operates at 690 Vso that it can use IGBT switches. For this reason, a 5-MVA transformer is necessary for connection to the 34.5-kV system.

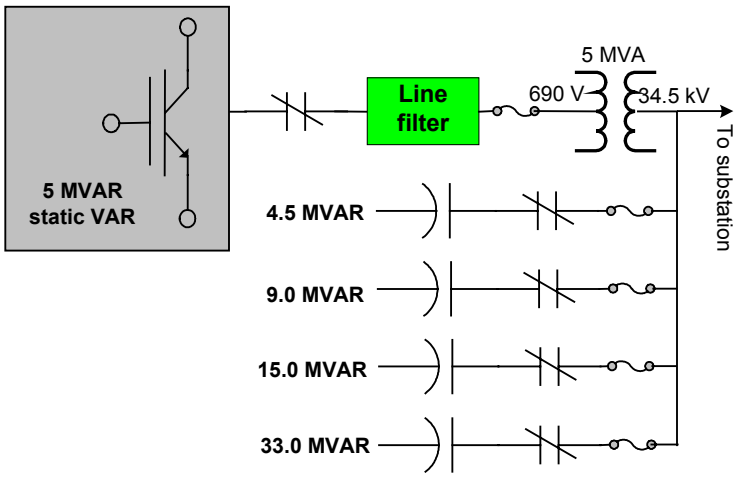

Figure 4-30. VAR control system for 100-MW wind farm (66 MVAR)

Costs of the VAR control system shown in Figure 4-30 are summarized in Table 4-24. William Erdman estimated these costs using the same methods used to estimate the PE system costs. Complete estimates are included in Appendix F. The estimated sales price of the 100-MW/66-MVAR wind farm VAR control system is about $760,000, based on a cost model using a 40% margin for the manufacturer, consistent with the PE estimates used in the study. The cost allocated to each 1.5-MW turbine in the wind farm is $11,500.

Table 4-24. VAR Control Cost Estimate for 66-MVAR System

	30% Margin	40% Margin	50% Margin
100-MW wind farm			
Direct variable materials, $[*]	389,031	389,031	389,031
Direct variable labor, $[†]	8,954	8,954	8,954
Direct fixed costs, $[‡]	59,698	59,698	59,698
Total direct costs, $	457,683	457,683	457,683
Gross margin, %[§]	30	40	50
Purchase price, $	653,833	762,805	915,366
Cost per 1.5-MW turbine, $ (÷66)	**9,907**	**11,558**	**13,869**

[*] Includes 3% freight in.
[†] Assumes 30% fringe benefits and 70% utilization, includes final assembly, board test, and final test.
[‡] This number can vary significantly; 15% is used here.
[§] Gross margin = (sales price - direct cost)/sales price.

5. Baseline Drive Train

The baseline drive train design is similar to the 1.5-MW variable-speed turbine designs currently produced by GE Wind in the United States and several turbine manufacturers in Europe. Detailed preliminary design estimates were developed for the baseline drive train. These estimates served as a reference point for the comparative evaluation of all the other drive train designs investigated during the study.

5.1 Baseline 1.5-MW System Description

The baseline drive train is illustrated in Figure 5-1, and Figure 5-2 is a diagram of the system. This bedplate design uses a three-point suspension to transmit rotor loads to the tower. Two elastomeric mounts, which minimize acoustic noise transmission, support a gearbox with integrated rear mainshaft bearings. The mainshaft front bearing provides the third support point. The gearbox has a ratio of 73:1, to step up the low-speed shaft input to the 900–1500 rpm range necessary for the 6-pole, doubly fed induction generator. The generator is mounted to the bedplate through isolation mounts, also to minimize noise transmission. The nacelle has a large fiberglass cover that carries no load.

The generator stator is electrically connected directly to the grid through the turbine pad mount transformer. The generator rotor is connected to a PE system that supplies the variable frequency and variable voltage necessary to operate the generator at variable speed. Under rated conditions, approximately 2/3 of the doubly fed generator power is output from the stator and 1/3 comes from the rotor. This system minimizes the power that must be converted by the PE system, minimizing the cost and improving the PE system efficiency at full power.

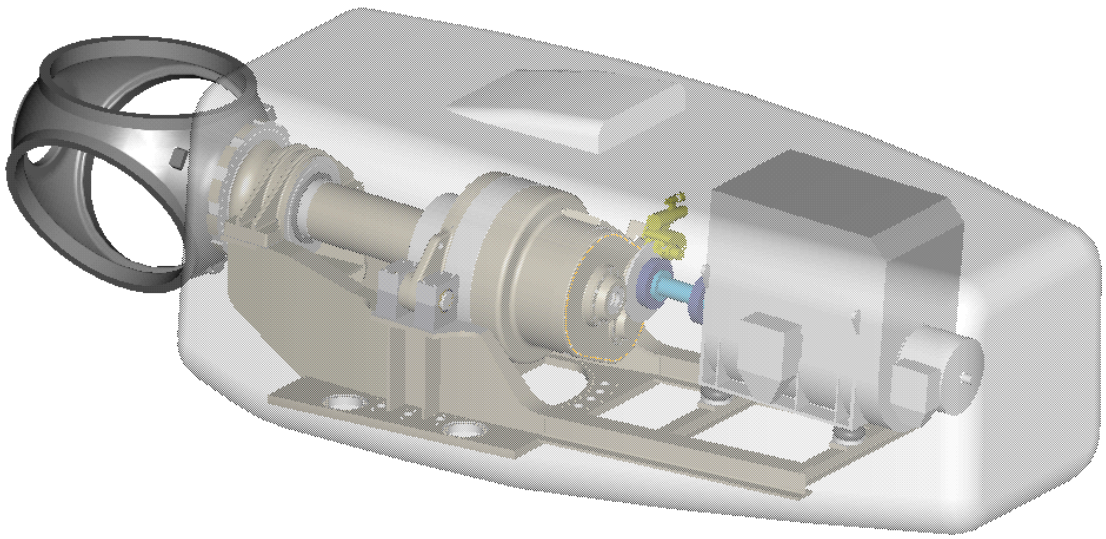

Figure 5-1. WindPACT 1.5-MW baseline drive train

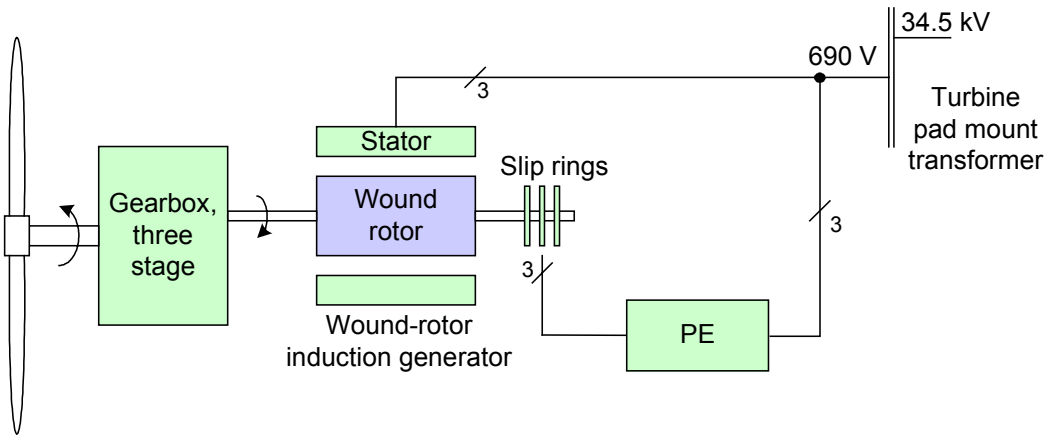

Figure 5-2. Baseline system diagram

5.2 Baseline Design Alternatives

Four variations of the WindPACT baseline architecture, described in the preceding section, were investigated as part of this study, and results are presented elsewhere in this report:

1. **Integrated baseline:** See Section 6. This design uses an integrated structure with the same generator and electrical topology.
2. **Klatt-EDI generator:** See Section 11. This design replaces the generator and PE system with the Klatt-EDI generator and its associated PE system.
3. **HDJ generator:** See Section 12. This design replaces the generator and PE system with the HDJ variable-slip induction generator.
4. **Henderson torque-limiting gearbox:** See Section 13. This design uses a modified baseline gearbox with hydraulic torque limiting and a fixed-speed generator.

Many other alternatives to the WindPACT baseline architecture use similar mechanical designs with alternative generator and electrical systems. Some of the possible alternatives are described below:

- **Fixed-speed and dual-speed architectures:** These architectures use line-connected, squirrel-cage induction generators without power converters. The dual-speed architectures use either a single, two-speed induction generator or a primary, full-rated generator together with a secondary, low-speed generator that has a lower rating. These architectures are available from a number of manufacturers.

- **Induction generators with controlled slip energy dissipation:** These systems use a wound-rotor induction generator with additional electronically controlled rotor resistance to provide variable slip and thus limited variable-speed operation (but only above the generator synchronous speed). The benefits of operation below synchronous speed cannot be attained. The generator slip energy is dissipated in the resistance. These systems do provide generator torque control to reduce gearbox loads but do not provide variable-speed operation below the generator synchronous speed with the associated increased aerodynamic efficiency. The Vestas Opti-slip system (Vestas Wind Systems A/S, Denmark) is an example of this architecture.

- **Squirrel-cage generators with full power electronics:** These systems use a squirrel-cage induction generator with an IGBT PWM voltage source converter. The IGBT system is required to provide field-oriented control for the squirrel-cage induction generator. These systems provide full variable-speed operation down to zero speed. They are seldom used in current wind turbine designs because the full-rated PE system is expensive, making the total generator plus PE cost more expensive than the baseline system. The limited speed range of the doubly fed baseline system is adequate for variable-speed energy capture purposes.

These alternatives were not investigated in this study but are described more fully in Dubois (2000) and Hau (2000). These architectures were outside the scope of this study because (1) most do not provide full variable-speed operation; (2) they are well understood in the industry, are being built, or have been built in the past; and (3) they are not expected to have significant COE benefits relative to the selected baseline (although modest improvements may be possible for some of the designs).

5.3 Baseline Design and Component Estimates

Whenever possible, component designs and estimates for the baseline system were based on existing knowledge of components used in current wind turbine designs. Several of the electrical components were estimated directly by industry partners who supply components to existing turbine manufacturers. In other cases, consultants participating in the study were familiar with the existing designs and able to provide estimates on that basis. For the most part, the emphasis was on following existing industry practice, assuming that the turbine manufacturers have largely optimized the baseline design.

5.3.1 Baseline Mechanical Design and Component Estimates

Figure 5-3 shows the mechanical design of the baseline drive train. The bearing, mainshaft, and gearbox designs are described in the following subsections.

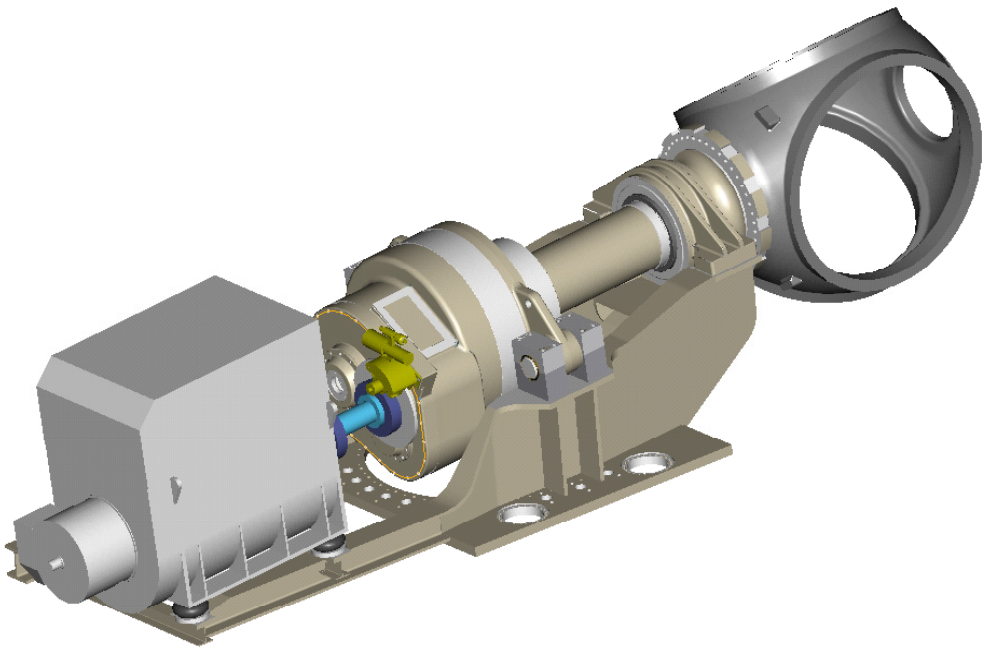

Figure 5-3. Baseline drive train mechanical design

5.3.1.1 Mainshaft and Front Bearing

The mainshaft connects the rotor to the gearbox and is in turn supported by a spherical roller bearing located in a pillow block. This custom pillow block is fastened to the bedplate and supports the majority of rotor forces and moments.

This configuration is used only on the baseline machine. The cost is based on estimated mass and the unit/mass multiplier for machined components described in Section 4.6.

5.3.1.2 Gearbox

PEI developed a detailed design for the baseline gearbox in Pro/E. The design is based on typical industry designs and the turbine loads described in Section 3.3. Figure 5-4 shows a cutaway view of the Pro/E model.

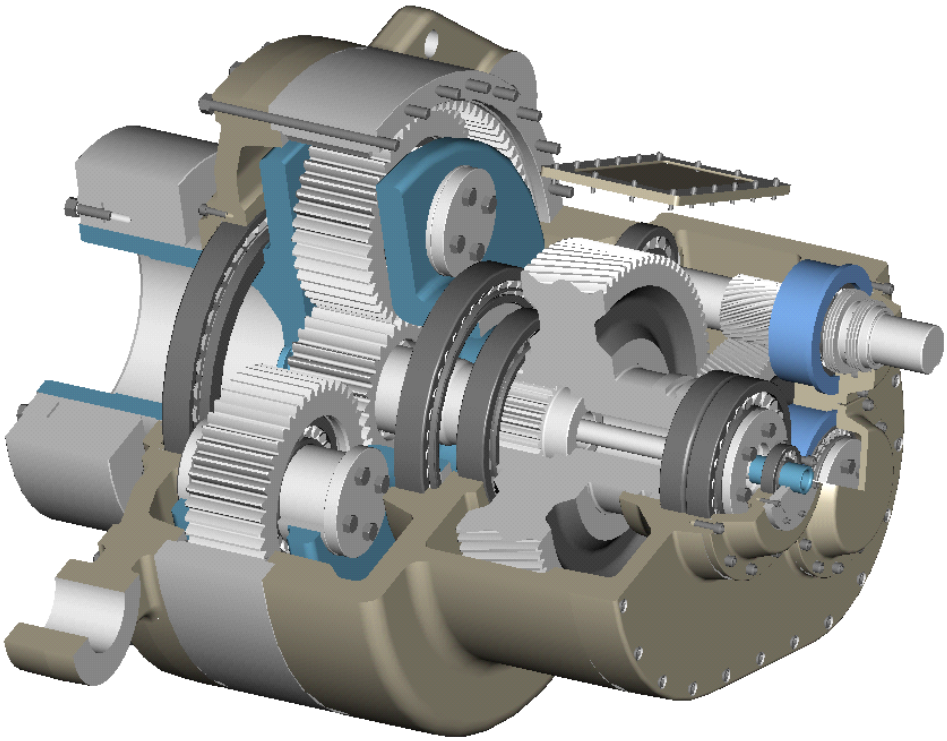

Figure 5-4. Baseline gearbox

The baseline gearbox consists of one planetary section, the first stage, and two additional stages of parallel-shaft helical gears. The input from the mainshaft is fixed to the first-stage carrier with a shrink disc. The gearbox carrier bearings, housed in a member with opposing torque arms, form the support for the mainshaft rear. The torque arms are fitted to the bedplate on pins with elastomeric bushings. This mounting helps to attenuate structural borne vibrations, which is useful for meeting stringent noise standards.

The sun pinion is spline-connected to the first helical stage. This connection provides a degree of freedom for the inevitable positional displacement of the sun pinion, which is critical for equalizing tooth forces. The connection does, however, cause positional displacement to slope the sun pinion axis. This sensitivity to manufacturing deviations is managed by extreme precision in component machining.

Output to the generator is offset, making the mainshaft center line clear of the high-speed shaft. This leaves enough room for the slip ring assembly. The gearbox center line must accommodate a conduit of electrical or hydraulic lines, or both, which must be connected to the rotor hub interior.

Using the method described in Section 4.6, Milwaukee Gear estimated the baseline gearbox costs based on a BOM and on Pro/E subcomponent drawings. Appendix D includes the BOM and the selling price estimate for the baseline gearbox.

5.3.1.3 Bedplate

The bedplate, shown in Figure 5-3, was designed as a welded steel component. A first-order analysis based on the loads described in Section 3.3 was used to size the structural members. A Pro/E solid model confirmed that the resulting mass is consistent with published nacelle weights for similar bedplates used in existing turbine designs. The cost estimates given in Appendix D were based on the estimated weight and a cost of $1.55/lb, based on known industry costs for similar bedplates purchased by existing turbine manufacturers from U.S. and Canadian fabricators.

5.3.1.4 Nacelle Cover

The nacelle cover was modeled in Pro/E and the mass was calculated based on this model. The costs were estimated using the calculated mass with added hardware costs, as described in Section 4.6.

5.3.2 Baseline Electrical Design and Component Estimates

Figure 5-5 is a simplified diagram of the WindPACT baseline electrical system. A detailed one-line diagram is included in Appendix I. The generator is a 1500-kW, 6-pole, 690-V line-line wound-rotor induction generator with external connections to the rotor through slip rings. Thus the synchronous speed for 60-Hz operation of this 6-pole generator is 1200 rpm. The generator has a rotor-to-stator turns ratio of 3:1, making the rotor voltage equal the stator voltage (690 V) when the generator slip is 0.33. When the generator speed is above or below the normal 900–1500 rpm operational range, the slip exceeds 0.33 and the rotor voltage exceeds 690 V. The generator stator is connected to the low-voltage side of the turbine pad mount transformer through a circuit breaker and contactor. The contactor is opened when the generator speed is less than 900 rpm because below this speed the generator rotor voltage would otherwise be excessive. The generator rotor is connected directly to the PE system.

The PE system includes two voltage-source PWM inverters interconnected by an 1100-V DC bus. One inverter is connected to the generator rotor through a crowbar and fuse protection circuit included in the PE system. This protection is necessary to protect the IGBT bridge from excessive rotor voltage that, because of the effective 3:1 transformer ratio, will be applied if the generator stator is connected to the line at low speed. The PE system also includes an output inductor, necessary to filter PWM current ripple, an input filter, and an input contactor.

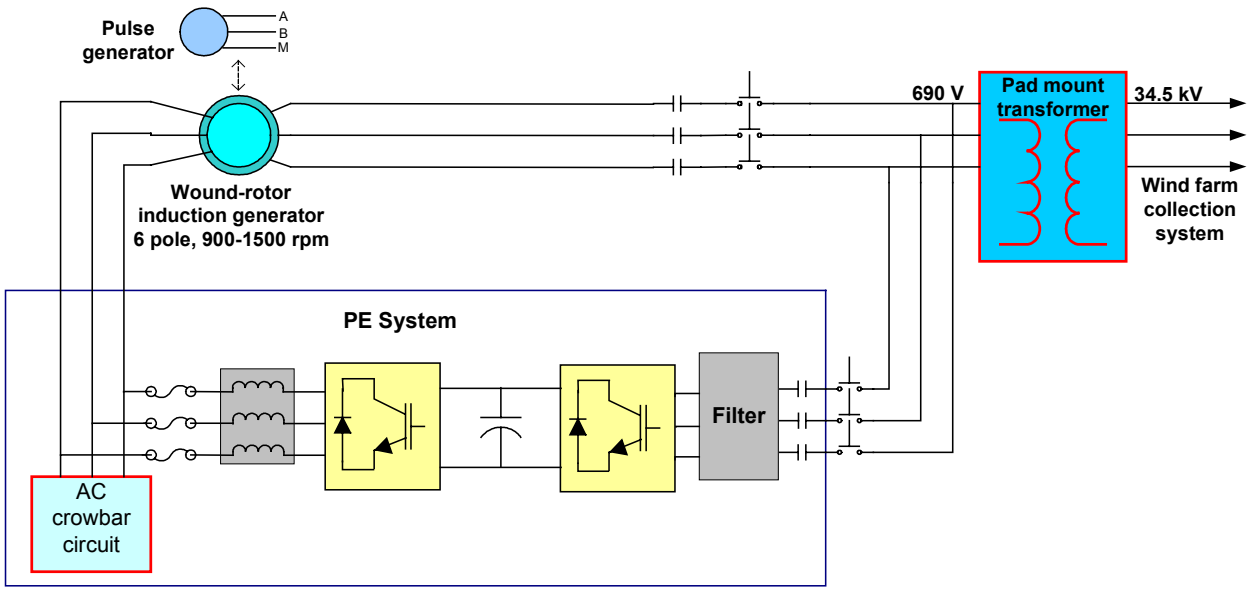

Figure 5-5. Baseline electrical system

The operation of the baseline doubly fed generator and PE system is described in detail in Muller, Deicke, and De Doncker (2002) and Mikhail et al. (2000). The PE control system monitors the generator rotor position with a shaft-mounted pulse generator (shaft position encoder). Field orientation is used to control generator torque per a command from the turbine control system. The generator PWM inverter is controlled to provide all generator magnetization current through the rotor, to give a nominal stator power factor of unity for the stator. The inverter also has the capability of providing additional leading or lagging reactive current through the generator rotor to provide wind farm reactive power (VAR) control.

The pad mount transformer steps the 690-V turbine output up to the wind farm distribution voltage. This voltage typically ranges from 13.2 to 34.5 kV. A distribution voltage of 34.5 kV was assumed for this study because this voltage has become typical in most large wind farms that have been built recently. The wind farm distribution system connects the pad mount transformers to the wind farm substation. The substation transformer converts the distribution voltage to the transmission level. The wind farm distribution and substation costs are included as part of the balance-of-station costs in this study and were not estimated separately.

The following subsections describe the major electrical components of this system.

5.3.2.1 Generator

Table 5-1 lists the baseline generator specifications. These specifications are similar to those currently used in a number of European turbines, with the exception of the 60-Hz frequency for the intended U.S. application. Liquid cooling is assumed. The additional cost of an external liquid-air heat exchanger system is included as a separate ancillary component.

Table 5-1. Target Baseline Generator Specifications

Type	Wound-rotor induction generator
Rotor connection	Slip ring
Rotor position sensing	Shaft encoder
Voltage	690 line-line
Pole number	6
Frequency	60 Hz
Construction	IP54 protection
Cooling	Liquid

Several companies manufacture 1.5-MW wound-rotor induction generators with specifications comparable to those described above. Selling price information from three manufacturers was used for this study. The first two manufacturers currently supply generators to wind turbine manufacturers. The third manufacturer has not yet produced generators for this application but has substantial experience supplying similar machines for other industrial applications. Table 5-2 shows the generator prices. All quoted prices were based on quantities of between 100 and 600 per year, as would be typically sold to wind turbine manufacturers. Manufacturer #1 supplied a generator model that is a very close match to the WindPACT specifications. The generators quoted by Manufacturers #2 and #3 all have either four rather than six poles or voltages other than 690 V, but still give a general check against the selling price from Manufacturer #1.

Other information received informally has indicated that the selling price of this type of generator is in the $50,000 to $60,000 range. Taking this into consideration, an estimated cost of $60,000 was used for this study.

Table 5-2. Baseline Generator Quotations

Manufacturer	Frequency, Hz	Pole #	Voltage	Protection	Cooling	Frame Size	Mass, kg	Price, $
1	60	6	690	IP55	Air-air	560L	8300	61,000
1	60	6	690	IP55	Liquid	560M	7800	61,000
1	50	6	690	IP55	Air-air	560LX	8500	64,000
1	50	4	690	IP55	Air-air	500L	7100	53,000
2	60	4	575	IP54	Air-air	500	8200	60,000
3	60	4	2400	IP54	Air-air	500–1250		63,000
3	60	6	2400	IP54	Air-air	560–1250		70,000

Generator stator and rotor power, voltages, currents, losses, and efficiency were calculated with equations defining the power flow in induction generators. Appendix G contains these calculations and associated equations in spreadsheet format for each wind turbine operating point. The generator parameters used in these calculations were estimated from manufacturer data and adjusted as necessary for a full load efficiency of approximately 97% to match manufacturer efficiency data.

5.3.2.2 Power Electronics

The design and costs estimates for the baseline PE system are included in Appendix F. A 40% gross margin was assumed for the manufacturer to estimate the cost. As described in Section 4.9, Loher Drive

Systems and Siemens Energy and Automation also quoted prices (with the same 40% gross margin) for this PE system, and those quotes compared well to the Appendix F estimates.

The PE system efficiency was calculated at each wind turbine operating point based on the generator operating point and a PWM VSI loss model. Appendix G contains the calculations and associated equations.

5.3.2.3 Transformer

A cost of $22,500 was used for the baseline transformer. This price was an estimate that took into account the 1500-kW transformer prices shown in Table 4-23 in Section 4.11.2, adjusted with the following considerations:

- A 1580 kVA rating is assumed, which is necessary for 0.95-0.95 power factor VAR control.
- A 34.5-kV collection system voltage is assumed.
- The service factor is 1.15.
- Shipping costs must be added to FOB factory price.

The transformer costs for all other drive train designs were estimated relative to the baseline transformer cost.

5.3.2.4 Cable

Cable costs for the baseline system were as outlined in Section 4.11.1 and Table 4-22. These costs include the cables used for transferring the power from the generator at the top of the tower to the electrical enclosures at the base of the tower and for the small distance from the tower base to the pad mount transformer. The costs of the (typically buried) cables of the 34.5-kV power collection network are included in the balance-of-station costs.

5.3.2.5 Switchgear

The switchgear costs for the baseline system were estimated per the one-line diagram and the estimates are included in Appendix I. The switchgear category of system components includes the contactors, circuit breakers, fuses, cable terminal blocks, and other system protection and electrical control devices needed for system operation and protection. The major switchgear elements are depicted in the system electrical diagram of Figure 5-5. As the figure shows, the filter, the crowbar, and the voltage and current sensors are considered part of the PE system.

5.3.3 Ancillary Components

5.3.3.1 Cooling System

The baseline gearbox is sold with its own cooling system, which is included in the baseline gearbox price. The cost of a separate liquid generator cooling system is included as a separate line item and is based on size and cost methods described in Section 4.6.10 and a generator full load efficiency of 97%. These estimates are shown in Appendix D.

5.3.3.2 Brake System and Hydraulics

Figure 5-6 depicts the baseline brake system, and cost estimates are given in Appendix D. The brake system cost was calculated with the method described in Section 4.6.8. The baseline brake disc is mounted on the high-speed shaft, and because of the relatively high gearbox ratio of approximately 80:1, the torque requirement for this break is low. For this reason, the baseline brake system has a low cost relative to some of the other drive trains investigated, which have the brake discs mounted on lower speed shafts.

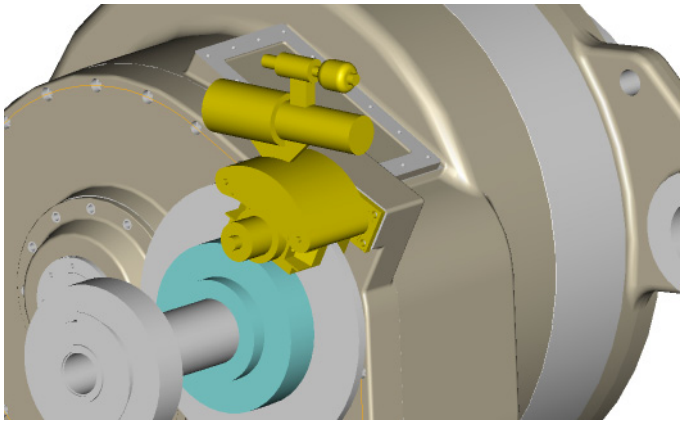

Figure 5-6. Baseline brake system

5.3.3.3 Coupling (High-Speed Shaft)

Appendix D also contains the high-speed coupling cost estimates, which were calculated with the method described in Section 4.6.7.

5.3.3.4 Drive Train Assembly and Test

Gearbox assembly and test is included in the gearbox cost estimate. The final drive train assembly and test estimates for the baseline system include the costs of assembling the driveline to the bedplate, painting the assembly, and testing the system.

5.4 Baseline Cost of Energy Results

The following subsections summarize the COE estimate for the baseline design along with the efficiency, energy production, component cost, and O&M estimates used for the COE estimate. Section 5.5 summarizes the scaling of the 1.5-MW estimates to 750-kW and 3.0-MW ratings.

5.4.1 Baseline Efficiency

Figure 5-7 illustrates the drive train efficiency versus input power for the baseline design on a component-by-component basis. Drive train efficiency is 93.8% at rated power but this decreases substantially below about 30% of rated power, primarily because of the reduced generator and PE efficiencies seen at lower power. The gearbox efficiency is approximately 98% at full power but does not decrease as much at lower power levels.

Values of generator and PE efficiencies are from the calculations given in Appendix G. The reduced generator and PE efficiencies at low power result from substantial fixed loss components caused primarily by losses associated with the magnetization component of the generator current. This current component flows in the generator rotor and is supplied by the rotor-fed power electronics. It causes resistive losses in the generator rotor and switching and conduction losses in the generator power electronic converter. The gearbox efficiency curve is from the measurements presented in GEC (2002) for a two-stage, 300-kW gearbox operated at variable speed.

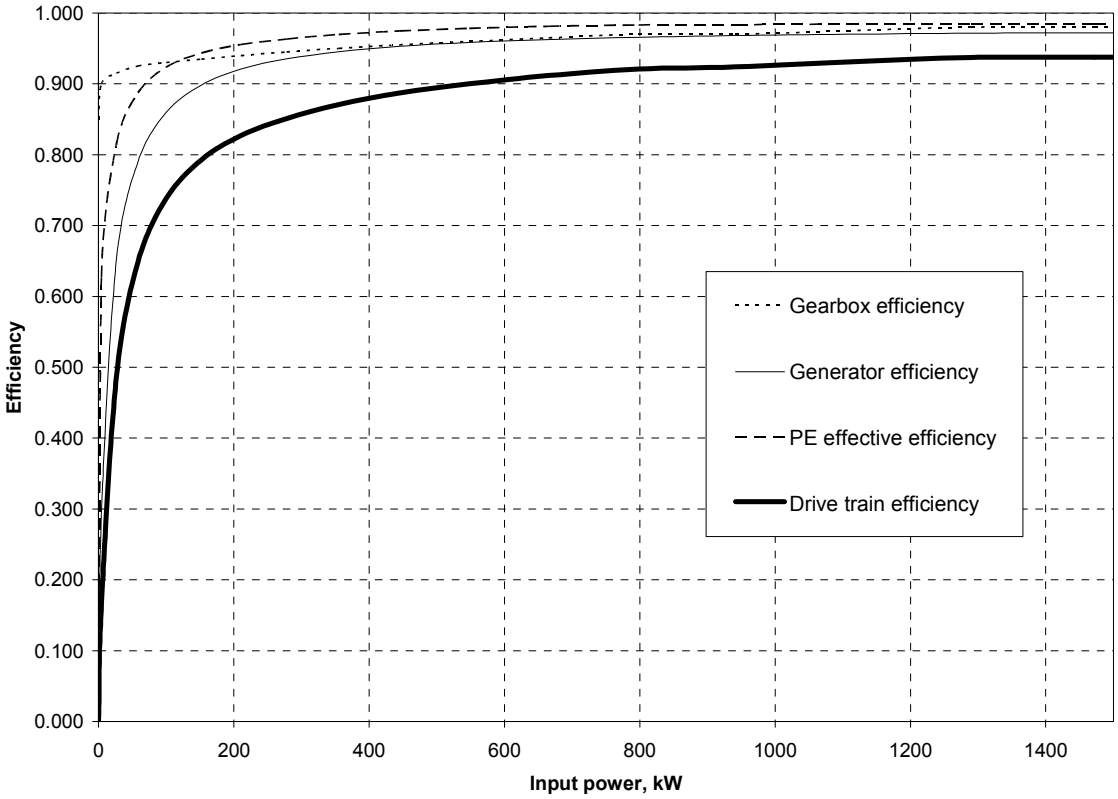

Figure 5-7. Baseline drive train efficiency by component

5.4.2 Baseline Gross Annual Energy Production

Table 5-3 gives the gross electrical energy production estimate for the baseline design for each wind speed bin. Because drive train efficiency losses are included in these binned values, they represent the annual electrical energy delivered at the output of the wind turbine generator. All other losses are calculated and included separately in the final cost of energy analysis (see Section 5.4.5).

The binned gross energy production estimates are shown graphically in Figure 5-8. The highest energy production occurs in the bins near the rated wind speed of 11.5 m/s. Almost half (48%) of the energy production occurs at the rated wind speed and above, where the turbine output is regulated to 1.5 MW. At lower wind speeds, the reduced energy production results from both decreasing rotor power and decreasing drive train efficiency. For wind speeds above the rated wind speed, the wind speed frequency distribution declines rapidly. Even though such winds are more energetic, their reduced number of hours per year results in an associated rapid decline in their annual energy contribution.

Table 5-3. Baseline Drive Train GAEP

Wind Speed Bin Center, m/s	Rotor Speed, rpm	Rotor Power, kW	Drive Train Efficiency	Output Power, kW	# of Hours per Year	Energy Production	
						MWh	Fraction of Total, %
3.0	12.28	6.7	0.000	0.0	297.5	0	0.00
3.5	12.28	27.2	0.165	4.5	333.1	1	0.03
4.0	12.28	54.4	0.486	26.5	363.0	10	0.18
4.5	12.28	90.2	0.649	58.5	386.9	23	0.41
5.0	12.28	136.0	0.738	100.5	404.7	41	0.74
5.5	12.28	191.6	0.793	151.8	416.5	63	1.15
6.0	12.28	254.2	0.827	210.2	422.4	89	1.62
6.5	12.42	326.4	0.851	277.8	422.7	117	2.14
7.0	13.37	407.7	0.871	355.0	417.8	148	2.71
7.5	14.33	501.4	0.887	444.7	408.3	182	3.31
8.0	15.28	608.6	0.900	547.8	394.7	216	3.95
8.5	16.24	729.9	0.912	665.4	377.7	251	4.59
9.0	17.19	866.5	0.921	797.9	357.8	286	5.21
9.5	18.15	1019.1	0.924	941.5	335.9	316	5.77
10.0	19.10	1188.6	0.931	1106.5	312.4	346	6.31
10.5	20.06	1375.9	0.937	1289.7	288.0	371	6.78
11.0	20.47	1569.8	0.938	1471.9	263.2	387	7.07
11.5	20.47	1600.0	0.938	1500.0	238.5	358	6.53
12.0	20.47	1600.0	0.938	1500.0	214.4	322	5.87
12.5	20.47	1600.0	0.938	1500.0	191.2	287	5.23
13.0	20.47	1600.0	0.938	1500.0	169.1	254	4.63
13.5	20.47	1600.0	0.938	1500.0	148.4	223	4.06
14.0	20.47	1600.0	0.938	1500.0	129.3	194	3.54
14.5	20.47	1600.0	0.938	1500.0	111.7	168	3.06
15.0	20.47	1600.0	0.938	1500.0	95.8	144	2.62
15.5	20.47	1600.0	0.938	1500.0	81.6	122	2.23
16.0	20.47	1600.0	0.938	1500.0	69.0	103	1.89
16.5	20.47	1600.0	0.938	1500.0	57.9	87	1.58
17.0	20.47	1600.0	0.938	1500.0	48.2	72	1.32
17.5	20.47	1600.0	0.938	1500.0	39.9	60	1.09
18.0	20.47	1600.0	0.938	1500.0	32.7	49	0.90
18.5	20.47	1600.0	0.938	1500.0	26.7	40	0.73
19.0	20.47	1600.0	0.938	1500.0	21.6	32	0.59
19.5	20.47	1600.0	0.938	1500.0	17.4	26	0.48
20.0	20.47	1600.0	0.938	1500.0	13.9	21	0.38
20.5	20.47	1600.0	0.938	1500.0	11.0	16	0.30
21.0	20.47	1600.0	0.938	1500.0	8.6	13	0.24
21.5	20.47	1600.0	0.938	1500.0	6.8	10	0.18
22.0	20.47	1600.0	0.938	1500.0	5.2	8	0.14
22.5	20.47	1600.0	0.938	1500.0	4.0	6	0.11
23.0	20.47	1600.0	0.938	1500.0	3.1	5	0.08
23.5	20.47	1600.0	0.938	1500.0	2.4	4	0.06
24.0	20.47	1600.0	0.938	1500.0	1.8	3	0.05
24.5	20.47	1600.0	0.938	1500.0	1.3	2	0.04
25.0	20.47	1600.0	0.938	1500.0	1.0	1	0.03
25.5	20.47	1600.0	0.938	1500.0	0.7	1	0.02
26.0	20.47	1600.0	0.938	1500.0	0.5	1	0.01
26.5	20.47	1600.0	0.938	1500.0	0.4	1	0.01
27.0	20.47	1600.0	0.938	1500.0	0.3	0	0.01
27.5	20.47	1600.0	0.938	1500.0	0.2	0	0.01
11.5-27.5	20.47	1600.0	0.938	1500.0	1754.6	2632	48.0
					Total GAEP =	**5479**	**MWh**

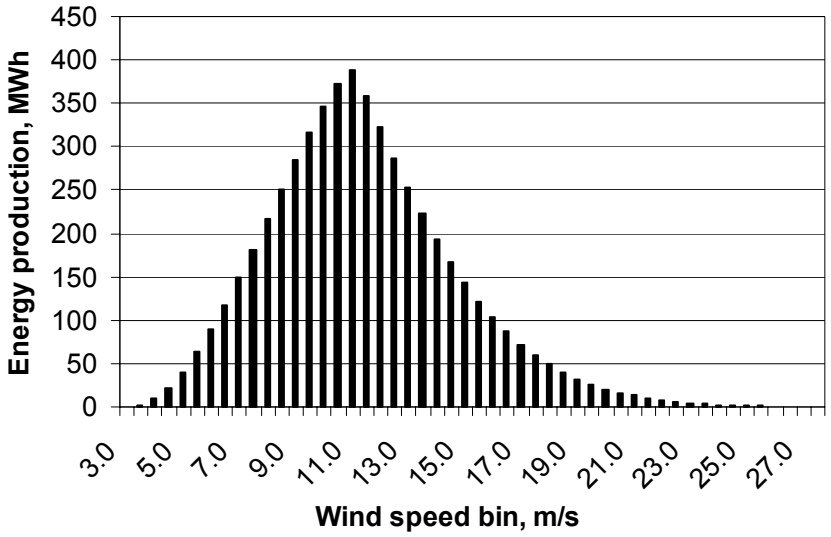

Figure 5-8. Baseline energy production by bin

5.4.3 Baseline Component Costs

Component costs for the baseline drive train are itemized in Table 5-4. All turbine and wind farm system components with costs that are directly dependent on the drive train design are included. To arrive at a representative total system cost and to properly account for differences in non-drive-train system components among the various drive train designs, all other wind turbine and wind farm subsystem costs are included. For this reason, the pad mount transformer, power factor correction capacitors, substation VAR control, cable, and switchgear are included even though they might not otherwise be considered part of the drive train. The highest cost component is the gearbox, which at $120,000 accounts for 28% of the drive train cost. The three highest cost components are the gearbox, the generator, and the power electronics, which together account for $242,000, or 57% of the drive train cost.

Table 5-4. Baseline Drive Train Component Costs

Component	Cost, $
Transmission system	**155,000**
Gearbox components	120,000
Mainshaft	20,000
Mainshaft support bearing and block	12,000
Elastomeric mounting system	3,000
Generator Isolation Mounts	1,000
Support structure (bedplate)	**34,000**
Generator cooling system	**2,400**
Brake system with hydraulics	**1,000**
Coupling (generator to gearbox)	**2,000**
Nacelle cover	**17,000**
Generator (wound rotor induction)	**60,000**
Power electronics	**62,000**
0.95–0.95 substation VAR control	**Not applicable**
Transformer	**23,000**
Cable	**18,000**
Switchgear	**12,000**
Other subsystems	**25,000**
Drive train assembly and test	**8,000**
Total	**420,000**

Note: All costs rounded.

5.4.4 Baseline Operations and Maintenance Costs

Table 5-5 shows the annual O&M costs and the LRC, both as cost per year and normalized by the annual energy capture of the turbine. Unscheduled maintenance, the largest component of O&M, is also larger than the LRC. Complete details of the baseline drive train O&M model are included in Appendix J.

Table 5-5. Baseline O&M and LRC Estimates

	$/yr	$/kWh
Unscheduled maintenance	12,103	0.0025
Scheduled maintenance	6,004	0.0012
Operations	6,501	0.0013
Subtotal, O&M (excluding LRC)	**24,608**	**0.0051**
LRC (major overhauls)	**5,124**	**0.0011**
Total O&M and LRC	29,732	0.0061

The scheduled and unscheduled maintenance costs, combined with LRC estimates from Table 5-5, are broken down by major turbine and drive train component in Figure 5-9. The operations estimate is not included, because breakdown by component is not possible. The drive train transmission is the single largest item, followed by the yaw drive and bearing. The generator, power electronics, and blades all make significant contributions.

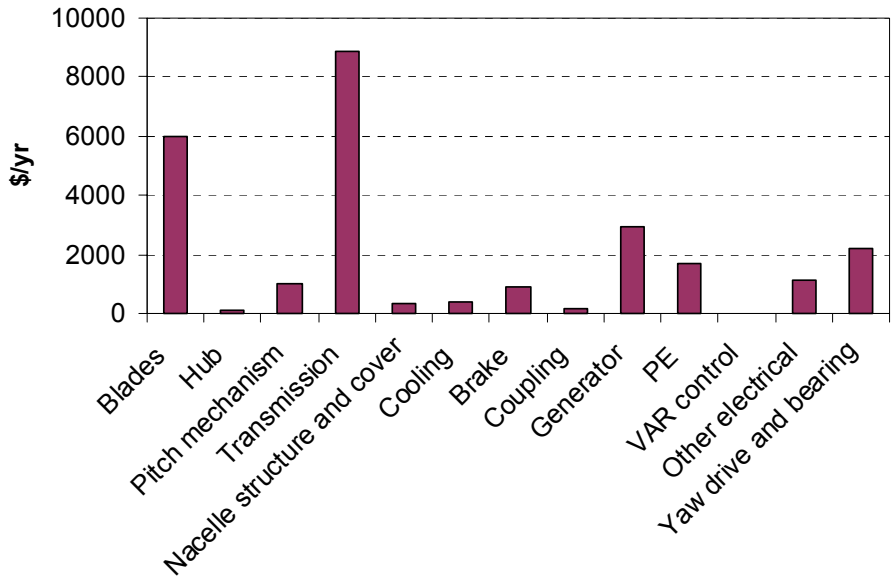

Figure 5-9. Scheduled plus unscheduled maintenance costs and LRC by baseline component

5.4.5 Baseline Cost of Energy Estimates

Table 5-6 gives COE estimates for the baseline design. Included in these COE estimates are a 95% availability factor and wind farm losses of 7%. The wind farm losses include those associated with the power collection system, the substation, array effects, controller actions, and others. Recall that only losses internal to the drive train were included in the gross energy production estimate, described in Section 5.4.2. Recognition of these loss factors external to the wind turbine reduces the gross energy production value to the net AEP value shown in Table 5-6.

The COE estimate for the baseline design is 0.0358 $/kWh. The drive train components alone account for 25.6% of the COE. In addition, the turbine manufacturer's 30% overhead and profit accounts for 7.7% of the COE. This item is approximately proportional to drive train component cost, because rotor and tower costs are not included. A significant portion of both the O&M and LRC are also dependent on the drive train design and component costs. Together, O&M and LRC account for 17% of the COE.

Table 5-6. Baseline Drive Train COE Estimates

	Cost, $	% of COE
Capital Costs		
Turbine	**1,001,491**	**61.0**
Rotor	**248,000**	**15.1**
Drive train and nacelle	**430,778**	**25.6**
Yaw drive and bearing	**16,000**	**1.0**
Control, safety system	**7,000**	**0.4**
Tower	**184,000**	**11.2**
Turbine manufacturer's overhead and profit (30%, tower, rotor, and transformer excepted)	**126,229**	**7.7**
Balance of station	**358,000**	**21.8**
ICC	**1,359,491**	**82.8**
AEP		
Ideal annual energy output, kWh	5,479,000	
Availability, fraction	0.95	
Losses, fraction	0.07	
AEP, kWh	**4,840,697**	
Replacement costs, LRC, $/yr	**5,124**	**3.0**
FCR, fraction/yr	**0.106**	
O&M, $/kWh	**0.0051**	**14.2**
COE = O&M + ((FCRxICC)+LRC)/AEP	**0.0358**	

5.5 Baseline Scaling to 750 kW and 3 MW

The baseline drive train estimates were extended to 750 kW and 3 MW with several techniques for the different components. PEI and Milwaukee Gear estimated the transmission components in detail, using a BOM similar to those shown in Appendix D. Structural components were modeled in Pro/E and masses calculated with the same methods used to estimate the 1.5-MW components.

Table 5-7 summarizes the results of this scaling process, and these results are compared graphically in Figure 5-10 in terms of the drive train COE. The drive train COE represents the portion of the turbine COE attributed to the drive train capital cost alone. Relative to the 1.5-MW single-stage, baseline drive train, the 750-kW version is characterized by a slightly higher normalized capital cost (in dollars per kilowatt) and a higher COE. Again, relative to the 1.5-MW system, the 3-MW variation has a comparable capital cost and COE. The entries in Table 5-7 give some insight into the reasons for these cost relationships. It appears that the transmission system and bedplate diminish in normalized capital cost as the power rating increases from 750 kW to 1.5 MW, but no further decrease occurs as the power rating is increased from 1.5 MW to 3 MW. The rest of the subsystems have comparable normalized capital costs at all three sizes.

Table 5-7. Baseline Drive Train Component Cost Scaling to 750 kW and 3 MW

	750 kW		1.5 MW		3 MW		Method
	Cost, $	Cost/kW	Cost, $	Cost/kW	Cost, $	Cost/kW	
Transmission system	$82,554	110	155,939	104	320,182	107	
Gearbox components	*63,475*	*85*	*123,043*	*82*	*254,061*	*85*	PEI input
Mainshaft	*10,420*	*14*	*17,966*	*12*	*36,112*	*12*	PEI input
Mainshaft support bearing	*6,786*	*9.0*	*11,700*	*7.8*	*23,516*	*7.8*	PEI input
Elastomeric mounting system	*1,583*	*2.1*	*2,730*	*1.8*	*5,487*	*1.8*	PEI input
Generator isolation mounts	*290*	*0.4*	*500*	*0.3*	*1,006*	*0.3*	PEI input
Support structure (bedplate)	*19,778*	*26*	*34,100*	*23*	*68,541*	*23*	PEI input
Generator cooling system	*1,373*	*1.8*	*2,422*	*1.6*	*3,814*	*1.3*	PEI input
Brake system with hydraulics	*520*	*0.7*	*1,445*	*1.0*	*2,312*	*0.8*	PEI input
Coupling (generator to gearbox)	*1,225*	*1.6*	*2,382*	*1.6*	*4,424*	*1.5*	PEI input
Nacelle cover	*7,795*	*10*	*17,322*	*12*	*24,251*	*8.1*	PEI input
Generator (WR induction)	31,000	41	60,000	40	140,000	47	OEM Development Corp. input
Power electronics	*31,500*	*42*	*61,800*	*41*	*118,500*	*40*	OEM input
Power factor correction capacitors	*NA*		*NA*		*NA*		
0.95–0.95 substation VAR control	*NA*		*NA*		*NA*		
Transformer	*11,250*	*15*	*22,500*	*15*	*45,000*	*15*	Power rating
Cable	*8,909*	*12*	*17,817*	*12*	*35,634*	*12*	Power rating
Switchgear	*6,196*	*8.3*	*12,392*	*8.3*	*24,784*	*8.3*	Power rating
Other subsystems	*12,500*	*17*	*25,000*	*17*	*50,000*	*17*	Power rating
Drive train assembly and test	*6,446*	*9*	*8,030*	*5.4*	*9,560*	*3.2*	PEI input
Drive train and Nacelle total	**221,046**	**295**	**421,149**	**281**	**847,001**	**282**	

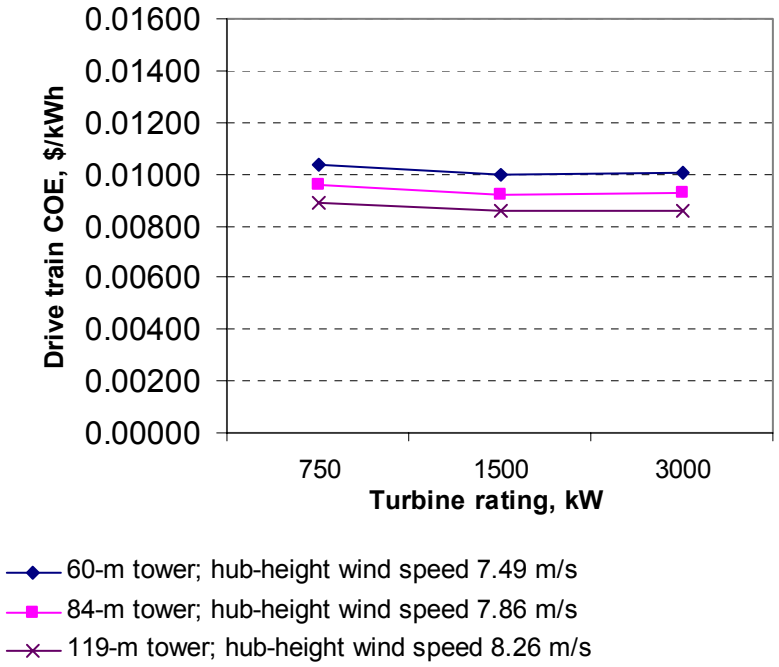

Figure 5-10. Baseline drive train COE scaling at different hub height wind speeds

6. Integrated Baseline Drive Train

The integrated baseline design is an alternative to the baseline. The latter uses a conventional bedplate design that supports the gearbox and other major structural components whereas the former integrates the bedplate with the major structural components. The integrated baseline was investigated to provide a direct comparison between a bedplate and an integrated design. Integrated designs, in general, make more efficient use of materials and have the potential to reduce costs. They have the disadvantage of using custom components that may not be available from multiple sources. Most of the designs investigated for this study, including the single PM, direct drive, multi-PM, and multi-induction, are integrated designs chosen to save material costs. The comparison of the integrated baseline to the baseline design provides insight into the COE savings that may be attributed to integration alone.

6.1 Integrated Baseline System Description

Figure 6-1 illustrates the 1.5-MW integrated baseline drive train. A system diagram, identical to the system diagram for the baseline system, is given as Figure 6-2. This design combines the integrated construction of the single-stage gearbox used in the single PM drive train with a conventional secondary two-stage gear train and face-mounted generator. A short-coupled mainshaft is supported by tapered roller bearings, which in turn are supported by a housing that is common with the gearbox. A tubular, stressed-skin nacelle supports the gearbox housing. The same electrical system design as the baseline drive train is used, including a doubly fed induction generator and a partially rated IGBT PE system.

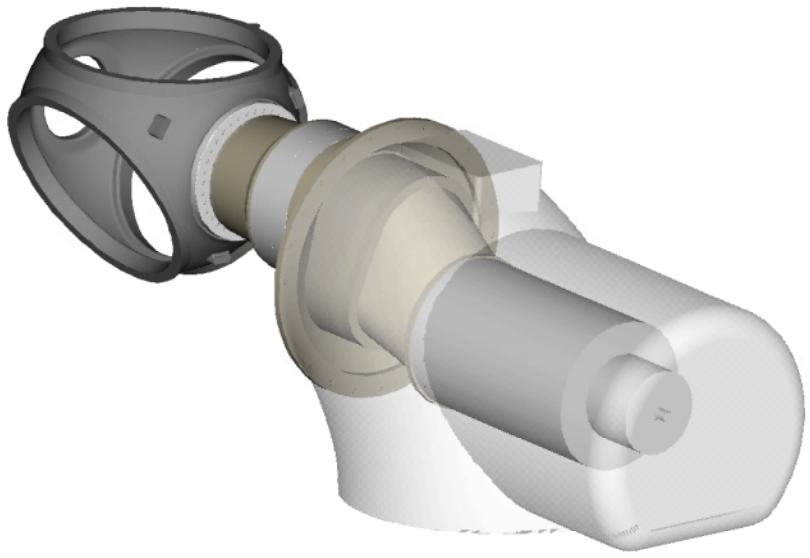

Figure 6-1. WindPACT integrated baseline drive train

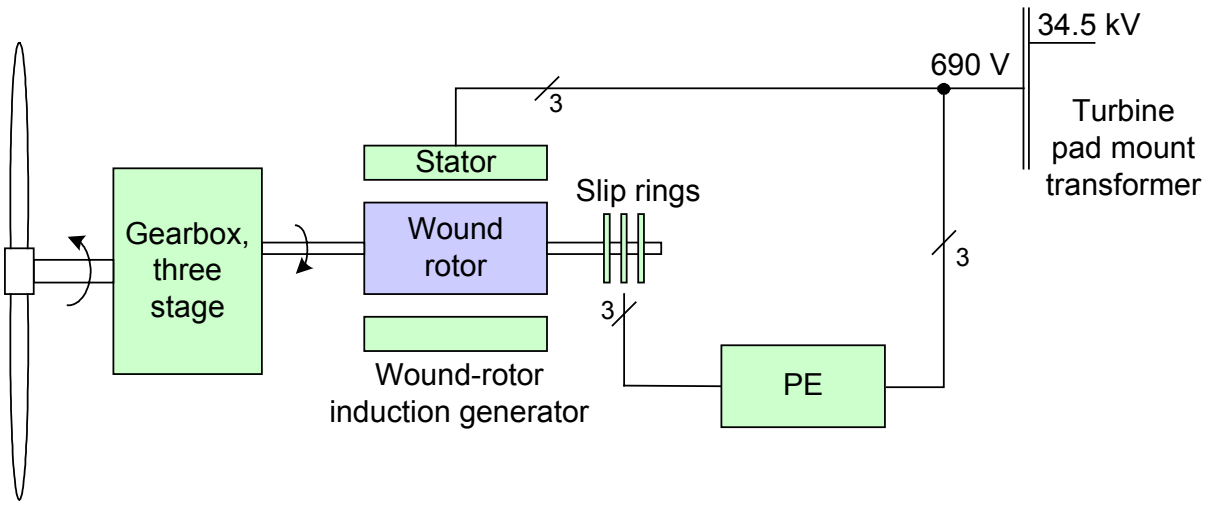

Figure 6-2. Integrated baseline system diagram

6.2 Integrated Baseline Component Designs and Estimates

Estimates for the integrated baseline design are based either on a Pro/E mechanical model that PEI developed, or where parts are similar, component estimates that were made for the baseline or other designs.

6.2.1 Integrated Baseline Mechanical Design and Component Estimates

Figure 6-3 shows the mechanical design of the integrated baseline drive train. The design and associated cost estimates for each of the mechanical components are described in the subsections that follow.

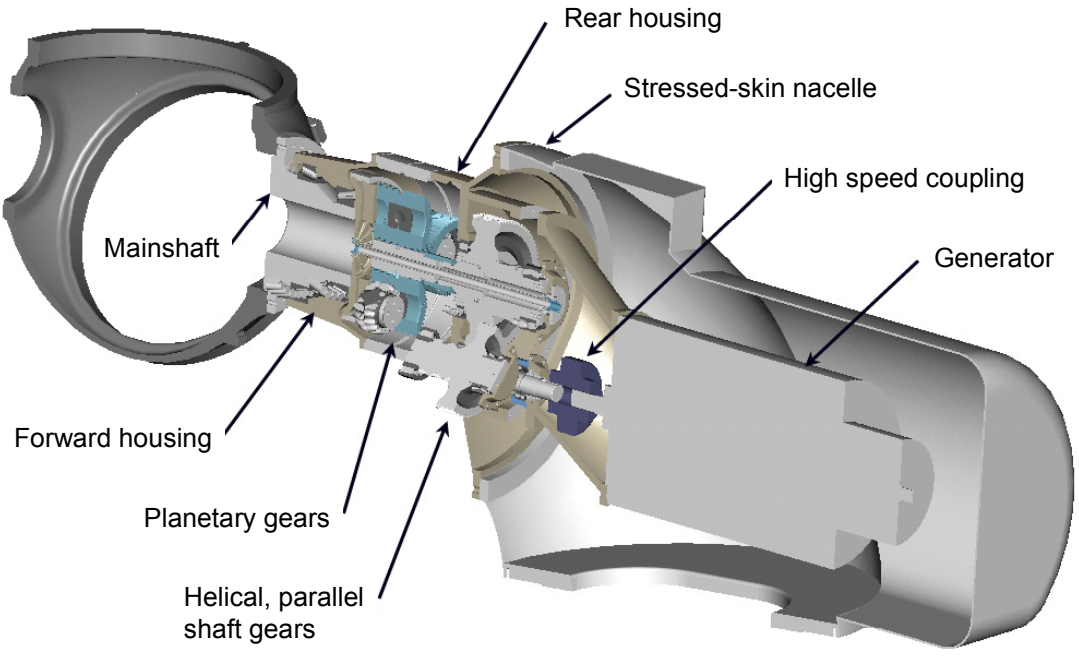

Figure 6-3. Integrated baseline drive train mechanical design

6.2.1.1 Mainshaft and Bearings

The integrated baseline mainshaft and support bearings are identical to the designs used for the single PM drive train, described in Section 7.3.1.1. The ductile iron shaft directly couples to the gearbox planetary stage. The weight was determined from the Pro/E solids model and the cost calculated with the methods described in Section 4.6.

6.2.1.2 Gearbox

The gearbox consists of a single stage of double helical gears arranged in a planetary configuration. Output from the planetary stage is further increased in speed by two parallel-shaft helical gear stages.

The gear case has an integral flange that connects to a stressed-skin nacelle structure. The parallel shaft helical gear stages are connected to the same casing. The casing carries an adapter for the face-mounted generator. The output from the final helical gear stage is sealed from the generator adapter. The generator shaft and high-speed pinion shaft are coupling-connected.

Milwaukee Gear estimated the cost of this gearbox, including assembly to the nacelle structure. Appendix D contains a BOM.

6.2.1.3 Structural Nacelle

The structural nacelle directly supports the driveline and couples to the yaw bearing. FEA and known material properties were used to investigate the concept for feasibility. Costs were estimated using estimated masses from a Pro/E model and the method described in Section 4.6 to estimate large castings.

In the integrated baseline design, a large rear opening is provided to allow service. In general, the stressed-skin nacelle has the advantage of reducing material costs compared to a standard bedplate design but has the disadvantage of restricted room to work. For example, should a hoist be desired, a larger nacelle casting would be needed to accommodate it. In this case the stressed-skin nacelle may be disadvantageous compared with the bedplate configuration.

6.2.2 Integrated Baseline Electrical Design and Component Estimates

Because all components except the generator are identical, the baseline drive train electrical system estimates were used for the integrated baseline. The integrated baseline uses a C-face mounted generator in place of the foot-mounted version used for the baseline design. As the change in cost for the different mounting is not expected to be significant, the baseline generator cost was used for the integrated baseline.

6.2.3 Integrated Baseline Ancillary Components

All ancillary components for the integrated baseline drive train, including the generator cooling system, parking brake, and coupling, are the same as those used in the baseline drive train.

6.3 Integrated Baseline Results

The following subsections summarize the COE estimate for the integrated baseline design along with the efficiency, energy production, component cost, and O&M estimates used for the COE estimate.

6.3.1 Integrated Baseline Efficiency and Gross Annual Energy Production

The efficiency and GAEP of the integrated baseline drive train were assumed to be the same as those of the baseline drive train. Baseline drive train efficiency and GAEP estimates are described in Sections 5.4.1 and 5.4.2.

6.3.2 Integrated Baseline Component Costs

Table 6-1 itemizes the component costs for the integrated baseline drive train. A comparison between these component costs and the corresponding costs for the baseline (bedplate version) drive train is given in Figure 6-4. The transmission system, support structure, and nacelle cover are less expensive for the integrated baseline design than for the baseline design; most of the other components have the same cost for both designs. The transmission system has reduced cost primarily because the short-coupled mainshaft and mainshaft bearings are less expensive than the corresponding baseline components. The structure costs are reduced because the structural nacelle design uses fewer materials than the bedplate and because the gearbox housing is used as part of the structure. The fiberglass nacelle cover is smaller and less expensive for the integrated baseline design.

Table 6-1. Integrated Baseline Drive Train Component Costs

Component	Cost, $
Transmission system	**120,000**
Gearbox components	120,000
Mainshaft	Included
Mainshaft support bearings and block	Included
Support structure (integrated nacelle)	**21,000**
External gearbox and generator cooling system	**3,000**
Brake system with hydraulics	**1,300**
Coupling (generator to gearbox)	**2,100**
Nacelle cover	**9,000**
Generator (WR induction)	**60,000**
Power electronics	**61,800**
0.95–0.95 substation VAR control	**NA**
Transformer	**23,000**
Cable	**18,000**
Switchgear	**12,000**
Other subsystems	**25,000**
Drive train assembly and test	**4,900**
Total	**361,000**

Note: All costs rounded.

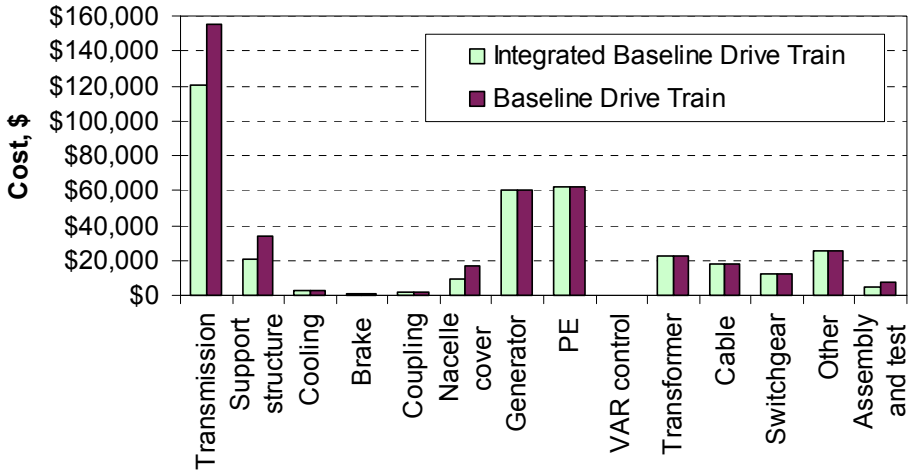

Figure 6-4. Integrated baseline and baseline component cost comparison

6.3.3 Integrated Baseline Operations and Maintenance Costs

Table 6-2 shows the three components of the integrated baseline O&M estimates along with LRC. The estimates are given both as cost per year and normalized by the annual energy capture of the turbine. Complete details of the integrated baseline drive train O&M model are included in Appendix J.

These estimates were made by modifying the baseline drive train estimates as follows:

- O&M related to the shaft and gearbox mounting was eliminated.
- Time to repair gearbox problems was increased because of the difficulty of removing the integrated gearbox.
- Additional equipment costs were included for gearbox repairs.

Table 6-2. Integrated Baseline O&M and LRC Estimates

	Integrated Baseline		Baseline
	$/yr	$/kWh	$/yr
Unscheduled maintenance	11,185	0.0017	12,103
Scheduled maintenance	5,791	0.0012	6,004
Operations	6,501	0.0013	6,501
Subtotal, O&M (excluding LRC)	**23,478**	**0.0043**	**24,608**
LRC (major overhauls)	**5,147**	**0.0009**	**5,124**
Total O&M and LRC	28,625	0.0052	29,732

The scheduled and unscheduled maintenance combined with LRC from Table 6-2 are compared to the corresponding baseline drive train estimates in Figure 6-5 on a component-by-component basis. Only drive train components are included because the contribution of other turbine components is the same for both designs. The integrated baseline transmission has a slightly lower estimate, but the estimates for all other components are the same.

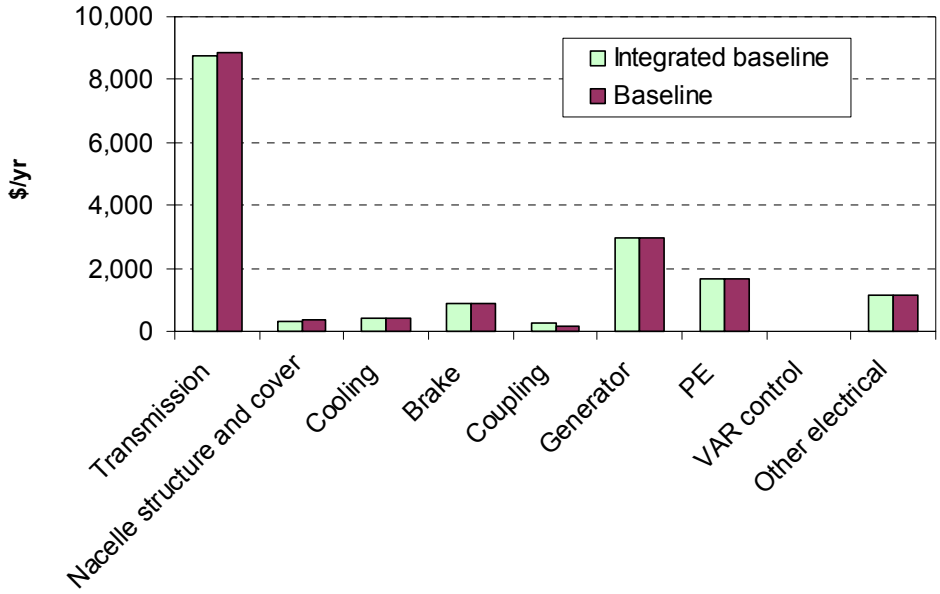

Figure 6-5. Scheduled and unscheduled maintenance costs and LRC, by component, compared to baseline

6.3.4 Integrated Baseline Cost of Energy Estimates

Table 6-3 presents the COE estimates for the integrated baseline design. The COE estimate for the integrated baseline design is 0.0339 $/kWh, approximately 5% less than the baseline COE of 0.0358 $/kWh. The lower COE for the integrated baseline may be attributed to the lower capital cost for this design. The annual energy capture is equal to the baseline design estimate.

Table 6-3. Integrated Baseline Drive Train COE Estimates

	Integrated Baseline Cost, $	% of COE	Baseline Cost, $
Capital Costs			
Turbine	**924,107**	**59.5**	1,001,491
Rotor	**248,000**	**16.0**	248,000
Drive train and nacelle	**360,736**	**23.2**	430,778
Yaw drive and bearing	**16,000**	**1.0**	16,000
Control, safety system	**7,000**	**0.5**	7,000
Tower	**184,000**	**11.8**	184,000
Turbine manufacturer's overhead and profit (30%, tower, rotor, and transformer excepted)	**108,371**	**7.0**	126,229
Balance of station	**358,000**	**23.0**	358,000
ICC	**1,282,107**	**82.5**	1,359,491
AEP			
Ideal annual energy output, kWh	5,479,000		5,479,000
Availability, fraction	0.95		0.95
Losses, fraction	0.07		0.07
Net AEP, kWh	**4,840,697**		4,840,697
Replacement costs, LRC, $/yr	**5,147**	**3.1**	5,124
FCR, fraction/yr	**0.106**		0.106
O&M, $/kWh	**0.0049**	**14.3**	0.0051
COE = O&M + ((FCRxICC)+LRC)/AEP	**0.0339**		0.0358

6.4 Integrated Baseline Scaling to 750 kW and 3 MW

No scaling estimates were made for the integrated baseline drive train.

7. Single PM Drive Train

The single PM drive train is an integrated design that uses a single-stage gearbox to drive a medium-speed PM generator. Detailed preliminary design estimates were made for both the mechanical and electrical design of this drive train. The estimated COE of this drive train is significantly lower than that of the baseline. This design was ultimately selected for detailed design and fabrication during Phase II of the study.

7.1 Single PM System Description

The 1.5-MW single PM generator drive train is illustrated in Figure 7-1, with a corresponding system diagram given in Figure 7-2. The 190-rpm, 72-pole, PM generator is driven by a single-stage gearbox with a ratio of approximately 9:1. The generator, gearbox, mainshaft, and mainshaft bearing are all integrated within a common housing. The size of the generator is minimized through integration of liquid cooling and because of its high diameter-to-length aspect ratio. The common generator-gearbox housing is supported by a tubular bedplate structure. The tower-top assemblies are enclosed with a nonstructural fiberglass nacelle cover.

The generator output is connected to the grid through a 1.5-MW PE control system used to implement variable-speed operation. To minimize the cost of the PE system, the SCR-SCR system described in Section 4.9.3.3 is used. This system uses passive SCR rectifiers at the generator side to create a DC current link. The energy stored in the decoupling current link is converted to 690 V AC by a line-commutated inverter. The pad mount transformer steps up the PE system voltage output to the 34.5-kV voltage of the wind farm power collection system. To filter the PE system harmonics, the wind farm transformer-power collection configuration system described in Section 4.9.3.4 and Appendix H is used. Recall that this system implements phase multiplication and harmonic suppression via groups of pad mount transformers, power factor correction capacitor banks, and substation VAR control components.

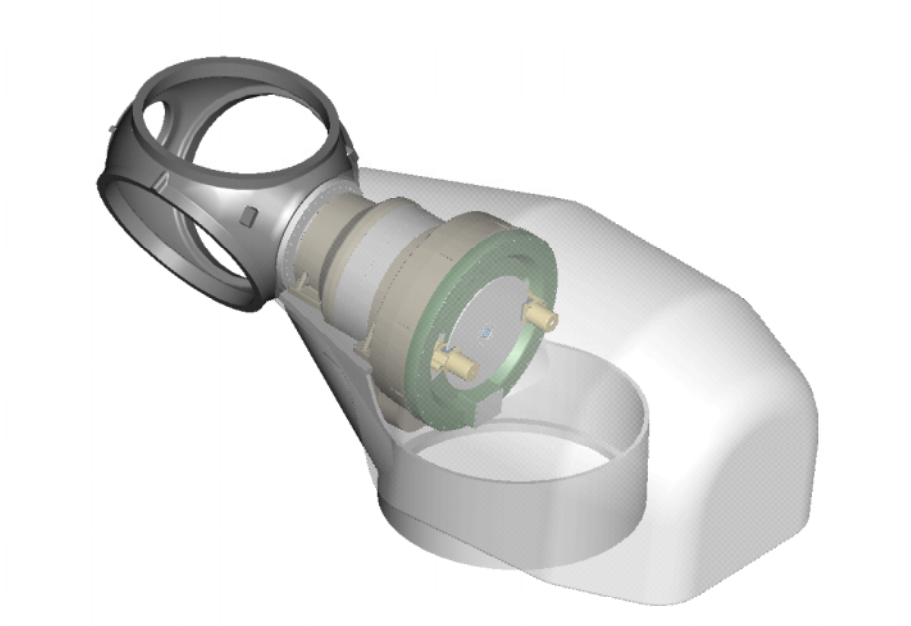

Figure 7-1. WindPACT single PM generator drive train

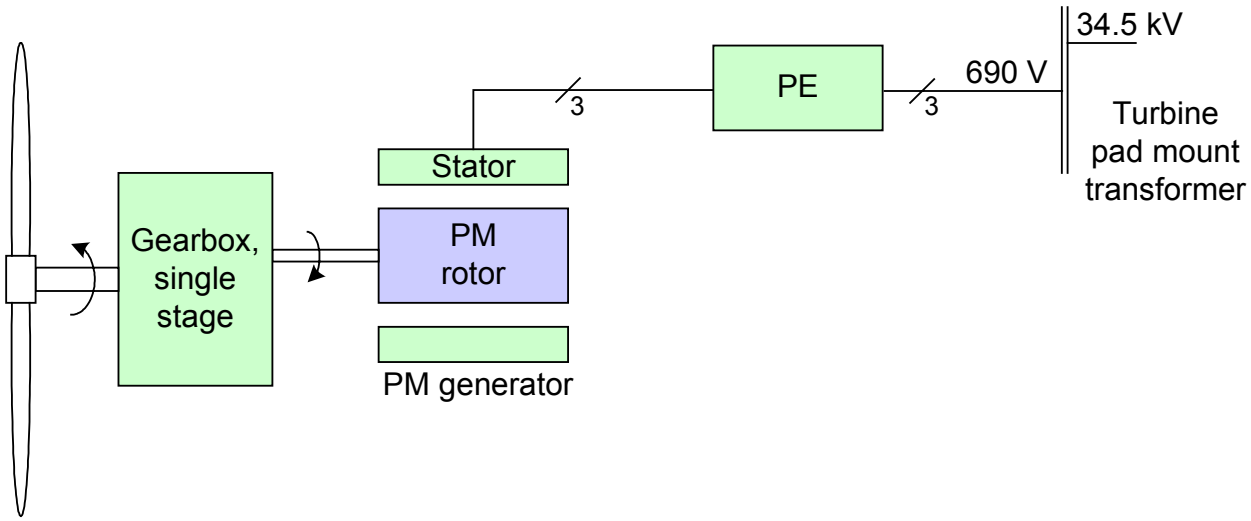

Figure 7-2. Single PM generator system diagram

7.2 Single PM Design Alternatives

A large number of design alternatives are available for the selected WindPACT single PM drive train design; many were considered during the study and some were investigated in detail. Some of the alternatives are described below along with the reasons they were not selected for the study.

- **Designs using structural nacelle covers:** Two designs using a tubular nacelle structure were initially investigated for the study. The first design, shown in Figure 7-3, uses the gearbox and generator housing as part of the structural load path that support the turbine rotor, in addition to using a tubular, cast iron structural nacelle cover. This design has the obvious advantage of minimizing the material in the structure and eliminating the fiberglass nacelle cover. The disadvantages of the design are (1) the difficulty of accessing or removing the gearbox for maintenance purposes, (2) the lack of working space in the nacelle for maintenance purposes, and (3) the need to design the gearbox and generator housing to minimize deformation resulting from structural loads. Cost estimates for this design were not significantly lower than the selected design shown in Figure 7-1.

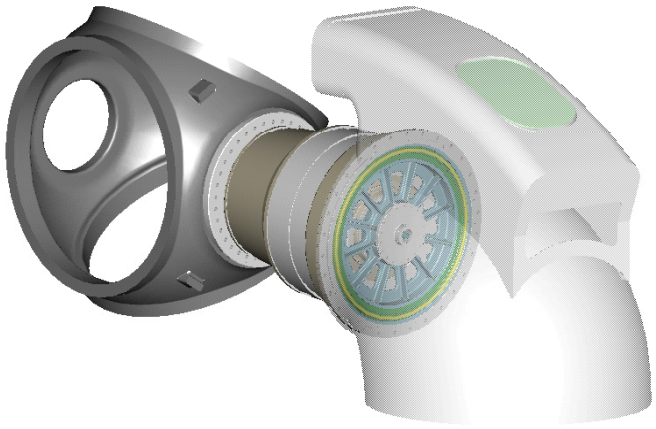

Figure 7-3. Single PM design with structural gearbox and generator housings

Figure 7-4 illustrates the second design, which uses a tubular, structural nacelle tower. This design does not use the gearbox or generator housings to carry the structural loads, but does use a tubular nacelle structure to eliminate the need for a separate nacelle cover. The disadvantage of this design is the lack of working space in the nacelle for maintenance purposes. Removal and replacement or on-site repair of the generator or gearbox would be difficult with this design. The cost estimates for this design were comparable to those for the selected design (Figure 7-1).

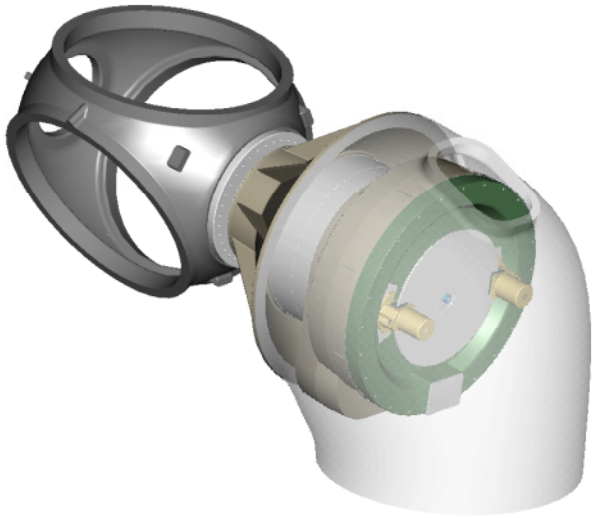

Figure 7-4. Single PM design with structural nacelle cover

- **Designs using a paired helical planetary gearbox:** Because small-diameter gearboxes were initially expected to be advantageous, the paired helical planetary gearbox shown in Figure 7-5 was investigated early in the study for use in the single PM drive train. This design uses dual sets of planetary gears to reduce the gearbox diameter. The dual gear sets increase the gear count, so gearboxes using this design cost more than conventional planetary designs. The most cost-effective single PM generator was ultimately determined to have a relatively large diameter, and to package best with similar diameter, conventional planetary gearboxes. The paired-helical design, then, showed no advantage for this application. The paired helical planetary design is covered by several patents held by Harrier Technologies, Inc., of Greenwich, Connecticut (Morrow 2001).

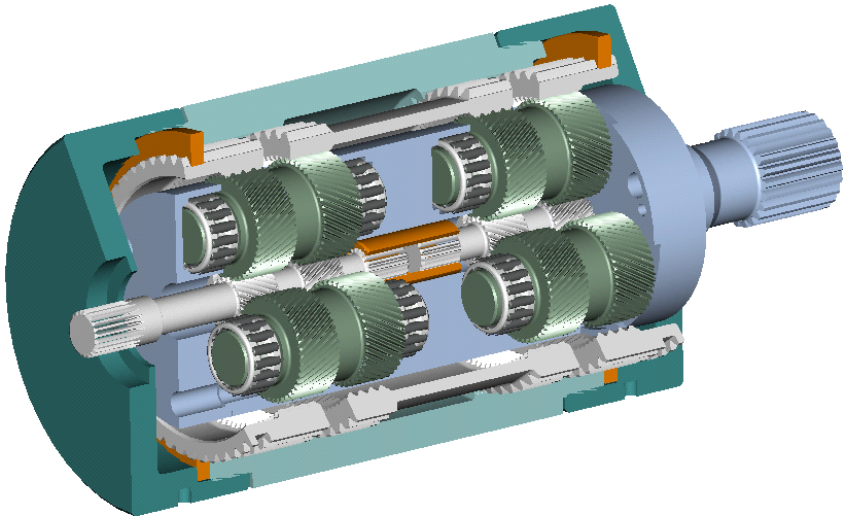

Figure 7-5. Paired helical planetary gearbox

- **Modular, bedplate designs without close-coupled mainshaft:** A conventional, modular design similar to the baseline design could be used. However, this approach was not investigated because the integrated approaches were expected to reduce the total component costs. These expectations were based on cost comparisons between the baseline and integrated baseline design.

- **Induction generators:** Induction generators were not considered for medium-speed designs because a large pole number is required. The efficiency and power factor of induction generators decreases in inverse proportion to the pole number because the magnetization current increases (Hefferman et al. 1996).

- **Electrically excited synchronous generators:** Early in the study, medium-speed, wound-field synchronous generators were determined to be less cost-effective than PM synchronous generators. For this reason, as described in Section 4.8.5, these generators were not investigated in detail.

- **Air-cooled generators:** Early in the study, Kaman investigated air-cooled medium-speed PM generators. Because they were found to be less cost-effective than liquid-cooled generators, this generator class was not selected for further design estimates, as described in Section 4.8.5.

- **Alternate PE systems:** The IGBT-IGBT and diode-IGBT PE systems described in Sections 4.9.3.1 and 4.9.3.2 were initially considered but were not selected based on the cost trade-offs described in Section 4.10.

7.3 Single PM Component Designs

Single PM component costs are dependent on the choice of gearbox ratio and generator diameter. Higher gearbox ratios increase the generator speed, decreasing the size and cost of the generator. However, higher gearbox ratios increase the gearbox size and cost. Larger generator diameters decrease the necessary generator length and active material cost, but drive up the structural costs to allow room for the larger housing. To analyze this design, preliminary estimates were made for a system using an 8:1 ratio gearbox that drives a 164-rpm, 2.3-m diameter generator. PEI developed a complete Pro/E model of this design, including a preliminary gearbox design. Kaman developed a preliminary generator design for this system. Using the Pro/E model, Milwaukee Gear estimated the cost to build the gearbox. The costs of other components were estimated from Pro/E mass and size calculations. Parameterized spreadsheets were then adapted from the base design to estimate component sizes, masses, and costs for other system diameters.

Using these spreadsheet tools, the minimum-cost single PM system was determined to have a 9.3:1 ratio gearbox and a 190-rpm, 2.0-m diameter generator. The Pro/E model was updated for this configuration, and the original spreadsheets were updated where they were inconsistent with the updated model.

The component designs applicable to the selected optimum design, a 9.3:1 gear ratio and 2.0-m diameter generator, are described in Sections 7.3.1 through 7.3.3. Section 7.3.4 gives the estimates for the selected design with other gear ratios and generator diameters. Associated spreadsheets are presented in Appendix C.

7.3.1 Mechanical Design

Figure 7-6 illustrates the mechanical design for the selected single PM system. A short mainshaft is supported by close-coupled, tapered roller bearings mounted in a housing that is common to both the gearbox and generator. The bearings share an oil lubrication system with the gearbox. The mainshaft drives the carrier of the planetary gearbox, which uses double-helical gears to minimize noise and eliminate the need for thrust bearings. The sun gear drives the shaft of the generator. The generator is a 72-pole, salient-pole, liquid-cooled PM generator. The generator bearings share a common oil lubrication system with the gearbox. The generator has a sealed rear cover for IP54 environmental protection. The parking brake disc is mounted to the generator shaft external to the rear cover.

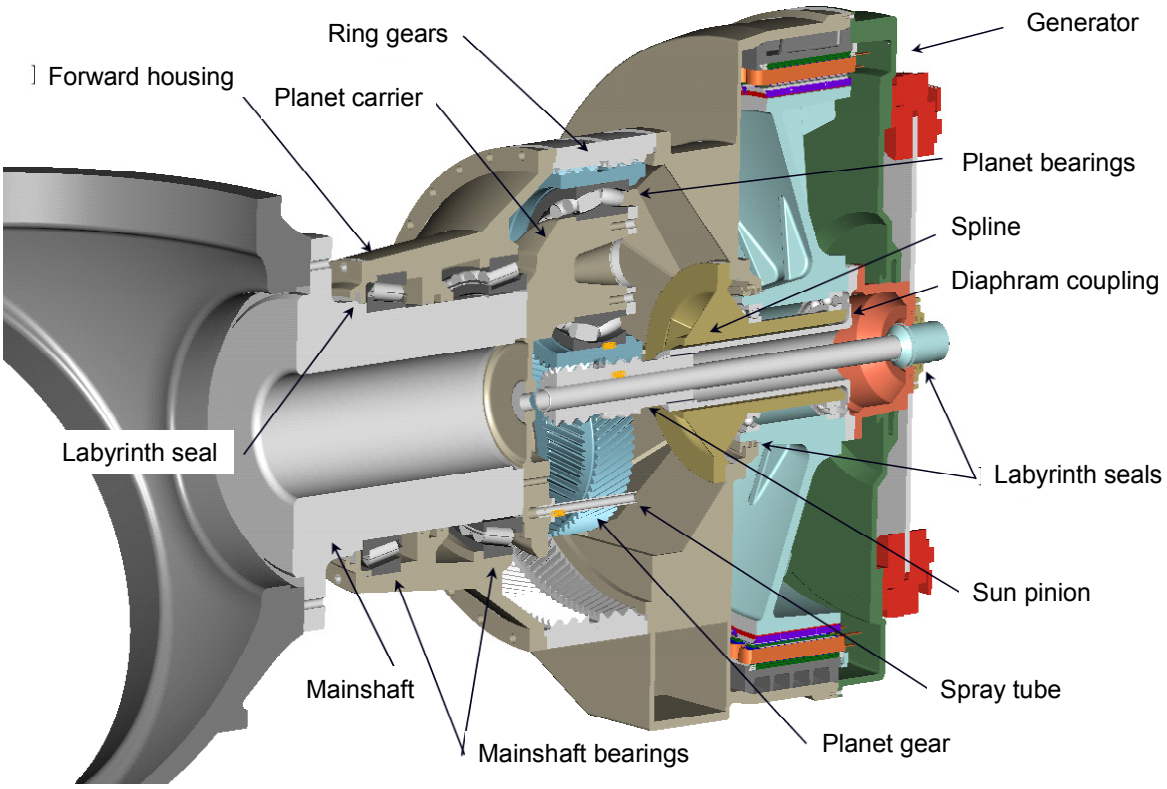

Figure 7-6. Single PM mechanical design

A complete Pro/E solid model was developed for this design. The weights of major components, such as the mainshaft, forward support housing, rear gear case, bedplate, carrier, and all the gears were accurately determined in the Pro/E solid model. Where specific quotes were not used, these weights were used to estimate component costs. The design and associated cost estimates for each of the mechanical components are described in the following subsections.

7.3.1.1 Mainshaft and Bearings

The internal construction is shown in Figure 7-7. Note the integral mainshaft and the use of separated tapered roller mainshaft bearings. These bearings are optimally suited for combined thrust and radial loads. By spreading the bearings apart, the large moments are correspondingly reduced. This permits the use of smaller diameter bearings compared to the case where the bearing separation is reduced, such as in back-to-back mounting. Smaller diameter bearings are preferred because (1) they are low in cost, with numerous suppliers; (2) they can be included in forced oil systems, which makes them easy to lubricate; and (3) they can use reliable labyrinth seals.

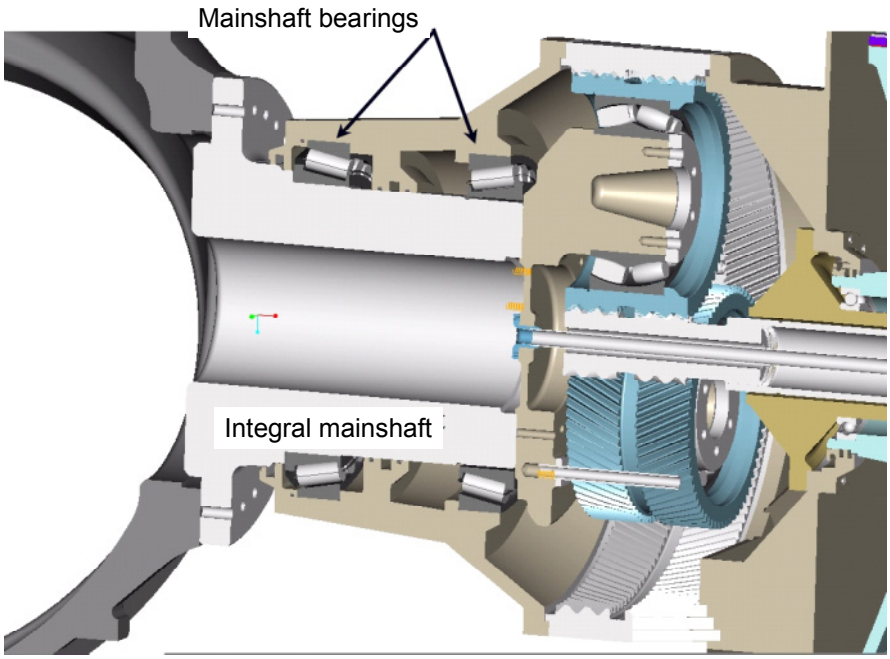

Figure 7-7. Single PM mainshaft and bearings

GEC completed an ADAMS™ computer model and analysis to produce a bearing load matrix suitable for analysis and design by specialists at the Timken Company. This analysis confirmed the suitability of the tapered roller bearing arrangement used in this design. The selected bearings are near optimal for size and taper angle, and are part of a standard engineered and tooled product. Timkin provided the estimated selling prices of these bearings for the study.

The mainshaft is a machined casting. Cost estimates were made based on mass estimates from the Pro/E solid model and the casting and machining costs per unit mass described in Section 4.6. The estimates are included in Appendix C.

7.3.1.2 Gearbox

Figures 7-6 and 7-7 show the single PM gearbox, which consists of a single stage of double-helical gears, arranged in a planetary configuration. The gearbox ratio is 9.16:1.

Because of the large ratio, the planets are large as well, which allows a single spherical planet bearing to carry the applied load. The bearing is conservatively rated, with an L10 life (life based on 90% survival reliability) of greater than 175,000 hours. The single spherical bearing design allows the planet axis to adjust itself to equalize tooth loads even when the carrier is deflected. The significant advantages of this configuration are reported in Jens Fisker (2001). The sun pinion is fully floating and decoupled from the output by a tubular torque-transmitting member.

The tubular torque-transmitting member (torque tube) acts as a diaphragm coupling and as a torsionally soft spring. This member incorporates a shear section, protecting the gearing from loads that might yield the teeth. The yield capacity of the gears is approximately seven times the rated torque. The torque tube will be designed at 4.5 times rated torque, which results in a reserve of approximately 155% relative to the gear teeth yield. The torque tube will decouple the sun pinion and allow positional displacement of the sun pinion spline axis. Figure 7-8 depicts the spring rate.

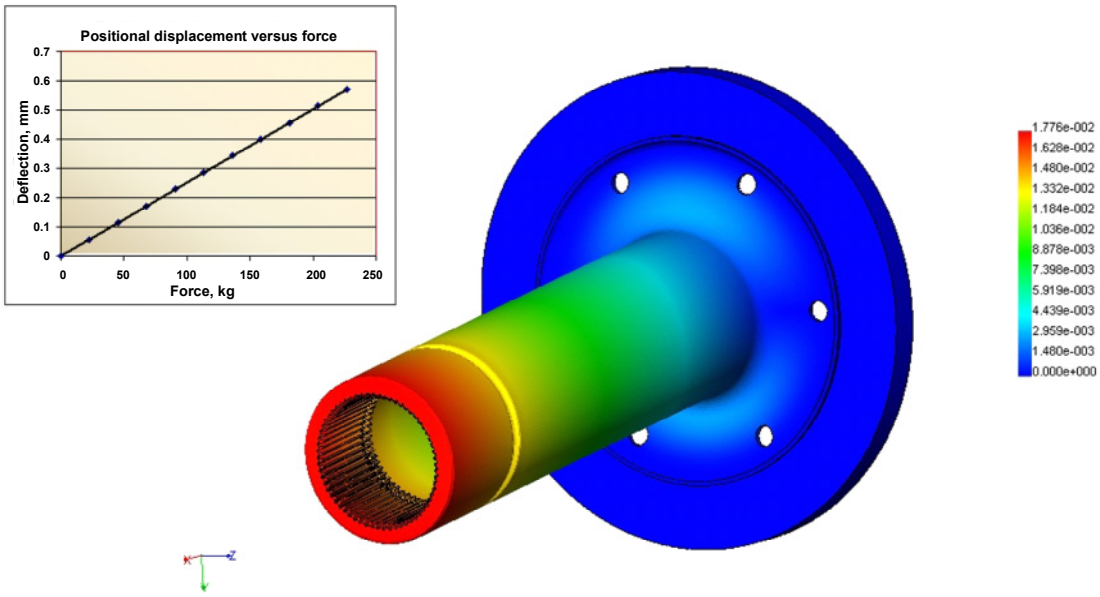

Figure 7-8. Force versus displacement of spline on torque tube

The torque tube flexes in the diaphragm section, which is designed for infinite life by maintaining fatigue stresses below the endurance limit.

The torque tube can be removed from the rear of the machine. The shear notch is positioned so that the parted torque tube will not enter the transmission, and debris is collected for removal during torque tube replacement. Shearing of the torque tube is not expected during normal operation, including most generator or control system shorts.

The generator is integrated to the gearbox, with the stator preassembled to a wet jacket and the rotor mounted to a hollow stub shaft attached to the back wall of the gearbox.

Gear mesh velocity is only 2.76 m/s (350 ft/min), an advantageously low value for precision gearing. Additionally, the double-helical system has axial overlap ratio values greater than 4.0. As one result, this design achieves very low noise levels without requiring vibrational isolation of the gearbox from its bedplate.

All of the internal rotating components are pressure-lubricated, including the mainshaft bearings and the generator bearings. This fact addresses the lubrication and sealing problems associated with grease-lubricated bearings in more conventional architectures. The pressure lubrication includes filtration and cooling to meet the requirements of the AGMA/AWEA 6006-Axx standard for wind turbine gearboxes.

The gears run in an essentially dry-sump mode, reducing churning losses. For start-up and safety, there is a small lubricant pool at the bottom of the ring gears, just enough to dip the planet bearings. The pressurized lubricant is fed through a rotating manifold to the rotating planet carrier, allowing continuous spray lubrication of the planets, the sun tooth meshes, and the planet bearings.

Seals at the rotor mainshaft and between the gearbox and generator are reliable labyrinth type, with dirt-exclusion V-rings.

Milwaukee Gear used the method described in Section 4.6 to estimate the cost of the single PM gearbox. Appendix D gives the BOM and the selling price estimate for this gearbox.

7.3.1.3 Generator Mechanicals

Figure 7-9 illustrates the mechanical design of the generator. The generator stator and rotor are subassemblies that easily mount and dismount for service. The stator consists of an iron ring with its outside exposed to the cooling medium. The inside of the ring holds the pole pieces to which coils are attached. The stator subassembly is held round and concentric with steep-taper location surfaces, each containing O-rings to seal the coolant.

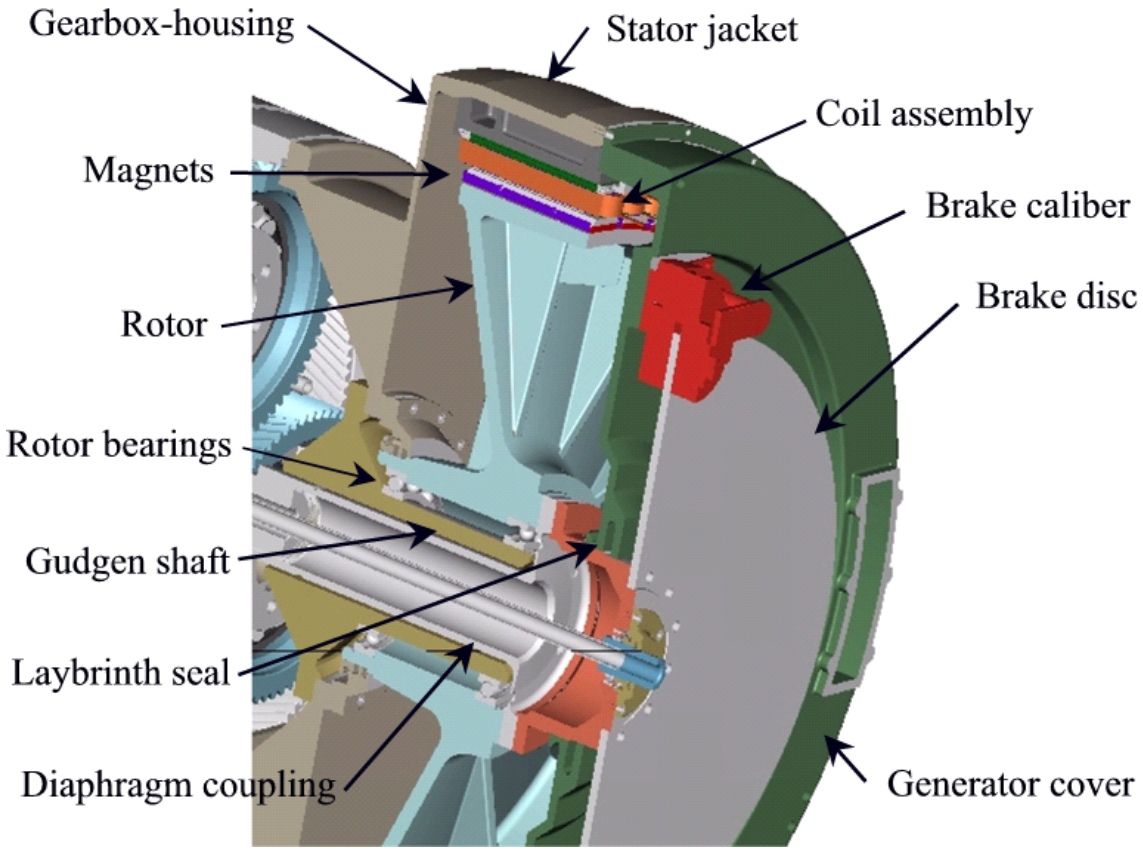

Figure 7-9. Single PM generator

The rotor is directly mounted to a gudgeon shaft through ball bearings that receive cooled and filtered oil from the pressure lubrication system. After passing through the bearings, the oil returns by gravity to the sump.

The generator is fitted with an iron cover that creates an IP54 rated enclosure and provides support for the parking brakes.

The generator mechanicals are primarily fabricated of machined castings with some purchased components. The cost estimates found in Appendix C were based on the estimated masses determined from the Pro/E solid model and on the cost per unit weight for castings and machining described in Section 4.6. Estimates for the purchased components were based on quoted prices for the particular component, or in some cases, on estimates for similar components used in the baseline design.

7.3.1.4 Support Structure

The mainshaft is integrated with the gearbox. As a consequence, the gearbox housing is a structural member. It is a ductile iron casting. Front and rear sections have integral feet that are bolted to the bedplate. The bedplate is a relatively simple design, with provisions for interfacing to the yaw bearing and yaw drives, and for attachment to the integrated drive train. FEA was used to obtain an optimized, long-life design of the bedplate, and to determine its mass. Figure 7-10 gives an example of this analysis.

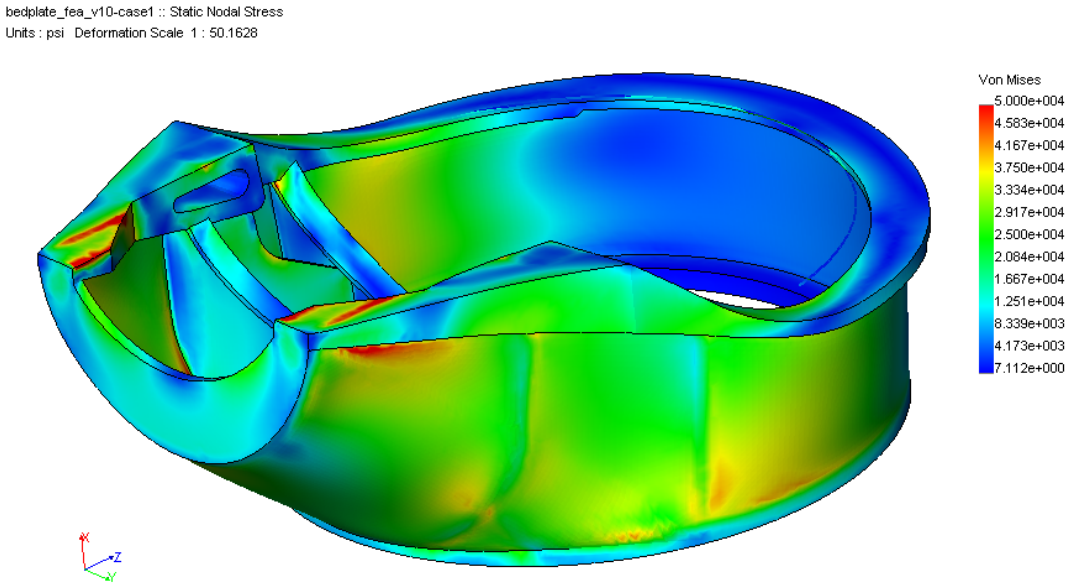

Figure 7-10. FEA of the single PM bedplate

The cost of the support structure was estimated using the mass calculated from the Pro/E solid model and applying the unit mass per cost for castings to the calculated mass, as described in Section 4.6.3. These estimates are included in Appendix C.

7.3.2 Electrical

Figure 7-11 is a simplified diagram of the single PM electrical system, including the associated wind farm system components. Appendix I contains a detailed one-line diagram of the turbine electrical system. The generator is a 1500-kW, 72-pole permanent magnet synchronous generator with an output voltage of approximately 600 V rms line to line at rated speed and load. The generator output is connected to an SCR rectifier-SCR inverter PE system that converts the variable-frequency, variable-voltage AC generator output to 690-V, 60-Hz AC power. The operation of the SCR-SCR converter is described in Section 4.9.3.

A contactor at the generator side of the PE system disconnects the generator when the system is shut down and fuses open in the case of a PE system failure. A contactor at the line side of the PE system is opened when the system is shut down. A circuit breaker protects against PE system failures and also acts as a manual disconnect. The 690-V PE system output is stepped up to the 34.5-kV wind farm collection system voltage by a pad mount transformer.

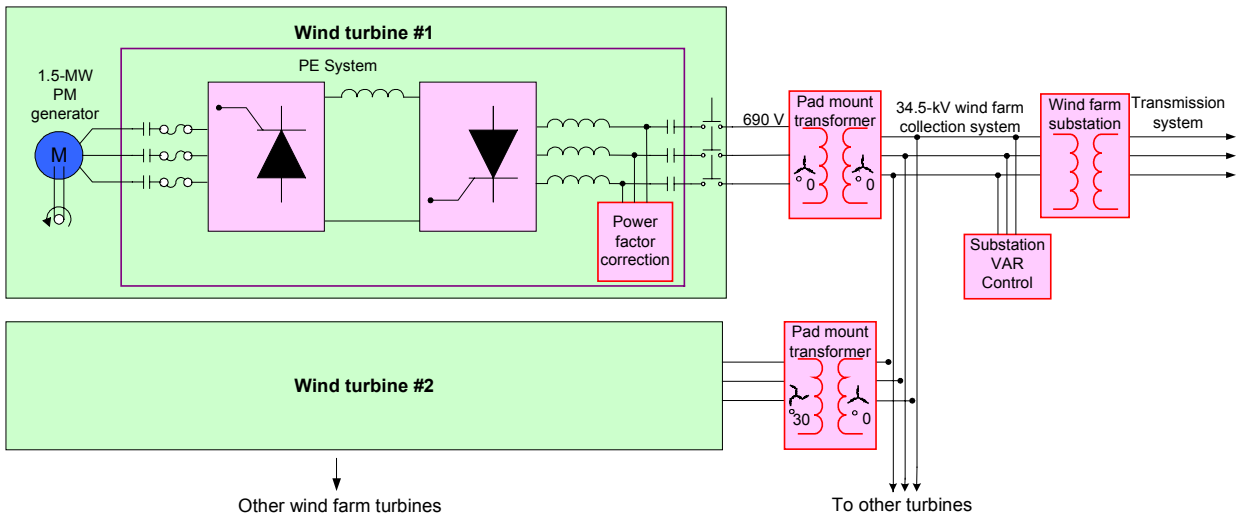

Figure 7-11. Single PM electrical system

Because the output of the SCR-SCR PE system does not have sinusoidal currents, it has high levels of current harmonics. In addition, the power factor is less than unity and changes with the DC bus voltage and therefore with generator and turbine rotor speed. To correct these power quality problems, a special configuration of turbine pad mount transformers, power factor correction, and VAR control in the wind farm collection system has been designed. This system provides power quality meeting IEEE 519 with 0.95-0.95 power factor control at the output of the wind farm substation.

This distributed harmonic filtering and suppression system is described in more detail in Section 4.9.3.4 and Appendix H. Two different types of pad mount transformers are used alternately throughout the wind farm to provide 12-pulse multiplication, which cancels the lower order current harmonics in the collection system. Switched capacitors at each turbine partially correct the wind farm power factor and provide some filtering of the current harmonics. A VAR control system included at the substation supplies the balance of the required power factor correction.

Descriptions and cost estimates of the major electrical components are given in the subsections that follow. Most of the wind farm collection system costs are included as part of the balance-of-station costs and not estimated separately. Costs of the pad mount transformer, power factor correction capacitors, and VAR control system are itemized separately because these components are unique to this electrical design.

In addition to the electrical system described above, the single PM design was analyzed with two alternative electrical systems based on the IGBT-IGBT and diode-IGBT PE designs described in Sections 4.9.3.1 and 4.9.3.2. Drive train system estimates that compare the economics of those two systems to those of the selected SCR-SCR based system are described in Section 4.10.

7.3.2.1 Generator Active Magnetics

PEI did the mechanical design of the generator and made the associated cost estimates, which are described in Section 7.3.1.3. Kaman did the estimates for the generator active magnetic components, as well as a preliminary design of the active magnetics for a 160-rpm, 2.3-m diameter, liquid-cooled, salient-pole generator. This generator design is optimized for interface with passive-rectified PE systems such as the selected SCR-SCR converter. A detailed description of this design and the associated cost estimates are included in Section 4.8 and Appendix E. This design was later scaled to the selected 190-rpm, 2.0-m

diameter size with the unit-pole scaling technique described in Section 4.8.6. The scaling estimates for this generator size are included in Appendix C.

7.3.2.2 Power Electronics

The SCR-SCR PE system design and cost estimates are described in Sections 4.9.3.3 and 4.10 and a BOM is included in Appendix F.

7.3.2.3 Switchgear

A one-line diagram for the electrical system of the single PM drive train using the SCR-SCR PE system is included in Appendix I, along with a BOM for the switchgear. The single most expensive item is the main 1600-A circuit breaker at the PE system output. The estimate also includes a fusible generator disconnect, which may be required for positive disconnection of the PM generator during maintenance. Unlike an induction generator, PM generators produce voltage when rotated, even when disconnected.

7.3.2.4 Cable

The cable estimates for the single PM drive train are described in Section 4.11.1 for PM generators using an SCR-SCR PE system. This estimate assumes the electrical system shown in the one-line diagram in Appendix I. The generator rectifier is placed near the generator, at the top of the tower. Cables carrying the rectified DC current run down the tower to the SCR line-commutated inverter located at the bottom of the tower. The entire PE system could also be located together, either at the top or bottom of the tower, but in this case, more cables will be needed in the tower, increasing the cable costs.

7.3.2.5 Pad Mount Transformer

The single PM pad mount transformer is estimated relative to the baseline pad mount transformer cost. The SCR-SCR system uses pairs of two different transformer types positioned throughout the wind farm, as described in Section 4.9.3.4. The average cost of these transformers is assumed to be 15% higher than the baseline transformer because (1) half the transformers require a nonstandard zig-zag winding, estimated to increase individual transformer cost by approximately 6% based on the quotations described in Section 4.11.2; (2) increased harmonic currents in the SCR-SCR transformers increase cooling requirements; and (3) production volumes for each transformer type will be 50% of the baseline production volumes.

7.3.2.6 VAR Control

VAR control cost estimates are described in Section 4.11.3.

7.3.3 Ancillary Components

7.3.3.1 Gearbox and Generator Cooling System

The estimated required heat capacity for the gearbox heat exchanger system is 21.7 hp. Cost estimates based on this capacity were calculated using the methods described in Section 4.6.9.

The generator cooling is based on the value of predicted efficiency at nominal rating, which is 97.4%. The capacity, then, is 52.3 hp. Cost estimates based on this capacity were calculated using the methods described in Section 4.6.10.

7.3.3.2 Brake System

A brake system, which can be seen in Figure 7-9, is applied to the generator rotor. The brake disc is attached to a hub that shares the bolted joint connecting the torque tube to the generator rotor. Because the gear ratio of the single PM system is 9.3:1 compared to about 80:1 for the baseline system, the brake torque—and therefore brake cost—is significantly higher. The method for calculating brake system cost is described in Section 4.6.8.

7.3.3.3 Assembly and Test

Because the gearbox comes from the manufacturer as an assembled unit, the gearbox assembly cost is included in the gearbox cost estimate. This figure includes the labor to complete the unit, including assembly of the integrated generator and the gearbox to its bedplate.

7.3.4 System Optimization for Gear Ratio and Generator Diameter

As described at the beginning of Section 7.3, the system was optimized to determine the gearbox ratio and generator diameter ultimately chosen for the single PM design.

The system optimization was necessary because generator cost is strongly affected by the air-gap velocity and radius. The most electrically efficient system uses large-diameter, short generator rotors at the highest rpm. Increasing the generator diameter drives the generator cost down, but the increased size adds cost to structural components. Increasing the gear ratio permits faster generator rpm, which reduces generator costs but increases gear costs.

A spreadsheet was used to compute these relationships based on parametric configuration and design rules sufficient to obtain air-gap areas, weights, and estimated costs.

7.3.4.1 Details of the Parametric Study

The parametric worksheet is included in Appendix C, along with a detailed description of the variables and calculations.

The parametric worksheet is based on a range of gearbox ratios. Because large planet gears are required to facilitate large bearings with adequate life, the minimum ratio considered was 7.8:1. The maximum ratio is determined by the point where the planets collide, and from experience, is limited to 10.6:1.

As the gear ratio increases, increasing generator speed reduces the mass and the cost of the active magnetic material. The gearbox cost, however, trends up because the gearbox mass increases as the square of diameter. The parametric worksheet calculates the gear ratio that is most cost-effective.

The ring gear diameter is computed based on the smallest gear set volume in which AGMA/AWEA 6006 aspect rules for gear face width to pitch diameter are met. The generator air-gap diameter is computed as a fraction of the ring gear diameter. This keeps the gearbox and generator diameter in proportion, allowing efficient use of a common housing for the gearbox and generator. The air-gap diameter is then rounded to the nearest 0.2 m. By iteration, the lowest system cost range has a ring gear diameter to air-gap diameter ratio of between 1.3 and 1.8.

With the ring gear diameter and air-gap diameter known, the size and mass of the required complementing components are calculated for each ratio. Totaling the cost yields the gear ratio of minimum system cost. As a check of the results, one design size was fully developed in Pro/E and the resulting masses were compared to those parametrically calculated.

7.3.4.2 Results of the Parametric Study

The parametric study results are shown in Figure 7-12.

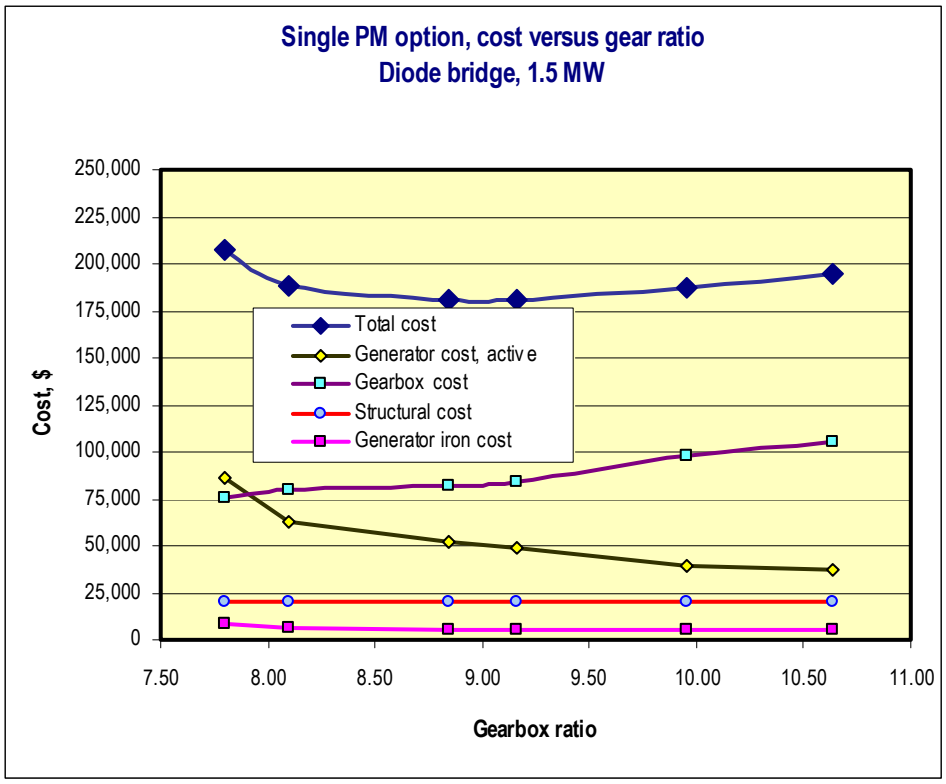

Figure 7-12. Results of single PM parametric study

7.4 Single PM Drive Train Results

The subsections that follow summarize all COE production estimates for the selected single PM generator drive train, as described in Sections 7.1 and 7.3. The COE of the single PM design using two alternative PE systems is presented in Section 4.10.

7.4.1 Single PM Efficiency

Figure 7-13 shows the drive train efficiency versus input power for the single PM design on a component-by-component basis. The total baseline drive train efficiency is shown for comparison. The efficiency of the single PM design is higher than that of the baseline design at all power levels, with the largest differences seen at low power. Most of this improvement can be attributed to increased efficiency in the generator and power electronics. Magnetization current in the baseline doubly fed induction generator causes a significant fixed loss at all power levels. This loss component does not exist in the single PM design's PM generator. The efficiency of the line-commutated SCR PE system is higher than that of the baseline IGBT PE system for two reasons: the SCRs have negligible switching losses and they do not need to supply magnetization current to the PM generator. In addition, with a reduced number of stages, the single PM gearbox has higher efficiency than the baseline gearbox.

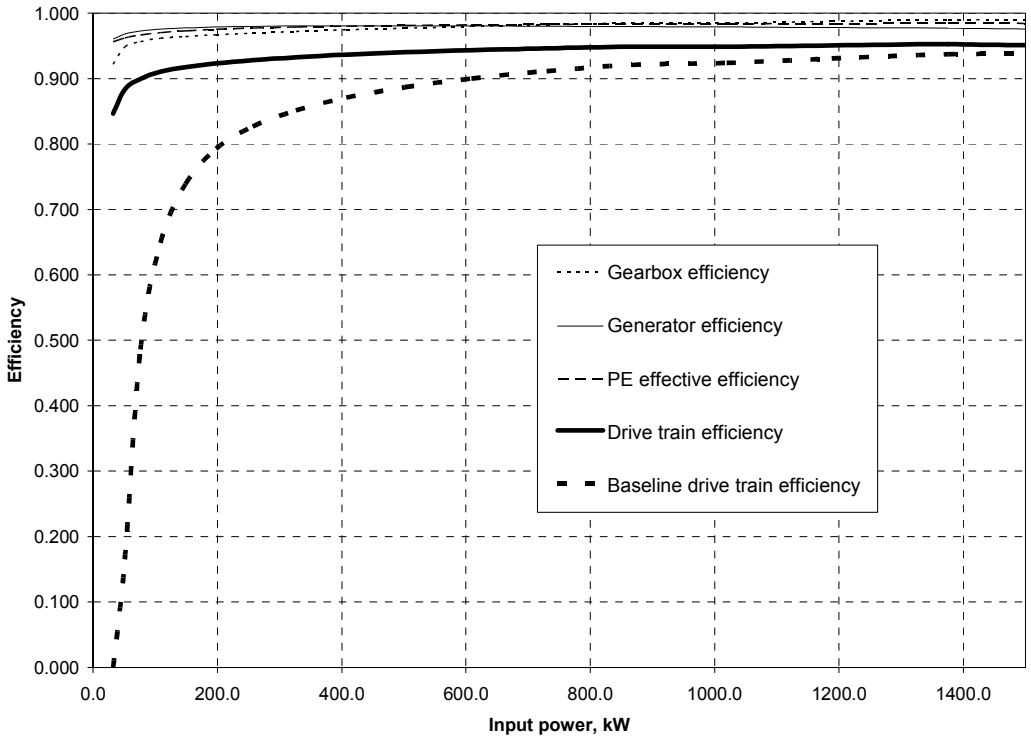

Figure 7-13. Single PM drive train efficiency by component

7.4.2 Single PM Gross Annual Energy Production

Table 7-1 presents the gross energy production estimate for the single PM design for each wind speed bin. As with all other systems, because drive train efficiency losses are recognized, the gross production value is referenced to the electrical output of the generator. All other losses are incorporated separately in the final COE analysis. The wind speed bins from 11.5 m/s to the cut-out speed of 27.5 m/s are aggregated in a single row. The energy productions for those wind speed bins are identical to those for the baseline turbine, shown in Table 5-3, with the rotor speed at rated and the output power regulated to 1.5 MW by the pitch system. The total GAEP from the single PM design is estimated at 5660 MWh. This value is approximately 3.3% higher than the estimated production of 5479 MWh for the baseline design. This is all the result of differences in the overall system efficiency.

Table 7-1. Single PM Drive Train GAEP

Wind Speed Bin Center, m/s	Rotor Speed, rpm	Rotor Power, kW	Drive Train Efficiency	Output Power, kW	# of Hours per Year	Energy Production	
						MWh	Fraction of Total, %
3.0	5.73	32.1	0.847	27.2	297.5	8	0.14
3.5	6.69	51.0	0.884	45.0	333.1	15	0.27
4.0	7.64	76.1	0.900	68.4	363.0	25	0.44
4.5	8.60	108.3	0.910	98.6	386.9	38	0.67
5.0	9.55	148.6	0.917	136.3	404.7	55	0.97
5.5	10.51	197.8	0.923	182.6	416.5	76	1.34
6.0	11.46	256.7	0.928	238.3	422.4	101	1.78
6.5	12.42	326.4	0.933	304.4	422.7	129	2.27
7.0	13.37	407.7	0.937	381.9	417.8	160	2.82
7.5	14.33	501.4	0.940	471.4	408.3	192	3.40
8.0	15.28	608.6	0.943	574.1	394.7	227	4.00
8.5	16.24	729.9	0.946	690.7	377.7	261	4.61
9.0	17.19	866.5	0.949	822.2	357.8	294	5.20
9.5	18.15	1019.1	0.949	966.9	335.9	325	5.74
10.0	19.10	1188.6	0.951	1130.1	312.4	353	6.24
10.5	20.06	1375.9	0.952	1310.4	288.0	377	6.67
11.0	20.47	1569.8	0.950	1490.7	263.2	392	6.93
11.5–27.5	20.47	1580.0	0.949	1500.0	1754.6	2632	46.5
					Total GAEP =	**5660**	**MWh**

The energy production values for the single PM and baseline designs are compared by wind speed bin in Figure 7-14. Above wind speeds of 11.0 m/s, the values are equal for both designs, so those bins are not shown. At 11.0 m/s and below, the single PM design produces more energy because the drive train efficiency is higher. Note the benefits of the single PM design at lower wind speeds.

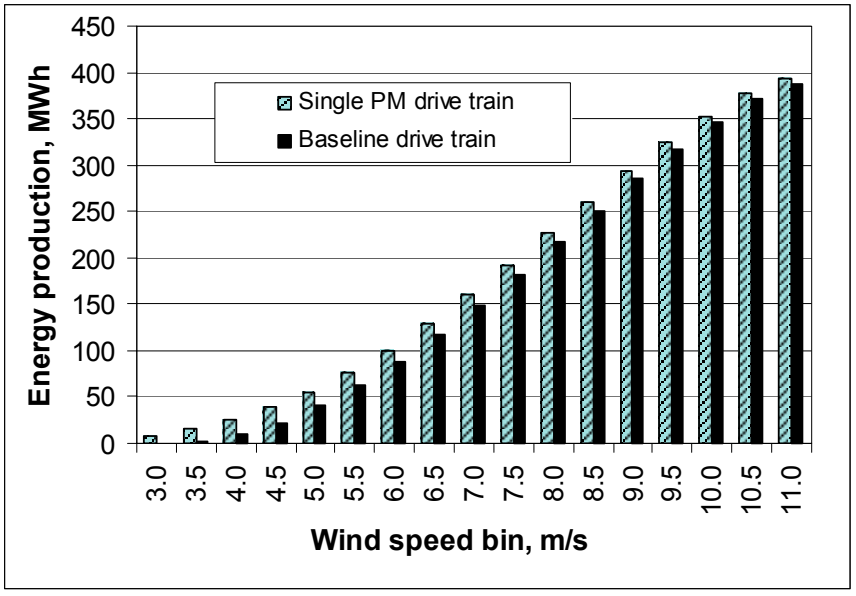

Figure 7-14. Single PM and baseline energy production by bin

7.4.3 Single PM Component Costs

Table 7-2 itemizes the component costs for the single PM drive train. Because this design uses an integrated gearbox and generator with a common housing, all generator structural components are included in the transmission system category. Only the generator active magnetic components are included in the generator category.

Table 7-2. Single PM Drive Train Component Costs

Component	Cost, $
Transmission system	**90,000**
Gearbox components	84,000
Mainshaft	included
Generator iron components	6,000
Mainshaft bearings	Included
Support structure (integrated nacelle)	**20,000**
Cooling system	**4,400**
Gearbox cooling	1,400
Generator cooling	3,100
Brake system with hydraulics	**3,200**
Coupling (generator to gearbox)	**NA**
Nacelle cover	**8,200**
Generator	**54,000**
Power electronics	**53,000**
0.95–0.95 substation VAR control	**12,000**
Transformer	**26,000**
Cable	**16,000**
Switchgear	**10,000**
Other subsystems	**25,000**
Drive train assembly and test	**5,500**
Total	**327,000**

Note: All costs rounded.

Figure 7-15 compares the component costs itemized in Table 7-2 to the baseline component costs. This design shows a significant cost benefit in the transmission system, support structure, and nacelle cover. The transmission system cost is reduced because only a single gearbox stage is necessary for the medium-speed generator. Furthermore, the integrated design with a close-coupled mainshaft reduces the mainshaft and mainshaft bearing costs. The support structure and nacelle cover costs also are reduced because this design is more compact than the baseline design.

The single PM generator costs include the active magnetic components only, with $6,000 of generator structure included in the transmission system category. Taking this into account, generator costs are comparable to the baseline estimates. The line-commutated SCR PE inverter costs are lower than those for the baseline doubly fed PE system. However, the SCR inverter requires that power factor correction and VAR control be added. As a result of all these factors, the cost of the entire PE and electrical systems are comparable for the single PM and baseline designs.

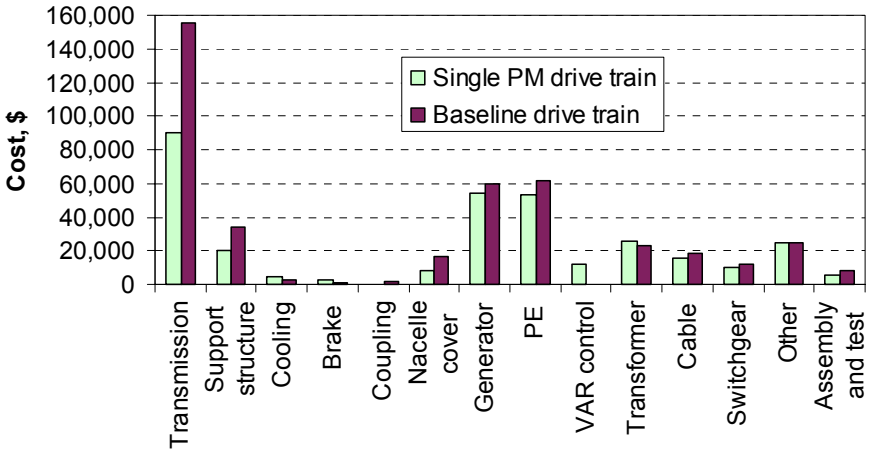

Figure 7-15. Single PM and baseline component cost comparison

7.4.4 Single PM Operations and Maintenance Costs

The three components of the baseline O&M estimates along with LRC are shown in Table 7-3, both as cost per year and normalized by the annual energy capture of the turbine. Unscheduled maintenance, as the largest component of O&M, is also larger than the LRC. Complete details of the single PM drive train O&M model are included in Appendix J.

These estimates were made by modifying the baseline drive train estimates as follows:

- All O&M related to the shaft, the coupling, and the gearbox mounting was deleted.
- Component replacement costs were updated with the single PM cost estimates.
- A gearbox failure rate of 66% of the baseline was used to account for fewer stages.
- A generator failure rate of 75% of baseline was used to account for higher expected PM generator reliability.
- Equipment and labor costs were increased for gearbox repair because removal and replacement is more difficult in the integrated single PM design.

Table 7-3. Single PM O&M and LRC Estimates

	Single PM		Baseline
	$/yr	$/kWh	$/yr
Unscheduled maintenance	8,768	0.0017	12,103
Scheduled maintenance	5,895	0.0012	6,004
Operations	6,501	0.0013	6,501
Subtotal, O&M (excluding LRC)	**21,165**	**0.0043**	**24,608**
LRC (major overhauls)	**4,792**	**0.0009**	**5,124**
Total O&M and LRC	25,956	0.0052	29,732

The scheduled and unscheduled maintenance costs, combined with the LRC from Table 7-3, are compared to the corresponding baseline drive train estimates in Figure 7-16 on a component-by-component basis. Only drive train components are included because the contribution of other turbine

components is the same for both designs. The contributions from the transmission system and generator are lower for the single PM design but contributions from the other components are similar.

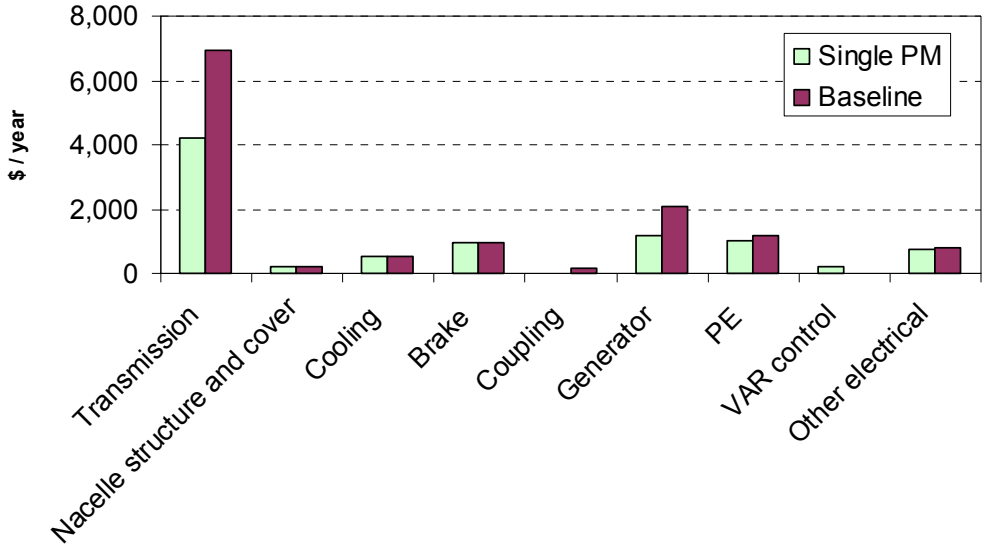

Figure 7-16. Scheduled and unscheduled maintenance costs and LRC compared to baseline by component

7.4.5 Single PM Cost of Energy Estimates

COE estimates for the single PM design are shown in Table 7-4. The COE estimate for this design is 0.0313 $/kWh, a reduction of approximately 13% relative to the 1.5-MW baseline estimate. There are three primary reasons for this COE benefit:

- Decreased drive train component costs, primarily because of reduced transmission system and support structure costs (see Figure 7-15)
- Increased energy capture, resulting from higher generator and PE system efficiency
- Reduced O&M costs and LRC, because of reduced maintenance time and lower component costs.

Table 7-4. Single PM Drive Train COE Estimates, Compared to Baseline

	Single PM		Baseline
	Cost, $	% of COE	Cost, $
Capital Costs			
Turbine	**876,236**	**59.2**	1,001,491
Rotor	**248,000**	**16.8**	248,000
Drive train and nacelle	**327,358**	**22.1**	430,778
Yaw drive and bearing	**16,000**	**1.1**	16,000
Control, safety system	**7,000**	**0.5**	7,000
Tower	**184,000**	**12.4**	184,000
Turbine manufacturer's overhead and profit (30%, tower, rotor, and transformer excepted)	**93,878**	**6.3**	126,229
Balance of station	**358,000**	**24.2**	358,000
ICC	**1,234,236**	**83.4**	1,359,491
AEP			
Ideal annual energy output, kWh	5,660,000		5,479,000
Availability, fraction	0.95		0.95
Losses, fraction	0.07		0.07
Net AEP, kWh	**5,000,610**		4,840,697
Replacement costs, LRC, $/yr	**4,792**	**3.1**	5,124
FCR, fraction/yr	**0.106**		0.106
O&M, $/kWh	**0.0042**	**13.5**	0.0051
COE = O&M + ((FCRxICC)+LRC)/AEP	**0.0313**		0.0358

7.5 Single PM Drive Train Scaling to 750 kW and 3 MW

Using similar techniques to those described in Section 7.3.4 and Appendix C to optimize the 1.5-MW single PM design, this drive train size and performance were extended to 750 kW and 3 MW output ratings. The PM generator estimates were scaled using the unit-pole scaling technique described in Section 4.8.6. The transmission system and support structure were scaled with the calculation methods described in Appendix C. The electrical system components, other than the generator, were scaled by power rating.

Table 7-5 summarizes the results of this scaling process. These results are compared graphically in Figure 7-17 in terms of the drive train COE. The drive train COE represents the portion of the turbine COE attributed to the drive train capital cost alone. Relative to the 1.5-MW, single-stage PM drive train, the 750-kW version is characterized by a slightly higher normalized capital cost (in dollars/kilowatt) and a higher COE. Again, relative to the 1.5-MW system, the 3-MW variation has a comparable, even slightly lower capital cost and COE. The entries in Table 7-5 give some insight into the reasons for these cost relationships. It appears that several major, costly structural and electrical subsystems diminish in normalized capital cost as the power rating increases. These include the support structure and generator.

Table 7-5. Single PM Drive Train Component Cost Scaling to 750 kW and 3 MW

	750 kW		1.5 MW		3 MW		Method
	Cost, $	Cost/ kW	Cost, $	Cost/kW	Cost, $	Cost/ kW	
Transmission system	53,379	71	98,551	66	214,036	71	
Gearbox components	*45,745*	*61*	*81,629*	*54*	*176,211*	*59*	PEI input
Mainshaft	*Included*		*Included*		*Included*		PEI input
Generator iron components	*7,634*	*10.2*	*16,922*	*11.3*	*37,825*	*12.6*	PEI input
Mainshaft bearings	*Included*		*Included*		*Included*		PEI input
Support structure	*22,024*	*29*	*26,018*	*17*	*37,252*	*12*	PEI input
Gearbox and generator cooling system	*1,616*	*2.2*	*3,231*	*2.2*	*6,462*	*2.2*	Power rating
Brake system with hydraulics	*6,000*	*8.0*	*2,925*	*2.0*	*15,000*	*5.0*	PEI input
Coupling	*NA*	*NA*	*NA*	*NA*	*NA*	*NA*	
Nacelle cover	*5,575*	*7*	*5,945*	*4*	*6,984*	*2.3*	PEI input
Generator	30,767	41	54,355	36	89,870	30	Unit-pole scaling
Power electronics	*26,560*	*35*	*53,119*	*35*	*106,238*	*35*	Power rating
0.95–0.95 substation VAR control	*5,779*	*8*	*11,557*	*8*	*23,114*	*8*	Power rating
Transformer	*12,938*	*17*	*25,875*	*17*	*51,750*	*17*	Power rating
Cable	*8,023*	*11*	*16,046*	*11*	*32,092*	*11*	Power rating
Switchgear	*5,233*	*7.0*	*10,465*	*7.0*	*20,930*	*7.0*	Power rating
Other subsystems	*12,500*	*17*	*25,000*	*17*	*50,000*	*17*	Power rating
Drive train assembly and test	*2,763*	*4*	*5,525*	*3.7*	*11,050*	*3.7*	PEI input
Drive train and nacelle total	**193,154**	**258**	**338,612**	**226**	**664,778**	**222**	

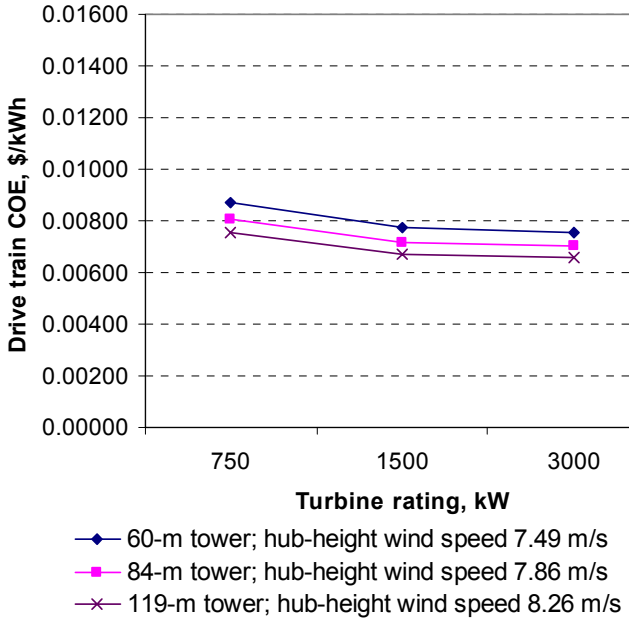

Figure 7-17. Single PM drive train COE scaling for different hub height wind speeds

8. Direct Drive Drive Train

The direct drive drive train uses a low-speed PM generator directly driven by the mainshaft. Several European manufacturers have built prototype or production turbines using similar configurations, and for that reason, detailed preliminary design estimates of this design were made during the study. However, these estimates show that the direct drive design has a higher COE than the baseline drive train because of the high cost of the low-speed generator.

8.1 Direct Drive System Description

Figure 8-1 illustrates the 1.5-MW direct drive drive train, and Figure 8-2 is the system diagram. A 20.5-rpm, 96-pole, 4-m diameter PM generator is directly driven by the turbine rotor. The generator size is minimized by incorporating liquid cooling and a high diameter-to-length aspect ratio.

The generator output is connected to the grid through a 1.5-MW, variable-speed PE system and a pad mount transformer. The entire electrical system for the direct drive design is identical to that for the single PM design and described in Section 7.

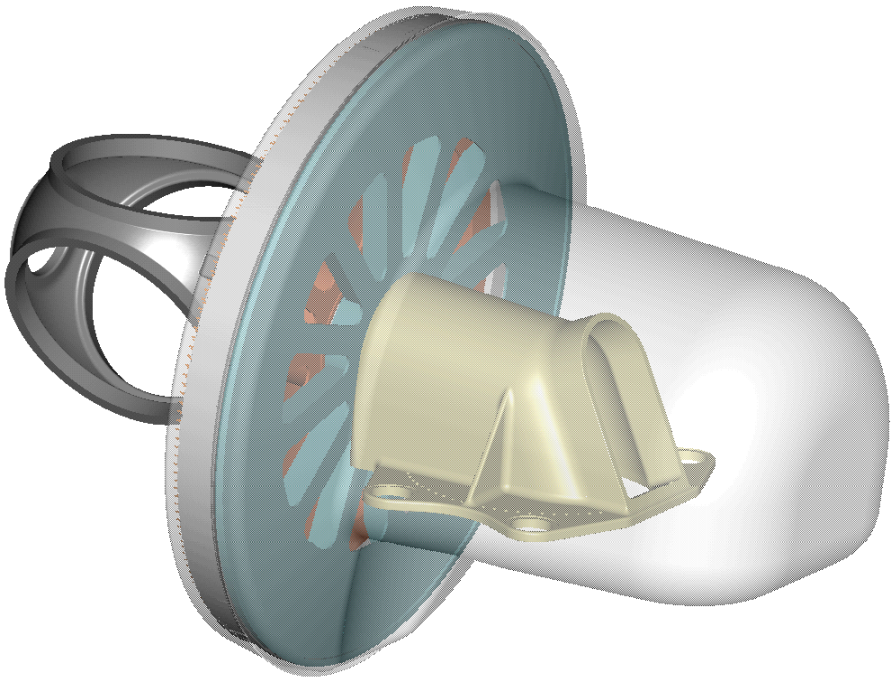

Figure 8-1. WindPACT direct drive drive train

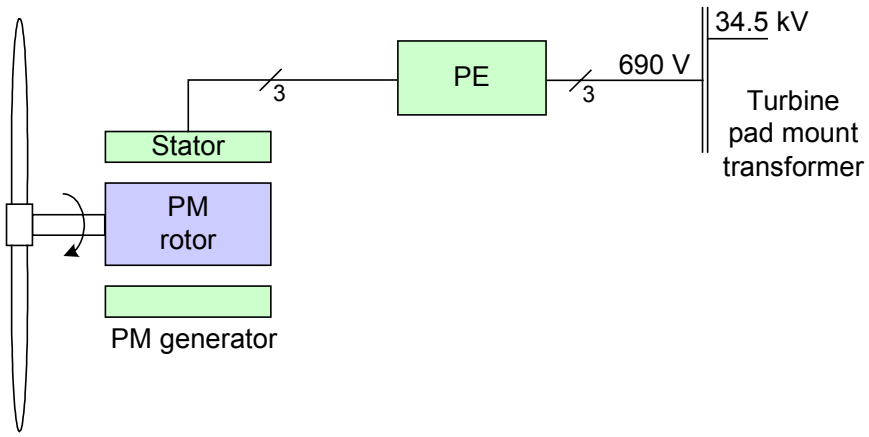

Figure 8-2. Direct drive system diagram

8.2 Direct Drive Design Alternatives

Several alternatives to the selected direct drive design are described here. They were briefly investigated early in the study as part of a rapid evaluation aimed at selecting a configuration that appeared to offer the most performance and economic potential. Some of the alternatives examined, along with the reasons that they were not selected for the study, are described below:

- **Designs using a long mainshaft:** Direct drive machines with a mainshaft extending from the rotor hub, across the tower top, and terminating on the opposite, downwind side with an overhung generator have been described. The advantage of this type of machine appears to be in the serviceability of the generator rotor. The rotor can easily be removed from the mainshaft as a single piece without disturbing other components. After an initial evaluation, this design was not developed further because of the higher costs of the long shaft and the structure required to transfer the torque across the tower top.

- **Designs using large-diameter bearings:** Large-diameter bearings allow novel designs for connecting the rotor hub to the tower support structure. The preliminary analysis indicated that a significant reduction in cost was not likely because of the high cost of the special large bearings required. Additionally, solving problems of lubrication and sealing of these large bearings would require significant development work. Because the benefits were not obvious and the risk was seen as relatively large, a conventional bearing arrangement was chosen.

- **Synchronous wound-field generators:** Medium-speed, wound-field synchronous generators were determined to be less cost-effective than PM synchronous generators early in the study, so they were not investigated further. Wound-field generators have lower efficiency resulting from losses in the field winding. Lower practical limits for the size of the field winding make pole pitches of less than about 100 mm impractical (Grauers 1996a, 1996b). PM excitation eliminates these problems. In the past, the cost of high-density permanent magnets was very high. However, the cost has recently declined significantly, making PM machines practical and cost-effective.

- **Air-cooled generators:** Kaman investigated air-cooled medium-speed generators and found them to be less cost-effective than liquid-cooled generators. The results of Kaman's investigations are described in the company's report, included in Appendix J. Air-cooled

generators are larger, require more material content, and increase the difficulty of removing heat from the nacelle enclosure relative to liquid-cooled generators.

- **Alternate PE systems:** The IGBT-IGBT and diode-IGBT PE systems described in Sections 4.9.3.1 and 4.9.3.2 were initially considered but were not selected, based on the economic comparison described in Section 4.10.

8.3 Direct Drive Component Designs

Direct drive component costs are dependent on the chosen generator diameter. Within limits, larger generator diameters decrease the necessary generator length and active magnetic material costs, but increase the structural costs. In addition, direct drive generators with diameters larger than 4.0 m require special methods for transport or must be designed as modules that can be broken down for shipping.

To analyze the direct drive PM system, PEI made preliminary estimates for a 5.275-m diameter system. Based on the active magnetic materials design Kaman supplied, PEI developed a Pro/E model. Using the unit-pole scaling method described in Section 4.8.6, generator estimates were made by scaling the Kaman 2.3-m, 160-rpm single PM generator design. Cost estimates for components were based on mass and size values from the Pro/E model together with material cost data from similar designs.

Parameterized spreadsheets were then developed from the base 5.275-m design to estimate component sizes, masses, and costs for other generator diameters using component mass ratios. These spreadsheets, presented in Appendix C, indicated that the minimum cost direct drive system would have a generator diameter of 5.5 m. Because of transportation considerations, this diameter was not considered practical. A 4-m diameter was ultimately chosen, and the spreadsheet cost estimates for that system diameter were used.

8.3.1 Mechanical Design

Figure 8-3 shows the mechanical design for the selected direct drive system. A tower-top structural housing, which provides a base for the yaw drives and the stationary mainshaft, attaches to the yaw bearing.

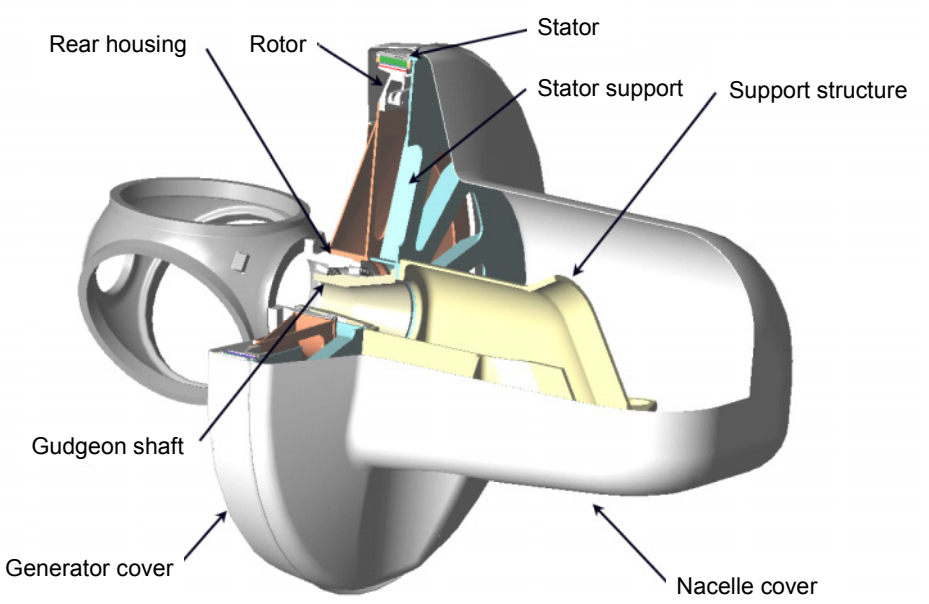

Figure 8-3. Direct drive mechanical design

Around the shaft, in an inverted arrangement, a torque tube is mounted on tapered roller bearings. This tube connects to the mainshaft on one side, and to the generator rotor on the other. The support structure is designed to permit the large-diameter rotor and stator discs to clear the tower. This lowers the generator's rotational axis relative to the tower top, reducing loads on the support structure.

A nacelle cover protects the rotor and stator. The front section rotates and overlays the rear, stationary section, which has a labyrinth seal to prevent water intrusion. The rear of the nacelle cover offers a protected work area and a location for electrical equipment.

8.3.1.1 Mainshaft and Bearings

Figure 8-4 shows the mainshaft and bearings, which are essentially an inverted version of the system developed for the single PM medium-speed design. The tapered roller bearings are engineered to meet the specified life. They are commercially available as a standard product. The connecting torque tube is made of ductile iron. Cost estimates for these components are included in Appendix C. The methods used are described in Sections 4.6.3 and 4.6.4 for large, machined castings and in Section 4.6.5 for bearings.

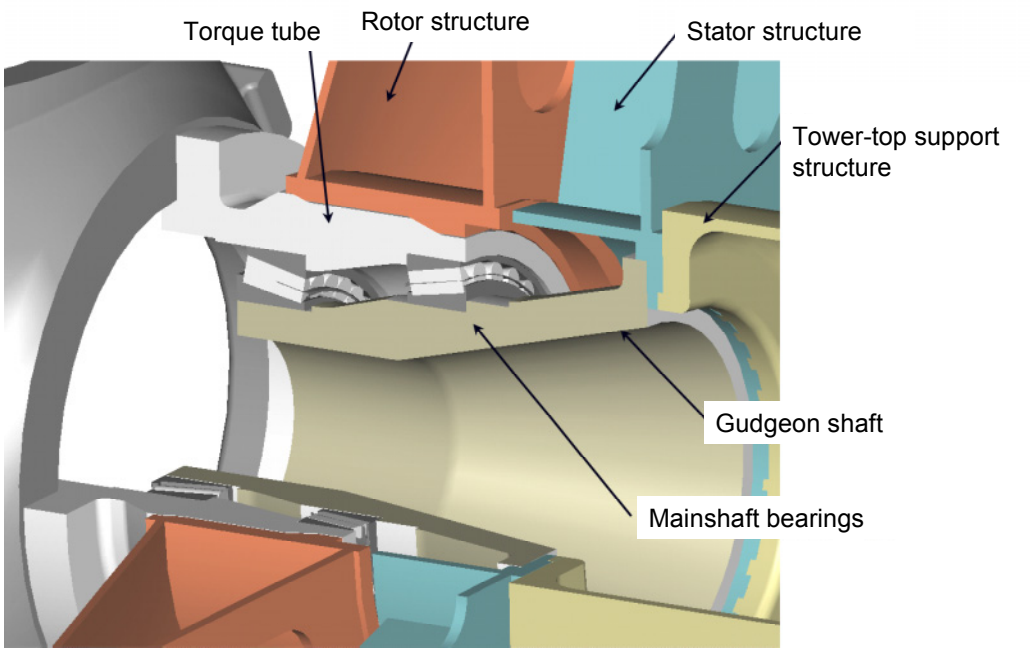

Figure 8-4. Section view of mainshaft area

8.3.1.2 Generator Mechanicals

The mechanical design of the direct drive generator, shown in Figure 8-5, consists of an air-cooled rotor connected to the torque tube. The stator, located outside the rotor, consists of a support structure attached to the tower-top housing, which has machined steep-tapered conical seats. The active magnetics—the stator unit-pole assemblies—are fastened to a steel or iron ring that has matching steep tapered conical surfaces. Channels in the outside of this ring are coolant fluid passages. They are sealed by O-rings in the conical fits. This design allows separate stator ring assembly or maintenance service, or both, without removal of the main structural member.

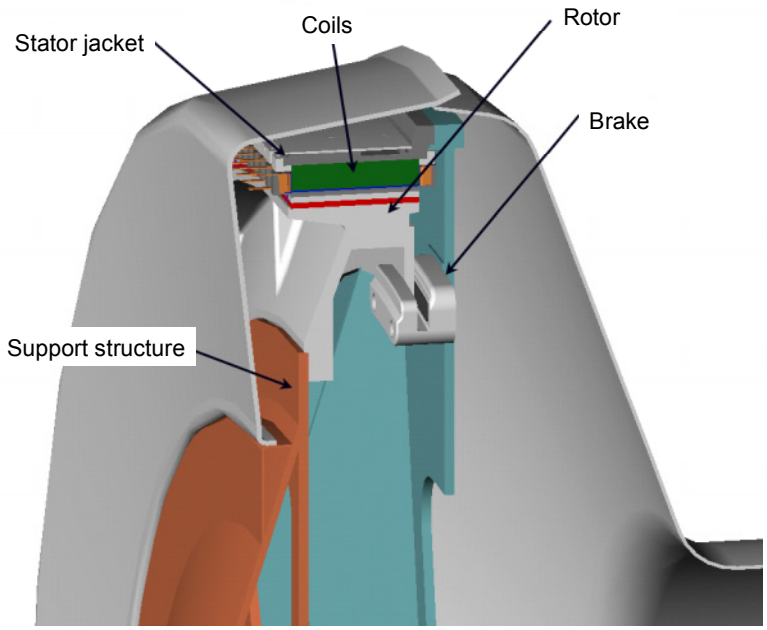

Figure 8-5. Direct drive generator mechanicals

The fiberglass shroud forms a labyrinth seal that allows some air exchange but prevents direct contact of stator windings to cooling air.

The weight of the generator components was calculated for a variety of air-gap diameters, and Appendix C includes the calculations. The required mass of the active magnetic material, the rotor and stator masses, and the variable portion of the support structure are shown for each air-gap diameter. Costs are calculated using the appropriate unit/mass multiplier for castings and machining described in Sections 4.6.3 and 4.6.4. The rotor and the stator ring, as described above, are included in the generator cost. The remaining structure and the torque tube are included in the support structure cost.

8.3.1.3 Support Structure

The support structure consists of a tower-top cast ductile housing that includes the interface for yaw drives and yaw bearings. A second interface receives the nonrotating bearing support member (the gudgeon shaft) that receives the rotor bearings. Both of these members were held constant in size for a variety of air-gap diameters. Pro/E models were used to determine the mass properties, which were used to calculate cost with the appropriate unit/mass multiplier for castings and machining described in Sections 4.6.3 and 4.6.4.

8.3.2 Electrical System

Aside from the generator itself, the direct drive electrical system is identical to that described in Section 7.3.2 for the single PM generator. The single PM component costs for the SCR-SCR PE system, switchgear, cable, pad mount transformer, power factor correction, and VAR control, described in Sections 7.3.2.2 through 7.3.2.6, were all used for the direct drive estimates.

8.3.2.1 Generator Active Magnetics

PEI did the mechanical design of the generator and made the associated cost estimates, which are described in Section 8.3.1.2. Cost estimates for the generator active magnetics were scaled from Kaman estimates for the 2.3-m diameter, 160-rpm single PM design using the unit-pole scaling methods

described in Section 4.8.6. These calculations are included in the parametric spreadsheets developed by PEI and included in Appendix C. The estimated cost of the active magnetics for the 4.0-m diameter generator is $284,000. Detailed descriptions of the generator active magnetics design are included in Sections 4.8.4 and Appendix E.

As described in Section 4.8.6, the unit-pole scaling method is expected to be most accurate when applied to the scaling of generators with similar air-gap velocities because the generator then operates at the same frequency. The direct drive system has an air-gap velocity of 6 m/s, compared to an air-gap velocity of 18 m/s for the base, single-stage gearbox-generator drive train that has a 2.3-m diameter and a 160-rpm generator. The air-gap velocity and the operating frequency of the direct drive generator are significantly lower than those for the generator used on the single PM gearbox. As a consequence, the generator estimates are not expected to be as accurate as the PM generator estimates for the single PM and multi-PM drive train designs. However, the scaling methods remain useful and valid for an approximate estimate of the costs.

The Large Machines Division of Siemens Automation and Drives, Berlin, Germany, furnished a comparative check of the WindPACT direct drive generator estimates described above. Siemens gave an estimate for a similar 1500-kW wind turbine generator based on a preliminary design. Table 8-1 outlines the specifications of this generator. The Siemens generator is cooled by forced air and the WindPACT generator is cooled by liquid, but the diameter and rated speeds are similar. The estimated price for the complete Siemens generator, including structure and active magnetic costs, is approximately $400,000 in large production volumes. The equivalent estimate for the WindPACT generator, including the generator structure cost, is $336,000. The Siemens estimate confirms that the WindPACT estimates, although approximate, are most likely in the correct range. If anything, the estimates may be slightly low.

Table 8-1. Siemens Direct Drive Generator Comparison

	WindPACT	Siemens
Output power (turbine)	1.5 MW	1.5 MW
Speed	20.5 rpm	20 rpm
Air-gap diameter	3.7 m	3.3 m
Overall diameter	4.0 m	4.0 m
Mass		62,000 kg
Cooling	Liquid	Air-air heat exchanger
PE system	SCR	IGBT
Full load efficiency	94.5	93.5
Generator structure cost, $	52,000	
Active magnetic cost, $	284,000	
Total generator cost, $	336,000	400,000

8.3.3 Ancillary Components

8.3.3.1 Generator Cooling System

The generator cooling requirements are based on the predicted 94.4% efficiency at rated power. The required cooling system capacity is thus 118 hp. Estimates, based on this capacity, were calculated using the methods described in Section 4.6.10. A cost adder of $550 was applied to the standard calculation to account for the large radius of cooling line plumbing.

8.3.3.2 Brake System

Based on methods described in Section 4.6.8, a parking brake cost was computed, as listed in Appendix C. For this analysis, the brake rotor was not assumed to be a conventional disc, but segments integral with the large rotor. This design can be seen in Figure 8-5, and the cost estimate reflects this difference.

8.3.3.3 Assembly and Test

Assembly and test costs are given in Appendix C. There is no gearbox assembly. The costs shown in the spreadsheet are for labor to complete the unit, including assembly of the generator stator to its frame.

8.3.4 System Optimization for Generator Diameter

The direct drive concept was investigated to determine cost trade-offs for various generator diameters before the 4.0-m diameter design described in the preceding subsections was selected. The system optimization was necessary because generator cost is strongly affected by the air-gap velocity and radius. The generators that cost the least have large diameters and short lengths. Increasing the generator diameter drives the generator cost down, but the increased size adds to the cost of the structural components.

Spreadsheet tools were developed and used to compute these trade-off relationships. The tools incorporate parametric design rules that enable the design configuration to be defined in sufficient detail to obtain masses, areas, and estimated costs.

8.3.4.1 Details of the Parametric Study

The spreadsheet is included in Appendix C, along with a line-by-line description of the equations used.

8.3.4.2 Results of the Parametric Study

Figure 8-6 shows the results of the parametric study for generator ODs ranging from 3.5 to 7.5 m. The results show that the active magnetic costs decrease and the structure costs increase as the diameter increases. The generator with the minimum total cost has a diameter of approximately 5.5 m. Generators of this diameter would be very difficult to transport. Modular construction is possible, enabling the generator to be transported in pieces, but the additional cost of this construction is expected to be higher than that of simply using a smaller diameter generator. For this reason, a 4.0-m generator was selected. The 4.0-m generator has a total cost that is approximately $40,000 higher than that of the 5.5-m diameter generator.

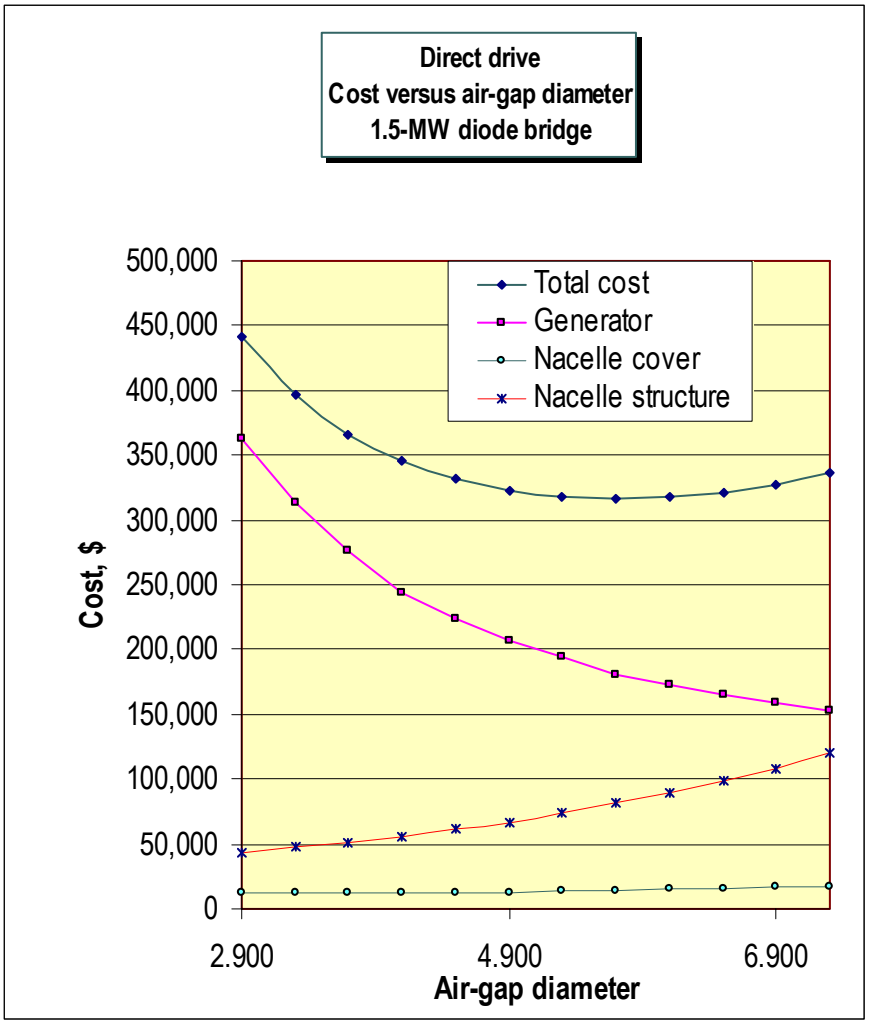

Figure 8-6. Results of direct drive parametric study

8.4 Direct Drive Drive Train Results

The following subsections summarize all of the COE production estimates for the selected direct drive design, as described in Sections 8.1 and 8.3.

8.4.1 Direct Drive Drive Train Efficiency

On a component-by-component basis, the direct drive drive train efficiency as a function of input power is shown in Figure 8-7. For comparison, the total drive train efficiency of the baseline system is given in the figure. The efficiency of the direct drive design is lower than that of the efficiency of the baseline design at rated power but is significantly higher at reduced power levels. The improvement at the lower power levels results from elimination of the gearbox and the increased efficiency in the generator and power electronics. Magnetization current losses in the baseline doubly fed induction generator cause significant fixed losses at all power levels. Such losses do not exist in the direct drive PM generator. The efficiency of the line-commutated SCR PE system is higher than that of the baseline IGBT PE system. This results from negligible switching losses of the SCRs and the absence of any requirement for the supply of magnetization current to the PM generator.

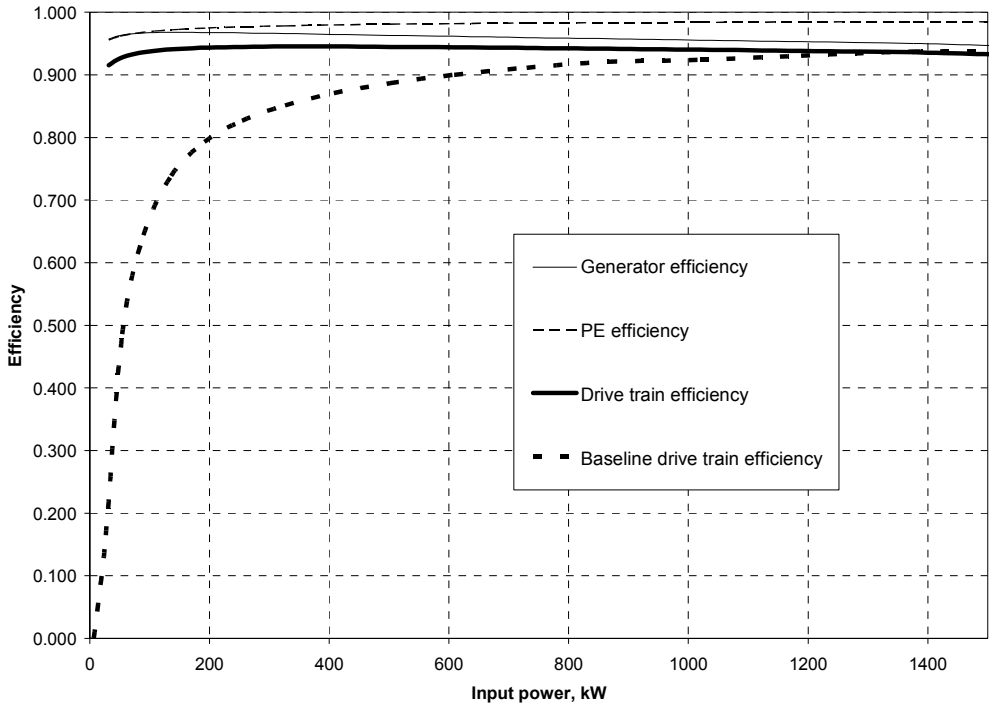

Figure 8-7. Direct drive drive train efficiency by component

8.4.2 Direct Drive Gross Annual Energy Production

Table 8-2 gives the GAEP estimate for the direct drive design for each wind speed bin. Because drive train efficiency losses are included, these estimates refer to the electrical output of the power electronics that process the generator's variable-frequency, variable-voltage power. All other losses are calculated separately in the final COE analysis. Wind speed bins ranging from 11.5 m/s to the cut-out speed of 27.5 m/s are aggregated in a single row. The energy production estimates for those wind speed bins are identical to those for the baseline turbine, shown in Table 5-3, with the rotor speed at rated power and the output power regulated to 1.5 MW by the pitch system. The total GAEP from the direct drive design is estimated to be 5648 MWh. This value is approximately 3.0% higher than the estimated production of 5479 MWh for the baseline design. The improvement results from the higher efficiency of the direct drive system.

Table 8-2. Direct Drive Drive Train GAEP

Wind Speed Bin Center, m/s	Rotor Speed, rpm	Rotor Power, kW	Drive Train Efficiency	Output Power, kW	# of Hours per Year	Energy Production	
						MWh	Fraction of Total, %.
3.0	5.73	32.1	0.915	29.4	297.5	9	0.15
3.5	6.69	51.0	0.926	47.2	333.1	16	0.28
4.0	7.64	76.1	0.934	71.0	363.0	26	0.46
4.5	8.60	108.3	0.938	101.6	386.9	39	0.70
5.0	9.55	148.6	0.942	139.9	404.7	57	1.00
5.5	10.51	197.8	0.944	186.6	416.5	78	1.38
6.0	11.46	256.7	0.945	242.5	422.4	102	1.81
6.5	12.42	326.4	0.945	308.5	422.7	130	2.31
7.0	13.37	407.7	0.945	385.4	417.8	161	2.85
7.5	14.33	501.4	0.945	473.8	408.3	193	3.43
8.0	15.28	608.6	0.944	574.6	394.7	227	4.02
8.5	16.24	729.9	0.943	688.4	377.7	260	4.60
9.0	17.19	866.5	0.942	816.0	357.8	292	5.17
9.5	18.15	1019.1	0.940	958.1	335.9	322	5.70
10.0	19.10	1188.6	0.938	1115.3	312.4	348	6.17
10.5	20.06	1375.9	0.936	1288.0	288.0	371	6.57
11.0	20.47	1569.8	0.931	1461.0	263.2	385	6.81
11.5–27.5	20.47	1614.8	0.929	1500.0	1754.6	1755	31.1
					Total GAEP =	**5648**	**MWh**

The GAEP estimates made for the direct drive and baseline designs are compared by wind speed bin in Figure 8-8. Above wind speeds of 11.0 m/s, the energy production values are equal for both designs, so those bins are not shown. The energy production of the direct drive design is slightly lower at 10.5 and 11.0 m/s. However, for wind speeds below 10.0 m/s, the direct drive production is significantly higher than that of the baseline because of the higher efficiency.

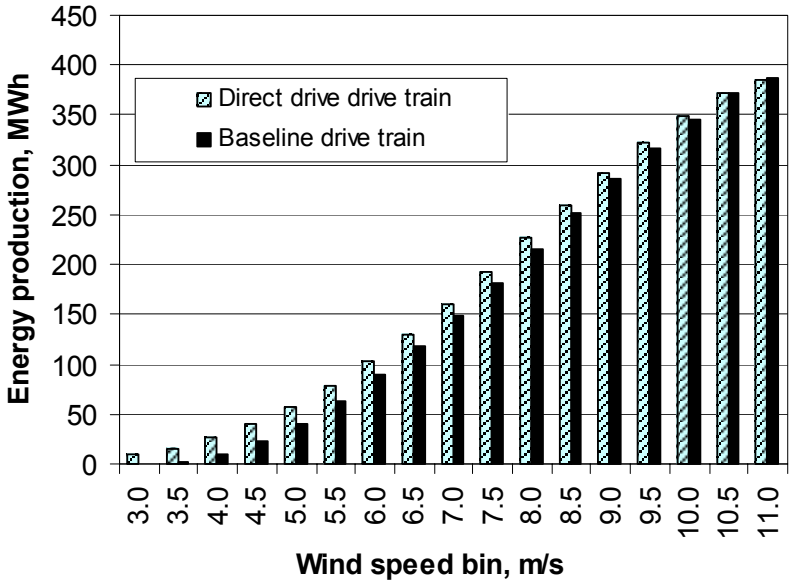

Figure 8-8. Direct drive and baseline energy production by bin

8.4.3 Direct Drive Drive Train Component Costs

Component costs for the 1.5-MW direct drive drive train are itemized in Table 8-3. Design details and estimation methods are described in Section 8.3. Generator costs appear in two categories, the generator mechanicals and the generator active magnetics.

Table 8-3. Direct Drive Drive Train Component Costs

Component	Cost, $
Transmission system	**NA**
Support structure	**55,000**
Mainshaft	4,300
Generator mechanicals	51,000
Generator cooling system	**3,400**
Brake system with hydraulics	**12,400**
Coupling (generator to gearbox)	**NA**
Nacelle cover	**14,000**
Generator active magnetics	**304,000**
Power electronics	**53,000**
0.95–0.95 substation VAR control	**12,000**
Transformer	**26,000**
Cable	**16,000**
Switchgear	**10,000**
Other subsystems	**25,000**
Drive train assembly and test	**9,400**
Total	**540,000**

Note: All costs rounded.

In Figure 8-9, the component costs itemized in Table 8-3 are compared to the baseline component costs. The table clearly shows that the savings in gearbox and related transmission system costs are not enough to offset the increased generator costs of the direct drive system. The support structure for the direct drive system includes the generator mechanicals and is higher for that reason. The costs that are not related to the generator are similar. The differences among electrical system costs are the same as for the single PM design, with the SCR-SCR PE costs being lower than the baseline doubly fed PE converter. However, additional power factor and VAR control components are necessary, making the total electrical system costs approximately the same.

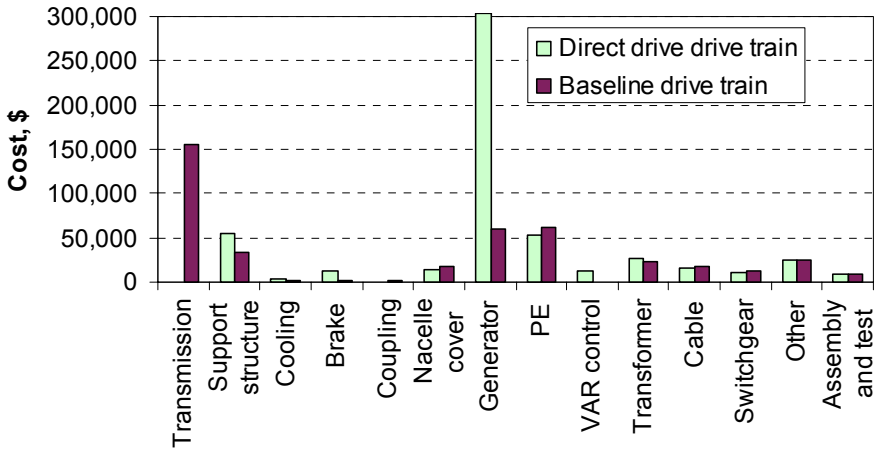

Figure 8-9. Direct drive and baseline component cost comparison

8.4.4 Direct Drive Operations and Maintenance Costs

The three components of the direct drive O&M estimates along with LRC are shown in Table 8-4, both as cost per year and normalized by the annual energy capture of the turbine. Complete details of the direct drive drive train O&M model are included in Appendix J.

These estimates were made by modifying the baseline drive train estimates as follows:

- All gearbox-related O&M costs were deleted.
- A generator failure rate equal to 120% of the baseline generator failure rate was used. The PM generator construction is expected to be more reliable, all else being equal, but the direct drive generator has a much higher pole count and therefore more windings.
- The generator repair cost was set to 30% of the complete generator cost. A segmented stator construction is planned so sections can be replaced in the field.
- The LRC was adjusted to include a rebuild of the generator at 25 years.

Table 8-4. Direct Drive O&M and LRC Estimates

	Direct Drive		Baseline
	$/yr	$/kWh	$/yr
Unscheduled maintenance	12,396	0.0025	12,103
Scheduled maintenance	4,803	0.0010	6,004
Operations	6,501	0.0013	6,501
Subtotal, O&M (excluding LRC)	**23,700**	**0.0048**	**24,608**
LRC (major overhauls)	**5,550**	**0.0011**	**5,124**
Total O&M and LRC	29,250	0.0059	29,732

The scheduled and unscheduled maintenance costs, combined with the LRC from Table 8-4, are compared to the corresponding baseline drive train estimates on a component-by-component basis in Figure 8-10. Only drive train components are included because the other turbine components are assumed to be the same for both designs. The contribution from the transmission system is eliminated for the direct drive design, but the contribution from the direct drive generator is much higher than that of the baseline.

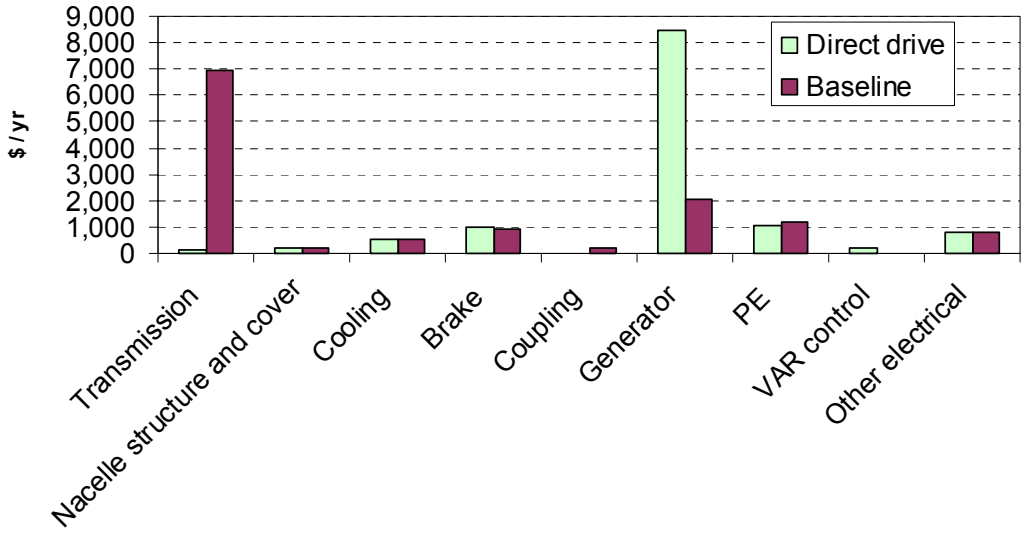

Figure 8-10. Direct drive scheduled and unscheduled maintenance costs and LRC compared to baseline by component

8.4.5 Direct Drive Cost of Energy Estimates

Table 8-5 gives the COE estimates for the direct drive design. The COE estimate for the direct drive design is 0.0378 $/kWh, approximately 6% higher than the baseline. The increase in COE is due to the approximately 11% higher capital cost of the direct drive system, which reflects the higher cost of the generator. The AEP of the direct drive system is approximately 3% higher than that of the baseline, which partially offsets the increased capital cost.

Table 8-5. Direct Drive Drive Train COE Estimates, Compared to Baseline

	Direct Drive		Baseline
	Cost, $	% of COE	Cost, $
Capital Costs			
Turbine	**1,152,659**	**64.5**	1,001,491
Rotor	**248,000**	**13.9**	248,000
Drive train and nacelle	**539,991**	**30.2**	430,778
Yaw drive and bearing	**16,000**	**0.9**	16,000
Control, safety system	**7,000**	**0.4**	7,000
Tower	**184,000**	**10.3**	184,000
Turbine manufacturer's overhead and profit (30%, tower, rotor, and transformer excepted)	**157,668**	**8.8**	126,229
Balance of station	**358,000**	**20.0**	358,000
ICC	**1,510,659**	**84.5**	1,359,491
AEP			
Ideal annual energy output, kWh	5,648,000		5,479,000
Availability, fraction	0.95		0.95
Losses, fraction	0.07		0.07
Net AEP, kWh	**4,990,008**		4,840,697
Replacement costs, LRC, $/yr	**5,550**	**2.9**	5,124
FCR, fraction/yr	**0.106**		0.106
O&M, $/kWh	**0.0047**	**12.6**	0.0051
COE = O&M + ((FCRxICC)+LRC)/AEP	**0.0378**		0.0358

8.5 Direct Drive Drive Train Scaling to 750 kW and 3 MW

The procedures used for scaling the 1.5-MW direct drive design and costs to the 750 kW and 3 MW power levels are the same as employed for the single PM drive train. They are described in Section 7.5 and adapted here. The generator diameter for each scaling size was limited to 4.0 m because of transportation limitations.

Table 8-6 summarizes the results of this scaling process, and the results are compared graphically in terms of the drive train COE in Figure 8-11. The drive train COE represents the portion of the turbine COE attributed to the drive train capital cost alone. Relative to the 1.5-MW direct drive drive train, the 750-kW version is characterized by a lower normalized capital cost (in dollars/kilowatt) and a lower COE. Again, relative to the 1.5-MW system, the 3-MW variation has a higher capital cost and COE. The entries in Table 8-6 give some insight into the reasons for these cost relationships. The generator is the largest cost item and has, by far, the largest effect on total costs. The normalized capital cost of the generator increases substantially with increasing turbine size. The limited 4.0-m generator diameter increases the generator cost at the large sizes, causing much of this effect. Larger diameter generators may be feasible if modular construction is used to allow shipping in multiple pieces. The cost of modular construction was not investigated for this study.

Table 8-6. Direct Drive Drive Train Component Cost Scaling to 750 kW and 3 MW

	750 kW		1.5 MW		3 MW		Method
	Cost, $	Cost/kW	Cost, $	Cost/kW	Cost, $	Cost/kW	
Transmission system	NA	NA	NA	NA	NA	NA	
Support structure	34,951	47	55,234	37	98,438	33	PEI input
Generator structure	*32,656*	*44*	*50,958*	*34*	*88,671*	*30*	PEI input
Mainshaft	*2,295*	*3.1*	*4,276*	*2.9*	*9,767*	*3.3*	PEI input
Generator cooling system	*1,680*	*2.2*	*3,359*	*2.2*	*6,718*	*2.2*	PEI input
Brake system with hydraulics	*6,190*	*8.3*	*12,380*	*8.3*	*24,760*	*8.3*	PEI input
Coupling	*NA*	*NA*	*NA*	*NA*	*NA*	*NA*	
Nacelle cover	*9,702*	*13*	*13,556*	*9*	*20,443*	*6.8*	PEI input
Generator	117,431	157	303,997	203	905,843	302	Unit-pole scaling
Power electronics	*26,560*	*35*	*53,119*	*35*	*106,238*	*35*	Power rating
0.95–0.95 substation VAR control	*5,779*	*7.7*	*11,557*	*7.7*	*23,114*	*7.7*	Power rating
Transformer	*12,938*	*17*	*25,875*	*17*	*51,750*	*17*	Power rating
Cable	*8,023*	*11*	*16,046*	*11*	*32,092*	*11*	Power rating
Switchgear	*5,233*	*7*	*10,465*	*7*	*20,930*	*7*	Power rating
Other subsystems	*12,500*	*17*	*25,000*	*17*	*50,000*	*17*	Power rating
Drive train assembly and test	*4,702*	*6*	*9,403*	*6.3*	*18,806*	*6.3*	PEI input
Drive train and nacelle total	**245,686**	**328**	**539,991**	**360**	**1,359,132**	**453**	

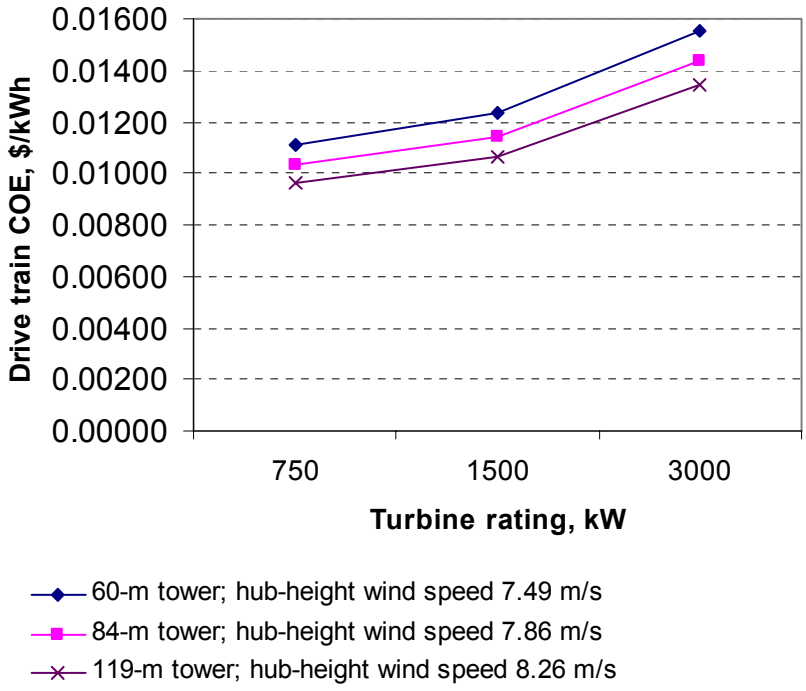

Figure 8-11. Direct drive drive train COE scaling for different hub height wind speeds

9. Multi-PM Drive Train

The multi-PM drive train is an integrated design that uses multiple PM generators driven by a common gearbox. Initial estimates indicated that this design has a favorable COE compared to the baseline design. A preliminary design was developed for this reason, although a detailed design was not developed for the entire PE system. Final estimates confirm the low COE, which results from the low cost of the multiple-output gearbox in combination with a high generator efficiency.

9.1 Multi-PM System Description

The 1.5-MW multi-PM generator drive train is illustrated in Figure 9-1 with a system diagram shown in Figure 9-2. Six 325-rpm, 250-kW PM generators are driven by pinions from a common bullgear that is driven by a turbine rotor through a close-coupled mainshaft. The generators, gearbox, mainshaft, and mainshaft bearings are all integrated within a common housing. The system and generator sizes are minimized by integrating liquid cooling and the large diameter-to-length aspect ratio of the generators.

Each of the generator outputs is connected to a dedicated PE converter. They rectify the AC output of each generator and couple the power to a common DC bus. To minimize the cost of these converters, passive SCR rectifiers are used for the generator converters. The common DC bus power is converted to AC power by a grid PE inverter, the output of which is connected to the turbine pad mount transformer. Again to minimize the PE system cost, SCR line-commutated inverters are used for the grid PE system.

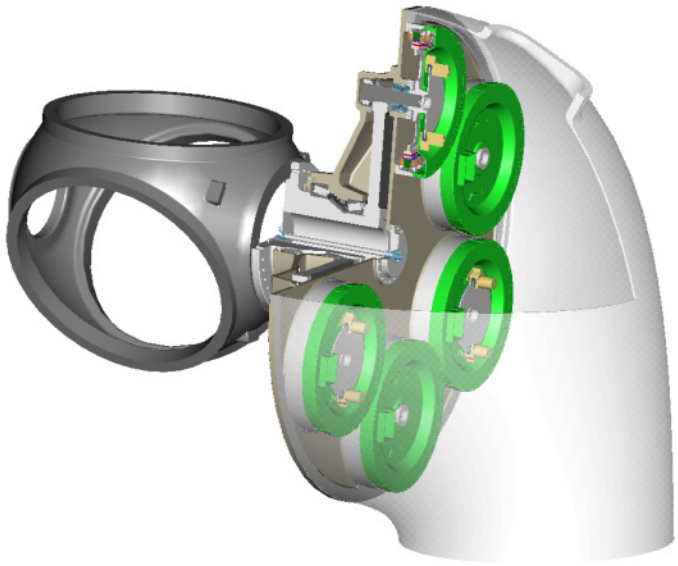

Figure 9-1. WindPACT multi-PM generator drive train

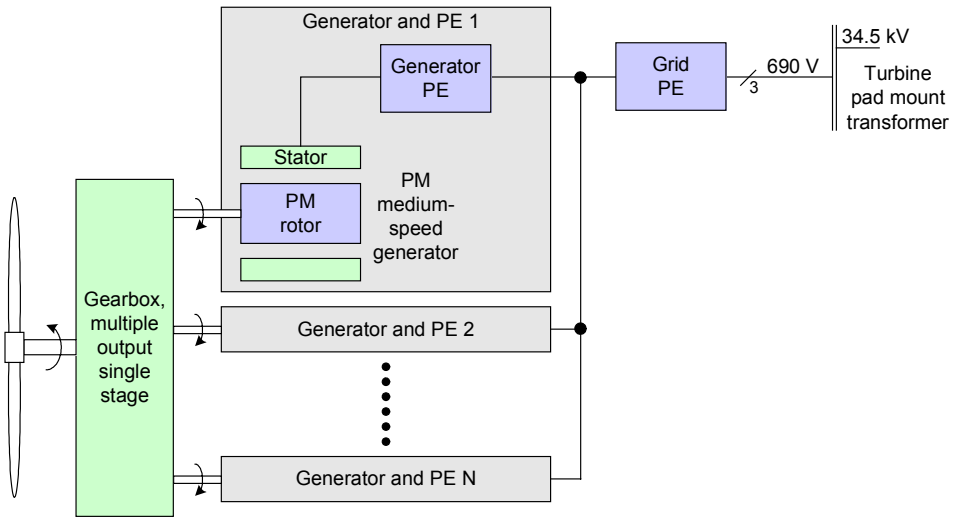

Figure 9-2. Multi-PM generator system diagram

9.2 Multi-PM Design Alternatives

The WindPACT multi-PM drive train described in the preceding section could be designed in a number of different ways. Many alternatives were considered early in the study before focusing on the selected design. Some of the alternative multi-PM designs considered, along with the reasons that they were considered less attractive for this study, are described below:

- **Modular bedplate designs:** An integrated design was selected over the bedplate approach because the integrated design clearly minimizes the material cost and therefore has the potential to minimize the turbine production cost in high-volume production.

- **Large-diameter bearings:** A number of design alternatives are possible with large-diameter structural members, mainshafts, and mainshaft bearings. These systems are less attractive because of potential problems with bearing deformations and bearing lubrication.

- **Standard-frame National Electric Manufacturers Association (NEMA) PM generators:** Standard-frame generators could be used to make it easier to procure generators from multiple sources. Standard generator frames were not used for the PM generators in this study because they would have higher material costs resulting from a lower diameter-to-length ratio than the optimized, custom designs. In high-volume production, the increased material cost would increase the cost of these generators.

- **Synchronous wound-field generators:** Synchronous generators are readily available in the size ranges considered. They have relatively low cost because they are produced in high volumes for other applications. In general, these generators have lower efficiency at partial loads—because of rotor excitation losses—than the PM generators. The relatively lower cost advantage was not expected to make up for the reduced turbine energy capture.

- **Alternate PE systems:** The IGBT-IGBT and diode-IGBT PE systems described in Sections 4.9.3.1 and 4.9.3.2 were initially considered but were not selected because of the cost trade-offs described in Section 4.10. The IGBT-IGBT system has additional cost with dedicated converters required for each generator in the multi-PM system, which makes this approach even less attractive.

9.3 Multi-PM Component Designs

Multi-PM component costs are highly dependent on the choice of system diameter and the number of generators. To analyze this design, preliminary estimates were made for a six-generator, 4.0-m diameter base system. PEI developed a complete Pro/E model of the mechanical design and determined component sizes and masses. Parameterized spreadsheets were then developed from the base design to estimate component sizes, masses, and costs for other system diameters and numbers of generators. The spreadsheet component cost estimates are based on the ratios of component masses to the masses of similar baseline or single PM components, for which detailed cost estimates had been made. Using these spreadsheets, the minimum-cost multi-PM system was determined to have six generators and a 3.5-m diameter.

The component designs developed for the six-generator, 3.5-m diameter system are described in Sections 9.3.1 through 9.3.3. Estimates for other system diameters and numbers of generators, including the lowest cost system with six generators and 4.0-m diameter, are described in Section 9.3.4.

9.3.1 Mechanical Design

The general design of this configuration follows the precept of shared function and material wherever possible so as to reduce mass and cost. This implies a high degree of integration. The mainshaft functions as the carrier of the hub and also of the bullgear. The gear casing forms the envelope of the gears but also serves as the generator frame.

9.3.1.1 Bearings and Mainshaft

Figure 9-3 shows the internal construction of this design. The bearing arrangement and estimates from the single PM design, described in Section 7.3.1.1, is used. Note the integral mainshaft and the use of separated tapered roller mainshaft bearings. These bearings are ideal for handling combined thrust and radial loads. By spreading the bearings apart, large moments are reduced. This permits the use of smaller diameter bearings compared to the case where the bearings are closely spaced, as in back-to-back mounting. The smaller diameter bearings were preferred because (1) they are lower in cost, with numerous suppliers; (2) they can be included in forced-oil systems and therefore are easy to lubricate; and (3) they can use reliable labyrinth seals.

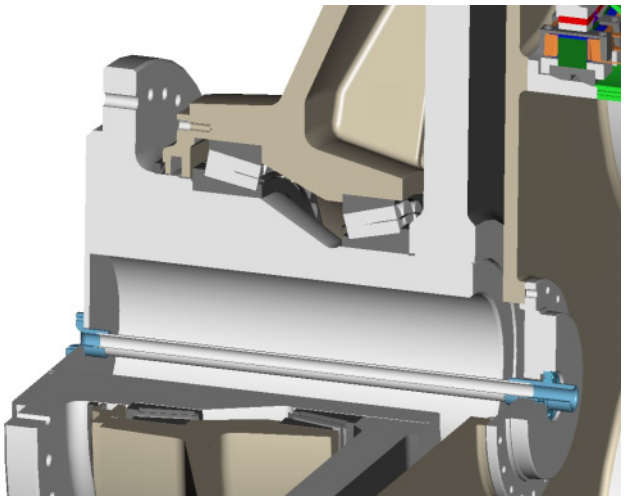

Figure 9-3. Section view of multi-PM mainshaft area

9.3.1.2 Gears

Gear design is based on AGMA 2001 C95 ratings (ANSI/AGMA 1995), utilizing a Miners Rule analysis and GEARTECH 218 software (Geartech Software, Inc., Townsend, MT). For preliminary design, the design meets the 30-yr life objective, with a design margin of 20% (safety factor of 1.2) to allow for load uncertainty and for conservatism.

The helical involute gears are designed with a conservative aspect ratio of approximately 1:1. Helical overlaps are approximately 2.0. A quality level of AGMA 2000, Class 12 is assumed. Gearing meets the requirements of AGMA 2001 C95 Grade 2.

9.3.1.3 Generator Mechanicals

The generator stator and rotor are subassemblies that mount and dismount easily for service. The stator consists of an iron ring with its outside exposed to the cooling medium. The inside supports the pole pieces to which coils are attached. The stator subassembly is held round and concentric with steep-tapered location surfaces, each containing O-rings to seal the liquid coolant.

The rotor is directly mounted to a pinion shaft through roller bearings. The bearings are included in the pressure lubrication system, receiving cooled and filtered oil. After passing through the bearings, the oil returns by gravity to the sump.

The generator is fitted with an iron cover that creates an IP54 rated enclosure and also provides support for the parking brakes. These details can be seen in Figure 9-4.

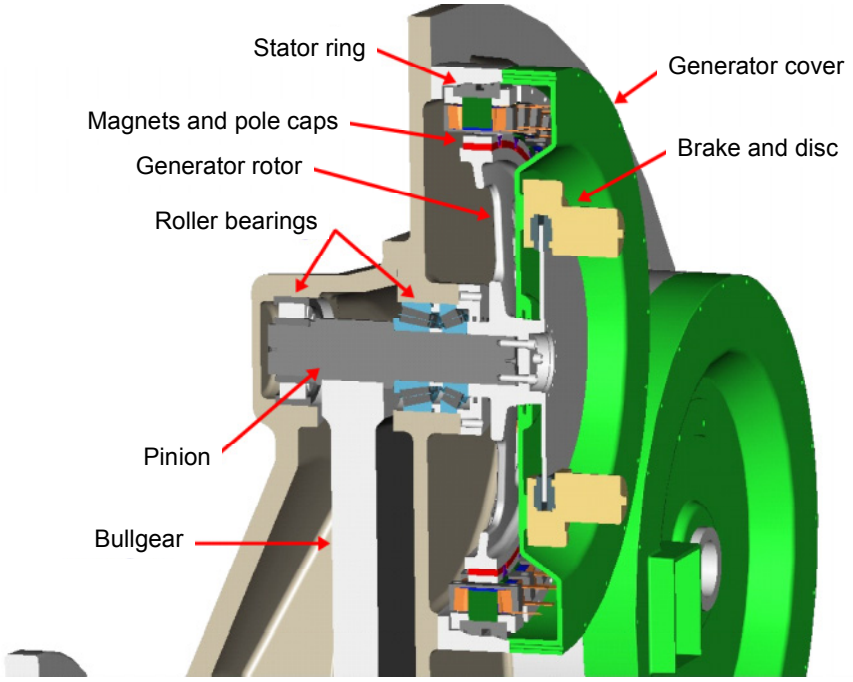

Figure 9-4. Section view through generator

9.3.1.4 Stressed-Skin Nacelle

This system is supported by a aggregated nacelle that acts as an enclosure as well as a structural support for the transfer of rotor loads. This component was developed in sufficient detail to validate the concept. Loads are described in Section 3.3.

Figure 9-5 shows the results of a preliminary FEA analysis.

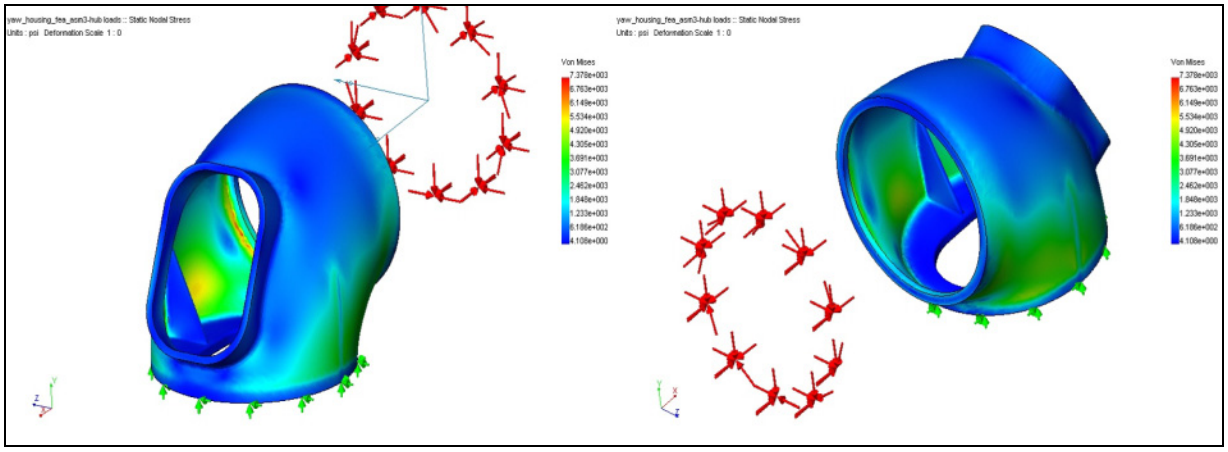

Figure 9-5. FEA on stressed-skin nacelle

For this analysis, an equivalent fatigue load was computed for each axis with a material exponent of 8. The moments and forces were combined per Germanischer Lloyd rules (Germanisher Lloyd 1999) and applied at the rotor hub center line. A conservative allowable stress of 7,500 psi was used to develop the section sizes.

9.3.1.5 Stressed-Skin Nacelle

For the multi-PM stressed-skin nacelle, the outer surface is also the enclosure that protects the machinery from the external weather environment. There is a large opening used for assembly access and for housing cooling equipment. This may include scoop-like ducts to provide sufficient area and velocity of cooling air along with the necessary cover. Any necessary covers and ducts would be built of fiberglass.

The masses of the cover and duct assembly are estimated as a ratio of the stressed-skin structural nacelle mass. This is a first-order estimate, following the general size of the system. Cost is computed from this mass estimate using the fiberglass cost per kilogram values described in Section 4.6.11.

9.3.2 Electrical

The electrical system costs for the multi-PM drive train are expected to be similar to those of the single PM generator drive train, with the exception of the generator. Costs were therefore estimated from the single PM electrical costs and were not further analyzed.

9.3.2.1 Generator

The costs of the generator active magnetics were estimated using the unit-pole scaling method described in Section 4.8.6. The unit-pole cost scaling, including calculations of the generator active magnetics and the generator structural costs, is included in the parametric spreadsheets described in Section 9.3.4. The generator mechanicals are included as part of the integrated mechanical design, as described in Section 9.3.1.3.

9.3.2.2 Power Electronics

The multi-PM system is expected to use an SCR-SCR PE system very similar to the system described in Section 7.3.2.2 for the single PM system. Figure 9-2 shows a PE system with individual generator converters and a common grid inverter. This PE system would require a large number of generator SCRs with lower ratings. This would increase the PE cost relative to a single larger system of equivalent total capacity, although the increase is expected to be small. It is also possible to directly connect all the multiple generator outputs in parallel and use a single generator inverter, if the generator rotors are all aligned to the same position. In this case the same single PM PE system could be used as is. Further investigation is needed to determine the best system. For simplicity, the single PM PE system cost was used for the multi-PM system

9.3.2.3 Switchgear

Each PM generator in the multi-PM system will require a separate fused disconnect or equivalent protection and disconnect device. The single PM system requires a single fused disconnect. All other switchgear components are assumed to be identical for both systems. The single PM switchgear costs are described in Section 7.3.2.3. The single fused disconnect has an estimated cost of $1500. The cost of six fused disconnects with 17% of the single disconnect rating is estimated at $3600, giving a net increase of $2100 for the multi-PM switchgear cost relative to the single PM switchgear cost.

9.3.2.4 Cable, Transformer, Power Factor Correction, and VAR Control

The cable, transformer, and VAR control costs for the multi-PM system are assumed to be the same as the estimates made for the single PM system in Section 7.3.2.

9.3.3 Ancillary Components

9.3.3.1 Gearbox and Generator Cooling System

The estimated heat capacity for the gearbox heat exchanger system is 21.7 hp. Based on this capacity, cost estimates were calculated using the methods described in Section 4.6.9.

The generator cooling is based on the value of predicted efficiency at nominal rating, which is 97.4%. The capacity, then, is 52.3 hp. Cost estimates, based on this capacity, were calculated using the methods described in Section 4.6.10.

9.3.3.2 Brake System

A brake system, which can be seen in Figure 9-4, is applied to the rotor of every other generator. Brake system costs were calculated using the method described in Section 4.6.8.

9.3.3.3 Assembly and Test

The multi-PM gearbox, being integral with the mainshaft and generator components, is designed for assembly by the integrator of the mechanical system. For this reason, the costs of gearbox assembly are included in the drive train assembly and test category for this drive train. The methods described in Section 4.6.6 were used to calculate the gearbox assembly costs.

9.3.4 System Optimization for Generator Number and Diameter

As described at the beginning of Section 8.3, the multi-PM system was optimized to determine the generator number and system diameter before the six-generator, 3.5-m diameter design described in the preceding subsection was selected. This optimization was done using the parametric spreadsheet included in Appendix C.

The system optimization was necessary because generator cost is strongly affected by the air-gap velocity and radius. The most efficient system uses large-diameter, short generator rotors at the highest rpm. Increasing the system diameter drives the generator cost down, but the increased size adds cost to structural components. Increasing size also permits higher gear ratios and faster generator rpm. This reduces the generator cost while the expensive bullgear is gaining in diameter and cost. Increasing the gear diameter and reducing its face width is less cost efficient than the opposite.

Adding more generators reduces the gear mesh torque, allowing smaller pinions and higher gear ratio. This is a favorable trend for individual pinion cost, but is countered by the costs of the additional pinions, bearings, and assembly. With the greater ratio and air-gap velocity, generator costs are reduced, but are offset by the increased per-generator fixed cost of the end turns and assembly.

The spreadsheet used to compute these relationships is based on parametric design rules that develop the design configuration sufficient to obtain weight areas and to estimate cost.

9.3.4.1 Details of the Parametric Study

The 3.5-m diameter parametric worksheet is included in Appendix C, along with a detailed description of the variables and calculations. An equivalent worksheet was used for each diameter. The input is defined as the radius over the outside of the generator housing (r_outside). See Figure 9-6 for a schematic of the system.

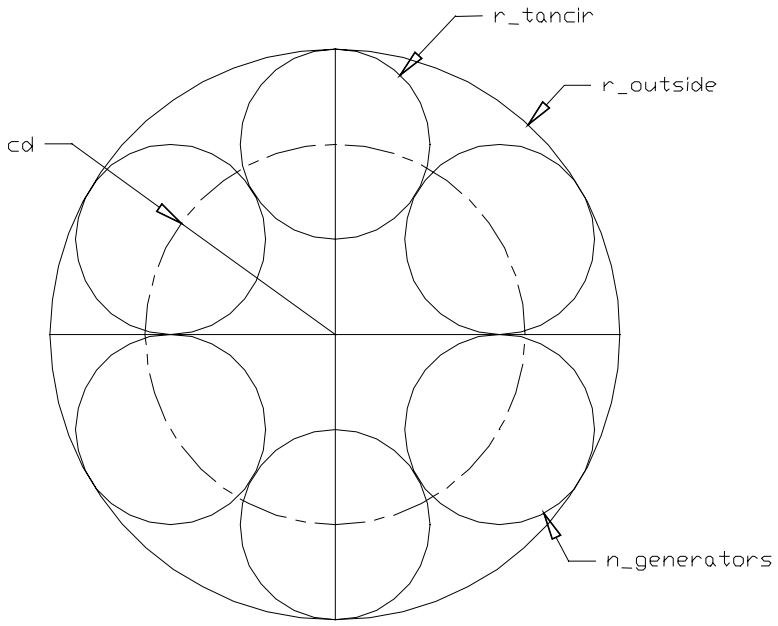

Figure 9-6. Schematic of system

The number of generators is varied from 3 to 14 per system in each worksheet. The system diameter is varied from 3.0 m to 4.5 m. The ranges are chosen to find the lowest system cost and to visualize the curve slope, or sensitivity, of the competing variables.

This analysis did not include any electrical components other than the generator. The PE system, transformer, cable, and switchgear costs were assumed to be constant and were not included in this analysis.

9.3.4.2 *Results of the Parametric Study*

Figure 9-7 shows the results in terms of the total cost for the analyzed components. The results show the minimum cost at approximately six generators with a system radius of 1.75 m (3.5-m diameter).

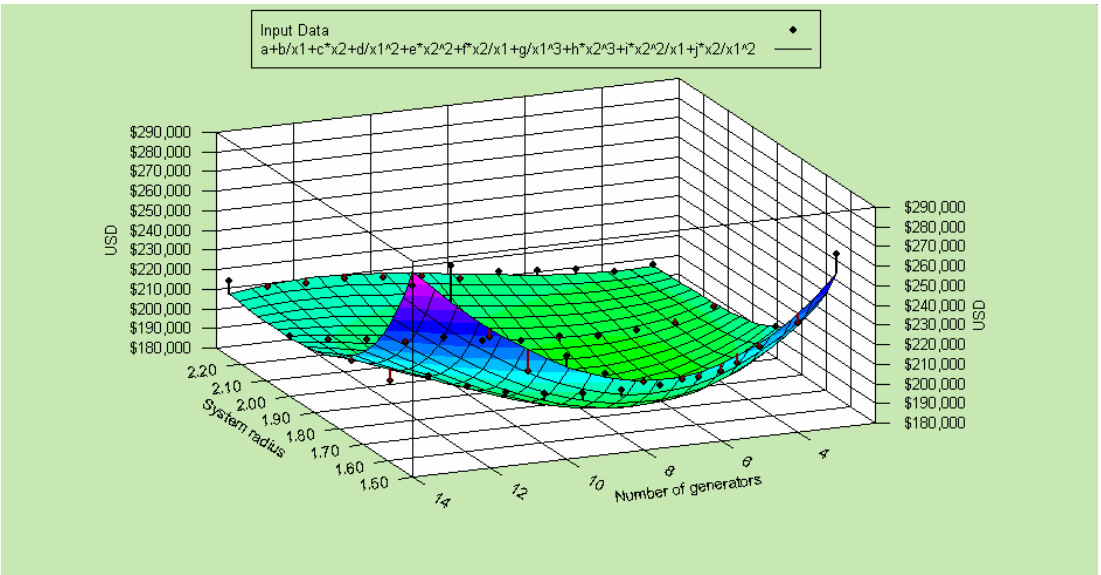

Figure 9-7. Three-dimensional representation of multi-PM optimization results

Cost curves for different numbers of generators are shown in Figure 9-8 at the 3.5-m system diameter, along with the component costs for the six-generator, minimum cost system. The generator costs change significantly with system diameter and to a large extent determine the optimum number of generators.

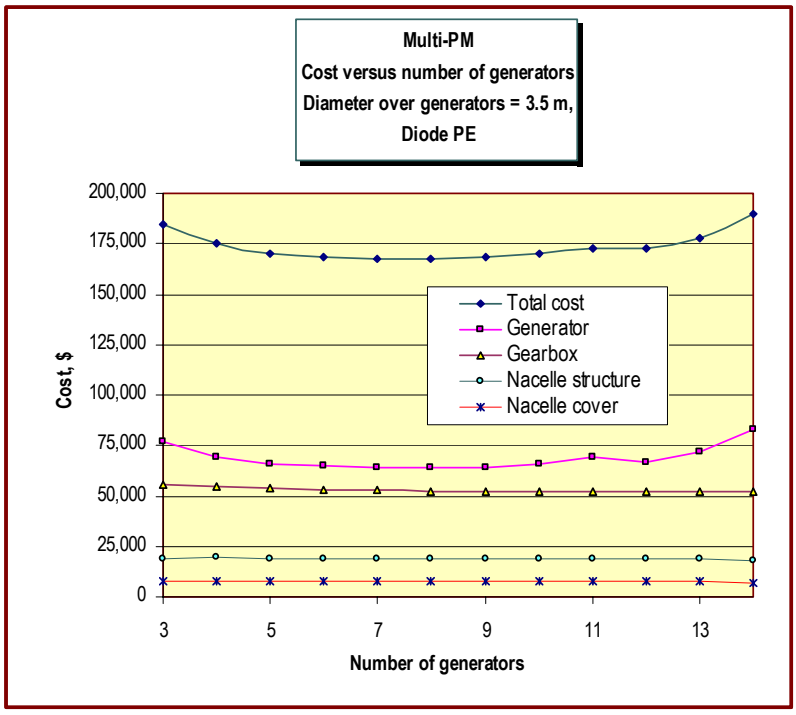

Figure 9-8. Summary results for 3.5-m diameter system

9.4 Multi-PM Results

The following subsections summarize all cost and energy production estimates for the 1.5-MW multi-PM generator drive train design described in Sections 9.1 and 9.3.

9.4.1 Multi-PM Efficiency

Figure 9-9 shows the drive train efficiency versus input power for the multi-PM design on a component-by-component basis. For comparison, the total drive train efficiency of the baseline system is given. The multi-PM drive train efficiency is higher than that of the baseline design at all power levels, with the largest differences seen at low power. The multi-PM system efficiency is similar to the single PM system efficiency described in Section 7.4.1. The efficiency is higher than that of the baseline for the same reasons, the absence of magnetization current in the PM generators and lower losses in the SCR PE system.

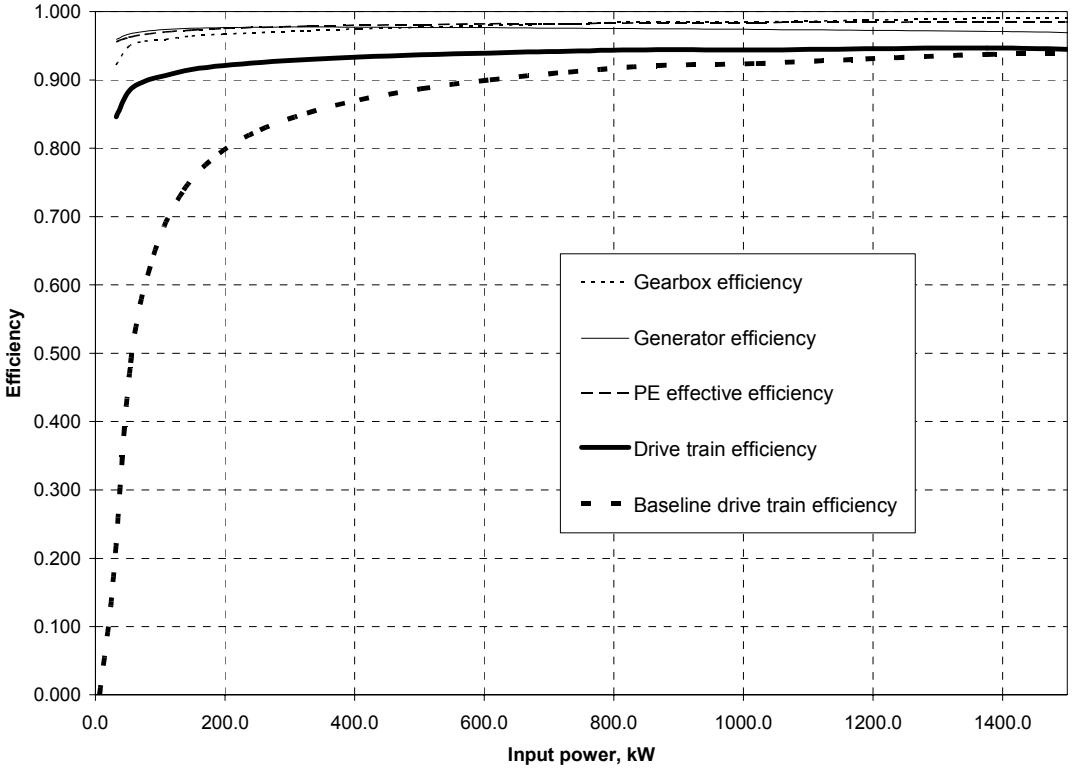

Figure 9-9. Multi-PM drive train efficiency by component

9.4.2 Multi-PM Gross Annual Energy Production

Table 9-1 presents the gross energy production estimate for the multi-PM design for each wind speed bin. Drive train efficiency losses are included in this estimate. All other losses are calculated separately in the final COE analysis. The wind speed bins from 11.5 m/s to the cut-out speed of 27.5 m/s are aggregated in a single row. The energy production values for these wind speed bins are identical to those for the baseline turbine, shown in Table 5-3, with the rotor speed at rated and the output power regulated to 1.5 MW by the pitch system. The total GAEP from the multi-PM design is estimated to be 5628 MWh, approximately 2.7% higher than the estimated production of 5479 MWh for the baseline design.

Table 9-1. Multi-PM Drive Train GAEP

Wind Speed Bin Center, m/s	Rotor Speed, rpm	Rotor Power, kW	Drive Train Efficiency	Output Power, kW	# of Hours per year	Energy Production	
						MWh	Fraction of Total %
3.0	5.73	32.1	0.846	27.1	297.5	8	0.14
3.5	6.69	51.0	0.883	45.0	333.1	15	0.27
4.0	7.64	76.1	0.898	68.3	363.0	25	0.44
4.5	8.60	108.3	0.906	98.2	386.9	38	0.67
5.0	9.55	148.6	0.915	136.0	404.7	55	0.98
5.5	10.51	197.8	0.921	182.1	416.5	76	1.35
6.0	11.46	256.7	0.926	237.7	422.4	100	1.78
6.5	12.42	326.4	0.930	303.5	422.7	128	2.28
7.0	13.37	407.7	0.933	380.6	417.8	159	2.83
7.5	14.33	501.4	0.937	469.7	408.3	192	3.41
8.0	15.28	608.6	0.940	571.8	394.7	226	4.01
8.5	16.24	729.9	0.942	687.7	377.7	260	4.61
9.0	17.19	866.5	0.944	818.3	357.8	293	5.20
9.5	18.15	1019.1	0.944	961.9	335.9	323	5.74
10.0	19.10	1188.6	0.946	1123.9	312.4	351	6.24
10.5	20.06	1375.9	0.947	1302.8	288.0	375	6.67
11.0	20.47	1569.8	0.944	1481.2	263.2	390	6.93
11.5-27.5	20.47	1590.7	0.943	1500.0	1301.7	2632	46.77
					Total GAEP =	**5628**	**MWh**

Figure 9-10 compares the AEP estimates for the multi-PM and baseline designs by wind speed bin. Above wind speeds of 11.0 m/s, the energy production values are equal for both designs, so those bins are not shown. At 11.0 m/s and below, the multi-PM design produces more energy because the drive train efficiency is higher.

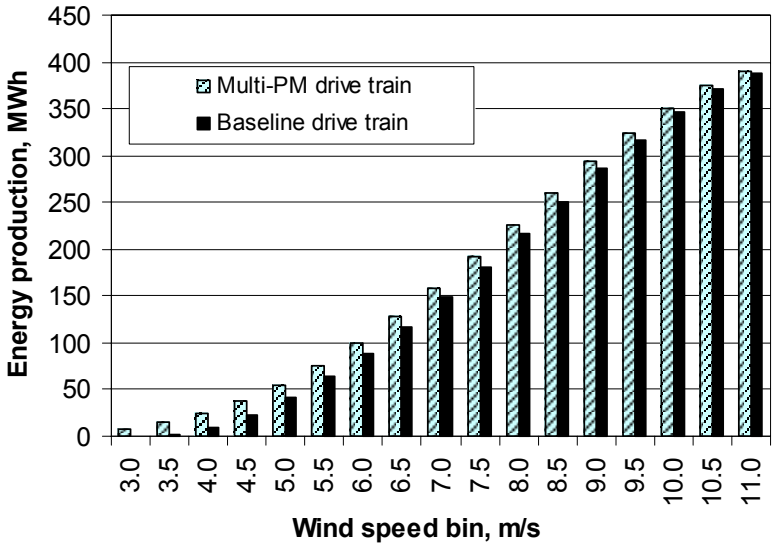

Figure 9-10. Multi-PM and baseline energy production by bin

9.4.3 Multi-PM Component Costs

Component costs for the multi-PM drive train are itemized in Table 9-2. Because this design uses an integrated gearbox and multiple generators with a common gearbox and generator interface housing, all generator structural components are included in the transmission system category. Only the generator active magnetic components are included in the generator category.

Table 9-2. Multi-PM Drive Train Component Costs

Component	Cost, $
Transmission system	**58,000**
Gearbox components	53,000
Mainshaft	5,000
Support structure (integrated nacelle)	**19,000**
Cooling system	**5,300**
Gearbox	2,200
Generator	3,100
Brake system	**5,600**
Coupling (generator to gearbox)	**NA**
Nacelle cover	**7,300**
Generator	**78,000**
Power electronics	**53,000**
0.95–0.95 substation VAR control	**12,000**
Transformer	**26,000**
Cable	**16,000**
Switchgear	**13,000**
Other subsystems	**25,000**
Drive train assembly and test	**7,900**
Total	**325,000**

Note: All costs rounded.

Figure 9-11 compares the component costs itemized in Table 9-2 to the baseline component costs. This design has significantly lower transmission system costs than the baseline system. The transmission system cost is reduced primarily because (1) only a single gearbox stage is necessary for the medium-speed generators and (2) the gear design with a single large bullgear driving multiple pinions has lower material content and simpler construction. The integrated design with a close-coupled mainshaft also reduces cost relative to the baseline bedplate system. The stressed-skin nacelle used in the integrated design has lower support structure costs.

Part of the cost savings in the transmission system is offset by higher generator costs for the multi-PM design relative to the baseline. This results from the inefficiencies of building small generators with proportionally higher end turn material, terminations, and housing costs.

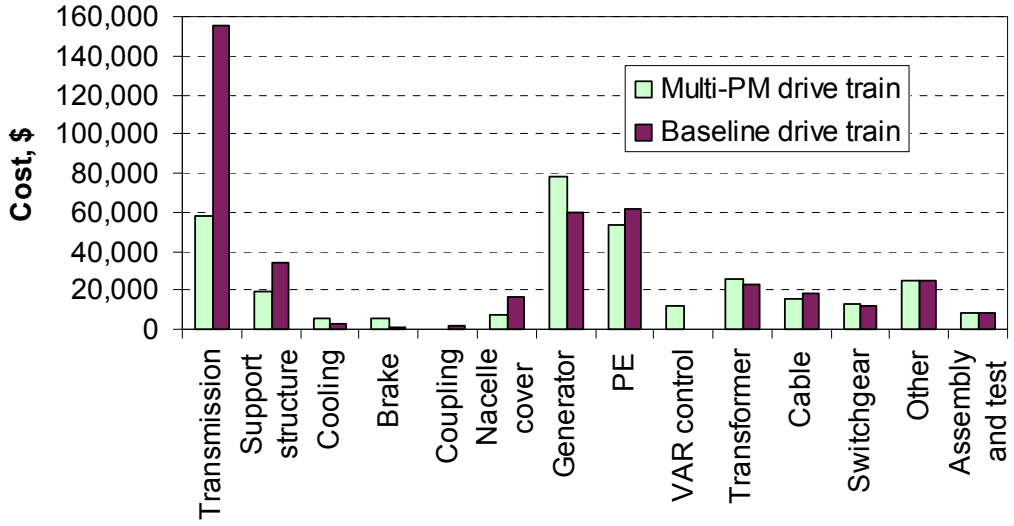

Figure 9-11. Multi-PM and baseline component cost comparison

9.4.4 Multi-PM Operations and Maintenance Costs

The three components of the multi-PM O&M estimates, along with the LRC, are shown in Table 9-3, both as cost per year and normalized by the annual energy capture of the turbine. Complete details of the multi-PM drive train O&M model are included in Appendix J.

These estimates were made by modifying the baseline drive train estimates as follows:

- A generator repair cost of 75% of new spare cost (compared to 50% for baseline) was used because the smaller, lower cost generators will require higher labor costs to repair relative to the spare cost.
- A gearbox failure rate of 66% of the baseline gearbox was used to account for the simple gearbox with fewer stages.
- A generator failure rate of 75% of the baseline was used to account for the expected higher reliability of the PM generators.
- Scheduled maintenance was increased for the additional generators.

- O&M was eliminated for the coupling and gearbox mounting, which are not part of the multi-PM design.
- Generator replacement equipment costs were eliminated because an on-board hoist could be used to change multi-PM generators.
- The gearbox replacement duration and staffing was increased to take into account the difficulty of replacing the integrated gearbox.

Table 9-3. Multi-PM O&M and LRC Estimates

	Multi PM		Baseline
	$/yr	$/kWh	$/yr
Unscheduled maintenance	9,675	0.0019	12,103
Scheduled maintenance	7,228	0.0014	6,004
Operations	6,501	0.0013	6,501
Subtotal, O&M (excluding LRC)	**23,404**	**0.0047**	**24,608**
LRC (major overhauls)	**4,516**	**0.0009**	**5,124**
Total O&M and LRC	27,921	0.0056	29,732

The multi-PM scheduled and unscheduled maintenance costs, combined with the LRC from Table 9-3, are compared to the corresponding baseline drive train estimates in Figure 9-12 on a component-by-component basis. Only drive train components are included because the cost contribution of other turbine components is the same for both designs. The contribution from the multi-PM transmission system is lower than that from the baseline, but the contribution from the multi-PM generators is higher.

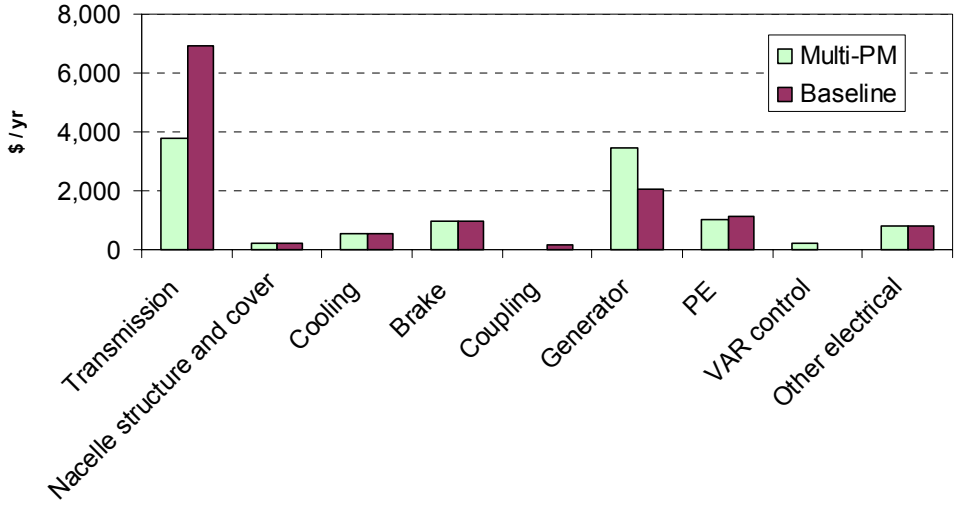

Figure 9-12. Scheduled and unscheduled maintenance costs and LRC compared to baseline by component

9.4.5 Multi-PM Cost of Energy Estimates

Table 9-4 presents the COE estimates for the multi-PM design. The COE estimate for this design is 0.0317 $/kWh, a reduction of approximately 11% relative to the 1.5-MW baseline estimate. This COE benefit is realized for three primary reasons:

- Decreased drive train component costs, primarily as a result of decreased transmission system and support structure costs (see Figure 9-11).
- Increased energy capture, resulting from higher generator and PE system efficiencies.
- Reduced O&M costs and LRC, reflecting reduced maintenance time and lower component costs.

Table 9-4. Multi-PM Drive Train COE Estimates, Compared to Baseline

	Multi-PM		Baseline
	Cost, $	% of COE	Cost, $
Capital Costs			
Turbine	**872,718**	**58.4**	1,001,491
Rotor	**248,000**	**16.6**	248,000
Drive train and nacelle	**324,652**	**21.7**	430,778
Yaw drive and bearing	**16,000**	**1.1**	16,000
Control, safety system	**7,000**	**0.5**	7,000
Tower	**184,000**	**12.3**	184,000
Turbine manufacturer's overhead and profit (30%, tower, rotor, and transformer excepted)	**93,878**	**6.2**	126,229
Balance of station	**358,000**	**23.9**	358,000
ICC	**1,230,718**	**82.3**	1,359,491
AEP			
Ideal annual energy output, kWh	5,628,000		5,479,000
Availability, fraction	0.95		0.95
Losses, fraction	0.07		0.07
Net AEP, kWh	**4,977,685**		4,840,697
Replacement costs, LRC, $/yr	**4,516**	**2.9**	5,124
FCR, fraction/yr	**0.106**		0.106
O&M, $/kWh	**0.0047**	**14.8**	0.0051
COE = O&M + ((FCRxICC)+LRC)/AEP	**0.0317**		0.0358

9.5 Multi-PM Scaling to 750 kW and 3 MW

To scale the 1.5-MW multi-PM design to the smaller and larger sizes, the techniques described in Section 9.3.4 and Appendix C were used. These techniques are designed to optimize the 1.5-MW design for different numbers of generators and diameters. Spreadsheets similar to the one shown in Appendix C were developed for the two scaling sizes, and the number of generators and the system diameter was optimized for both scaling sizes. The optimum 750-kW system uses six generators and has a 2.75-m diameter. The optimum 3000-kW system uses seven generators and has a 4.0-m diameter.

Table 9-5 summarizes the results of this scaling process. These results are compared graphically in terms of the drive train COE in Figure 9-13. The drive train COE represents the portion of the turbine COE attributed to the drive train capital cost alone. Relative to the 1.5-MW multi-PM drive train, the 750-kW version is characterized by a higher normalized capital cost (in dollars/kilowatt) and a higher COE. The 3-MW variation has a capital cost and a COE that are approximately equal to those of the 1.5-MW system. The entries in Table 9-5 give some insight into the reasons for these cost relationships. It appears that several major costly subsystems, including the transmission system, support structure, and nacelle cover, diminish in normalized capital cost as the power rating increases from 750 kW to 1.5 MW.

However, these subsystems do not diminish in cost further as the power rating is increased from 1.5 MW to 3 MW, giving no advantage to increasing the power rating beyond 1.5 MW.

Table 9-5. Multi-PM Drive Train Component Cost Scaling to 750 kW and 3 MW

	750 kW		1.5 MW		3 MW		Method
	Cost, $	Cost/kW	Cost, $	Cost/kW	Cost, $	Cost/kW	
Transmission system	32,590	43	57,728	38	116,960	39	
Gearbox components	*29,793*	*40*	*53,184*	*35*	*91,379*	*30*	PEI input
Mainshaft	*2,797*	*4*	*4,544*	*3*	*25,581*	*9*	PEI input
Support structure (integrated nacelle)	*13,262*	*18*	*18,671*	*12*	*37,831*	*13*	PEI input
Gearbox and generator cooling system	*3,123*	*4.2*	*5,341*	*3.6*	*5,795*	*1.9*	PEI input
Brake system with hydraulics	*3,161*	*4.2*	*6,698*	*4.5*	*9,510*	*3.2*	PEI input
Coupling	*NA*		*NA*		*NA*		
Nacelle cover	*6,173*	*8*	*7,299*	*5*	*8,828*	*2.9*	PEI input
Generators	40,980	55	77,965	52	182,392	61	Unit-pole scaling
Power Electronics	*26,560*	*35*	*53,119*	*35*	*106,238*	*35*	Power rating
0.95–0.95 substation VAR control	*5,779*	*8*	*11,557*	*8*	*23,114*	*8*	Power rating
Transformer	*12,938*	*17*	*25,875*	*17*	*51,750*	*17*	Power rating
Cable	*8,023*	*11*	*16,046*	*11*	*32,092*	*11*	Power rating
Switchgear	*5,233*	*7.0*	*10,465*	*7.0*	*20,930*	*7.0*	Power rating
Other subsystems	*12,500*	*17*	*25,000*	*17*	*50,000*	*17*	Power rating
Drive train assembly and test	*7,704*	*10*	*7,888*	*5.3*	*8,814*	*2.9*	PEI input
Drive train and nacelle total	**178,024**	**237**	**237**	**216**	**654,254**	**218**	

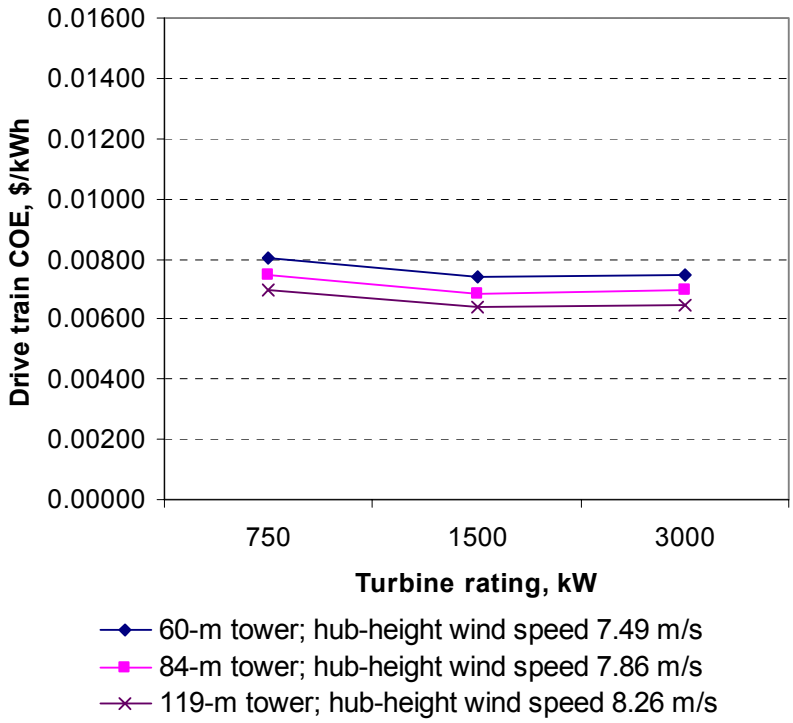

Figure 9-13. Multi-PM drive train COE scaling for different hub height wind speeds

10. Multi-Induction Drive Train

The multi-induction drive train is similar to the multi-PM drive train, using induction generators and an additional gearbox stage in place of the medium speed multi-PM generators. Initial estimates showed that this design has a favorable cost of energy relative to the baseline design and a detailed preliminary design was developed for that reason. Final estimates confirm the low cost of energy, which results primarily from the low cost of the multiple-output gearbox.

10.1 Multi-Induction System Description

The 1.5-MW multi-induction generator drive train is illustrated in Figure 10-1, and a system diagram is shown in Figure 10-2. The mechanical design is similar to the multi-PM drive train design described in Section 9. The same short-coupled mainshaft with bearings integrated into a common housing with the gearbox is used. Like the multi-PM design, the gearbox has a single, large-diameter bullgear driving multiple pinions. In the case of the multi-induction design, however, the pinions drive multiple secondary, parallel axis gear stages that are integrated into the same housing as the first stage. Each gearbox output drives a generator. The generators are electrically connected directly to the grid through the pad mount transformer. No variable-speed power electronics are used, so the design operates at constant speed.

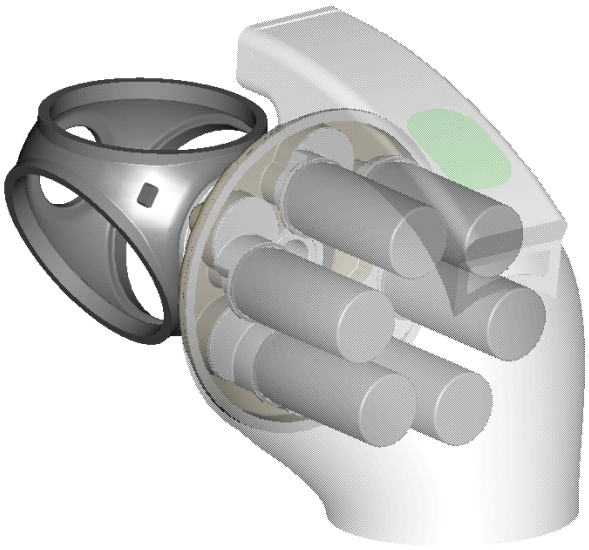

Figure 10-1. WindPACT multi-induction generator drive train

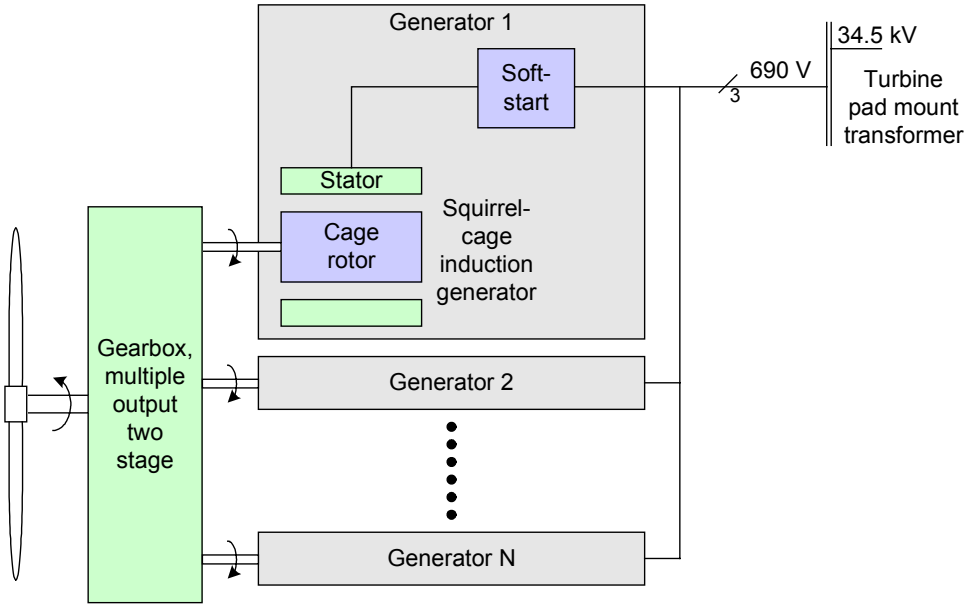

Figure 10-2. Multi-induction generator system diagram

10.2 Multi-Induction Design Alternatives

The WindPACT multi-induction drive train described in the preceding subsection could be designed in a number of different ways. Several alternatives were considered early in the study before focusing on the selected design. Some of these design alternatives are described below, along with the reasons that they were considered less attractive than the design selected for this study:

- **Modular bedplate design:** The bedplate multi-induction design shown in Figure 10-3 was considered early in the study. This design uses a bedplate structure similar to the baseline drive train to support a double-sided gearbox and generator arrangement. The second stages of the gearbox in this design are not integrated with the main gearboxes but are separate units. A 12-generator design is shown in the figure, but other numbers of generators were also investigated. This design was not selected because initial estimates showed the component costs to be higher than those of the selected integrated design.

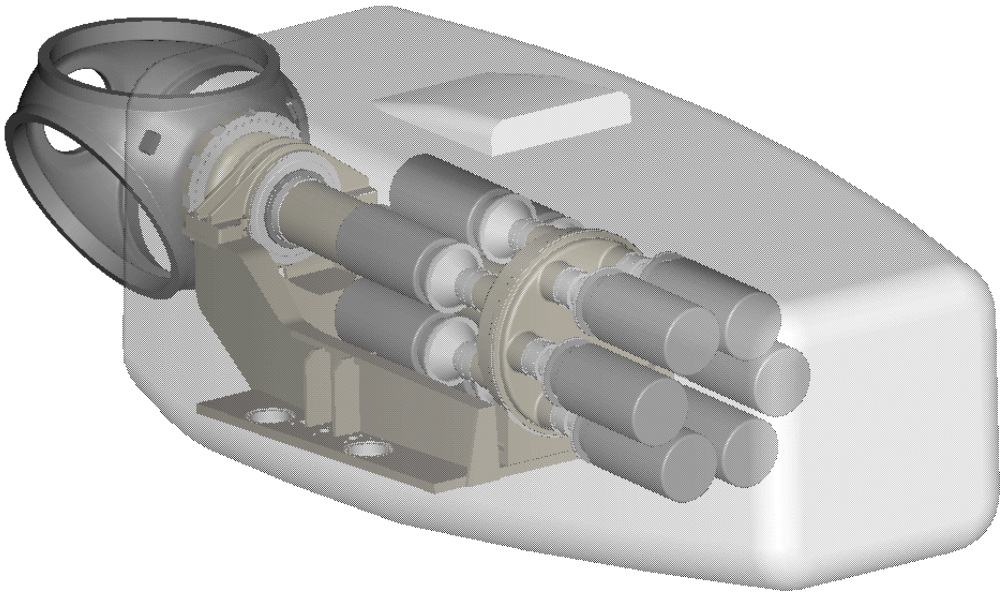

Figure 10-3. Bedplate multi-induction design

- **Variable-speed power electronics with doubly fed induction generators:** The feasibility of using multiple doubly fed induction generators, each controlled by a partially rated variable-speed PE system, was considered. This system would be the equivalent to the baseline generator and PE system. However, the costs of both the wound-rotor generators and the variable-speed electronics increase substantially for multiple generators, making this system less cost-effective than the fixed-speed system that was chosen.

- **Variable-speed power electronics with squirrel-cage induction generators:** Multiple squirrel-cage induction generators with full-rated variable-speed power electronics were considered. However, the cost of the power electronics for this system does not make it cost-effective compared to the selected fixed-speed design.

- **Squirrel-cage generators with variable-voltage torque control:** A low-cost SCR-based PE system capable of limiting gearbox torque by controlling the voltage of the squirrel-cage induction generators was investigated. This system does not give variable-speed performance below rated speed, but it does allow the speed to increase in a limited range above rated to limit torque. Figure 10-4 shows the circuit for one generator phase. This system takes advantage of the increase in breakdown torque and associated change in the speed-torque relationship of induction machines that results from the reduction in terminal voltage. To allow a speed variation above rated of approximately 10% while maintaining rated torque, the terminal voltage of the generator must be reduced by approximately 40%. Although this system does appear to be feasible, rough estimates indicated that it was less cost-effective than the selected fixed-speed system.

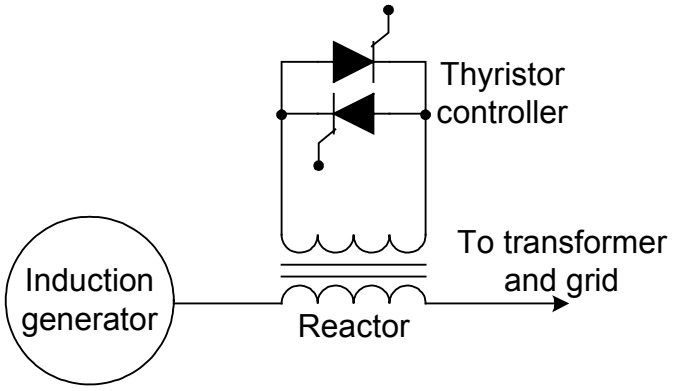

Figure 10-4. Thyristor voltage control system, one of three phases

10.3 Multi-Induction Component Designs

A similar approach was used to analyze the multi-induction component costs to the approach taken for the multi-PM analysis. Both systems have component costs that are highly dependent on the choice of system diameter and number of generators. Preliminary estimates were initially made for a six-generator, 2.85-m diameter base system. PEI developed a complete Pro/E model of the mechanical design and determined component sizes and masses. Parameterized spreadsheets were then developed from the base design to estimate component sizes, masses, and costs for other system diameters and numbers of generators. The spreadsheet estimates are based on the ratios of component masses to the masses of similar components used in other designs for which detailed cost estimates had been developed. Using these spreadsheets, the minimum-cost multi-induction system, at 1.5 MW, was determined to have eight generators and a 2.5-m diameter.

The component designs developed for the six-generator, 2.85-m diameter system are described in Sections 9.3.1 through 9.3.3. Estimates for other system diameters and numbers of generators, including the lowest cost system with eight generators and 2.5-m diameter, are given in Section 9.3.4.

All multi-induction design estimates were made using load estimates for the baseline system. These load estimates were modified for the lack of torque limiting without a variable-speed PE system. Annual energy capture calculations, as described in Section 10.5.2, were made for fixed-speed operation at 17.2 rpm, a reduction of approximately 15% from the baseline rated speed of 20.5 rpm. The additional loading resulting from the reduced operating speed was neglected. This approximation favors the multi-induction system.

10.3.1 Mechanical Design

Figure 10-5 depicts the mechanical design. The general design of this configuration follows the principle of shared function material wherever possible, an approach that is intended to reduce mass and cost and that leads to a high degree of integration. The mainshaft functions as the carrier of the hub and also of the bullgear. The gear casing is the envelope of gears but also serves as the generator frame.

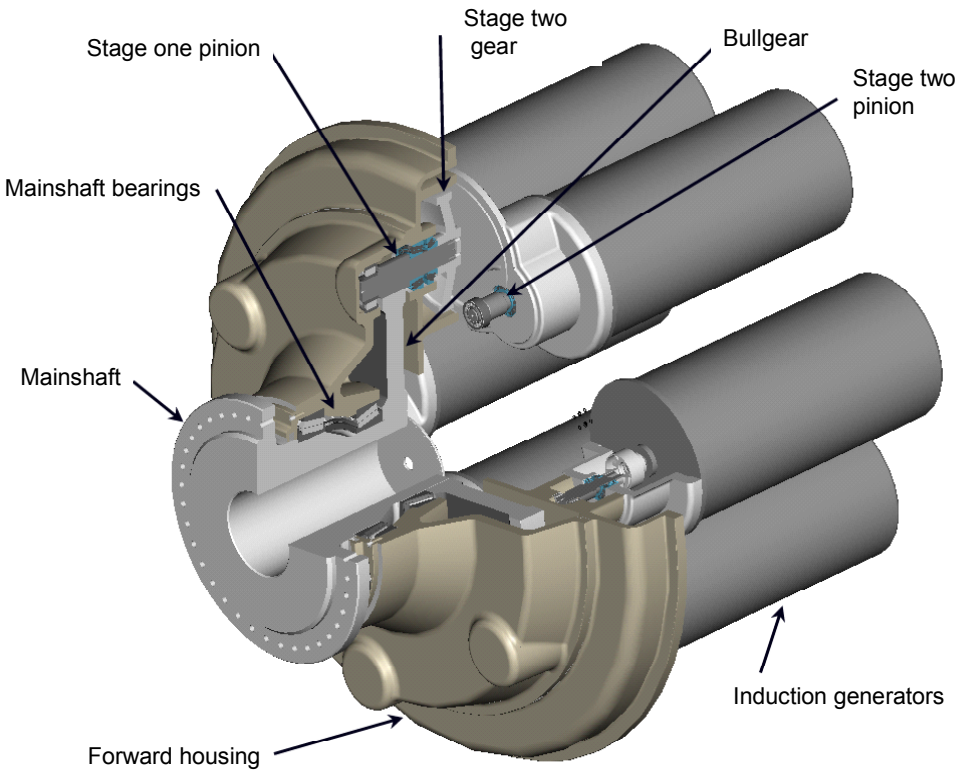

Figure 10-5. Multi-induction drive train mechanical design

10.3.1.1 Bearings, Mainshaft

Figure 10-6 illustrates the internal construction. The bearing arrangement and estimates from the single PM design, described in Section 7.3.1.1, is used. Note the integral mainshaft and use of separated tapered-roller mainshaft bearings. These bearings are ideal for handling combined thrust and radial loads. By spreading the bearings apart, large moments are reduced. This permits the use of smaller diameter bearings compared to the case where the bearings are closely spaced, as in back-to-back mounting. The smaller diameter bearings were preferred because (1) they are lower in cost, with numerous suppliers; (2) they can be included in forced-oil systems and are therefore easy to lubricate; and (3) they can use reliable labyrinth seals.

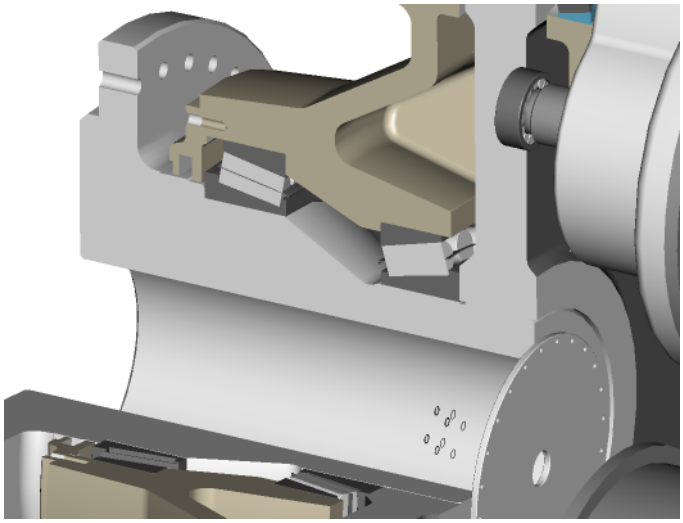

Figure 10-6. Section close-up of multi-induction mainshaft

10.3.1.2 Gears

To account for the lack of generator torque control in this configuration, the standard load profile, as described in Section 3.3, was factored by the ratio 750:550. This ratio represents the typical capacity upgrade for gearboxes designed for variable-pitch, single-speed induction machines, reapplied to variable-pitch, variable-speed, torque-controlled machines.

Gear design is based on AGMA 2001 C95 ratings, utilizing a Miners Rule analysis and GEARTECH 218 software. For preliminary design, the design meets the 30-yr life objective, with a design margin of 20% (Sf = 1.2) to allow for load uncertainty and for conservatism. The significant factors such as J and I are derived from the sample rating and used in the parametric spreadsheets to accurately estimate gear size in the 120 configurations analyzed.

The helical involute gears are designed with a conservative aspect ratio of approximately 1:1. Helical overlaps are approximately 2.0. A quality level of AGMA 2000, Class 12 is assumed. Gearing meets the requirements of AGMA 2001 C95 Grade 2.

10.3.1.3 Stressed-Skin Nacelle

This system is supported by an aggregated nacelle, which acts as an enclosure as well as a structural support for rotor loads. This component was developed with sufficient detail to validate the concept. Loads are described in Section 3.3.

Figure 10-7 shows the results of a preliminary FEA analysis.

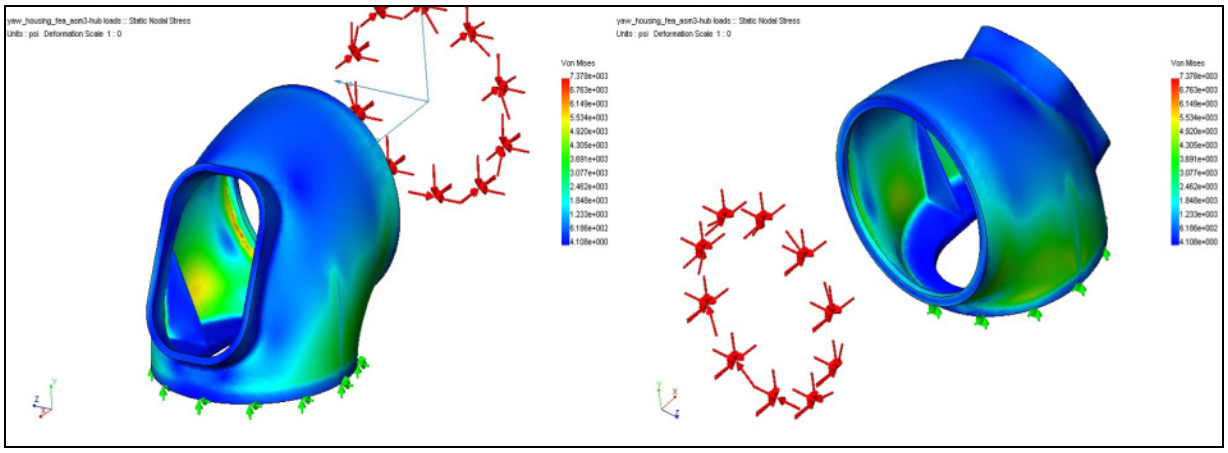

Figure 10-7. FEA on stressed-skin nacelle

For this analysis, an equivalent fatigue load in each axis was computed with a material exponent of 8. The moments and forces were combined per Germanischer Lloyd rules, and applied at the rotor hub center line. A conservative allowable stress of 7,500 psi is used to develop the section sizes.

10.3.1.4 Nacelle Cover

For the multi-induction stressed-skin nacelle, the outer surface is also the enclosure that separates the machinery from the outdoors. There is, however, a large opening used for assembly access and for housing cooling equipment. This may include scoop-like ducts to provide sufficient area and velocity of cooling air along with the necessary cover. Any required covers and ducts will be built of fiberglass.

The mass of this cover and duct assembly is estimated as a ratio of the stressed-skin structural nacelle mass. This is a first-order estimate following the general size of the system. Cost is computed from this mass estimate using the fiberglass cost per kilogram rate described in Section 4.6.11.

10.3.2 Electrical System

The multi-induction electrical system is shown in Figure 10-8, and Appendix I includes a complete one-line diagram. Each 690-V squirrel-cage induction generator is connected to a soft-start controller through a contactor and circuit breaker. The soft-starts are used to incrementally engage and disengage the generators as the turbine output power changes with wind speed. At the turbine cut-in wind speed, only one generator is engaged. As wind speed increases, additional generators are incrementally engaged until at rated wind speed, all the generators are engaged. Incremental engagement is used to keep the generators operating near their rated power level to maximize efficiency. The soft-start circuits are connected to the generators through a contactor and circuit breaker. The soft-starts are connected to the pad mount transformer through a common circuit breaker. Power factor correction capacitors are connected to the 690-V side of the pad mount transformer to correct the power factor of the induction generators to 0.95 lagging. Wind farm VAR control is used to provide 0.95 lagging–0.95 leading power factor at the substation.

Individual components of this system and the cost estimates for each are described in the subsections that follow.

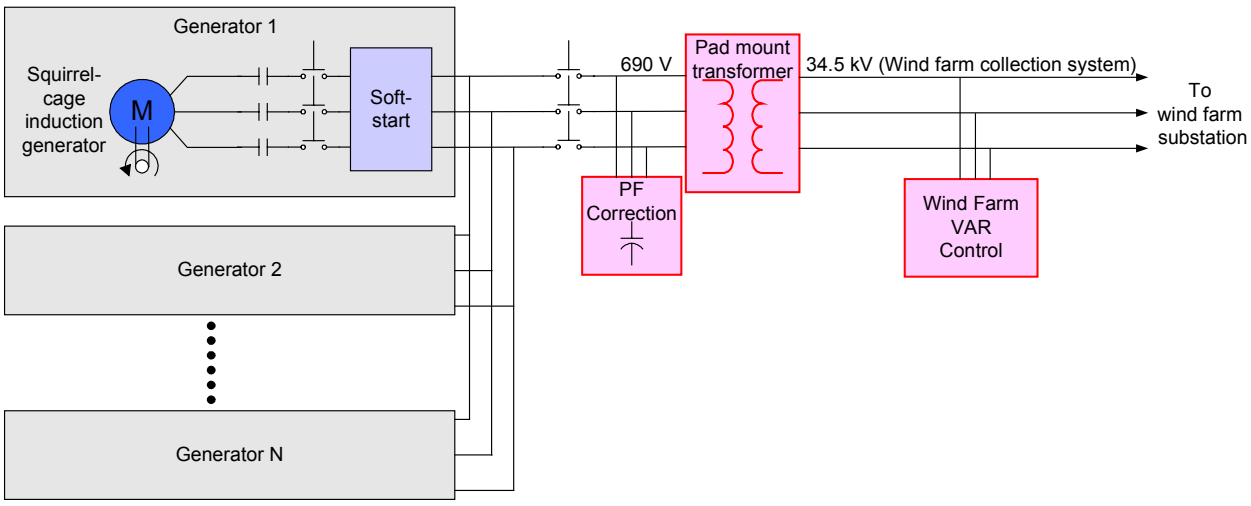

Figure 10-8. Multi-induction electrical system

10.3.2.1 Generator

The multi-induction generator specifications are listed in Table 10-1. These requirements are similar to those for generators used in a number of European turbines, with the exception that the specified frequency is 60 Hz for the intended U.S. application. The cost of an external liquid cooling system is included as a separate item in the WindPACT estimates, although liquid cooled generators in the smaller sizes are less common and air cooling could be used.

Table 10-1. Multi-Induction Generator Specifications

Type	Squirrel-Cage Induction Generator
Voltage	690 V line-line
Pole number	4
Frequency	60 Hz
Construction	IP54 protection
Cooling	Air or liquid

Several manufacturers produce squirrel-cage induction generators with specifications similar to those described above in the 75-kW to 500-kW range of ratings necessary for a 3- to 20-generator, 1.5-MW design. The same three manufacturers that supplied information for the baseline generator provided price quotes and other information, and Table 10-2 gives the quoted generator prices. The first two manufacturers currently supply generators to wind turbine manufacturers, although the U.S. division of Manufacturer #2, which quoted the squirrel-cage prices, has not yet built generators for the wind application. The third manufacturer has not yet produced generators for wind turbines. All quoted prices were based on 1500-kW turbine quantities of between 100 and 600 per year and for generators sold to turbine manufacturers. The quotes from the first manufacturer are clearly much lower than the other two. A sales manager familiar with recently negotiated sales to the wind industry quoted these prices informally. Most likely these prices include the true discounts given to turbine original equipment manufacturers; the other two manufacturers supplied quotes that were not discounted appropriately. For this reason, the quotes from Manufacturer #1 were considered more reliable and were used directly for the cost estimates in the study.

All three manufacturers quoted prices for air-cooled generators. Manufacturer #1 quoted 50-Hz generator prices, which should be slightly more expensive than 60-Hz equivalents.

Table 10-2. Squirrel-Cage Generator Quotations

Rating, kW	Manufacturer #1, $	Manufacturer #2, $	Manufacturer #3, $
500	15,714	36,547	28,000
375	11,249	28,547	17,680
300	8,857	25,534	13,400
250	7,540	22,384	12,150
150	4,215	17,203	9,420
100	2,762		8,250
75	2,071		7,150

Notes: All quotes are for 4-pole, IP54, flanged air-cooled generators. Manufacturer #1 generators are 50 Hz. Generators from manufacturers #2 and #3 are 60 Hz.

Figure 10-9 shows the total cost of the complete 1500-kW generator set using different numbers of generators. The Manufacturer #1 quotes from Table 10-2 are used. The total generator cost is approximately $40,000 to $50,000 regardless of the number of generators used. The total generator cost increases slightly for the largest machines. The smaller generators have the benefit of higher quantity production for other applications, either for generator components or in some cases, for assembled generators.

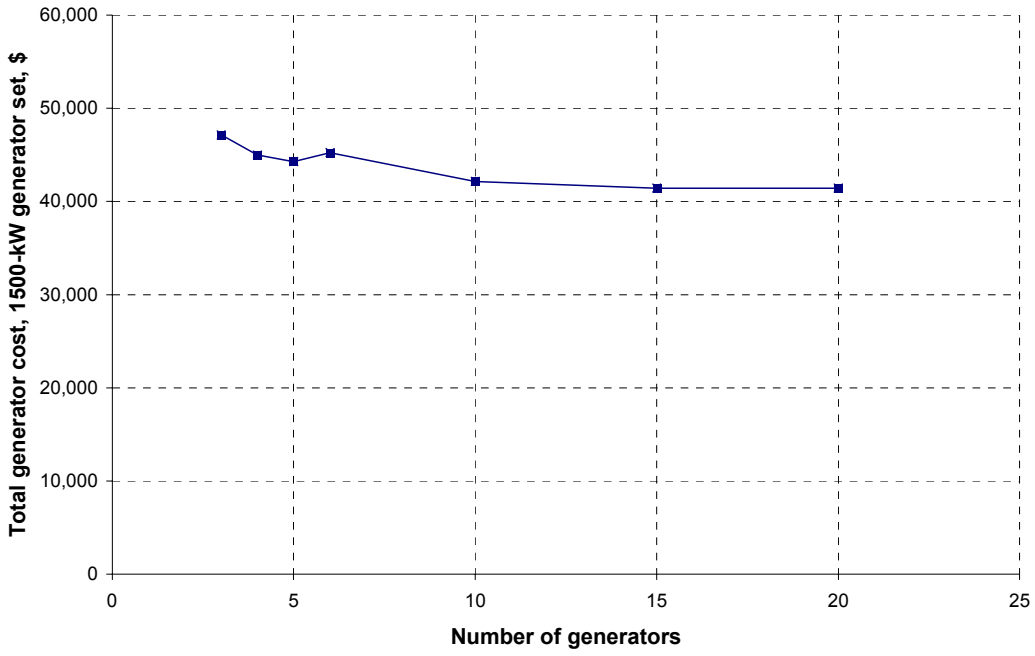

Figure 10-9. Total squirrel-cage generator (1.5 MW) cost versus number of generators

Efficiency and power factor data were provided by Manufacturer #1 for the complete range of generators. Table 10-3 lists the full load efficiencies and power factors for generators rated from 75 kW to 1.5 MW. The efficiency is lower for the smaller generators. Power factor does not change significantly with generator size. Figure 10-10 shows the normalized efficiency and power factor versus load curves, and this figure is applicable to all the generator sizes listed in Table 10-3. The full load efficiency or power factor for a specific generator may be multiplied by the normalized curves to give the specific curves applicable to each generator size.

Table 10-3. Full Load Efficiency and Power Factor for Different Generator Sizes

Rating, kW	Efficiency, Rated Load	Power Factor, Rated Load
1500	97.1	0.87
1000	96.6	0.86
750	97.1	0.88
500	96.8	0.87
300	96.5	0.87
250	96.4	0.87
150	95.6	0.86
100	95.1	0.88
75	94.6	0.88

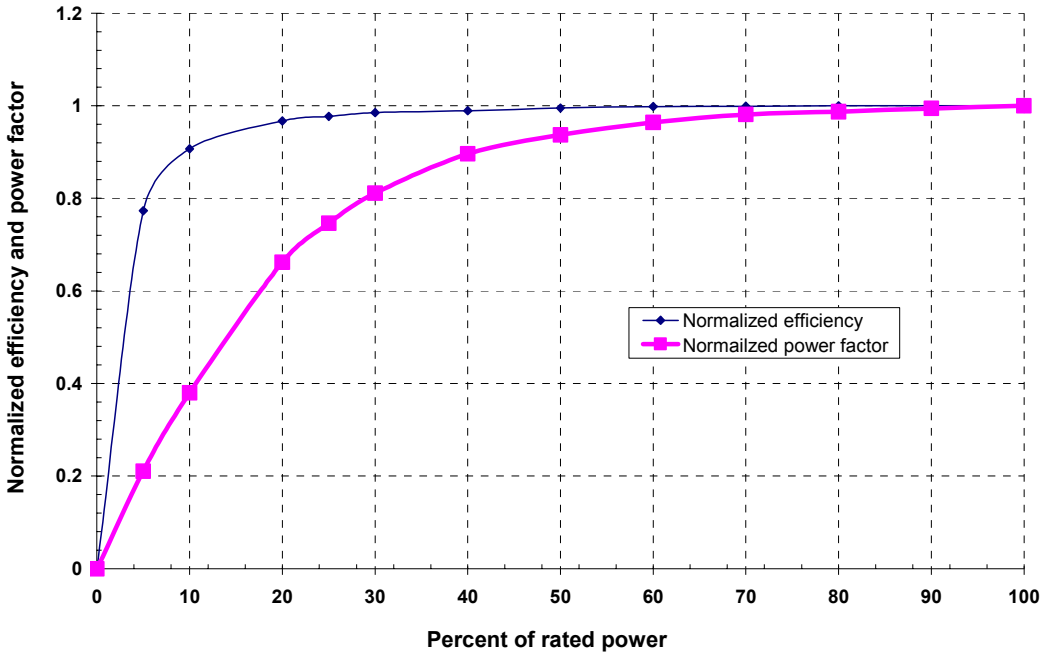

Figure 10-10. Normalized efficiency and power factor versus load

The multi-induction system is operated with incrementally engaged generators to maximize generator efficiency at lower wind speeds. Calculations of the generator efficiency for this system are included in Appendix G, and the resulting efficiency curve is included in Figure 10-14 along with the multi-induction results. These calculations are based on the efficiency data and curves provided in Table 10-3 and Figure 10-10.

10.3.2.2 Soft-Start and Power Factor Correction

Soft-start and power factor correction estimates made for the Henderson drive train, described in Section 13.3.3, were used for the multi-induction drive train. These soft-start estimates are for a single 1.5-MW generator. Estimates for multiple generators were not made.

10.3.2.3 Switchgear

A complete one-line diagram and switchgear estimate for a six-generator system is included in Appendix I. The highest cost items are the individual contactors and circuit breakers necessary for each generator. Switchgear costs were estimated only for the six-generator system and the same estimate was used for other systems with different numbers of generators.

10.3.2.4 Cable

The multi-induction cable estimate is included in Section 4.11.1. The required cable for this system is approximately the same as the one used in the baseline system.

10.3.2.5 Pad Mount Transformer

The multi-induction design uses the same pad mount transformer as the baseline design.

10.3.2.6 VAR Control

The cost of substation VAR control was included in the multi-induction estimates because the turbine electrical system does not include a PE converter that furnishes that function. VAR control system estimates are described in Section 4.11.3.

10.3.3 Ancillary Components

10.3.3.1 Gearbox Cooling System

The estimated heat capacity for the gearbox cooler is 21.7 hp. Using the calculation methods described in Section 4.6.9, costs were estimated based on this capacity.

10.3.3.2 Generator Cooling System

Because the induction generators are air-cooled, an external liquid-cooling system is unnecessary.

10.3.3.3 Brake System

A detailed brake design was not developed for the multi-induction design. Brakes can be implemented either at the generator coupling or within the generators. The specific number of brake discs and calipers varies depending on the number of generators. Brake system cost estimates are included in the spreadsheets shown in Appendix C and were calculated using the methods described in Section 4.6.8.

10.3.3.4 Assembly and Test

The gearbox, being integral with the mainshaft and generator components, is based on assembly at the integrator of the mechanical system. For this, the methods described in Section 4.6.6 for the gearbox section were used, and the system-level assembly was added as shown in the parametric spreadsheets.

10.3.4 System Optimization for Generator Number and Diameter

Parameterized Excel spreadsheets were developed from the base 2.85-m diameter, six-generator design described in the previous sections to estimate component sizes, masses, and costs for other system

diameters and numbers of generators. The spreadsheet estimates are based on the ratios of component masses to the masses of similar components used in other designs, for which detailed cost estimates had been made. Using these spreadsheets, the minimum cost multi-induction system, at 1.5 MW, was determined to have eight generators and a 2.5-m diameter. A three-dimensional graphic, shown in Figure 10-12, was developed to visualize cost relationship to generator count and system size.

10.3.4.1 Details of the Parametric Study

The 2.5-m diameter parametric worksheet is included in Appendix C, along with a detailed description of the variables and calculations. The spreadsheets cover all combinations. In some cases the generators interfere; these cells are marked by highlighting. An equivalent worksheet was used for each diameter. The input is defined as the radius over the outside of the generator housing (r_outside; see Figure 10-11).

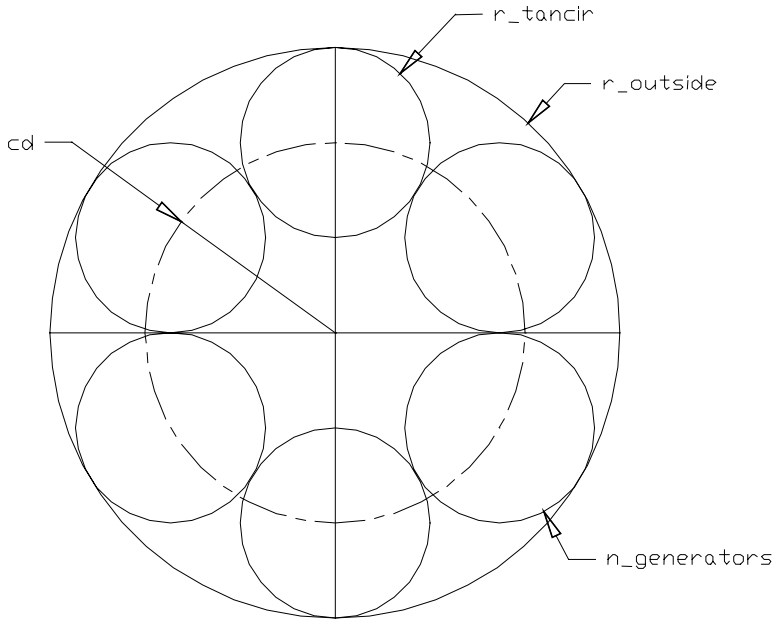

Figure 10-11. Schematic of system

The number of generators is varied from 3 to 14 per system in each worksheet. The system diameter is varied from 2.0 m to 4.0 m. The ranges are chosen to find the lowest system cost and to visualize the curve slope, or sensitivity, of the competing variables.

This analysis did not include any electrical components other than the generator. The PE system, transformer, cable, and switchgear costs were assumed to be constant and not included in this analysis.

10.3.4.2 Results of the Parametric Study

Figure 10-12 shows the results in terms of the total cost for the analyzed components. The results show the minimum cost at approximately 12 generators with a system radius of 1.25 m (2.5-m diameter). However, these results do not include the impact of system complexity on O&M. As Figure 10-12 shows very little cost penalty associated with reducing the number of generators to eight, this was selected as the preferred configuration.

Cost curves of individual system components are shown in Figure 10-13 at the 2.5-m system diameter. The total costs are largely driven by the gearbox cost, which increases significantly when fewer than eight or nine generators are used.

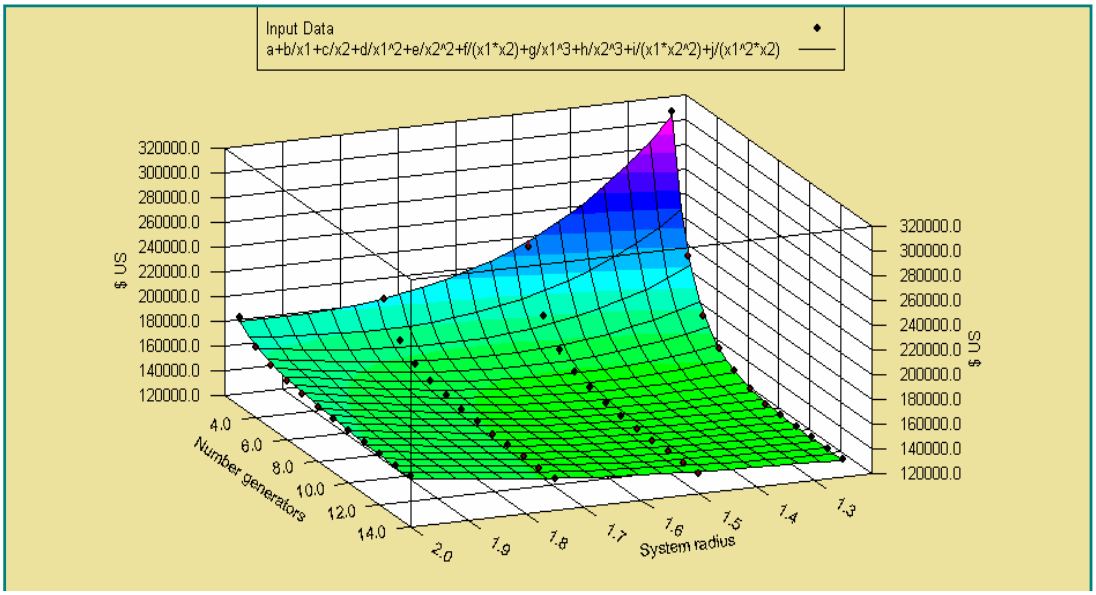

Figure 10-12. Three-dimensional representation of multi-induction optimization results

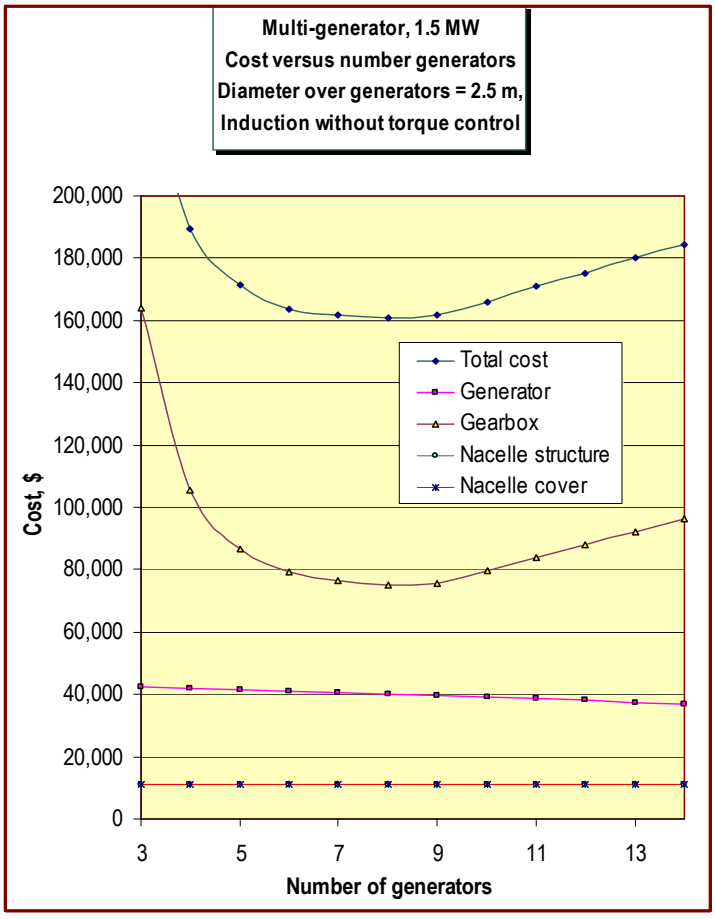

Figure 10-13. Summary of results for 2.5-m diameter system

10.4 Multi-Induction Controls Investigation

Clipper Windpower, LLC, investigated control methods for the multi-induction generator drive train. The results are applicable to both the selected design described in Section 9.3 and the alternative bedplate design shown in Figure 9-3. The primary objectives of this investigation were:

- To determine the inherent torque-matching between parallel, line-connected, mass-manufactured induction generators.
- To determine the feasibility of incrementally engaging the generators with increasing power to maximize efficiency at low system loads.
- To develop appropriate controls giving dynamic generator slip control to allow for gust energy absorption.

To perform this investigation, Clipper built and tested a lab-scale multi-induction generator system. This system used a gearbox with six pinions coupled to a large bullgear. One pinion was driven by a 3-kW, variable-speed drive motor. The remaining pinions drove five 0.5-kW squirrel-cage induction generators. The generators were either directly connected to the three-phase, 480-V utility power or were driven by an experimental PE system. A programmable Labview control system was used to monitor the generators and control the power electronics.

Clipper and NREL funded this investigation on a cost-share basis, and the detailed results are proprietary to Clipper. All results were disclosed to NREL and GEC under a proprietary agreement among the three parties, but are not described in this report. The general results were:

- Excellent load torque-matching was measured among the five parallel, line-connected induction generators. Standard induction generators with no modifications were tested.
- Incremental engagement of multiple generators is a feasible method for maximizing generator efficiency at low power. A system using stator voltage modulation during the engagements was demonstrated, which smoothly brought individual generators on and off line.
- A control scheme that makes use of stator voltage control was developed. This system gives a viable means of controlling generator torque.
- Voltage control of induction generators has significant positive impacts on both generator efficiency and power factor.

10.5 Multi-Induction Results

The following subsections summarize all cost and energy production estimates for the 1.5-MW multi-induction generator drive train design described in Sections 10.1 and 10.3.

10.5.1 Multi-Induction Efficiency

Figure 10-14 shows drive train efficiency versus input power on a component-by-component basis, with the total drive train efficiency of the baseline system given for comparison. The multi-induction drive train efficiency is approximately equal to the baseline design's efficiency at medium to rated power but has reduced efficiency below approximately 10% power. Several factors determine the multi-induction design's efficiency:

- The system operates at fixed speed, which increases gearbox losses at low power relative to the variable-speed baseline drive train. The fixed-speed gearbox efficiency measurements presented in GEC (2002) were used for these estimates.
- There are no variable-speed power electronics, eliminating associated losses.
- Smaller generators are used; each has lower full-load efficiency than the baseline generator.

- The generators are incrementally engaged, as described in Sections 10.3.2 and 10.3.2.1, which operates each connected generator at a higher percentage of rated power than the generator in an equivalent, single generator turbine at partial load.

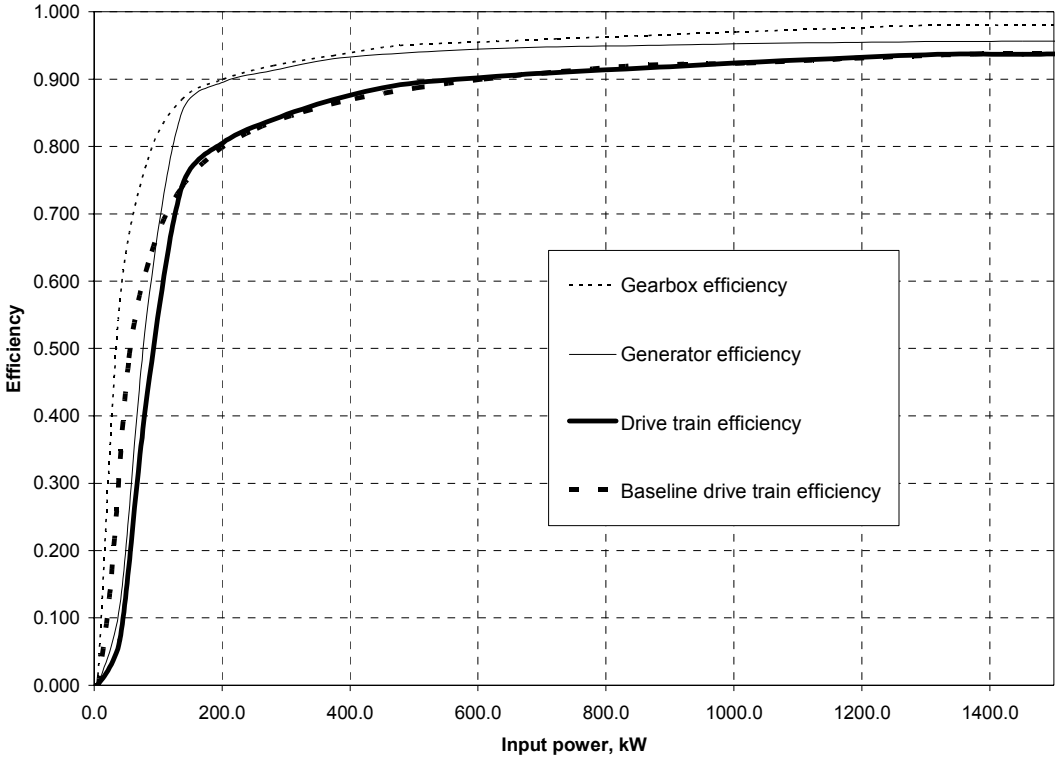

Figure 10-14. Multi-induction drive train efficiency by component

10.5.2 Multi-Induction Gross Annual Energy Production

Table 10-4 shows the ideal energy production estimate for each wind speed bin. Drive train efficiency losses are included in this estimate. All other losses are calculated separately in the final COE analysis. The wind speed bins from 12.0 m/s to the cut-out speed of 27.5 m/s are aggregated in a single row. The energy productions for those wind speed bins are identical to those for the baseline turbine, shown in Table 5-3, with the rotor speed at rated and the output power regulated to 1.5 MW by the pitch system. The total GAEP from the multi-induction design is estimated at 5273 MWh, which is approximately 4% less than the estimated production of 5479 MWh for the baseline design. The multi-induction has lower energy capture than the baseline system because it is a constant-speed design, with no variable speed below rated wind speed. The efficiency of the multi-induction design is also lower than that of the baseline design below about 10% power, as shown in Figure 10-14, but this has less effect on energy capture.

An optimization of the constant operating speed for the multi-induction design was necessary to maximize the GAEP. The variable-speed baseline design operates at a constant rotor TSR to operate at a maximum blade performance coefficient (C_p) at all wind speeds below rated. The multi-induction design, by comparison, has a rotor TSR that changes with wind speed because of the constant-speed operation. The optimum TSR and maximum C_p therefore occur at only one wind speed, and the C_p decreases as the wind speed increases or decreases from this optimum point. This effect reduces the GAEP of the multi-induction design relative to the baseline design. To determine the optimum fixed operating speed for the

multi-induction design, the GAEP was iteratively calculated and the fixed speed was adjusted. The energy production is maximized at a fixed operating speed of 17.2 rpm, which is about 84% of the 20.5-rpm rated speed for the baseline design. These effects can be seen in Figure 10-15, which compares the energy production of the multi-induction to that of the baseline designs by wind speed bin (below rated wind speed). Above rated wind speed, the power output is regulated to 1.5 MW and the energy production levels of the two designs are equal. The energy production levels of the two designs are also approximately equal at a wind speed of 9.0 m/s. At this wind speed, the baseline design operates at approximately 17.2 rpm, the same speed as the multi-induction design. Consequently, both designs operate with the same optimum rotor TSR. The slight difference in energy production results from the different drive train efficiencies. At higher and lower speeds, however, the multi-induction design operates away from optimum TSR, producing less energy than the baseline design. Adjusting the multi-induction operating speed to 17.2 rpm puts the wind speed for optimum blade performance near the middle of the subrated wind speed range, maximizing the annual energy capture.

To simplify the optimization described above, the small amount of speed change that results from generator slip was neglected and a fixed rotor speed was used for all wind speed bins.

Table 10-4. Multi-Induction Drive Train GAEP

Wind Speed Bin Center, m/s	Rotor Speed, rpm	Rotor Power, kW	Drive Train Efficiency	Output Power, kW	# of Hours per Year	Energy Production	
						MWh	Fraction of Total, %
3.0	17.20	0.0	0.000	0.0	297.5	0	0.00
3.5	17.20	0.0	0.000	0.0	333.1	0	0.00
4.0	17.20	5.1	0.000	0.0	363.0	0	0.00
4.5	17.20	40.2	0.067	2.7	386.9	1	0.02
5.0	17.20	83.7	0.437	36.6	404.7	15	0.28
5.5	17.20	137.2	0.740	101.6	416.5	42	0.80
6.0	17.20	201.9	0.806	162.8	422.4	69	1.30
6.5	17.20	280.0	0.840	235.2	422.7	99	1.89
7.0	17.20	373.1	0.870	324.5	417.8	136	2.57
7.5	17.20	478.5	0.892	426.7	408.3	174	3.30
8.0	17.20	598.1	0.902	539.4	394.7	213	4.04
8.5	17.20	724.0	0.910	658.9	377.7	249	4.72
9.0	17.20	866.4	0.917	794.5	357.8	284	5.39
9.5	17.20	1003.3	0.924	927.1	335.9	311	5.91
10.0	17.20	1153.4	0.931	1073.3	312.4	335	6.36
10.5	17.20	1317.7	0.937	1234.4	288.0	355	6.74
11.0	17.20	1451.5	0.937	1360.2	263.2	358	6.79
11.5	17.20	1591.7	0.938	1493.0	238.5	356	6.75
12.0-27.5	17.20	1599.1	0.938	1500.0	1516.1	2274	43.1
					Total GAEP =	**5273 MWh**	

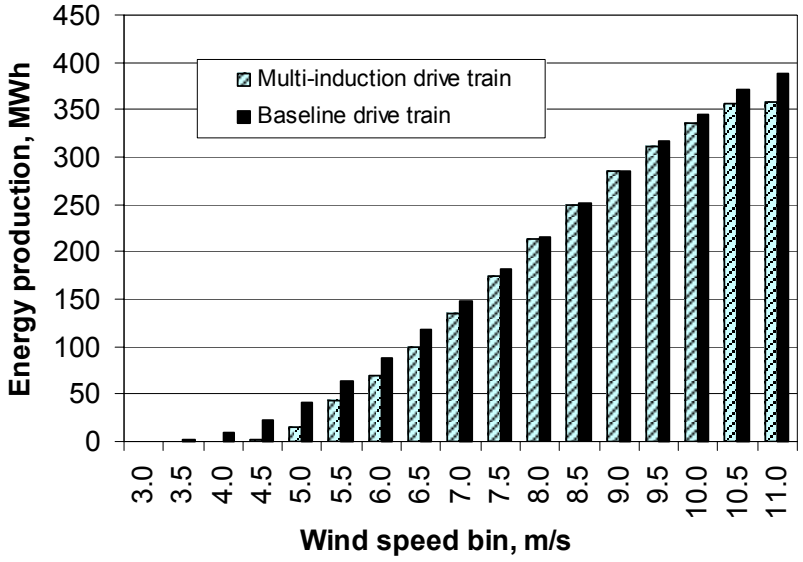

Figure 10-15. Multi-induction and baseline energy production by bin

10.5.3 Multi-Induction Component Costs

Component costs for the multi-induction drive train are itemized in Table 10-5.

Table 10-5. Multi-Induction Drive Train Component Costs

Component	Cost, $
Transmission system	**80,000**
Gearbox components	75,000
Mainshaft	4,500
Support structure (integrated nacelle)	**11,000**
External gearbox and generator cooling system	**4,400**
Gearbox cooling	2,200
Generator cooling	2,200
Brake system with hydraulics	**2,800**
Coupling (generator to gearbox)	**1,800**
Nacelle cover	**13,100**
Generators	**40,000**
Power electronics (soft-start & power factor caps)	**17,048**
0.95–0.95 substation VAR control	**12,000**
Transformer	**23,000**
Cable	**18,000**
Switchgear	**22,000**
Other subsystems	**25,000**
Drive train assembly and test	**10,200**
Total	**279,000**

Note: All costs rounded.

The component costs itemized in Table 10-5 are compared to the baseline component costs in Figure 10-16. The multi-induction design has a significantly lower component cost total than the baseline. Most of the difference can be attributed to savings in the transmission system and the elimination of the PE system. The transmission system cost is reduced primarily because the gear design with a single large bullgear driving multiple pinions and secondary gear sets has low material content and a simple construction relative to other gear designs. The integrated design with a close-coupled mainshaft also reduces cost relative to the baseline bedplate system. The stressed-skin nacelle used in the integrated design has lower support structure costs.

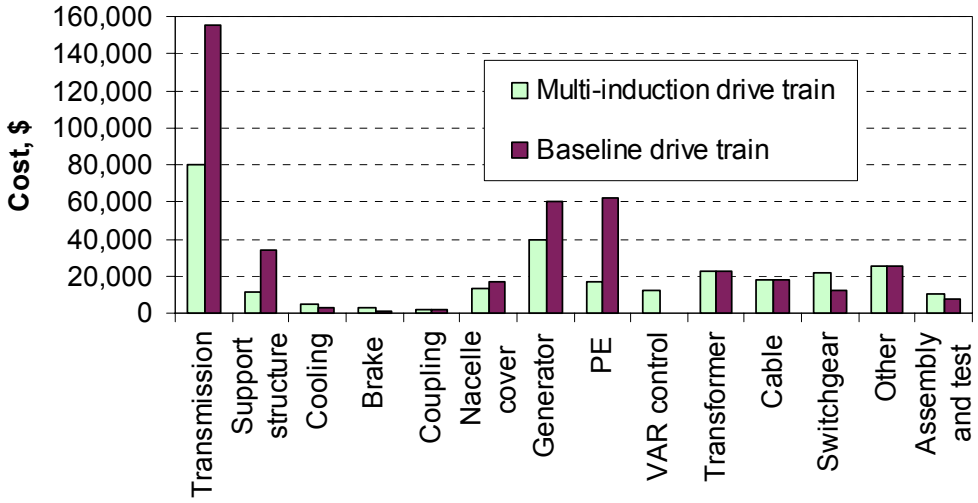

Figure 10-16. Multi-induction and baseline component cost comparison

10.5.4 Multi-Induction Operations and Maintenance Costs

The three components of the multi-induction O&M estimates, along with LRC, are shown in Table 10-6, both as cost per year and normalized by the annual energy capture of the turbine. Complete details of the multi-induction drive train O&M model are included in Appendix J.

These estimates were made by modifying the baseline drive train estimates as follows:

- A generator repair cost of 75% of new spare cost (compared to 50% for baseline) was used.
- A gearbox failure rate of 66% of the baseline gearbox was used to account for the simple gearbox design.
- Scheduled maintenance was increased for the additional generators.
- O&M was eliminated for the coupling and gearbox mounting, which are not part of the multi-induction design.
- Generator replacement equipment costs were eliminated because an on-board hoist could be used to change multi-induction generators.
- The gearbox replacement duration and staffing were increased to take into account the difficulty of replacing the integrated gearbox.

Table 10-6. Multi-Induction O&M and LRC Estimates

	Multi Induction		Baseline
	$/yr	$/kWh	$/yr
Unscheduled maintenance	9,097	0.0019	12,103
Scheduled maintenance	7,254	0.0016	6,004
Operations	6,501	0.0013	6,501
Subtotal, O&M (excluding LRC)	**22,852**	**0.0048**	**24,608**
LRC (major overhauls)	**4,738**	**0.0010**	**5,124**
Total O&M and LRC	27,590	0.0058	29,732

The multi-induction scheduled and unscheduled maintenance costs, combined with the LRC from Table 10-6 are compared to the corresponding baseline drive train estimates in Figure 10-17 on a component-by-component basis. Only drive train components are included because the contribution of other turbine components is the same for both designs. The cost contribution from the multi-induction transmission and PE systems is lower than in the baseline, and the contributions from the remainder of the components are similar.

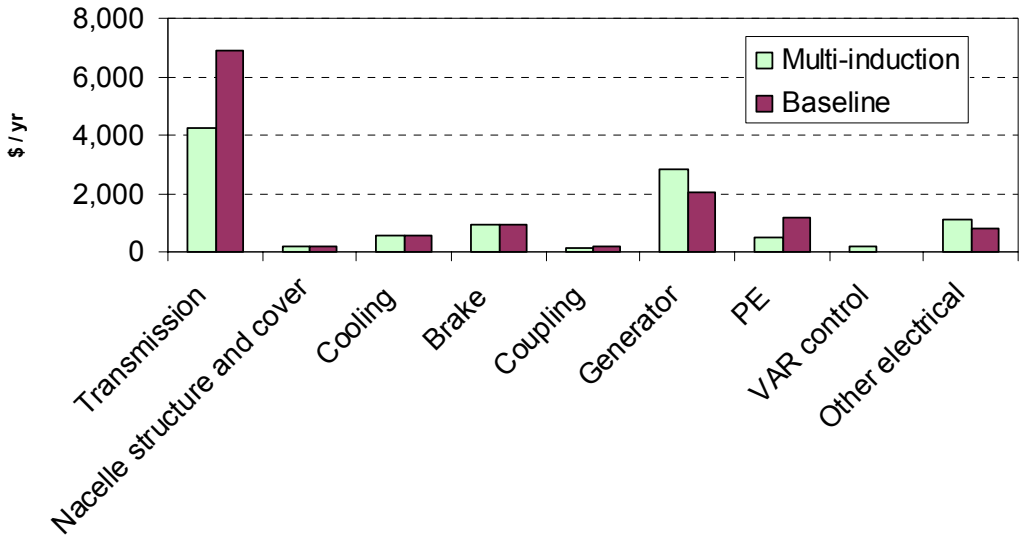

Figure 10-17. Scheduled and unscheduled maintenance costs and LRC compared to baseline by component

10.5.5 Multi-Induction Cost of Energy Estimates

Table 10-7 gives the COE estimates for the multi-induction design. The COE estimate for this design is 0.0325 $/kWh, a reduction of approximately 9% relative to the baseline estimate. This decrease in COE results from the decreased capital costs in the drive train. The multi-induction drive train cost is $279,000, nearly 35% less than the baseline cost of $431,000. This cost reduction results primarily from savings in the transmission system and the elimination of the PE system, as described in Section 10.5.3. This cost savings is partially offset by the AEP, which is approximately 4% lower than that of the baseline.

Table 10-7. Multi-Induction Drive Train COE Estimates, Compared to Baseline

	Multi-Induction		Baseline
	Cost, $	% of COE	Cost, $
Capital Costs			
Turbine	**815,032**	**56.8**	1,001,491
Rotor	**248,000**	**17.3**	248,000
Drive train and nacelle	**279,499**	**19.5**	430,778
Yaw drive and bearing	**16,000**	**1.1**	16,000
Control, safety system	**7,000**	**0.5**	7,000
Tower	**184,000**	**12.8**	184,000
Turbine manufacturer's overhead and profit (30%, tower, rotor, and transformer excepted)	**80,533**	**5.6**	126,229
Balance of station	**358,000**	**25.0**	358,000
ICC	**1,173,032**	**81.8**	1,359,491
AEP			
Ideal annual energy output, kWh	5,272,000		5,479,000
Availability, fraction	0.95		0.95
Losses, fraction	0.07		0.07
Net AEP, kWh	**4,657,812**		4,840,697
Replacement costs, LRC $/yr	**4,738**	**3.1**	5,124
FCR, fraction/yr	**0.106**		0.106
O&M, $/kWh	**0.0049**	**15.1**	0.0051
COE = O&M + ((FCRxICC)+LRC)/AEP	**0.0325**		0.0358

10.6 Multi-Induction Scaling to 750 kW and 3 MW

To scale the multi-induction design to the smaller and larger sizes, the techniques described in Section 10.3.4 and Appendix C were used. These techniques were designed to optimize the 1.5-MW design for different numbers of generators and diameters. Similar spreadsheets to the one shown in Appendix C were developed for the two scaling sizes and the numbers of generators and the system diameter were optimized for both scaling sizes. The optimum 750-kW system uses four generators and has a 2.0-m diameter. The optimum 3000-kW system uses ten generators and has a 3.5-m diameter.

Table 10-8 summarizes the results of this scaling process, and these results are compared graphically in terms of the drive train COE in Figure 10-18. The drive train COE represents the portion of the turbine COE attributed to the drive train capital cost alone. Relative to the 1.5-MW direct drive drive train, the 750-kW version is characterized by a higher normalized capital cost (in dollars/kilowatt) and a lower COE. Relative to the 1.5-MW design, the 3-MW variation has a lower capital cost and COE. Table 10-8 gives some insight into the reasons for these cost relationships. It appears that several major, costly subsystems diminish in normalized capital cost as the power rating increases. These include the transmission system, support structure, and nacelle cover.

Table 10-8. Multi-Induction Drive Train Component Cost Scaling to 750 kW and 3 MW

	750 kW		1.5 MW		3 MW		Method
	Cost ($)	Cost/kW	Cost ($)	Cost/kW	Cost ($)	Cost/kW	
Transmission system	53,003	71	79,771	53	152,612	51	
Gearbox components	*50,206*	*67*	*75,227*	*50*	*127,031*	*42*	PEI input
Mainshaft	*2,797*	*4*	*4,544*	*3*	*25,581*	*9*	PEI input
Support structure (integrated nacelle)	*9,086*	*12*	*11,092*	*7*	*22,058*	*7*	PEI input
Gearbox and generator cooling system	*3,636*	*4.8*	*4,482*	*3.0*	*6,173*	*2.1*	PEI input
Brake system with hydraulics	*1,757*	*2.3*	*2,763*	*1.8*	*3,743*	*1.2*	PEI input
Coupling (generators to gearbox)	*883*	*1.2*	*1,765*	*1.2*	*2,933*	*1.0*	
Nacelle cover	*11,849*	*16*	*13,094*	*9*	*17,039*	*5.7*	PEI input
Generators (squirrel cage induction)	19,982	27	39,965	27	82,841	28	Manufacturer data
Power electronics	*8,524*	*11*	*17,048*	*11*	*34,096*	*11*	Power rating
0.95–0.95 Substation VAR Control	*5,779*	*8*	*11,557*	*8*	*23,114*	*8*	Power rating
Transformer	*11,250*	*15*	*22,500*	*15*	*45,000*	*15*	Power rating
Cable	*8,909*	*12*	*17,817*	*12*	*35,634*	*12*	Power rating
Switchgear	*11,206*	*14.9*	*22,411*	*14.9*	*44,822*	*14.9*	Power rating
Other subsystems	*12,500*	*17*	*25,000*	*17*	*50,000*	*17*	Power rating
Drive train assembly and test	*7,339*	*10*	*10,234*	*6.8*	*11,929*	*4.0*	PEI input
Drive train and nacelle total	**165,702**	**221**	**279,499**	**186**	**531,994**	**177**	

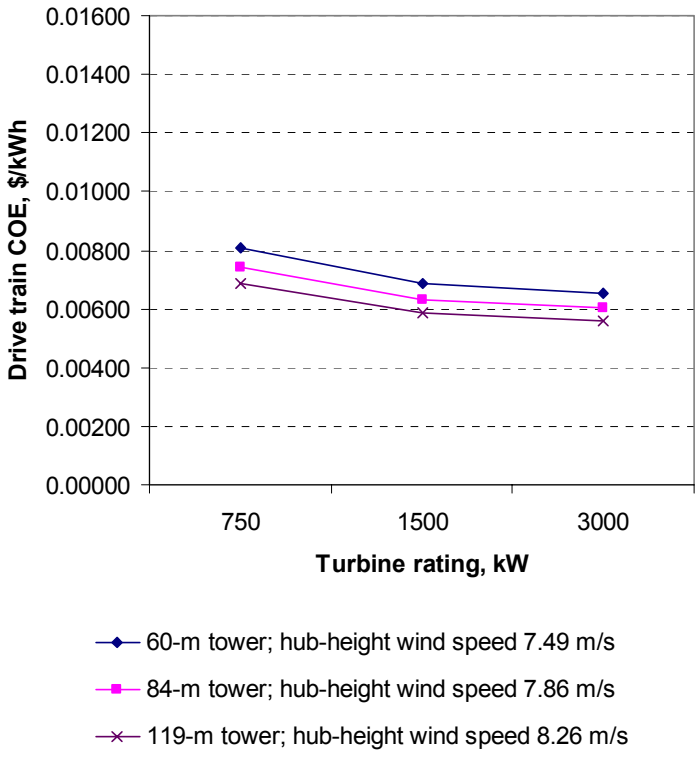

Figure 10-18. Multi-induction drive train COE scaling for different hub height wind speeds

11. Klatt Generator Drive Train

The Klatt drive train is a modification of the baseline drive train with the baseline generator and electrical system replaced with the Klatt system. Initial conceptual design estimates for the Klatt design showed that the Klatt drive train did not have a lower COE than the baseline system. For this reason, further preliminary designs were not developed for the Klatt design. This section describes the conceptual design estimates made for this drive train early in the study.

11.1 Klatt System Description

The Klatt drive train uses the Klatt integrated generator and PE system. The Klatt generator was invented and patented by Fred Klatt of EDI. This system uses a wound-rotor induction generator modified with a high-frequency rotating transformer and an integrated PE system. Figure 11-1 is a system diagram of this drive train. Together with the baseline gearbox, the system is operated in variable-speed mode over the same 900- to 1500-rpm generator speed range.

The Klatt generator provides variable speed and torque control equivalent to that of the baseline, but eliminates the generator slip rings and shaft encoder used in the baseline system. The stator of the Klatt generator is electrically connected to the grid through the turbine pad mount transformer. The generator rotor is connected to one side of a co-rotating, three-phase, high-frequency transformer through four bidirectional IGBT switches per phase. These switches convert the rotor power to a higher frequency, typically several kilohertz. Because the rotating transformer is operated at a relatively high frequency, it can be made small enough to be mounted in place of the standard slip ring assembly. The high-frequency power from the rotating transformer is converted back to 60-Hz power with four bidirectional IGBT switches per phase on the stationary side of the transformer and connected to the grid through the turbine pad mount transformer.

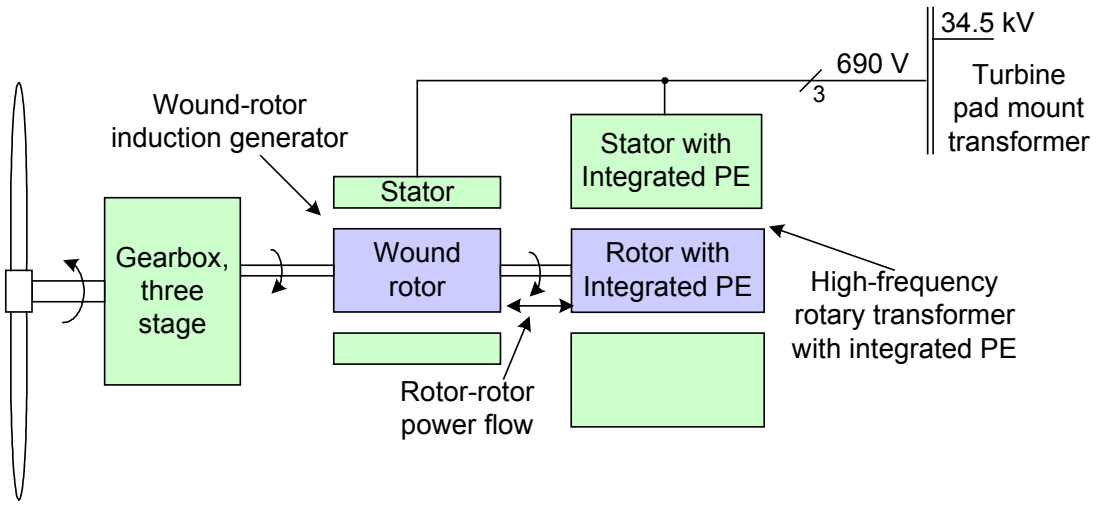

Figure 11-1. Klatt generator system diagram

11.2 Klatt Generator Component Designs

11.2.1 Klatt Drive Train Mechanical Design

The mechanical design of the Klatt generator drive train is identical to that of baseline, described in Section 5.3.1. Because the Klatt generator is expected to provide torque-limiting equivalent to that supplied by the baseline generator with PE control, loads are the same for both systems.

11.2.2 Klatt Generator Electrical Design

OEM Development Corporation investigated the Klatt generator and PE system for this study. Fred Klatt furnished information on the system to OEM and GEC, and EDI was paid a consulting fee for the time spent supplying that information. OEM analyzed the system to the extent necessary to evaluate the performance, cost, and feasibility of the system for the 1.5-MW wind turbine application.

The Klatt generator and PE system is covered by several patents (Klatt 1984; Klatt 1987; Klatt 1993a; Klatt 1993b). Significant aspects of the system control are not covered by these patents and are trade secrets of EDI. EDI disclosed some of these trade secrets to OEM and GEC under a proprietary agreement made among the three companies to allow OEM to evaluate the system for the study. These aspects of the system operation are not described in this report.

All electrical system components other than the generator and PE system, including cable and switchgear, are assumed to have approximately equal cost and performance to those of the baseline.

11.2.2.1 Klatt Generator and PE System: Theory of Operation

The Klatt generator is a modification of the baseline wound-rotor induction generator, which uses slip rings, a shaft encoder, and conventional, stationary-frame power electronics to control and convert the rotor power. The Klatt modification eliminates the slip rings and shaft encoder. The stationary-frame power electronics and its associated control are replaced with a distributed PE-magnetics subsystem for processing the rotor power and transferring it to the stationary frame. The subsystem elements include:

- Power electronics, associated sensors, and control electronics in the rotating frame
- A high-frequency (nominally several kHz) rotary power transformer
- Similar PE circuitry in the stationary frame
- Communication between the rotating and stationary frame control electronics.

Through the application of communication and signal modulation theory to the control of the added power components, this arrangement is able to process the rotor power and couple it to the stator and grid through the same pad mount transformer used for the baseline. According to EDI, the system offers a number of attractive performance characteristics. These include four-quadrant, variable-speed operation with intrinsic synchronization to the grid frequency and phase, as well as torque control with no shaft position encoder and without the conventional field-oriented control algorithm used in the baseline.

To achieve this, the rotor power is fed to a PE circuit in the rotating frame. This circuit, the power modulator-demodulator (modem) transforms the slip power (at the baseband slip frequency) to a higher frequency, amplitude-modulated power signal. The modulating frequency (the carrier frequency) is considerably higher than the highest operational slip frequency. A typical value of the carrier frequency might be 1000 Hz. This value will be used for illustrative purposes.

Through this process, the rotor power (at the slip frequency) is transformed to a 1000-Hz, amplitude-modulated, bipolar wave form whose envelope is the (lower frequency) slip wave form.

The modulated slip power wave form is fed to the rotating winding of the high-frequency (1000 Hz) rotary transformer. This winding and the associated modem power electronics are turning at the rotor speed. The associated magnetic flux is intercepted by the stationary winding of the rotary transformer and represents transferred slip power.

Similar modem power electronics in the stationary frame then demodulate the coupled high-frequency signal. With appropriate phase shifting, the demodulation is done synchronously with the modulation accomplished in the rotating frame. The result, according to analysis presented by EDI, is that the slip wave form is transformed to the grid frequency, then synchronized and coupled to the grid. The high-frequency modulation is isolated to the high-frequency rotating transformer and sindusoidal wave forms are supplied to both the power grid and generator windings.

The high-frequency modulator circuit required for the Klatt rotating transformer is shown in Figure 11-2 for one of the three phases on one side of a transformer winding. The rotating and stationary side of the transformer both use the same switch topology. The entire three-phase system requires six of the circuits shown in the figure. This switch topology is similar to circuits that have been proposed for stationary high-frequency transformers (Kang, Enjeti, and Pitel 1999). The power wave form must be bipolar with no average DC component to avoid saturation of the transformer core with attendant loss of the magnetic properties. Each switch, then, must be bidirectional and controlled. This requires two active devices, typically IGBTs, driven by a common gate driver. Each phase winding of a three-phase rotor requires eight actively controlled switches and four gate drivers. The entire three-phase, rotating transformer requires 48 actively controlled switches and 24 gate drivers.

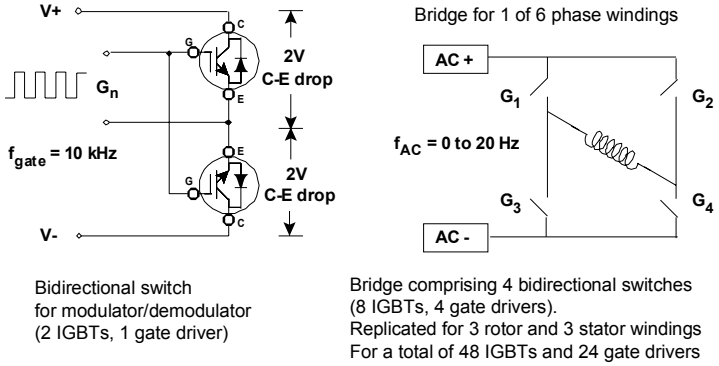

Figure 11-2. Basic switch module of the Klatt-EDI modulator consisting of two semiconductor switches

As noted, EDI, through the work of Klatt, has performed extensive analyses of the operation and performance of the Klatt machine. EDI has fabricated and demonstrated the operation of this system in a small machine. The techniques by which four-quadrant operation and torque control are achieved were cited as proprietary to EDI.

11.2.2.2 Klatt Generator and PE System: Advantages and Disadvantages

The advantages of the Klatt system relative to the baseline generator and power electronic system are:

- The generator slip rings are eliminated.
- The generator shaft encoder is eliminated.

- The DC link stage and associated capacitor is eliminated.
- Synchronized switching of the high-frequency transformer eliminates the conventional field-oriented control algorithm and simplifies the control system.
- Synchronized switching isolates most of the high-frequency currents to the rotating transformer.

The Klatt system is expected to have torque control equivalent to that of the baseline. Although careful design of the power electronics will be required to achieve this, the Klatt system has the potential to have equal efficiency to the baseline. At this point, however, relative to the baseline system, the Klatt system does not appear to offer further performance advantages.

The disadvantages of the Klatt system are all associated with increased complexity relative to the baseline. The Klatt system requires more active switches, switches in the rotating portion of the high-frequency transformer, and communication between the rotating and stationary portion of the transformer. Some of the related design issues are described in the following subsection.

11.2.2.3 Klatt Generator and PE System: Design Issues

Several design issues are associated with the Klatt system. These issues may be grouped into the four areas described below:

- **Integrity of the rotating-frame power electronics:** For a 6-pole machine having a synchronous speed of 1200 rpm and a 33% speed range about synchronous, the maximum speed is 1600 rpm. For the power levels of interest in this study, the semiconductor switches and associated support components are not small in either mass or physical size. Centripetal forces, then, are expected to form an important aspect of the design of the rotating frame power electronics.

- **Heat removal from the rotating frame power electronics:** For a 500-kW rotating frame power processing system operating at 500 kW, each 1% of inefficiency will generate 5 kW of heat. Because of the need to supply reactive power, a system rated at 500 kW may have a 750-kVA apparent power rating with associated increases in current. On this basis, each 1% of system inefficiency will generate approximately 7 kW of heat. For the power electronics of the Klatt configuration, a maximum efficiency of 98% can be expected, with half of the losses in the rotating frame. This implies the requirement to remove at least 5 to 7 kW of heat from the rotating frame components.

- **High-frequency rotating transformer design:** This design issue, of how to achieve minimal transformer losses at the relatively high frequency of operation, is fairly tractable. Although the nominal frequency is 1000 Hz, the transformer materials and windings must accommodate harmonics that carry significant power up into the several kilohertz region. The 1000-Hz switching frequency and its spectrum impose thickness requirements on the magnetic steel laminations and on the loss characteristics of the magnetic steel. It may also be necessary to utilize Litz wire for the windings to minimize losses associated with skin-effect crowding of the current within the conductor volume. Even though these design issues are straightforward, they add cost implications relative to the baseline wound-rotor generator and power-processing configuration.

- **Stationary–rotating frame communication:** Reliable digital communication between the stationary frame and the controller of the rotating frame power electronics is necessary. Optical and radio-frequency (RF) techniques are possible. Optical communication using focused light-emitting diodes (LEDs) or solid-state lasers are readily achievable. Reliable communication is at risk as the optical fiber, lenses, or other components become occluded by the dust, oil mist, and

other forms of contamination inherent in wind turbine systems. RF techniques have a relative advantage in that they do not suffer from occlusion by dust and other contaminants. However, because the RF communication system must operate in an environment that is electromagnetically noisy, both physical shielding and robust error correction techniques will be needed.

Although each of these items may pose challenging design issues at the power levels of interest, there are engineering approaches to each that can provide tractable solutions.

11.2.2.4 Klatt Generator and PE Cost Estimates

The Klatt generator, minus integrated PE costs, was assumed to have a high volume production cost of $60,000, equal to that of the baseline generator. The Klatt generator uses the baseline stator and wound rotor. The Klatt generator eliminates the shaft encoder and slip rings but requires a rotating transformer. The cost of the rotating transformer, minus electronics, was assumed to be equal to the costs of the baseline generator slip ring and encoder.

Because the Klatt system requires a greater number of active switches, the high-volume production cost of the Klatt PE system was assumed to be higher than that of the baseline. Both systems transfer the same amount of power from the generator rotor. Appendix F contains a schematic of the baseline PE system, which has a total of 12 IGBT switches. The Klatt system uses 48 switches in all. The cost of the Klatt PE system was assumed to be 20% higher than that of the baseline, and was estimated at $74,000, compared to the baseline PE estimate of $62,000.

11.3 Klatt Generator Results

The following subsections summarize the COE estimate for the Klatt design along with the efficiency, energy production, component cost, and O&M estimates used to make this COE estimate. These estimates were made as part of a conceptual design phase early in the study. Because detailed preliminary design estimates were not made for the Klatt design, these estimates were developed with less detail than corresponding estimates made for several other designs investigated during the study.

The AEP and O&M costs were not estimated for the Klatt design, so the baseline estimates were used as best-case approximations. All component costs other than those of the PE system are identical to the baseline. The estimated Klatt PE system costs are 20% higher than those of the baseline. Although this is a rough approximation, it is considered to be extremely unlikely that the Klatt system could be designed to have lower PE system costs than the baseline. The higher PE costs, all else being equal, result in a higher COE for the Klatt system.

11.3.1 Klatt Efficiency and Gross Annual Energy Production

Efficiency was not calculated for the Klatt drive train, so the efficiency of the baseline system was used to analyze this design. For this reason, the GAEP of the 1.5-MW Klatt design was assumed to be equal to the baseline design. Efficiency curves and GAEP estimates for the baseline are included in Sections 5.4.1 and 5.4.2, respectively.

11.3.2 Klatt Component Costs

Table 11-1 itemizes the component costs for the 1.5-MW Klatt drive train. All component costs are the same as for the baseline, with the exception of the PE system cost, which is 20% higher than the baseline. These data are compared directly to the baseline system in the bar chart shown in Figure 11-3.

Table 11-1. Klatt Drive Train Component Costs

Component	Cost, $
Transmission system	**155,000**
Gearbox components	120,000
Mainshaft	20,000
Mainshaft support bearing and block	12,000
Elastomeric mounting system	2,700
Generator Isolation Mounts	500
Support structure (bedplate)	**34,000**
Generator cooling system	**2,400**
Brake system with hydraulics	**1,400**
Coupling (generator to gearbox)	**2,400**
Nacelle cover	**17,000**
Generator	**60,000**
Power electronics	**74,000**
0.95–0.95 substation VAR control	**NA**
Transformer	**23,000**
Cable	**18,000**
Switchgear	**12,000**
Other subsystems	**25,000**
Drive train assembly and test	**8,000**
Total	**433,000**

Note: All costs rounded.

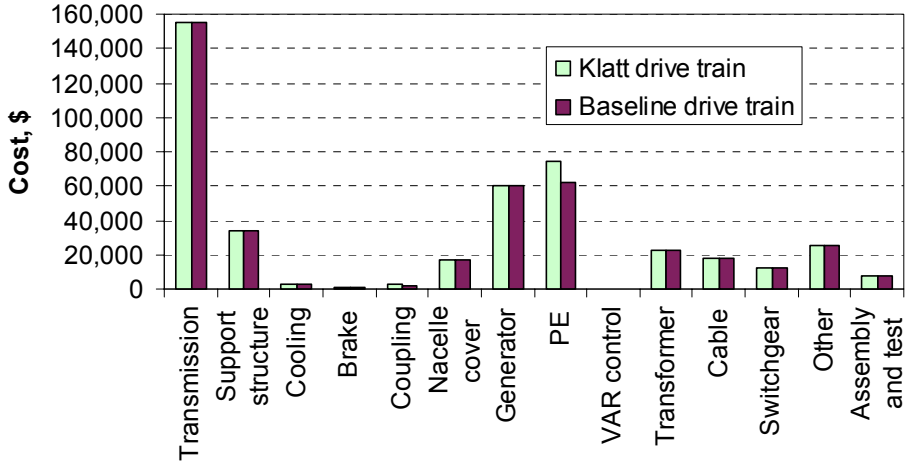

Figure 11-3. Klatt and baseline component cost comparison

11.3.3 Klatt Operations and Maintenance Costs

Because the O&M costs of the Klatt drive train were not modeled, the O&M costs of the baseline drive train were used to analyze the Klatt design. Because of the parts count and the rotating-frame power

electronics, this assumption is believed to be conservative. Baseline O&M estimates are described in Section 5.4.4.

11.3.4 Klatt Cost of Energy Estimates

COE estimates for the Klatt drive train are shown in Table 11-2. The COE estimate for this design is 0.0361 $/kWh, approximately 1% higher than the estimate for the baseline.

Table 11-2. Klatt Drive Train COE Estimates, Compared to Baseline

	Klatt		Baseline
	Cost, $	% of COE	Cost, $
Capital Costs			
Turbine	**1,017,559**	**61.4**	1,001,491
Rotor	**248,000**	**15.0**	248,000
Drive train and nacelle	**432,622**	**26.1**	430,778
Yaw drive and bearing	**16,000**	**1.0**	16,000
Control, safety system	**7,000**	**0.4**	7,000
Tower	**184,000**	**11.1**	184,000
Turbine manufacturer's overhead and profit (30%, tower, rotor, and transformer excepted)	**129,937**	**7.8**	126,229
Balance of station	**358,000**	**21.6**	358,000
ICC	**1,375,559**	**83.0**	1,359,491
AEP			
Ideal annual energy output, kWh	5,479,000		5,479,000
Availability, fraction	0.95		0.95
Losses, fraction	0.07		0.07
Net AEP, kWh	**4,840,697**		4,840,697
Replacement costs, LRC, $/yr	**5,124**	**2.9**	5,124
FCR, fraction/yr	**0.106**		0.106
O&M, $/kWh	**0.0051**	**14.1**	0.0051
COE = O&M + ((FCRxICC)+LRC)/AEP	**0.0361**		0.0358

11.4 Klatt Scaling to 750 kW and 3 MW

For the reasons indicated, scaling estimates were not made for the Klatt drive train.

12. Heller-De Julio Drive Train

The HDJ drive train is a modification of the baseline drive train with the generator and PE system replaced with the HDJ generator. Initial conceptual design estimates for the HDJ showed an unfavorable COE for this design compared to the baseline. For this reason, further preliminary designs were not developed for the HDJ. This section describes the conceptual design estimates made for this design early in the study.

12.1 HDJ Generator System Description

The HDJ drive train has a mechanical design identical to that of the baseline. Only the generator and electrical system are modified. The HDJ variable-slip induction generator is a modification of the baseline wound-rotor induction generator. This generator is connected directly to the grid through a pad mount transformer. Variable-speed power electronics are not used.

Figure 12-1 is a system diagram for this drive train. The HDJ generator is a wound-rotor induction machine with a rotor circuit that has been modified to achieve a passive, variable-slip characteristic. It does not provide variable-speed operation below rated speed, but does provide torque-dependent variable compliance above rated speed to reduce gearbox torque transients during wind gusts. The HDJ generator is covered by several patents held by the Heller-De Julio Corporation (Wallace et al. 1999; Wallace et al. 2000).

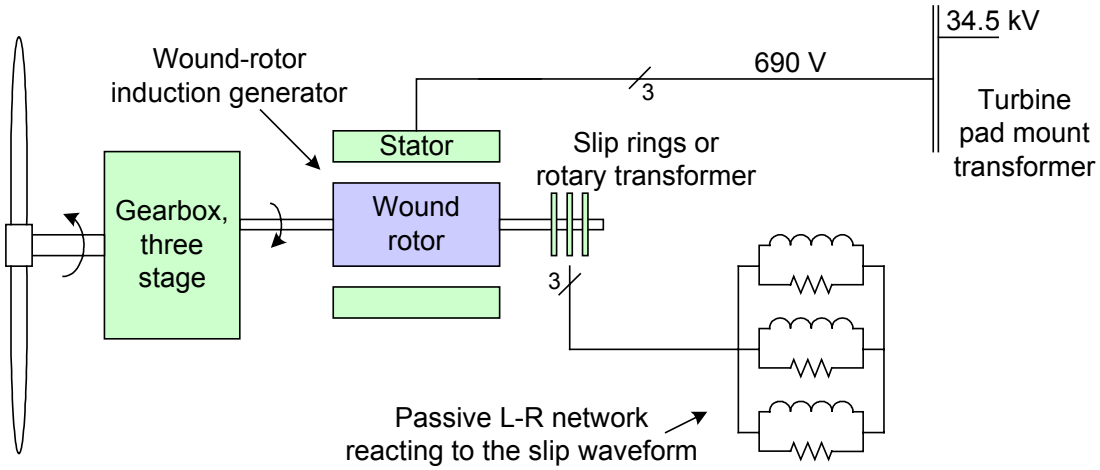

Figure 12-1. HDJ generator system diagram

12.2 HDJ Generator Component Designs

The Heller-De Julio Corporation was contracted to write a report for this study describing the use of its generator for the baseline turbine application. This report is included in Appendix L. Alan Wallace of Oregon State University, Corvallis, and James Oliver of Jarsco Engineering, Corona, California, assisted the corporation with this report. The report provides component costs, efficiency, and other performance estimates for the 1500-kW HDJ system and compares the estimates to other drive train systems. The generator cost and efficiency estimates from that report were used to analyze this drive train for the study.

12.2.1 HDJ Drive Train Mechanical Design

The mechanical design of the HDJ generator drive train has the same architecture as the baseline drive train described in Section 5. However, several minor differences in the mechanical system result from the different generator characteristics:

- The HDJ generator does not provide actively controlled, perfect torque limiting during wind gusts. As a consequence, the resulting loads are slightly higher for the HDJ gearbox, mainshaft, and structure than for the baseline.

- In common with the speed-power characteristics of a squirrel-cage induction generator, from synchronous speed to the speed at which rated power is achieved, the HDJ design operates over a very narrow speed range. Compared to the variable-speed operation of the baseline system, the HDJ generator runs at essentially constant speed. However, over its narrow speed range, the losses within the L-R (inductance and resistance) network do vary. To maximize energy capture, the HDJ system was analyzed with a rated speed of 18.6 rpm, approximately 10% below the baseline rated speed of 20.5 rpm. This causes a corresponding torque increase. The selection of the 18.6-rpm rated speed is described in Section 12.3.2.

- Because the HDJ generator operates at a lower speed than the baseline generator, a lower gear ratio is needed for the HDJ system. When the turbine operates at rated output, the 6-pole HDJ generator runs at a rated speed of approximately 1310 rpm. By comparison, the 6-pole baseline generator operates supersynchronously with a speed of 1500 rpm, as controlled by the doubly fed power electronics, when the turbine is operating at rated output.

For this study, the baseline costs for all mechanical components, other than the gearbox, were used to estimate the HDJ drive train costs. The additional loading resulting from the reduced operating speed and the increased torques was neglected. This approximation is favorable to the HDJ system. The HDJ gearbox costs were adjusted relative to the baseline gearbox costs as described in the subsection that follows.

12.2.1.1 Gearbox Estimates

The HDJ generator does not limit torque in the same way that the baseline variable-speed system does. Because the HDJ generator is high slip, the rotor speed will increase with positive wind gusts. However, based on the slope of the slip curve, the torque also will increase. To estimate the increase in gearbox cost that results from this effect, an approximate analysis was carried out.

The baseline torque load spectrum was binned by both torque level and rpm. For each bin in the baseline spectrum, a bin with an equivalent power was calculated using the HDJ torque-speed slip curve. The torque levels calculated in this way were used in a fatigue analysis. As part of the WindPACT rotor study (Malcolm and Hansen 2002), a curve fit was made from a range of gearbox designs to determine the relationship between gear stress levels and gearbox mass. This relationship was used to determine the required additional mass to meet fatigue life requirements in the analysis described above. The result was a required increase in mass of approximately 7%, which translates directly to the cost increase.

The Heller-De Julio report indicated that the torque transients will be lower than expected from the generator slip curve alone because the rotor inductance does not allow fast changes in generator rotor current. This effect was not included in the analysis. The assumptions of the analysis are probably somewhat optimistic, however, for predicting the torque transients of the generator based on the slip curve alone. This is because the baseline torque load spectrum, which assumes perfect torque limiting, is used in the analysis.

12.2.2 HDJ Drive Train Electrical Design

A detailed one-line diagram was not developed for the HDJ system. Cost estimates of the electrical system were based on modifications to the baseline component costs with information provided in the Heller-De Julio report (Appendix L). The baseline variable-speed PE system was eliminated. Costs were added for capacitors to correct the generator power factor, and costs were also included for substation VAR control. This is consistent with estimates for the other WindPACT drive trains that do not have PE systems capable of providing active VAR control. The rest of the electrical system costs, including cable and switchgear costs, were considered to be the same as the baseline estimates.

A soft-start circuit to limit generator in-rush current and associated torque transients during start-up has not been included in the estimates. The in-rush current is limited by the added passive components in the rotor circuit of the generator. Heller-De Julio estimates the in-rush current at start-up to be less than the rated current of the generator.

The HDJ design has been estimated with a 690-V electrical system to be consistent with the other designs investigated for the study. The HDJ system, without the need for a PE system, could be built with a medium-voltage (2400 or 4160 V) generator output. The use of medium voltage would reduce the cost of cables and the pad mount transformer; however, medium-voltage switchgear and additional maintenance personnel training would be required.

12.2.2.1 HDJ Generator: Theory of Operation

The HDJ generator is a wound-rotor induction machine with a rotor circuit that has been modified to achieve a passive, variable-slip characteristic. This slip characteristic provides a speed-dependent, variable compliance to limit gearbox torques without the need for variable-speed power electronics. The compliance is supplied over the limited range of speeds above synchronous speed comparable to the range associated with slip operation of a conventional squirrel-cage induction machine.

The slip varies with speed such that at speeds near synchronous, the slip is small, providing only limited compliance and low losses. At speeds that are significantly above synchronous, the generator is characterized by high slip and a correspondingly high compliance presented to the balance of the drive train. The slip and compliance benefits are accompanied by higher losses. As shown in Figure 12-1, this passive, speed-dependent, variable-slip characteristic is implemented by placing a parallel inductance and resistance network in each of the three phases of the rotor winding.

The operation can be understood with reference to Equation 12-1. The impedance of the added parallel resistor/capacitor network is given by the expression

$$Z = \frac{j\omega LR}{R + j\omega L} = \frac{R}{\left(1 + R \big/ j\omega L\right)} \qquad (12\text{-}1)$$

where the slip frequency $\omega = 2\pi f_s = 2\pi/T_s$ and T_s denotes the period corresponding to the slip frequency.

The operation of the HDJ machine can be illustrated by considering two limiting cases based on the value of the ratio ($R/j\,\omega\,L$). Because the resistance R and the inductance L are fixed, this dimensionless ratio varies inversely as the slip frequency, proportional to the generator speed relative to the synchronous speed.

Limiting Case 1: Operation Near Synchronous Speed: For this limiting case, the value of the ratio ($R/j\ \omega_s\ L$) is much greater than unity:

$$\text{For } \frac{R}{j\omega_s L} >> 1 \qquad Z = j\omega_s L \quad and \quad T_s >> \frac{L}{R}$$

For this limiting case, the machine is operating near the synchronous speed ω_s; that is, with a small slip frequency and a large slip period T_s. The impedance of the parallel inductance branch is very small relative to the resistive branch. The inductive impedance effectively shorts the resistive branch. For this case, there is very little compliance. However, near synchronous speed, very little compliance is necessary or desirable because the wind turbine is operating in Region II, which is the rising part of the power curve. The HDJ machine behaves as a classical squirrel-cage induction machine with very low slip. The losses are small.

Limiting Case 2: Operation Above Synchronous Speed, Near Rated Power: For this limiting case, the value of the ratio ($R/j\ \omega_s\ L$) is much less than unity:

$$\text{For } \frac{R}{j\omega_s L} << 1 \qquad Z = R \quad and \quad T_s << \frac{L}{R}$$

For this limiting case, the machine is operating significantly above the synchronous speed ω_s; that is, with a larger slip frequency and a smaller slip period T_s. This implies that the machine is operating at or near rated power.

The relatively high slip frequency causes the parallel inductance branch to have a high value of impedance relative to the resistive branch. Consequently, the resistance dominates and the machine appears as a classical medium- or high-slip induction machine. The resistance provides compliance that acts to relieve the drive train of the buildup of impulsive torque transients associated with incident wind gusts. On the other hand, according to classical induction machine theory, the losses are proportional to the slip. Although the slip results in desirable drive train compliance, there also are associated losses and the counterpart to those losses, reduced efficiency.

In comparison with the baseline system (a wound-rotor induction machine with partial-rated power electronics to process the rotor power), the HDJ machine offers simplicity in its characteristic of passive adjustable slip. The slip, compliance, and losses are small when the wind turbine is operating at low power near the generator's synchronous speed. The slip increases as the generator moves toward its full-rated power. This yields increasing drive train compliance, which is desirable. However, to the extent that the wind turbine spends an appreciable fraction of time at or near its rated power, losses are inescapable.

12.2.2.2 HDJ Generator Estimates

The Heller-De Julio Corporation describes three generators with different slip versus speed characteristics in its report (Appendix L). Each uses a different inductance and resistance selection. The 10% slip generator gives the greatest compliance and the lowest gearbox loads, but has the lowest efficiency. The 8% and 5% slip generators offer lower compliance but higher efficiency. For this study, the 10% slip generator initial presented by Heller-De Julio was evaluated. It gives enough compliance so that gearbox loads are only modestly higher than the baseline gearbox loads.

Because power dissipated in the added rotor circuit resistance will be significant for a 1.5-MW generator, Heller-De Julio representatives propose mounting the resistors external to the generator. Connections to the generator rotor can be made through slip rings, as shown in Figure 12-1, or with a rotary transformer. If a rotary transformer is used, it is possible to integrate the circuit inductance into the transformer. The

rotary transformer with integrated inductance is assumed for Heller-De Julio's cost estimates. The external resistors do not need to be close to the generator and could be mounted external to the nacelle for cooling purposes.

In its report, the Heller-De Julio Corporation furnished estimates for the costs of modifying the 1500-kW baseline wound-rotor generator to incorporate a rotary transformer and external resistors. These estimates are based on high-volume production rates of 600 units per year. The company's estimate for the rotary transformer is $1500 and for the external resistors, the estimate is $15,000. Based on the study's estimate for the baseline generator—$60,000—the cost of the HDJ generator with rotary transformer and external resistors added was estimated at $66,500.

12.2.2.3 Power Factor Correction

For the purposes of comparison to other drive train designs, the power factor capacitor estimates were made using the same methods used to estimate PE systems throughout the study. The assumption was made that these components would be assembled in a common enclosure by an electrical system manufacturer, who would then sell the assembled unit to the turbine manufacturer. Table 12-1 presents the estimates for these components. Estimates are based on the estimate for 350 kVAR of correction capacitors and associated contactors and fuses included in the SCR-SCR PE system estimates in Appendix F. The amount of reactive power necessary to correct a 1500-kW, 0.87 power factor induction generator to 0.95 lagging power factor at full load is 350 kVAR. The wind farm VAR control system supplies the rest of the compensation.

Table 12-1. Power Factor Correction Estimate

Description	Quantity	Unit Cost, $	Extended Cost, $
Fuse and fuse holder, 50 A, 600 V	6	33	198
Fuse and fuse holder, 100 A, 690 V	3	33	99
Fuse and fuse holder, 200 A, 690 V	3	33	99
Contactor, 50 A, 690 V, 3-Pole	2	111	222
Contactor, 100 A, 690 V, 3-Pole	1	212	212
Contactor, 200 A, 690 V, 3-Pole	1	334	334
Capacitor, 50 kVAR, 690 V, three-phase	2	200	400
Capacitor, 100 kVAR, 690 V, three-phase	1	400	400
Capacitor, 200 kVAR, 690 V, three-phase	1	800	800
Enclosure	1	900	900
Material cost total			**3,763**
Gross margin = 40%*			
Sales price to turbine manufacturer			**6,271**

*Gross margin = (sales price - material cost) ÷ sales price

12.3 HDJ Results

The following subsections summarize the COE estimate for the 1.5-MW HDJ design along with the efficiency, energy production, component cost, and O&M estimates used for the COE estimate.

Detailed, preliminary design estimates were not made for this drive train, and this section presents the results of conceptual design estimates made early in the study. These estimates were made with less detail than corresponding estimates made for several other designs investigated during the study.

12.3.1 HDJ Efficiency

Figure 12-2 shows drive train efficiency versus input power on a component-by-component basis, with the total drive train efficiency of the baseline system shown for comparison. The HDJ drive train efficiency is lower than that of the baseline above about 50% power, and approximately equal to the baseline at lower powers. The lower efficiency at higher power results primarily from the relatively low efficiency of the HDJ generator. The efficiency curves for the 10% slip version of this generator provided by the Heller-De Julio Corporation in its report (Appendix L) were used for these estimates. The gearbox efficiency for this system is lower than that of the baseline at low input power. This results from the operating speed of the variable-speed baseline drive train, which is lower than the fixed-speed HDJ drive train at low wind speeds. The fixed-speed gearbox efficiency measurements presented in GEC (2002) were used for these estimates.

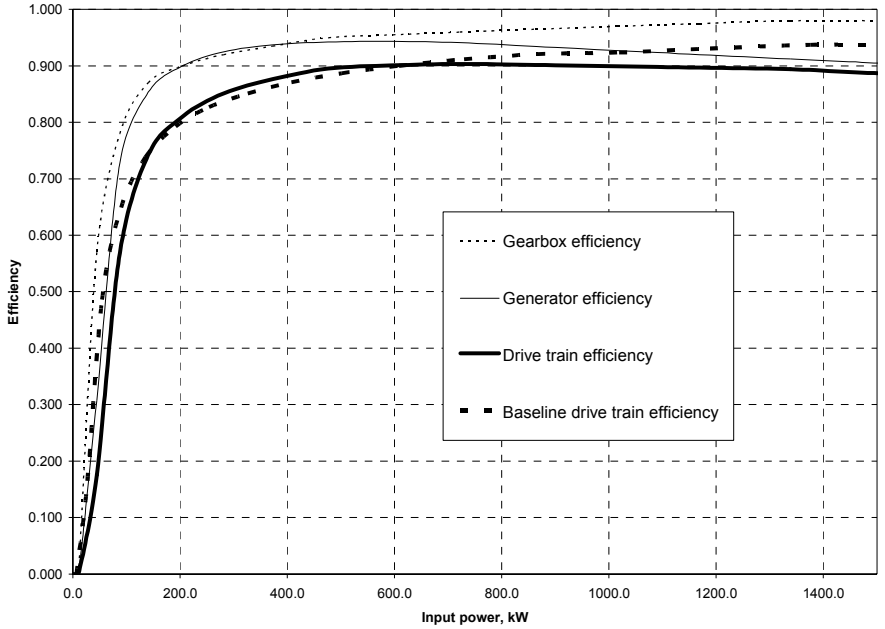

Figure 12-2. HDJ drive train efficiency by component

12.3.2 HDJ Gross Annual Energy Production

Table 12-2 shows the GAEP estimate for the HDJ design for each wind speed bin. Because drive train efficiency losses are included, these estimates reflect the binned energy at the output of the wind turbine generator. All other losses are calculated separately in the final COE analysis. The wind speed bins from 12.0 m/s to the cut-out speed of 27.5 m/s are aggregated in a single row. The energy production levels for those wind speed bins are identical to those for the baseline turbine, shown in Table 5-3, with the rotor speed at rated and the output power regulated to 1.5 MW by the pitch system. The total GAEP from the HDJ design is estimated at 5248 MWh, which is approximately 4% less than the estimated production of 5479 MWh for the baseline.

The HDJ has lower energy capture than the baseline for two reasons: (1) the HDJ design is essentially a constant-speed design below rated power, although there is some speed variation resulting from the 10% generator slip; and (2) the HDJ drive train has lower efficiency than the baseline above about 50% power, as shown in Figure 12-2. The HDJ design does allow the rotor speed to increase above rated to limit torque during wind gusts. However, the additional energy captured during this speed increase is dissipated and not converted to usable energy.

The energy production estimates shown in Table 12-2 take into account the 10% speed variation caused by generator slip. The rotor speed is 16.9 rpm when the generator has zero slip, at no load. The speed increases with added generator slip, the slip being proportional to rotor torque, until a rated speed of 18.6 rpm is reached under rated conditions, with 10% slip. The rated speed of 18.6 rpm was selected to maximize the energy capture of the turbine, using an optimization method similar to that described in Section 10.5.2 for the fixed-speed multi-induction drive train. This rotor speed is approximately 10% lower than the baseline rated speed of 20.5 rpm.

Table 12-2. HDJ Drive Train GAEP

Wind Speed Bin Center, m/s	Rotor Speed, rpm	Rotor Power, kW	Drive Train Efficiency	Output Power, kW	# of Hours per Year	Energy Production	
						MWh	Fraction of total, %
3.0	16.80	0.0	0.000	0.0	297.5	0	0.00
3.5	16.80	0.0	0.000	0.0	333.1	0	0.00
4.0	16.81	10.1	0.000	0.0	363.0	0	0.00
4.5	16.85	44.6	0.175	0.0	386.9	0	0.00
5.0	16.90	87.7	0.568	49.8	404.7	20	0.38
5.5	16.96	140.5	0.742	104.3	416.5	43	0.83
6.0	17.03	204.4	0.810	165.5	422.4	70	1.33
6.5	17.11	281.3	0.851	239.4	422.7	101	1.93
7.0	17.21	372.9	0.877	326.8	417.8	137	2.60
7.5	17.32	476.5	0.895	426.5	408.3	174	3.32
8.0	17.45	596.7	0.901	537.6	394.7	212	4.04
8.5	17.59	721.6	0.904	652.0	377.7	246	4.69
9.0	17.73	862.8	0.902	778.0	357.8	278	5.30
9.5	17.89	1014.8	0.900	912.8	335.9	307	5.84
10.0	18.04	1169.0	0.897	1048.7	312.4	328	6.24
10.5	18.21	1338.3	0.894	1196.4	288.0	345	6.56
11.0	18.39	1523.4	0.886	1349.6	263.2	355	6.77
11.5	18.48	1701.1	0.882	1500.0	238.5	358	6.82
12.0–27.5	18.48	1701.1	0.882	1500.0	1516.1	2274	43.3
					Total GAEP =	**5248**	**MWh**

The energy production estimates of the HDJ and baseline designs are compared by wind speed bin in Figure 12-3. Above 11.5 m/s wind speeds, the energy production estimates are equal for both designs, so those bins are not shown. At each wind speed bin shown, the HDJ system has a lower energy capture than the baseline. The difference is greatest at the low wind speeds near cut-in and at the higher wind speeds near rated.

At those wind speeds, the HDJ system has a rotor TSR that is the furthest from optimum. The 10% speed range of the HDJ system varies from 16.9 rpm at cut-in to 18.6 rpm at rated. The 18.6-rpm rated speed is approximately 10% less than the 20.5-rpm rated speed for the baseline system. The 20.5-rpm speed gives an optimum TSR near rated. If that speed is used for the HDJ system, energy capture will be higher near rated and drop off more quickly at lower wind speeds. With the selected speed range, the energy capture is lower near the high end. However, the additional energy capture at lower speeds maximizes the total energy capture across the entire wind profile.

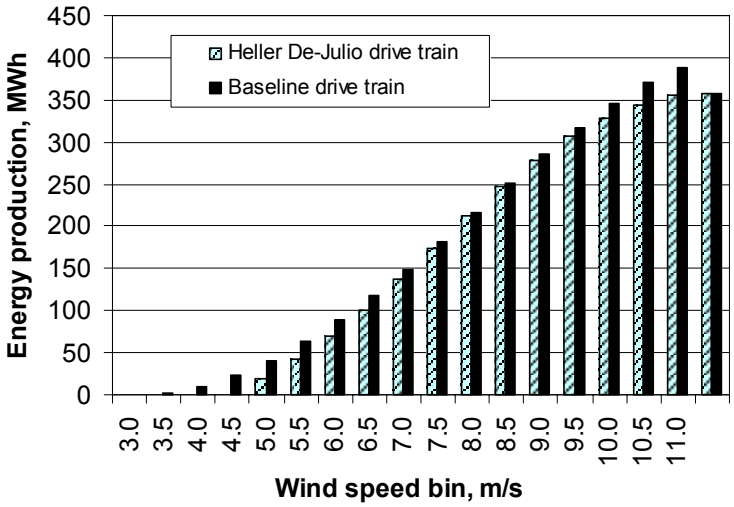

Figure 12-3. HDJ and baseline energy production by bin

12.3.3 Heller-De Julio Component Costs

Component costs for the HDJ drive train are itemized in Table 12-3. These data are compared directly to the baseline system in the bar chart shown in Figure 12-4. Component costs for the HDJ drive train system are approximately 6% less than those of the baseline because of savings in PE costs, but these savings are offset by the addition of power factor correction and VAR control costs. Gearbox costs are also higher than the baseline because of additional loads.

Table 12-3. HDJ Drive Train Component Costs

Component	Cost, $
Transmission system	**166,000**
Gearbox components	131,000
Mainshaft	20,000
Mainshaft support bearing and block	12,000
Elastomeric mounting system	2,700
Generator isolation mounts	500
Support structure (bedplate)	**34,000**
Generator cooling system	**2,400**
Brake system with hydraulics	**1,400**
Coupling (generator to gearbox)	**2,400**
Nacelle cover	**17,000**
Generator	**77,000**
Power electronics (power factor caps)	**6,000**
0.95–0.95 substation VAR control	**12,000**
Transformer	**23,000**
Cable	**18,000**
Switchgear	**12,000**
Other subsystems	**25,000**
Drive train assembly and test	**8,000**
Total	**404,000**

Note: All costs rounded.

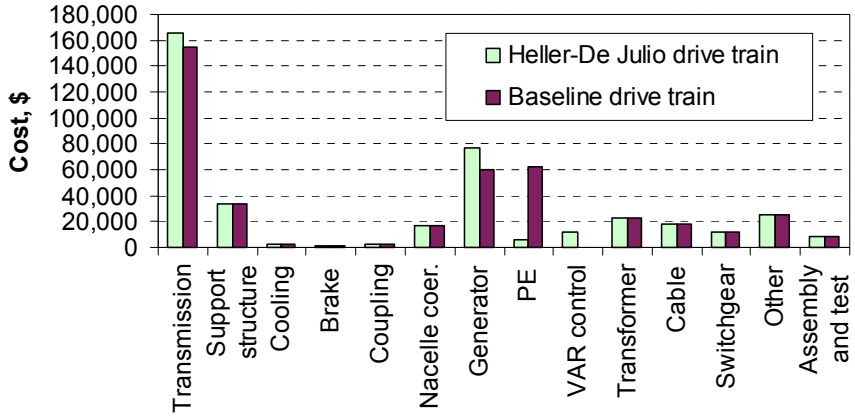

Figure 12-4. HDJ and baseline component cost comparison

12.3.4 Heller-De Julio Operations and Maintenance Costs

O&M costs of the HDJ drive train were not modeled. The annual O&M cost per year of the baseline drive train was used for analysis of the HDJ design. Baseline O&M estimates are described in Section 5.4.4. Because the AEP of the HDJ is lower than that of the baseline, the O&M costs as normalized by the AEP (in dollars/kilowatt) are higher for the HDJ than for the baseline.

The O&M costs of the HDJ system may be lower than those of the baseline because the baseline includes a PE system and the HDJ design does not. The baseline O&M estimates, itemized in Appendix J, include $1,030/yr in unscheduled maintenance and $130/yr in scheduled maintenance for the PE system. This adds to $1,160/yr, or approximately 5% of the $24,600 total O&M estimate for the baseline system.

12.3.5 HDJ Cost of Energy Estimates

Table 12-4 gives the COE estimates for the HDJ drive train. The COE estimate for this design is 0.0368 $/kWh, approximately 3% higher than the baseline estimate. The higher COE estimate results from lower energy capture for the HDJ compared with the baseline. As described in Section 12.3.2, the lower energy capture of the HDJ results from the (1) absence of significant variable-speed operation below rated, and (2) lower efficiency at higher powers. The initial capital cost of the HDJ system is less than the baseline, but not low enough to make up for the lost energy production.

It is expected that lower slip versions of the HDJ generator may give more favorable COE estimates. The generator efficiency will be higher, giving a higher AEP. However, component costs will also increase because of lower compliance to wind gusts and higher loads. The higher energy production may offset the higher costs. It is not expected that this trend will result in a COE significantly lower than that of the baseline.

The maintenance advantages of eliminating the PE system in the HDJ have not been taken into account in these estimates. The baseline O&M estimates, which include PE system maintenance, were used for these estimates. As described in Section 12.3.4, the power electronics account for approximately 5% of the baseline O&M costs. A 5% reduction in the O&M estimates will result in a reduction of approximately 1% in the COE estimate.

Table 12-4. HDJ Drive Train COE Estimates, Compared to Baseline

	Heller-De Julio		Baseline
	Cost, $	% of COE	Cost, $
Capital Costs			
Turbine	**976,983**	**60.4**	1,001,491
Rotor	**248,000**	**15.3**	248,000
Drive train and nacelle	**404,077**	**25.0**	430,778
Yaw drive and bearing	**16,000**	**1.0**	16,000
Control, safety system	**7,000**	**0.4**	7,000
Tower	**184,000**	**11.4**	184,000
Turbine manufacturer's overhead and profit (30%, tower, rotor, and transformer excepted)	**117,906**	**7.3**	126,229
Balance of station	**358,000**	**22.1**	358,000
ICC	**1,334,983**	**82.6**	1,359,491
AEP			
Ideal annual energy output, kWh	5,248,000		5,479,000
Availability, fraction	0.95		0.95
Losses, fraction	0.07		0.07
Net AEP, kWh	**4,636,608**		4,840,697
Replacement costs, LRC, $/yr	**5,124**	**3.0**	5,124
FCR, fraction/yr	**0.106**		0.106
O&M, $/kWh	**0.0053**	**14.4**	0.0051
COE = O&M + ((FCRxICC)+LRC)/AEP	**0.0368**		0.0358

12.4 Heller-De Julio Scaling to 750 kW and 3 MW

No scaling estimates were made for the HDJ drive train.

13. Henderson Drive Train

The Henderson drive train is a modification of the baseline drive train, using a hydraulic torque-limiting system to replace the variable-speed power electronics. Initial conceptual design estimates for the Henderson design indicated that the COE for this design is comparable to that of the baseline. Significant improvements over the baseline COE were not anticipated, so further preliminary designs were not developed for this design. This section describes the conceptual design estimates made for this design early in the study.

13.1 Henderson System Description

The Henderson drive train is illustrated in Figure 13-1, and Figure 13-2 is a system diagram. The Henderson drive train is the same as the baseline, except that the gearbox, generator, and PE system have been replaced with the proprietary Henderson torque-limiting gearbox and a fixed-speed, grid-connected squirrel-cage induction generator.

The Henderson gearbox is a modification of the baseline gearbox. The third parallel gear stage of the baseline is replaced by a planetary stage with a secondary power takeoff from a rotating annulus gear. The secondary takeoff drives a hydraulic pump, which is part of a torque-limiting hydraulic system that allows the annulus gear to slip when the torque exceeds a set level. The system provides torque limiting to reduce gearbox loads without a variable-speed PE system. In this regard, the Henderson approach is functionally comparable to the incorporation of a fluid coupling between the baseline gearbox and the squirrel-cage induction generator.

Although the Henderson design does provide desirable torque limiting, the technique does not capture the additional energy associated with variable-speed operation. The Henderson system is covered by a U.S. patent held by Geoff Henderson, Christchurch, New Zealand (Henderson 1992).

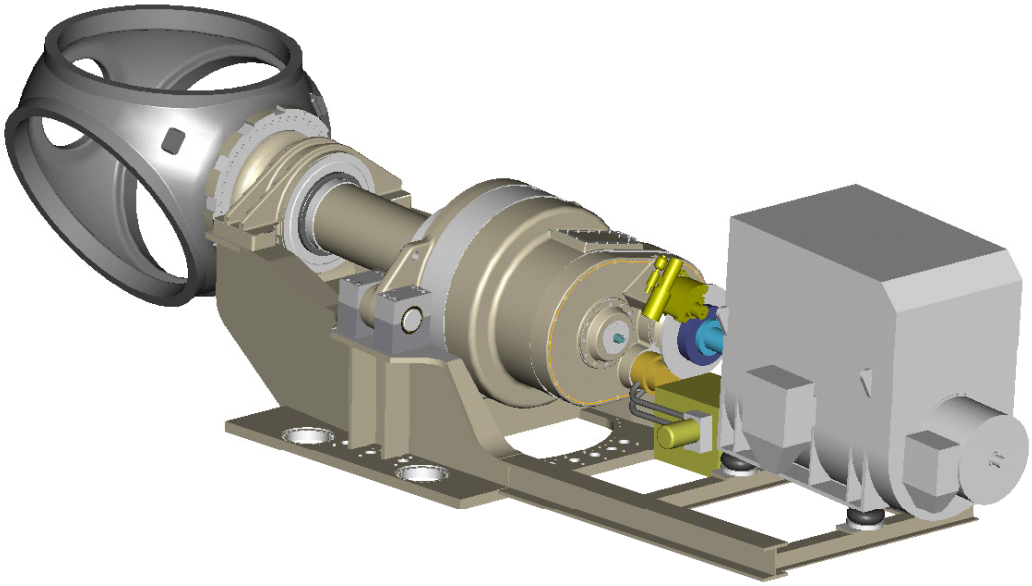

Figure 13-1. WindPACT Henderson drive train

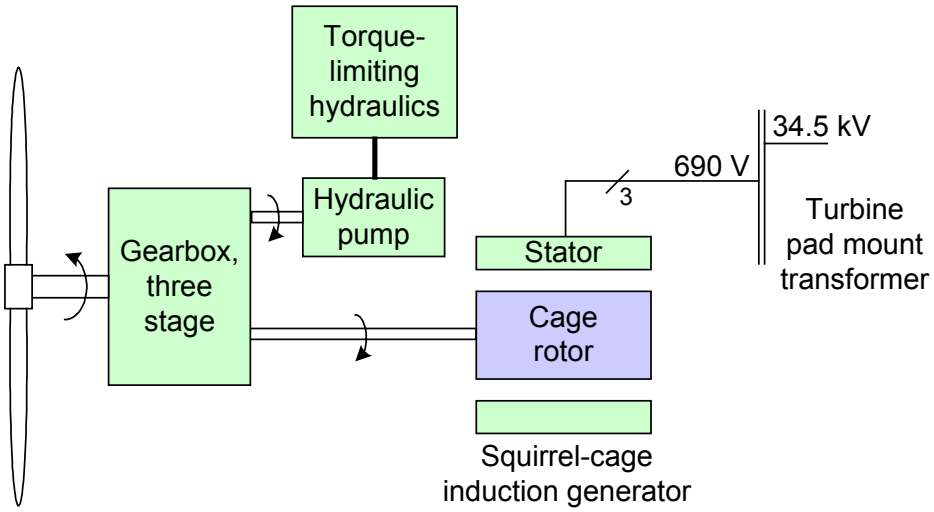

Figure 13-2. Henderson torque-limiting gearbox system diagram

13.2 Henderson Design Alternatives

The only significant alternative considered in the study for the Henderson drive train was the use of a synchronous generator in place of the squirrel-cage induction generator. Geoff Henderson recommended using a synchronous generator. Because the torque-limiting hydraulics limit the gearbox torque, the slip compliance of induction generators is not necessary in the Henderson system. Synchronous generators have performance advantages over induction generators because reactive power is controlled by the field-

winding control. This allows the power factor to be controlled without power factor correction capacitors and enables leading power factor operation and VAR generation.

A synchronous generator was not chosen for the Henderson design because IP54 sealed-construction synchronous generators are significantly more expensive than IP54 induction generators. However, the use of an open-construction, IP23 (IEC 2001) synchronous generator was estimated and the COE was found to be lower than that resulting from the use of an IP23 induction generator. This is because open-construction IP23 synchronous generators are manufactured in quantity and are available at lower prices than IP23 induction generators.

Open-construction, IP23 generators were not considered for the WindPACT study, however. This decision reflects field experience with stator winding failures resulting from environmental contaminants and the effects of vibration. Such failures have resulted in IP54 generators becoming standard for virtually all wind turbine designs.

13.3 Henderson Component Designs

Geoff Henderson of Wind Torque Limited (WTL) supplied information about the Henderson system to GEC, and WTL was paid a consulting fee for the time involved. GEC analyzed the system with the assistance of PEI, who estimated costs for the modified baseline gearbox, and Phil Forde and Associates, LLC, who were contracted to estimate the hydraulic system costs.

13.3.1 Henderson Drive Train Mechanical Design

The mechanical design of the Henderson drive train has the same architecture as the baseline drive train, described in Section 5. Several minor differences in the mechanical system result from the Henderson torque-limiting system:

1. The gearbox is modified and the hydraulic torque-limiting system is added.

2. The Henderson design runs at fixed speed below rated. To maximize energy capture, the Henderson system was analyzed with a fixed speed of 17.2 rpm, approximately 15% below the baseline rated speed of 20.5 rpm. This causes a corresponding torque increase, with drive train cost implications. The selection of the 17.2-rpm fixed speed is described in Section 10.5.2 for the multi-induction drive train, which is also a fixed-speed design and was analyzed in the same way.

3. The Henderson design limits torque at the high-speed stage of the gearbox; the baseline design limits torque at the air gap of the generator. This reduces the gearbox torque by eliminating the additional torques caused by acceleration of the generator inertia during wind gusts.

4. The rated speed of a 4-pole induction generator is approximately 1820 rpm; the rated speed of the baseline generator is 1500 rpm (synchronous speed is 1200 rpm for the 6-pole machine analyzed), so a higher gear ratio is needed for the Henderson system.

For this study, with the exception of the gearbox, the baseline costs for all mechanical components were used to estimate the Henderson drive train costs. Both the additional loading caused by item #2 above and the reduced loading resulting from item #3 above were neglected. This approximation is expected to be favorable to the Henderson system because rough estimates show the additional loads resulting from item #2 to be greater than the reduced loads resulting from item #3. A detailed estimate was made for the Henderson gearbox, as described in the following subsection, based on the baseline load estimates.

13.3.1.1 Henderson Gearbox

The Henderson gearbox configuration, shown in Figure 13-3, is identical to the baseline transmission for the first two stages. The third and final stage is reconfigured with a planetary differential. The planetary differential splits the output power, similar to an automotive differential. This device allows one output to speed up while retarding the other. Because the toothed device has no slip capability, the sum of the two outputs always equals the input.

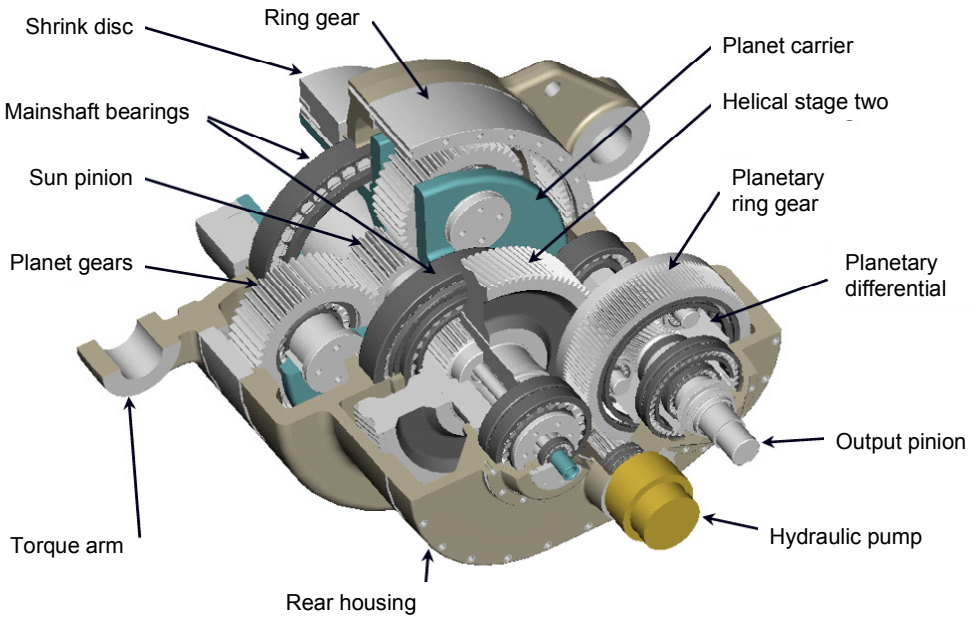

Figure 13-3. Henderson gearbox

Figure 13-3 illustrates the planetary differential output stage. In a conventional planetary stage with the power input at the planet carrier, the ring gear is fixed. In this case the output is at the sun pinion, and the speed increase is proportional to the gear ratio. In the Henderson gearbox, the ring gear may be stationary or it may rotate, depending on the pump-driven hydraulic circuit. Any rotation of the ring gear subtracts from the output speed.

The gears in the Henderson gearbox output stage were designed with the same design rules used for other gears in the system. To simplify the bearing reaction, spur gearing was used. High-speed output stages for wind turbine transmissions typically use helical gears to limit audible noise. The use of spur gears would ultimately require further development and testing to validate noise characteristics, but this was not done as part of this study. Converting the output stage design to use helical gears would likely increase the size and the cost of the Henderson gearbox.

13.3.1.2 Henderson Torque-Limiting Hydraulics

Geoff Henderson supplied specifications and descriptions of the torque-limiting hydraulics. Based on these specifications, Phil Forde and Associates estimated costs for the 1.5-MW WindPACT design.

The torque-limiting hydraulic system is described in three documents: U.S. Patent 5,140,170 (Henderson 1992), WTL S1509 “Wind Torque Limited, 1.5 MW Torque Limiting Hydraulics,” and WTL S1506 “Wind Torque Limited, 1.5 MW Torque Limiting Gearbox.” The last two documents were developed for this study and are included in Appendix M.

The hydraulic torque-limiting system's primary component is a low-speed, high-pressure pump equipped with control valves to provide the desired torque reaction to the annulus gear. The pump will run with limited slip until the pump torque (fluid pressure) reaches a preset value, after which it is not allowed to increase further. When this occurs, the rotor accelerates and the blade pitch is then used to control the speed.

The low-speed, high-pressure pump is driven by a pinion gear meshed with the ring gear of the drive train gearbox. The system also includes the following components: a pressure relief valve, in-line variable-flow restrictors, a fluid filter, an oil-to-air heat exchanger, and a thermostatic mixing valve. The mixing valve directs the hot fluid through the heat exchanger when the fluid temperature reaches a predetermined threshold value.

The fluid discharging from the pump encounters an adjustable fluid restriction that permits the pump-induced reaction torque characteristics to be shaped to some degree. The primary fluid restriction path is paralleled with a second restriction path to decrease the pump outlet pressure when the fluid is cold and quite viscous (wind turbine start-up). This second parallel path remains connected until the fluid temperature reaches a value that can be adjusted in the field via the settings of the temperature switch. When the threshold temperature level is reached, the secondary parallel path is disconnected by the actuation of the solenoid valve. Normally this secondary flow path then remains out of the circuit until the next start-up sequence when the fluid is cold.

The system described above is connected into a closed circuit, meaning that the fluid recirculates quite rapidly from the pump outlet back to the pump inlet without flowing through a fluid reservoir. However, some fluid is discharged from the closed circuit by means of internal leakage of the pump. That fluid does return to a reservoir, and is replenished into the closed circuit by an external source of low-pressure fluid. The external source of fluid is directed into the pump inlet using a pressure-reducing and -relieving valve that limits the pump inlet pressure to a desired range. The pressure range is adjustable within the limits of the pressure-reducing and -relieving valve and the magnitude of the external source of pressure.

Phil Forde and Associates developed the hydraulic schematic diagram shown in Figure 13-4 for the torque-limiting concept. The pump is shown on the diagram with an identifier name of PMP 1. The gearbox ring gear powers the pump drive pinion at a speed set by the drive train slip (governed by blade pitch control). The rotation of the pump causes a fluid flow to be discharged from the pump outlet. If the resistance of the fluid flow becomes too great, the system relief valve PRV 3 opens up and directs the fluid flow past the control restrictions NV 7-1 and NV 7-2 to a low-pressure region of the closed circuit.

The torque required to drive the pump is proportional to the size of the pump's displacement and to the resistance to the fluid flow exiting the pump outlet. The size of pump PMP 1 is expressed in cubic inches per revolution. This pump is a fixed-displacement pump, so the torque required to drive the pump is proportional to the outlet fluid flow resistance, expressed in pounds per square inch. The pump outlet pressure is limited by the relief valve PRV 3, which limits the pump drive torque, and thus the drive train reaction torque. The relief valve PRV 3 is a cartridge-style valve. It is incorporated into a circuit manifold MFD 2, which is fastened directly to the pump's inlet-outlet-porting interface. Note that the spring chamber of the relief valve PRV 3 is referenced to the pump inlet pressure to avoid the effects of system back-pressure on relief valve performance.

The outlet flow from pump PMP1 normally goes to the torque control manifold MFD 6. If the fluid is warm, the only passage available to it is the path through variable restrictions NV 7-2 and NV 7-1. Variable-flow restrictors NV 7-2 and NV 7-1 are used to adjust the pump outlet pressure at a given pump

speed (pump output flow rate). Because their settings affect the conditions under which the relief valve PRV 3 will open, these restrictors control the conditions when the torque limiting takes place.

If the fluid temperature is low, the resistance of the flow through the flow restrictions NV 7-2 and NV 7-1 will be high, which results in torque limitation caused by the relatively high fluid viscosity. This causes the torque limitation to vary from the system design values. Before temperature switch TS 9 is actuated, a parallel path exists for the fluid flow through flow restriction NV 7-3 and solenoid valve SV 8. This will continue until the fluid temperature warms up to the normal level. At the temperature switch setting, the solenoid valve is energized to shut valve SV 8 and force the pump outlet flow to be channeled to the path of NV 7-2 and NV 7-1 only. This mode of operation provides for normal torque-limiting control.

Pump outlet flow that exits manifold MFD 6 is directed to the fluid filter FLT 10 where the particulate matter in the fluid is removed and stored in the filter element media. As the filter element captures particulate matter, the resistance to fluid flow through the filter assembly increases. A visual readout displays the amount of flow resistance when the system is running. In addition, the increasing pressure drop caused by the collected contaminants will eventually trigger a differential pressure switch that informs the wind turbine control system that the filter element needs servicing. If the visual display and the differential pressure switch are ignored, the fluid will bypass the filter element, nullifying most of the effectiveness of the filter assembly.

Downstream of the filter assembly is the heat exchanger EXCH 11 and thermostatic control valve VLV 12. When the fluid is cold, the exchanger will be bypassed by the action of valve VLV 12. This allows the fluid to warm up to a normal level rapidly. When the fluid temperature reaches the maximum desired temperature, all the fluid will be directed through the exchanger; none will bypass the exchanger.

After passing through the heat exchanger, the fluid returns to the pump inlet at manifold MFD2. Depending on the operating conditions of fluid viscosity and pump speed, among others, the pressure at the pump inlet may be low, permitting insufficient pump filling. The low inlet pressure would be detrimental to the life of the pump. Adequate pressure and quantity of fluid is provided by feeding the pump inlet with another source of fluid external to the closed circuit. This replaces the fluid that exited the closed circuit via the pump case drain. The valve that controls this added supply of fluid is the valve PCV 4 located in manifold MFD 2 that is mounted on the pump.

Hydraulic System Cost Estimate

Table 13-1 gives Phil Forde and Associates' cost estimates for the 1.5-MW hydraulic system. These estimates are based on the hydraulic schematic described in the preceding subsection. A hydraulic power unit, necessary to provide the circuit make-up fluid for the hydraulic torque-limiting system, is included in these estimates. The power unit estimate is based on a variable-volume pump powered by a 5-hp electric motor mounted on a 25-gal reservoir with standard accessories. The estimates are based on a production rate of ten units per month.

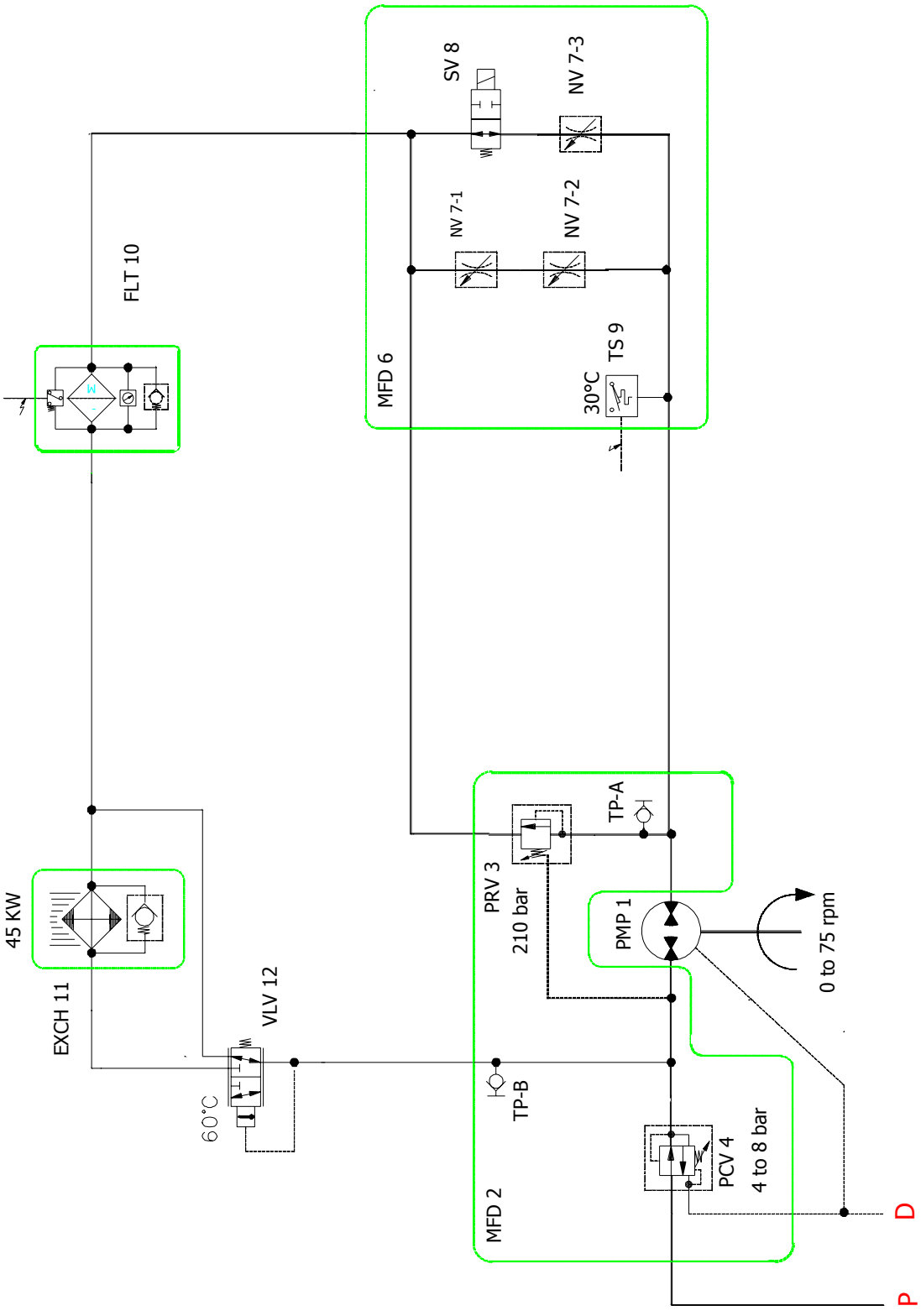

Figure 13-4. Hydraulic schematic

Table 13-1. Hydraulic Torque-Limiting System Components and Production Costs

Item	Description	Manufacturer's Model	Cost, $
1	Low-speed, high-pressure piston pump	Poclain Hydraulics Model MS18-0-1-1-1-A18-2-A-5-0-2568	5,560
2	Valve manifold, pump mounted	Custom design for this application	249
3	Relief valve cartridge	Sun Hydraulics Model RVGD - LWN	192
4	Pressure-reducing, pressure-relieving valve cartridge	Sun Hydraulics Model PPFB - LBN	79
5	Pressure test quick connect	Schroeder Industries Model 2101 - 01 - 21.00	25
6	Valve manifold, torque control	Custom design for this application	197
7	Needle valve cartridge	Sun Hydraulics Model NFCC - LCN	67
8	Bypass valve	Sun Hydraulics Model DLDA - MHN - 224 - (24 VDC)	82
9	Temperature switch	Barksdale Model ML1H - 203S - WS	279
10	Hydraulic pressure filter	Schroeder Industries Model LF1 - KS3 - 5 - MS - D	275
11	Hydraulic fluid to air cooler without fan, with b-pass check valve	OilAir Hydraulics Model 539033 - SAE	594
12	Mixing valve, thermostatically controlled	Fluid Power Energy Model S1010J16T50140	249
13	Fluid conductors and fittings	Various Parker products	840
14	Hydraulic power unit, 5 hp		2,500
	Assembly and test	NA	400
		Sub-total:	11,588
	Installation and Functional Test		1,000
		Total System Installed Costs	12,588

Notes:
Component costs include multiple quantity when required.
Costs noted are for production rate of 10 systems per month
Project costs at 50 systems per month are at 85% of costs listed.

13.3.2 Henderson Drive Train Electrical Design

A detailed one-line diagram was not developed for the Henderson system. Cost estimates of the electrical system were based on modifications to the baseline component costs. The baseline wound-rotor induction generator was replaced with a squirrel-cage induction generator, and the variable-speed PE system was eliminated. Costs were added for a soft-start module to limit in-rush currents during start-up and for capacitors to correct power factor. Power factor capacitor costs from the SCR-SCR PM generator system used in the single PM drive train (correction from 0.85 power factor) were used. Costs were included also for substation VAR control, consistent with estimates for other drive trains that do not have IGBT, PWM PE converters capable of providing active VAR control. The rest of the electrical system costs, including cable and switchgear costs, were approximated with the baseline estimates.

13.3.2.1 Henderson Generator

Table 13-2 gives the generator specifications for the 1.5-MW Henderson drive train. Liquid cooling is assumed and the additional costs of an external liquid heat exchanger and piping are included as a separate item in the ancillary component estimates.

Table 13-2. Target 1.5-MW Generator Specifications

Type	Squirrel-cage induction generator
Voltage	690 V line-line
Pole number	4
Frequency	60 Hz
Construction	IP54 protection
Cooling	Liquid

Several manufacturers offer generators with specifications similar to those described above. Quotes from two manufacturers were used for this study. The first is currently a supplier to wind turbine manufacturers. The second has not yet produced generators for this application. Table 13-3 shows the quoted generator prices. All quoted prices were based on quantities of between 100 and 600 per year, sold to turbine manufacturers. None of the quoted generators is an exact match for the specifications listed in Table 13-2. Both generators quoted by Manufacturer #1 are 50-Hz generators. Generators for 60-Hz operation are expected to be slightly lower in cost. The generator quoted by Manufacturer #2 is a 2400-V generator, and a 690-V generator should be more expensive. The liquid-cooled generator is less expensive than the air-cooled generator, possibly because it has a smaller frame size.

Taking the data in Table 13-3 into account, a cost of $42,000 was used for the 1.5-MW squirrel-cage generator.

Table 13-3. Squirrel-Cage Generator Quotes

Manufacturer	Frequency, Hz	Pole #	Voltage	Protection	Cooling	Frame Size	Price, $
1	50	4	690	IP55	Air-air	500 M	41,900
1	50	4	690	IP55	Liquid	450 L	37,600
2	60	4	2400	IP54	Air-air	500–1120	41,750

Generator efficiency was estimated using a full-load efficiency value of 97.1% provided by Manufacturer #1, together with the normalized, partial-load efficiency curves used for the multi-induction generators shown in Figure 10-10. Manufacturer #1 gave a power factor estimate of 0.87 at full load.

13.3.3 Soft-Start, Power Factor Correction, and VAR Control

For the purposes of comparison to other drive train designs, the soft-start and power factor capacitor estimates were made using the same methods used to estimate PE systems throughout the study. The assumption was made that these components would be assembled in a common enclosure by an electrical system manufacturer, who would then sell the assembled unit to the turbine manufacturer. Table 13-4 presents the estimates for these components. The soft-start controller was assumed to consist of six SCRs and associated components along with a parallel contactor. Component estimates from the SCR-SCR PE system included in Appendix F were used. Power factor correction capacitor estimates are based on the estimate for 350 kVAR of correction capacitors and the associated contactors and fuses included in the SCR-SCR PE system estimates in Appendix F. The amount of reactive power necessary to correct a

1500-kW induction generator with a power factor of 0.87, 0.95 lagging power factor at full load is 350 kVAR. The wind farm VAR control system provides the rest of the compensation.

Table 13-4. Soft-Start and Power Factor Correction Estimate

Description	Quantity	Unit Cost, $	Extended Cost, $
Assembly, SCR, three-phase	1	3,109	3,109
Contactor, 1500 A, 1000 V, 3-pole, line	1	2,480	2,480
Soft-start total (1.5 MW)			**5,589**
Fuse and fuse holder, 50 A, 690 V	6	33	198
Fuse and fuse holder, 100 A, 690 V	3	33	99
Fuse and fuse holder, 200 A, 690 V	3	33	99
Contactor, 50 A, 690 V, 3-pole	2	111	222
Contactor, 100 A, 690 V, 3-pole	1	212	212
Contactor, 200 A, 690 V, 3-pole	1	334	334
Capacitor, 50 kVAR, 690 V, three-phase	2	200	400
Capacitor, 100 kVAR, 690 V, three-phase	1	400	400
Capacitor, 200 kVAR, 690 V, three-phase	1	800	800
Power factor correction total (350 kVAR)			**2,764**
Enclosure	1	1,876	**1,876**
Material cost total			**10,229**
Gross margin = 40%*			
Sales price to turbine manufacturer			**17,048**

*Gross margin = (sales price - material cost) ÷ sales price

The wind farm VAR control estimates described in Section 4.11.3 were used for this drive train.

13.3.4 Henderson Drive Train Ancillary Components

All ancillary component costs for the Henderson drive train were assumed to be the same as for the baseline drive train estimates. These items include the costs for the gearbox and generator cooling system, the brake and hydraulics system, the high-speed coupling, and assembly.

13.4 Henderson Results

The subsections that follow summarize the COE estimate for the 1.5-MW Henderson design along with the efficiency, energy production, component cost, and O&M estimates used for the COE estimate. Detailed, preliminary design estimates were not made for the Henderson drive train. The results of conceptual design estimates, made early in the study, are presented in this section. These estimates were made with less detail than corresponding estimates made of some of the other designs investigated during the study.

13.4.1 Henderson Efficiency

Figure 13-5 shows the drive train efficiency versus input power on a component-by-component basis, with the total drive train efficiency of the baseline shown for comparison. The Henderson drive train efficiency is slightly higher than that of the baseline at medium to rated power but has reduced efficiency below approximately 10% of rated power. Several factors determine the Henderson efficiency:

- The system operates at fixed speed, which increases gearbox losses at low power relative to the variable-speed baseline drive train. The fixed-speed gearbox efficiency measurements presented in GEC (2002) were used for these estimates.
- There are no variable-speed power electronics, eliminating associated losses.
- Hydraulic system losses are introduced, resulting from the associated slip.

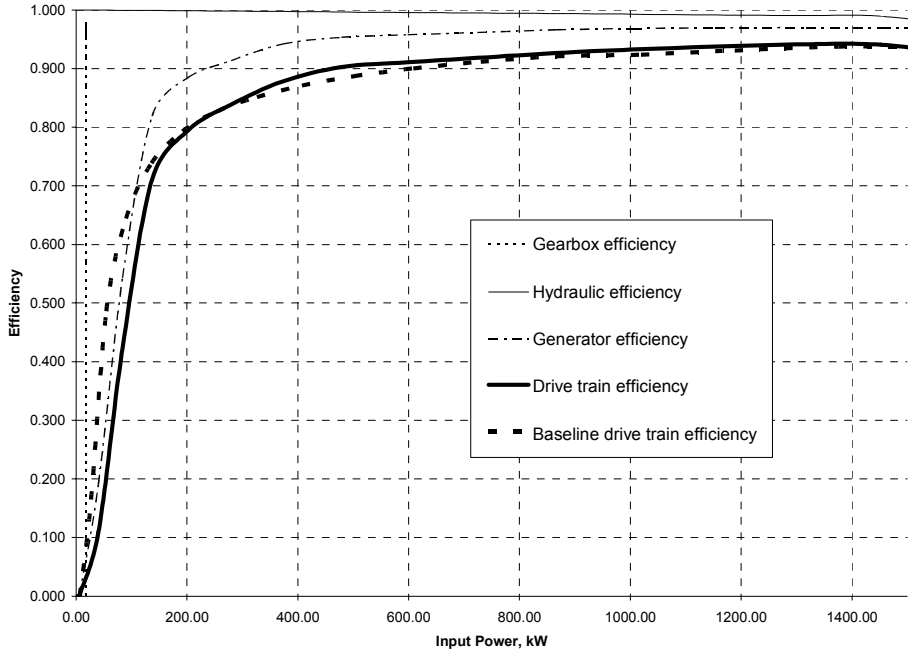

Figure 13-5. Henderson drive train efficiency by component

13.4.2 Henderson Gross Annual Energy Production

The GAEP estimate for the Henderson design is shown for each wind speed bin in Table 13-5. Because these values represent the generator electrical output, drive train efficiency losses are included in this estimate. All other losses (those external to the drive train) are calculated separately in the final COE analysis. The wind speed bins from 12.0 m/s to the cut-out speed of 27.5 m/s are aggregated in a single row. The energy production values for those wind speed bins are identical to those for the baseline turbine (see Table 5-3) with the rotor speed at rated and the output power regulated to 1.5 MW by the pitch system.

The Henderson design's total GAEP is estimated at 5283 MWh, which is approximately 4% less than the estimated production of 5479 MWh for the baseline design. The Henderson design has lower energy capture than the baseline system because the Henderson design does not operate at variable speed in Region II, when the output power is below rated. There are also minor efficiency differences between the Henderson design and the baseline design, as shown in Figure 13-5, but the effects of these differences are less significant.

To simplify calculations, generator slip was neglected and a fixed rotor speed was used for all wind speed bins. To optimize the constant-speed operation, the fixed rotor speed was adjusted to maximize the energy capture of the turbine. This is the same optimization that was done for the fixed-speed multi-induction drive train, which is described in Section 10.5.2. A rotor speed of 17.2 rpm maximized the energy capture. This rotor speed is lower than the baseline rated speed of 20.5 rpm, resulting in relatively higher drive train torques and costs.

Table 13-5. Henderson Drive Train GAEP

Wind Speed Bin Center, m/s	Rotor Speed, rpm	Rotor Power, kW	Drive Train Efficiency	Output Power, kW	# of Hours per Year	Energy Production	
						MWh	Fraction of Total, %
3.0	17.20	0.0	0.000	0.0	297.5	0	0.00
3.5	17.20	0.0	0.000	0.0	333.1	0	0.00
4.0	17.20	5.1	0.000	0.0	363.0	0	0.00
4.5	17.20	40.2	0.109	4.4	386.9	2	0.03
5.0	17.20	83.7	0.423	35.4	404.7	14	0.27
5.5	17.20	137.2	0.712	97.6	416.5	41	0.77
6.0	17.20	201.9	0.795	160.5	422.4	68	1.28
6.5	17.20	280.0	0.839	234.8	422.7	99	1.88
7.0	17.20	373.1	0.878	327.6	417.8	137	2.59
7.5	17.20	478.5	0.902	431.8	408.3	176	3.34
8.0	17.20	598.1	0.910	544.5	394.7	215	4.07
8.5	17.20	724.0	0.918	664.8	377.7	251	4.75
9.0	17.20	866.4	0.926	802.6	357.8	287	5.44
9.5	17.20	1003.3	0.932	935.4	335.9	314	5.95
10.0	17.20	1153.4	0.937	1081.1	312.4	338	6.39
10.5	17.20	1317.7	0.941	1240.6	288.0	357	6.76
11.0	17.20	1451.5	0.941	1365.2	263.2	359	6.80
11.5	17.20	1591.7	0.922	1467.7	238.5	350	6.63
12.0–27.5	17.20	1626.8	0.922	1500.0	1516.1	2274	43.0
					Total GAEP =	**5283 MWh**	

Figure 13-6 compares the energy production values of the Henderson and baseline designs by wind speed bin. For wind speeds above 11.5 m/s, the energy production values are equal for both designs, so those bins are not shown. At each wind speed bin shown, the Henderson system has a lower energy capture than the baseline system. The difference is greatest at the low wind speeds near cut-in and the higher wind speeds near rated. At those wind speeds, the Henderson system has a rotor TSR that is the furthest from optimum. The rotor speed for the Henderson system was decreased to 17.2 rpm, approximately 15% less than the 20.5-rpm rated speed for the baseline system. The 20.5-rpm speed gives an optimum TSR near rated. If that speed is used for the Henderson system, energy capture will be higher near rated and drop off faster at lower wind speeds. With the rotor speed fixed at 17.2 rpm, the energy capture is lower near the high end. However, the additional energy capture at lower speeds maximizes the total energy capture across the entire wind profile.

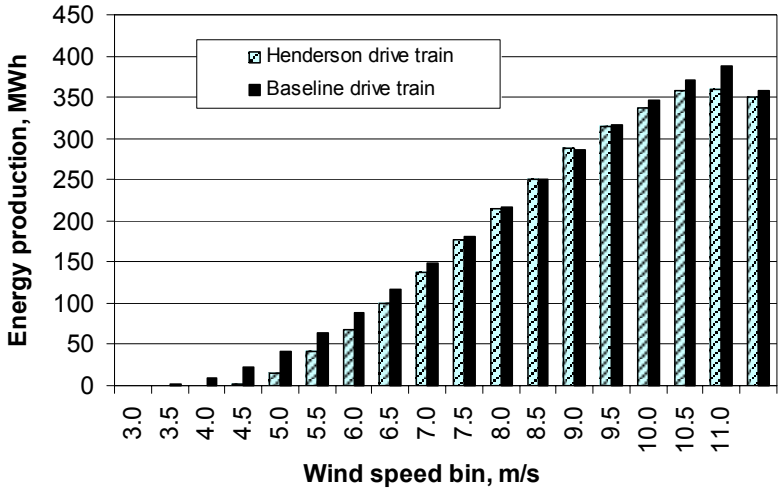

Figure 13-6. Henderson and baseline energy production by bin

13.4.3 Henderson Component Costs

Component costs for the Henderson drive train are itemized in Table 13-6. These data are compared directly to the baseline system in the bar chart given in Figure 13-7. Component costs for the Henderson drive train system are approximately 8% less than those for the baseline system, primarily because of reduced generator costs and the absence of costs for the power electronics. These cost savings are offset to some extent by the addition of soft-start, power factor correction and VAR control costs, along with additional costs in the transmission system for the more complicated gearbox and the hydraulic system.

Table 13-6. Henderson Drive Train Component Costs

Component	Cost, $
Transmission system	**178,000**
Gearbox components	130,000
Mainshaft	20,000
Mainshaft support bearing and block	12,000
Elastomeric mounting system	2,700
Generator isolation mounts	500
Torque-limiting hydraulics	13,000
Support structure (bedplate)	**34,000**
Generator cooling system	**2,400**
Brake system with hydraulics	**1,400**
Coupling (generator to gearbox)	**6,000**
Nacelle cover	**17,000**
Generator	**42,000**
Power electronics (soft-start and power factor caps only)	**17,000**
0.95–0.95 substation VAR control	**12,000**
Transformer	**23,000**
Cable	**18,000**
Switchgear	**12,000**
Other subsystems	**25,000**
Drive train assembly and test	**8,000**
Total	**396,000**

Note: All costs rounded.

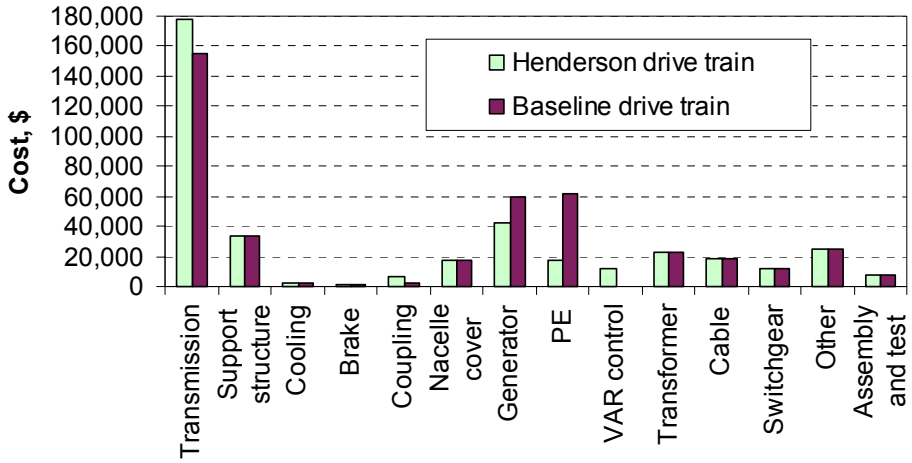

Figure 13-7. Henderson and baseline component cost comparison

13.4.4 Henderson Operations and Maintenance Costs

O&M costs for the Henderson drive train were not modeled. The annual O&M cost per year of the baseline drive train was used to analyze the Henderson design. Baseline O&M estimates are given in Section 5.4.4. Because the AEP of the Henderson drive train is lower than that of the baseline, the O&M costs expressed per energy production, or dollars per kilowatt-hour, are higher for the Henderson drive train than for the baseline.

13.4.5 Henderson Cost of Energy Estimates

Table 13-7 presents the COE estimates for the Henderson drive train. The COE estimate for this design is 0.0363 $/kWh, approximately 1% higher than the estimate for the baseline. The higher COE estimate results from lower energy capture for the Henderson drive train relative to the baseline. As described in Section 13.4.2, the Henderson design has lower energy capture because it does not operate with variable speed in Region II. The initial capital cost of the Henderson system is slightly less than that of the baseline, but not low enough to make up for the difference in energy production.

Table 13-7. Henderson Drive Train COE Estimates, Compared to Baseline

	Henderson		Baseline
	Cost, $	% of COE	Cost, $
Capital Costs			
Turbine	**965,893**	**60.2**	1,001,491
Rotor	**248,000**	**15.4**	248,000
Drive train and nacelle	**395,546**	**24.6**	430,778
Yaw drive and bearing	**16,000**	**1.0**	16,000
Control, safety system	**7,000**	**0.4**	7,000
Tower	**184,000**	**11.5**	184,000
Turbine manufacturer's overhead and profit (30%, tower, rotor, and transformer excepted)	**115,347**	**7.2**	126,229
Balance of station	**358,000**	**22.3**	358,000
ICC	**1,323,893**	**82.5**	1,359,491
AEP			
Ideal annual energy output, kWh	5,283,000		5,479,000
Availability, fraction	0.95		0.95
Losses, fraction	0.07		0.07
Net AEP, kWh	**4,667,531**		4,840,697
Replacement costs, LRC, $/yr	**5,124**	**3.0**	5,124
FCR, fraction/yr	**0.106**		0.106
O&M, $/kWh	**0.0053**	**14.5**	0.0051
COE = O&M + ((FCRxICC)+LRC)/AEP	**0.0363**		0.0358

13.5 Henderson Scaling to 750 kW and 3 MW

No scaling estimates were made for the Henderson drive train.

14. Summary

14.1 Summary of Cost of Energy Estimates

The drive train component cost estimates, AEP estimates, O&M and LRC estimates, and the resulting COE are summarized for each of the candidate drive trains in Table 14-1. The cost of energy estimate for three of the drive train designs, the single PM, multi-PM, and multi-induction, are substantially lower than the baseline COE. The single PM COE estimate is the lowest, at 87% of the baseline. The multi-induction drive train has the lowest drive train component cost, but this design also has a lower energy capture because of its constant-speed operation, offsetting some of the benefits in the COE estimate. The direct drive, Klatt, HDJ, and Henderson designs all have higher COE estimates than the baseline. This is caused by higher component costs for the direct drive and Klatt designs, and lower energy production, primarily as a result of constant-speed operation, for the HDJ and Henderson designs. The integrated baseline design has a COE estimate that is approximately 5% lower than the baseline, which results from a lower drive train component cost accruing from the benefits of integration. Based on these results and other factors, the single PM configuration was selected for detailed design and testing as part of this project.

The COE estimates in Table 14-1 are consistently lower than those being realized in existing U.S. wind farms, for several reasons:

- To be consistent with other WindPACT study results, the FCR NREL specified at the beginning of the project, 10.6%, was used for all estimates. As described in Section 4.2.2, NREL's current (2002) FCR estimates have increased to 11.8%.
- The turbine rotor was not marked up for the turbine manufacturer's overhead and profit in any of the estimates for consistency with other WindPACT results, as described in Section 4.2.1.
- The balance-of-station cost estimate of $240,000/MW is low compared to most wind farms. This estimate was used for consistency with other WindPACT studies.

Because each of these factors was applied consistently to all estimates, the COE numbers still correctly state the relative merits of each drive train design.

14.2 Summary of Scaling Estimates to 750 kW and 3 MW

The drive train cost estimates for each design at 750 kW, 1.5 MW, and 3 MW are shown together in Figure 14-1 and Figure 14-2 in terms of the drive train cost of energy and normalized cost per kilowatt, respectively. The drive train COE is the portion of the turbine COE that is attributed to the drive train capital cost. A constant hub height of 84 m is used for all sizes to eliminate the effects of height differences on wind speed in the COE calculations. All designs except the direct drive show a decreasing drive train COE and a normalized cost per kilowatt from 750 kW to 1.5 MW and an approximately level COE from 1.5 MW to 3 MW. The direct drive is an exception, increasing in COE and normalized cost as turbine size increases. This result is caused by limiting the diameter of the direct drive generators to 4.0 m, a practical limit for transportation purposes. These generators have an optimum diameter that is larger than 4.0 m.

Note that the results shown in Figure 14-1 and Figure 14-2 do not necessarily reflect the COE trends when scaling an entire wind turbine system. As turbine sizes increase, the costs of rotors and other elements of the system may rise more rapidly than the energy production for the system. The most cost-effective wind turbine size for a given wind energy project will most probably depend on site-specific wind resources, transportation logistics, and construction issues.

Table 14-1. Summary of Results

	Baseline	Integrated Baseline	Direct Drive	Single PM	Multi-PM	Multi-Induction	Klatt	Heller-De Julio	Henderson
Transmission system, $	155,000	120,000	NA	90,000	58,000	80,000	155,000	166,000	178,000
Support structure, $	34,000	21,000	55,000	20,000	19,000	11,000	34,000	34,000	34,000
External cooling system, $	2,400	3,000	3,400	4,400	5,300	4,500	2,400	2,400	2,400
Brake, $	1,400	1,300	12,400	3,200	5,600	2,800	1,400	1,400	1,400
Coupling, $	2,400	2,100	NA	NA	NA	1,800	2,400	2,400	6,000
Nacelle cover, $	17,000	9,000	14,000	8,200	7,000	13,100	17,000	17,000	17,000
Generator, $	60,000	60,000	304,000	54,000	78,000	40,000	60,000	77,000	42,000
Power electronics, $	62,000	62,000	53,000	53,000	53,000	17,000	74,000	6,000	17,000
Substation VAR control, $	NA	NA	12,000	12,000	12,000	12,000	NA	12,000	12,000
Transformer, $	23,000	23,000	26,000	26,000	26,000	23,000	23,000	23,000	23,000
Cable, $	18,000	18,000	16,000	16,000	16,000	18,000	18,000	18,000	18,000
Switchgear, $	12,000	12,000	10,000	10,000	13,000	22,000	12,000	12,000	12,000
Other subsystems, $	25,000	25,000	25,000	25,000	25,000	25,000	25,000	25,000	25,000
Drive train assembly and test, $	8,000	4,900	9,400	5,500	7,900	10,200	8,000	8,000	8,000
Drive train component cost total	**420,000**	**361,000**	**540,000**	**327,000**	**325,000**	**279,000**	**433,000**	**404,000**	**396,000**
Percentage of baseline drive train cost	**100**	**86**	**129**	**78**	**77**	**66**	**103**	**96**	**94**
AEP, kWh)	**4.841E+06**	**4.841E+06**	**4.990E+06**	**5.001E+06**	**4.978E+06**	**4.658E+06**	**4.841E+06**	**4.637E+06**	**4.668E+06**
Percentage of baseline AEP	**100**	**100**	**103**	**103**	**103**	**96**	**100**	**96**	**96**
Replacement costs, LRC ($/yr))	**5100**	**5100**	**5600**	**4800**	**4500**	**4700**	**5100**	**5100**	**5100**
O&M, $/yr)	**24600**	**23500**	**23700**	**21200**	**23400**	**22900**	**24600**	**24600**	**24600**
O&M, $/kWh	**0.0051**	**0.0049**	**0.0047**	**0.0042**	**0.0047**	**0.0049**	**0.0051**	**0.0053**	**0.0053**
COE, $/kWh	**0.0358**	**0.0339**	**0.0378**	**0.0313**	**0.0317**	**0.0325**	**0.0361**	**0.0368**	**0.0363**
Percentage of baseline COE	**100**	**95**	**106**	**87**	**89**	**91**	**101**	**103**	**101**

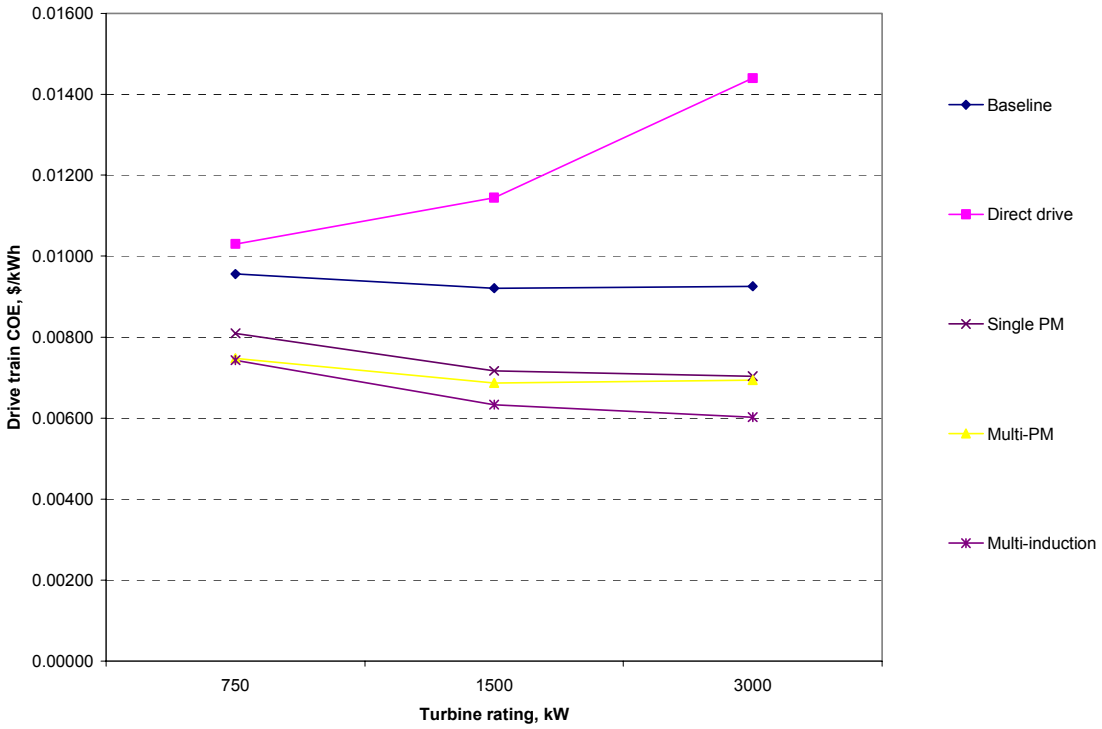

Figure 14-1. Drive train COE scaling for 84-m hub height

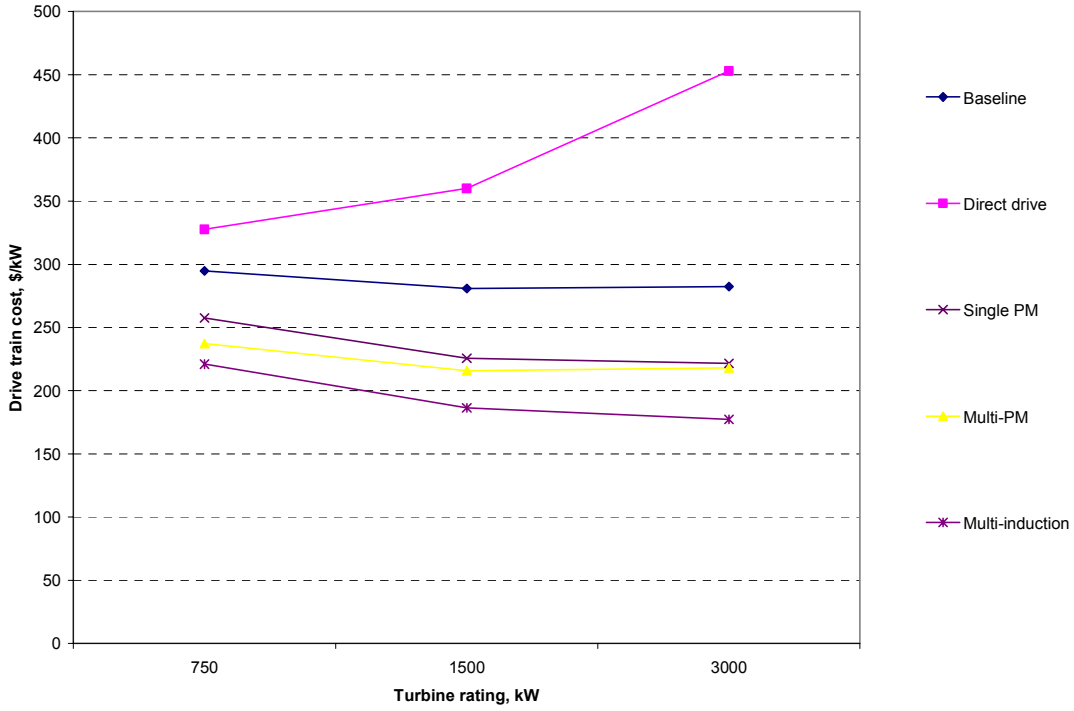

Figure 14-2. Drive train cost per kilowatt scaling

15. List of Abbreviations

AC	alternating current
AEP	annual net energy production
AGMA	American Gear Manufacturers Association
AWEA	American Wind Energy Association
BOM	bill of materials
COE	cost of energy
DC	direct current
EDI	Engineering Devices, Inc.
EMF	electromagnetic field
EPRI	Electric Power Research Institute
FCR	fixed charge rate
FEA	finite element analysis
GAEP	gross annual energy production
GCT	gate controlled thyristor
GEC	Global Energy Concepts, LLC
HDJ	Heller-De Julio
hp	horsepower
ICC	initial capital cost
IEEE	Institute of Electrical and Electronic Engineers
IGBT	insulated gate bipolar transistor
LED	light-emitting diode
LRC	levelized replacement cost
NA	not applicable
NEMA	National Electric Manufacturers Association
NREL	National Renewable Energy Laboratory
NeFeB	Neodymium Iron Boron
O&M	operations & maintenance
OEM	OEM Development Corporation
PE	power electronics
PEI	Powertrain Engineers, Inc.
PID	proportional integral derivative
PM	permanent magnet
PWM	pulse width modulation
RF	radio frequency

rms	root mean square
rpm	revolutions per minute
SCR	silicon controlled rectifier
VAR	volt ampere reactive
VSI	voltage-source inverter
WindPACT	Wind Partnerships for Advanced Component Technologies
WTL	Wind Torque Limited

16. References

AGMA/AWEA (1997). *Recommended Practices for Design and Specification of Gearboxes for Wind Turbine Generator Systems, 921-A97.* Alexandria, VA: AGMA.

ANSI/AGMA (1995). *Fundamental Rating Factors and Calculation Methods for Involute Spur and Helical Gear Teeth, 2001 C-95.* Alexandria, VA: AGMA.

ANSI/AGMA (1997). *Design and Selection of Components for Enclosed Gear Drives, 6001-D97.* Alexandria, VA: AGMA.

ANSI/AGMA (1992). *A Rational Procedure for Preliminary Design of Minimum Volume Gears, 901-A92.* Alexandria, VA: AGMA.

ASTM (1993). *Standard Specification for Ductile Iron Castings, ASTM A536-84.* West Conshohocken, PA: ASTM.

Avolio, S.; Palmari, C., Honorati, O., Pincella, C., Zanotti, P., and Torri, C. (1993). "Power Conversion for the Connection to the Medium-Voltage Grid of a Variable Speed Wind Generator." In *Proceedings European Wind Energy Conference '93,* Lubeck-Travemunde, Germany, p.646.

Chan, Z.; Spooner, E. (1998). "Grid Interface Options for Variable-Speed, Permanent-Magnet Generators." In *IEE Proceedings on Power Applications* 145(4):273. IEE, London, UK, available at http://www.ieee.org/.

Cohen, J., Hock, S., and Codogan, J. (1989). "A Methodology for Computing Wind Turbine Cost of Electricity Using Utility Economic Assumptions." In *Windpower '89 Proceedings.* NREL/TP-257-3628. Golden, CO: NREL.

DIN (1997). *Spherical Graphite Cast Iron, EN1563.* Berlin, Germany. Deutsches Institute fur Normung.

Dubois, M. (2000). *Review of Electromechanical Conversion in Wind Turbines*. TU Delft Report EPP00.R03, 2000. Delft, The Netherlands: TU Delft University. Available at http://ee.its.tudelft.nl/epp/Pb_003_1.PDF.

Erdman, W.; Lettenmaier, T., and Chapman, J. (2002). "A Unique Variable-Speed Wind Farm Design Using Line-Commutated SCR Converters." In *Proceedings of Global Windpower Conference 2002, April 2-5, Paris, France*. European Wind Energy Association, 26 Rue du Trone, Brussels, Belgium.

GEC (2002). *Laboratory Testing of Drivetrain Component Efficiencies for Constant-Speed and Variable-Speed Wind Turbines*. NREL/SR-500-30117. Golden, CO: NREL. Available at http://www.osti.gov/bridge.

Germanisher Lloyd (1999). *Rules and Regulations, Non-Marine Technology,* Germanisher Lloyd, Vorsetzen 32, D-20459 Hamburg, Germany.

Grauers, A. (1996a). "Generators for Gearless Wind Energy Converters." Presented at the 1996 European Union Wind Energy Conference.

Grauers, A. (1996b). *Design of Direct-Driven Permanent-Magnet Generators for Wind Turbines*, Ph.D. Thesis, Chalmers University, Goteborg, Sweden.

Hau, E. (2000). *Wind Turbine Fundamentals, Technologies, Application, Economics*. New York: Springer-Verlag Berlin Heidelberg.

Heffernan, R.; Chrenko, R, Gamble, C. R., Heberle, D., Holley, W., Javier, B., Konconis, D., and Mills, R. (1996). *Direct-Drive Wind Turbine Feasibility Study*. Report TR-104911. Palo Alto, CA: EPRI.

Henderson, G.M. U.S. Patent No. 5,140,170 (August 18, 1992).

HYDAC International (2002). "SC and OK Series Air Cooled Oil Coolers." Glendale Heights, IL: HYDAC International.

IEC (1998). *Safety of Wind Turbine Conversion Systems, 61400-1.* International Electrotechnical Commission, Geneva, Switzerland, available at www.iec.ch

IEC (2001). *Degrees of Protection Provided by Enclosures (IP Code), 60529, Ed. 2.1*, International Electrotechnical Commission, Geneva, Switzerland, available at www.iec.ch

IEEE (1992). IEEE Reccomended Practices and Requirements for Harmonic Control in Electrical Power Systems, IEEE 519-1992, Institute of Electrical and Electronics Engineers, 347 East 47th Street, New York, NY, available at www.ieee.org.

ISO (1998). *Roller Bearings – Dynamic Load Ratings and Rating Life, ISO 281.* International Organization for Standardization, Geneva, Switzerland.

Jens Fisker (2001). "Face Load Distribution of Spherical Supported Planet Gears." M.Sc. research paper. Presented to committee members of AGMA/AWEA 6006, August 17.

Jones, R.; Smith, G.A. (1993). "High Quality Mains Power from Variable Speed Turbines." In proceedings of *International Conference on Renewable Energy – Clean Power,* p. 202-206., IEE, London, UK, , available at www.ieee.org.

KTR Corporation (2003). *Rotex Couplings*. Michigan City, IN: KTR Corporation. Available at www.ktr.com.

Kang, M.; Enjeti, P.; Pitel, I. (1999). "Analysis and Design of Electronic Transformers for Electric Power Distribution System." *IEEE Transactions on Power Electronics* 14(6):1133, available at www.ieee.org/.

Klatt, F. U.S. Patent No. 4,459,530. (July 10, 1984).

Klatt, F. U.S. Patent No. 4,634,950. (January 6, 1987).

Klatt, F. U.S. Patent No. 5,237,255. (August 17, 1993).

Klatt, F. U.S. Patent No. 5,243,268. (September 7, 1993).

Krishnan, R.; Rim, G.-H. (1989). "Performance and Design of a Variable Speed Constant Frequency Power Conversion Scheme with a Permanent Magnet Synchronous Generator." In *Conference Record of the 1989 IEEE Industry Applications Society Annual Meeting* 1:45, Institute of Electrical and Electronics Engineers, 347 East 47th Street, New York, NY, available at www.ieee.org.

Malcolm, D.J.; Hansen, A.C. (2002). *WindPACT Turbine Rotor Design Study*. Golden, CO: NREL.

Mikhail, A., Cristenson, C., Cousineau, K., Erdman, W., and Holley, W. U.S. Patent No. 6,137,187. (October 24, 2000).

Mohan, N., Undeland, T., Robbins, W. (1995). *Power Electronics: Converters, Applications, and Design*. New York: John Wiley & Sons.

Morrow, W., U.S. Patent No. 6,179,743. (January 30, 2001).

Muller, S.; Deicke, M.; De Doncker, R. (2002). "Doubly Fed Induction Generator Systems for Wind." *IEEE Industry Applications Magazine*, May/June:26, Institute of Electrical and Electronics Engineers, 347 East 47th Street, New York, NY, available at www.ieee.org.

NFPA. (2002). *National Electric Code*. 2002 edition. Quincy, MA: NFPA.

Richardson, D. and Erdman, W. U.S. Patent No. 5,083,039. (January 21, 1992).

SAE (1993). *Automotive Gray Iron Castings, SAE J431.* Warrendale, PA: SAE, Inc.

Short, W.; Packey, D., and Holt, T. (1995). *A Manual for the Economic Evaluation of Energy Efficiency and Renewable Energy Technologies*. NREL/TP-462-5173. Golden, CO: NREL. Available at http://www.osti.gov/bridge.

Vachon, W. (2002). "Long-Term O&M Costs of Wind Turbines Based on Failure Rates and Repair Costs." Presented at Windpower 2002, American Wind Energy Association, Annual Conference, June 2–5.

Wallace, A. et al. U.S. Patent No. 5,986,438. (November 16, 1999).

Wallace, A. et al. U.S. Patent No. 6,163,137. (December 19, 2000).

Appendix A

WindPACT Drive Train System Specification and Design Criteria

N60001-C

Drive Train System Specification and Design Criteria

Approvals

Tim McCoy	9/24/02
Originator	Date
Terry Lettenmaier	9/24/02
Checker	Date
Robert Poore	9/24/02
Project Manager	Date

Revision Block

Revision	Release Date	Pages Affected
A-original	February, 27, 2001	
B	June 26, 2002	3, 4, 6
C	September 24, 2002	2, 3, 4, 5, 6, 7, 8

Prepared by:

Global Energy Concepts, LLC
5729 Lakeview Drive NE Suite 100
Kirkland, Washington 98033-7340
(425) 822-9008

1. General

1.1 Background

The United States Department of Energy (DOE) through the National Renewable Energy Laboratory (NREL) has implemented the Wind Partnership for Advanced Component Technologies (WindPACT) program. This program will explore advanced technologies for improving the cost of energy from wind turbines. As part of this program, Global Energy Concepts, LLC (GEC) was awarded contract number YAM-0-30209, "WindPACT Advanced Wind Turbine Drive Train Designs" to research advanced drive train components for utility-scale wind turbines. This project will be broken into three distinct phases. In Phase I, GEC will perform preliminary designs of several innovative drive train architectures. At the conclusion of Phase I, NREL will select one of the architectures for further development in Phase II. In Phase III, a prototype of the selected design will be built and tested.

The turbine ratings covered by this specification, as per the focus of the WindPACT program, are 750 kW, 1500 kW, and 3000 kW.

1.2 Purpose and Scope

This document presents the general specifications and design criteria for drive train components and subsystems. This specification will include general operational, environmental, and engineering requirements. It is intended that this specification be applied throughout all phases of the project, although amendment may be necessary as the project progresses.

1.3 Applicability

These requirements are broadly applicable to all of the components and subsystems proposed for use across the full range of power ratings. These specifications apply primarily to equipment in the nacelle of the turbine, but also to a large extent to equipment in the tower or on the ground.

1.4 References

1. International Electrotechnical Commission, *Wind Turbine Generator System–Part 1: Safety Requirements*, International Standard 61400-1, 2nd Edition, 1998.
2. Germanisher Lloyd, *Rules and Regulations, IV–Non-Marine Technology, Part 1–Wind Energy,* 1999.
3. International Standards Organization, *General Principles on the Reliability of Structures*, ISO 2394.
5. *IEEE Recommended Practices and Requirements for Harmonic Control in Electrical Power Systems*, IEEE Standard No. 519-1992.
6. AGMA/AWEA-921-A97, *Standard for Design and Specification of Gearboxes for Wind Turbine Generator Systems*.
7. ANSI/AGMA 2001-C95, *Fundamental Rating Factors and Calculation Methods for Involute Spur and Helical Gear Teeth.*
8. ANSI C84.1-1995, Electric Power Systems and Equipment – Voltage Ratings (60 Hz).

2. Wind Turbine Design and Operation

2.1 Turbine Architecture and System Design

The following turbine architectural and system design assumptions are being made:

- Three blade, upwind rotor with independent full-span blade pitch control
- Variable speed except where specifically indicated
- Mechanical parking brake rated at turbine nominal rated torque
- Cone angle fixed at zero degrees
- Nacelle tilt angle fixed at 5 degrees (hub up)
- Tubular steel tower

2.2 Machine Characteristics

The four baseline ratings will have the specifications found in Table 2-1. Figure 2-1 depicts the ideal variable-speed operational curve for the 1500 kW rating.

Table 2–1. Baseline Turbine Specifications

Rating, kW	750	1500	3000
Rotor Diameter, m	50	70	99
Design tip speed ratio	7.0	7.0	7.0
Rated wind speed, m/s	11.5 m/s	11.5 m/s	11.5 m/s
Theoretical minimum operating rpm (n_1)*	8.0	5.7	4.1
Rated rpm	28.6	20.5	14.5
Maximum operating rpm (n_2=1.07*rated)	30.6	21.9	15.5
PE system trip rpm (=1.14*rated)	32.6	23.4	16.5
Safety system activation rpm (n_a=1.2*n_2)	36.7	26.3	18.6
Maximum overspeed design rpm (n_{max}=1.3*n_2)	39.8	28.5	20.2
Hub height, m	60	84	119
Hub height V_{ave}, m/s**	7.5	7.9	8.3
Cut in W.S., m/s	3.0	3.0	3.0
Cut out W.S., m/s	26.3	27.6	29.0

* Actual minimum rpm will vary depending on capability of PE system

** For production estimates only, see Table 3-2 for design wind regime

2.3 Operational Characteristics

The drive train components and subsystems shall be designed for safe operation for a wide range of possible configurations and control strategies. The turbine will have the following operational characteristics:

- Standalone automatic operation, including startup and shutdown. This does not include fault resets or maintenance
- Start up accomplished through blade pitch control
- Normal shutdown accomplished through blade pitch control only
- Emergency shutdown accomplished through blade pitch control only

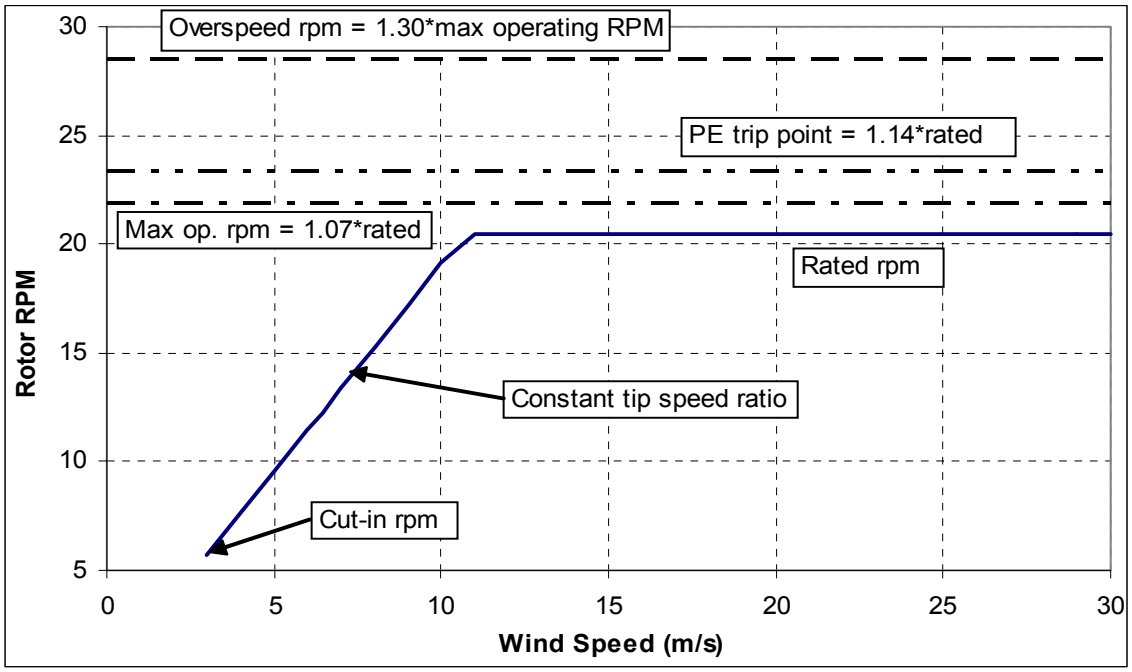

Figure 2–1. RPM vs. wind speed for the 1500 kW wind turbine operating in the theoretical optimum variable-speed range

Table 2-2 defines the short- and long-term transient cycles for the turbine to be used for a design basis:

Table 2–2. Cycle Counts for Transient Events

Event	Count
Normal start-stop cycles/hour	3
Emergency stops/hour	3
Normal start-stop cycles/year	2000
Emergency stops/year	100
Electrical faults (LOL)	10

2.4 Non-Operational Characteristics

The following describes the possible modes that the turbine may be in when not in power production operation or in transition. The drive train components and subsystems shall be able to accommodate these modes without damage or otherwise diminished life expectancy. This may be accomplished through either design or specified procedures:

- Low wind idling: blades pitched to allow for speed ramp up if winds permit. This state could persist for multiple consecutive days with input speeds ranging from 0 to cut-in rpm.
- High wind parked: blades pitched to minimize thrust loads and mechanical brake applied, turbine will start when winds drop below specified threshold. This state could persist for multiple consecutive hours.
- Any wind parked: turbine faulted and not operational, mechanical brake applied and blades pitched to minimize thrust. This state could persist for multiple consecutive days with no rotation.
- Maintenance: turbine parked and locked out. Regular maintenance intervals are anticipated to be approximately 6 months.

3. Drive Train Design Requirements

3.1 Life

The drive train components shall be designed to withstand the specified operational and non-operational loads and environment for a period of 20 years.

3.2 Design Criteria

All designs shall meet the IEC 61400-1 [1] design code for wind turbine generator systems. The IEC 61400-1 requires a 'limit states' design approach which is based on ISO 2394 *General Principles on Reliability for Structures* [3]. To ensure an acceptably low probability of failure, the limit state design requires that uncertainties and variabilities in loads and materials are accounted for by partial safety factors.

The IEC 61400-1 requires different safety factors to be applied according to the type of analysis (ultimate versus fatigue), the type of component (fail-safe versus non fail-safe), and the type of load (aerodynamic, gravity, etc.). These shall be used for all designs where no other explicit design standard is in place.

3.3 Wind Regimes

Two separate wind regimes will be used: one for design and the other for performance evaluation. Drive train components shall be designed for an IEC Class II design site per reference [1]. The Class II site is defined by the parameters given in Table 3-1, where all values are for hub height. All design wind conditions will be derived using the parameters of Table 3-1, according to the definitions and equations contained in reference 1.

Table 3–1. Design Site Wind Definition

Hub height reference wind speed, V_{ref}	42.5 m/s
Hub height average wind speed, V_{ave}	8.5 m/s
Turbulence parameters, A I_{15}	0.18
a	2
Weibull shape factor, k	2 (Rayleigh)
Design air density at sea level standard atmospheric conditions, ρ_{air}	1.225 kg/m^3

For performance and economic evaluation, the annual wind distribution in Table 3-2 will be used as required by the project statement of work.

Table 3–2. Performance Evaluation Wind Definition

10 m average wind speed, V_{ave}	5.8 m/s
Weibull shape factor, k	2 (Rayleigh)
Wind shear exponent	0.143
Design air density at sea level standard atmospheric conditions, ρ_{air}	1.225 kg/m^3

3.4 Physical Environment

The anticipated target region for deployment of wind turbines in the near future in the United States is the Midwest. As such, the drive train components shall be designed to withstand the following ambient environmental conditions:

- Maximum operating temperature: +50°C
- Minimum operating temperature: -20°C
- Minimum survivability temperature: -40°C
- Humidity: 0 to 100% condensing
- Industrial and environmental dust environment and industrial airborne pollution including possible electrically conducting airborne contaminants
- Mild vibration environment
- Altitude above sea level to 2000 m

3.5 Gearing Requirements

All gearing shall be evaluated in conformance with AGMA/AWEA–921-A97 [6] and ANSI/AGMA 2001-C95 [7]. Gear ratings shall be done using Miner's rule analysis of the torque load profile provided in the loads documentation.

3.6 Electrical Requirements

The drive train electrical output shall be designed to produce power in accordance with the following electrical characteristics.

- Nominal wind turbine system connection to site distribution: 3 phase, 60 Hz, 34.5 kVAC
- Voltage tolerances shall be per ANSI C84.1-1995 [8]
- Frequency tolerances typical for U.S. utilities
- Power factor shall be > 0.95 at full load
- Maximum harmonic distortion: shall conform with IEEE *Recommended Practices and Requirements for Harmonic Control in Electrical Power Systems*; IEEE Standard No. 519-1992

3.6.1 Electrical System Protection

The wind turbine control and electrical subsystems shall include provisions for detection of and protection against at least the following conditions:

- Over and under voltage as required by specific equipment
- Over and under frequency as required by specific equipment
- Voltage surge
- Loss of phase and phase reversal
- Overcurrent due both to overload and short circuits
- Ground fault

The electrical protection system shall conform with applicable, NEC, ANSI, IEEE, and typical local codes and specifications.

The electrical protection system shall include surge suppression to protect the controls and electrical system from over voltages that may originate in either the utility grid or on the wind turbine.

3.6.2 Grounding and Shielding

The grounding arrangement specified shall be sufficient to meet or exceed the NEC and typical applicable local codes and requirements.

The grounding and shielding arrangement will be sufficient for reliable operation in an electrically noisy environment.

3.7 Lightning

Wind turbines are often installed in locations with significant lightning activity. It shall be assumed that primary lightning protection is in place for the blades, nacelle and tower. This protection will route the majority of the current through designated conductors and metallic structure.

However, the possibility exists for substantial induced voltage and current effects. Mechanical and electrical equipment shall be protected so that they will be undamaged during most lightning events. Ideally the equipment will survive in a mode allowing for a continuation or resumption of automatic operation without manual intervention.

3.8 Control and Protection Requirements

In general, the purpose of the wind turbine control and protection systems is to control the operation of the wind turbine, minimize component damage in the event of failures, and maintain the wind turbine in a non-hazardous condition at all times. The control and protection systems shall detect all unsafe conditions and cause the machine to cease operation and/or return to a safe or non-hazardous condition.

A safe turbine condition will be assured despite the failure of any one “fail-safe” component, part, or power source. IEC 61400-1 defines a “fail-safe” structural component as one whose failure does not lead rapidly to the failure of a major part of the turbine.

The probability of multiple failures resulting in an unsafe condition will be reduced by automatic detection of component failures to the extent practical. The simultaneous failures of two components shall not be considered unless there is statistical correlation between the two failures.

For the drive train, all necessary sensing and actuation equipment that is required to meet the above general requirements for the wind turbine shall be specified. If controls are specifically provided as part of the drive train subsystem, they shall meet the above requirements and in addition meet the following:

- The effects of electrical noise and EMI from power electronics switching must be taken into account in the design of control and communication electronics.

3.9 Audible Noise Requirements

Specific noise requirements are generally governed by the location at which the turbine is installed. However, as noise is an important issue, consideration will be given to minimization and isolation of noise sources. Gearboxes shall be tested to AGMA specification 6025-690, latest revision, with maximum allowed sound level of 80 dbA at 1.5 m from any point of the transmission. Additionally, no pure tone shall exceed background noise level by more than 5 dbA.

3.10 Maintenance and Safety Characteristics

The drive train components shall be designed with the following maintenance and safety characteristics.

- Manual emergency stop buttons in readily accessible locations at nacelle and ground levels
- Automatic shutdown when a fault condition occurs
- Accommodation of local and remote monitoring of performance and operational status
- Accommodation of local and remote control of the turbine's operational status
- Attachment points on all components requiring material(s) handling devices
- Attachment points for personnel working on machine where appropriate
- Alternative means to lock machine rotation for maintenance, such lock being on the low-speed side of the gearbox
- Capability to record, store, and present system fault information following a shutdown

3.11 Common Practice for Finishes

All material not naturally corrosion resistant shall be treated or finished to protect surface/functional integrity. Finishes should have a minimum life of twenty years.

4. QUALITY ASSURANCE

Quality assurance and inspection shall be an integral part of the design, procurement, manufacture, installation, operation, and maintenance of the drive train components. While these considerations are outside the scope of the current study, vendors and products shall meet quality requirements of ISO 9000.

Appendix B

WindPACT 1.5 MW Structural and Drive Train Loads Specification

N60003 Rev. A

1.5 MW Structural and Drive Train Loads Specification

Approvals

Tim McCoy	March 5, 2001
Originator	Date
David Malcolm	March 5, 2001
Checker	Date
Robert Poore	March 5, 2001
Project Manager	Date

Revision Block

Revision	Release Date	Pages Affected
A-original	March 5, 2001	

Global Energy Concepts, LLC
5729 Lakeview Drive NE Suite 100
Kirkland, Washington 98033-7340
(425) 822-9008

Table of Contents

List of Figures

List of Tables

1. Purpose and Scope

1.1 Purpose

This document presents the loads to be used for the design of the WindPACT drive train supporting structures and the baseline drive train at the 1.5 MW rating. The loads specified in this document are intended to ensure that the designs meet or exceed the design requirements.

1.2 Scope

This document defines turbine load cases to be used in developing the conceptual and preliminary designs at the 1.5 MW rating. The information presented here is intended to establish a set of loads for the major structural components between the rotor hub and tower top. This document also specifies the required partial safety factors for loads and materials.

Additionally, the torque histogram for the baseline and the bearing load histogram for the medium and low speed configurations are presented. These histograms are potentially applicable to other drive train configurations, but in cases other than that specified their use must be justified by the analyst.

2. Normative and Applicable References

2.1 Normative References

The primary normative references are listed below:

1. N60001, *Drive Train System Specification and Design Criteria*, Global Energy Concepts, February 27, 2001.
2. IEC 61400-1 ed. 2, *Safety of Wind Turbine Generator Systems*, International Electrotechnical Commission, 1998.
3. ISO 2394, *General Principles on Reliability for Structures*, 2nd Ed, October, 1986.
4. Germanisher Lloyd, *Rules and Regulations, IV –Non-Marine Technology, Part 1 –Wind Energy,* 1999.

2.2 Other Applicable References

5. NREL, *Guideline DG03: Wind Turbine Design - Yaw and Pitch Rolling bearing Life*, Draft, June 10, 1999.
6. *Wind PACT Rotor – FAST_AD of 15A07C06, turb. and gust runs*, Windward Engineering, January 22, 2001, Stored on Compact Disc.
7. Wilson, R.E., Freeman, L.N., Walker, S.N., and Harman, C.R., "Users' manual for the FAST advanced dynamics code," OSU/NREL report 95-01, September 1995
8. Hansen, Craig, "User's Guide for YawDyn and AeroDyn for ADAMS," University of Utah, January 1996.

3. Definitions and Symbols

3.1 Definitions

Characteristic (or Representative) values are actual values that have been obtained by direct calculation or measurement. The characteristic loads are those that are actually expected to occur (with no additional safety factors). If there is a distribution of values, the characteristic value is chosen to represent a prescribed probability of occurrence.

Design values are obtained by applying the appropriate partial safety factors to the characteristic values. Design values have often been referred to as factored values. The factored value terminology will not be used in this document. The intent is that the design analyst will use these values directly in calculations without requiring additional factors on the loads.

3.2 Symbols and Abbreviations

3.2.1 Symbols and units

Symbol	Description	Units
a	Slope parameter for turbulence standard deviation model	none
c	Weibull distribution parameter, related to annual average wind speed	m/s
k	Weibull distribution shape parameter	none
I_{15}	Turbulence intensity characteristic value defined at 15 m/s	%
F	Force	N
M	Moment	N m
T	Torque	N m
P	Power	kW or W
V_{ave}	Annual average wind speed for the design wind regime	m/s
V_{en}	Expected extreme wind speed for a return period of n years	m/s
V_{ref}	Reference wind speed, 10 minute average	m/s
θ	Pitch angle	degrees
γ_f	Partial safety factor for loads	none
γ_n	Partial safety factor for consequences of failure	none

3.2.2 Subscripts

b	blade coordinates
h	hub coordinates
n	nacelle coordinates
s	shaft coordinates
t	tower/ground coordinates
x	local x-direction
y	local y-direction
z	local z-direction
N	Number of years in return period

3.2.3 Abbreviations

COR	Center of Rotation
ECD	Extreme Coherent gust with Direction change
ECG	Extreme Coherent Gust
EDC_N	Extreme Direction Change over Nyear return period
EOG_N	Extreme Operating Gust over Nyear return period
EWM	Extreme Wind speed Model
EWS	Extreme Wind Shear
NTM	Normal Turbulence Model
NWP	Normal Wind Profile
LC	Design Load Case, specifically from IEC 61400-1 Table 2
Sta	Station, either blade radial station in % of radius or tower station in meters
w.r.t.	With Respect to
WTGS	Wind Turbine Generator System

4. Background

4.1 Design Site Class

The turbine loads analysis is based on an IEC 61400-1 class II design site. The details of this class are found in Table 4-1.

Table 4–1. Class II Design Site Definition

Parameter	Value	Reference
V_{ref}	42.5 m/s	Class II
V_{ave}	8.5 m/s	Class II
I_{15}	0.18	Type A turbulence
a	2	Type A turbulence
Weibull k	2.0	Rayleigh distribution
Weibull c	9.59 m/s	

4.2 Compliance with Applicable Standards

The loads presented in this document are a partial representation of the requirements of the IEC 61400-1 standard. This representation has been selected based on experience as to which conditions are typical design drivers. Full compliance with IEC 61400-1 is beyond the scope of this project. Additional system specifications for environmental and electrical conditions can be found in reference 1.

5. Baseline Wind Turbine Technical Description

5.1 Turbine Configuration

The basic turbine configuration is described in Table 5-1.

Table 5–1. Turbine Characteristics

Item	Description
Wind Turbine Class (IEC 61400-1)	II
Design Life (years)	20
General Configuration:	
Manufacturer and Model	Generic
Top level drawing	Excel Spreadsheet: InputData1.5A07C06.xls
Orientation	Upwind
Rotor Diameter (m)	70.0
Hub Height (m)	84.0
Performance:	
Rated Electrical Power (kW)	1500
Rated Wind Speed (m/s)	11.5
Cut-in Wind Speed (m/s)	3.0
Cut-out Wind Speed (m/s)	27.6
Extreme Wind Speed (m/s)	59.5
Blade:	
Manufacturer, Model of Blades	Griffin
Length (m)	33.35
Material	Fiberglass Composite
Mass (kg)	4182
Rotor:	
Number of Blades	3
Swept Area (m^2)	3848.5
Rated Rotational Speed (rpm)	20.5
Design Maximum Rotational Speed (rpm)	33.3
Rotor Hub Type (e.g. rigid, teeter)	Rigid
Coning Angle (deg)	0
Tilt Angle (deg)	5
Rated Blade Pitch Angle (deg), + to feather	2.68
Direction of Rotation (looking downwind)	Clockwise
Rotor mass incl. Blades (kg)	31400
Hub cg to yaw axis distance (m)	3.5

Drive Train:	
Gearbox Manufacturer, Type, Ratio	
Generator: Manufacturer, Type	
Generator: Voltage , Frequency	
Generator: Synchronous, Rated and Max Speed	1800
Low speed shaft diameter (m)	0.570
Low speed shaft length (m)	2.100
Upwind bearing dist from yaw axis (m)	2.450
Downwind bearing dist from yaw axis (m)	0.700
Nacelle (not incl rotor) cg dist from yaw (m)	0.000
Braking System:	
Parking / Service Brake: Manufacturer, Type, Location	High speed shaft if available, otherwise low speed shaft
Normal Shutdown Brake: Manufacturer, Type, Location	None
Emergency Shutdown Brake: Manufacturer, Type, Location and Torque Time History	None
Yaw System:	
Wind Direction Sensor	Vane
Yaw Control Method (passive, active)	Active
Yaw Actuator (electrical, hydraulic)	Electrical
Yaw Brake: Manufacturer, Type, Location	
Control / Electrical System:	
Controller: Manufacturer, Type	Microcomputer
Software: Release, Version Number	
Monitoring System: Manufacturer, Type	
Power Regulation	Full span independent blade pitch
Over speed Control	Full span pitch
Generator Connection	3 phase
Power Factor Compensation	> 0.95
Generator Phase Connection (Delta/Wye)	
Electrical Output: Voltage, Frequency, phase	
Grid Tolerances (voltage, frequency)	
Tower:	
Tower Type	Tubular steel
Height (m)	82.3
Top diameter (m)	2.700
Top wall thickness (mm)	10.8
Bottom diameter (m)	5.720
Bottom wall thickness (mm)	18.9
Tower head mass (kg)	80872
Tower mass (kg)	137837

5.2 Control System

The control system for the baseline turbine is described below. It is anticipated that this control strategy will be maintained for most of the drive train configurations. If control is expected to be substantially different and have an effect on the loads, the loads can be modified with appropriate justification and documentation.

The generator torque control and blade pitch control are essentially independent. The simulation of generator control is a torque speed curve spline fit from a look up table. This is reasonable since the real response is so quick. The torque increases parabolically from a "cut-in" rpm to rated rpm at which point the torque rises only very slowly with rpm. This slight rise gives better damping than a flat line. This method serves to both keep the rotor operating at a specified tip speed ratio and peak Cp and to limit torque excursions above rated.

The blade pitch is used to control rotor speed with a set point at nominal rated rpm (20.5 for the 1.5 MW). Below rated power the blade pitch position is held at a mechanical limit and so does not vary. Above rated power the blades pitch to keep the rotor at the rated rpm. The simulation uses a PID control algorithm applying the gains to the speed error and computing a demanded pitch setting which is fed to an actuator algorithm. The pitch actuator is simulated with another PID loop that computes blade pitching torque from pitch error. The pitching torque is applied to the simulated mechanical system which calculates blade pitch states and other turbine states from the equations of motion in FAST/ADAMS and the AeroDyn routines [7,8].

The net effect is that below rated power the aerodynamic torque is balanced with the generator torque in such a way that it operates at a constant tip speed ratio. Above rated power wind gusts are absorbed in rotor speed increases until the pitch system can catch up and slow the rotor down by reducing the aerodynamic power input.

6. Analysis Description

6.1 Turbine Modeling

6.1.1 Coordinate Systems

The coordinate systems for the various subassemblies are described in Tables 6-1 and 6-2 and depicted in Figure 6-1.

Table 6–1. Coordinate System Definitions

	Tower		Nacelle		Shaft/hub	
Subscript	(t)		(n)		(s)	
Origin	Tower center at base		Intersection of the tower and shaft centerlines		Intersection of the shaft centerline and hub center	
Rotation reference	Ground, no rotation		Yaw angle w.r.t. tower z axis, left handed, tilt angle w.r.t. tower y axis		Azimuth angle w.r.t. nacelle x axis, right handed	
	Orientation	Positive	Orientation	Positive	Orientation	Positive
X	Along wind, horizontal	Down wind	Along shaft centerline, tilted 5°	Rotor to nacelle	Along shaft centerline, tilted 5°	Rotor to nacelle
Y	Cross wind, horizontal	Right hand rule	Perpendicular to shaft, horizontal	Right hand rule	Perpendicular to x and y	Right hand rule
Z	Vertical	Up	Tilted 5° from vertical	Up	In line with blade 1	C.O.R to blade 1

Table 6–2. Coordinate System Angle Definitions

	Description
Yaw angle	Yaw angle is the rotation of the nacelle coordinates relative to the fixed tower coordinates about the tower z axis. Negative angle is a right handed rotation, positive angle is clockwise when viewed from above. Zero degrees of yaw aligns the tower and nacelle y axis. The nacelle x and z axes are rotated around the common tower/nacelle y axes by the tilt angle.
Azimuth angle	Azimuth angle is the rotation of the shaft coordinates relative to the nacelle coordinates about their common x axis. Positive angle is a right handed rotation, a clockwise rotation when viewed from upwind. Zero degrees of azimuth corresponds to parallel shaft and nacelle x, y, and z axes with blade 1 vertically up.

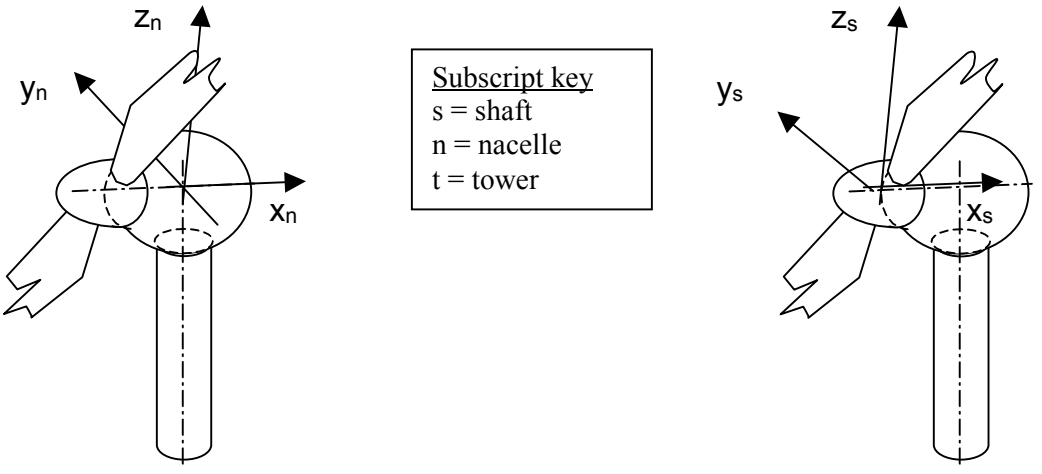

Figure 6–1. Coordinate systems for the rotating shaft, nacelle, and tower

6.2 Data Processing

6.2.1 Ultimate loads

The ultimate design loads presented later in this document were developed from the ADAMS time series outputs using the following approach:

1. Scan the time series for the peak value of each signal, including some composite signals such as the net force vector (Fxy) and net moment vector (Mxy) magnitudes at each load application point.
2. While scanning, multiply by the appropriate partial safety factor for load, 1.35 as detailed in Table 6-3. This allows evaluation of the peak design load rather than the peak characteristic load.
3. For the peak of each signal, store the values of the other load components associated with the corresponding load application point.
4. Output design load combinations at each load application point corresponding to the peak of each of the load signals at that application point.

Table 6–3. Partial Safety Factors for Ultimate Loads

Load Source	Factor
Aerodynamic loads	1.35
Operational loads	1.35
Gravity loads	1.35
Inertial loads	1.35

6.2.2 Fatigue loads

Fatigue loads are generated by rainflow counting each load signal from each run of the ADAMS time series output that are specified for fatigue in the IEC standard. Table 6-4 shows the amount of simulation time (30 minutes = three 10 minute simulations) for the normal operating runs. The multipliers in Table 6-4 are determined from the design site wind distribution as the number of hours in the wind speed range shown in the table. This multiplier is the ratio of the simulation time to the number of hours in 20 years in the given wind speed interval.

Table 6–4. Design Site Weighting for ADAMS Runs for IEC Load Case 1.1

Simulation Wind Speed, m/s	Wind Distribution Range, m/s	Simulation time in minute	Multiplier
8	3.5 to 8.5	30	147238.9
12	8.5 to 12.5	30	95710.4
16	12.5 to 16.5	30	45882.0
20	16.5 to 20.5	30	14476.6
24	20.5 to 27.5	30	3515.7

The full spectrum of rainflow counts for each load are used to calculate an equivalent fatigue load using a range of SN curve slopes, m. The fatigue equivalent loads are calculated as follows:

$$R_{eq} = \left[\frac{\sum (n_i R_i^m)}{N_{eq}} \right]^{(1/m)}$$

where R_{eq} is the equivalent fatigue load range, N_{eq} = 20*3600*8760 = 630,720,000 cycles/lifetime is based on 1 Hz cycles, and n_i is the number of lifetime cycles at load range R_i. Note that this formulation is useful only if the SN curve is of the form $N=aS^{-m}$ and has no endurance limit or other changes in slope. To determine life as a fraction of 20 years, apply the equation

$$Life = a(uR_{eq})^{-m} / N_{eq}$$

where a is the intercept of the SN curve and u is the stress per unit load for the given part. This yields life in years.

7. Load Case Descriptions

7.1 Load Case Parameters and Run Summary

Table 7-1 describes the load cases run, including the partial load factors used to obtain the design loads.

Table 7–1. Load Case Run Summary

IEC Load Case	Analysis Type	Partial Load Factor	Turbine State	Wind Model	Comments
1.1	Ultimate	1.35	Operating	NTM, V_{avg} = 8,12,16,20,24 m/s	3 runs each at 5 wind speeds
1.2	Fatigue	1.0	Operating	NTM, V_{avg}= 8,12,16,20,24 m/s	Same results as for LC 1.1
1.3a	Ultimate	1.35	Operating	ECD, V_{avg}= 12 m/s, neg wind dir	
1.3b	Ultimate	1.35	Operating	ECD, V_{avg}= 16 m/s, neg wind dir	
1.3c	Ultimate	1.35	Operating	ECD, V_{avg}= 20 m/s, neg wind dir	
1.3d	Ultimate	1.35	Operating	ECD, V_{avg}= 24 m/s, neg wind dir	
1.3e	Ultimate	1.35	Operating	ECD, V_{avg}= 12 m/s, pos wind dir	
1.3f	Ultimate	1.35	Operating	ECD, V_{avg}= 16 m/s, pos wind dir	
1.3g	Ultimate	1.35	Operating	ECD, V_{avg}= 20 m/s, pos wind dir	
1.3h	Ultimate	1.35	Operating	ECD, V_{avg}= 24 m/s, pos wind dir	
1.5a	Ultimate	1.35	Operating	EOG1, V_{avg}= 12 m/s	
1.5b	Ultimate	1.35	Operating	EOG1, V_{avg}= 16 m/s	
1.5c	Ultimate	1.35	Operating	EOG1, V_{avg}= 20 m/s	
1.5d	Ultimate	1.35	Operating	EOG1, V_{avg}= 24 m/s	
1.6a	Ultimate	1.35	Operating	EOG50, V_{avg}= 12 m/s	
1.6b	Ultimate	1.35	Operating	EOG50, V_{avg}= 16 m/s	
1.6c	Ultimate	1.35	Operating	EOG50, V_{avg}= 20 m/s	
1.6d	Ultimate	1.35	Operating	EOG50, V_{avg}= 24 m/s	
1.7a	Ultimate	1.35	Operating	EHS, neg, V_{avg} = 12 m/s	
1.7b	Ultimate	1.35	Operating	EHS, neg, V_{avg} = 16 m/s	
1.7c	Ultimate	1.35	Operating	EHS, neg, V_{avg} = 20 m/s	
1.7d	Ultimate	1.35	Operating	EHS, neg, V_{avg} = 24 m/s	
1.7e	Ultimate	1.35	Operating	EHS, pos, V_{avg} = 12 m/s	
1.7f	Ultimate	1.35	Operating	EHS, pos, V_{avg} = 16 m/s	
1.7g	Ultimate	1.35	Operating	EHS, pos, V_{avg} = 20 m/s	
1.7h	Ultimate	1.35	Operating	EHS, pos, V_{avg} = 24 m/s	
1.7i	Ultimate	1.35	Operating	EVS, V_{avg} = 12 m/s	
1.7j	Ultimate	1.35	Operating	EVS, V_{avg} = 16 m/s	
1.7k	Ultimate	1.35	Operating	EVS, V_{avg} = 20 m/s	
1.7l	Ultimate	1.35	Operating	EVS, V_{avg} = 24 m/s	

Table 7-1. Load Case Run Summary (cont.)

1.8a	Ultimate	1.35	Operating	EDC1, neg, V_{avg} = 12 m/s,	
1.8b	Ultimate	1.35	Operating	EDC1, neg, V_{avg} = 16 m/s,	
1.8c	Ultimate	1.35	Operating	EDC1, neg, V_{avg} = 20 m/s,	
1.8d	Ultimate	1.35	Operating	EDC1, neg, V_{avg} = 24 m/s,	
1.8e	Ultimate	1.35	Operating	EDC1, pos, V_{avg} = 12 m/s,	
1.8f	Ultimate	1.35	Operating	EDC1, pos, V_{avg} = 16 m/s,	
1.8g	Ultimate	1.35	Operating	EDC1, pos, V_{avg} = 20 m/s,	
1.8h	Ultimate	1.35	Operating	EDC1, pos, V_{avg} = 24 m/s,	
1.8i	Ultimate	1.35	Operating	EDC50, neg, V_{avg} = 12 m/s,	
1.8j	Ultimate	1.35	Operating	EDC50, neg, V_{avg} = 16 m/s,	
1.8k	Ultimate	1.35	Operating	EDC50, neg, V_{avg} = 20 m/s,	
1.8l	Ultimate	1.35	Operating	EDC50, neg, V_{avg} = 24 m/s,	
1.8m	Ultimate	1.35	Operating	EDC50, pos, V_{avg} = 12 m/s,	
1.8n	Ultimate	1.35	Operating	EDC50, pos, V_{avg} = 16 m/s,	
1.8o	Ultimate	1.35	Operating	EDC50, pos, V_{avg} = 20 m/s,	
1.8p	Ultimate	1.35	Operating	EDC50, pos, V_{avg} = 24 m/s,	
1.9a	Ultimate	1.35	Operating	ECG, V_{init} = 12 m/s	
1.9b	Ultimate	1.35	Operating	ECG, V_{init} = 16 m/s	
1.9c	Ultimate	1.35	Operating	ECG, V_{init} = 20 m/s	
1.9d	Ultimate	1.35	Operating	ECG, V_{init} = 24 m/s	
6.1	Ultimate	1.35	Parked	NTM, V_{avg} = 50 m/s,V_{max}=59.5 m/s	5 runs with different turbulent seeds

8. Ultimate Design Loads

8.1 Application

The ultimate design loads are applicable to all of the structural elements supporting the drive train. While the drive train and its supporting structure may vary, the assumption is that these structural loads will be approximately constant.

8.2 Design Load Tables

8.2.1 Rotating Hub and Shaft

Table 8-1 presents the design loads for the shaft in the rotating frame. The application point is the center of the hub, geometry as detailed in Table 5-1. The bold entries are the peaks (minimum and maximum) for the load component and the combinations are in the rows. The Fyz and Myz are the resultant moments formed by the square root of the sum of the squares of the two indicated vectors.

Table 8–1. Shaft Design Loads at Hub Center - Rotating

		Fx, N	Fy, N	Fz, N	Mx, N m	My, N m	Mz, N m	Fyz, N	Myz, N m
Fx	Min	**-0.7**	446.0	-11.4	1,002.1	363.0	474.5	446.2	597.5
	Max	**409.2**	-290.7	-345.1	1,155.6	194.8	58.4	451.2	203.4
Fy	Min	144.2	**-502.7**	43.4	1,053.0	1,244.2	80.3	504.6	1,246.8
	Max	129.7	**494.2**	-28.4	1,028.2	-770.6	599.1	495.1	976.1
Fz	Min	129.9	85.5	**-513.0**	1,064.6	-400.8	505.4	520.1	645.1
	Max	151.3	-15.8	**498.3**	1,118.2	108.9	-732.4	498.5	740.4
Mx	Min	75.8	-450.1	-60.2	**195.2**	95.8	192.2	454.1	214.8
	Max	207.9	409.3	-248.3	**1,269.0**	-54.6	687.7	478.7	689.9
My	Min	80.1	80.7	427.0	1,023.3	**-3,388.5**	86.9	434.6	3,389.6
	Max	97.6	105.0	-458.9	1,047.1	**2,142.4**	1,483.7	470.7	2,606.0
Mz	Min	89.0	-438.1	-78.1	1,026.5	1,352.7	**-3,007.8**	445.0	3,298.0
	Max	72.6	352.4	-239.9	1,006.6	1,487.7	**2,951.1**	426.3	3,304.9
Fyz	Max	129.9	85.5	-513.0	1,064.6	-400.8	505.4	**520.1**	645.1
Myz	Max	80.1	80.7	427.0	1,023.3	-3,388.5	86.9	434.6	**3,389.6**

8.2.2 Bedplate

Tables 8-2 and 8-3 present the design loads for the nacelle at two points: the center of the hub and the yaw bearing center, geometry as detailed in Table 5-1. The bold entries are the peaks (minimum and maximum) for the load component and the combinations are in the rows. The Fyz and Myz are the resultant moments formed by the square root of the sum of the squares of the two indicated vectors.

Table 8–2. Nacelle Design Loads at Hub Center – Nonrotating

		Fx, N	Fy, N	Fz, N	Mx, N m	My, N m	Mz, N m	Fyz, N	Myz, N m
Fx	Min	**-0.7**	3.2	-446.2	1,002.1	486.2	-347.3	446.2	597.5
	Max	**409.2**	-1.3	-451.2	1,155.6	111.9	169.8	451.2	203.4
Fy	Min	100.3	**-135.5**	-442.1	1,045.4	2,963.0	213.9	462.3	2,970.7
	Max	80.5	**117.6**	-441.1	1,023.0	-2,734.5	-1,030.6	456.5	2,922.3
Fz	Min	129.9	17.6	**-519.8**	1,064.6	-331.2	553.6	520.1	645.1
	Max	104.1	-26.5	**-371.0**	1,123.5	1,183.1	-1,667.8	371.9	2,044.9
Mx	Min	75.8	5.8	-454.1	**195.2**	-179.4	118.2	454.1	214.8
	Max	207.9	-40.6	-477.0	**1,269.0**	591.8	354.4	478.7	689.9
My	Min	79.2	98.3	-452.9	1,018.0	**-2,875.3**	-665.3	463.5	2,951.3
	Max	80.1	-105.9	-421.5	1,023.3	**3,377.3**	-288.5	434.6	3,389.6
Mz	Min	128.4	-15.7	-419.5	1,011.0	471.6	**-1,997.1**	419.8	2,052.0
	Max	125.7	-20.4	-485.3	1,027.5	33.8	**1,632.2**	485.8	1,632.6
Fyz	Max	129.9	17.6	-519.8	1,064.6	-331.2	553.6	**520.1**	645.1
Myz	Max	80.1	-105.9	-421.5	1,023.3	3,377.3	-288.5	434.6	**3,389.6**

Table 8–3. Nacelle Design Loads at Yaw Bearing

		Fx, N	Fy, N	Fz, N	Mx, N m	My, N m	Mz, N m	Fxy, N	Mxy, N m
Fx	Min	**-18.0**	3.0	-1,101.3	1,002.1	-1,045.3	-328.5	18.2	1,448.1
	Max	**389.9**	-1.2	-1,142.1	1,155.6	-845.2	53.7	389.9	1,431.7
Fy	Min	83.1	**-135.4**	-1,106.1	1,045.4	1,562.0	420.4	158.9	1,879.5
	Max	78.9	**117.8**	-1,096.6	1,037.1	-3,919.1	-1,108.0	141.8	4,053.9
Fz	Min	105.8	17.9	**-1,185.8**	1,064.6	-1,629.5	296.2	107.2	1,946.4
	Max	93.1	-26.5	**-1,035.6**	1,123.5	0.6	-1,239.0	96.7	1,123.5
Mx	Min	57.7	5.8	-1,115.9	**195.2**	-1,613.2	60.4	58.0	1,625.0
	Max	187.1	-40.1	-1,150.3	**1,269.0**	-770.3	277.8	191.4	1,484.5
My	Min	66.1	84.0	-1,118.2	1,011.4	**-4,343.0**	-680.4	106.9	4,459.2
	Max	64.8	-106.2	-1,083.6	1,023.3	**2,038.5**	-21.7	124.4	2,280.9
Mz	Min	127.4	-3.5	-1,068.0	1,021.7	-609.7	**-2,033.0**	127.5	1,189.8
	Max	104.6	-20.2	-1,151.3	1,027.5	-1,506.6	**1,602.0**	106.5	1,823.6
Fxy	Max	389.9	-1.2	-1,142.1	1,155.6	-845.2	53.7	**389.9**	**1,431.7**
Mxy	Max	66.1	84.0	-1,118.2	1,011.4	-4,343.0	-680.4	**106.9**	**4,459.2**

9. Fatigue Loads

9.1 Application

The structural fatigue loads are applicable to all of the structural elements supporting the drive train. While the drive train and its supporting structure may vary, the assumption is that these structural fatigue loads will be approximately constant. The torque histogram, however, is intended only for use with the baseline drive train configuration. Its use with any other configuration must be justified by the analyst.

9.2 Equivalent Structural Fatigue Loads

The equivalent fatigue loads for each structural load component are given in Table 9-1. These are intended to be used either for preliminary analysis or where the SN curve is of the form and with the restrictions discussed in Section 6.2.2. These are essentially design loads, however additional factors may need to be applied as described in Section 10.

Table 9–1. Equivalent Structural Fatigue Loads

		SN Curve Slope					
		3	6	9	12	15	18
Shaft Rotating	Fx, kN	39	76	101	118	131	141
	Fy, kN	415	528	573	597	611	622
	Fz, kN	416	529	573	597	612	622
	Mx, kN m	96	199	284	344	388	421
	My, kN m	519	826	1,078	1,304	1,508	1,688
	Mz, kN m	518	829	1,099	1,338	1,539	1,703
Shaft Non-Rot	Fx, kN	39	76	101	118	131	141
	Fy, kN	19	27	36	45	53	59
	Fz, kN	21	28	36	45	52	59
	Mx, kN m	96	199	284	344	388	421
	My, kN m	423	706	979	1,214	1,408	1,568
	Mz, kN m	418	684	927	1,122	1,277	1,401
Yaw Brng	Fx, kN	39	75	100	117	130	140
	Fy, kN	18	26	35	43	50	57
	Fz, kN	20	27	36	45	52	59
	My, kN m	435	721	999	1,244	1,449	1,620
	Mz, kN m	417	679	919	1,113	1,267	1,391

9.3 Gearbox Torque-Speed Histogram

A histogram of the gearbox torque loads is given in Table 9-2.

9.4 Bearing Load Histograms

Tables 9-3 to 9-5 present bearing radial and thrust loads for the special configuration mainshaft required for the direct drive and medium speed architectures. These loads are <u>not</u> applicable to the baseline turbine. They are based on hub center to bearing distances of 1.1 m and 1.61 m.

Table 9–2. Gearbox Torque-Speed Histogram, Lifetime Hours

Torque	RPM->	9	11	13	15	17	19	21	23
kN m	Totals	570	10571	17779	27523	18574	26303	56131	377
10	0.0	0.0	0.0	0.0	0.0	0.0	0.0	0.0	0.0
30	0.0	0.0	0.0	0.0	0.0	0.0	0.0	0.0	0.0
50	0.0	0.0	0.0	0.0	0.0	0.0	0.0	0.0	0.0
70	0.0	0.0	0.0	0.0	0.0	0.0	0.0	0.0	0.0
90	0.0	0.0	0.0	0.0	0.0	0.0	0.0	0.0	0.0
110	0.0	0.0	0.0	0.0	0.0	0.0	0.0	0.0	0.0
130	0.0	0.0	0.0	0.0	0.0	0.0	0.0	0.0	0.0
150	233.3	233.3	0.0	0.0	0.0	0.0	0.0	0.0	0.0
170	473.9	225.9	248.0	0.0	0.0	0.0	0.0	0.0	0.0
190	1944.8	110.5	1834.3	0.0	0.0	0.0	0.0	0.0	0.0
210	2556.3	0.0	2556.3	0.0	0.0	0.0	0.0	0.0	0.0
230	2460.5	0.0	2455.6	4.9	0.0	0.0	0.0	0.0	0.0
250	3393.6	0.0	2735.5	658.1	0.0	0.0	0.0	0.0	0.0
270	3646.6	0.0	707.2	2939.4	0.0	0.0	0.0	0.0	0.0
290	3914.2	0.0	34.4	3879.8	0.0	0.0	0.0	0.0	0.0
310	3906.9	0.0	0.0	3906.9	0.0	0.0	0.0	0.0	0.0
330	3816.0	0.0	0.0	3742.3	73.7	0.0	0.0	0.0	0.0
350	3859.1	0.0	0.0	2133.9	1725.2	0.0	0.0	0.0	0.0
370	4948.6	0.0	0.0	503.4	4445.2	0.0	0.0	0.0	0.0
390	4988.2	0.0	0.0	9.8	4978.3	0.0	0.0	0.0	0.0
410	5238.6	0.0	0.0	0.0	5238.6	0.0	0.0	0.0	0.0
430	4951.5	0.0	0.0	0.0	4928.4	23.1	0.0	0.0	0.0
450	5183.0	0.0	0.0	0.0	4498.1	684.9	0.0	0.0	0.0
470	3900.1	0.0	0.0	0.0	1540.8	2359.4	0.0	0.0	0.0
490	3604.5	0.0	0.0	0.0	87.3	3517.2	0.0	0.0	0.0
510	3538.6	0.0	0.0	0.0	7.7	3530.8	0.0	0.0	0.0
530	2818.4	0.0	0.0	0.0	0.0	2814.1	4.3	0.0	0.0
550	2315.0	0.0	0.0	0.0	0.0	2283.4	31.6	0.0	0.0
570	2550.3	0.0	0.0	0.0	0.0	2105.2	445.0	0.1	0.0
590	2857.4	0.0	0.0	0.0	0.0	1033.2	1822.9	1.2	0.0
610	2260.0	0.0	0.0	0.0	0.0	198.6	2057.5	3.9	0.0
630	2643.6	0.0	0.0	0.0	0.0	22.4	2607.2	14.0	0.0
650	2783.2	0.0	0.0	0.0	0.0	1.4	2729.8	51.2	0.7
670	3332.3	0.0	0.0	0.0	0.0	0.0	3101.3	228.6	2.5
690	5861.1	0.0	0.0	0.0	0.0	0.0	4725.4	1128.6	7.2
710	9799.5	0.0	0.0	0.0	0.0	0.0	4924.3	4851.2	24.0
730	15768.8	0.0	0.0	0.0	0.0	0.0	2751.6	12954.3	62.9
750	18703.0	0.0	0.0	0.0	0.0	0.0	879.5	17729.8	93.7
770	12942.7	0.0	0.0	0.0	0.0	0.0	180.4	12663.0	99.2
790	4898.0	0.0	0.0	0.0	0.0	0.0	31.2	4808.6	58.1
810	1310.4	0.0	0.0	0.0	0.0	0.0	9.1	1281.4	19.9
830	311.3	0.0	0.0	0.0	0.0	0.0	1.0	304.3	6.0
850	85.6	0.0	0.0	0.0	0.0	0.0	0.3	82.9	2.5
870	22.3	0.0	0.0	0.0	0.0	0.0	0.1	21.9	0.3
890	4.1	0.0	0.0	0.0	0.0	0.0	0.0	4.0	0.1
910	1.2	0.0	0.0	0.0	0.0	0.0	0.0	1.1	0.0
930	0.5	0.0	0.0	0.0	0.0	0.0	0.0	0.5	0.0

Table 9–3. Direct Drive Upwind Main Bearing Radial Load-Speed Histogram, Lifetime Hours

(Note that these loads include rotor weight but not shaft, gearbox, or other supported weight)

Radial	RPM->	9	11	13	15	17	19	21	23
kN	Totals	569.7	10571.4	17778.6	27523.4	18573.7	26302.5	56130.7	377.3
50	456.5	0.0	0.0	0.0	7.4	20.6	77.4	350.1	1.0
150	1498.6	0.0	0.0	0.0	31.2	35.4	265.6	1156.2	10.3
250	2684.9	0.0	0.0	0.0	113.6	164.3	512.9	1878.7	15.4
350	4132.4	0.0	7.4	19.6	171.0	295.7	914.7	2698.3	25.7
450	6295.9	0.0	19.6	174.3	455.6	578.3	1270.8	3773.0	24.4
550	8778.9	0.0	235.7	481.3	1009.5	780.5	1724.7	4527.8	19.3
650	12364.3	4.9	574.6	1014.2	1906.9	1376.4	2245.7	5217.7	24.0
750	16540.0	44.2	1095.2	1942.4	3126.3	2084.1	2562.7	5656.4	28.8
850	19508.4	27.0	1522.5	3020.4	3887.8	2518.8	2747.0	5739.5	45.4
950	20922.7	29.5	1775.4	3361.7	4612.2	2611.2	2891.6	5600.5	40.6
1050	19930.2	142.4	2050.4	2870.6	4617.1	2530.5	2691.5	4992.7	34.9
1150	15687.2	93.3	1554.4	2357.4	3281.6	1979.5	2281.2	4105.2	34.6
1250	11163.5	66.3	854.5	1301.5	2244.9	1424.6	1963.7	3281.6	26.3
1350	7428.6	117.9	589.3	682.7	1156.8	974.5	1486.3	2404.3	16.9
1450	4513.2	44.2	203.8	375.7	527.5	585.0	1064.3	1703.2	9.5
1550	2522.7	0.0	36.8	142.4	215.0	326.3	671.0	1121.9	9.2
1650	1408.9	0.0	27.0	34.4	84.5	169.6	393.4	696.0	4.0
1750	826.5	0.0	14.7	0.0	38.5	63.7	240.0	466.0	3.5
1850	482.2	0.0	9.8	0.0	17.8	23.8	134.5	295.6	0.7
1950	286.2	0.0	0.0	0.0	8.4	9.8	69.5	198.0	0.5
2050	162.0	0.0	0.0	0.0	2.8	11.2	40.6	106.9	0.5
2150	101.2	0.0	0.0	0.0	4.2	5.6	16.9	73.7	0.8
2250	59.5	0.0	0.0	0.0	2.8	2.8	13.3	40.1	0.5
2350	34.3	0.0	0.0	0.0	0.0	1.4	10.5	22.3	0.1
2450	13.4	0.0	0.0	0.0	0.0	0.0	4.5	8.9	0.0
2550	9.8	0.0	0.0	0.0	0.0	0.0	2.8	6.9	0.1
2650	6.1	0.0	0.0	0.0	0.0	0.0	2.3	3.7	0.1
2750	2.8	0.0	0.0	0.0	0.0	0.0	1.1	1.5	0.1
2850	3.1	0.0	0.0	0.0	0.0	0.0	1.1	2.0	0.0
2950	1.4	0.0	0.0	0.0	0.0	0.0	0.4	1.0	0.0
3050	0.8	0.0	0.0	0.0	0.0	0.0	0.2	0.6	0.0
3150	0.3	0.0	0.0	0.0	0.0	0.0	0.1	0.2	0.0
3250	0.3	0.0	0.0	0.0	0.0	0.0	0.1	0.1	0.0
3350	0.3	0.0	0.0	0.0	0.0	0.0	0.2	0.1	0.0
3450	0.1	0.0	0.0	0.0	0.0	0.0	0.0	0.1	0.0

Table 9–4. Direct Drive Downwind Main Bearing Radial Load-Speed Histogram, Lifetime Hours

(Note that these loads include rotor weight but not shaft, gearbox, or other supported weight)

Radial	RPM->	9	11	13	15	17	19	21	23
kN	Totals	569.7	10571.4	17778.6	27523.4	18573.7	26302.5	56130.7	377.3
50	1653.6	0.0	4.9	36.8	117.5	210.2	372.5	906.8	4.9
150	5103.8	0.0	51.6	164.5	455.5	606.4	1007.2	2804.2	14.4
250	9067.3	0.0	262.7	510.8	1184.5	907.0	1750.1	4424.5	27.7
350	13717.6	14.7	739.1	1173.8	2095.5	1557.0	2436.5	5664.5	36.4
450	18561.4	39.3	1149.2	2217.4	3509.3	2187.9	2897.9	6521.1	39.3
550	21648.2	24.6	1618.2	3236.5	4152.7	2756.9	3046.6	6762.9	49.8
650	22522.6	56.5	1912.9	3487.0	4864.8	2557.4	3076.7	6523.1	44.1
750	20587.7	164.5	2092.2	2698.7	4383.5	2543.1	2951.4	5715.8	38.6
850	15944.9	63.8	1323.6	2136.4	3006.2	2002.6	2497.9	4866.8	47.6
950	11148.9	90.9	707.2	1144.3	2082.5	1300.4	2048.0	3752.1	23.5
1050	7357.4	100.7	530.4	552.5	975.1	877.4	1517.8	2785.0	18.6
1150	4351.8	14.7	105.6	294.7	413.1	520.1	1063.7	1929.0	10.8
1250	2599.3	0.0	29.5	115.4	163.0	313.3	691.9	1276.7	9.5
1350	1443.3	0.0	24.6	9.8	63.8	144.3	384.3	812.7	3.8
1450	872.5	0.0	17.2	0.0	27.0	42.0	242.1	540.7	3.6
1550	494.8	0.0	2.5	0.0	15.4	18.2	135.8	321.2	1.8
1650	311.1	0.0	0.0	0.0	4.2	16.8	72.4	217.0	0.7
1750	168.7	0.0	0.0	0.0	2.8	5.6	43.4	116.3	0.6
1850	117.4	0.0	0.0	0.0	7.0	4.2	22.7	82.7	0.9
1950	71.5	0.0	0.0	0.0	0.0	2.8	19.0	49.4	0.3
2050	33.2	0.0	0.0	0.0	0.0	0.0	9.7	23.4	0.1
2150	19.0	0.0	0.0	0.0	0.0	0.0	6.2	12.8	0.0
2250	11.2	0.0	0.0	0.0	0.0	0.0	2.6	8.4	0.1
2350	8.7	0.0	0.0	0.0	0.0	0.0	2.4	6.0	0.2
2450	3.9	0.0	0.0	0.0	0.0	0.0	1.7	2.1	0.0
2550	2.6	0.0	0.0	0.0	0.0	0.0	0.7	1.8	0.0
2650	2.1	0.0	0.0	0.0	0.0	0.0	0.5	1.5	0.0
2750	0.8	0.0	0.0	0.0	0.0	0.0	0.2	0.6	0.0
2850	0.9	0.0	0.0	0.0	0.0	0.0	0.2	0.7	0.0
2950	0.3	0.0	0.0	0.0	0.0	0.0	0.1	0.2	0.0
3050	0.4	0.0	0.0	0.0	0.0	0.0	0.2	0.2	0.0
3150	0.1	0.0	0.0	0.0	0.0	0.0	0.0	0.0	0.0
3250	0.045	0.0	0.0	0.0	0.0	0.0	0.0	0.0	0.0

Table 9–5. Direct Drive Main Bearing Thrust Load-Speed Histogram, Lifetime Hours

Thrust	RPM->	9	11	13	15	17	19	21	23
kN	Totals	569.7	10571.4	17778.6	27523.4	18573.7	26302.5	56130.7	377.3
5	0.4	0.0	0.0	0.0	0.0	0.0	0.0	0.4	0.0
15	1.7	0.0	0.0	0.0	0.0	0.0	0.4	1.3	0.0
25	8.6	0.0	0.0	0.0	0.0	0.0	1.5	7.0	0.1
35	30.8	0.0	0.0	0.0	0.0	0.0	5.9	24.7	0.2
45	192.8	63.8	22.1	0.0	0.0	0.0	22.5	83.2	1.2
55	1028.0	243.1	542.7	0.0	0.0	0.0	44.5	194.0	3.7
65	3697.0	201.4	2843.6	100.7	0.0	0.0	110.3	436.2	4.9
75	5095.2	39.3	3017.9	920.9	0.0	0.0	212.5	894.3	10.3
85	7899.8	22.1	2907.4	2924.6	76.1	0.0	359.0	1588.8	21.6
95	9349.3	0.0	1053.5	4874.4	356.0	0.0	513.4	2513.1	39.0
105	10752.9	0.0	167.0	4658.3	1751.7	6.7	773.6	3362.6	33.1
115	12610.1	0.0	17.2	2733.1	4656.0	70.1	902.1	4173.5	58.0
125	14337.8	0.0	0.0	1306.4	6910.1	397.2	942.0	4710.6	71.5
135	15088.5	0.0	0.0	248.0	7078.0	1444.0	893.5	5393.8	31.2
145	13828.2	0.0	0.0	12.3	4634.7	3015.2	1092.8	5044.2	29.0
155	11830.8	0.0	0.0	0.0	1691.7	4281.5	1241.5	4576.0	40.1
165	9934.4	0.0	0.0	0.0	330.7	3918.0	1496.6	4174.9	14.2
175	8656.8	0.0	0.0	0.0	38.2	2753.9	2117.4	3732.2	15.0
185	8422.2	0.0	0.0	0.0	0.0	1752.6	3180.3	3485.3	4.0
195	7650.5	0.0	0.0	0.0	0.0	616.8	3932.7	3100.9	0.0
205	5908.7	0.0	0.0	0.0	0.0	235.4	3074.8	2598.5	0.0
215	4981.4	0.0	0.0	0.0	0.0	78.1	2600.5	2302.8	0.0
225	3519.9	0.0	0.0	0.0	0.0	4.2	1656.9	1858.8	0.0
235	1890.0	0.0	0.0	0.0	0.0	0.0	762.8	1127.2	0.0
245	800.6	0.0	0.0	0.0	0.0	0.0	276.2	524.4	0.0
255	253.8	0.0	0.0	0.0	0.0	0.0	65.2	188.6	0.0
265	53.1	0.0	0.0	0.0	0.0	0.0	21.0	32.2	0.0
275	4.2	0.0	0.0	0.0	0.0	0.0	2.8	1.4	0.0

10. Material Factors

Material factors required by IEC 61400-1 are not included in the design loads provided herein. These factors should be applied based on the requirements of 61400-1 which are dependent on situation and material. Where recognized codes are available (such as for gearing) the practices of established design codes should be used. For design in steel or iron, the values from Table 10-1 should be used. If other materials are used, material factors shall be obtained from IEC 61400-1, Table 4. In addition, for fatigue, as shown in Table 10-1, there is a factor for consequence of failure.

Table 10–1. Partial Safety Factors for Materials

	Component Class	
Partial Factor	Failsafe	Non-Failsafe
Ultimate, γ_m	1.10	1.10
Fatigue, γ_m	1.10	1.10
Fatigue - consequences of failure, γ_n	1.00	1.15

Appendix C

Mechanical Design Parametric Spreadsheets

Appendix C

C.1 Single PM Generator Parametric Spreadsheet

In the text that follows, each line of the design spreadsheet for the single PM Generator drive train model is broken out and expanded into an annotated form. Moving down these notes is analogous to moving down one of the design worksheets line by line. Most named variables are defined when first presented. Otherwise, their definitions should be present at the top of the design worksheet where declarations occur, or later in the appendix text. The units are in parentheses at the right.

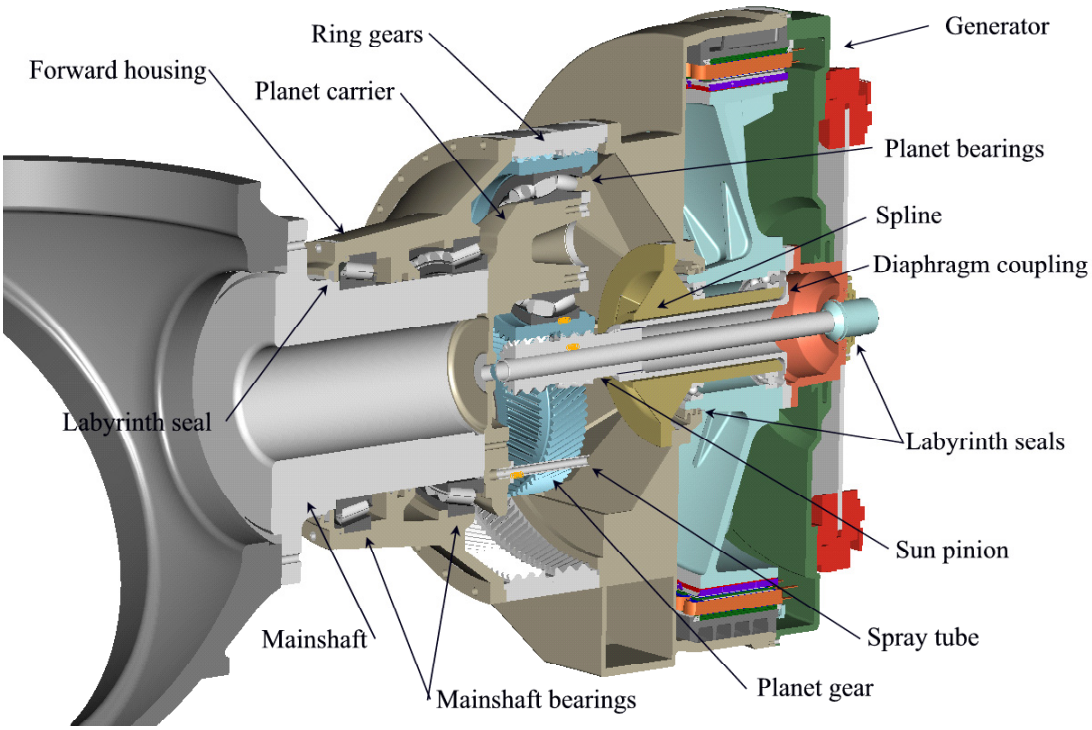

Figure C.1-1. Cutaway view of the Single PM Drive Train

The ratio between the rotor and the generator rpm, the total gear ratio of the system, is used as a parameter of the single PM drive train design spreadsheet and is named *Ratio*.

C.1.1 System Design

The sun to pinion aspect ratio is calculated:

Aspect ratio = 0.5 • gear face / pinion PD

Generator rpm is calculated based on the fixed rotor rpm (20.5 rpm) and the parameter gear ratio:

Gen rpm = Ratio • rotor rpm *(rpm)*

The airgap velocity is calculated:

Airgap velocity = airgap diameter • PI() • generator rpm *(m/s)*

The generator mechanical torque is calculated from the mechanical rotor torque, Qmech, and the gear ratio:

Generator torque = Qmech / Ratio *(N•m)*

The electrical rotor torque is calculated:

Electrical rotor torque = electrical input power • 9594 / rotor rpm *(kW)*

The generator electrical torque is calculated:

Generator electrical torque = electrical rotor torque / Ratio *(kW)*

The stator diameter is calculated from the dimensions of the ring gear and then rounded to the nearest tenth of a meter:

Stator diam = round(ring gear diam • 25.4 • airgap to ring gear diam ratio, -2) / 1000 (m)

A rough airgap diameter is calculated by subtracting the slot depth (*sd*) and stator back iron thickness (*bis)* from the stator diameter:

Airgap diameter = stator diameter – (2 • (sd + bis) / 1000) *(m)*

The airgap radius is computed directly from the diameter:

Airgap radius = 0.5 • airgap diameter *(m)*

The number of poles which will fit inside the airgap diameter while keeping an even number of poles is calculated:

Number of poles = ROUND((0.5 • airgap diam • 1000 • PI() / pole pitch), 0) • 2

An exact airgap is then calculated based on the actual number of poles which were found above:

Corrected airgap = number of poles • pole pitch / PI() *(mm)*

The frequency of the electricity is calculated from the generator rpm and the number of poles:

Frequency = (number of poles / 2) • gen rpm / 60 *(Hz)*

The power per pole pair (*Pr*) is calculated:

Pr = electrical input power / (number of poles / 2) *(kW)*

The frequency at rated is compared to the frequency of a reference baseline turbine for scaling purposes:

Wu = frequency / 76.5 Hz *(none)*

The power per pole pair is compared to that of a reference baseline turbine:

Pu = Pr / 53.571 kW *(none)*

An intermediate impedance (*Zsu*) is calculated in order to size the generator:

Zsu = 0.09268 + 0.000095 • number of poles • generator rpm *(ohms)*

C.1.2 Generator Design

The airgap length can then be calculated based on the design parameters of power per pole, frequency, and impedance limit:

$$Airgap\ length = 250 \bullet (Z_{su} + (Z_{su}^{\ 2} + 2.4 \bullet 0.0662 \bullet W_u^{\ 2} / P_u)^{0.5}) / (2 \bullet W_u^{\ 2} / P_u) \quad (mm)$$

The airgap area is computed as the area of a cylinder:

Airgap area = PI() • (corrected airgap diameter / 1000) • airgap length *(m^2)*

C.1.3 Variable Dimensions

The radius to the outside of the wet sleeve (*R1*) is calculated so as to sit just outside the stator back iron:

R1 = stator diameter / (2 • 1000) + 30 *(mm)*

The structural casing outside radius (*R2*) differs from the wet sleeve radius by the casing wall thickness:

R2 = R1 + 30 *(mm)*

The structural casing flange outer radius (*R3*) is based on the structural casing outside radius plus the flange thickness:

R3 = R2 + 30 *(mm)*

The back wall outer radius (R4) is equivalent to the structural casing outside radius:

R4 = R2 *(mm)*

The structural attachment radius (*R5*) is based on the structural attachment flange radius plus a clearance for the bolt pattern:

R5 = R3 + 100 *(mm)*

The length inside the structural casing (*L1*) is calculated from the airgap length, plus clearances to the back and front walls:

L1 = airgap length + 44 + 125 *(mm)*

The attachment flange thickness is constant:

L2 = 40 *(mm)*

The rear wall thickness (*L3*) is an independent variable which increases with gear ratio.

The rotor rim outer radius is smaller than the airgap radius by the magnet thickness (mag_thick):

Rotor Rim outer radius = airgap radius – mag_thick *(mm)*

The rotor rim inner radius is calculated:

Inner radius = rotor rim outer radius – bir – (airgap length / 4) • TAN(0.2) *(mm)*

The average thickness of the rotor web (*L5*) is set to be one-fifth the airgap length, and no smaller than 25 mm:

L5 = IF(0.2 • airgap length > 25, 0.2 • airgap length, 25) *(mm)*

C.1.4 Fixed-Weight Calculations

The fixed weights for the retainer, mainshaft, bearings, and other miscellaneous hardware all come from Milwaukee Gear estimate 46325 obtained by GEC[1]. The fixed weight of the gearbox is a sum of the fixed weights of the retainer, mainshaft, and bearings and other miscellaneous hardware.

[1] See attached quote (Table C.1-1).

C.1.5 Variable Weight Calculations

The variable weight front casing supports the rotor hub and attaches to the planetary gear system. The first term (1500 kg) accounts for the constant rotor support section of the casing. The second expression calculates the weight contributed by the attachment to the planetary gears. It uses a combined constant (density • pi) = 0.8, a wall thickness of 1.5, and a factor of 0.4536 = kg/lb to convert to kilograms giving:

$$Front\ casing = 1550 + (((Structural\ attachment\ radius / 25.4)^2 - 27.5^2) \bullet 0.8 \bullet 1.5) \bullet 0.4536 \quad (kg)$$

The weight calculation of the generator casing (also denoted structural casing) is broken into four parts.

The first term (*W1*) calculates the weight of the outside wrapper:

$$W1 = (R2^2 - R1^2) \bullet PI() \bullet L1 \quad (mm^3)$$

The second term (*W2*) calculates the attachment flange on the aft end of the outside wrapper:

$$W2 = (R3^2 - R2^2) \bullet PI() \bullet L2 \quad (mm^3)$$

The third term (*W3*) calculates the contribution of the front face of the generator casing:

$$W3 = (R3^2 - 165^2) \bullet PI() \bullet L3 \quad (mm^3)$$

The fourth term (*W4*) calculates the inner tube which supports the generator bearings:

$$W4 = (165^2 - 125^2) \bullet PI() \bullet airgap\ length \bullet 1000 \quad (mm^3)$$

Summing the four terms and multiplying by density gives the total weight:

$$Generator\ casing\ wt = (W1 + W2 + W3 + W4) \bullet 7.197 \times 10^{-6} kg / mm^3 \bullet 0.6 \bullet 2.5 \ (kg)$$

The carrier weight is calculated by summing the weight of the back plate and the weight of the three cylindrical, hollow planet gear supports:

$$Carrier\ weight = 1600 \bullet 0.4536 + (ring\ gear\ diameter - 49) \bullet (ring\ gear\ diameter \bullet PI()) \bullet 3 \bullet 0.26 \bullet 0.4536 \quad (kg)$$

The ring gear weight calculates surface area of the gear teeth, and then multiplies by an average depth of 3.1 in. and a density of 0.283 lb / in³:

$$Ring\ gear\ weight = ((ring\ gear\ diameter + 3) \bullet PI() \bullet (gear\ face + 1) \bullet 3.1 \bullet 0.283) \bullet 0.4536 \quad (kg)$$

The planet gear weight is calculated by computing the planet gear diameter as a function of the ring gear diameter and the pinion pitch diameter, and then multiplying by face width and density:

$$Planets\ weight = ((ring\ gear\ diameter - pinion\ PD) / 2 \bullet PI() \bullet (gear\ face + 1) \bullet 2.75 \bullet 0.283 \bullet 3) \bullet 0.4536 \quad (kg)$$

The sun pinion is weight calculated as a hollow cylinder, with an added weight of 177 lb to account for the extension on the pinion where the generator linkage attaches:

$$Sun\ pinion\ weight = (117 + ((pinion\ PD / 2)^2 - 1.375^2) \bullet 0.889 \bullet gear\ face) \bullet 0.4536 \quad (kg)$$

The following components are summed as variable-weight gearbox components: front casing, generator casing, carrier, ring gears, planet gears, and sun pinion. The total weight of the gearbox is then calculated from the variable-weight and fixed-weight components from above.

C.1.6 Nacelle Design

The nacelle dimensions of length, width and height are all functions of the structural attachment radius (*R5*):

$$Nacelle\ length = 3.5 \bullet R5 \bullet 1.25 / 1000 \quad (m)$$

$$Nacelle\ width = R5 \bullet 1.25 / 1000 \quad (m)$$

$$Nacelle\ height = R5 \bullet 1.25 / 1000 \quad (m)$$

The nacelle weight can then be calculated based on the calculated dimensions:

$$Nacelle\ weight = (2 \bullet length \bullet width + 2 \bullet width \bullet height + 2 \bullet height) \bullet 0.015 \bullet nacelle\ density \quad (kg)$$

C.1.7 Generator Weight Calculations

The rotor weight is calculated in four terms. The first (*W5*) computes the volume of the rotor rim which holds the magnets:

$$W5 = (R5^2 - R6^2) \bullet PI() \bullet (airgap\ length + 5) \quad (mm^3)$$

The second term calculates the volume of the web which extends from the rotor rim inner radius (*R6*) to the rotor hub and has an average thickness of rotor web (L5):

$$W6 = (R6^2 - 240^2) \bullet PI() \bullet L5 \quad (mm^3)$$

The third term computes the volume of the web, where it joins the hub:

$$W7 = ((airgap\ radius \bullet 0.2)^2 \bullet PI() \bullet L5 \bullet 6) \quad (mm^3)$$

The fourth term computes the volume of the rotor hub:

$$W8 = (240^2 - 200^2) \bullet PI() \bullet (airgap\ length + 95) \quad (mm^3)$$

The volumes are summed and converted to weights:

$$Rotor\ weight = (W5 + W6 - W7 + W8) \bullet 0.000007197 \quad (kg)$$

The weight of the generator cover which covers up the aft side of the generator is calculated from the structure radius to the wet sleeve (R1) and the attachment flange thickness (L2). It is shaped as a uniform disk with a thick attachment rim:

$$Generator\ cover\ weight = (((R1 + 75)^2 - R1^2) \bullet PI() \bullet L2 + (R1^2 - 200^2) \bullet PI() \bullet (L2 \bullet 0.5) \bullet 1.25) \bullet 0.000007197 \quad (kg)$$

The stator jacket weight is calculated by subtracting the space for the windings from a circular band of outer radius R1:

$$Stator\ jacket\ weight = ((R1^2 - Airgap\ radius^2) \bullet PI() \bullet (Airgap\ length + 44) - (R1^2 - Airgap\ radius^2) \bullet PI() \bullet (Airgap\ length - 40) \bullet 0.5) \bullet 0.000007197 \quad (kg)$$

The total weight of the generator iron is calculated:

$$Generator\ iron = rotor\ weight + generator\ cover\ weight + stator\ jacket\ weight \quad (kg)$$

The support structure weight is calculated from interpolation of a best-fit line using the attachment diameter as the parameter:

Support structure = (0.625 • (attachment diameter • 12)² – 59.12 • (attachment diameter • 12) + 10498) • 0.4536 *(kg)*

C.1.8 Assembly Labor Time

Assembly labor time is fixed across all gear ratio and generator sizes.

C.1.9 Cost Calculations

The system assembly cost is figured by adding the time for all assembly tasks and using a rate of $65/hr. The gearbox fixed cost is taken from Milwaukee Gear quote 46325[2]. The gearbox variable cost is calculated from the total variable weight of gearbox components and a cost of $5.34/kg.

The generator iron cost is calculated using weight as a parameter in the cost equation:

Generator iron cost = (0.00000017 • (gen iron wt)² – 0.001172 • (gen iron wt)² + 3.837) • gen iron wt *($)*

The active material and generator assembly cost is calculated from a best fit line:

Generator mat'ls and ass'ly = 21034.66 • airgap length^(11.60346 / airgap length) • airgap area • 1.09 *($)*

The nacelle cover cost is calculated using the weight as a parameter for estimating material and shipping cost:

Nacelle cover cost = nacelle weight • cost / kg + nacelle weight • freight rate + additional hardware cost *($)*

The bedplate structure cost is fixed at $20,000 across all gear ratios. Similarly, the brake cost is fixed at $6,160 corresponding to three calipers, a disk diameter of 600 mm, and a cost of $2,053/caliper.

The cooling system cost is calculated:

Cooling cost = 500 + 1.25 • electrical input power + 0.4 • airgap diameter *($)*

The total cost is calculated:

Total cost = gearbox + generator iron + active materials and assembly + nacelle cover + bedplate structure + brake + cooling *($)*

[2] See the attached quote (Table C.1-1), which was used to create the Single PM bill of materials.

Table C.1-1. Bill of Materials for the Single PM Generator

Inquiry 46325

Assem. No.	Part Number	Inquiry Item	Descriptions	Quantity per box	Price per pc	Total Price
1	SK01138-7	1.01	Main shaft	1	$4,195.15	$4,195.15
2	SK01138-3	1.02	Forward bearing retainer	1	$820.57	$820.57
3	SK01138-1	1.03	Forward housing	1	$2,137.29	$2,137.29
4	SK01138-4	1.04	Carrier	1	$3,368.17	$3,368.17
5	SK01138-8	1.05	L.H. ring gear	1	$4,526.89	$4,526.89
6	SK01138-9	1.06	R.H. ring gear	1	$4,300.30	$4,300.30
7	SK01138-2	1.07	Rear housing	1	$1,739.29	$1,739.29
8	SK01138-5	1.08	Rear bearing retainer	1	$1,881.49	$1,881.49
9	SK051701-9	1.09	Coupling, input	1	$1,140.91	$1,140.91
10	SK051701-10	1.10	Spherical bearing, planetary	3	$1,043.61	$3,130.84
11	SK051701-11	1.11	Cap	3	$89.69	$269.07
12	SK01138-11R	1.12	R.H. planetary gear	3	$1,150.09	$3,450.27
13	SK01138-11l	1.13	L.H. planetary gear	3	$1,150.09	$3,450.27
14	SK051701-14	1.14	Generator retainer	1	$572.61	$572.61
15						
16	SK01138-13	1.16	Generator shaft coupling	1	$400.00	$400.00
17	SK051701-17	1.17	Generator outer tapered bearing	1	$818.14	$818.14
18	SK051701-18	1.18	Generator bearing retainer	1	$156.73	$156.73
19	SK051701-19	1.19	Adaptor tube	1	$96.00	$96.00
20	SK051701-20	1.20	Tube, roller bearing	1	$40.00	$40.00
21	SK01138-12L	1.21	L.H. sun gear	1	$336.63	$336.63
22	SK01138-12R	1.22	R.H. sun gear	1	$630.59	$630.59
23	SK01138-6	1.23	Labyrinth	1	$405.41	$405.41
24	SK051701-24	1.24	Generator coupling	1	$444.49	$444.49
25	SK051701-25	1.25	Generator inner tapered bearing	1	$818.14	$818.14
26						
		1.27	Various purchased Items	N/A		
27			Forward mainshaft bearing	1	$9,523.77	$9,523.77
28			Rear mainshaft bearing	1	$8,162.35	$8,162.35
	SK01138-12	1.97	Sun gear assembly	1	$101.81	$101.81
	SK01138-11	1.98	Planetary gear assembly	3	$448.75	$1,346.25
45			Assembly labor	40	$65.00	$2,600.00
46			Test, 6 h total	6	$65.00	$390.00
44			Lube system	1	$2,700.00	$2,700.00
49			Paint, prepare for ship	1	$1,350.00	$1,350.00
					Total	$65,303.43
			Mark-up	25%	Sell price	$81,629.29

Medium Speed Weight and Cost Calculations 1.5 MW Design, Diode Bridge

Rotor rpm =	20.5		Gap shear stress =	0.048625847	n/mm2
Mechanical input power =	1621.0	kW	Stator pole height =	80	mm
Mechanical rotor torque =	755,297	Nm	Air gap =	5	mm
Electricall input power =	1,500	kW	Slot depth =	60	mm
Electrical rotor torque =	702,000	Nm	Stator back iron =	20	mm
Air gap to ring gear dia ratio =	1.43		Structure wall thickness =	65	mm
Magnet + pole cap thickness =	35	mm	Rotor back iron thickness =	25	mm
Pole pitch =	120.0537	mm	Gap shear stress =	7.057	psi

System Design

Ratio =	7.80	8.05	8.84	9.1580	9.96	10.64
Sun pinion aspect ratio =	1.9302	1.2147	1.0601	1.0412	0.7070	0.6621
Gen rpm =	159.9	165.1	181.3	187.7	204.1	218.1
Air gap velocity, m/min =	572.7	798.7	990.8	1085.2	1500.2	1740.5
Gen mechanical torque, Nm =	96,833	93,791	85,422	82,474	75,871	70,987
Gen electrical torque, Nm =	90,000	87,172	79,394	76,654	70,517	65,977
Stator dia, m =	1.300	1.700	1.900	2.000	2.500	2.700
Air gap diameter, m =	1.1400	1.5400	1.7400	1.8400	2.3400	2.5400
Air gap radius, mm =	573	764	879	917	1185	1261
No of poles =	30	40	46	48	62	66
Corrected air gap diameter, mm =	1146	1529	1758	1834	2369	2522
Frequency, Hz =	39.98	55.03	69.48	75.10	105.44	119.97
Pr =	100.00	75.00	65.22	62.50	48.39	45.45
Wu =	0.52	0.72	0.91	0.98	1.38	1.57
Pu =	1.87	1.40	1.22	1.17	0.90	0.85
Zsu, ohms =	0.55	0.72	0.88	0.95	1.29	1.46

Generator Design

Air gap length, m =	0.955	0.500	0.337	0.297	0.161	0.132
Air gap length, mm =	955	500	337	297	161	132
Air gap, m^2 =	3.440	2.403	1.863	1.713	1.200	1.049

Variable Dimmensions

R1, structure radius to wet sleeve, mm =	680	880	980	1,030	1,280	1,380
R2, structural casing outside radius, mm =	710	910	1,010	1,060	1,310	1,410
R3, structural casing, flange outer radius, mm =	740	940	1,040	1,090	1,340	1,440
R4, back wall outer radius, mm =	710	910	1,010	1,060	1,310	1,410
R5 srtuctural attachment radius, mm =	840	1,040	1,140	1,190	1,440	1,540
L1, length, inside structural casing, mm =	1,124	669	506	466	330	301
L2, attachment flange thickness, mm =	40	40	40	40	40	40
L3, rear wall thickness, mm =	25	27	30	32	35	40
R5, rotor rim outer radius, mm =	538	729	844	882	1150	1226
R6, rotor rim inner radius, mm =	465	679	802	842	1116	1194
L5, ave thickness of rotor web, mm =	191	100	67	59	32	26

Medium Speed Weight and Cost Calculations 1.5 MW Design, Diode Bridge

Rotor rpm =	20.5		Gap shear stress =	0.048625847	n/mm2
Mechanical input power =	1621.0	kW	Stator pole height =	80	mm
Mechanical rotor torque =	755,297	Nm	Air gap =	5	mm
Electricall input power =	1,500	kW	Slot depth =	60	mm
Electrical rotor torque =	702,000	Nm	Stator back iron =	20	mm
Air gap to ring gear dia ratio =	1.43		Structure wall thickness =	65	mm
Magnet + pole cap thickness =	35	mm	Rotor back iron thickness =	25	mm
Pole pitch =	120.0537	mm	Gap shear stress =	7.057	psi

System Design						
Ratio =	7.80	8.05	8.84	9.1580	9.96	10.64

Fixed Weight Calculations						
Fixed weight, retainer, kg =	121.2	121.2	121.2	121.2	121.2	121.2
Fixed weight, mainshaft, kg =	2053.3	2053.3	2053.3	2053.3	2053.3	2053.3
Fixed weight, bearings, misc and hardware, kg =	1580	1580	1580	1580	1580	1580
Fixed weight, gearbox, kg =	3754.5	3754.5	3754.5	3754.5	3754.5	3754.5

Variable Weight Calculations						
Variable weight, front casing, kg =	1,734	2,052	2,236	2,334	2,890	3,142
Variable weight, generator casing, kg =	2,466	2,276	2,314	2,456	3,141	3,800
Variable weight, carrier, kg =	193	600	886	1,017	2,207	2,746
Variable weight, ring gears, kg =	1,017	1,056	1,027	1,049	1,055	1,066
Variable weight, planet gears, kg =	1,001	1,122	1,117	1,150	1,207	1,233
Variable weight, sun pinion, kg =	93	111	104	103	109	105
Variable weight, gearbox components, kg =	6,503	7,216	7684	8,109	10,608	12,092
Total weight, gearbox components, kg =	10,258	10,971	11439	11,863	14,363	15,847

Nacelle Design						
Nacelle length, m =	3.68	4.55	4.99	5.21	6.30	6.74
Nacelle width, m =	1.05	1.30	1.43	1.49	1.80	1.93
Nacelle height, m =	1.05	1.30	1.43	1.49	1.80	1.93
Nacelle weight, kg =	304.77	451.48	535.53	580.23	830.47	943.04

Generator Weight Calculations						
Variable weight, rotor, kg =	2360	1643	1318	1233	1006	920
Variable weight, generator cover, kg =	336	540	658	722	1082	1246
Variable weight, stator jacket, kg =	1638	1352	988	1057	768	925
Total weight, generatoe iron, kg =	4334	3534	2965	3011	2856	3091

Variable weight, support structure, kg =	4,208	4,429	4,593	4,688	5,293	5,597

Medium Speed Weight and Cost Calculations 1.5 MW Design, Diode Bridge

Rotor rpm =	20.5		Gap shear stress =	0.048625847	n/mm2
Mechanical input power =	1621.0	kW	Stator pole height =	80	mm
Mechanical rotor torque =	755,297	Nm	Air gap =	5	mm
Electricall input power =	1,500	kW	Slot depth =	60	mm
Electrical rotor torque =	702,000	Nm	Stator back iron =	20	mm
Air gap to ring gear dia ratio =	1.43		Structure wall thickness =	65	mm
Magnet + pole cap thickness =	35	mm	Rotor back iron thickness =	25	mm
Pole pitch =	120.0537	mm	Gap shear stress =	7.057	psi

System Design						
Ratio =	7.80	8.05	8.84	9.1580	9.96	10.64

Assembly Labor Time						
Assemble box to nacelle, h =	15.0	15.0	15.0	15.0	15.0	15.0
Assemble generator, wire system, h =	25.0	25.0	25.0	25.0	25.0	25.0
Assemble cooling, aux equip, h =	25.0	25.0	25.0	25.0	25.0	25.0
Test and paint, h =	20.0	20.0	20.0	20.0	20.0	20.0
Nacelle assembly, total, h =	85.0	85.0	85.0	85.0	85.0	85.0

Cost Calculations						
System assembly cost, USD =	$5,525	$5,525	$5,525	$5,525	$5,525	$5,525
Gearbox, fixed cost, USD =	$41,170	$41,170	$41,170	$41,170	$41,170	$41,170
Gearbox variable cost, USD =	$34,700	$38,502	$41,001	$43,267	$56,603	$64,521
Total gearbox, USD =	$75,870	$79,672	$82,171	$84,436	$97,772	$105,691
Generator iron cost, USD =	$8,455.04	$6,426.48	$5,504.16	$5,568.51	$5,359.41	$5,683.18
Active mat and assem generator cost, USD =	$85,718	$63,642	$52,174	$49,055	$39,665	$36,914
Nacelle cover cost, USD =	$4,914	$6,660	$7,660	$8,192	$11,170	$12,509
Bedplate structure cost, USD =	$20,000	$20,000	$20,000	$20,000	$20,000	$20,000
Brake, USD =	$6,160	$6,160	$6,160	$6,160	$6,160	$6,160
Cooling, USD =	$2,834	$2,986	$3,078	$3,109	$3,323	$3,384
Total cost, USD =	$209,475	$191,072	$182,272	$182,045	$188,974	$195,866

C.2 Direct Drive Generator Parametric Spreadsheet

The direct drive generator design was optimized by power output and generator diameter. Each worksheet computes design parameters, weight and cost for a range of power outputs of 0.75 MW, 1.5 MW, 2.25 MW and 3.0 MW as well as generator radii. In the text that follows, each line of one design spreadsheet for the direct drive generator is broken out and expanded into an annotated form. Moving down these notes is analogous to moving down one of the design worksheets line by line. Most named variables are defined when first presented. Otherwise, their definitions should be present at the top of the design worksheet where declarations occur, or later in the appendix text. The units are in parentheses at the right.

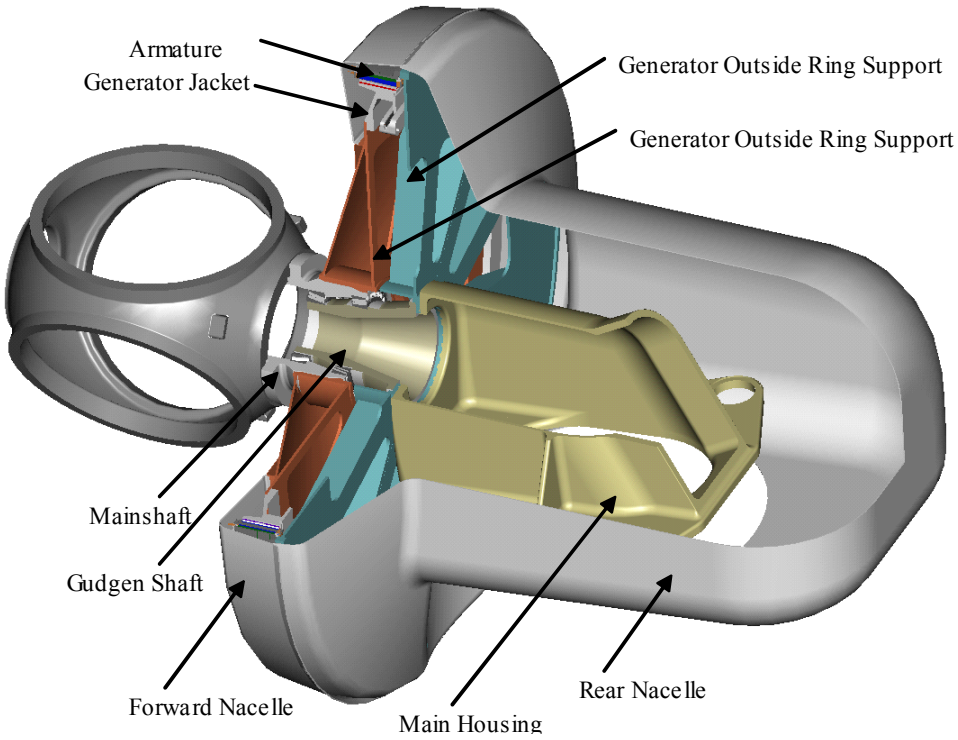

Figure C.2-1. Cutaway view of the direct drive generator showing part names of some major weight contributors

C.2.1 System Design

The number of generators, *ng* is constant across all radii in the direct drive design. The electrical requirement, per generator:

$$kW\_gen\_e = kW\_e / ng \qquad (kW)$$

The approximate distance over the stator, *r_tancir*, is varied across the design worksheet. Based on that distance over the stator, and constrained by constants t-jacket and h_gen_od_wall for housing wall thicknesses, the nominal airgap diameter is computed:

$$Nominal\ airgap\ diam = INT(40 \bullet (r\_tancir - (t\_jacket + h\_gen\_od\_wall + h\_pole) / 1000)) / 20 \qquad (m)$$

With the salient pole design, the near-optimum pole spacing is nearly constant, allowing the number of poles, *np*, to be computed using the nominal airgap diameter and the pole pitch (*pip*):

np = ROUND((0.5 • nominal airgap diam • 1000 • PI() / pip), 0) • 2 *(mm)*

The frequency at rated (*fe*) can then be calculated using the number of poles:

fe = rpm_rotor • np / 120 *(Hz)*

The power per pole pair (*Pr*) is calculated:

Pr = kW_gen_e / (np / 2) *(kW)*

The frequency at rated is compared to the frequency of a reference medium-speed turbine for scaling purposes:

Wu = fe / 76.5 Hz *(none)*

The power per pole pair is compared to that of a reference medium speed turbine:

Pu = Pr / 53.571 kW *(none)*

An intermediate impedance (*Zsu*) is calculated in order to size the generator:

Zsu = 0.09268 + 0.000095 • np • rpm_rotor *(ohms)*

C.2.2 Generator Design

The actual airgap diameter, *D_ag*, is found by recalculating the airgap diameter, based on computed pole number and pitch:

D_ag = np • pip / (PI() • 1000 *(m)*

The pole stack length (*L_stack*) is computed:

L_stack = 250 • ((Zsu + (Zsu^2 + 8 • 0.3 • 0.066 • Wu^2 / Pu)^0.5) / (2 • Wu^2 / Pu)) *(mm)*

The total active area is calculated:

A_ag = D_ag • PI() • (L_stack / 1000) • ng *(m²)*

The generator outside diameter is calculated from the airgap diameter and the stator's composite thickness:

D_gen = D_ag • 1000 + 2 • (h_pole + t_jacket + h_gen_od_wall) *(mm)*

The electrical torque is calculated from the power rating of the generator and its rotational rate:

Q_e = kW_gen_e • 9549 / rpm_rotor *(Nm)*

The shear stress is calculated by taking the torque imparted across the airgap radius and dividing by the total active area:

Sigma = ng • Q_e / (A_ag • 1000 • (D_ag • 1000 / 2)) *(mPa)*

C.2.3 Variable Dimensions

The rear mainshaft bearing is sized to be proportional to the front mainshaft bearing by a factor of 1.3:

d_ms_r = d_ms_f • 1.3 *(mm)*

The rear mainshaft bearing is sized from a best fit line which is based on bearing weight and size data:

$$d\_ms\_f = 314.521 + 0.17359 \bullet kW\_m + (-0.00000043 / kW\_m^2) \quad (mm)$$

The attachment diameter calculation is similar to the generator outside diameter, with a 80 mm clearance:

$$D\_attachment = D\_ag \bullet 1000 + 2 \bullet h\_pole + 2 \bullet t\_jacket + 2 \bullet h\_gen\_od\_wall + 80 \quad (mm)$$

The generator jacket height is constant across all radii:

$$h\_jacket = 32 \quad (mm)$$

The diameter of the rotating spider, the web supporting the rotor iron and magnetics, is calculated as 80% of the airgap diameter:

$$D\_ri = 0.8 \bullet D\_ag \bullet 1000 \quad (mm)$$

The diameter of the armature rotor is back calculated from the airgap diameter minus the airgap and magnetics stack-up:

$$D\_arm\_rotor = D\_ag \bullet 1000 - 2 \bullet (h\_magwithcap + gap) \quad (mm)$$

The diameter of the inner rim of the rotor differs from the armature diameter by the thickness of the back iron:

$$D\_inner\_rim = D\_arm\_rotor - 2 \bullet bir \quad (mm)$$

The mean inner rim diameter of the rotor iron is calculated:

$$D\_rmi = IF(D\_inner\_rim - (L\_stack \bullet 0.176) < D\_ri, D\_ri, D\_inner\_rim - (L\_stack \bullet 0.176)) \quad (mm)$$

The brake disc pitch diameter is set to be 250 mm smaller than the mean inner rim diameter:

$$r\_caliper = (D\_rmi - 250) / 1000 \quad (m)$$

The number of brake calipers (n_calipers) is an input to the design worksheet.

C.2.4 Weight Calculations

The main housing, main shaft, and gudgeon shaft weights are calculated using weight model equations which take the generator wattage as an input:

$$Main\ housing\ weight = 5204 \bullet (kW\_gen\_e / 1500)^0.8978 \quad (kg)$$

$$Mainshaft\ weight = 1851 \bullet (kW\_gen\_e / 1500)^0.8978 \quad (kg)$$

$$Gudgeon\ shaft\ weight = 1429 \bullet (kW\_gen\_e / 1500)^0.8978 \quad (kg)$$

The rotating spider weight is calculated in two parts. First, the weight of the shaft portion is calculated:

$$W_1 = (((d\_ms\_f \bullet 1.24) / 2)^2 - (d\_ms\_f \bullet 1.12 / 2)^2) \bullet d\_ms\_f \bullet PI() \bullet k\_cd \bullet 1.09 \quad (kg)$$

The weight of the web is calculated next:

$$W_2 = ((0.375 \bullet D\_ag \bullet 1000)^2 - (d\_ms\_f \bullet 1.24 / 2)^2) \bullet 0.05 \bullet d\_ms\_f \bullet PI() \bullet k\_cd \bullet 1.09 \quad (kg)$$

The weights are totaled:

$$Spider\ weight = (W_1 + W_2) \quad (kg)$$

The armature rotor weight is calculated in three parts. The first term calculates a roughed out doughnut shape of outer diameter D_arm_rotor and inner diameter D_rmi:

$$W_3 = ((D\_arm\_rotor / 2)^2 - (D\_rmi / 2)^2) \cdot (L\_stack + 4) \cdot 40 \cdot PI() \cdot k\_cd \quad (kg)$$

The second term is calculated:

$$W_4 = ((((D\_inner\_rim - D\_ri) / (2 \cdot 0.707)) / 2)^2 - (0.5 \cdot D\_ri)^2) \cdot 40 \cdot PI() \cdot k\_cd \quad (kg)$$

The third term is calculated:

$$W_5 = ((D\_ri / 2)^2 - (D\_ri / 2\text{-}75)^2) \cdot 40 \cdot PI() \cdot k\_cd \quad (kg)$$

The weights are totaled:

$$Armature\ weight = (W_3 + W_4 + W_5) \quad (kg)$$

The generator jacket is weight calculated by taking a doughnut with outer diameter equal to the airgap and a height of 1.5 times the jacket height, and then subtracting an interior portion. It then becomes an inner tube. The full ring is calculated:

$$W_6 = (((D\_ag \cdot 1000 + 3 \cdot h\_jacket) / 2)^2 - (D\_ag \cdot 1000 / 2)^2) \cdot (L\_stack + 48) \cdot PI() \cdot k\_cd \cdot ng \quad (kg)$$

The inner portion is calculated:

$$W_7 = (((D\_ag \cdot 1000 + 2 \cdot h\_jacket) / 2)^2 - ((D\_ag \cdot 1000 + h\_jacket) / 2)^2) \cdot (L\_stack - 30) \cdot 0.3 \cdot PI() \cdot k\_cd \cdot ng \quad (kg)$$

The interior portion is subtracted out giving:

$$Generator\ jacket\ weight = (W_6 - W_7) \quad (kg)$$

The generator outside ring support weight is calculated in three parts. The outer flange is weight calculated:

$$W_8 = ((D\_attachment / 2)^2 - (D\_attachment / 2\text{-}40)^2) \cdot 60 \cdot PI() \cdot k\_cd \cdot 1.09 \cdot 1.25 \quad (kg)$$

The web is weight calculated:

$$W_9 = ((D\_attachment / 2\text{-}40)^2 - (0.66 \cdot d\_ms\_r)^2) \cdot 0.035 \cdot d \cdot PI() \cdot k\_cd \cdot 1.09 \cdot 1.25 \quad (kg)$$

The hub portion is weight calculated:

$$W_{10} = ((0.66 \cdot d\_ms\_r)^2 - (d\_ms\_r / 2)^2) \cdot 60 \cdot PI() \cdot k\_cd \cdot 1.09 \cdot 1.25 \quad (kg)$$

The weights are summed:

$$Generator\ outside\ ring\ support\ weight = (W_8 + W_9 + W_{10}) \quad (kg)$$

The mainshaft bearing weights are calculated from a curve fit of bearing weight versus diameter data:

$$Mainshaft\ bearing\ weight = 3.258 \cdot d\_ms\_f^{0.6956} + 3.258 \cdot d\_ms\_r^{0.6956} \quad (kg)$$

The retainer weight is calculated from a curve fit of weight versus generator power data:

$$Retainer\ weight = 115 \cdot (kW\_gen\_e / 1500)^{0.8978} \quad (kg)$$

The forward nacelle cover is weight calculated in two parts. The front facing ring is calculated:

$$W_{11} = (((D\_gen + 250) / 2)^2 - ((d\_ms\_r + 1000) / 2)^2) \cdot 8 \cdot PI() \cdot 1690 / 1000^3 \quad (kg)$$

The outer wrapper is then calculated:

$$W_{12} = (D\_gen + 250) \bullet (L\_stack + 500) \bullet 8 \bullet PI() \bullet 1690 / 1000\text{^}3 \quad (kg)$$

The weights are summed:

$$Nacelle\ weight = (W_{11} + W_{12}) \quad (kg)$$

The rear nacelle cover is calculated in two parts. The outer wrapper where the rear nacelle meets the front nacelle:

$$W_{13} = (D\_gen + 250) \bullet (L\_stack + 500) \bullet PI() \bullet 8 \bullet 1690 / 1000\text{^}3 \quad (kg)$$

The cylindrical portion of the nacelle covering the main housing is calculated:

$$W_{14} = (2000 \bullet 3000) \bullet PI() \bullet 8 \bullet 1690 / 1000\text{^}3 \quad (kg)$$

The weights are summed:

$$Rear\ nacelle\ weight = (W_{13} + W_{14}) \quad (kg)$$

The brake disk weight is calculated from the caliper radius determined above:

$$Brake\ disk\ weight = r\_caliper \bullet 1000 \bullet 2 \bullet PI() \bullet 25 \bullet 220 \bullet k\_cd \bullet 1.09 \quad (kg)$$

C.2.5 Cost Calculations

For most items, the cost calculations are based on the weight of the item and a rate ($/kg). The cost for parts such as the rotating spider is calculated by scaling the rate down for larger diameters. The $/kg rate is scaled by comparing the airgap diameter to a 1.5 meter baseline. The mainshaft bearing cost calculations are computed using curve fits of cost and weight data.

Table C.2-1. Cost Data for Direct Drive Design

Item	Basis	Rate
Main housing USD	weight • rate	$2.31
Mainshaft USD	weight • rate	$2.31
Gudgeon shaft USD	weight • rate	$2.31
Rotating spider USD	weight • rate • (D_ag / 1.5)^0.33	$2.31
Gen jacket USD	weight • rate • (D_ag / 1.5)^0.33	$2.31
Gen outside ring support USD	weight • rate • (D_ag / 1.5)^0.33	$2.31
Mainshaft bearings USD	0.000287 • E50^2.72	
Retainer, mainshaft USD	weight • rate	$2.31
Nacelle covers USD	weight • rate • (D_ag / 1.5)^0.33	$11.90
Assemble and test, USD	time • rate • (D_ag / 1.5)^0.33	$65.00
Transport premium USD	IF(D_attachment>4115,3500,0) • (D_ag / 1.5)^0.33	
Generator active magnetics USD	21034.66 • L_stack^(11.60346 / L_stack) • A_ag • 1.09	
Brake system	=8011 • 2.7183^(0.000123 • D_inner_rim)	

C.2.6 Assembly Labor Time

Assembly labor and time is based on a fixed minimum amount for assembly, plus a variable amount of time which depends on the airgap diameter.

Table C.2-2. Assembly Labor Data for Direct Drive Design

Item	Basis
Assemble main structure (h)	35 + 2 • D_ag
Assemble generator to system (h)	15 + 2 • D_ag
Assemble cooling, aux equip (h)	5 + 4 • D_ag
Test and paint (h)	16 + 2 • D_ag
Nacelle assembly, total (h)	Sum of above

Direct Drive with Diodes 0.75 MW

Mainshaft rpm =	20.5		Caliper force/unit =	200,000	N	Matl const, ductile =	7.197E-06	
Design kW, mechanical =	1574	kW	Magnet + pole cap thickness =	35.0	mm	Structural gen OD wall thick, min =	35.0	mm
Design kW, electrical =	1,500	kW	Stator pole height =	80.0	mm	Pole pitch =	120.0537	mm
Rotor back iron =	25.00	mm	Airgap =	5.0	mm	Size exponent =	0.33	
Gap shear stress =	0.06	mPa	Slot depth =	60.0	mm	base diameter =	1.5	m
Jacket thickness =	30.0	mm	Stator back iron =	20.0	mm	Torque at rated =	698,707	Nm

System Design												
Generators per system =	1	1	1	1	1	1	1	1	1	1	1	1
kW per generator =	1500.0	1500.0	1500.0	1500.0	1500.0	1500.0	1500.0	1500.0	1500.0	1500.0	1500.0	1500.0
Approximate radius over stator, m =	1.600	1.800	2.000	2.200	2.400	2.600	2.800	3.000	3.200	3.400	3.600	3.800
Nominal airgap dia, m =	2.900	3.300	3.700	4.100	4.500	4.900	5.300	5.700	6.100	6.500	6.900	7.300
Poles per generator =	76	86	96	108	118	128	138	150	160	170	180	192
Frequency at rated, Hz =	13.0	14.7	16.4	18.5	20.2	21.9	23.6	25.6	27.3	29.0	30.8	32.8
Pr =	39.47	34.88	31.25	27.78	25.42	23.44	21.74	20.00	18.75	17.65	16.67	15.63
Wu =	0.17	0.19	0.21	0.24	0.26	0.29	0.31	0.33	0.36	0.38	0.40	0.43
Pu =	0.74	0.65	0.58	0.52	0.47	0.44	0.41	0.37	0.35	0.33	0.31	0.29
Zsu =	0.24	0.26	0.28	0.30	0.32	0.34	0.36	0.38	0.40	0.42	0.44	0.47

Generator Design												
Actual airgap diameter, m =	2.904	3.286	3.669	4.127	4.509	4.891	5.274	5.732	6.114	6.496	6.879	7.337
Pole stack length, mm =	1579.4	1185.2	921.4	706.5	580.2	485.1	411.8	344.0	299.7	263.6	233.8	204.3
Active area, per generator, m^2 =	14.4106	12.237	10.620	9.161	8.219	7.454	6.822	6.195	5.757	5.380	5.051	4.709
Total active area, m^2 =	14.4106	12.2366	10.6198	9.1607	8.2191	7.4544	6.8222	6.1953	5.7575	5.3800	5.0513	4.7091
Generator outside diameter, mm =	3194.3	3576.4	3958.6	4417.1	4799.3	5181.4	5563.6	6022.1	6404.3	6786.4	7168.6	7627.1
Electrical torque, Nm =	698,707	698,707	698,707	698,707	698,707	698,707	698,707	698,707	698,707	698,707	698,707	698,707
Shear stress, mPa =	0.03339	0.03475	0.03587	0.03696	0.03770	0.03832	0.03884	0.03935	0.03970	0.03998	0.04022	0.04044

Variable Dimensions												
Mainshaft bearing dia, front, mm =	764	764	764	764	764	764	764	764	764	764	764	764
Mainshaft bearing dia, rear, mm =	588	588	588	588	588	588	588	588	588	588	588	588
Attachment diameter to nacelle, mm =	3274	3656	4039	4497	4879	5261	5644	6102	6484	6866	7249	7707
Generator jacket thickness, mm =	32	32	32	32	32	32	32	32	32	32	32	32
Diameter of rotating spider, mm =	2323	2629	2935	3302	3607	3913	4219	4586	4891	5197	5503	5870
Diameter of armature rotor, mm =	2824	3206	3589	4047	4429	4811	5194	5652	6034	6416	6799	7257
Diameter of rotating iron, inner rim, mm =	2774	3156	3539	3997	4379	4761	5144	5602	5984	6366	6749	7207
Mean inner rim dia, rotor iron, mm =	2496	2948	3376	3873	4277	4676	5071	5542	5932	6320	6707	7171
Brake disc pitch dia, m =	2.246	2.698	3.126	3.623	4.027	4.426	4.821	5.292	5.682	6.070	6.457	6.921
Number brake calipers =	5	5	5	5	4	4	4	4	4	3	3	2

Direct Drive with Diodes 0.75 MW

Mainshaft rpm =	20.5		Caliper force/unit =	200,000	N	Matl const, ductile =	7.197E-06	
Design kW, mechanical =	1574	kW	Magnet + pole cap thickness =	35.0	mm	Structural gen OD wall thick, min =	35.0	mm
Design kW, electrical =	1,500	kW	Stator pole height =	80.0	mm	Pole pitch =	120.0537	mm
Rotor back iron =	25.00	mm	Airgap =	5.0	mm	Size exponent =	0.33	
Gap shear stress =	0.06	mPa	Slot depth =	60.0	mm	base diameter =	1.5	m
Jacket thickness =	30.0	mm	Stator back iron =	20.0	mm	Torque at rated =	698,707	Nm

System Design

Approximate radius over stator, m =	1.600	1.800	2.000	2.200	2.400	2.600	2.800	3.000	3.200	3.400	3.600	3.800

Weight Calculations

Main housing, kg =	5204	5204	5204	5204	5204	5204	5204	5204	5204	5204	5204	5204
Mainshaft, kg =	1,851	1,851	1,851	1,851	1,851	1,851	1,851	1,851	1,851	1,851	1,851	1,851
Gudgen shaft, kg =	1,429	1,429	1,429	1,429	1,429	1,429	1,429	1,429	1,429	1,429	1,429	1,429
Rotating spider, kg =	1,117	1,759	2,188	2,783	3,349	3,981	4,680	5,610	6,464	7,391	8,392	9,694
Armature rotor, kg =	15,741	10,833	7,877	5,704	4,541	3,727	3,137	2,624	2,306	2,056	1,856	1,664
Generator jacket , kg =	4,718	4,045	3,551	3,112	2,835	2,614	2,435	2,262	2,145	2,047	1,965	1,882
Gen outside ring support, kg =	2,331	2,893	3,514	4,339	5,093	5,906	6,780	7,908	8,915	9,981	11,108	12,539
Mainshaft bearings, kg =	605	605	605	605	605	605	605	605	605	605	605	605
Retainer, maishaft, kg =	115	115	115	115	115	115	115	115	115	115	115	115
Nacelle cover forward, kg =	397	396	409	437	469	507	551	610	663	721	783	861
Nacelle cover, rear, kg =	559	529	509	494	487	482	480	480	481	483	486	490
Brake disc, kg =	214	297	402	547	659	769	877	1,004	1,110	1,215	1,320	1,445
Total, kg =	34,067	29,658	27,251	26,074	25,977	26,421	27,267	28,699	30,178	31,883	33,793	36,335

Cost Calculations

Main housing, USD =	$12,021	$12,021	$12,021	$12,021	$12,021	$12,021	$12,021	$12,021	$12,021	$12,021	$12,021	$12,021
Mainshaft, USD =	$4,276	$4,276	$4,276	$4,276	$4,276	$4,276	$4,276	$4,276	$4,276	$4,276	$4,276	$4,276
Gudgen shaft, USD =	$3,301	$3,301	$3,301	$3,301	$3,301	$3,301	$3,301	$3,301	$3,301	$3,301	$3,301	$3,301
Rotating spider, USD =	$3,210	$5,265	$6,790	$8,979	$11,125	$13,582	$16,369	$20,172	$23,742	$27,695	$32,045	$37,812
Gen jacket, USD =	$13,553	$12,103	$11,018	$10,041	$9,416	$8,918	$8,517	$8,134	$7,879	$7,671	$7,502	$7,343
Gen outside ring support, USD =	$6,698	$8,656	$10,904	$13,997	$16,916	$20,153	$23,716	$28,434	$32,742	$37,400	$42,414	$48,910
Mainshaft bearings, USD =	$17,676	$17,676	$17,676	$17,676	$17,676	$17,676	$17,676	$17,676	$17,676	$17,676	$17,676	$17,676
Retainer,mainshaft, USD =	$266	$266	$266	$266	$266	$266	$266	$266	$266	$266	$266	$266
Nacelle covers, USD =	$12,665	$12,295	$12,212	$12,371	$12,662	$13,063	$13,556	$14,249	$14,901	$15,614	$16,383	$17,375
Assemble and test, USD =	$8,087	$8,746	$9,403	$10,191	$10,851	$11,513	$12,178	$12,982	$13,657	$14,335	$15,019	$15,846
Transport premium, USD =	$0	$0	$0	$4,888	$5,033	$5,170	$5,300	$5,448	$5,565	$5,677	$5,785	$5,910
Generator active magnetics, USD =	$348,772	$300,689	$265,343	$233,927	$214,020	$198,163	$185,338	$172,974	$164,617	$157,655	$151,827	$146,055
Brake system, USD =	$11,269	$11,811	$12,380	$13,098	$13,728	$14,389	$15,082	$15,957	$16,725	$17,530	$18,373	$19,439
Total cost, USD =	$441,794	$397,104	$365,589	$345,033	$331,291	$322,491	$317,596	$315,889	$317,368	$321,117	$326,890	$336,230

Direct Drive with Diodes 0.75 MW

Mainshaft rpm =	20.5		Caliper force/unit = Magnet + pole cap	200,000	N	Matl const, ductile = Structural gen OD wall	7.197E-06	
Design kW, mechanical =	1574	kW	thickness =	35.0	mm	thick, min =	35.0	mm
Design kW, electrical =	1,500	kW	Stator pole height =	80.0	mm	Pole pitch =	120.0537	mm
Rotor back iron =	25.00	mm	Airgap =	5.0	mm	Size exponent =	0.33	
Gap shear stress =	0.06	mPa	Slot depth =	60.0	mm	base diameter =	1.5	m
Jacket thickness =	30.0	mm	Stator back iron =	20.0	mm	Torque at rated =	698,707	Nm

System Design

Approximate radius over stator, m =	1.600	1.800	2.000	2.200	2.400	2.600	2.800	3.000	3.200	3.400	3.600	3.800

Assembly Labor Time

Assemble mainstructure, h =	40.8	41.6	42.3	43.3	44.0	44.8	45.5	46.5	47.2	48.0	48.8	49.7
Assemble generator to system, h =	20.8	21.6	22.3	23.3	24.0	24.8	25.5	26.5	27.2	28.0	28.8	29.7
Assemble cooling, aux equip, h =	16.6	18.1	19.7	21.5	23.0	24.6	26.1	27.9	29.5	31.0	32.5	34.3
Test and paint, h =	21.8	22.6	23.3	24.3	25.0	25.8	26.5	27.5	28.2	29.0	29.8	30.7
Nacelle assembly, total, h =	100.0	103.9	107.7	112.3	116.1	119.9	123.7	128.3	132.1	136.0	139.8	144.4

Costs for Graphs

Generators, USD =	$362,325	$312,792	$276,361	$243,968	$223,437	$207,081	$193,855	$181,107	$172,496	$165,326	$159,330	$153,398
Mainshaft, USD =	$4,276	$4,276	$4,276	$4,276	$4,276	$4,276	$4,276	$4,276	$4,276	$4,276	$4,276	$4,276
Nacelle cover, USD =	$12,665	$12,295	$12,212	$12,371	$12,662	$13,063	$13,556	$14,249	$14,901	$15,614	$16,383	$17,375
Nacelle structure, USD =	$43,171	$47,185	$50,958	$56,240	$61,305	$66,999	$73,350	$81,870	$89,748	$98,359	$107,723	$119,986
Transport prem, USD =	$0	$0	$0	$4,888	$5,033	$5,170	$5,300	$5,448	$5,565	$5,677	$5,785	$5,910
Assemble and test, USD =	$8,087	$8,746	$9,403	$10,191	$10,851	$11,513	$12,178	$12,982	$13,657	$14,335	$15,019	$15,846
Brake system, USD =	$11,269	$11,811	$12,380	$13,098	$13,728	$14,389	$15,082	$15,957	$16,725	$17,530	$18,373	$19,439
Total, USD =	$441,794	$397,104	$365,589	$345,033	$331,291	$322,491	$317,596	$315,889	$317,368	$321,117	$326,890	$336,230

C.3 Multi Generator Permanent Magnet Parametric Spreadsheet

The multi gen permanent magnet generator design was optimized by power output, outer radius and number of generators. In the text that follows, each line of one design spreadsheet for the multi gen permanent magnet generator is broken out and expanded into an annotated form. Moving down these notes is analogous to moving down one of the design worksheets line by line. Most named variables are defined when first presented. Otherwise, their definitions should be present at the top of the design worksheet where declarations occur, or later in the appendix text. The units are in parentheses at the right.

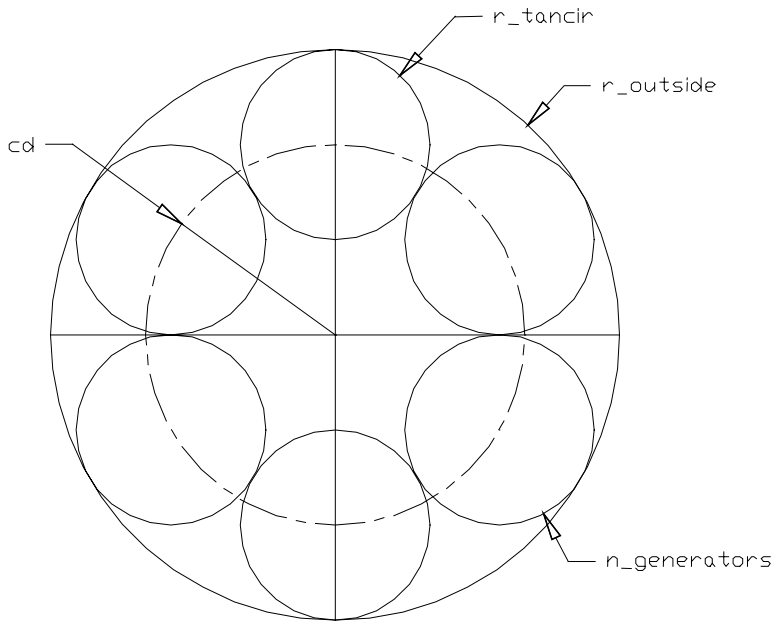

Figure C.3-1. Schematic of generator layout and related variables

C.3.1 System Design

The number of generators (*ng*) is an input to the design.

The electrical requirement, per generator:

$$kW\_gen\_e = kW\_e / ng \qquad (kW)$$

The load spectrum has been analyzed using Miners Rule theory to yield an equivalent load suitable for this analysis. The equivalent mechanical design load is given: *kW_m*

Mechanical power per generator is computed:

$$kW\_gen\_m = kW\_m / ng / 0.7457 \qquad (kW)$$

With the system radius known, the pitch circle of tangent circles is determined for each number of generators. The radius, r_tancir is computed:

$$r\_tancir = r\_outside \bullet SIN(PI() / ng) / (1 + SIN(PI() / ng)) \qquad (mm)$$

Based on the pitch circle of the generators and constrained by constants *t_jacket* and *h_gen_od_wall* for housing wall thicknesses, the nominal airgap diameter is computed and rounded to the nearest five hundredths:

A_g_nominal = INT(40 • (r_tancir – (t_jacket + h_gen_od_wall + h_pole) / 1000)) / 20 (m)

With the salient pole design, the near-optimum pole spacing is nearly constant, allowing the number of poles, *np*, to be computed. *Pip* is the pole pitch:

np = ROUND((0.5 • D14 • 1000 • PI() / pip), 0) • 2 *(mm)*

The frequency at rated (*fe*) can then be calculated using the number of poles:

fe = rpm_rotor • np / 120 *(Hz)*

The power per pole pair (*Pr*) is calculated:

Pr = kW_gen_e / (np / 2) *(kW)*

The frequency at rated is compared to the frequency of a reference medium-speed turbine for scaling purposes:

Wu = fe / 76.5 Hz *(none)*

The power per pole pair is compared to that of a reference medium-speed turbine:

Pu = Pr / 53.571 kW *(none)*

An intermediate impedance (*Zsu*) is calculated in order to size the generator:

Zsu = 0.09268 + 0.000095 • np • rpm_rotor *(ohms)*

C.3.2 Generator Design

The actual airgap diameter, *D_ag* , is found by recalculating the airgap diameter, based on computed pole number and pitch:

D_ag = np • pip / (PI() • 1000) *(mm)*

And using an input design factor for airgap shear stress (*sigma*), the stack length of stator poles is computed:

L_stack = Q_e / (PI() • D_ag • (D_ag / 2) • sigma • 1000) *(mm)*

And the total actual area of magnetic material for all generators:

A_ag_gen = A_ag • ng *(m^2)*

With the airgap diameter and stack length known, the airgap area is computed:

A_ag = D_ag • PI() • (L_stack / 1000) *(m^2)*

The generator outside diameter and the inputs *h_pole, t_jacket,* and *h_gen_od_wall* are used to determine housing weight:

D_gen = D_ag • 1000 + 2 • (h_pole + t_jacket + h_gen_od_wall) *(mm)*

With the pinion and generator rotor speed known, the generator electrical torque, *Q_e*, is computed:

Q_e = kW_gen_e • 9549 / rpm_pinion *(Nm)*

C.3.3 Gear Design

From the given system diameter and the radius of tangent circles, we compute the center distance:

$$CD = (r\_outside - r\_tancir) \bullet 1000 \quad (mm)$$

With pinion diameter known, and the center distance set as the radius of tangent circles, the pinion rpm is calculated:

$$rpm\_pinion = rpm\_rotor \bullet d\_gear / d\_pinion \quad (rpm)$$

The pinion torque is taken directly from the iterative solver section below:

$$Q\_pinion = pinion\ torque \quad (N \bullet m)$$

The load on the pinion bearings is computed by taking the torque transmitted and then dividing by the pinion radius:

$$wt = (Q\_pinion \bullet 2 / (d\_pinion / 1000)) / 1000 \quad (kN)$$

To determine required dynamic capacity based on $p = .3$ for roller bearings when wt is known:

$$C_{dynamic} = (6 \bullet rpm\_pinion)^{0.3} \bullet ((wt^2 + (wt \bullet 0.48)^2)^{0.5}) / 2 \quad (N)$$

The gear ratio (mg) is calculated from the pinion rpm and the mainshaft rpm input:

$$mg = rpm\_pinion / mainshaft\ rpm \quad (none)$$

C.3.4 Variable Dimensions

The pinion pitch diameter is calculated from the iteration variable x and the centerline distance:

$$d\_pinion = CD / x \quad (mm)$$

The gear pitch diameter is calculated from the centerline distance and the pinion pitch diameter:

$$D\_gear = 2 \bullet CD - d\_pinion \quad (mm)$$

The gearset face width is calculated using the pinion diameter and an adjustment factor of 1.05:

$$face = ROUND(1.05 \bullet d\_pinion, -0.5) \quad (mm)$$

The rear mainshaft bearing is sized from a best fit line based on bearing load and size data:

$$d\_ms\_r = 314.521 + 0.17359 \bullet kW\_m + (-0.00000043 / kW\_m^2) \quad (mm)$$

The front mainshaft bearing is sized to be proportional to the front mainshaft bearing by a factor of 1.3:

$$d\_ms\_f = d\_ms\_r \bullet 1.3 \quad (mm)$$

The attachment diameter to the nacelle can be calculated with the diameter of the generator and centerline distance known:

$$D\_attachment = CD \bullet 2 + D\_gen + 235 \quad (mm)$$

The generator jacket thickness, h_jacket, is an input to the design.

The diameter of the rotor iron can be calculated from the airgap diameter and the height of the magnetics and airgap:

$$D\_ri = D\_ag \bullet 1000 - 2 \bullet gap - 2 \bullet h\_magwithcap \quad (mm)$$

The mean inner rim diameter can then be calculated from the rotor iron diameter:

$$D\_rmi = (D\_ri - 2 \bullet bir - L\_stack \bullet 0.5 \bullet 0.267) \quad (mm)$$

C.3.5 Weight Calculations

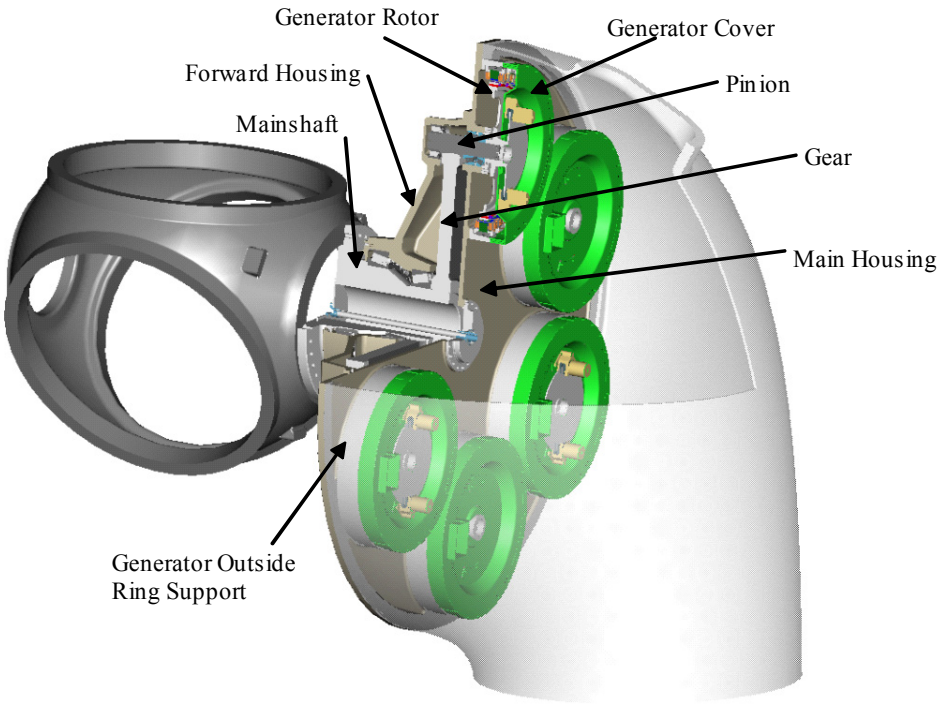

Figure C.3-2. Cutaway view of Multi Gen PM showing part names of some major weight contributors

With the attachment diameter known, the main housing is weight calculated. The front wall flange is computed first, with the wall thicknesses based on a ratio of the attachment diameter:

$$W_1 = (((0.5 \bullet D\_attachment)^2)-(0.44 \bullet D\_attachment)^2) \bullet 0.012 \bullet D\_attachment \bullet PI() \bullet k\_cd \quad (kg)$$

The remaining wall with hole is calculated:

$$W_2 = ((0.44 \bullet D\_attachment)^2 \bullet 0.008 \bullet D\_attachment - ((D\_attachment - 2.2 \bullet D\_gen)/2)^2 \bullet 0.008 \bullet D\_attachment) \bullet PI() \bullet k\_cd \quad (kg)$$

The attachment bosses are weight calculated:

$$W_3 = ((0.5 \bullet D\_gen)^2 - (0.45 \bullet (D\_ag + 2 \bullet h\_jacket))^2) \bullet 0.01 \bullet D\_attachment \bullet PI() \bullet k\_cd \quad (kg)$$

The results are summed:

$$Main\ housing\ weight = (W_1 + W_2 + W_3) \quad (kg)$$

The forward housing, which contains the main shaft bearings, is weight calculated in three parts; the flange from 1447mm on out is calculated first:

$$W_3 = ((CD + 165)^2 – 732^2) \cdot 38 \cdot PI() \cdot k\_cd \quad (kg)$$

The attachment wrapper is calculated:

$$W_4 = (CD + 185) \cdot 2 \cdot (d\_pinion + 150) \cdot 32 \cdot PI() \cdot k\_cd \quad (kg)$$

The constant weight of the hub is an input:

$$W_5 = 1750 \quad (kg)$$

They are summed:

$$Forward\ housing\ weight = (W_3 + W_4 + W_5) \quad (kg)$$

Generator jackets are weight calculated in two parts. First the solid ring is computed:

$$W_6 = (((D\_ag \cdot 1000 + 2 \cdot h\_jacket\ ) / 2)^2 - (D\_ag \cdot 1000/2)^2) \cdot (L\_stack + 48) \cdot PI() \cdot k\_cd \cdot ng \quad (kg)$$

Then the hollow portion of jacket is computed:

$$W_7 = (((D\_ag \cdot 1000 + 2 \cdot h\_jacket) / 2)^2 – ((D\_ag \cdot 1000 + h\_jacket) / 2)^2) \cdot (L\_stack – 30) \cdot 0.3 \cdot PI() \cdot k\_cd \cdot ng \quad (kg)$$

The hollow portion is subtracted:

$$Generator\ jacket\ weight = (W_6 – W_7) \quad (kg)$$

The generator outside ring support is computed:

$$Ring\ support\ weight = (((D\_gen) / 2)^2 – ((D\_ag \cdot 1000 + 2 \cdot h\_jacket + 2 \cdot h\_pole) / 2)^2) \cdot (L\_stack + 130) \cdot PI() \cdot k\_cd \cdot ng \quad (kg)$$

Generator rotors are weight calculated in three parts. The rim (W_8), the hub (W_9), and the spokes (W_{10}) are all broken out:

$$W_8 = ((D\_ag \cdot 500)^2 – (D\_ag \cdot 0.94 \cdot 500)^2) \cdot L\_stack \cdot PI() \cdot k\_cd \cdot ng \quad (kg)$$

$$W_9 = ((0.75 \cdot d\_pinion)^2 – (0.5 \cdot d\_pinion)^2) \cdot 1.25 \cdot L\_stack \cdot PI() \cdot k\_cd \cdot ng \quad (kg)$$

$$W_{10} = ((D\_ag \cdot 0.94 \cdot 500)^2 – (0.75 \cdot d\_pinion)^2) \cdot 0.1 \cdot L\_stack \cdot PI() \cdot k\_cd \cdot ng \quad (kg)$$

They are summed:

$$Generator\ rotor\ weight = (W_8 + W_9 + W_{10}) \quad (kg)$$

Generator retainers are a fixed weight of 18 kg each, thus:

$$Retainers\ weight = 18 \cdot ng. \quad (kg)$$

Generator covers are weight calculated in two parts. First the wrapper (W_{11}) and then the wall and hub (W_{12}) are calculated:

$$W_{11} = ((D\_gen / 2)^2 – ((D\_gen – 2 \cdot h\_gen\_od\_wall\text{-}10) / 2)^2) \cdot 25 \cdot PI() \cdot k\_cd \cdot ng \quad (kg)$$

$$W_{12} = (((D\_gen / 2)^2 – 125^2) \cdot 12.5 \cdot PI() \cdot k\_cd + 168750 \cdot k\_cd) \cdot ng \quad (kg)$$

The results are summed:

Generator cover weight = (W_{11} + W_{12}) *(kg)*

From the 3D model, the main shaft is constant for all sizes:

Mainshaft weight = 2170 *(kg)*

From the mainshaft bearing sizes already computed, a weight is now computed. This is a curve fit of weight and size data:

Mainshaft bearings weight =3.258 • d_ms_f^0.6956 + 3.258 • d_ms_r^0.6956 *(kg)*

Main shaft retainers are weight calculated in three parts. The end plate (W_{13}), the outer flange (W_{14}) and a constant portion (W_{15}) are all calculated:

W_{13} = *((d_ms_r • 0.6)^2 – (d_ms_r • 0.4)^2) • 25 • PI() • k_cd* *(kg)*

W_{14} = *(((d_ms_r • 0.75)^2 – 6000) • 40) • PI() • k_cd* *(kg)*

W_{15}= *100* *(kg)*

The results are summed:

Mainshaft retainer weight = W_{13}+ W_{14}+ W_{15} *(kg)*

A hub with seal envelopes each generator shaft at exit of the gear casing. They are weight-calculated:

W_{16} = *(200 / 2)^2 • 35 • PI() • k_cd • ng* *(kg)*

W_{17} = *((180 / 2)^2 • 25) • PI() • k_cd • ng* *(kg)*

The results are summed:

Hub with seal weight = W_{16} + W_{17} *(kg)*

The nacelle support structure is based on its attachment diameter. The variable weight is curve fitted from 3D modeling work. The weight is computed:

Nacelle support structure weight = 0.00037 • D_attachment^2 – 0.82725 • D_attachment + 4585 *(kg)*

The gear weight is based on gears with 80% web thickness and approximately 570 mm bore. A hub begins at 650 mm, and the rim extends 38 mm below pitch diameter. K_cd is a material constant of ductile iron in kg/mm^3 and is equal to 0.000007197. The correction factor for steel is 1.09. The weight is:

Gear weight = (((d_gear / 2)^2 – 81225) • PI() • face • k_cd – (((d_gear – 75) / 2)^2 – 105625) • PI() • (face / 5) • k_cd) • 1.09 *(kg)*

The pinion weights are estimated by calculating their volume, then multiplying by density:

Pinion wt = ((d_pinion • 0.35)^2 • 1.1 • face + ((d_pinion / 2)^2 • face)+ ((d_pinion • 0.35)^2 • L_stack)) • PI() • k_cd • ng • 1.09 *(kg)*

The pinion bearing load is derived from obtaining 100,000 h, L_{10} life. With the catalog rating based on 1 m cycles, we calculate a cycle ratio based on rpm and 100,000 h:

$$r = \frac{100{,}000 \cdot 60 \cdot rpm}{1{,}000{,}000} = 6\ rpm$$

For L_{10} life of required cycles:

$$L_{10} = \left(\frac{C}{P}\right)^{p} \cdot r \cdot rpm$$

Pinion bearing weight is then calculated based on curve fit of weight and size data:

Pinion bearing wt = 1.76E – 12 • C_dyn^4 – 1.98E-08 • C_dyn ^3 + 6.90E-05 • C_dyn ^2 – 1.00E-02 • C_dyn + 1.61 *(kg)*

The nacelle cover weight is ten percent of the nacelle support structure weight:

Nacelle cover weight = 0.1 • nacelle support structure *(kg)*

C.3.6 Cost Calculations

Most cost calculations are based on the weight of the item and a curve fit of cost versus weight data.

Table C.3-1. Cost Data for Multi-PM Drive Train Design

Item	Cost Basis
Main housing USD	= (0.00000017 • weight^2-0.001172 • weight+3.837) • weight
Forward housing USD	= (0.00000017 • weight ^2-0.001172 • weight +3.837) • weight
Gen jacket USD	= (0.00000017 • weight ^2-0.001172 • weight +3.577) • weight
Gen outside ring support USD	= (0.00000017 • weight ^2-0.001172 • weight +3.577) • weight
Generator rotors USD	= (0.00000017 • weight ^2-0.001172 • weight +3.577) • weight
Retainers, generator rotors USD	= (0.00000017 • weight ^2-0.001172 • weight +3.577) • weight
Generator cover USD	= (0.00000017 • weight ^2-0.001172 • weight +3.577) • weight
Mainshaft USD	= (0.00000017 • weight ^2-0.001172 • weight +3.837) • weight
Mainshaft bearings USD	= weight • 29$/kg
Retainer, mainshaft USD	= (0.00000017 • weight ^2-0.001172 • weight +3.577) • weight
Hubs with seal USD	= (0.00000017 • weight ^2-0.001172 • weight +3.577) • weight
Support nacelle structure USD	= (0.00000017 • weight ^2-0.001172 • weight +3.837) • weight
Gear USD	= weight • 5.456+882
Pinions USD	= weight • 5.456+882
Pinion bearings USD	= weight • ng • 2 • 14.81$/kg
Nacelle cover USD	= weight • 11.90 $/kg
Assemble and test USD	= nacelle assembly total time • 65 $/hr
Brake cost	= 57.18 • ng ^2-1069.24 • ng +9955.12
Gearbox cooling, lube	= $2,235.41 (from ancillary systems cost models)
Transport premium USD	= IF(D_attachment > 4115,3500,0)
Generator active magnetics USD	= 16925.6 • L_stack^(12.95559 / L_stack) • A_ag • 1.08

C.3.7 Assembly and Labor

The assembly of the main box depends primarily on the number of generators:

Main box assembly time =30 + 1.5 • ng • 2 *(h)*

The generator assembly also depends on the number of generators:

Generator assembly time = 4 • ng *(h)*

The time to assemble to the nacelle only depends on attachment diameter, which is fairly constant across a single worksheet:

Assemble to nacelle time = 5 + d_attachment / 1000 *(h)*

The cooling system and auxiliary equipment assembly depends on both attachment diameter and number of generators:

Assemble cooling system =4 • (D_attachment / 1000) + 2 • ng *(h)*

As does the test and paint time:

Test and paint time =12 + 0.75 • (D_attachment / 10000) • 2 • ng *(h)*

C.3.8 Iterative Solver Section

The gear set power capacity is computed for each of the number of generators. The capacity is computed by incrementing an index variable, *x*, which increases the pinion pitch diameter until the computed capacity per generator is equal to the required power capacity per generator. Based on given factors for geometry (*J-fact*), allowable stress (*Sat*), and estimated face contact factor (*Km*), the power capacity is estimated:

Gear power capacity = rpm_pinion • d_p^3 • J_fact • Km / (126000 • N_min • 1.25) *(HP)*

Delta power checks to make sure that the power found by iteration matches the input power. *X* is the incremented variable used in iteration. *CD* is calculated from the generator layout:

CD =(r_outside – r_tancir) • 1000/25.4 *(in)*

The pinion pitch diameter is calculated:

Pinion PD = CD / x *(in)*

The mesh force is calculated:

Mesh force = 2 • kW_gen_m • 63025 / rpm_pinion / pinion pd *(lbf)*

The pinion torque is calculated from the mechanical horsepower per generator and the pinion rpm:

Pinion torque = kW_gen_m • 63025 / rpm_pinion *(lb-in)*

Single Side Multi-Gen with Diodes Dia over generators = 3.25

Mainshaft rpm =	20.5	Outer radius =	1.62 m			Matl const, ductile =	0.000007197
Design kW, mechanical =	1574 kW	Magnet + pole cap =	35.0 mm			Structural genOD wall thick, min =	35.0 mm
Design kW, electrical =	1500 kW	Stator pole height =	80.0 mm	Aspect ratio =	1.25	J factor =	0.53
Rotor back iron =	25.0 mm	Airgap =	5.0 mm			Design root stress =	42000 psi
Gap shear stress =	5E-02 mPa	Slot depth =	60.0 mm			Min teeth =	21
Jacket thickness =	30.0 mm	Stator back iron =	20.0 mm			Pole pitch =	120.054 mm

System Design												
Generators per system =	3	4	5	6	7	8	9	10	11	12	13	14
kW per generator =	500.0	375.0	300.0	250.0	214.3	187.5	166.7	150.0	136.4	125.0	115.4	107.1
Mechanical HP per gen =	703.6	527.7	422.2	351.8	301.5	263.9	234.5	211.1	191.9	175.9	162.4	150.8
Radius of tangent circles, m =	0.752	0.671	0.600	0.540	0.490	0.448	0.413	0.382	0.356	0.333	0.313	0.295
Nominal airgap dia, m =	1.200	1.050	0.900	0.750	0.650	0.600	0.500	0.450	0.400	0.350	0.300	0.250
Poles per generator =	32	28	24	20	18	16	14	12	10	10	8	6
Frequency at rated, Hz =	39.9	48.5	53.4	54.1	57.0	57.8	56.5	53.3	48.3	52.0	44.4	35.4
Pr =	31.25	26.79	25.00	25.00	23.81	23.44	23.81	25.00	27.27	25.00	28.85	35.71
Wu =	0.52	0.63	0.70	0.71	0.75	0.76	0.74	0.70	0.63	0.68	0.58	0.46
Pu =	0.58	0.50	0.47	0.47	0.44	0.44	0.44	0.47	0.51	0.47	0.54	0.67
Zsu =	0.55	0.65	0.70	0.71	0.74	0.75	0.74	0.70	0.64	0.69	0.60	0.50
Generator Design												
Actual airgap diameter, m =	1.223	1.070	0.917	0.764	0.688	0.611	0.535	0.459	0.382	0.382	0.306	0.229
Pole stack length, mm =	281.9	198.8	168.5	166.3	150.3	146.0	151.7	168.9	203.4	173.1	233.6	363.1
Active area, per generator, m^2 =	1.0831	0.668	0.485	0.399	0.325	0.280	0.255	0.243	0.244	0.208	0.224	0.262
Total active area, m^2 =	3.2492	2.6725	2.4273	2.3953	2.2731	2.2438	2.2954	2.4338	2.6860	2.4939	2.9167	3.6620
Generator outside diameter, mm =	1512.9	1360.0	1207.1	1054.3	977.9	901.4	825.0	748.6	672.1	672.1	595.7	519.3
Electrical torque, Nm =	31,912	17,226	10,728	7,352	5,382	4,132	3,288	2,689	2,248	1,914	1,653	1,445
Shear stress, mPa =	0.04819	0.04819	0.04819	0.04819	0.04819	0.04819	0.04819	0.04819	0.04819	0.04819	0.04819	0.04819
Gear Design												
Centerdistance, mm =	868.155	948.974	1020.289	1080.000	1129.799	1171.635	1207.135	1237.570	1263.914	1286.920	1307.173	1325.131
Pin rpm =	149.61	207.88	267.02	324.71	380.19	433.29	484.06	532.62	579.13	623.76	666.66	707.98
Pinion torque, Nm =	33,487	18,076	11,258	7,715	5,648	4,336	3,450	2,822	2,359	2,008	1,734	1,516
Wt, kN =	320	212	155	120	98	82	70	62	55	49	44	41
Required pinion bearing load, kN =	1,365	999	785	647	551	481	427	384	350	321	297	276
Gear ratio =	7.30	10.14	13.03	15.84	18.55	21.14	23.61	25.98	28.25	30.43	32.52	34.54
Variable Dimensions												
Pinion PD, mm =	209.24	170.37	145.49	128.27	115.60	105.86	98.09	91.74	86.42	81.90	77.99	74.58
Gear pitch dia, mm =	1527.07	1727.58	1895.09	2031.73	2143.99	2237.41	2316.18	2383.40	2441.41	2491.94	2536.35	2575.68
Gear set facewidth, mm =	220.00	179.00	153.00	135.00	121.00	111.00	103.00	96.00	91.00	86.00	82.00	78.00
Mainshaft bearing dia, rear, mm =	588	588	588	588	588	588	588	588	588	588	588	588
Mainshaft bearing dia, front, mm =	764	764	764	764	764	764	764	764	764	764	764	764
Attachment diameter to nacelle, mm =	3484	3493	3483	3449	3472	3480	3474	3459	3435	3481	3445	3405
Generator jacket thickness, mm =	32	32	32	32	32	32	32	32	32	32	32	32
Diameter of rotor iron, mm =	1143	990	837	684	608	531	455	379	302	302	226	149
Mean inner rim dia, rotor iron, mm =	1055	913	765	612	538	462	385	306	225	229	145	51

Single Side Multi-Gen with Diodes Dia over generators = 3.25

Mainshaft rpm =	20.5	Outer radius =	1.62 m			Matl const, ductile =	0.000007197
Design kW, mechanical =	1574 kW	Magnet + pole cap =	35.0 mm			Structural genOD wall thick, min =	35.0 mm
Design kW, electrical =	1500 kW	Stator pole height =	80.0 mm	Aspect ratio =	1.25	J factor =	0.53
Rotor back iron =	25.0 mm	Airgap =	5.0 mm			Design root stress =	42000 psi
Gap shear stress =	5E-02 mPa	Slot depth =	60.0 mm			Min teeth =	21
Jacket thickness =	30.0 mm	Stator back iron =	20.0 mm			Pole pitch =	120.054 mm

System Design												
Generators per system =	3	4	5	6	7	8	9	10	11	12	13	14
Weight Calculations												
Main housing, kg =	2,575	2,469	2,304	2,082	2,020	1,927	1,811	1,678	1,532	1,580	1,416	1,249
Forward housing, kg =	2,754	2,882	3,012	3,131	3,235	3,327	3,407	3,477	3,540	3,595	3,644	3,688
Generator jackets, kg =	794	705	671	669	656	656	668	694	740	715	793	948
Gen outside ring supports, kg =	1,364	1,302	1,307	1,355	1,383	1,431	1,498	1,596	1,749	1,735	1,985	2,505
Gen rotors, kg =	1,744	1,228	955	799	682	604	552	519	504	456	468	523
Retainers, generator rotors, kg =	54	72	90	108	126	144	162	180	198	216	234	252
Generator covers, kg =	575	629	631	590	599	590	564	524	473	516	448	374
Mainshaft, kg =	2,170	2,170	2,170	2,170	2,170	2,170	2,170	2,170	2,170	2,170	2,170	2,170
Mainshaft bearings, kg =	605	605	605	605	605	605	605	605	605	605	605	605
Retainers, maishaft, kg =	309	309	309	309	309	309	309	309	309	309	309	309
Hubs with seal, kg =	37.5	50.0	62.5	75.0	87.4	99.9	112.4	124.9	137.4	149.9	162.4	174.9
Support nacelle structure, kg =	6,194	6,210	6,192	6,134	6,174	6,186	6,177	6,150	6,109	6,189	6,126	6,057
Gear, kg =	2,039	2,182	2,280	2,335	2,346	2,355	2,350	2,326	2,318	2,286	2,262	2,221
Pinions, kg =	385.78	266.72	207.38	175.92	149.77	133.87	124.25	119.52	121.34	107.70	117.26	142.96
Pinion bearings, per bearing, kg =	72.4	42.5	27.4	19.0	13.9	10.7	8.4	6.9	5.7	4.9	4.2	3.7
Nacelle cover, kg =	619	621	619	613	617	619	618	615	611	619	613	606
Total, kg =	22,582	21,998	21,662	21,358	21,341	21,316	21,271	21,217	21,237	21,360	21,457	21,925
Cost Calculations												
Main housing, USD =	$5,011	$4,888	$4,698	$4,443	$4,370	$4,258	$4,114	$3,941	$3,739	$3,807	$3,566	$3,296
Forward housing, USD =	$5,229	$5,392	$5,570	$5,742	$5,903	$6,053	$6,192	$6,319	$6,437	$6,545	$6,645	$6,738
Gen jacket, USD =	$2,187	$1,999	$1,923	$1,918	$1,889	$1,890	$1,917	$1,974	$2,073	$2,020	$2,184	$2,482
Gen outside ring support, USD =	$3,131	$3,046	$3,053	$3,117	$3,155	$3,217	$3,300	$3,415	$3,580	$3,566	$3,812	$4,278
Generator rotors, USD =	$3,575	$2,940	$2,495	$2,196	$1,949	$1,771	$1,645	$1,564	$1,528	$1,405	$1,435	$1,575
Retainers, generator rotors, USD =	$190	$252	$313	$373	$432	$491	$549	$607	$664	$720	$775	$830
Generator cover, USD =	$1,703	$1,829	$1,833	$1,736	$1,759	$1,736	$1,674	$1,577	$1,448	$1,557	$1,382	$1,182
Mainshaft, USD =	$4,544	$4,544	$4,544	$4,544	$4,544	$4,544	$4,544	$4,544	$4,544	$4,544	$4,544	$4,544
Mainshaft bearings, USD =	$17,542	$17,542	$17,542	$17,542	$17,542	$17,542	$17,542	$17,542	$17,542	$17,542	$17,542	$17,542
Retainer,mainshaft, USD =	$999	$999	$999	$999	$999	$999	$999	$999	$999	$999	$999	$999
Hubs with seal, USD =	$132	$176	$219	$262	$304	$346	$388	$429	$470	$510	$551	$591
Support nacelle structure, USD =	$19,203	$19,340	$19,180	$18,671	$19,022	$19,133	$19,050	$18,813	$18,460	$19,153	$18,608	$18,022
Gear, USD =	$12,006	$12,786	$13,322	$13,624	$13,684	$13,732	$13,705	$13,572	$13,530	$13,357	$13,222	$13,001
Pinions, USD =	$2,987	$2,337	$2,013	$1,842	$1,699	$1,612	$1,560	$1,534	$1,544	$1,470	$1,522	$1,662
Pinion bearings, USD =	$6,433	$5,040	$4,061	$3,378	$2,887	$2,524	$2,248	$2,035	$1,867	$1,733	$1,626	$1,540
Nacelle cover, USD =	$7,371	$7,390	$7,368	$7,299	$7,347	$7,362	$7,351	$7,318	$7,270	$7,365	$7,290	$7,208
Assemble and test, USD =	$6,044	$6,666	$7,282	$7,888	$8,516	$9,137	$9,754	$10,366	$10,975	$11,614	$12,216	$12,816
Brake cost, USD =	$7,262	$6,593	$6,038	$5,598	$5,272	$5,061	$4,964	$4,981	$5,112	$5,358	$5,718	$6,193
Gearbox cooling, lube, USD =	$2,235	$2,235	$2,235	$2,235	$2,235	$2,235	$2,235	$2,235	$2,235	$2,235	$2,235	$2,235
Transport premium, USD =	$0	$0	$0	$0	$0	$0	$0	$0	$0	$0	$0	$0
Generator active magnetics, USD =	$76,972	$68,976	$65,812	$65,220	$64,012	$63,826	$64,424	$65,932	$68,883	$67,044	$72,146	$82,608
Total cost, USD =	$184,756	$174,972	$170,502	$168,627	$167,521	$167,472	$168,157	$169,697	$172,900	$172,543	$178,020	$189,341

	System Design											
Generators per system =	3	4	5	6	7	8	9	10	11	12	13	14
	Assembly Labor Time											
Assemble main box, h =	39.0	42.0	45.0	48.0	51.0	54.0	57.0	60.0	63.0	66.0	69.0	72.0
Assemble generators, h =	12.0	16.0	20.0	24.0	28.0	32.0	36.0	40.0	44.0	48.0	52.0	56.0
Assemble to nacelle, h =	8.5	8.5	8.5	8.4	8.5	8.5	8.5	8.5	8.4	8.5	8.4	8.4
Assemble cooling, aux equip, h =	19.9	22.0	23.9	25.8	27.9	29.9	31.9	33.8	35.7	37.9	39.8	41.6
Test and paint, h =	13.6	14.1	14.6	15.1	15.6	16.2	16.7	17.2	17.7	18.3	18.7	19.1
Nacelle assembly, total, h =	93.0	102.6	112.0	121.4	131.0	140.6	150.1	159.5	168.8	178.7	187.9	197.2
	Iterative Solver Section, To Find Size to Equal Power Required											
Gear power capacity, kW =	944	708	566	472	404	354	315	283	257	236	218	202
Delta power, kW =	0.000	0.000	0.000	0.000	0.000	0.000	0.000	0.000	0.000	0.000	0.000	0.000
x, incr =	105.387	141.482	178.124	213.861	248.234	281.131	312.581	342.663	371.478	399.126	425.705	451.303
CD, mm =	868.155	948.974	1,020.289	1,080.000	1,129.799	1,171.635	1,207.135	1,237.570	1,263.914	1,286.920	1,307.173	1,325.131
Pinion PD, mm =	209.240	170.367	145.491	128.270	115.604	105.856	98.091	91.735	86.421	81.898	77.993	74.580
Mesh force, N =	320,099	212,210	154,762	120,295	97,711	81,927	70,348	61,527	54,605	49,039	44,475	40,667
Pinion torque, Nm =	33,487	18,076	11,258	7,715	5,648	4,336	3,450	2,822	2,359	2,008	1,734	1,516
	Costs for Graphs											
Generator, active, USD =	$76,972	$68,976	$65,812	$65,220	$64,012	$63,826	$64,424	$65,932	$68,883	$67,044	$72,146	$82,608
Generator, iron, USD =	$7,655	$7,020	$6,564	$6,223	$6,029	$5,889	$5,787	$5,722	$5,713	$5,702	$5,776	$6,068
Gearbox, USD =	$55,705	$54,442	$53,713	$53,184	$52,779	$52,519	$52,284	$52,021	$51,943	$51,764	$51,720	$51,882
Mainshaft, USD =	$4,544	$4,544	$4,544	$4,544	$4,544	$4,544	$4,544	$4,544	$4,544	$4,544	$4,544	$4,544
Nacelle cover, USD =	$7,371	$7,390	$7,368	$7,299	$7,347	$7,362	$7,351	$7,318	$7,270	$7,365	$7,290	$7,208
Assemble & Test, USD =	$6,044	$6,666	$7,282	$7,888	$8,516	$9,137	$9,754	$10,366	$10,975	$11,614	$12,216	$12,816
Brakes, USD =	$7,262	$6,593	$6,038	$5,598	$5,272	$5,061	$4,964	$4,981	$5,112	$5,358	$5,718	$6,193
Nacelle structure, USD =	$19,203	$19,340	$19,180	$18,671	$19,022	$19,133	$19,050	$18,813	$18,460	$19,153	$18,608	$18,022
Transport prem, USD =	$0	$0	$0	$0	$0	$0	$0	$0	$0	$0	$0	$0
Total, USD =	$184,756	$174,972	$170,502	$168,627	$167,521	$167,472	$168,157	$169,697	$172,900	$172,543	$178,020	$189,341

C.4 Multi-Induction Drive Train Parametric Spreadsheet

In the text that follows, each line of the design spreadsheet for the multi induction drive train model is broken out and expanded into an annotated form. Moving down these notes is analogous to moving down one of the design worksheets line by line. Most named variables are defined when first presented. Otherwise, their definitions should be present at the top of the design worksheet where declarations occur, or later in the appendix text. The units are in parentheses at the right.

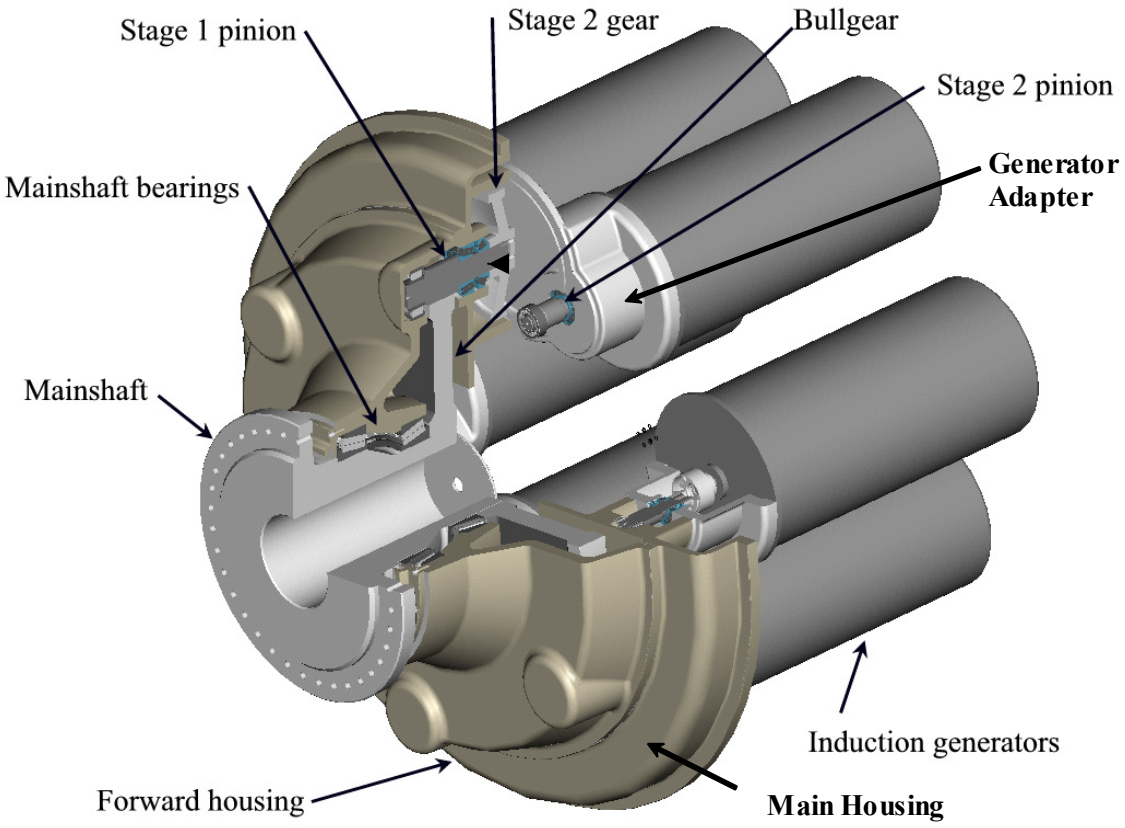

Figure C.4-1. Cutaway view of the Multi-Induction drive train showing housing and gear naming conventions

C.4.1 System Design

The number of generators (*ng*) is an input to the design spreadsheet.

The mechanical power per generator is calculated based on the total mechanical power:

Mechanical HP, nominal = kW_m / ng / 0.7457 *(hp)*

The electrical requirement, per generator, based on the total electrical design kW:

kW_gen_e = kW_e / ng *(kW)*

The actual mechanical power per generator is calculated:

HP_gen_m = Q_factor • Mechanical HP, nominal *(hp)*

To determine the size of the gearbox and the spacing of the generators, a circle with radius r_tancir is computed which spaces the generators such that they are just touching. It is computed from a given outer radius, as well as the number of generators:

r_tancir = (Outer Radius • sin (PI / ng)) / (1 + sin(PI / ng)) *(m)*

The outside diameter of the generator, the generator frame dimension, is computed using a step function which depends on the design kW of the generators:

IF Generator kW < 91 then D_frame = 550 *(mm)*

IF Generator kW < 201 then D_frame= 622 *(mm)*

IF Generator kW < 316 then D_frame = 700 *(mm)*

IF Generator kW < 451 then D_frame = 740 *(mm)*

IF Generator kW < 561 then D_frame = 820 *(mm)*

IF Generator kW < 901 then D_frame = 920 *(mm)*

IF Generator kW > 901 then D_frame = 1015 *(mm)*

The clearance between the calculated generator frame diameter and the tangent circle radius is checked:

L_clear = 2 • R_tancir • 1000 – D_frame *(mm)*

The second stage gear ratio is calculated using the input synchronous rpm (rpm_sync):

mg_2 = IF(rpm_sync / rpm_pinion > 1, rpm_sync / rpm_pinion, 0) *(rpm)*

C.4.2 Gear Design, Stage 1

The centerline distance is converted to mm from the iterative solver section:

CD (metric) = CD English • 25.4 *(mm)*

The gear ratio is calculated from the design input mainshaft rpm and the iterated pinion rpm:

mg = rpm_pinion / mainshaft rpm *(rpm)*

The pinion rpm is calculated from drive train dimensions found in the iterative solver section:

rpm_pinion = mainshaft rpm(CD • 2 / pinion PD-1)

The pinion torque is converted to metric from the iterative solver section:

Q_pinion = pinion torque • 0.11298 *(Nm)*

The radial load on the pinion bearings (*wt*) is calculated:

wt =(Q_pinion • 2 / (d_pinion / 1000)) / 1000 *(kN)*

The total load on the stage one pinion bearing accounting for all directions:

Required pinion bearing load = (6 • rpm_pinion)^0.3 • ((wt^2 + (wt • 0.48)^2)^0.5) / 2 *(kN)*

The pinion PD is converted to metric units from the iterative solver section:

d_pinion (metric) = Pinion PD • 25.4 *(mm)*

The gear pitch diameter (d_gear) is calculated from the pinion pitch diameter and the CD:

d_gear = (2 • CD – d_pinion) *(mm)*

The gearset face width is calculated by scaling and rounding the pinion PD:

face = ROUND(1.05 • d_pinion, -0.5) *(mm)*

C.4.3 Gear Design, Stage 2

The stage 2 centerline distance is converted to mm from the iterative solver section:

CD_2 (metric) = stage 2 CD English • 25.4 *(mm)*

The stage 2 gear ratio is displayed again here, without a change in calculation method.

The stage 2 pinion rpm is calculated:

rpm_pinion_2 = mg_2 • rpm_pinion *(rpm)*

The pinion torque is converted from the iterative solver section:

Q_pinion_2 = stage 2 pinion torque • 0.11298 *(Nm)*

The radial load on the pinion bearings (*wt*) is calculated:

wt_2 = (Q_pinion_2 • 2 / (d_pinion_2 / 1000)) / 1000 *(kN)*

The total load on the stage one pinion bearing accounting for all directions:

Required pinion bearing load = (6 • rpm_pinion_2)^0.3 • ((wt_2^2 + (wt_2 • 0.48)^2)^0.5) / 2 *(kN)*

The pinion PD is converted to metric units from the iterative solver section:

d_pinion_2 (metric) = stage 2 pinion PD • 25.4 *(mm)*

The gear pitch diameter (d_gear_2) is calculated from the pinion pitch diameter and the CD:

d_gear_2 = (2 • CD_2 – d_pinion_2) *(mm)*

The gearset face width is calculated by scaling and rounding the pinion PD:

face_2 = ROUND(1.05 • d_pinion_2, -0.5) *(mm)*

C.4.4 Variable Dimensions

The rear mainshaft bearing is sized from a best fit line based on bearing load and size data:

d_ms_r = 314.521 + 0.17359 • kW_m + (-0.00000043 / kW_m^2) *(mm)*

The front mainshaft bearing is sized to be proportional to the front mainshaft bearing by a factor of 1.3:

d_ms_f = d_ms_r • 1.3 *(mm)*

The attachment diameter to the nacelle can be calculated with the generator spacing and centerline distance known:

D_attachment = 2 • (CD + r_tancir • 1000 + 75) *(mm)*

The secondary gearbox wall thickness (t_wall) is an input.

The generator adapter size is based on the outside diameter of the generator:

$$d\_adapter = 0.7 \bullet D\_frame \quad (mm)$$

C.4.5 Weight Calculations

The main housing is weight calculated in four terms:

$$W_1 = ((0.5 \bullet D\_attachment)^2 - (0.44 \bullet D\_attachment)^2) \bullet 0.012 \bullet D\_attachment \bullet PI() \bullet k\_cd \quad (kg)$$

$$W_2 = (0.44 \bullet D\_attachment)^2 \bullet 0.008 \bullet D\_attachment \bullet PI() \bullet k\_cd \quad (kg)$$

$$W_3 = ((D\_attachment - 4.5 \bullet r\_tancir \bullet 1000) / 2)^2 \bullet 0.008 \bullet D\_attachment \bullet PI() \bullet k\_cd \quad (kg)$$

$$W_4 = ((r\_tancir \bullet 1000)^2 - (0.45 \bullet (1.6 \bullet r\_tancir \bullet 1000))^2) \bullet 0.01 \bullet D\_attachment \bullet PI() \bullet k\_cd \quad (kg)$$

The terms are summed:

$$Main\ housing\ weight = W_1 + W_2 - W_3 + W_4 \quad (kg)$$

The forward housing is weight calculated in three parts. The weight of the front face is calculated:

$$W_5 = ((CD + 165)^2 - 732^2) \bullet 38 \bullet PI() \bullet k\_cd \quad (kg)$$

Then the weight of the wrapper is calculated:

$$W_6 = (CD + 185) \bullet 2 \bullet (d\_pinion + 150) \bullet 32 \bullet PI() \bullet k\_cd \quad (kg)$$

And then the fixed portion which supports the mainshaft is included from a 3D model:

$$W_7 = 1750 \quad (kg)$$

The weights are summed:

$$forward\ housing\ weight = W_5 + W_6 + W_7 \quad (kg)$$

The mainshaft is weight calculated by scaling the rear bearing diameter to calculate various portions:

$$W_8 = (0.85 \bullet d\_ms\_r)^2 \bullet 0.06 \bullet d\_ms\_r \bullet PI() \bullet k + \quad (kg)$$

$$W_9 = (1.1 \bullet d\_ms\_r)^2 \bullet 0.14 \bullet d\_ms\_r \bullet PI() \bullet k + \quad (kg)$$

$$W_{10} = (0.7 \bullet d\_ms\_r)^2 \bullet 0.2 \bullet d\_ms\_r \bullet PI() \bullet k + \quad (kg)$$

$$W_{11} = (0.65 \bullet d\_ms\_r)^2 \bullet 0.25 \bullet d\_ms\_r \bullet PI() \bullet k + \quad (kg)$$

$$W_{12} = (0.57 \bullet d\_ms\_r)^2 \bullet 0.35 \bullet d\_ms\_r \bullet PI() \bullet k + \quad (kg)$$

$$W_{13} = (0.5 \bullet d\_ms\_r)^2 \bullet 0.5 \bullet d\_ms\_r \bullet PI() \bullet k - \quad (kg)$$

$$W_{14} = (0.35 \bullet d\_ms\_r)^2 \bullet 1.49 \bullet d\_ms\_r \bullet PI() \bullet k\_cd \quad (kg)$$

The weights are summed:

$$Mainshaft\ weight = W_8 + W_9 + W_{10} + W_{11} + W_{12} + W_{13} - W_{14} \quad (kg)$$

The secondary housing base is weight calculated:

$$W_{14} = PI() \bullet 2 \bullet r\_tancir \bullet 1000 \bullet t\_wall \bullet face\_2 \bullet k\_cd \quad (kg)$$

$$W_{15} = ((r\_tancir \bullet 1000)^2 - (d\_pinion\_2 / 2)^2) \bullet PI() \bullet t\_wall \bullet 1.2 \bullet k\_cd \quad (kg)$$

$$W_{16} = (d\_pinion\_2 \bullet 1.25) \bullet PI() \bullet t\_wall \bullet face\_2 \bullet k\_cd) \quad (kg)$$

The weights are summed and scaled by the number of generators:

$$Secondary\ housing\ base\ weight = (W_{14} + W_{15} + W_{16}) \bullet ng \quad (kg)$$

The secondary housing cover is weight calculated:

$$W_{17} = ((r\_tancir \bullet 1000)^2 - (d\_pinion\_2 / 2)^2) \bullet PI() \bullet t\_wall \bullet 1.2 \bullet k\_cd \quad (kg)$$

$$W_{18} = (d\_pinion\_2 \bullet 1.25) \bullet PI() \bullet t\_wall \bullet 2 \bullet k\_cd \quad (kg)$$

The weights are summed:

$$Secondary\ housing\ cover\ weight = (W_{17} + W_{18}) \bullet ng \quad (kg)$$

The generator adapter section is weight calculated:

$$W_{19} = ((D\_frame / 2)^2 - (d\_adapter / 2)^2) \bullet 1.5 \bullet t\_wall \bullet PI() \bullet k\_cd \quad (kg)$$

$$W_{20} = ((d\_adapter / 2)^2 - ((d\_adapter - 2.5 \bullet t\_wall) / 2)^2) \bullet D\_frame \bullet PI() \bullet k\_cd \quad (kg)$$

The weights are summed and scaled by the number of generators:

$$Generator\ adapter\ weight = (W_{19} + W_{20}) \bullet ng \quad (kg)$$

The mainshaft bearings are weight calculated from a curve fit of weight versus size data:

$$Mainshaft\ bearing\ weight = 3.258 \bullet d\_ms\_f^{0.6956} + 3.258 \bullet d\_ms\_r^{0.6956} \quad (kg)$$

The retainer mainshaft is a constant for all numbers of generators.

The hubs with seal are weight calculated:

$$Hub\ with\ seal\ weight = ((200 / 2)^2 \bullet 35 + (180 / 2)^2 \bullet 25) \bullet PI() \bullet k\_cd \bullet ng \quad (kg)$$

The nacelle support structure is weight calculated using a curve fit of weight versus size data:

$$Nacelle\ support\ structure\ weight = 0.00037 \bullet D\_attachment^2 - 0.82725 \bullet D\_attachment + 4585 \quad (kg)$$

The main gear weight is calculated as a solid disk with inset faces subtracted off:

$$W_{21} = ((d\_gear / 2)^2 - 81225) \bullet PI() \bullet face \bullet k\_cd \quad (kg)$$

$$W_{22} = (((d\_gear - 75) / 2)^2 - 105625) \bullet PI() \bullet (face/2) \bullet k\_cd \quad (kg)$$

The weights are subtracted:

$$Main\ gear\ weight = W_{21} - W_{22} \quad (kg)$$

The stage 1 pinions are weight calculated in three sections, according to the portion which rides in the bearings, the portion which is toothed, and the portion which supports the second stage gear (respectively):

$$W_{23} = (d\_pinion \bullet 0.35)^2 \bullet 1.1 \bullet face \bullet PI() \bullet k\_cd \quad (kg)$$

$$W_{24} = ((d\_pinion / 2)^2 \bullet face) \bullet PI() \bullet k\_cd \quad (kg)$$

W_{25} = ((d_pinion • 0.35)^2 • face_2) • PI() • k_cd (kg)

The weights are summed and scaled by number of generators:

Stage 1 pinions weight = (W_{23} + W_{24} + W_{25}) • ng (kg)

The stage 1 and 2 pinion bearing mass calculations use a curve fit of weight data that depends on the dynamic capacity of the bearing:

Bearing weight = 1.764326187E – 12 • C_dynamic^4 + -0.00000001981162673 • C_dynamic^3 + 0.00006906735072 • C_dynamic^2 + -0.01000661195 • C_dynamic + 1.60807798 (kg)

The stage 2 gears are weight calculated:

Stage 2 gears weight = ((d_gear_2 / 2)^2 – (d_pinion_2 • 0.4)^2) • face_2 • PI() • k_cd • 1.09 • ng (kg)

The stage 2 pinions are weight calculated:

Stage 2 pinions weight = (d_pinion_2 / 2)^2 • PI() • 3 • face_2 • k_cd • 1.09 • ng (kg)

The nacelle cover weight is based on the nacelle support structure weight:

Nacelle cover weight = (0.1 • Support nacelle structure) / 0.4536 (kg)

The weights of all parts are totaled and the weights of the pinion bearings are scaled by (one less than the number of generators):

Total = sum of all lines in weight table + (stage 1 + stage 2 pinion bearings weight) • (ng – 1) (kg)

C.4.6 Cost Calculations

Most cost calculations are based on the weight of the item and a curve fit of cost versus weight data.

Table C.4-1. Cost Data for Multi-Induction Generator Drive Train Design

Item	Cost Basis
Main housing USD	= (0.00000017 • weight^2-0.001172 • weight+3.837) • weight
Forward housing USD	= (0.00000017 • weight ^2-0.001172 • weight +3.837) • weight
Mainshaft USD	= (0.00000017 • weight ^2-0.001172 • weight +3.577) • weight
Secondary housing base USD	= (0.00000017 • weight ^2-0.001172 • weight +3.577) • weight
Secondary housing cover USD	= (0.00000017 • weight ^2-0.001172 • weight +3.577) • weight
Gen adaptor section USD	= (0.00000017 • weight ^2-0.001172 • weight +3.577) • weight
Mainshaft bearings USD	= weight • 29$/kg
Retainer, mainshaft USD	= (0.00000017 • weight ^2-0.001172 • weight +3.577) • weight
Hubs with seal USD	= (0.00000017 • weight ^2-0.001172 • weight +3.577) • weight
Support nacelle structure USD	= (0.00000017 • weight ^2-0.001172 • weight +3.837) • weight
Main gear USD	= weight • 5.456+882
Stage 1 pinions USD	= ((weight/ng) • 5.456+882) • ng
Stage 1 pinion bearings USD	= (0.004 • weight+12.612) • weight • ng
Stage 2 gears USD	= ((weight/ng) • 5.456+881) • ng
Stage 2 pinions USD	= ((weight/ng) • 5.456+881) • ng
Stage 2 pinion bearings USD	= (0.004 • weight+12.612) • weight • ng
Nacelle cover USD	= weight • 11.90 $/kg
Assemble and test USD	= nacelle assembly total time • 65 $/hr
Transport premium USD	= IF(D_attachment>4115,$3500,0)
Brake cost USD	= (100+0.64 • (Q_pinion_2 • 4000/(D_frame-150))^0.68+(D_frame-150) • 0.046) • INT((ng+1)/2)+750
Generators USD	= (29.231 • kW_gen_e-485.25) • ng

C.4.7 Assembly and Labor

The assembly of the main box depends primarily on the number of generators:

Main box assembly time = 30 + 1.5 • ng • 2 *(h)*

The time to assemble to the nacelle only depends on the attachment diameter, which is fairly constant across a single worksheet:

Assemble to nacelle time = 5 + d_attachment/1000 *(h)*

The cooling system and auxiliary equipment assembly depends on both attachment diameter and number of generators:

Assemble cooling system =4 • (D_attachment / 1000) + 1.5 • ng *(h)*

As does the test and paint time:

Test and paint time =25 + 0.75 • (D_attachment / 10000) • ng *(h)*

The generator assembly also depends on the number of generators:

Generator assembly time = 3 • ng *(h)*

The total nacelle assembly time is the sum of all assembly and labor rows above.

C.4.8 Iterative Solver Section

The gear set power capacity is computed for each of the number of generators. The capacity is computed by incrementing an index variable, x, which increases the pinion pitch diameter until the computed capacity per generator is equal to the required power capacity per generator. Based on given factors for geometry (J-fact), allowable stress (Sat), estimated face contact factor (Km), and minimum number of teeth (N_min), the power capacity is estimated:

Gear power capacity = rpm_pinion • stage 1 pinion PD^3 • $J_fact • Km /(126000 • N_min • 1.25) *(hp)*

Delta power checks to make sure that the power found by iteration matches the input power:

Delta power = HP_gen_m – gear power capacity *(hp)*

X is the incremented variable used in iteration. CD is calculated from the generator layout:

CD = (r_outside – r_tancir) • 1000 / 25.4 *(in)*

The pinion pitch diameter is calculated:

Stage 1 pinion PD = CD / x *(in)*

The mesh force is calculated:

Mesh force =2 • kW_gen_m • 63025 / rpm_pinion/pinion PD *(lbf)*

The pinion torque is calculated from the mechanical horsepower per generator and the pinion rpm:

Pinion torque = kW_gen_m • 63025 / rpm_pinion *(lb-in)*

The gear set power capacity calculation for stage 2 is similar to stage 1, except the synchronous rpm is used instead of the pinion rpm:

Gear power capacity = rpm_sync• stage 2 pinion PD^3 • $J_fact • Km / (126000 • N_mi_2 • 1.25 *(hp)*

Delta power again checks to make sure that the power found by iteration matches the input power:

Delta power = HP_gen_m – gear power capacity *(hp)*

X is the incremented variable used again in iteration. It is a centerline distance. *CD Stage 2* is set equal to *x*. The stage 2 pinion PD is calculated:

Pinion PD = 2 • (CD Stage 2 / (mg_2 + 1)) *(in)*

The mesh force is calculated:

Mesh force = HP_gen_m • 2 • 63025 / (rpm_sync • stage 2 pinion PD) *(lbf)*

The stage 2 pinion torque is calculated from the mechanical horsepower per generator and the input rpm:

Pinion torque = HP_gen_m • 63025 / rpm_sync *(lb-in)*

Single Side Multi-Gen with Induction Motors Dia over generators = 2.5 m

Mainshaft rpm =	20.5		Outer radius =	1.25 m	Matl const, ductile =	7.197E-06
Design kW, mechanical =	1574	kW	Increased torque factor =	1.3636364	J factor =	0.53
Design kW, electrical =	1,500	kW	Root stress stg 2 =	50000	Root stress stg 1 =	42000
Sync rpm =	1800		Min teeth stg 2 =	22	Min teeth stg 1 =	21

System Design											
Design intent, no generators =	3	4	5	6	7	8	9	10	11	12	13	14
Generators per system =	3	4	5	6	7	8	9	10	11	12	13	14
Mechanical HP, nominal =	703.6	527.7	422.2	351.8	301.5	263.9	234.5	211.1	191.9	175.9	162.4	150.8
kW per generator =	500.0	375.0	300.0	250.0	214.3	187.5	166.7	150.0	136.4	125.0	115.4	107.1
Mechanical HP per gen =	959.5	719.6	575.7	479.7	411.2	359.8	319.8	287.8	261.7	239.9	221.4	205.6
Radius of tangent circles, m =	0.580	0.518	0.463	0.417	0.378	0.346	0.319	0.295	0.275	0.257	0.241	0.228
Generator frame dia, mm =	820	740	700	700	700	622	622	622	622	622	622	622
Clearance between generators, mm =	340	296	225	133	56	70	15	-32	-72	-108	-139	-167
Stage 2 ratio required =	29.526	19.594	14.647	11.763	9.893	8.588	7.626	7.626	7.626	7.626	7.626	7.626

Gear Design, Stage 1												
Centerdistance, mm =	669.873	732.233	787.260	833.333	871.758	904.039	931.432	954.915	975.242	992.994	1008.621	1022.477
Gear ratio =	2.97	4.48	5.99	7.46	8.88	10.22	11.51	11.51	11.51	11.51	11.51	11.51
Pin rpm =	60.96	91.86	122.89	153.03	181.95	209.60	236.02	236.02	236.02	236.02	236.02	236.02
Pinion torque, Nm =	112,067	55,779	33,357	22,323	16,092	12,223	9,649	8,684	7,895	7,237	6,680	6,203
Wt, kN =	664.8	417.5	296.4	226.7	182.3	151.8	129.6	113.8	101.3	91.2	82.9	75.9
Stg 1 required pinion bearing load, kN =	2,166.0	1,538.4	1,191.6	973.7	824.5	716.2	633.9	556.5	495.3	445.9	405.3	371.2
Pinion PD, mm =	337.14	267.18	225.10	196.90	176.55	161.08	148.87	152.63	155.87	158.71	161.21	163.42
Gear pitch dia, mm =	1002.60	1197.28	1349.42	1469.77	1566.97	1647.00	1713.99	1757.20	1794.61	1827.28	1856.03	1881.53
Gear set facewidth, mm =	354.00	281.00	236.00	207.00	185.00	169.00	156.00	160.00	164.00	167.00	169.00	172.00

Gear Design, Stage 2												
Centerdistance, mm =	1595.433	977.944	689.756	529.432	429.229	361.353	312.610	312.610	312.610	312.610	312.610	312.610
Gear ratio =	29.5259	19.5944	14.6471	11.7627	9.8928	8.5876	7.6265	7.6265	7.6265	7.6265	7.6265	7.6265
Pin rpm =	1800	1800	1800	1800	1800	1800	1800	1800	1800	1800	1800	1800
Pinion torque, Nm =	3,796	2,847	2,277	1,898	1,627	1,423	1,265	1,139	1,035	949	876	813
Wt, kN =	72.62	59.95	51.66	45.75	41.28	37.76	34.91	31.42	28.57	26.18	24.17	22.44
Required pinion bearing load, kN =	653.26	539.25	464.72	411.53	371.34	339.71	314.05	282.65	256.95	235.54	217.42	201.89
Pinion PD, mm =	104.53	94.97	88.16	82.97	78.81	75.38	72.48	72.48	72.48	72.48	72.48	72.48
Gear pitch dia, mm =	3086.34	1860.92	1291.35	975.90	779.65	647.33	552.74	552.74	552.74	552.74	552.74	552.74
Gear set facewidth, mm =	110.00	100.00	93.00	87.00	83.00	79.00	76.00	76.00	76.00	76.00	76.00	76.00

Variable Dimensions												
Mainshaft bearing dia, rear, mm =	588	588	588	588	588	588	588	588	588	588	588	588
Mainshaft bearing dia, front, mm =	764	764	764	764	764	764	764	764	764	764	764	764
Attachment diameter to nacelle, mm =	2650	2650	2650	2650	2650	2650	2650	2650	2650	2650	2650	2650
Secondary gearbox wall thickness, mm =	18	18	18	17	17	17	16	16	16	16	16	16
Gen adaptor diameter, mm =	574	518	490	490	490	435	435	435	435	435	435	435

Single Side Multi-Gen with Induction Motors			Dia over generators = 2.5 m		
Mainshaft rpm =	20.5		Outer radius =	1.25 m	Matl const, ductile =	7.197E-06
Design kW, mechanical =	1574	kW	Increased torque factor =	1.3636364	J factor =	0.53
Design kW, electrical =	1,500	kW	Root stress stg 2 =	50000	Root stress stg 1 =	42000
Sync rpm =	1800		Min teeth stg 2 =	22	Min teeth stg 1 =	21

	System Design											
Design intent, no generators =	3	4	5	6	7	8	9	10	11	12	13	14
Weight Calculations												
Main housing, kg =	1,033	1,002	960	915	870	828	788	752	719	688	660	635
Forward housing, kg =	2,491	2,535	2,596	2,657	2,712	2,762	2,805	2,866	2,920	2,968	3,011	3,049
Mainshaft, kg =	2,170	2,170	2,170	2,170	2,170	2,170	2,170	2,170	2,170	2,170	2,170	2,170
Secondary housing base, kg =	662	707	714	664	648	627	571	559	548	537	526	517
Secondary housing cover, kg =	489	520	519	476	457	437	392	373	355	338	322	308
Gen adaptor section, kg =	847	917	1,023	1,162	1,356	1,218	1,292	1,436	1,580	1,723	1,867	2,010
Mainshaft bearings, kg =	605	605	605	605	605	605	605	605	605	605	605	605
Retainer, maishaft, kg =	115	115	115	115	115	115	115	115	115	115	115	115
Hubs with seal, kg =	37	50	62	75	87	100	112	125	137	150	162	175
Support nacelle structure, kg =	4,991	4,991	4,991	4,991	4,991	4,991	4,991	4,991	4,991	4,991	4,991	4,991
Main gear, kg =	923	1,096	1,194	1,257	1,285	1,302	1,306	1,410	1,510	1,595	1,667	1,745
Stage 1 pinions, kg =	1,154	777	585	475	401	351	313	373	438	503	568	638
Stg 1 pinion bearings, per bearing, kg =	141	87	58	41	30	23	18	14	11	9	8	6
Stg 2 pinion bearings, per bearing, kg =	19	13	10	8	6	5	5	4	3	3	2	2
Stage 2 gears, kg =	19,353	8,520	4,763	3,049	2,162	1,618	1,273	1,415	1,556	1,698	1,839	1,981
Stage 2 pinions, kg =	67	67	67	66	67	66	66	74	81	89	96	103
Nacelle cover, kg =	1,100	1,100	1,100	1,100	1,100	1,100	1,100	1,100	1,100	1,100	1,100	1,100
Total, kg =	36,521	25,574	21,804	20,067	19,282	18,517	18,108	18,545	18,985	19,414	19,831	20,262
Cost Calculations												
Main housing, USD =	$2,901	$2,838	$2,753	$2,659	$2,563	$2,470	$2,380	$2,295	$2,216	$2,141	$2,071	$2,006
Forward housing, USD =	$4,913	$4,965	$5,037	$5,110	$5,177	$5,239	$5,294	$5,373	$5,444	$5,509	$5,568	$5,622
Mainshaft, USD =	$4,544	$4,544	$4,544	$4,544	$4,544	$4,544	$4,544	$4,544	$4,544	$4,544	$4,544	$4,544
Secondary housing base, USD =	$1,905	$2,004	$2,019	$1,908	$1,872	$1,825	$1,693	$1,664	$1,636	$1,609	$1,583	$1,559
Secondary housing cover, USD =	$1,490	$1,566	$1,563	$1,456	$1,407	$1,353	$1,232	$1,180	$1,130	$1,082	$1,037	$994
Gen adaptor section, USD =	$2,293	$2,425	$2,615	$2,841	$3,119	$2,925	$3,032	$3,223	$3,396	$3,554	$3,699	$3,836
Mainshaft bearings, USD =	$17,542	$17,542	$17,542	$17,542	$17,542	$17,542	$17,542	$17,542	$17,542	$17,542	$17,542	$17,542
Retainer,mainshaft, USD =	$396	$396	$396	$396	$396	$396	$396	$396	$396	$396	$396	$396
Hubs with seal, USD =	$132	$176	$219	$262	$304	$346	$388	$429	$470	$510	$551	$591
Support nacelle structure, USD =	$11,092	$11,092	$11,092	$11,092	$11,092	$11,092	$11,092	$11,092	$11,092	$11,092	$11,092	$11,092
Main gear, USD =	$5,919	$6,862	$7,398	$7,738	$7,893	$7,988	$8,007	$8,576	$9,118	$9,586	$9,978	$10,402
Stage 1 pinions, USD =	$8,942	$7,768	$7,604	$7,883	$8,363	$8,969	$9,644	$10,857	$12,089	$13,327	$14,564	$15,830
Stage 1 pinion bearings, USD =	$5,593	$4,533	$3,711	$3,115	$2,676	$2,343	$2,084	$1,797	$1,573	$1,395	$1,253	$1,138
Stage 2 gears, USD =	$108,233	$50,011	$30,394	$21,920	$17,961	$15,873	$14,877	$16,530	$18,183	$19,836	$21,489	$23,141
Stage 2 pinions, USD =	$3,007	$3,888	$4,769	$5,648	$6,531	$7,410	$8,291	$9,213	$10,134	$11,055	$11,976	$12,898
Stage 2 pinion bearings, USD =	$737	$676	$631	$596	$569	$549	$532	$488	$454	$429	$410	$396
Nacelle cover, USD =	$13,094	$13,094	$13,094	$13,094	$13,094	$13,094	$13,094	$13,094	$13,094	$13,094	$13,094	$13,094
Assemble and test, USD =	$6,822	$7,504	$8,187	$8,869	$9,552	$10,234	$10,917	$11,599	$12,282	$12,964	$13,647	$14,329
Transport premium, USD =	$0	$0	$0	$0	$0	$0	$0	$0	$0	$0	$0	$0
Brake cost, USD =	$2,183	$2,055	$2,546	$2,380	$2,757	$2,763	$3,119	$2,998	$3,324	$3,218	$3,522	$3,427
Generators, USD =	$42,391	$41,906	$41,420	$40,935	$40,450	$39,965	$39,479	$38,994	$38,509	$38,024	$37,538	$37,053
Total cost, USD =	$244,128	$185,843	$167,533	$159,988	$157,862	$156,918	$157,637	$161,882	$166,623	$170,906	$175,553	$179,890

Single Side Multi-Gen with Induction Motors Dia over generators = 2.5 m

Mainshaft rpm =	20.5		Outer radius =	1.25 m	Matl const, ductile =	7.197E-06
Design kW, mechanical =	1574	kW	Increased torque factor =	1.3636364	J factor =	0.53
Design kW, electrical =	1,500	kW	Root stress stg 2 =	50000	Root stress stg 1 =	42000
Sync rpm =	1800		Min teeth stg 2 =	22	Min teeth stg 1 =	21

	System Design											
Design intent, no generators =	3	4	5	6	7	8	9	10	11	12	13	14
Assembly Labor Time												
Assemble main box, h =	48.0	54.0	60.0	66.0	72.0	78.0	84.0	90.0	96.0	102.0	108.0	114.0
Assemble to nacelle, h =	7.7	7.7	7.7	7.7	7.7	7.7	7.7	7.7	7.7	7.7	7.7	7.7
Assemble cooling, aux equip, h =	15.1	16.6	18.1	19.6	21.1	22.6	24.1	25.6	27.1	28.6	30.1	31.6
Test and paint, h =	25.2	25.2	25.2	25.2	25.2	25.2	25.2	25.2	25.2	25.2	25.2	25.2
Assemble generators, h =	9.0	12.0	15.0	18.0	21.0	24.0	27.0	30.0	33.0	36.0	39.0	42.0
Nacelle assembly, total, h =	104.9	115.4	125.9	136.4	146.9	157.4	167.9	178.4	188.9	199.4	209.9	220.4
Iterative Solver Section, To Find Size to Equal Power Required												
Gear power capacity, kW =	959.5	719.6	575.7	479.7	411.2	359.8	319.8	344.6	367.1	387.5	406.1	423.1
Delta power, kW =	0.0	0.0	0.0	0.0	0.0	0.0	0.0	-56.8	-105.4	-147.7	-184.7	-217.5
x, incr =	1.986912764	2.740556	3.4973377	4.2323366	4.9378349	5.6122846	6.2565896	6.2565896	6.25658959	6.25658959	6.25658959	6.2565896
CD, in. =	26.3730	28.8281	30.9945	32.8084	34.3212	35.5921	36.6705	37.5951	38.3954	39.0943	39.7095	40.2550
Pinion PD, in. =	13.2733	10.5191	8.8623	7.7518	6.9507	6.3418	5.8611	6.0089	6.1368	6.2485	6.3468	6.4340
Mesh force, lbf =	149,461	93,869	66,629	50,977	40,985	34,119	29,143	25,583	22,773	20,502	18,632	17,066
Pinion torque, in.-lbf =	991,923	493,707	295,243	197,584	142,435	108,188	85,404	76,863	69,876	64,053	59,126	54,902
Gear power capacity, kW =	959.5	719.6	575.7	479.7	411.2	359.8	319.8	319.8	319.8	319.8	319.8	319.8
Delta power =	0.0	0.0	0.0	0.0	0.0	0.0	0.0	-32.0	-58.2	-80.0	-98.4	-114.2
x, incr =	62.81233524	38.501723	27.155758	20.843778	16.898785	14.226511	12.307476	12.307476	12.3074763	12.3074763	12.3074763	12.307476
CD stage 2, in. =	62.8123	38.5017	27.1558	20.8438	16.8988	14.2265	12.3075	12.3075	12.3075	12.3075	12.3075	12.3075
Pinion PD, in. =	4.1153	3.7390	3.4710	3.2664	3.1028	2.9677	2.8534	2.8534	2.8534	2.8534	2.8534	2.8534
Mesh force, lbf =	16,327	13,477	11,614	10,285	9,281	8,490	7,849	7,064	6,422	5,887	5,434	5,046
Pinion torque, in.-lbf =	33,595	25,196	20,157	16,798	14,398	12,598	11,198	10,079	9,162	8,399	7,753	7,199
Costs for Graphs												
Generators, USD =	$42,391	$41,906	$41,420	$40,935	$40,450	$39,965	$39,479	$38,994	$38,509	$38,024	$37,538	$37,053
Gearbox, USD =	$164,002	$105,649	$86,650	$79,073	$76,374	$75,227	$75,392	$79,561	$83,779	$87,970	$92,116	$96,350
Mainshaft, USD =	$4,544	$4,544	$4,544	$4,544	$4,544	$4,544	$4,544	$4,544	$4,544	$4,544	$4,544	$4,544
Nacelle cover, USD =	$13,094	$13,094	$13,094	$13,094	$13,094	$13,094	$13,094	$13,094	$13,094	$13,094	$13,094	$13,094
Assembly, USD =	$6,822	$7,504	$8,187	$8,869	$9,552	$10,234	$10,917	$11,599	$12,282	$12,964	$13,647	$14,329
Brake, USD =	$2,183	$2,055	$2,546	$2,380	$2,757	$2,763	$3,119	$2,998	$3,324	$3,218	$3,522	$3,427
Couplings, USD =	$1,268	$1,367	$1,467	$1,566	$1,666	$1,765	$1,864	$1,964	$2,063	$2,163	$2,262	$2,362
Nacelle structure, USD =	$11,092	$11,092	$11,092	$11,092	$11,092	$11,092	$11,092	$11,092	$11,092	$11,092	$11,092	$11,092
Cooling, USD =	$2,247	$2,247	$2,247	$2,247	$2,247	$2,247	$2,247	$2,247	$2,247	$2,247	$2,247	$2,247
Transport prem, USD =	$0	$0	$0	$0	$0	$0	$0	$0	$0	$0	$0	$0
Total, USD =	$247,643	$189,458	$171,247	$163,801	$161,775	$160,930	$161,749	$166,093	$170,934	$175,316	$180,062	$184,499

Appendix D

Gearbox Bill of Materials and Mechanical Cost Estimates

Baseline Drivetrain Gearbox BOM

Global Energy Concepts, LLC Baseline Project

Inquiry 46252

Assem. No.	*Part Number*	*Inquiry Item*	*Descriptions*	*Quantity per Box*	*Price per pc*	*Total Price*
1	SK01066-1	1.01	Ring Gear, internal	1	$9,031.25	$9,031.25
2	SK01066-10	1.02	Intermediate_gear	1	$2,102.06	$2,102.06
3	SK01066-11	1.03	Output_pinion	1	$653.52	$653.52
4	SK01066-9	1.04	Intermediate_pinion	1	$1,455.28	$1,455.28
5	SK01066-6	1.05	Jack_shaft	1	$1,056.88	$1,056.88
6	SK01066-8	1.06	Bull_gear	1	$4,540.36	$4,540.36
7	SK01066-5	1.07	Bull shaft	1	$4,140.93	$4,140.93
8	SK01066-4	1.08	Planet	3	$1,553.10	$4,659.30
9	SK01066-3	1.09	Planet_shaft	3	$587.24	$1,761.72
10	SK040501-1	1.10	Bearing cap, planet	3	$105.82	$317.46
11	SK040501-2	1.11	Spacer, planet	3	$238.17	$714.51
12	SK01066-7	1.12	Sun_gear	1	$1,405.80	$1,405.80
13	SK040501-3	1.13	Clamp, bull shaft bearing	1	$125.43	$125.43
14	SK040501-4	1.14	Cover, bull shaft	1	$382.99	$382.99
15	SK040501-5	1.15	Cover, seal	1	$96.35	$96.35
16	SK040501-6	1.16	Adapter, bearing	1	$376.92	$376.92
17	SK040501-7	1.17	Retainer, intermediate bearing	1	$86.62	$86.62
18	SK040501-8	1.18	Cover, intermediate bearing	1	$254.99	$254.99
19	SK040501-9	1.19	Spacer	1	$174.87	$174.87
20	SK040501-10	1.20	Cover, output seal	1	$298.97	$298.97
21	SK040501-11	1.21	Adapter, bearing	1	$335.24	$335.24
22	SK01066-14	1.22	Housing, cover	1	$2,591.00	$2,591.00
23	SK040501-13	1.23	Input bearing housing retainer	1	$734.23	$734.23
24	SK040501-14	1.24	Locking hub, taper	1	$2,090.43	$2,090.43
25	SK01066-2	1.25	Carrier	1	$6,995.40	$6,995.40
26	SK040501-15	1.26	Hub	1	$2,918.18	$2,918.18
27	SK01066-15	1.27	Housing, forward	1	$4,401.75	$4,401.75
28	SK01066-13	1.28	Housing, main	1	$8,073.00	$8,073.00
29	SK040501-18	1.29	Bearing, spacer	1	$39.86	$39.86
30	SK040501-19	1.30	Adapter, tube	1	$96.00	$96.00
31	SK040501-20	1.31	Mounting trunions	2	$675.00	$1,350.00
32	nu2338		Bearing, straight roller	1	$2,272.00	$2,272.00
33	nj330		Bearing, straight roller	1	$506.00	$506.00
34	23228		Bearing, spherical roller	1	$198.00	$198.00
35	93127cd, 39787		Bearing, taper roller	1	$593.76	$593.76
36	23156		Bearing, spherical roller	1	$1,094.00	$1,094.00
37	nu1076		Bearing, straight roller	1	$1,940.00	$1,940.00
38			Bearing, taper roller	1	$1,850.00	$1,850.00
39	24148		Bearing, spherical roller	3	$927.00	$2,781.00
40			Bearing, taper roller	1	$1,850.00	$1,850.00
41	SK040501-20	1.31	Retaining ring	1	$87.74	$87.74
42	nu315		Bearing, spherical roller	1	$41.00	$41.00
43		1.32	Various purchased Items	1	$550.00	$550.00
44			Various hardware	1	$900.00	$900.00
45			Lube system	1	$2,000.00	$2,000.00
47			Assembly and test	1	$6,000.00	$6,000.00
48			Shrink disc	1	$4,400.00	$4,400.00
49			Cooling radiator & fan	1	$3,720.54	$3,720.54
50			Paint, prepare for ship	1	$1,350.00	$1,350.00
	3.43				Total	$95,395.34
			Mark-up	25.79%	Sell price	$120,000.00

Baseline - Other Mechanical Components

Part Name	Qty per Box	Weight/Unit, lbm	Rate/Unit	Total Price
LS shaft	1	14,373	$1.40	$20,122
LS bearing	1	1190	$5.50	$6,545
LS bearing block	1	2291	$2.25	$5,155
Bedplate	1	22000	$1.55	$34,100
Elastomeric pins	2	165	$3.50	$1,155
Blocks for pins	2	450	$1.75	$1,575
Gen mounting isolators	4	1	$125.00	$500

Nacelle Cover

Based on estimate of length, height, width, meters

	Size	Cu m	Weight, kg	
Length =	4	0.7857	1328	
Width =	2.7			
Height =	2.7	$ cost	Freight $	Total $
Wall =	0.015	$15,204	$598	$17,322
Wall (inches) =	0.5			

Cost cu meter =	19350.5	USD
Density, cu meter =	1690	kg
Cost/ kg =	11.45	
Freight rate =	0.45	$/kg
Additional for hardware =	$1,520	

Gearbox Assembly

Baseline

Stages	1	2
Gears/stage	5	2
Stage assembly, ea	3	3
Stage assem, total	15	12
Variable, total	27	
Base time	15	
Test	6	
Tolal hours	48	
Crew Rate	125	
Total	$6,000	

Brake Worksheet

	Nominal Torque Rating					Svendborg Brake Model			
	521,000	521,000	521,000	521,000	Nm				
Disk dia, mm	Brake System Torque Capacity (Nm)				Disc mass	200	3000	300	500
400	108,800	544,000	1,196,800	2,176,000	17.9	$453	$1,203	$2,031	$3,831
600	172,800	864,000	1,900,800	3,456,000	40.3	$554	$1,304	$2,132	$3,932
800	236,800	1,184,000	2,604,800	4,736,000	71.7	$695	$1,445	$2,273	$4,073
1200	364,800	1,824,000	4,012,800	7,296,000	161.4	$1,098	$1,848	$2,676	$4,476
4000	1,260,800	6,304,000	13,868,800	25,216,000	1792.9	$8,440	$9,190	$10,018	$11,818
Fb brake =	8000	40000	88000	160000	Rated Q	8000	40000	88000	160000
No calipers =	1	1	1	1	mass	18.5	81	150	300
No discs =	1	1	1	1					
Selected disc size =	4000	800	600	400					
Gearbox ratio =	80	80	80	80					
System cost =	$ 8,439.86	$ 1,444.71	$ 2,131.53	$ 3,830.68					

Cost $/kg	$ 12.00	Brake caliper
Cost $/kg	$ 4.50	Brake disc

Cooling, Generator Fluid

HP	Mass kg	GPM	Calculated	Cost @ 20.00
18	117.6	28	50.1	$1,002.43
33	181.6	70	92.9	$1,858.42
45	288.0	70	121.1	$2,422.42
60	324.0	70	148.8	$2,976.43
80	380.0	70	172.7	$3,454.16

Integrated Baseline

Gearbox BOM and Assembly to Structural Nacelle

Assem. No.	*Part Number*	*Wt./ea., lb*	*Wt./ea., kg*	*Descriptions*	*Quantity per Box*	*Price per pc*	*Total Price*
2	New	9,515	4,316	Housing assembly	1	$8,396.29	$8,396.29
3	New	3,738	1,696	Adapter	1	$3,965.13	$3,965.13
4	SK01138-9	1,134	514	R.H. ring gear	1	$5,300.30	$5,300.30
5	SK01138-8	1,365	619	L.H. ring gear	1	$5,526.89	$5,526.89
6	SK01138-1	3,365	1,526	Forward housing	1	$3,730.69	$3,730.69
7	SK01138-7	4,159	1,887	Main shaft	1	$4,208.87	$4,208.87
8	SK01138-3	245	111	Forward bearing retainer	1	$383.28	$383.28
9	SK01138-4	1,527	693	Carrier	1	$2,151.90	$2,151.90
10	SK01138-11	707	321	Planetary gear	3	$2,748.93	$8,246.79
11	SK01138-5	616	279	Retainer, rear bearing	1	$911.68	$911.68
12	SK01138-12		0	Sun pinion	1	$1,069.03	$1,069.03
13	New	241	109	Conduit assembly	1		
14	SK051701-11	28	13	Planet bearing cap	3	$45.24	$135.73
15	SK01066-8	2,136	969	Bull gear	1	$4,375.52	$4,375.52
16	New	998	453	Bull shaft	1	$4,140.93	$4,140.93
17	SK01066-11	250	113	Output pinion	1	$653.52	$653.52
18	New	82	37	High speed adapter	1		
19	New	24	11	High speed labyrinth	1	$38.80	$38.80
20	SK01066-6	197	89	Jack shaft	1	$1,056.88	$1,056.88
21	SK01066-10	764	347	Intermediate gear	1	$2,102.06	$2,102.06
22	SK01066-9	476	216	Intermediate pinion	1	$1,455.28	$1,455.28
23	SK040501-3	26	12	Retainer, bull shaft bearing	1	$42.02	$42.02
24	SK040501-4	189	86	Cover, bull Shaft	1	$298.15	$298.15
25	SK040501-7	21	10	Retainer, intermediate bearing	1	$33.97	$33.97
26	New	101	46	Retainer, high speed bearing	1		
27	SK040501-8	105	48	Cover, intermediate bearing	1	$167.73	$167.73
28	New	23	10	Retainer, jack shaft	1		
29	nu1076			Bearing, straight roller	1	$1,940.00	$1,940.00
30	nu2336			Bearing, straight roller	1	$2,272.00	$2,272.00
31	nj330			Bearing, straight roller	1	$506.00	$506.00
32	23156cc			Bearing, spherical roller	1	$1,094.00	$1,094.00
33	23228			Bearing, spherical roller	1	$198.00	$198.00
35	nu315			Bearing, spherical roller	1	$41.00	$41.00
36	New			Rear, taper bearing	1	$8,354.00	$8,354.00
37	New			Forward mainshaft bearing	1	$7,362.00	$7,362.00
39	SK051701-10			Spherical bearing, planetary	3	$1,043.61	$3,130.83
44		1.32		Various purchased Items	1	$550.00	$550.00
45				Various hardware	1	$900.00	$900.00
46				Lube system	1	$3,720.54	$3,720.54
47				Assembly labor, gearbox	1	$6,000.00	$6,000.00
				Paint, prepare for ship	1	$1,350.00	$1,350.00
						Total	$95,809.80
				Gross mark-up	25%	Sell price	$119,762.25

Integrated Baseline - Other Mechanical Components

Nacelle Cover Cost Data				
Based on estimate of length, height, width, meters				
	Size	Cu m	Weight, kg	
Length =	2	0.4028	681	
Width =	2.6			
Height =	2.6	$ cost	Freight $	Total $
Wall =	0.0127	$7,795	306	$8,881
Wall (inches) =	0.5			
Cost cu meter =	19350.5	USD		
Density, cu meter =	1690	kg		
Cost/ kg =	$11.45			
Freight rate =	0.45	$/kg		
Additional for hardware =	$780			

Cooling, Generator Fluid					
HP	Mass lb	Mass kg	GPM	Calculated	Cost @ 20.00
18	117.6	53.3	28	50.1	$1,002.43
33	181.6	82.4	70	92.9	$1,858.42
45	288	130.6	70	121.1	$2,422.42
60.3	324	147.0	70	149.3	$2,986.48
80	380	172.4	70	172.7	$3,454.16

	System Assembly		
	Hours	Rate	$
Assemble system	25	$125	$3,125
Paint	12	$65	$780
Test	8	$125	$1,000
Totals	45		$4,905

Brake Worksheet

	Nominal Torque Rating					Svendborg Brake model			
	384,275	384,275	384,275	384,275	lb-ft				
	4,611,300	4,611,300	4,611,300	4,611,300	lb-in				
	521,000	521,000	521,000	521,000	Nm				
Disk dia, mm	Brake System Torque Capacity				Disc mass	200	3000	300	500
400	435,200	544,000	1,196,800	2,176,000	17.9	$453	$1,203	$2,031	$3,831
600	691,200	864,000	1,900,800	3,456,000	40.3	$554	$1,304	$2,132	$3,932
800	947,200	1,184,000	2,604,800	4,736,000	71.7	$695	$1,445	$2,273	$4,073
1200	1,459,200	1,824,000	4,012,800	7,296,000	161.4	$1,098	$1,848	$2,676	$4,476
4000	5,043,200	6,304,000	13,868,800	25,216,000	1792.9	$8,440	$9,190	$10,018	$11,818
Fb brake =	8000	40000	88000	160000	Rated Q	8000	40000	88000	160000
No calipers =	4	1	1	1	mass	18.5	81	150	300
No discs =	1	1	1	1					
Selected disc size =	600	600	800	600		Cost $/kg	$12.00	Brake caliper	
Gearbox ratio =	80	80	80	80		Cost $/kg	$4.50	Brake disc	
System cost	$1,220	$1,304	$2,273	$3,932					

	Gearbox Assembly	
	Baseline (125/hr)	
Stages	1	2
Gears/stage	5	2
Stage assembly, ea	3	3
Stage assem, total	15	12
Variable, total	27	
Base time	15	
Test	6	
Tolal hours	48	
Crew rate	125	
Total	$6,000	

Couplings, Ka = 1.5, rpm = 1,800					
kW rating	Torque, lb-in	Weight, lbm	$/lb	Projected $	Calc cost
250	17,601	149	$3.50	$522.84	$522.03
375	26,401	195	$3.50	$683.01	$683.58
500	35,202	241	$3.50	$843.18	$845.13
600	42,242	278	$3.50	$971.31	$974.37
750	52,802	292	$3.50	$1,022.00	$1,168.23
1,000	70,403	440	$3.50	$1,540.00	$1,491.33
1,500	105,605	594	$3.50	$2,079.00	$2,137.53
2,000	140,807	890	$3.50	$3,115.00	$2,783.73
3,000	211,210	1,116	$3.50	$3,906.00	$4,076.13

Single PM Gearbox, Mainshaft, and Bearing BOMs

Inquiry 46325 Global Energy Concepts, LLC

Assem. No.	Part Number	Inquiry Item	Descriptions	Quantity per Box	Price per pc	Total Price	Mass ea-kg	Mass total
4	SK01138-4	1.04	Carrier	1	$2,259.65	$2,259.65	692.8	692.8
5	SK01138-8	1.05	L.H. ring gear	1	$4,479.44	$4,479.44	1,307.0	1,307.0
6	SK01138-9	1.06	R.H. ring gear	1	$4,300.30	$4,300.30	1,124.0	1,124.0
7	SK01138-2	1.07	Rear housing	1	$4,993.27	$4,993.27	2,591.0	2,591.0
10	SK051701-10	1.10	Spherical bearing, planetary	3	$1,043.61	$3,130.84		0.0
11	SK051701-11	1.11	Cap	3	$89.69	$269.07	18.0	54.0
12	SK01138-11R	1.12	R.H. planetary gear	3	$1,150.09	$3,450.27		0.0
13	SK01138-11l	1.13	L.H. planetary gear	3	$1,150.09	$3,450.27		0.0
14	SK051701-14	1.14	Generator retainer	1	$572.61	$572.61	45.0	45.0
16	SK01138-13	1.16	Generator shaft coupling	1	$400.00	$400.00	40.0	40.0
17	SK051701-17	1.17	Generator outer tapered bearing	1	$818.14	$818.14	6.5	6.5
18	SK051701-18	1.18	Generator bearing retainer	1	$156.73	$156.73	69.8	69.8
19	SK051701-19	1.19	Adaptor tube	1	$96.00	$96.00	12.0	12.0
20	SK051701-20	1.20	Tube, roller bearing	1	$40.00	$40.00	3.0	3.0
21	SK01138-12L	1.21	L.H. sun gear	1	$336.63	$336.63		0.0
22	SK01138-12R	1.22	R.H. sun gear	1	$630.59	$630.59		0.0
23	SK01138-6	1.23	Labyrinth	1	$405.41	$405.41	69.8	69.8
24	SK051701-24	1.24	Generator coupling	1	$444.49	$444.49	12.0	12.0
25	SK051701-25	1.25	Generator inner tapered bearing	1	$818.14	$818.14	6.5	6.5
		1.27	Various purchased Items	N/A				
21a	SK01138-12	1.97	Sun gear assembly	1	$101.81	$101.81	115.3	115.3
3	SK01138-1	1.03	Forward housing	1	$4,051.03	$4,051.03	1,661.0	1,661.0
12a	SK01138-11	1.98	Planetary gear assembly	3	$448.75	$1,346.25		
					Total	$36,550.94	Variable items	7,809.6
			Mark-up	0.25	Sell price	$45,688.67		
						$5.95		
1	SK01138-7	1.01	Main shaft	1	$4,265.66	$4,265.66	2,053.3	2,053.3
2	SK01138-3	1.02	Forward bearing retainer	1	$663.30	$663.30	121.2	121.2
27			Forward mainshaft bearing	1	$9,523.77	$9,523.77	825.0	825.0
28			Rear mainshaft bearing	1	$8,162.35	$8,162.35	755.0	755.0
45			Assembly labor, test	42	$125.00	$5,250.00		
44			Lube system	1	$3,720.54	$3,720.54		
49			Paint, prepare for ship	1	$1,350.00	$1,350.00		
					Total	$32,935.62	Fixed items	3,754.5
			Mark-up	$0.25	Sell price	$41,169.53	Total	11,564
					Rate/kg	$10.97		Mass, kg

Appendix E

Kaman Electromagnetics PM Generator Design

Unit Pole Model

Nov 27, 2001

Rev 5B

Kaman Aerospace

Peter Mongeau **Jan Janda**

Salient Pole Geometry

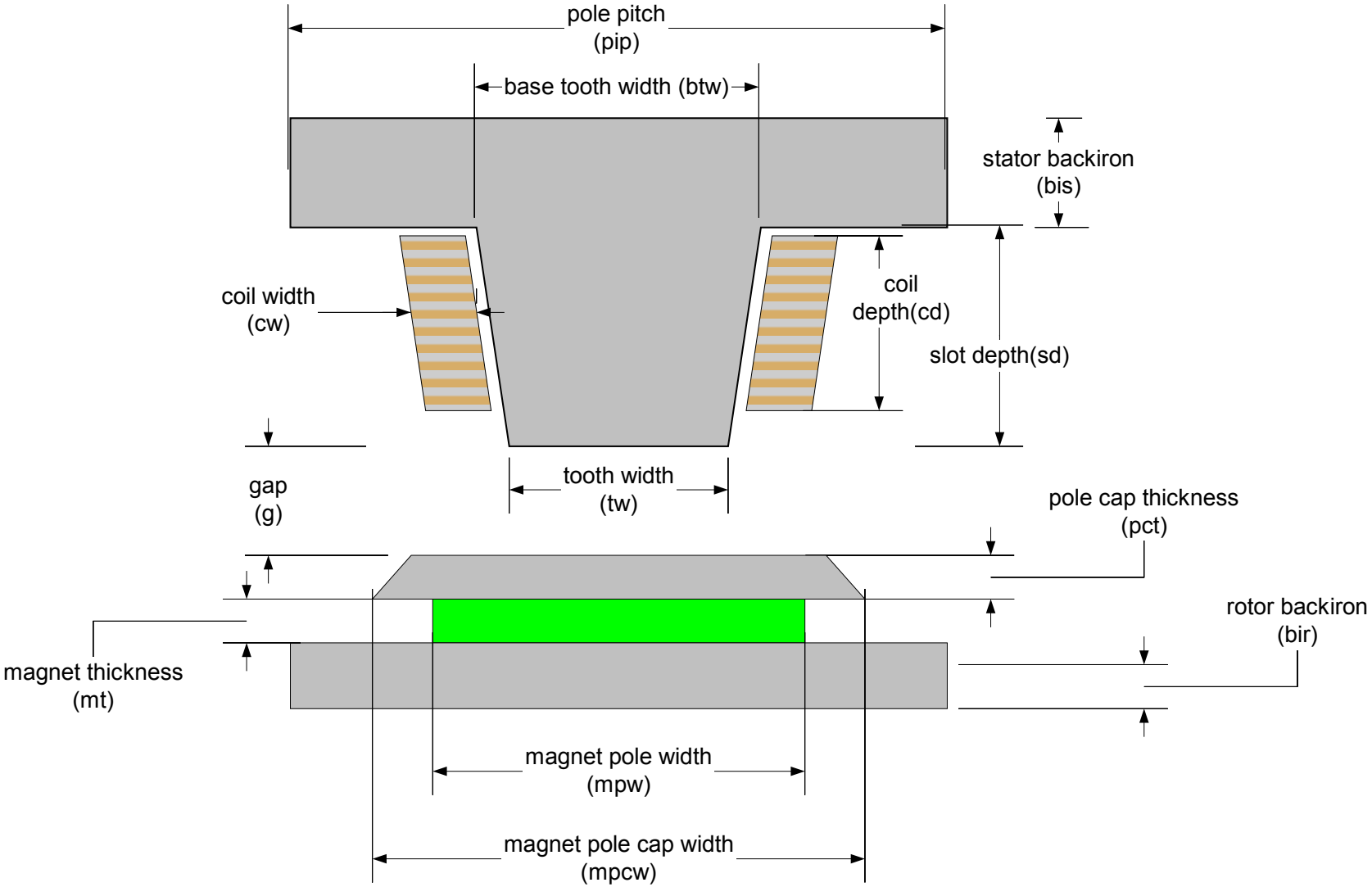

Formed Coil Construction

- Coils made from edge wound rectangular cross-section copper
- Turn-to-turn insulation installed after forming
- Mechanically clamped onto core
- Coil jumpers brazed and wrap insulated in place
- Low cost standard construction

Core Losses

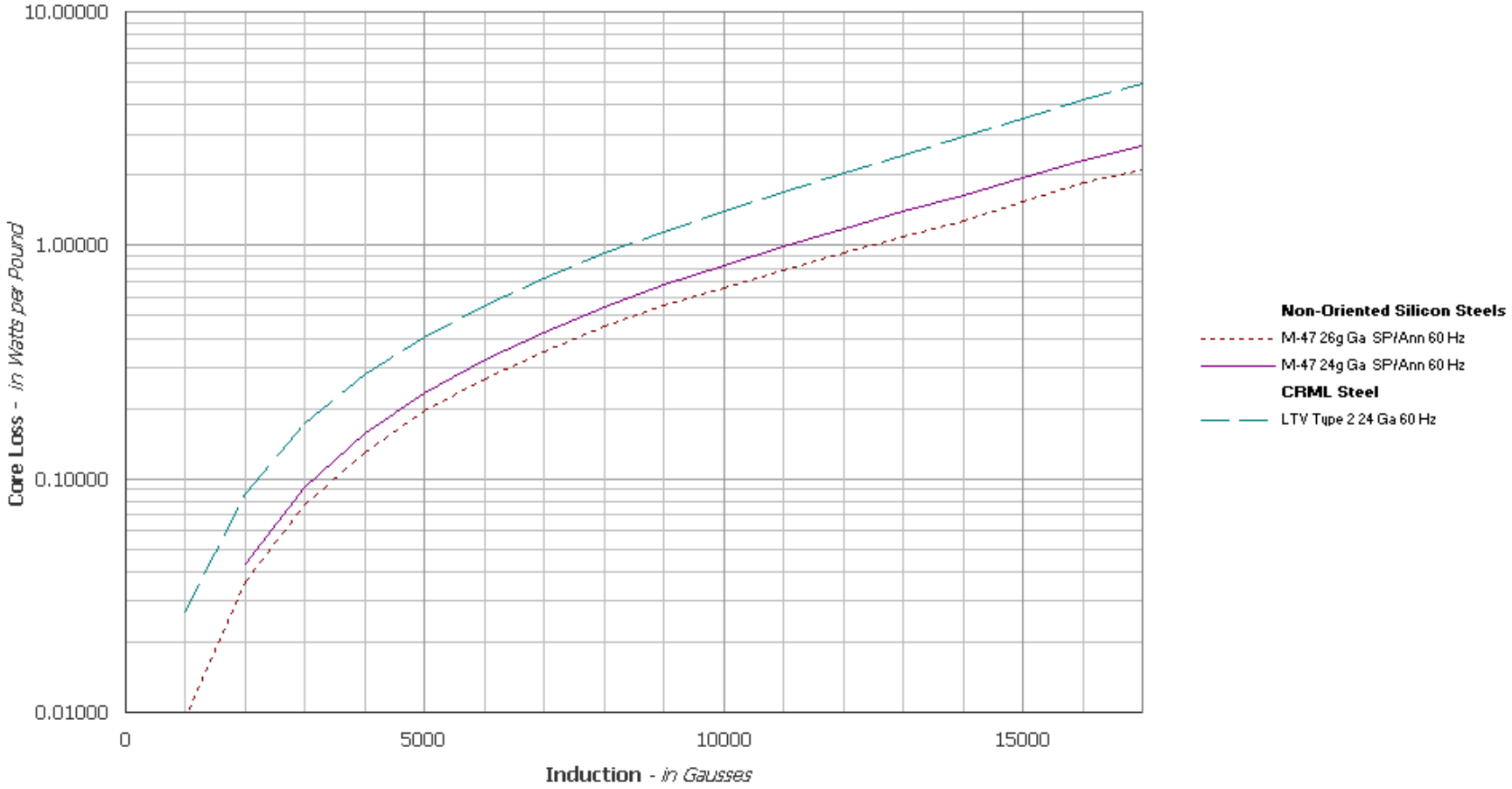

- 24 Ga (23.5 mils) low carbon steel (M-64) baseline
- Reference core loss is 3.5 Watts/lb @ 1.5 T, 60 Hz
- M47 is acceptable cost and better loss: 2 Watts/lb @ 1.5 T, 60 Hz

Magnet Selection

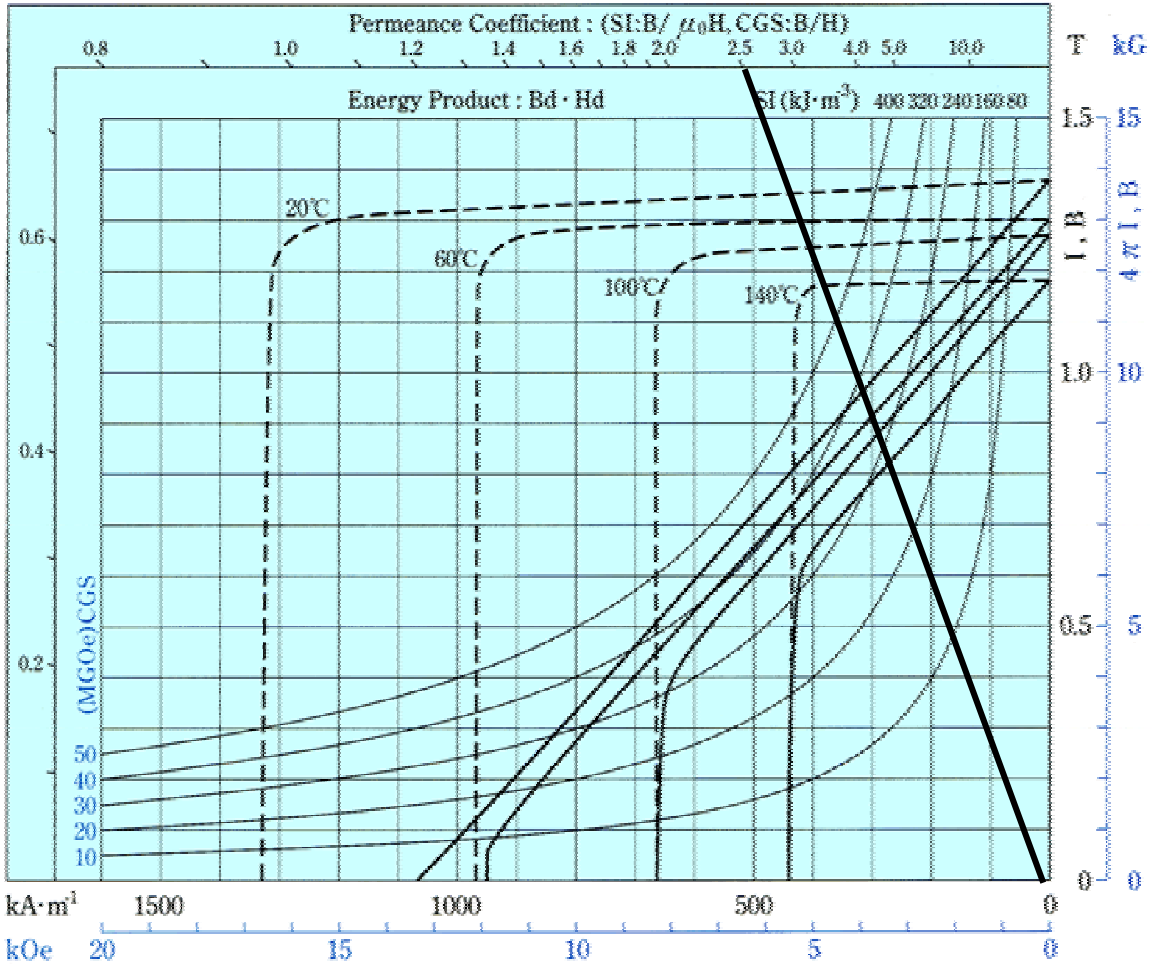

- High grade Neodymium magnet
  - 1.3 T @ 60 C
  - Maximum reversible operating temperature of 100°C
  - Maximum no load temperature of 140°C

2D FEA Model

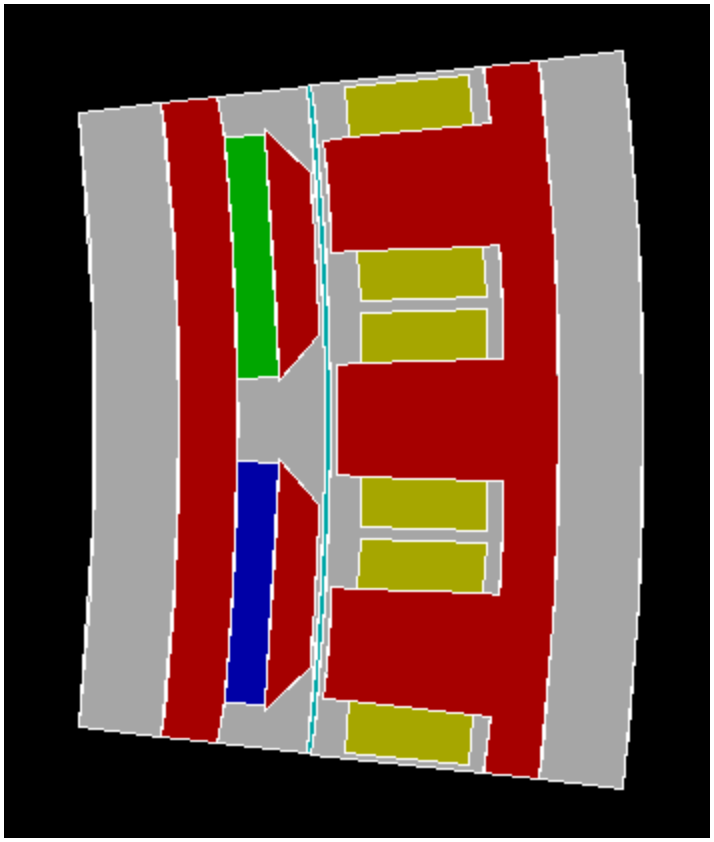

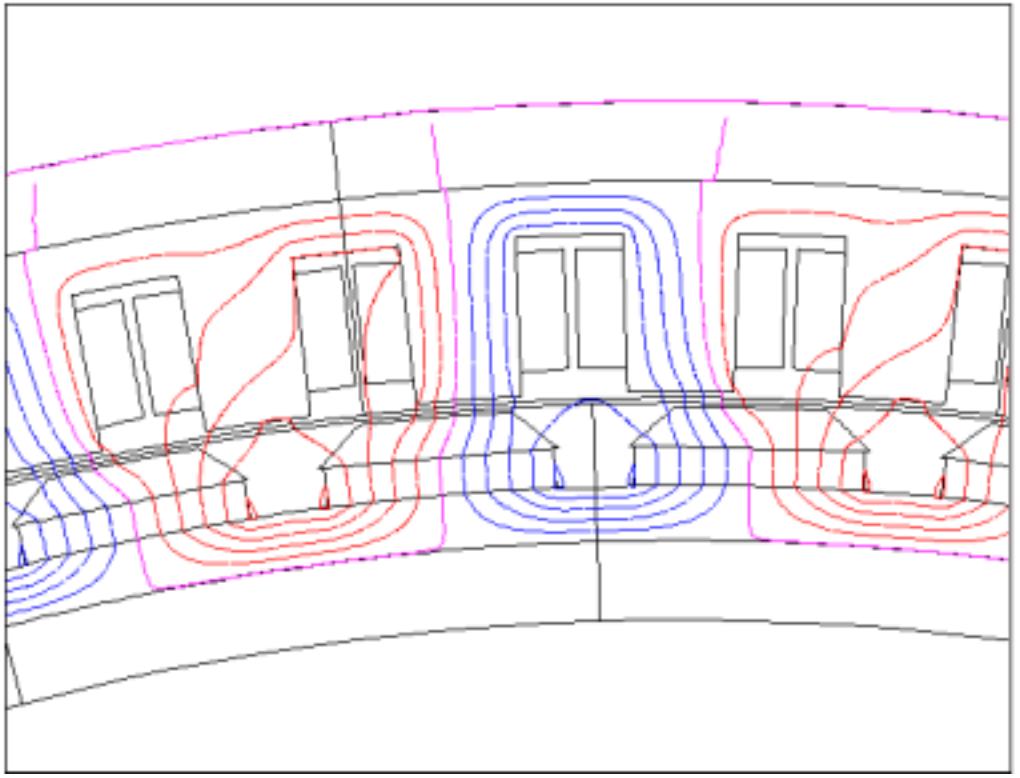

- 2D model with non-linear steel and conductive magnets

FEA Model: Circuits

Rectifier Bridge

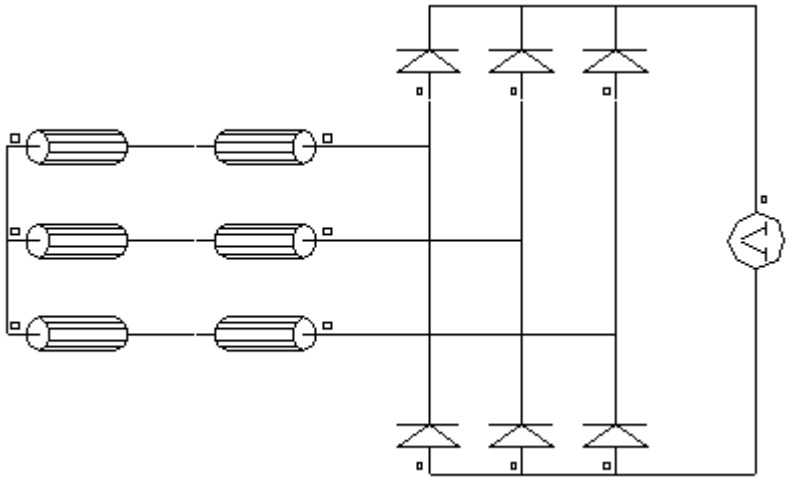

Back EMF

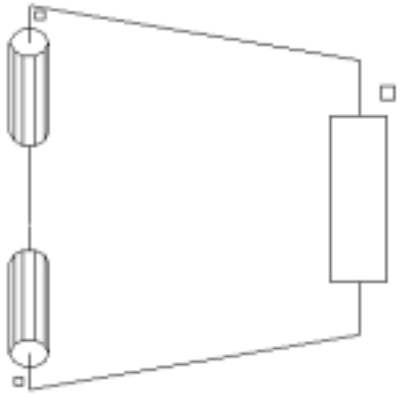

Inductance

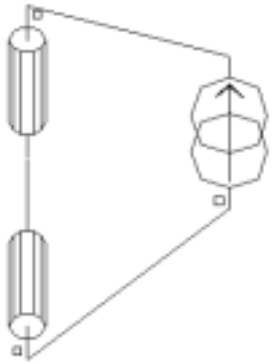

Inverter Coupled FEA Model Results: No load

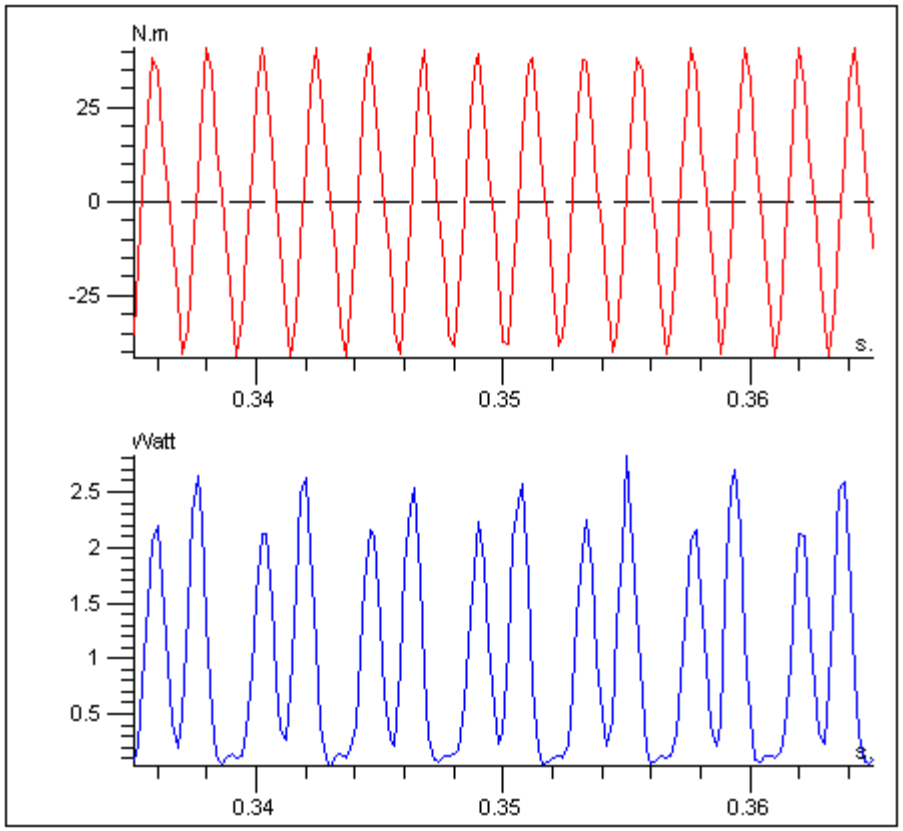

Pole Pair Cogging Torque:
± 41 Nm

Total cogging torque:
1148 Nm, ± 1.3% PU

Magnet pole heating @ 164 rpm:
1.0 watt per pole
56 watts per rotor

Note: Non-excited results (i.e. no stator currents)

Inverter Coupled FEA Model Results: No load @164 rpm

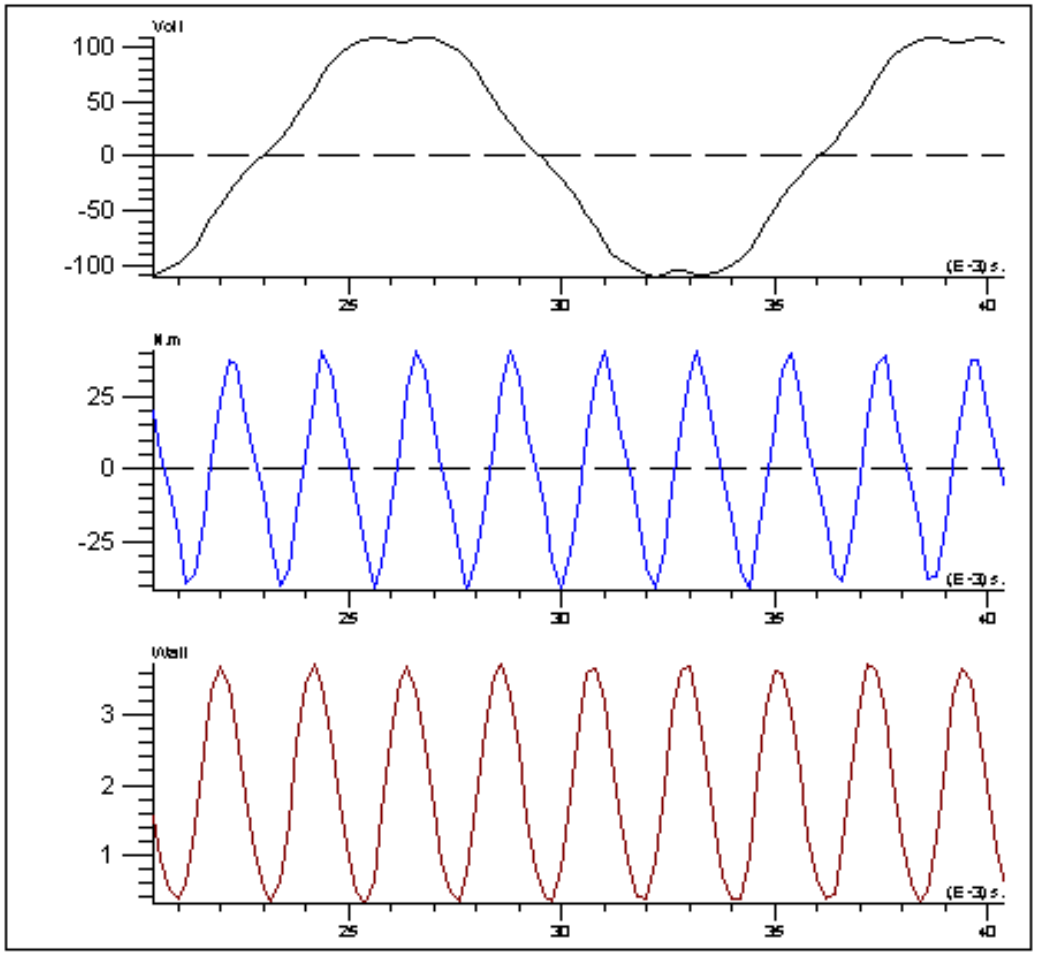

Stator pole VBEMF:
~ 110 Volt pk
@ 24 turns per pole

Cogging Torque:
~ ± 41 Nm per pole pair
1.15 kNm total (1.3%PU)

Magnet Losses:
2 watt per pole pair
56 watts per rotor

Note: Non-excited results (i.e. no stator currents)

Inverter Coupled FEA Model Results: Inductance

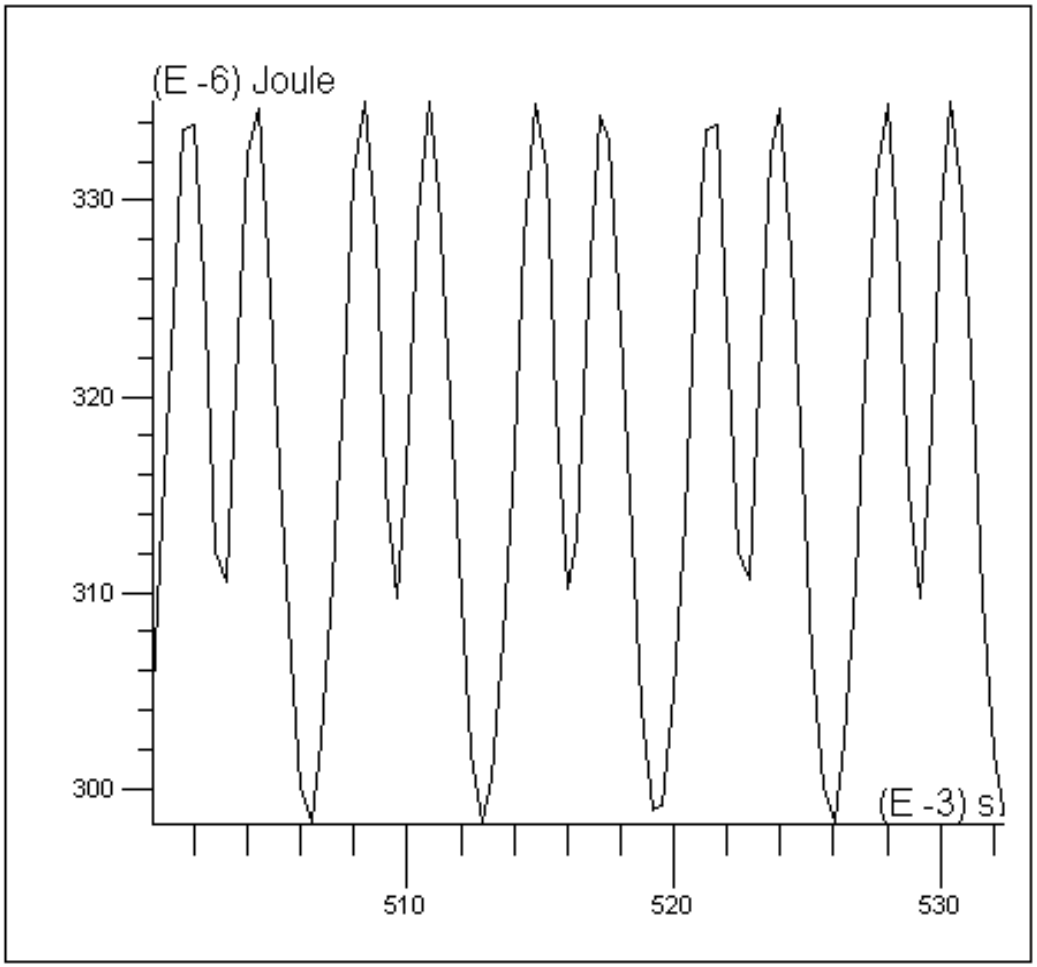

FEA Inductance:

630 µH per pole @ 24 turns

Turn Adjusted:

turn adjusted for 600 volts BEMF (130 turns)

18.5 mH per pole

662 µH per phase

Inverter Coupled Saturation Effects

@ 0.025 PU current

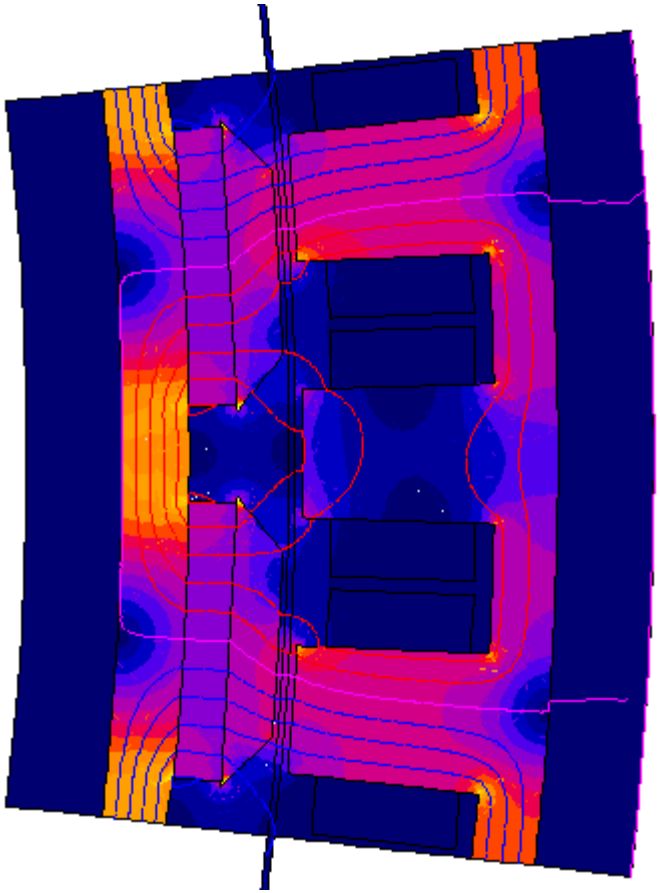

@ 2.25 PU current

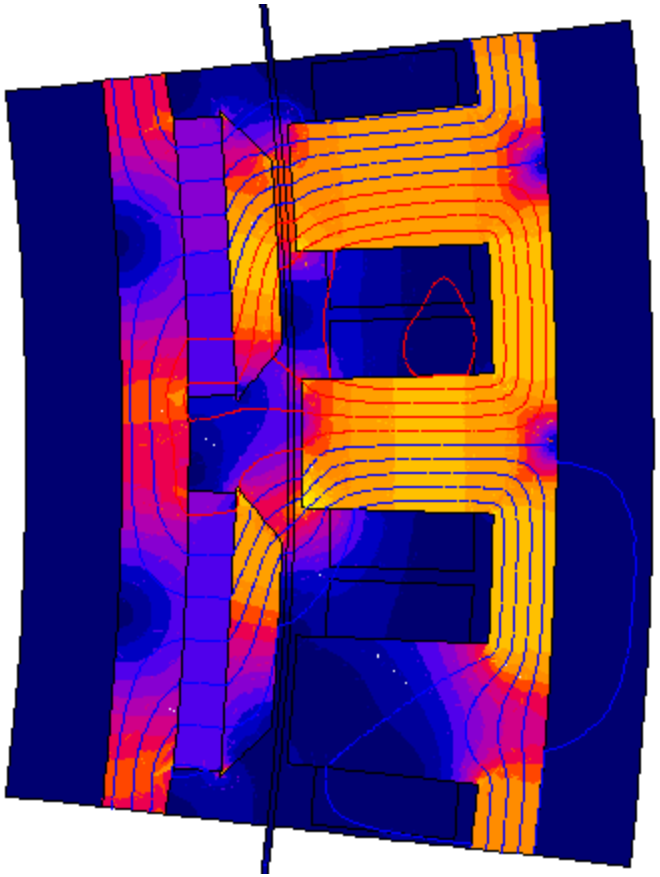

Inverter Coupled Saturation Effects

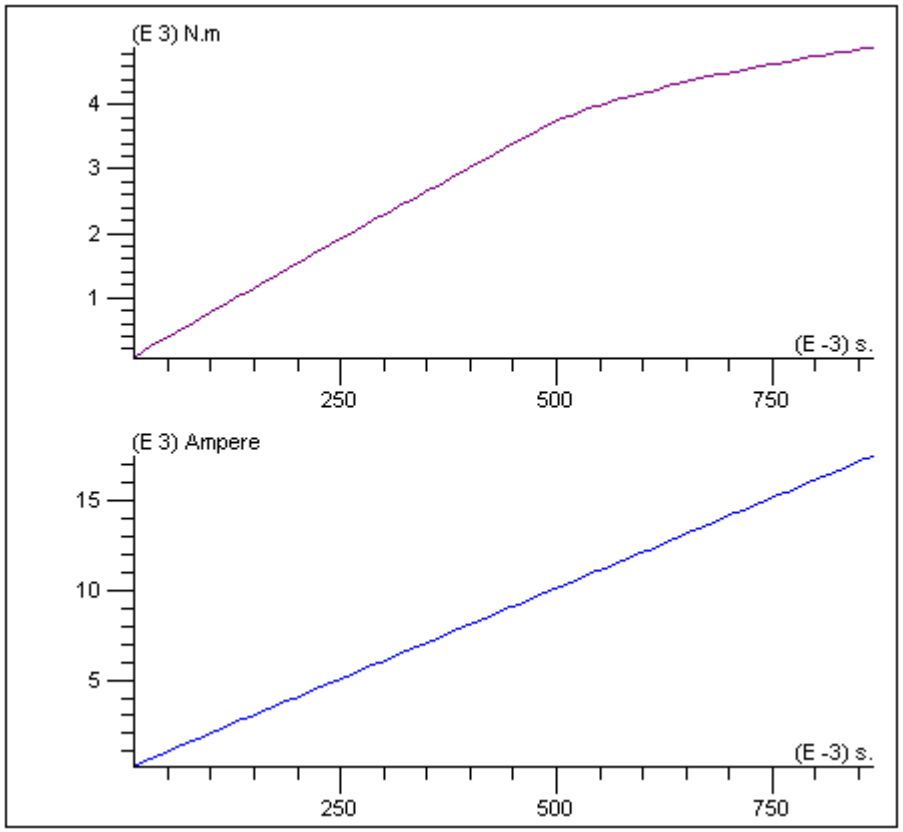

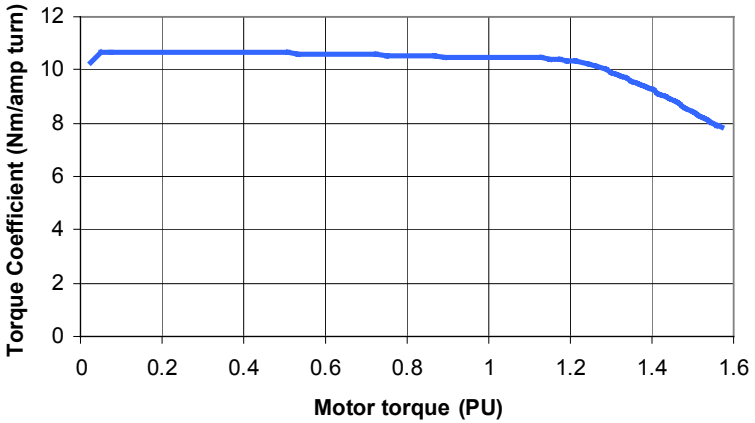

- Acceptable saturation at 1.0 PU torque
- Saturation onset at 1.2 PU torque

Rectifier Model

Thevenin Equivalent Model

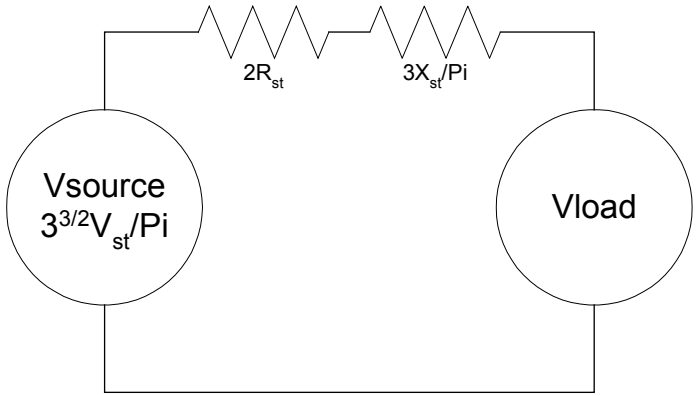

Explicit Circuit Simulation

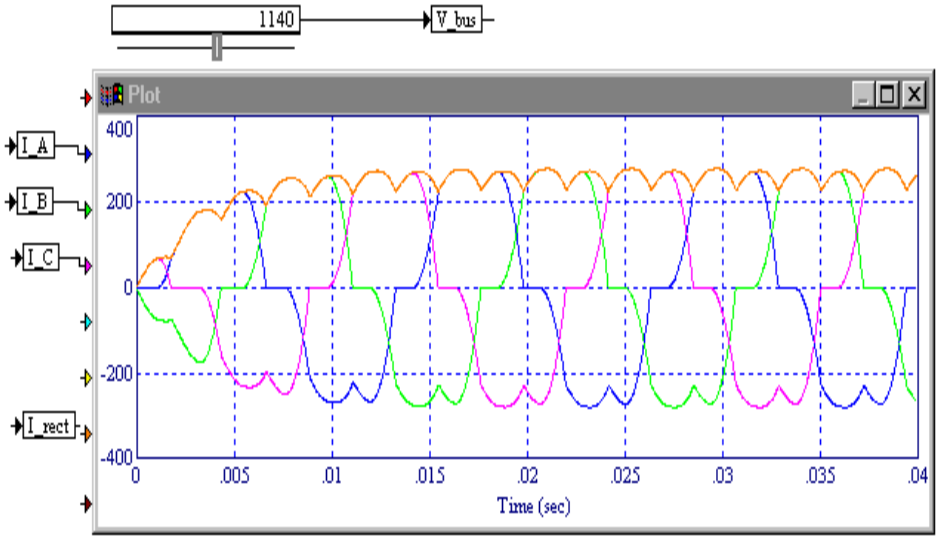

Rectifier Penalty

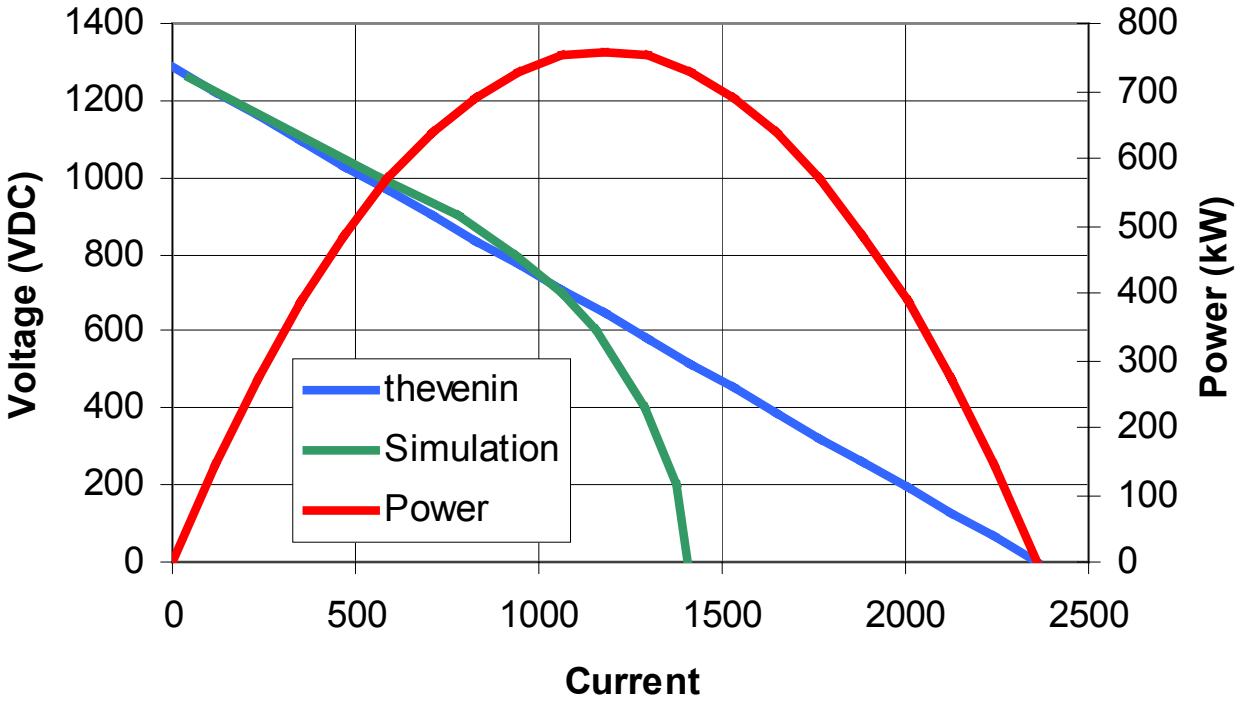

- Current point design can only reach 50% power objective with rectifier bridge converter and baseline parameters

Diode Coupled FEA Model Results: No load

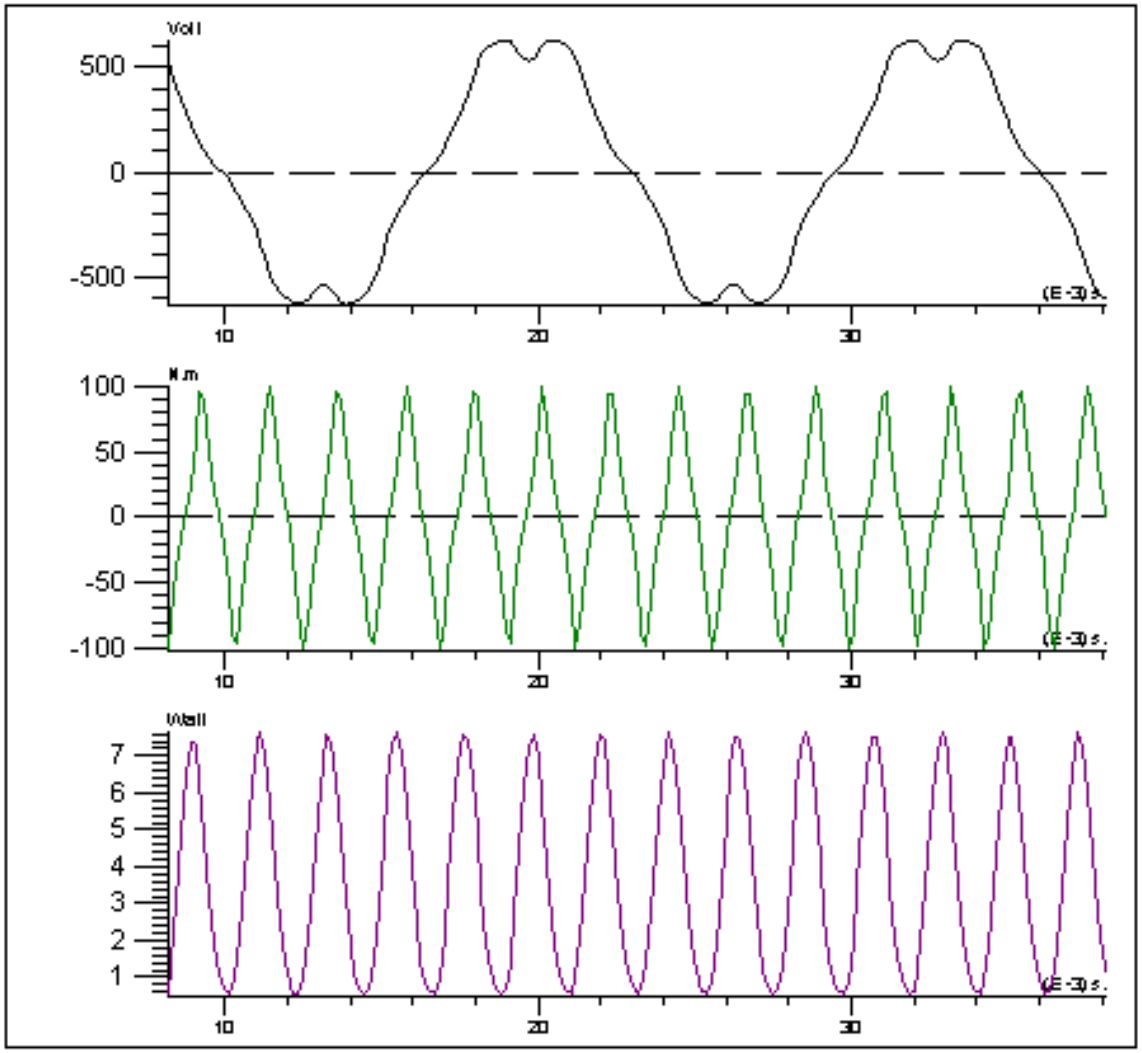

VBEMF:

~ 600 volts per phase

Cogging torque:

±2400 NM (2.7% PU)

Low magnet heating:

~ 103 W total

Per pole pair results shown

Diode Coupled FEA Model Results: Inductance

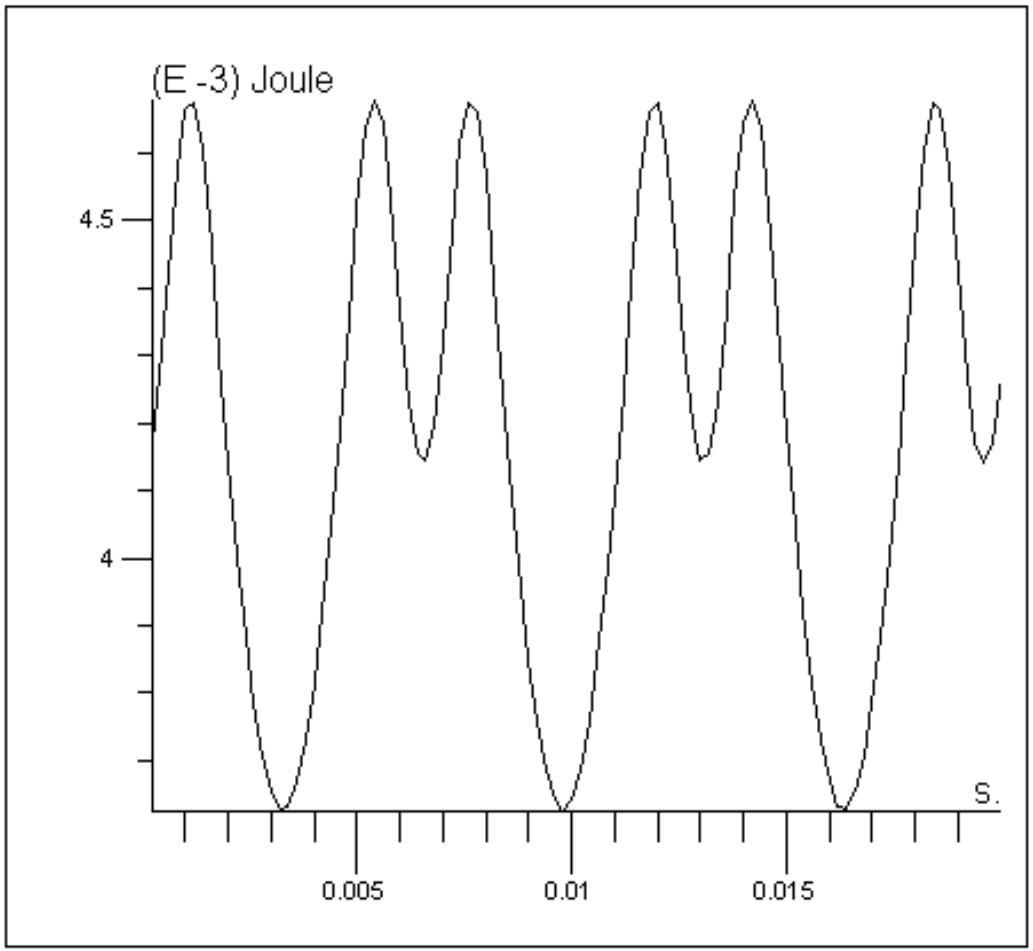

- FEA Pole Inductance (single pole @ 75 turns): 8.05 mH
  - 288 μH per phase
  - Turn count adjusted for 600 volt peak phase voltage @164 rpm

Diode Coupled FEA Model Results: @ 1100 Vbus

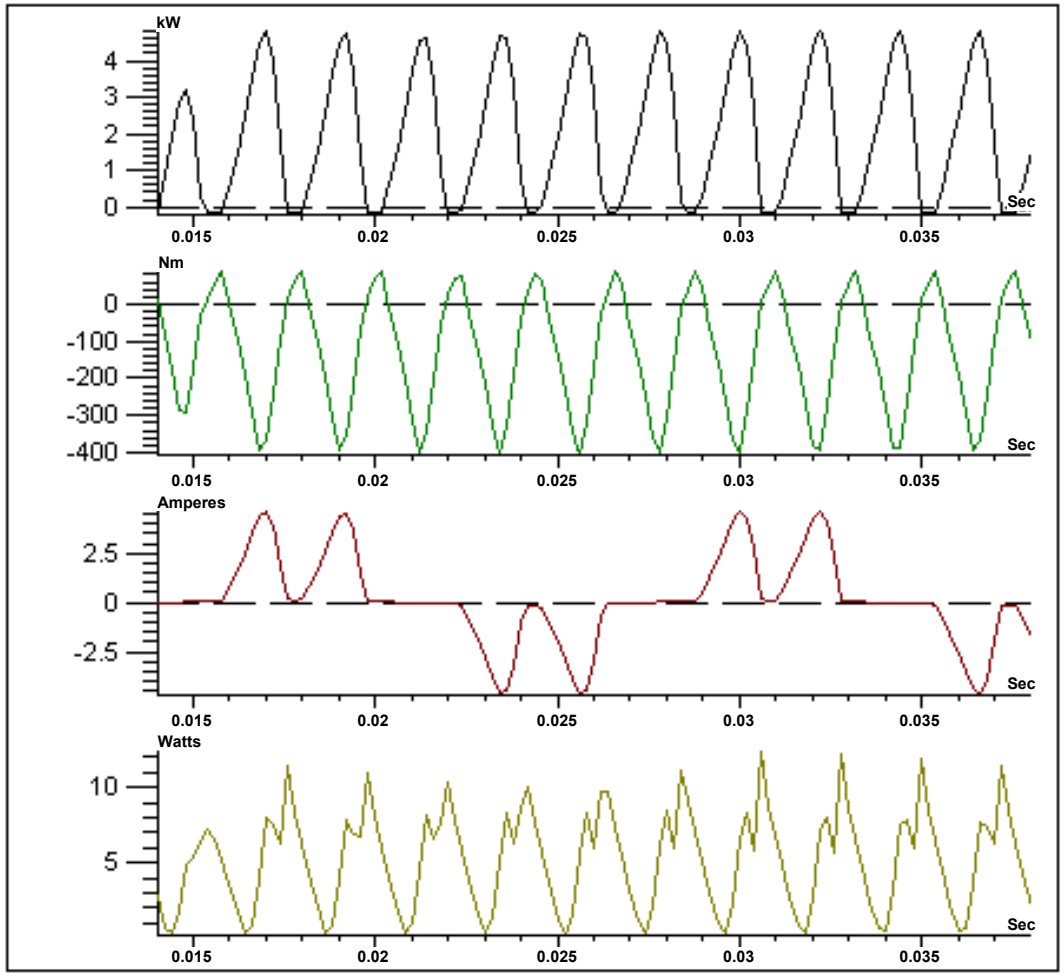

Power:

- 980 VDC bus
- 3 phase WYE bridge
- 2.0 kW per pole pair
- 55 kW total

Torque:

- ~132 Nm per pole pair
- 3.7 kNm total

Coil Current:

- ~5 amps pk
- 2 amps rms

Magnet Losses:

- ~5.3 Watts per pole pair
- 147 Watts total

All results are on a rotor pole pair basis (1 pair of 28 in reference baseline)

Turn count (N=75) adjusted to get ~ 600 Volt open circuit

Diode Coupled FEA Model Results: @ 980 Vbus

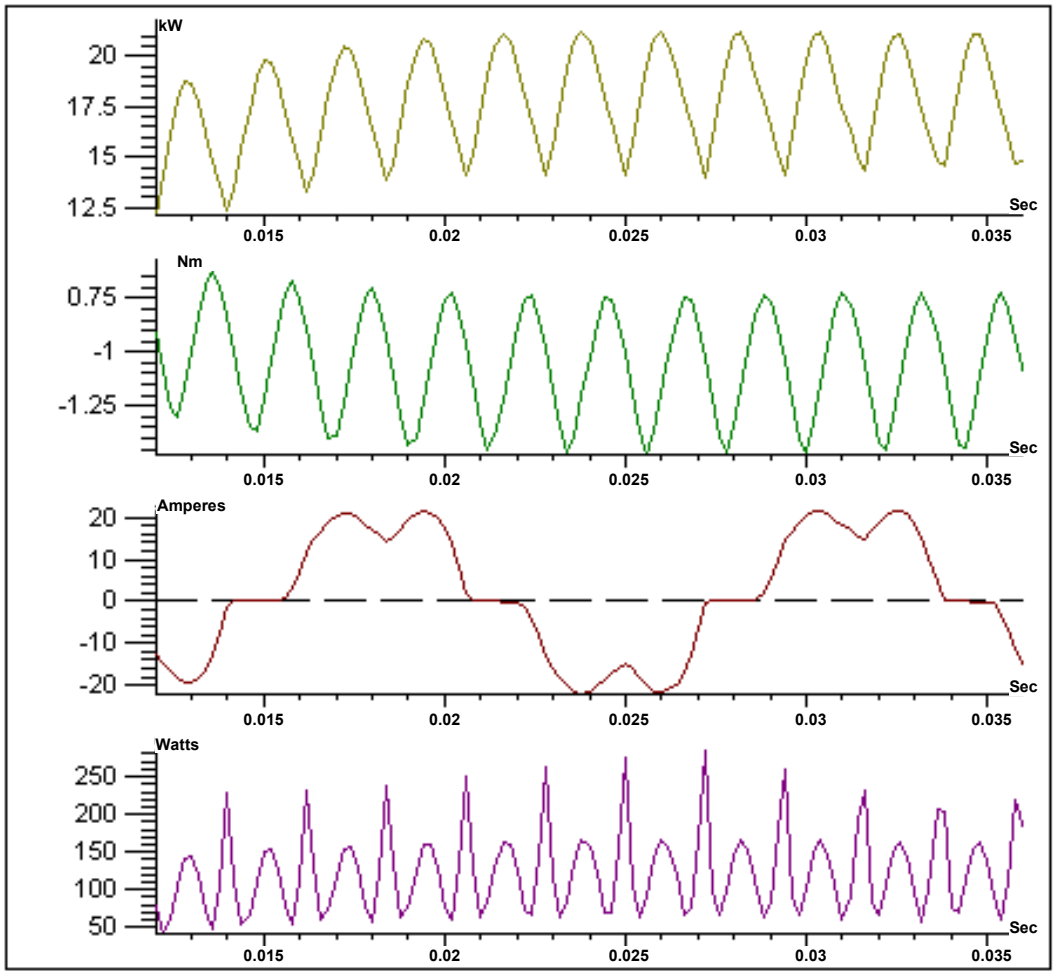

Power:

- 980 VDC bus
- 3 phase WYE bridge
- 17.7 kW per pole pair
- 496 kW total

Torque:

- ~1.05 kNm per pole pair
- 29.4 kNm total

Coil Current:

- ~21 amps pk
- 13 amps rms

Magnet Losses:

- ~67 Watts per pole pair
- 1865 Watts total

All results are on a rotor pole pair basis (1 pair of 28 in reference baseline)

Turn count (N=75) adjusted to get ~ 600 Volt open circuit

Diode Coupled FEA Model Results: @ 860 Vbus

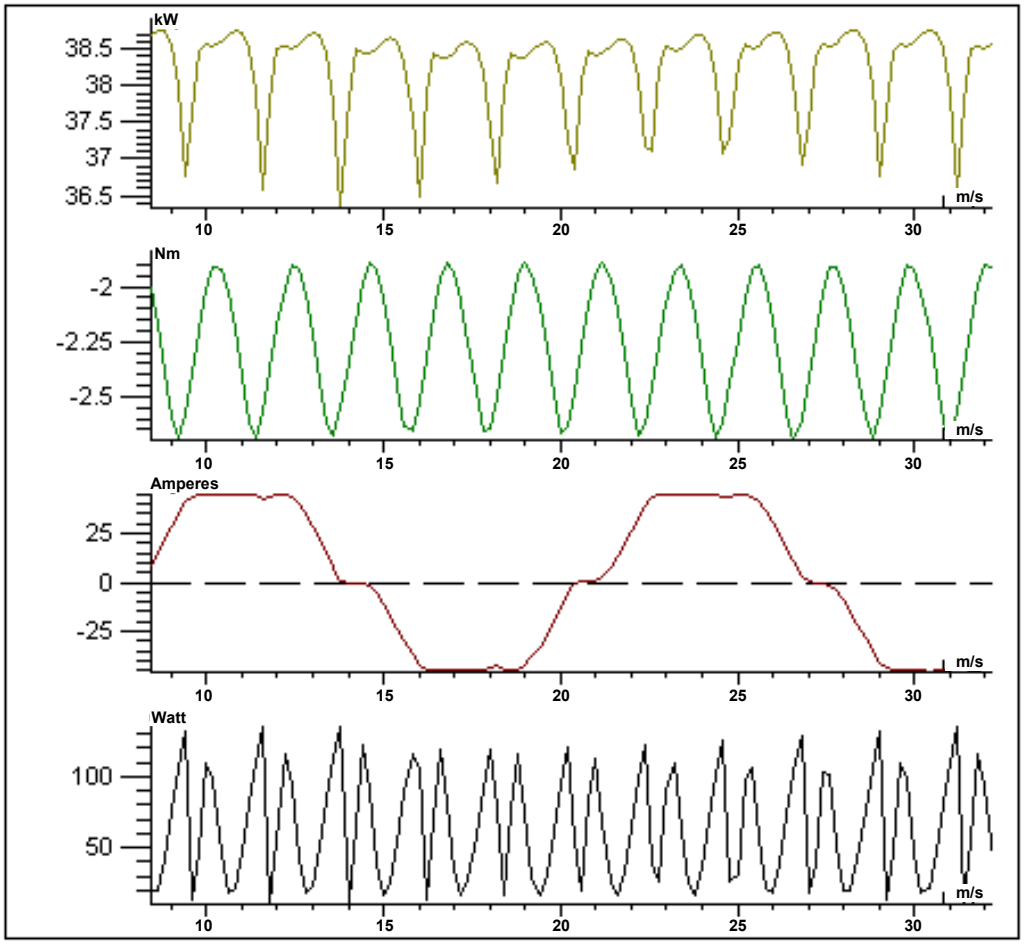

Power:

- 860 VDC bus
- 3 phase WYE bridge
- 38.2 kW per pole pair
- 1.07 MW total

Torque:

- ~2.27 kNm per pole pair
- 63.3 kNm total

Coil Current:

- ~45 amps pk
- 30 amps rms

Magnet Losses:

- ~65 Watts per pole pair
- 1820 Watts total

All results are on a rotor pole pair basis (1 pair of 28 in reference baseline)

Turn count (N=75) adjusted to get ~ 600 Volt open circuit

Diode Coupled FEA Model Results: @ 740 Vbus

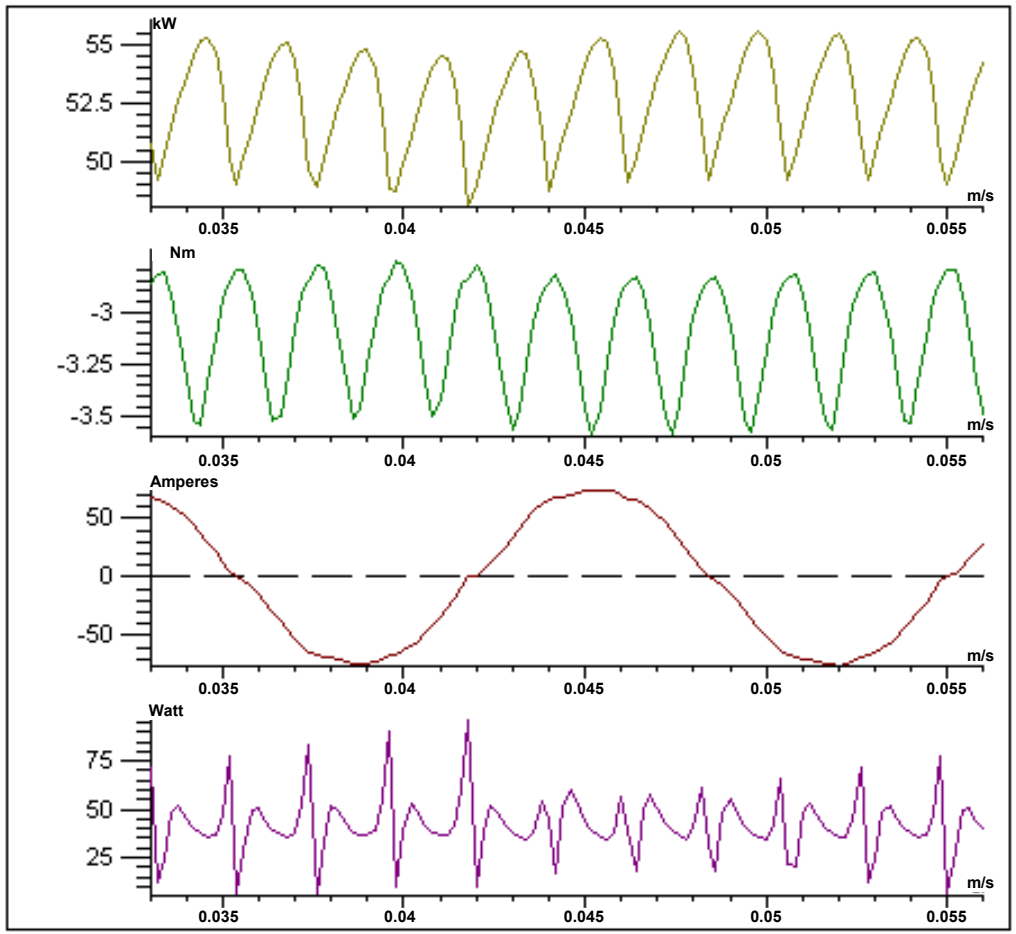

Power:

- 740 VDC bus
- 3 phase WYE bridge
- 52.6 kW per pole pair
- 1.47 MW total

Torque:

- ~3.11 kNm per pole pair
- 87.1 kNm total

Phase Current:

- ~75 amps pk
- 47 amps rms

Magnet Losses:

- ~42 Watts per pole pair
- 1176 Watts total

All results are on a rotor pole pair basis (1 pair of 28 in reference baseline)

Turn count (N=75) adjusted to get ~ 600 Volt open circuit

Diode Coupled FEA Model Results: @ 550 Vbus

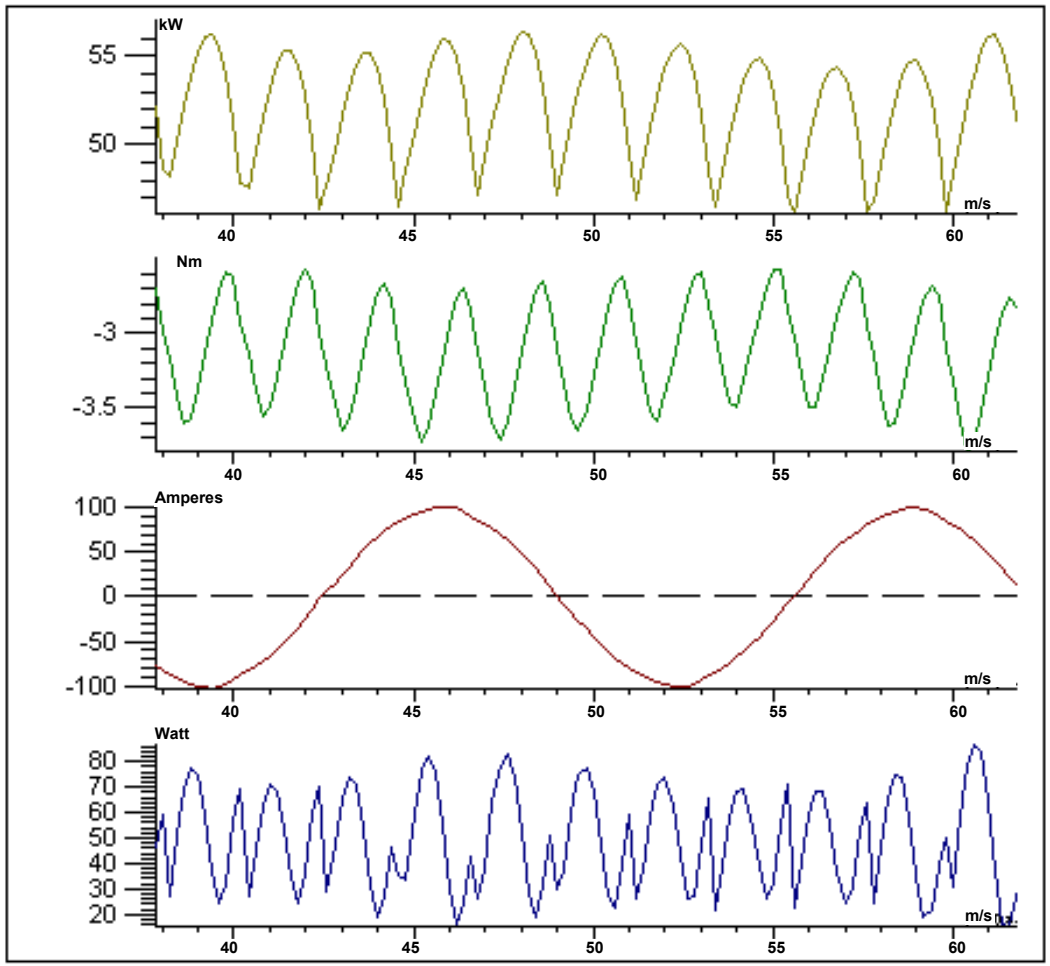

Power:

- 550 VDC bus
- 3 phase WYE bridge
- 52.2 kW per pole pair
- 1.46 MW total

Torque:

- ~3.12 kNm per pole pair
- 87.4 kNm total

Phase Current:

- ~102 amps pk
- 62 amps rms

Magnet Losses:

- ~49 Watts per pole pair
- 1372 Watts total

All results are on a rotor pole pair basis (1 pair of 28 in reference baseline)

Turn count (N=75) adjusted to get ~ 600 Volt open circuit

Baseline Circuit Parameters

Parameter	inverter coupled baseline	Diode coupled baseline
Phase voltage coefficient	600	600
Phase inductance (μH)	662	288
Phase resistance (mΩ)	12.3	5.72
Stack Length (mm)	200	250
Matched Power (kW)	750	1710
Approx cost	$34,585	$49,285

- Turn Count adjusted for 600 volt pk phase voltage @ 164 rpm
- Sine fundamental of phase voltage is substantially higher than peak due to 3rd harmonic component
- Matched power is higher due to 3rd harmonic
- End turns increase resistance to ~ 1.39 X of 2D model for diode coupled design

Diode Coupled Model: Load Characteristics

DC Voltage (volts)	Bus Current (amps)	Power (kW)	Phase Current (Arms)	Ohmic Losses (kW)	Core Losses (kW)	Magnet Losses (kW)	Total Losses (kW)	Efficiency
1200	0	0	0	0	7.69	0.10	7.8	0.0%
1100	50	55	45	0	7.69	0.15	7.9	87.5%
980	506	496	364	2	7.69	1.87	11.8	97.7%
860	1244	1070	849	12	7.69	1.82	21.9	98.0%
740	1986	1470	1318	30	7.69	1.18	38.7	97.4%
550	2655	1460	1736	52	7.69	1.37	60.8	96.0%

- M47 assumed for core loss
  - No adjustment for armature effects
- Magnet eddy current losses can probably be reduced with further pole shaping

Inverter Coupled Cost Breakdown

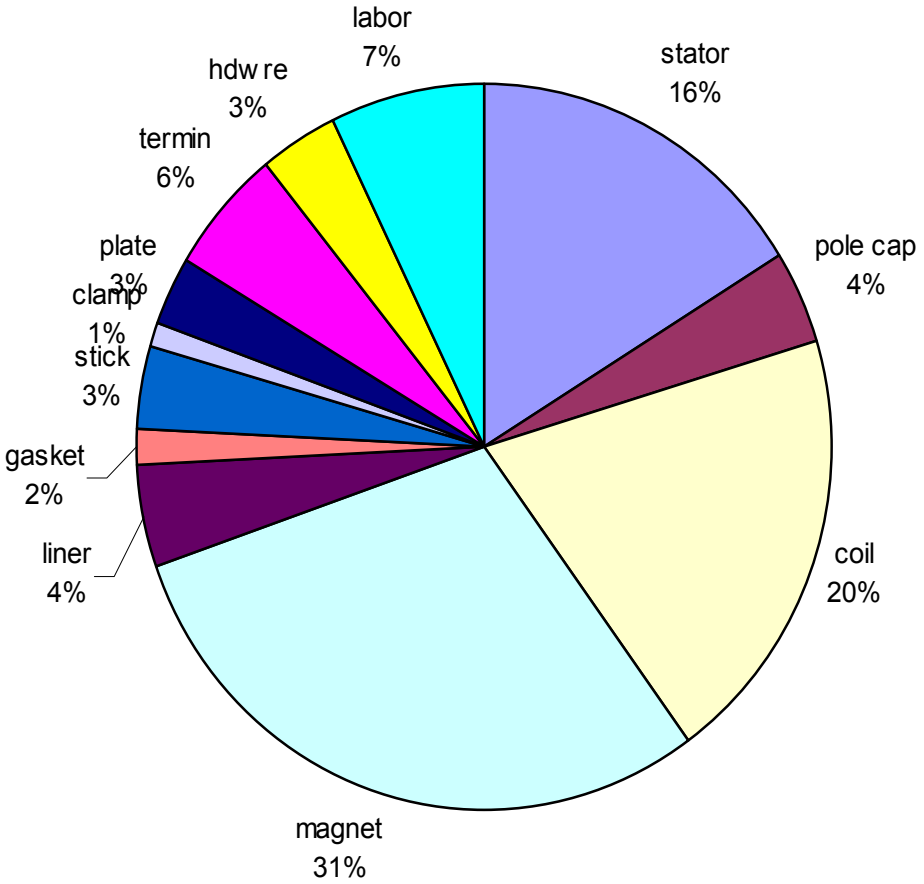

Tooling, warranty and NRE not included

Cost vs Length Tradeoffs

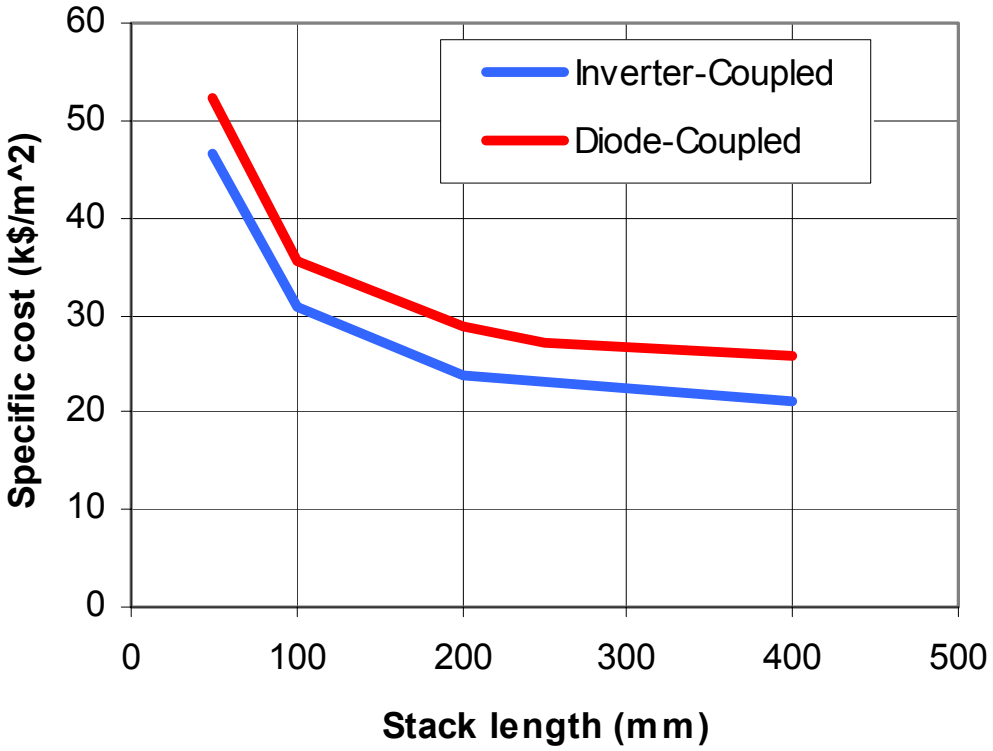

Thermal Management

- Cooling of the generator magnetics is via indirect conduction to a liquid cooled stator housing
- Materials, dimensions and assembly are optimized to facilitate heat transfer to the jacket
- Windings do not require any air-circulation for cooling
  - Minimal end turns minimize losses and facilitate conduction to the stack
- Indirect conduction cooling is well understood and is common practice in PM machines
  - Thin backiron of PM machines enables effective thermal conduction to stator OD

Thermal Model

2D FEA Model

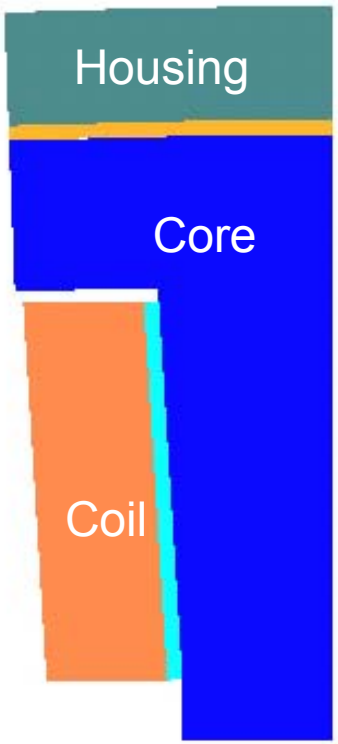

Mesh

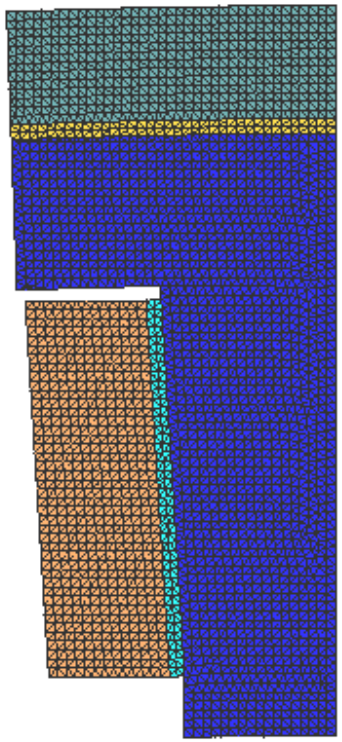

Results

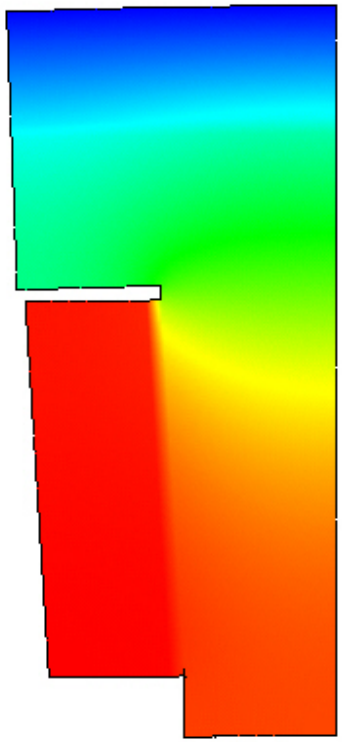

- Average wire temperature is ~ 40°C above housing OD @ 1.5 MW
- Peak end turn temperature will be ~ 10°C above average
- Fluid ΔTs not included
- Insulation system is rated for 180°C , recommend Tmax of 160 °C

Appendix F

Power Electronic and VAR Control Estimates

Baseline System Drive Topology

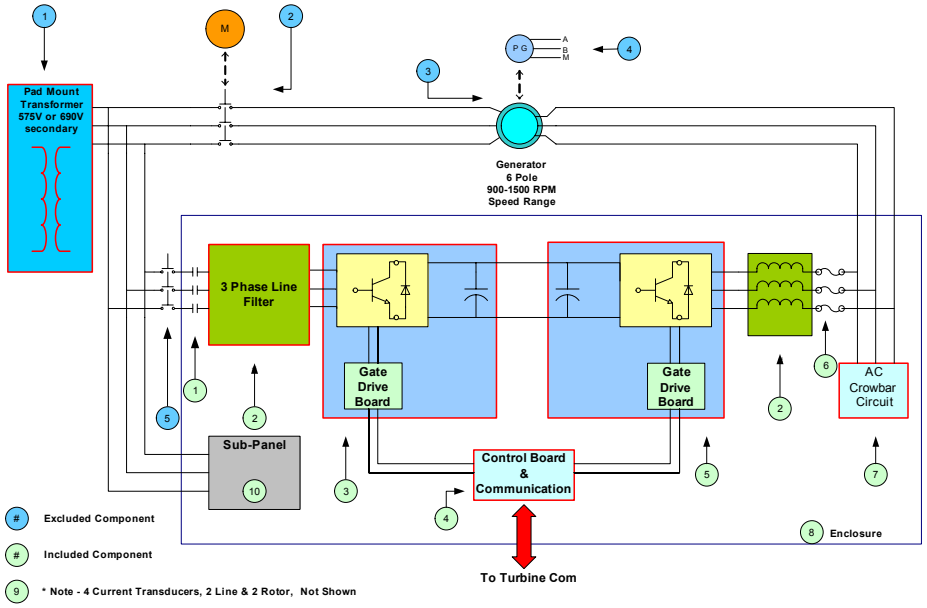

Baseline System
Bill of Materials (BOM)

Item #	Qty	Description	Unit Cost	Extended Cost
1	1	Contactor, 525 A, 1000 VAC, 3-pole	$811.00	$811.00
2	1	Line Filter, 3-Phase	$7,540.00	$7,540.00
3	1	Assy, Matrix, 3-Phase, Line	$5,964.00	$5,964.00
4	1	Generator Control Board	$1,887.00	$1,887.00
5	1	Assy, Matrix, 3-Phase, Rotor	$5,964.00	$5,964.00
6	1	Fuse, 600 A, 1000 VAC, 3-pole	$281.00	$281.00
7	1	AC Crow bar Circuit	$3,216.00	$3,216.00
8	1	Enclosure	$3,157.00	$3,157.00
9	4	Current transducers, 2 Line, 2 Rotor	$268.00	$1,072.00
10	1	Sub-Panel	$1,300.00	$1,300.00
		Total		**$31,192.00**

Baseline System
3-Phase IGBT Line/Rotor Side Matrix

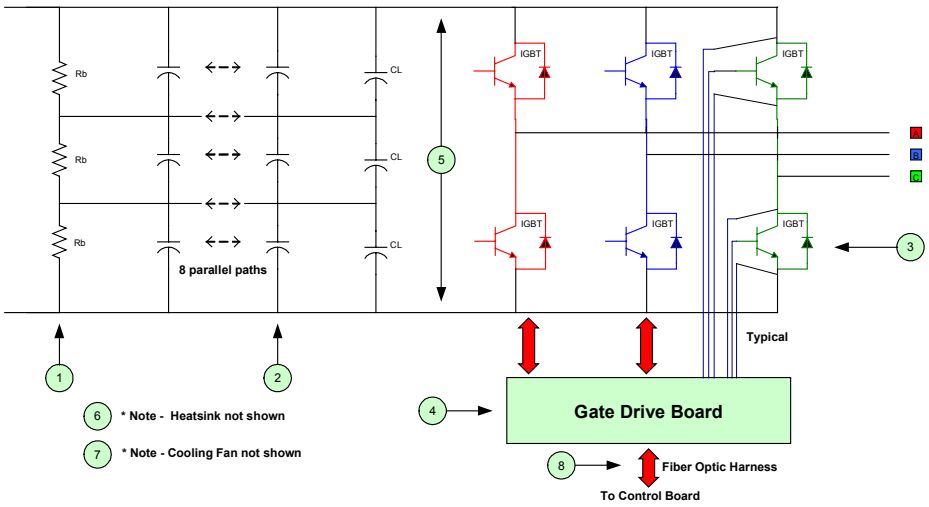

Baseline System
3-Phase IGBT Line & Rotor Matrix
BOM

Item #	Qty	Description	Unit Cost	Extended Cost
1	3	Resistor, Balance	$1.66	$5.00
2	24	Capacitor, 5500 uF, 450 Volt	$35.40	$850.00
3	6	IGBT, 1600 A, 1700 Volt	$406.00	$2,436.00
4	1	Gate Drive Board, Hex	$404.00	$404.00
5	1	Assy, Laminated Bus	$900.00	$900.00
6	1	Heatsink	$630.00	$630.00
7	1	Cooling Fan	$514.00	$514.00
8	1	Fiber Optic Harness	$225.00	$225.00
		Total		**$5,964.00**

Baseline System
3-Phase Line Side Filter

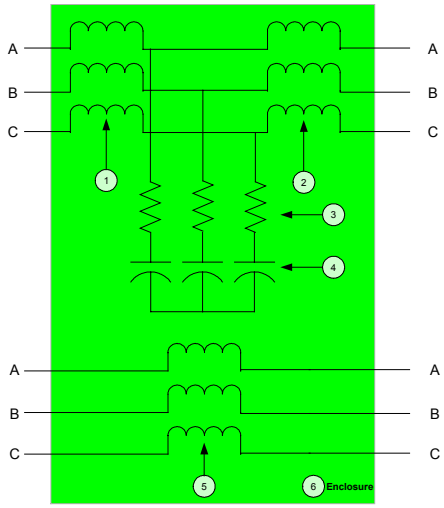

Baseline System - Rev. 4.0 5

Baseline System
3-Phase Line Side Filter
BOM

Item #	Qty	Description	Unit Cost	Extended Cost
1	1	Inductor, Reactor, Line, 250uH, 3-phase	$1,847.00	$1,847.00
2	1	Inductor, Reactor, PWM, 250uH, 3-phase	$2,243.00	$2,243.00
3	3	Resistor, Stainless, 3-phase, .1 OHM/phase	$76.00	$228.00
4	1	Capacitor, 20.8 KVAR, 3-phase, 690 Volt	$172.00	$172.00
5	1	Inductor, Rotor, 3-phase	$1,638.00	$1,638.00
6	1	Enclosure	$1,412.00	$1,412.00
		Total		**$7,540.00**

Baseline System - Rev. 4.0 6

Baseline System
Sub-Panel
BOM

Item #	Qty	Description	Unit Cost	Extended Cost
1	1	Fab, Panel, Pow er Dist	$127.00	$127.00
2	1	Sw itch, Disconnect, 80 A, 1000V	$36.00	$36.00
3	2	Circuit Breaker, 30A, 1000V	$152.00	$152.00
4	3	Fuse, 30A, 1000V	$12.00	$36.00
5	3	Fuseblock, 100A, 1000V	$21.00	$63.00
6	2	Res, 40 OHM, 250 W	$57.00	$114.00
7	2	Cap, Electrolytic, 3300 uF,	$23.00	$46.00
8	1	Assy, Harness, Main	$282.00	$282.00
9	1	Circuit Breaker, 20A, 1000V	$152.00	$152.00
10	1	Circuit Breaker, 2A, 1000V	$100.00	$100.00
11	4	SSR, 12A, 400 VDC, MOSFET OUT	$23.00	$92.00
12	1	Transformer, Control	$100.00	$100.00
		Total		**$1,300.00**

Baseline System - Rev. 4.0 7

Baseline System Pricing Estimates

Baseline System			
Direct Variable Materials[1]	$ 31,192	$ 31,192	$ 31,192
Direct Variable Labor[2]	$ 1,040	$ 1,040	$ 1,040
Direct Fixed Costs[3]	$ 4,835	$ 4,835	$ 4,835
Total Direct Costs	$ 37,067	$ 37,067	$ 37,067
Gross Margin[4]	30%	40%	50%
Purchase Price	**$ 52,953**	**$ 61,778**	**$ 74,134**

[1]Includes 3% freight in.
[2]Assumes 30% fringe benefits and 70% utilization, includes final assembly, board test, and final test.
[3]This number can vary significantly, 15% is used here.
[4]Gross Margin = (Sales Price - Direct Cost)/Sales Price

Baseline System - Rev. 4.0 8

1.5 MW PM SCR/SCR Drive Topology

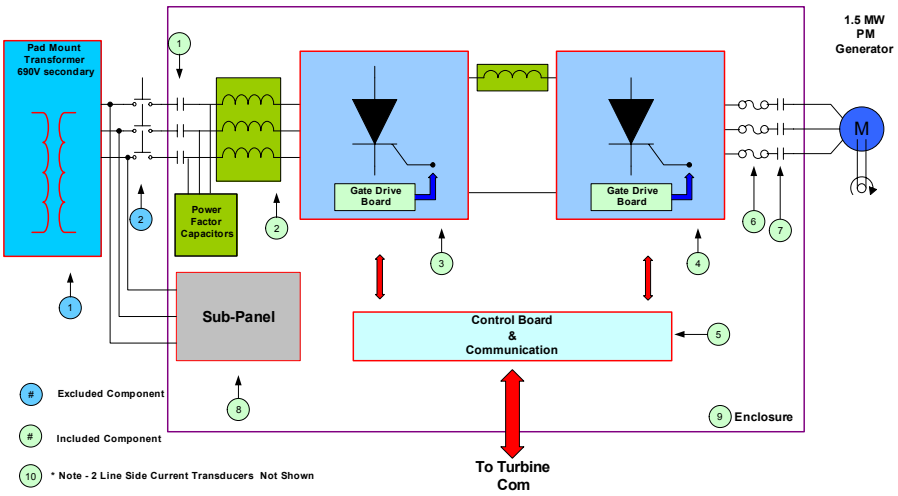

1.5 MW PM SCR/SCR Drive Bill of Materials (BOM)

Item #	Qty	Description	Unit Cost	Extended Cost
1	1	Contactor, 1500 A, 1000 VAC, 3-pole, Line	2,480.00	2,480.00
2	1	Line Inductor-3-Phase, DC Inductor, PF Capacitor Assy	8,877.00	8,877.00
3	1	Assy, SCR Matrix, 3-Phase, Line	3,109.00	3,109.00
4	1	Assy, SCR Matrix, 3-Phase, Rotor	3,109.00	3,109.00
5	1	Control Board	1,000.00	1,000.00
6	1	Fuse, 1500 A, 1000 VAC, 3-pole	281.00	281.00
7	1	Contactor, 1500 A, 1000 VAC, 3-pole, Gen	2,480.00	2,480.00
8	1	Enclosure	2,916.00	2,916.00
9	1	Sub-Panel	1,452.00	1,452.00
10	6	Current transformers, 2 Line	75.00	450.00
		Total		**26,154.00**

1.5 MW PM SCR/SCR Drive
3-Phase SCR Line/Gen Side Matrix

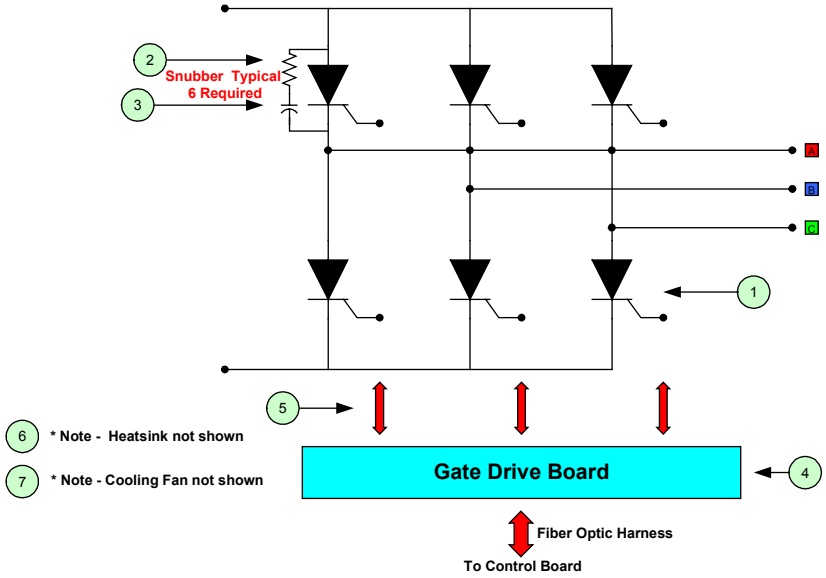

1.5 MW PM SCR/SCR Drive
3-Phase SCR Line Side Matrix
BOM

Item #	Qty	Description	Unit Cost	Extended Cost
1	6	SCR, 2500 A, 2400 V, C781	$240.00	$1,440.00
2	6	Resistor, Snubber, 33 Ohm	$2.50	$15.00
3	6	Capacitor, Snubber, .5 uF	$11.00	$66.00
4	1	Gate Drive Board	$404.00	$404.00
5	1	Gate Wire Harness	$112.00	$112.00
6	1	Heatsink, Clamps, Terminations	$700.00	$700.00
7	1	Cooling Fan & Switch Gear	$372.00	$372.00
		Total		**$3,109.00**

1.5 MW PM SCR/SCR Drive
3-Phase Line Side Inductor, PF Caps, & DC Reactor

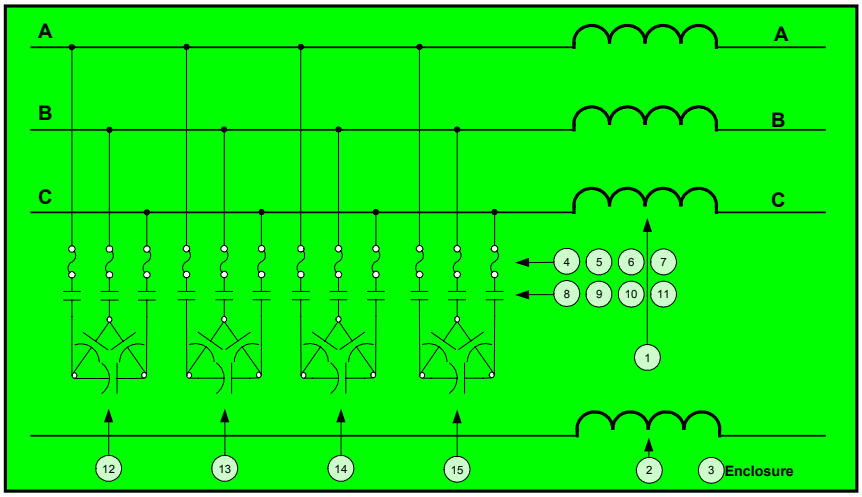

1.5 MW PM SCR/SCR Drive
3-Phase Line Side Inductor & DC Reactor
BOM

Item #	Qty	Description	Unit Cost	Extended Cost
1	1	Inductor, Line, 150 uH, 3-Phase	$2,212.00	$2,212.00
2	1	Inductor, DC, 2.5 mH, 1500 A	$2,025.00	$2,025.00
3	1	Enclosure	$1,876.00	$1,876.00
4,5	6	Fuse & Fuse Holder, 50 Amps, 690 Volts	$33.00	$198.00
6	3	Fuse & Fuse Holder, 100 Amps, 690 Volts	$33.00	$99.00
7	3	Fuse & Fuse Holder, 200 Amps, 690 Volts	$33.00	$99.00
8,9	2	Contactor, 50 Amps, 690 Volts, 3-Pole	$111.00	$222.00
10	1	Contactor, 100 Amps, 690 Volts, 3-Pole	$212.00	$212.00
11	1	Contactor, 200 Amps, 690 Volts, 3-Pole	$334.00	$334.00
12,13	2	Capacitor, 50 kVAR, 690 Volts, 3-Phase	$200.00	$400.00
14	1	Capacitor, 100 kVAR, 690 Volts, 3-Phase	$400.00	$400.00
15	1	Capacitor, 200 kVAR, 690 Volts, 3-Phase	$800.00	$800.00
		Total		**$8,877.00**

1.5 MW PM SCR/SCR Drive Sub-Panel BOM

Item #	Qty	Description	Unit Cost	Extended Cost
1	1	Fab, Panel, Pow er Dist	$127.00	$127.00
2	1	Sw itch, Disconnect, 80 A, 1000V	$36.00	$36.00
3	2	Circuit Breaker, 30A, 1000V	$152.00	$304.00
4	3	Fuse, 30A, 1000V	$12.00	$36.00
5	3	Fuseblock, 100A, 1000V	$21.00	$63.00
6	2	Res, 40 OHM, 250 W	$57.00	$114.00
7	2	Cap, Electrolytic, 3300 uF,	$23.00	$46.00
8	1	Assy, Harness, Main	$282.00	$282.00
9	1	Circuit Breaker, 20A, 1000V	$152.00	$152.00
10	1	Circuit Breaker, 2A, 1000V	$100.00	$100.00
11	4	SSR, 12A, 400 VDC, MOSFET OUT	$23.00	$92.00
12	1	Transformer, Control	$100.00	$100.00
		Total		**$1,452.00**

1.5 MW PM SCR/SCR Drive Pricing Estimates

1.5 MW Permanent Magnet Drive						
Direct Variable Materials[1]	$	26,154	$	26,154	$	26,154
Direct Variable Labor[2]	$	1,560	$	1,560	$	1,560
Direct Fixed Costs[3]	$	4,157	$	4,157	$	4,157
Total Direct Costs	$	31,871	$	31,871	$	31,871
Gross Margin[4]		30%		40%		50%
Purchase Price	**$**	**45,530**	**$**	**53,119**	**$**	**63,742**

[1]Includes 3% freight in.
[2]Assumes 30% fringe benefits and 70% utilization, includes final assembly, board test, and final test.
[3]This number can vary significantly, 15% is used here.
[4]Gross Margin = (Sales Price - Direct Cost)/Sales Price

1.5 MW Diode-IGBT Drive Topology

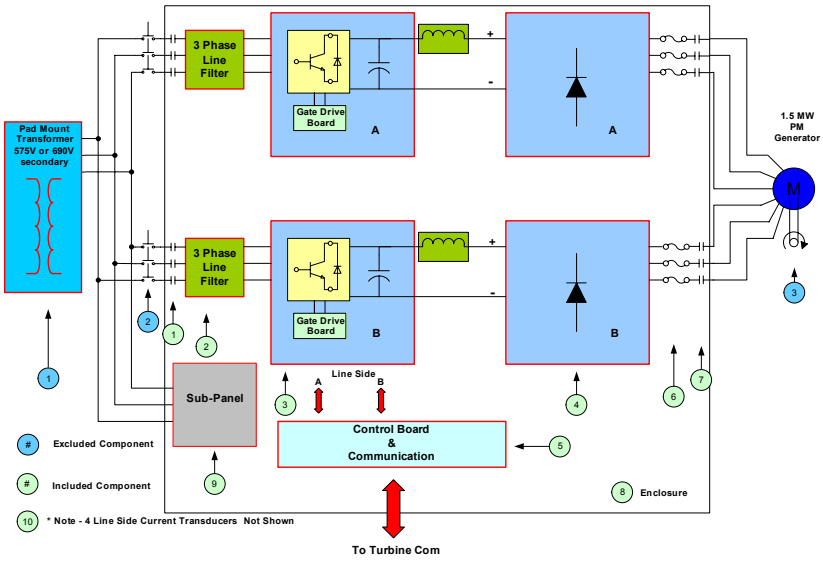

1.5 MW Diode-IGBT Drive Bill of Materials (BOM)

Item #	Qty	Description	Unit Cost	Extended Cost
1	2	Contactor, 800 A, 1000 VAC, 3-pole, Line	1,240.00	2,480.00
2	2	Line Filter, 3-Phase	7,238.00	14,476.00
3	2	Assy, Matrix, 3-Phase, Line	8,045.00	16,090.00
4	2	Assy, Diode Matrix, 3-Phase, Rotor	1,692.00	3,384.00
5	1	Control Board	1,400.00	1,400.00
6	2	Fuse, 900 A, 1000 VAC, 3-pole	281.00	562.00
7	2	Contactor, 800 A, 1000 VAC, 3-pole, Gen	1,240.00	2,480.00
8	1	Enclosure	2,916.00	2,916.00
9	1	Sub-Panel	1,300.00	1,300.00
10	4	Current transducers, 4 Line	268.00	1,072.00
		Total		**46,160.00**

1.5 MW Diode-IGBT Drive
3-Phase IGBT Line Side Matrix

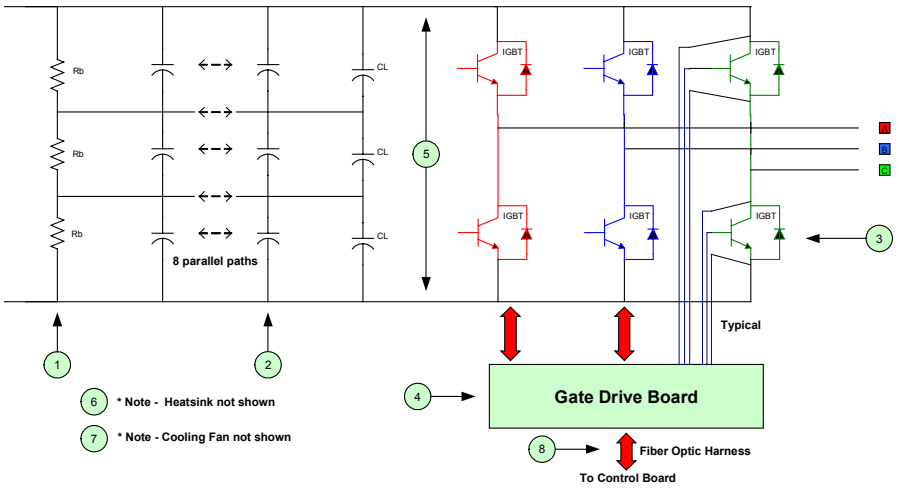

1.5 MW PM Diode-IGBT Drive
3-Phase IGBT Line Side Matrix
BOM

Item #	Qty	Description	Unit Cost	Extended Cost
1	3	Resistor, Balance	$1.66	$5.00
2	24	Capacitor, 6500 uF, 450 Volt	$40.40	$969.00
3	6	IGBT, 2400 A, 1700 Volt	$554.00	$3,324.00
4	1	Gate Drive Board, Hex	$404.00	$404.00
5	1	Assy, Laminated Bus	$1,232.00	$1,232.00
6	1	Heatsink	$1,372.00	$1,372.00
7	1	Cooling Fan	$514.00	$514.00
8	1	Fiber Optic Harness	$225.00	$225.00
		Total		**$8,045.00**

1.5 MW Diode-IGBT Drive
3-Phase Diode Bridge

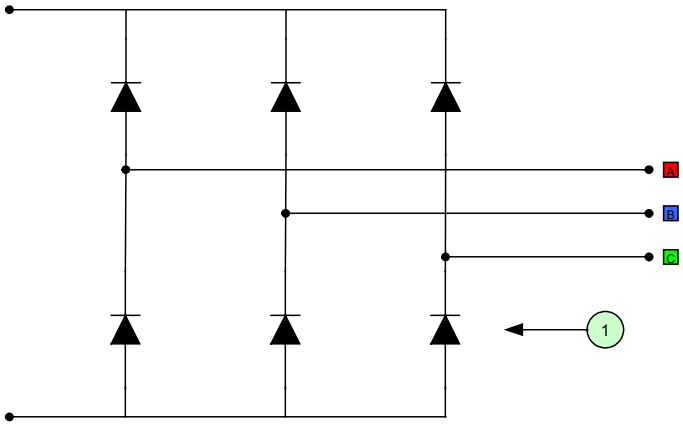

2 * Note - Heatsink not shown

3 * Note - Cooling Fan not shown

1.5 MW Diode-IGBT Drive
3-Phase Diode Bridge
BOM

Item #	Qty	Description	Unit Cost	Extended Cost
1	6	Diode, 1200 A, 2400 V, Fast Recovery	$120.00	$720.00
2	1	Heatsink, Clamps, Terminations	$600.00	$600.00
3	1	Cooling Fan & Switch Gear	$372.00	$372.00
		Total		**$1,692.00**

1.5 MW Diode-IGBT Drive
3-Phase Line Side Filter

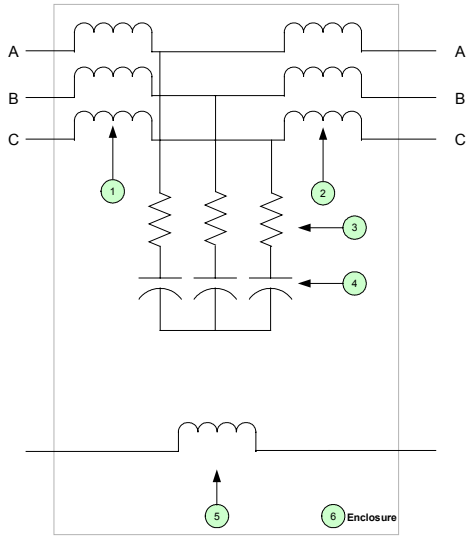

1.5 MW Diode-IGBT Drive
3-Phase Line Side Filter
BOM

Item #	Qty	Description	Unit Cost	Extended Cost
1	1	Inductor, Reactor, Line, 1000uH, 3-phase	$2,509.00	$2,509.00
2	1	Inductor, Reactor, PWM, 500uH, 3-phase	$1,374.00	$1,374.00
3	3	Resistor, Stainless, 3-phase, .1 OHM/phase	$76.00	$228.00
4	2	Capacitor, 20.8 KVAR, 3-phase, 690 Volt	$172.00	$344.00
5	1	Inductor, 500uH, 800 A	$2,025.00	$907.00
6	1	Enclosure	$1,876.00	$1,876.00
		Total		**$7,238.00**

1.5 MW Diode-IGBT Drive Sub-Panel BOM

Item #	Qty	Description	Unit Cost	Extended Cost
1	1	Fab, Panel, Pow er Dist	$127.00	$127.00
2	1	Sw itch, Disconnect, 80 A, 1000V	$36.00	$36.00
3	2	Circuit Breaker, 30A, 1000V	$152.00	$152.00
4	3	Fuse, 30A, 1000V	$12.00	$36.00
5	3	Fuseblock, 100A, 1000V	$21.00	$63.00
6	2	Res, 40 OHM, 250 W	$57.00	$114.00
7	2	Cap, Electrolytic, 3300 uF,	$23.00	$46.00
8	1	Assy, Harness, Main	$282.00	$282.00
9	1	Circuit Breaker, 20A, 1000V	$152.00	$152.00
10	1	Circuit Breaker, 2A, 1000V	$100.00	$100.00
11	4	SSR, 12A, 400 VDC, MOSFET OUT	$23.00	$92.00
12	1	Transformer, Control	$100.00	$100.00
		Total		**$1,300.00**

1.5 MW Diode-IGBT Drive Pricing Estimates

1.5 MW Permanent Magnet (2X) Drive			
Direct Variable Materials[1]	$ 46,160	$ 46,160	$ 46,160
Direct Variable Labor[2]	$ 1,560	$ 1,560	$ 1,560
Direct Fixed Costs[3]	$ 7,158	$ 7,158	$ 7,158
Total Direct Costs	$ 54,878	$ 54,878	$ 54,878
Gross Margin[4]	30%	40%	50%
Purchase Price	**$ 78,397**	**$ 91,463**	**$ 109,756**

[1]Includes 3% freight in.
[2]Assumes 30% fringe benefits and 70% utilization, includes final assembly, board test, and final test.
[3]This number can vary significantly, 15% is used here.
[4]Gross Margin = (Sales Price - Direct Cost)/Sales Price

1.5 MW IGBT-IGBT Drive Topology

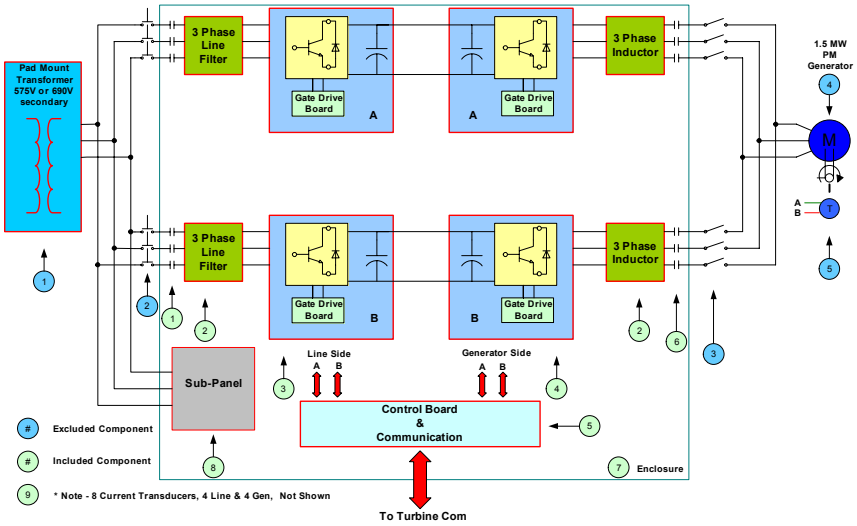

1.5 MW IGBT-IGBT Drive Bill of Materials (BOM)

Item #	Qty	Description	Unit Cost	Extended Cost
1	2	Contactor, 810 A, 600 VAC, 3-pole, Line	$1,240.00	$2,480.00
2	2	Line Filter, 3-Phase	$9,770.00	$19,540.00
3	2	Assy, Matrix, 3-Phase, Line	$6,783.00	$13,566.00
4	2	Assy, Matrix, 3-Phase, Rotor	$6,783.00	$13,566.00
5	1	Generator Control Board	$1,992.00	$1,992.00
6	2	Contactor, 810 A, 600 VAC, 3-pole, Line	$1,240.00	$2,480.00
7	1	Enclosure	$3,451.00	$3,451.00
8	1	Sub-Panel	$1,300.00	$1,300.00
9	8	Current transducers, 4 Line , 4 Gen	$268.00	$2,144.00
		Total		**$60,519.00**

1.5 MW IGBT-IGBT Drive
3-Phase IGBT Line/Gen Side Matrix

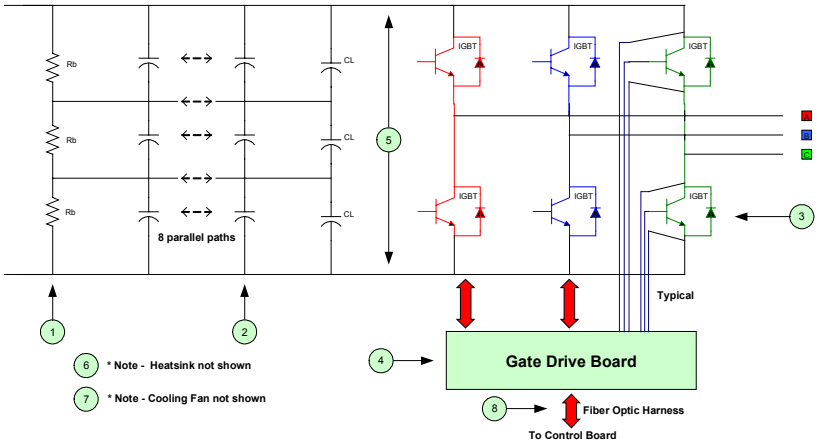

1.5 MW IGBT-IGBT Drive
3-Phase IGBT Line/Gen Side Matrix
BOM

Item #	Qty	Description	Unit Cost	Extended Cost
1	3	Resistor, Balance	$1.66	$5.00
2	24	Capacitor, 6500 uF, 450 Volt	$40.40	$969.00
3	6	IGBT, 2400 A, 1700 Volt	$496.00	$2,976.00
4	1	Gate Drive Board, Hex	$404.00	$404.00
5	1	Assy, Laminated Bus	$900.00	$900.00
6	1	Heatsink	$790.00	$790.00
7	1	Cooling Fan	$514.00	$514.00
8	1	Fiber Optic Harness	$225.00	$225.00
		Total		**$6,783.00**

1.5 MW IGBT-IGBT Drive
3-Phase Line Side Filter

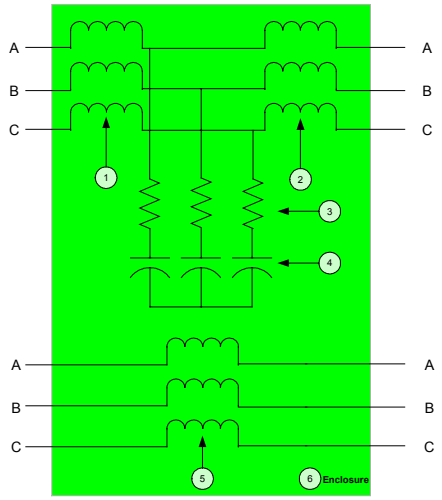

1.5 MW IGBT-IGBT Drive
3-Phase Line Side Filter
BOM

Item #	Qty	Description	Unit Cost	Extended Cost
1	1	Inductor, Reactor, Line, 250uH, 3-phase	$2,402.00	$2,402.00
2	1	Inductor, Reactor, PWM, 250uH, 3-phase	$2,916.00	$2,916.00
3	3	Resistor, Stainless, 3-phase, .1 OHM/phase	$76.00	$228.00
4	1	Capacitor, 20.8 KVAR, 3-phase, 690 Volt	$172.00	$172.00
5	1	Inductor, Reactor, Line, 250uH, 3-phase	$2,402.00	$2,402.00
6	1	Enclosure	$1,650.00	$1,650.00
		Total		**$9,770.00**

1.5 MW IGBT-IGBT Drive Sub-Panel BOM

Item #	Qty	Description	Unit Cost	Extended Cost
1	1	Fab, Panel, Pow er Dist	$127.00	$127.00
2	1	Sw itch, Disconnect, 80 A, 1000V	$36.00	$36.00
3	2	Circuit Breaker, 30A, 1000V	$152.00	$152.00
4	3	Fuse, 30A, 1000V	$12.00	$36.00
5	3	Fuseblock, 100A, 1000V	$21.00	$63.00
6	2	Res, 40 OHM, 250 W	$57.00	$114.00
7	2	Cap, Electrolytic, 3300 uF,	$23.00	$46.00
8	1	Assy, Harness, Main	$282.00	$282.00
9	1	Circuit Breaker, 20A, 1000V	$152.00	$152.00
10	1	Circuit Breaker, 2A, 1000V	$100.00	$100.00
11	4	SSR, 12A, 400 VDC, MOSFET OUT	$23.00	$92.00
12	1	Transformer, Control	$100.00	$100.00
		Total		**$1,300.00**

1.5 MW IGBT-IGBT Drive Pricing Estimates

1.5 MW IGBT-IGBT Drive						
Direct Variable Materials[1]	$	60,519	$	60,519	$	60,519
Direct Variable Labor[2]	$	1,560	$	1,560	$	1,560
Direct Fixed Costs[3]	$	9,312	$	9,312	$	9,312
Total Direct Costs	$	71,391	$	71,391	$	71,391
Gross Margin[4]		30%		40%		50%
Purchase Price	**$**	**101,987**	**$**	**118,985**	**$**	**142,782**

[1]Includes 3% freight in.
[2]Assumes 30% fringe benefits and 70% utilization, includes final assembly, board test, and final test.
[3]This number can vary significantly, 15% is used here.
[4]Gross Margin = (Sales Price - Direct Cost)/Sales Price

Wind Farm Power Factor and VAR Control System

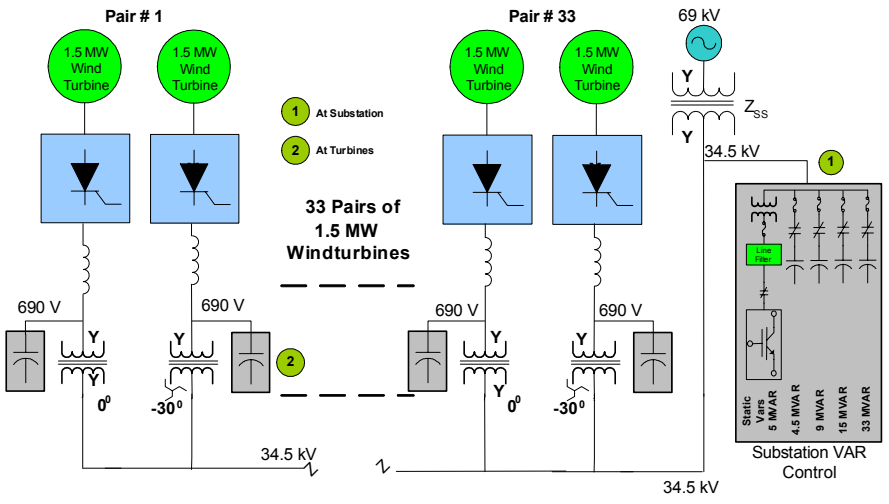

VAR Control Assembly – Cost per Turbine

Item #	Qty	Description		Unit Cost	Extended Cost
1	1	PF Correction ASSY - Substation		$762,805.00	$762,805.00
		Total			**$762,805.00**
		Cost for each turbine	**($762,805/66 Turbines)**		**$11,557.65**

3-Phase Power VAR Control Assembly
(1 for each substation)

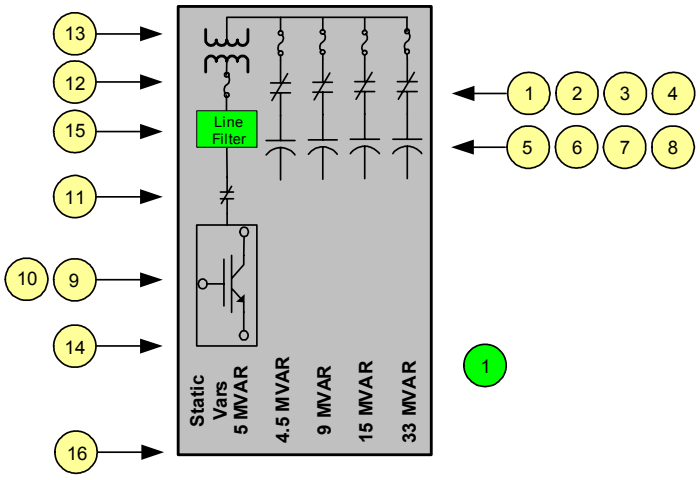

3-Phase Power VAR Control Assembly
Bill of Materials (BOM)

Item #	Qty	Description	Unit Cost	Extended Cost
1	1	100 A Fused - 400 A Contactor, 34.5 kV, 3-pole	$7,900.00	$7,900.00
2	1	200 A Fused - 400 A Contactor, 34.5 kV, 3-pole	$7,900.00	$7,900.00
3	1	400 A Fused - 400 A Contactor, 34.5 kV, 3-pole	$7,900.00	$7,900.00
4	1	400 A Fused - 400 A Contactor, 34.5 kV, 3-pole	$7,900.00	$7,900.00
5	9	Capacitors, 500kVAR, 34.5kV, (4.5MVAR)	$1,327.00	$11,943.00
6	18	Capacitors, 500kVAR, 34.5kV, (9.0MVAR)	$1,327.00	$23,886.00
7	30	Capacitors, 500kVAR, 34.5kV, (15.0MVAR)	$1,327.00	$39,810.00
8	66	Capacitors, 500kVAR, 34.5kV, (33.0MVAR)	$1,327.00	$87,582.00
9	10	IGBT Matrix, 1200 A, 1700 Volt	$5,442.00	$54,420.00
10	5	Control board	$1,892.00	$9,460.00
11	10	Contactor, 540 A, 600 VAC, 3-pole, Line	$692.00	$6,920.00
12	30	Fuseblock & Fuse, 500A, 1000V	$33.00	$990.00
13	1	Transformer, 5MVA	$42,000.00	$42,000.00
14	5	Enclosure, Static VAR	$2,200.00	$11,000.00
15	10	3-phase line filter	$5,302.00	$53,020.00
16	1	Enclosure, PF Correction Assy	$16,400.00	$16,400.00
		Total		**$389,031.00**

Static VAR
3-Phase IGBT Matrix

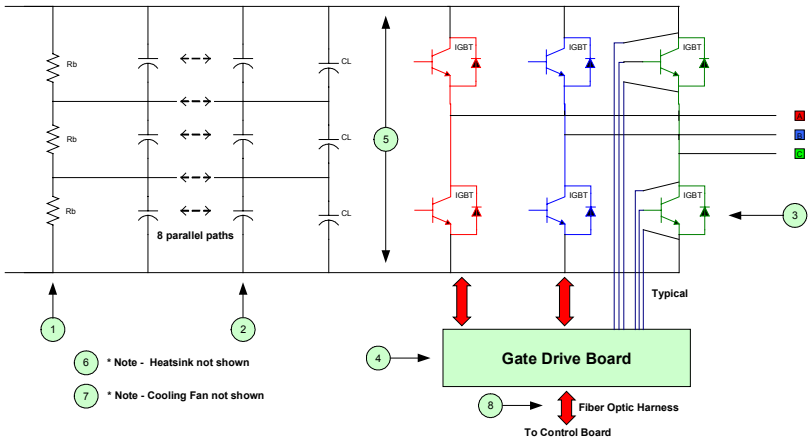

Static VAR
3-Phase IGBT Matrix
BOM

Item #	Qty	Description	Unit Cost	Extended Cost
1	3	Resistor, Balance	$1.66	$5.00
2	24	Capacitor, 5500 uF, 450 Volt	$35.40	$850.00
3	6	IGBT, 1200 A, 1700 Volt	$349.00	$2,094.00
4	1	Gate Drive Board, Hex	$404.00	$404.00
5	1	Assy, Laminated Bus	$900.00	$900.00
6	1	Heatsink	$450.00	$450.00
7	1	Cooling Fan	$514.00	$514.00
8	1	Fiber Optic Harness	$225.00	$225.00
		Total		**$5,442.00**

3-Phase Filter

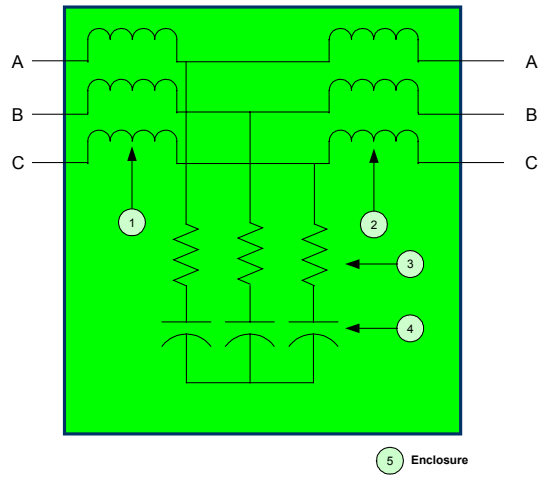

3-Phase Filter
BOM

Item #	Qty	Description	Unit Cost	Extended Cost
1	1	Inductor, Reactor, Line, 250uH, 3-phase	$1,547.00	$1,547.00
2	1	Inductor, Reactor, PWM, 250uH, 3-phase	$1,943.00	$1,943.00
3	3	Resistor, Stainless, 3-phase, .1 OHM/phase	$76.00	$228.00
4	1	Capacitor, 20.8 KVAR, 3-phase, 690 Volt	$172.00	$172.00
5	1	Enclosure	$1,412.00	$1,412.00
		Total		**$5,302.00**

VAR Control Pricing Estimates (100 MW Wind Farm)

PF Correction per Wind Turbine			
Direct Variable Materials[1]	$ 389,031	$ 389,031	$ 389,031
Direct Variable Labor[2]	$ 8,954	$ 8,954	$ 8,954
Direct Fixed Costs[3]	$ 59,698	$ 59,698	$ 59,698
Total Direct Costs	$ 457,683	$ 457,683	$ 457,683
Gross Margin[4]	30%	40%	50%
Purchase Price	**$ 653,833**	**$ 762,805**	**$ 915,366**

[1]Includes 3% freight in.
[2]Assumes 30% fringe benefits and 70% utilization, includes final assembly, board test, and final test.
[3]This number can vary significantly, 15% is used here.
[4]Gross Margin = (Sales Price - Direct Cost)/Sales Price

PF Correction - Rev. 4.7 9

Appendix G

Generator & PE Calculations

Baseline Generator Calculations

Wind Speed (m/s)	Rotor Speed W (rpm)	Gen Speed = (gear ratio)*(rotor speed)	Gen Slip = (gen synch speed - gen speed) /gen synch speed	Gen Input Power = (gearbox efficiency)*(rotor power)	Stator Power = (gen input power)/(1-slip)	Rotor Power = gen input power - stator power	Mag Current = line voltage/sqrt (3) / magnetizing reactance (referred to stator side) (A)	Stator Current = 1000 * stator pwr (kw) /(sqrt(3)*line-line voltage) Unity PF on stator side (A)	Stator DPF = stator displacement power factor= stator power/(sqrt(3)*stator voltage*stator current)	Rotor Freq. = ABS(slip)*60 (Hz)	Rotor Voltage = Rotor V (Volts line-line) = (rotor-stator turns ratio)*stator voltage*ABS(slip) (V)	Rotor Current = Rotor I (A) = sqrt(stator current^2 + mag current ^2)/rotor-stator turns ratio (PE controlled so unity PF on stator side) (A)	Rotor DPF = Rotor displacement power factor= ABS(rotor power)/(sqrt(3)*rotor voltage*rotor I)	Core Loss = constant	Stator Loss = Stator I^R loss (kW) = 3* (stator I(A))^2*.001*(stator R(ohms)) (I^2*R)	Rotor Loss = Windage loss (kW)= windage loss factor * gen speed (windage)	Rotor loss = Rotor I^2*R loss (kW) = 3* Rotor I(A)^2 * Rotor R * .0001 (I^2*R)	Total Gen Loss = Gen loss (total - kW) = Rotor I^2*R loss + Stator I^2*R loss + core loss + windage	Gen Efficiency = Generator efficiency = (gen input power - gen loss)/gen input power
3.0	12.28	900.0	0.25	5.7	7.6	-1.9	553.3	6.3	1.00	15.0	518	184	0.01	11.0	0.0	2.7	3.6	17.3	0.0%
3.5	12.28	900.0	0.25	24.4	32.6	-8.1	553.3	27.3	1.00	15.0	518	185	0.05	11.0	0.0	2.7	3.6	17.3	29.3%
4.0	12.28	900.0	0.25	49.8	66.4	-16.6	553.3	55.6	1.00	15.0	518	185	0.10	11.0	0.0	2.7	3.6	17.3	65.2%
4.5	12.28	900.0	0.25	83.4	111.2	-27.8	553.3	93.1	1.00	15.0	518	187	0.17	11.0	0.1	2.7	3.7	17.5	79.1%
5.0	12.28	900.0	0.25	126.5	168.7	-42.2	553.3	141.2	1.00	15.0	518	190	0.25	11.0	0.2	2.7	3.8	17.7	86.0%
5.5	12.28	900.0	0.25	179.1	238.8	-59.7	553.3	199.8	1.00	15.0	518	196	0.34	11.0	0.5	2.7	4.0	18.2	89.8%
6.0	12.28	900.0	0.25	239.0	318.6	-79.7	553.3	266.6	1.00	15.0	518	205	0.43	11.0	0.8	2.7	4.4	18.9	92.1%
6.5	12.42	910.1	0.24	308.5	406.7	-98.2	553.3	340.3	1.00	14.5	500	217	0.52	11.0	1.3	2.7	4.9	20.0	93.5%
7.0	13.37	980.1	0.18	387.3	474.2	-86.9	553.3	396.8	1.00	11.0	379	227	0.58	11.0	1.8	2.9	5.4	21.1	94.5%
7.5	14.33	1050.1	0.12	478.9	547.2	-68.3	553.3	457.9	1.00	7.5	259	239	0.64	11.0	2.4	3.2	6.0	22.6	95.3%
8.0	15.28	1120.2	0.07	584.2	625.9	-41.6	553.3	523.7	1.00	4.0	138	254	0.69	11.0	3.1	3.4	6.8	24.3	95.8%
8.5	16.24	1190.2	0.01	704.4	710.2	-5.8	553.3	594.3	1.00	0.5	17	271	0.73	11.0	4.0	3.6	7.7	26.3	96.3%
9.0	17.19	1260.2	-0.05	840.5	800.4	40.1	553.3	669.7	1.00	3.0	104	290	0.77	11.0	5.1	3.8	8.8	28.7	96.6%
9.5	18.15	1330.2	-0.11	988.5	891.8	96.7	553.3	746.2	1.00	6.5	225	310	0.80	11.0	6.3	4.0	10.1	31.4	96.8%
10.0	19.10	1400.2	-0.17	1158.9	993.2	165.7	553.3	831.1	1.00	10.0	345	333	0.83	11.0	7.9	4.2	11.6	34.7	97.0%
10.5	20.06	1470.2	-0.23	1348.4	1100.6	247.8	553.3	921.0	1.00	13.5	466	358	0.86	11.0	9.7	4.4	13.5	38.5	97.1%
11.0	20.47	1500.2	-0.25	1538.4	1230.6	307.9	553.3	1029.8	1.00	15.0	518	390	0.88	11.0	12.1	4.5	15.9	43.5	97.2%
11.5-27.5	20.47	1500.2	-0.25	1568.0	1254.2	313.8	553.3	1049.6	1.00	15.0	518	395	0.88	11.0	12.6	4.5	16.4	44.5	97.2%
8% overspeed	22.10	1619.9	-0.35	1568.0	1161.5	406.5	553.3	972.0	1.00	21.0	724	373	0.87	11.0	10.8	4.9	14.6	41.2	97.4%
14% overspeed	23.33	1710.1	-0.43	1568.0	1100.3	467.7	553.3	920.7	1.00	25.5	880	358	0.86	11.0	9.7	5.1	13.5	39.3	97.5%

Parameters Used for Calculations

Magnetizing reactance (referred to stator)	0.72 ohms	**Gearbox Ratio**	73.3
Stator leakage reactance	0.017 ohms	**Synchronous gen speed**	1200 rpm
Rotor/stator turns ratio	3	**Line-line output voltage**	690 volts
Rotor resistance (referred to rotor)	0.035 ohms	**Generator core losses (25%)**	11 kW
Stator resistance	0.0038 ohms	**Generator windage loss factor**	0.003 kW/rpm

Stator and rotor resistances are adjusted by a factor of 2.7 to account for stray load loss and give a full load efficiency of 97%.

Baseline PE System Calculations

Wind Speed (m/s)	From generator spreadsheet Rotor DPF DPFgen	Vgen = sqrt(2) * RMS rotor voltage (gen spreadsheet) Rotor Voltage (pk l-l) (V) Vgen	Igen = sqrt(2) * RMS rotor current (gen spreadsheet) Rotor Current (pk amps) (A) Igen	Mgen = Vgen/Vdc Gen Inverter Mod. Index Mgeninv	Gen inverter IGBT conduction loss = .001*(0.5*(VCEO*Igen/PI()+Rdigbt*Igen*Igen/4)+Mgeninv*DPFgen*(VCEO*Igen/8+1/3/PI()*Rdigbt*Igen*Igen)) Gen Inv IGBT Cond Loss (kW)	Gen inverter IGBT switching loss = .001*fpwm/PI()*(Eon+Eoff)*Igen/Inom*Vdc/Vnom Gen Inv IGBT Sw Loss (kW)	Gen inverter diode conduction loss = .001*(0.5*(Vd0*Igen/PI()+rd*Igen*Igen/4)-Mgeninv*DPFgen*(Vd0*Igen/8+1/3/PI()*rd*Igen*Igen)) Gen Inv Diode Cond Loss (kW)	Gen inverter diode switching loss = .001/PI()*fpwm*Erec*(0.45*Igen/Inom+0.55)*Vdc/Vnom Gen Inv Diode Sw Loss (kW)	Generator inverter total loss = 6*(IGBT cond loss + IGBT sw loss + diode cond loss + diode sw loss)+fixedloss Gen Inv Total Loss (kW) Pinvloss	Igrid = sqrt(2)*(ABS (rotor power) - 2*(gen inv total loss))/(SQRT(3)*690)) Grid Inverter Cur. (pk) (A) Igrid	DPFgridinv = ABS((gen rotor power) -2*(gen total inverter loss))/(SQRT(3)*Igrid/SQRT(2)*690) Grid Inverter DPF DPFgridinv	Grid inverter IGBT conduction loss = 0.001*(0.5*(VCEO*Igrid/PI()+Rdigbt*Igrid/4)+Mgridinv*DPFgridinv*(VCEO*Igrid/8+1/3/PI()*Rdigbt*Igrid)) Util Inv IGBT Cond loss (kW)	Gen inverter IGBT switching loss = 0.001*(fpwm/PI()*(Eon+Eoff)*Igrid/Inom*Vdc/Vnom) Util Inv IGBT Sw loss (kW)	Gen inverter diode conduction loss = 0.001*(0.5*(Vd0*Igrid/PI()+rd*Igrid*Igrid/4)-Mgridinv*DPFgridinv*(Vd0*Igrid/8+1/3/PI()*rd*Igrid*Igrid)) Util Inv Diode Cond loss (kW)	Gen inverter diode switching loss = 0.001*(1/PI()*fpwm*Erec*(0.45*Igrid/Inom+0.55)*Vdc/Vnom) Util Inv Diode Sw loss (kW)	Generator inverter total loss = 6*(IGBT cond loss + IGBT sw loss + diode cond loss + diode sw loss)+fixedloss Util Inv Total Loss (kW)	Filter losses = 0.001*0.077*((gen rotor current)/SQRT(2))^2 Filter Losses (kW)	Total PE loss = gen inverter loss + util inverter loss + filter loss Total PE Loss (kW)	PE effective efficiency = (generator input power - total PE loss)/generator input power PE Effective Efficiency
3	0.011	732	261	0.67	0.07	0.22	0.06	0.02	4.21	12	1.000	0.00	0.01	0.00	0.02	2.21	2.62	9.04	-59.3%
3.5	0.049	732	261	0.67	0.08	0.22	0.05	0.02	4.22	20	1.000	0.01	0.02	0.00	0.02	2.27	2.63	9.11	62.7%
4	0.100	732	262	0.67	0.08	0.22	0.05	0.02	4.23	30	1.000	0.01	0.02	0.00	0.02	2.35	2.65	9.22	81.5%
4.5	0.166	732	264	0.67	0.08	0.22	0.05	0.02	4.25	43	1.000	0.02	0.04	0.00	0.02	2.46	2.69	9.40	88.7%
5	0.247	732	269	0.67	0.09	0.22	0.05	0.02	4.29	60	1.000	0.03	0.05	0.00	0.02	2.59	2.79	9.68	92.4%
5.5	0.340	732	277	0.67	0.09	0.23	0.05	0.02	4.37	81	1.000	0.03	0.07	0.00	0.02	2.76	2.96	10.09	94.4%
6	0.434	732	290	0.67	0.10	0.24	0.05	0.02	4.48	105	1.000	0.05	0.09	0.01	0.02	2.96	3.23	10.67	95.5%
6.5	0.524	707	306	0.64	0.11	0.25	0.05	0.02	4.63	127	1.000	0.06	0.11	0.01	0.02	3.14	3.61	11.38	96.3%
7	0.583	536	321	0.49	0.12	0.27	0.05	0.02	4.75	114	1.000	0.05	0.09	0.01	0.02	3.03	3.97	11.75	97.0%
7.5	0.638	366	339	0.33	0.12	0.28	0.06	0.02	4.90	92	1.000	0.04	0.08	0.01	0.02	2.86	4.41	12.17	97.5%
8	0.687	195	359	0.18	0.12	0.30	0.07	0.02	5.07	61	1.000	0.03	0.05	0.00	0.02	2.60	4.97	12.63	97.8%
8.5	0.732	24	383	0.02	0.12	0.32	0.08	0.02	5.26	19	1.000	0.01	0.02	0.00	0.02	2.27	5.64	13.17	98.1%
9	0.771	147	410	0.13	0.14	0.34	0.08	0.02	5.51	34	1.000	0.01	0.03	0.00	0.02	2.39	6.46	14.35	98.3%
9.5	0.803	318	438	0.29	0.16	0.36	0.08	0.03	5.78	101	1.000	0.04	0.08	0.01	0.02	2.92	7.38	16.09	98.4%
10	0.832	488	471	0.44	0.19	0.39	0.08	0.03	6.11	182	1.000	0.08	0.15	0.01	0.02	3.60	8.53	18.24	98.4%
10.5	0.857	659	506	0.60	0.23	0.42	0.07	0.03	6.48	278	1.000	0.14	0.23	0.02	0.02	4.44	9.88	20.79	98.5%
11	0.881	732	551	0.67	0.27	0.46	0.07	0.03	6.92	348	1.000	0.18	0.29	0.02	0.02	5.07	11.69	23.68	98.5%
11.5-27.5	0.885	732	559	0.67	0.28	0.46	0.07	0.03	7.00	355	1.000	0.18	0.29	0.02	0.02	5.13	12.04	24.18	98.5%
8% overspeed	0.869	1024	527	0.93	0.29	0.44	0.04	0.03	6.75	465	1.000	0.25	0.38	0.03	0.03	6.16	10.70	23.61	98.5%
14% overspeed	0.857	1244	506	1.13	0.29	0.42	0.03	0.03	6.58	538	1.000	0.30	0.44	0.04	0.03	6.87	9.87	23.33	98.5%

Parameters Used for Calculations

Inverter parameters common to both bridges		Inverter parameters common to both bridges		Parameters specific to grid inverter	
DC bus voltage (volts)	**Vdc =** 1100	IGBT turn-on energy loss (Joules)	**Eon =** 3.50E-01	Grid RMS line-line voltage	**VgridRMS =** 690
PWM switching frequency - Hz	**fpwm =** 3000	IGBT turn-off energy loss (Joules)	**Eoff =** 5.00E-01	Modulation index; m = Vac/Vdc	**Mgridinv =** 0.887098
IGBT Vceo (fixed portion Vce - volts)	**VCEO =** 1.5	Current for Eon, Eoff (Amps)	**Inom =** 1200		
IGBT dynamic resistance (Ohms)	**rdigbt =** 1.36E-03	Voltage for Eon, Eoff (volts)	**Vnom =** 900		
Diode Vd0 (fixed portion Vd - volts)	**Vd0 =** 1.25	Diode recovery energy loss (Joules - at Inom, Vnom	**Erec =** 3.00E-02		
Diode dynamic resistance (Ohms)	**rddiode =** 5.00E-04	Fixed loss per bridge (fans, gate drivers, etc.- kW)	**fixedloss =** 2		

PM Generator Equivalent Circuit and Phaser Diagrams

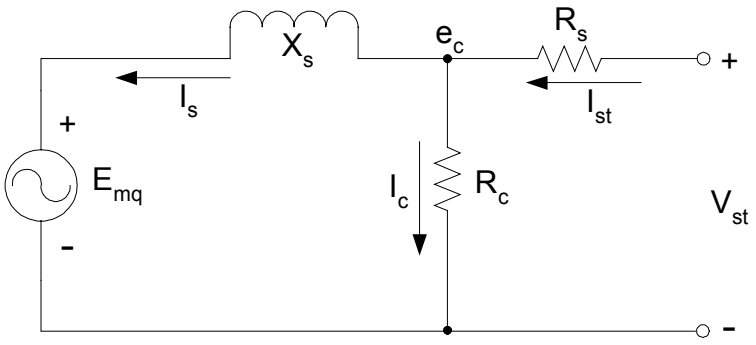

Figure G-1. PM Generator Per-Phase Equivalent Circuit

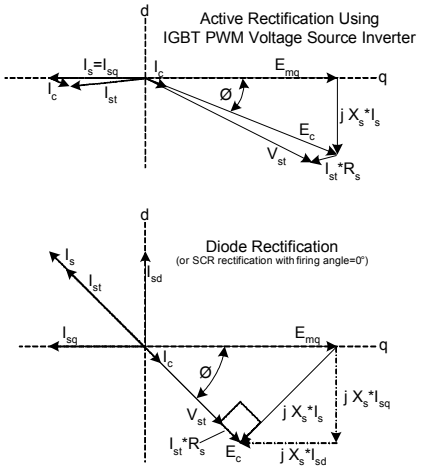

Figure A-2. PM Generator Phaser Diagrams

Single PM Generator Efficiency Calculations, SCR-SCR System

Wind Speed (m/s)	Rotor Speed (rpm)	Gen Spd (rpm)	Gen. Input Power	Gen. Freq.	Input Power	Core losses (kW) Eddy Loss	Hyst Loss	Core Loss	Phase React. (ohms)	Phase Voltage pk l-n	q-axis Current (A pk)	d-axis Current (A pk)		Internal Voltage pk l-n			Core Loss I (A pk)						pk l-n Terminal Voltage	Cu Loss (kW)	Gen. Eff.
		w = ratio*rotor speed	Pgenin = rotor power * gearbox efficiency	fe = p*w/120	Pin = Pgenin/(p/2)	eddy = eddyo*L/Lo*(fe/feo)^2	hyst = hysto*L/Lo*fe/feo	coreloss = eddy+hyst	Xs = 2*PI()*fe*Ls	Emq = Emqo*L/Lo*fe/feo*N/No	Isq = -1000*Pin/(3/2*Emq)	Isd = 0.5*(-Emq/Xs+SQRT((Emq/Xs)^2 -4*Isq^2))	Is = SQRT(Isd^2+Isq^2)	Ec = SQRT((Emq+Xs*Isd)^2+(Xs*Isq)^2)	cos = Ec/Emq	sin = SQRT(1-cos^2)	Ic = 1000*coreloss/(3/2*Ec)	Istq = Isq+Ic*cos	Istd = Isd+Ic*sin	Ist = SQRT(Istd^2+Istq^2)	Vstq = Ec*cos+Rs*Istq	Vstd = Ec*sin+Rs*Istd	Vst = SQRT(Vstd^2+Vstq^2)	Pcu = 3/2*Ist^2*Rs/1000	ngen = (Pin-coreloss-Pcu)/Pin
		w	Pgenin	fe	Pin	eddy	hyst.	coreloss	Xs	Emq	Isq	Isd	Is	Ec	cos	sin	Ic	Istq	Istd	Ist	Vstq	Vstd	Vst	Pcu	ngen
3.0	5.7	45.8	30	21.4	1.1	0.02	0.02	0.04	0.07	41.9	-16.8	-0.5	16.8	41.9	1.00	0.03	0.60	-16.2	-0.4	16.2	41.7	1.1	41.8	0.00	96.0%
3.5	6.7	53.5	48	25.0	1.7	0.02	0.03	0.05	0.08	48.9	-23.5	-0.9	23.5	48.9	1.00	0.04	0.64	-22.9	-0.9	22.9	48.6	1.9	48.7	0.01	96.8%
4.0	7.6	61.1	73	28.5	2.6	0.03	0.03	0.06	0.09	55.9	-31.0	-1.6	31.0	55.8	1.00	0.05	0.68	-30.3	-1.5	30.3	55.5	2.8	55.5	0.01	97.3%
4.5	8.6	68.8	104	32.1	3.7	0.03	0.03	0.07	0.10	62.9	-39.4	-2.5	39.5	62.8	1.00	0.06	0.72	-38.7	-2.5	38.8	62.3	4.0	62.4	0.02	97.6%
5.0	9.6	76.4	143	35.7	5.1	0.04	0.04	0.08	0.11	69.9	-48.8	-3.9	49.0	69.7	1.00	0.08	0.76	-48.1	-3.8	48.2	69.0	5.5	69.2	0.03	97.8%
5.5	10.5	84.0	191	39.2	6.8	0.05	0.04	0.09	0.12	76.9	-59.2	-5.7	59.5	76.5	1.00	0.10	0.81	-58.4	-5.6	58.7	75.6	7.3	75.9	0.05	97.9%
6.0	11.5	91.7	249	42.8	8.9	0.06	0.05	0.11	0.14	83.9	-70.7	-8.2	71.1	83.3	0.99	0.11	0.85	-69.8	-8.1	70.3	82.1	9.5	82.6	0.07	98.0%
6.5	12.4	99.3	317	46.4	11.3	0.07	0.05	0.12	0.15	90.9	-83.2	-11.4	83.9	90.0	0.99	0.14	0.89	-82.3	-11.3	83.0	88.4	12.1	89.2	0.10	98.0%
7.0	13.4	107.0	397	49.9	14.2	0.08	0.05	0.14	0.16	97.8	-96.7	-15.5	97.9	96.6	0.99	0.16	0.93	-95.8	-15.3	97.0	94.4	15.1	95.6	0.14	98.1%
7.5	14.3	114.6	490	53.5	17.5	0.09	0.06	0.15	0.17	104.8	-111.3	-20.7	113.2	103.1	0.98	0.18	0.98	-110.3	-20.5	112.2	100.2	18.6	101.9	0.19	98.1%
8.0	15.3	122.3	596	57.1	21.3	0.11	0.06	0.17	0.18	111.8	-127.0	-27.2	129.9	109.3	0.98	0.21	1.02	-126.0	-27.0	128.8	105.6	22.7	108.0	0.25	98.0%
8.5	16.2	129.9	717	60.6	25.6	0.12	0.06	0.19	0.19	118.8	-143.7	-35.4	148.0	115.4	0.97	0.24	1.07	-142.7	-35.1	146.9	110.6	27.2	113.9	0.32	98.0%
9.0	17.2	137.5	853	64.2	30.5	0.14	0.07	0.20	0.20	125.8	-161.5	-45.5	167.8	121.1	0.96	0.27	1.12	-160.4	-45.2	166.7	114.9	32.4	119.4	0.42	98.0%
9.5	18.1	145.2	1004	67.7	35.8	0.15	0.07	0.22	0.21	132.8	-180.0	-57.7	189.0	126.4	0.95	0.31	1.18	-178.8	-57.4	187.8	118.6	38.0	124.6	0.53	97.9%
10.0	19.1	152.8	1174	71.3	41.9	0.17	0.08	0.24	0.23	139.8	-199.9	-73.2	212.9	131.2	0.94	0.34	1.23	-198.8	-72.8	211.7	121.2	44.4	129.1	0.67	97.8%
10.5	20.1	160.5	1362	74.9	48.6	0.18	0.08	0.26	0.24	146.8	-221.0	-92.8	239.7	135.3	0.92	0.39	1.30	-219.8	-92.3	238.4	122.6	51.5	132.9	0.85	97.7%
11.0	20.5	163.7	1554	76.4	55.5	0.19	0.08	0.27	0.24	149.8	-247.1	-123.1	276.1	134.0	0.90	0.45	1.36	-245.9	-122.5	274.7	117.5	58.6	131.3	1.13	97.5%
11.5-27.5	20.5	163.7	1564	76.4	55.9	0.19	0.08	0.27	0.24	149.8	-248.7	-125.3	278.5	133.7	0.89	0.45	1.36	-247.5	-124.7	277.1	117.0	58.9	131.0	1.15	97.4%
8% overspeed	22.1	176.8	1564	82.5	55.9	0.22	0.09	0.31	0.26	161.7	-230.3	-102.8	252.2	147.7	0.91	0.41	1.41	-229.0	-102.2	250.8	132.6	59.1	145.2	0.94	97.8%
14% overspeed	23.3	186.6	1564	87.1	55.9	0.25	0.09	0.34	0.28	170.7	-218.2	-90.0	236.0	157.8	0.92	0.38	1.44	-216.8	-89.4	234.5	143.7	59.3	155.5	0.83	97.9%

Base machine quantities

Stator phase resistance (entire machine - ohms)	5.72E-03	Rsbase
Stator phase inductance (entire machine - Hy)	2.88E-04	Lsbase
Phase voltage (pk l-n) at rated speed	600	Emqbase
Machine pole connection	4 series, 7 parallel	
Base machine pole number	56	po
Rated speed	164	
Rated power output (kw)	1500	

Base machine pole pair quantities

Freq at rated speed (Hz)	76.5	feo = rated speed *po/120
Airgap length (m)	0.25	Lo
Turns ratio	1	No
Power output per pole pair (kw)	53.6	Pro = rated power/(po/2)
Stator per pole-pair phase resistance (ohms)	1.00E-02	Rso = 7/4*Rsbase
Stator per pole-pair phase inductance (Hy)	5.04E-04	Lso = 7/4*Lsbase
Fraction of winding copper in the slots	75%	ms
Fraction of winding copper in the end turns	25%	me
Pole pair eddy current loss (kw)	0.192	eddyo
Pole pair hysteresis loss (kw)	0.082	hysto
Phase voltage (pk l-n) at rated speed	150.0	Emqo = Emqbase/4

Scaled machine quantities

Airgap length	0.250	L
Turns ratio	1	N
Gearbox ratio	8	ratio
Pole number	56	p
Power output (kW)	1500	
Stator phase resistance (ohms)	1.00E-02	Rs = Rso*(me+ms*L/Lo)*(N/No)^2
Stator phase inductance (Hy)	5.04E-04	Ls = Lso*(L/Lo)*(N/No)^2

Single PM Power Electronics Efficiency Calculations, SCR-SCR System

Wind Speed (m/s)	RPM = rotor speed * gear ratio Gen Speed (rpm) RPM	From gen calculations Gen Power Output (kW) Pgout	emf = EMFllrated*SQRT(2) /SQRT(3)*RPM/rated RPM Gen EMF (pk l-n) emf	From gen calculations Gen Freq (Hz) Fgen	From gen calculations Gen Term DPF DPFgen	Vgen = emf*Vst/Emq Gen Volts (pk l-n) Vgen	Igen = SQRT(2)*1000*Pgout /(3*DPFgen*Vgen/SQRT(2)) Generator Output Current (pk amps) Igen	Vdc = 1.35*SQRT(3)/SQRT(2)*Vgen DC Bus Volts (volts) Vdc	Idc = 1000*Pgout/Vdc DC Bus I Idc	bridgeloss = 2*Vscr*Idc/1000 Bridge Loss (kW) bridgeloss	reactloss = Rreact*Idc^2/1000\ DC Reactor Loss (kW) reactloss	Pgridin = Pgout-bridgeloss-reactloss Grid Inverter Power Input (kW)	DPFgrid = 0.9*Vdc/(1.35*Vgrid) Grid Terminal DPF DPFgrid	Igrid = 1000*Q12/(SQRT(3)*Vgrid*DPFg Grid Current (RMS) Igrid	invloss = 2*Vscr*Idc/1000 Grid Inverter Loss (kW) invloss	PEloss = bridgeloss+reactloss+invloss Total PE Loss (kW) PEloss	PE efficiency = (Pgout-PEloss)/(Pgout) Total PE Efficiency
3	45.8	28	168	21.4	1.000	167	113	276	103	0.6	0.0	28	0.267	87	0.62	1.24	95.6%
3.5	53.5	47	196	25.0	1.000	195	160	322	145	0.9	0.0	46	0.311	124	0.87	1.77	96.2%
4	61.1	71	224	28.5	1.000	222	212	367	193	1.2	0.0	70	0.355	164	1.16	2.35	96.7%
4.5	68.8	102	252	32.1	1.000	250	271	413	246	1.5	0.1	100	0.399	210	1.48	3.02	97.0%
5	76.4	140	280	35.7	1.000	277	337	458	306	1.8	0.1	138	0.442	261	1.84	3.77	97.3%
5.5	84.0	187	308	39.2	1.000	304	411	502	373	2.2	0.1	185	0.485	319	2.24	4.61	97.5%
6	91.7	244	336	42.8	1.000	331	492	547	446	2.7	0.2	241	0.528	382	2.68	5.55	97.7%
6.5	99.3	311	364	46.4	1.000	357	581	590	527	3.2	0.3	308	0.570	451	3.16	6.60	97.9%
7	107.0	390	392	49.9	1.000	383	679	633	616	3.7	0.4	386	0.611	528	3.69	7.77	98.0%
7.5	114.6	480	420	53.5	1.000	408	785	674	712	4.3	0.5	476	0.652	611	4.27	9.06	98.1%
8	122.3	585	447	57.1	1.000	432	901	715	818	4.9	0.7	579	0.691	701	4.91	10.48	98.2%
8.5	129.9	703	475	60.6	1.000	456	1028	754	933	5.6	0.9	696	0.728	800	5.60	12.06	98.3%
9	137.5	836	503	64.2	1.000	478	1166	790	1058	6.3	1.1	829	0.763	908	6.35	13.82	98.3%
9.5	145.2	983	531	67.7	1.000	498	1314	824	1192	7.2	1.4	974	0.796	1023	7.15	15.73	98.4%
10	152.8	1148	559	71.3	1.000	517	1481	854	1344	8.1	1.8	1138	0.825	1154	8.06	17.93	98.4%
10.5	160.5	1331	587	74.9	1.000	532	1668	880	1513	9.1	2.3	1319	0.850	1299	9.08	20.45	98.5%
11	163.7	1515	599	76.4	1.000	525	1922	869	1744	10.5	3.0	1501	0.839	1497	10.46	23.96	98.4%
11.5-27.5	163.7	1524	599	76.4	1.000	524	1939	867	1759	10.6	3.1	1511	0.837	1510	10.55	24.20	98.4%
8% overspeed	176.8	1529	647	82.5	1.000	581	1755	961	1592	9.6	2.5	1517	0.928	1368	9.55	21.64	98.6%
14% overspeed	186.6	1531	683	87.1	1.000	622	1641	1029	1489	8.9	2.2	1520	0.994	1280	8.93	20.08	98.7%

Parameters used for PE efficiency calculations

AC grid voltage line-line RMS	Vgrid = 690
Average SCR voltage drop	Vd = 3
DC link inductor resistance (ohms)	Rreact = 0.001

Single PM Generator Efficiency Calculations, Diode-IGBT System

Wind Speed (m/s)	Rotor Speed (rpm)	Gen Speed (rpm)	Gen. Input Power	Gen. Freq.	Input Power	Core losses: Eddy Current	Core losses: Hyst.	Core Loss	Phase React.	Phase Voltage (pk l-n)	q-axis Current (A-pk)	d-axis Current (A-pk)	(A-pk)	Internal Voltage (pk l-n)			Core Loss I (A-pk)	(A-pk)	(A-pk)	(A-pk)	Cu Loss (kW)	Gen. Eff.
		w = gearbox ratio*rotor speed	Pgenin = rotor power*gearbox ratio	fe = p*w/120	Pin = Pgenin/(p/2)	eddy = eddyo*L/Lo*(fe/feo)^2	hyst = hysto*L/Lo*fe/feo	coreloss = eddy+hyst	Xs = 2*PI()*fe*Ls	Emq = Emqo*L/Lo*fe/feo*N/No	Ist = -1000*Pin/(3/2*Emq)	Isd = 0.5*(-Emq/Xs+SQRT((Emq/Xs)^2-4*Isq^2))	Is = SQRT(Isd^2+Isq^2)	Ec = SQRT((Emq+Xs*Isd)^2+(Xs*Isq)^2)	cos = Ec/Emq	sin = SQRT(1-cos^2)	Ic = 1000*coreloss/(3/2*Ec)	Istq = Isq+Ic*cos	Istd = Isd+Ic*sin	Ist = SQRT(Istd^2+Istq^2)	Pcu = 3/2*Ist^2*Rs/1000	ngen = (Pin-coreloss-Pcu)/Pin
		w	Pgenin	fe	Pin	eddy	hyst.	coreloss	Xs	Emq	Isq	Isd	Is	Ec	cos	sin	Ic	Istq	Istd	Ist	Pcu	ngen
3.0	10.3	82	30	38	1.1	0.05	0.04	0.09	0.12	75	-9	-0.1	9	75	1.00	0.02	0.79	-8.6	-0.1	8.6	0.00	91.5%
3.5	10.3	82	48	38	1.7	0.05	0.04	0.09	0.12	75	-15	-0.4	15	75	1.00	0.02	0.79	-14.6	-0.4	14.6	0.00	94.7%
4.0	10.3	82	73	38	2.6	0.05	0.04	0.09	0.12	75	-23	-0.9	23	75	1.00	0.04	0.79	-22.3	-0.8	22.3	0.01	96.3%
4.5	10.3	82	104	38	3.7	0.05	0.04	0.09	0.12	75	-33	-1.8	33	75	1.00	0.05	0.79	-32.2	-1.7	32.2	0.02	97.2%
5.0	10.3	82	143	38	5.1	0.05	0.04	0.09	0.12	75	-45	-3.4	46	75	1.00	0.07	0.79	-44.7	-3.3	44.8	0.03	97.7%
5.5	10.5	84	191	39	6.8	0.05	0.04	0.09	0.12	77	-59	-5.7	59	77	1.00	0.10	0.81	-58.4	-5.6	58.7	0.05	97.9%
6.0	11.5	92	249	43	8.9	0.06	0.05	0.11	0.14	84	-71	-8.2	71	83	0.99	0.11	0.85	-69.8	-8.1	70.3	0.07	98.0%
6.5	12.4	99	317	46	11.3	0.07	0.05	0.12	0.15	91	-83	-11.4	84	90	0.99	0.14	0.89	-82.3	-11.3	83.0	0.10	98.0%
7.0	13.4	107	397	50	14.2	0.08	0.05	0.14	0.16	98	-97	-15.5	98	97	0.99	0.16	0.93	-95.8	-15.3	97.0	0.14	98.1%
7.5	14.3	115	490	53	17.5	0.09	0.06	0.15	0.17	105	-111	-20.7	113	103	0.98	0.18	0.98	-110.3	-20.5	112.2	0.19	98.1%
8.0	15.3	122	596	57	21.3	0.11	0.06	0.17	0.18	112	-127	-27.2	130	109	0.98	0.21	1.02	-126.0	-27.0	128.8	0.25	98.0%
8.5	16.2	130	717	61	25.6	0.12	0.06	0.19	0.19	119	-144	-35.4	148	115	0.97	0.24	1.07	-142.7	-35.1	146.9	0.32	98.0%
9.0	17.2	138	853	64	30.5	0.14	0.07	0.20	0.20	126	-162	-45.5	168	121	0.96	0.27	1.12	-160.4	-45.2	166.7	0.42	98.0%
9.5	18.1	145	1004	68	35.8	0.15	0.07	0.22	0.21	133	-180	-57.7	189	126	0.95	0.31	1.18	-178.8	-57.4	187.8	0.53	97.9%
10.0	19.1	153	1174	71	41.9	0.17	0.08	0.24	0.23	140	-200	-73.2	213	131	0.94	0.34	1.23	-198.8	-72.8	211.7	0.67	97.8%
10.5	20.1	160	1362	75	48.6	0.18	0.08	0.26	0.24	147	-221	-92.8	240	135	0.92	0.39	1.30	-219.8	-92.3	238.4	0.85	97.7%
11.0	20.5	164	1554	76	55.5	0.19	0.08	0.27	0.24	150	-247	-123.1	276	134	0.90	0.45	1.36	-245.9	-122.5	274.7	1.13	97.5%
11.5-27.5	20.5	164	1617	76	57.7	0.19	0.08	0.27	0.24	150	-257	-137.1	291	132	0.88	0.47	1.38	-255.8	-136.5	289.9	1.26	97.3%
8% overspeed	22.1	177	1617	83	57.7	0.22	0.09	0.31	0.26	162	-238	-111.7	263	146	0.91	0.42	1.42	-236.7	-111.1	261.5	1.03	97.7%
14% overspeed	23.3	186	1617	87	57.7	0.25	0.09	0.34	0.28	170	-226	-97.8	246	156	0.92	0.40	1.45	-224.4	-97.2	244.6	0.90	97.9%

Base machine quantities

Stator phase resistance (entire machine - ohms)	5.72E-03	Rsbase
Stator phase inductance (entire machine - ohms)	2.88E-04	Lsbase
Phase voltage (pk l-n) at rated speed	600	Emqbase
Machine pole connection	4 series, 7 parallel	
Base machine pole number	56	po
Rated speed	164	
Rated power output (kW)	1500	

Base machine pole pair quantities

Freq at rated speed (Hz)	76.5	feo = RPM *po/120
Airgap length (m)	0.25	Lo
Turns ratio	1	No
Power output per pole pair (kW)	53.6	Pro
Stator per pole-pair phase resistance (ohms)	1.00E-02	Rso
Stator per pole-pair phase inductance (Hy)	5.04E-04	Lso
Fraction of winding copper in the slots	75%	ms
Fraction of winding copper in the end turns	25%	me
Pole pair eddy current loss (kW)	0.192	eddyo
Pole pair hysteresis loss (kW)	0.082	hysto
Phase voltage (pk l-n) at rated speed	150.0	Emqo

Scaled machine quantities

Airgap length	0.250	L
Turns ratio	1	N
Gearbox ratio	8	ratio
Pole number	56	p
Power output (kW)	1500	

Single PM Power Electronics Efficiency Calculations, Diode-IGBT System

Wind Speed	Gen Speed	Gen Pwr Out	Gen EMF	Gen Freq	Gen Term DPF	Gen Volts	Gen Output Current	DC Bus Volts	Bridge Loss	DC Bus Idc	Grid Inv. Pwr In	Grid Inv Mod. Index	Grid I	1/2 Igrid	Util Inv IGBT Cnd Loss	Util Inv IGBT Sw Loss	Util Inv Diode Cnd Loss	Util Inv Diode Sw Loss	Util inv Total Loss	Filter Loss	Total Loss	Total PE Eff
	RPM = rotor speed * gear ratio	From gen calcs	emf = EMFllrated*SQRT(2)/SQRT(3)*rpm /Rated RPM	From gen calcs	From gen calcs	Vgen = emf * Vst/Emq	Igen = SQRT(2)*1000*Pgout /(3*DPFgen*Vgen/SQRT(2))	Vdc = 1.35*SQRT(3)/SQRT(2)*Vgen	bridgeloss = 2*Vd/Vdc*Pgout	Idc = 1000*Pgout/Vdc	Pgridinv = Pgout-bridgeloss	Mgridinv = VgridRMS*SQRT(3)/Vdc	Igrid = SQRT(2)*1000*Pgridinv /(VgridRMS/SQRT(3))/3	Igrid2 = Igrid/2	IGBT cond loss = 0.5*(VCEO*Igrid2/PI() +Rdigbt*Igrid2^2/4)+Mgridinv*DPFutilinv *(VCEO*Igrid2/8+1/3/PI()*Rdigbt*Igrid2^2)	IGBT sw loss = fpwm/PI()*(Eon+Eoff) *Igrid2/Inom*Vdc/Vnom	Diode cond loss = 0.5*(Vd0*Igrid2/PI() +rd*Igrid2^2/4)-Mgridinv*DPFgrid *(Vd0*Igrid2/8+1/3/PI()*rd*Igrid2^2)	Diode sw loss = 1/PI()*fpwm*Erec	*(0.45*Igrid2/Inom+0.55)*Vdc/Vnom utilinvloss = IGBT cond loss + IGBT sw loss + diode cond loss + diode sw loss	filterloss = kfilter*Igrid^2	Total losses = bridgeloss+2*utilinvloss +filterloss	Efficiency = (Pgout-Total loss)/(Pgout)
(m/s)	(rpm)	(kW)	(pk l-n)	(Hz)		(pk l-n)	(pk A)	(V)	(kW)	(A)	(kW)		(pk A)	(pk A)	(watts)	(watts)	(watts)	(watts)	(kW)	(kW)	(kW)	
	RPM	Pgout	emf	Fgen	DPFgen	Vgen	Igen	Vdc	bridgeloss	Idc	Pgridinv	Mgridinv	Igrid	Igrid2					utilinvloss	filterloss		
3	82.0	27	300	38.3	1.000	300	60	496	0.2	55	27	1.22	63	31	15	7	1	8.9	2.2	0.0	4.6	83.0%
3.5	82.0	46	300	38.3	1.000	299	102	495	0.4	92	45	1.22	106	53	25	12	1	9.0	2.3	0.0	5.0	89.2%
4	82.0	70	300	38.3	1.000	299	156	494	0.6	142	69	1.23	162	81	39	18	1	9.1	2.4	0.1	5.4	92.2%
4.5	82.0	101	300	38.3	1.000	298	226	493	0.8	205	100	1.23	234	117	57	25	2	9.3	2.6	0.1	6.1	94.0%
5	82.0	140	300	38.3	1.000	298	314	492	1.1	284	139	1.23	324	162	81	35	3	9.6	2.8	0.3	6.9	95.0%
5.5	84.0	187	308	39.2	1.000	304	411	502	1.5	373	186	1.21	433	217	110	48	4	10.1	3.0	0.5	8.0	95.7%
6	91.7	244	336	42.8	1.000	331	492	547	1.8	446	242	1.11	565	282	142	68	10	11.4	3.4	0.8	9.4	96.1%
6.5	99.3	311	364	46.4	1.000	357	581	590	2.1	527	309	1.03	721	360	182	94	18	12.9	3.8	1.4	11.1	96.4%
7	107.0	390	392	49.9	1.000	383	679	633	2.5	616	387	0.96	903	452	230	126	27	14.5	4.4	2.1	13.4	96.6%
7.5	114.6	480	420	53.5	1.000	408	785	674	2.8	712	478	0.90	1114	557	289	166	40	16.3	5.1	3.2	16.2	96.6%
8	122.3	585	447	57.1	1.000	432	901	715	3.3	818	581	0.85	1356	678	361	214	55	18.3	5.9	4.8	19.8	96.6%
8.5	129.9	703	475	60.6	1.000	456	1028	754	3.7	933	699	0.80	1631	815	449	272	74	20.5	6.9	6.9	24.4	96.5%
9	137.5	836	503	64.2	1.000	478	1166	790	4.2	1058	832	0.77	1940	970	555	339	96	23.0	8.1	9.8	30.2	96.4%
9.5	145.2	983	531	67.7	1.000	498	1314	824	4.8	1192	978	0.74	2281	1141	681	416	122	25.7	9.5	13.5	37.2	96.2%
10	152.8	1148	559	71.3	1.000	517	1481	854	5.4	1344	1143	0.71	2666	1333	836	503	153	28.5	11.1	18.5	46.1	96.0%
10.5	160.5	1331	587	74.9	1.000	532	1668	880	6.1	1513	1325	0.69	3091	1545	1023	601	189	31.6	13.1	24.8	57.0	95.7%
11	163.7	1515	599	76.4	1.000	525	1922	869	7.0	1744	1508	0.70	3517	1759	1243	675	218	33.4	15.0	32.2	69.2	95.4%
11.5-27.5	163.7	1515	599	76.4	1.000	525	1922	869	7.0	1744	1508	0.70	3517	1759	1243	675	218	33.4	15.0	32.2	69.2	95.4%
8% OS	176.8	1574	647	76.4	1.000	558	1879	923	6.8	1704	1567	0.66	3655	1828	1289	746	244	36.3	15.9	34.7	73.3	95.3%
14% OS	186.6	1579	683	82.5	1.000	607	1733	1004	6.3	1572	1573	0.60	3669	1835	1261	815	265	39.6	16.3	35.0	73.9	95.3%

Inverter Parameters

PWM switching frequency - Hz	fpwm = 3000
IGBT Vceo (fixed portion Vce - volts)	VCEO = 1.5
IGBT dynamic resistance (Ohms)	rdigbt = 1.00E-03
Diode Vd0 (fixed portion Vd - volts)	Vd0 = 1.25
Diode dynamic resistance (Ohms)	rddiode = 3.00E-04
IGBT turn-on energy loss (Joules)	Eon = 2.00E-01

Inverter Parameters

IGBT turn-off energy loss (Joules)	Eoff = 3.00E-01
Current for Eon, Eoff (Amps)	Inom = 1200
Voltage for Eon, Eoff (volts)	Vnom = 900
Diode recovery energy loss (Joules - at Inom, Vnom)	Erec = 3.00E-02
Fixed loss per bridge (fans, gate drivers, etc. - watts)	fixedloss = 2000
Filter loss consant (filter loss = kfilter*Igrid^2)	kfilter = 2.60E-06

Other Parameters

Grid RMS line-line voltage	VgridRMS = 350
Grid inverter displacement PF	DPFgrid = 0.95
Gen emf at rated speed (L-N RMS)	EMFllrated = 734
Average diode voltage drop	Vd = 2
DC link inductor resistance (ohms)	Rreact = 0.001

Single PM Generator Efficiency Calculations, IGBT-IGBT System

Wind Speed (m/s)	Rotor Speed (rpm)	Gen Speed (rpm)	Gen. Input Power	Gen. Freq.	Input Power	Core losses: Eddy Current	Core losses: Hyst.	Core losses: Core (hyst+ eddy)	Phase React.	Phase Voltage pk l-n	Phase Current (amps)	Internal Voltage			Core Loss Current				Copper Loss (kW)	Generator Efficiency
		w = gearbox ratio*rotor speed	Pgenin = rotor power*gearbox ratio	fe = p*w/120	Pin = Pgenin/(p/2)	eddy = eddyo*L/Lo*(fe/feo)^2	hyst = hysto*L/Lo*fe/feo	coreloss = eddy+hyst	Xs = 2*PI()*fe*Ls	Emq = Emqo*L/Lo*fe/feo*N/No	Isq = -1000*Pin/(3/2*Emq)	Ec = SQRT(Emq^2+(Xs*Isq)^2)	cos = Emq/Ec	sin = SQRT(1-cos^2)	Ic = 1000*coreloss/(3/2*Ec)	Istq = Isq+Ic*cos	Istd = Ic*sin	Ist = SQRT(Istd^2+Istq^2)	Pcu = 3/2*Ist^2*Rs/1000	ngen = (Pin-coreloss-Pcu)/Pi
		w		fe	Pin	eddy	hyst.	coreloss	Xs (ohms)	Emq	Isq	Ec	cos	sin	Ic	Istq	Istd	Ist	Pcu	ngen
3.0	6	46	30	21.4	1.1	0.01	0.02	0.03	0.16	42	-17	42	1.00	0.06	0.48	-16	0.03	16	0.01	96.3%
3.5	7	53	48	25.0	1.7	0.02	0.02	0.04	0.18	49	-24	49	1.00	0.09	0.51	-23	0.04	23	0.02	96.8%
4.0	8	61	73	28.5	2.6	0.02	0.02	0.05	0.21	56	-31	56	0.99	0.11	0.54	-30	0.06	30	0.03	97.1%
4.5	9	69	104	32.1	3.7	0.03	0.03	0.05	0.23	63	-39	64	0.99	0.14	0.57	-39	0.08	39	0.05	97.2%
5.0	10	76	143	35.7	5.1	0.03	0.03	0.06	0.26	70	-49	71	0.98	0.18	0.60	-48	0.11	48	0.08	97.3%
5.5	11	84	191	39.2	6.8	0.04	0.03	0.07	0.29	77	-59	79	0.98	0.21	0.63	-59	0.13	59	0.11	97.3%
6.0	11	92	249	42.8	8.9	0.05	0.04	0.08	0.31	84	-71	87	0.97	0.25	0.65	-70	0.17	70	0.16	97.3%
6.5	12	99	317	46.4	11.3	0.06	0.04	0.10	0.34	91	-83	95	0.96	0.30	0.67	-83	0.20	83	0.22	97.2%
7.0	13	107	397	49.9	14.2	0.07	0.04	0.11	0.36	98	-97	104	0.94	0.34	0.69	-96	0.23	96	0.30	97.1%
7.5	14	115	490	53.5	17.5	0.07	0.05	0.12	0.39	105	-111	113	0.92	0.38	0.71	-111	0.27	111	0.40	97.1%
8.0	15	122	596	57.1	21.3	0.09	0.05	0.13	0.42	112	-127	124	0.90	0.43	0.72	-126	0.31	126	0.52	97.0%
8.5	16	130	717	60.6	25.6	0.10	0.05	0.15	0.44	119	-144	135	0.88	0.47	0.73	-143	0.35	143	0.66	96.8%
9.0	17	138	853	64.2	30.5	0.11	0.06	0.16	0.47	126	-162	147	0.86	0.51	0.74	-161	0.38	161	0.84	96.7%
9.5	18	145	1004	67.7	35.8	0.12	0.06	0.18	0.49	133	-180	160	0.83	0.56	0.74	-179	0.41	179	1.04	96.6%
10.0	19	153	1174	71.3	41.9	0.13	0.06	0.19	0.52	140	-200	174	0.80	0.60	0.74	-199	0.44	199	1.28	96.5%
10.5	20	160	1362	74.9	48.6	0.15	0.06	0.21	0.55	147	-221	190	0.77	0.63	0.74	-220	0.47	220	1.57	96.3%
11.0	20	164	1554	76.4	55.5	0.15	0.07	0.22	0.56	150	-247	203	0.74	0.68	0.72	-247	0.48	247	1.96	96.1%
11.5-27.5	20	164	1643	76.4	58.7	0.15	0.07	0.22	0.56	150	-261	209	0.72	0.70	0.70	-261	0.49	261	2.20	95.9%
8% overspeed	22	177	1643	82.5	58.7	0.18	0.07	0.25	0.60	162	-242	217	0.74	0.67	0.76	-241	0.51	241	1.88	96.4%
14% overspeed	23	186	1643	87.0	58.7	0.20	0.08	0.27	0.63	170	-229	224	0.76	0.65	0.81	-229	0.53	229	1.69	96.7%

Base machine quantities

Stator phase resistance (entire machine - ohms)	1.23E-02	
Stator phase inductance (entire machine - ohms)	6.62E-04	
Phase voltage (pk l-n) at rated speed	600	
Machine pole connection	4 series, 7 parallel	
Base machine pole number	56	po
Rated speed	164	
Rated power output (kW)	1500	

Base machine pole pair quantities

Freq at rated speed (Hz)	76.5	feo
Airgap length (m)	0.2	Lo
Turns ratio	1	No
Power output per pole pair (kW)	53.6	Pro
Stator per pole-pair phase resistance (ohms)	2.15E-02	Rso
Stator per pole-pair phase inductance (Hy)	1.16E-03	Lso
Fraction of winding copper in the slots	70%	ms
Fraction of winding copper in the end turns	30%	me
Pole pair eddy current loss (kW)	0.153	eddyo
Pole pair hysteresis loss (kW)	0.066	hysto
Phase voltage (pk l-n) at rated speed	150.0	Emqo

Scaled machine quantities

Airgap length	0.200	L
Turns ratio	1	N
Gearbox ratio	8	ratio
Pole number	56	p
Power output (kW)	1500	

Single PM Power Electronics Efficiency Calculations, IGBT-IGBT System

Wind Speed (m/s)	Gen Speed (RPM)	Gen Pwr Out (kW)	Gen EMF (pk l-n)	Gen Freq (Hz)	Gen Term DPF	Gen Volts (pk l-n)	Gen Term I (A pk)	Gen Inv Mod Index	Gen Inv IGBT Cond Loss (w)	Gen Inv IGBT Sw loss (w)	Gen Inv Diode Cond Loss (w)	Gen Inv Diode Sw loss (w)	Gen Inv loss (per inv) (kW)	Utility Inv Pwr in (kW)	Util Inv IGBT Cond Loss (w)	Util Inv IGBT Sw loss (w)	Util Inv Diode Cond Loss (w)	Util Inv Diode Sw loss (w)	Util Inv Loss (per inv) (kW)	Filter Loss (kW)	Total Loss (kW)	Total PE Eff.
	RPM = rotor speed * gear ratio	From gen calcs	emf = EMFllrated*SQRT(2)/SQRT(3)* RPM/rated RPM	From gen calcs	From gen calcs	Vgen = emf * Vst/Emq	Igen = SQRT(2)*1000*Pgout/ (3*DPFgen*Vgen/SQRT(2))	Mgeninv = Vgen*SQRT(3)/Vdc	0.5*(VCEO*(Igen/2)/PI()+ Rdigbt*(Igen/2* (Igen/2)/4)+ Mgeninv*DPFgen*(VCEO* (Igen/2)/8+1/3/PI()*Rdigbt*(Igen/2)^2)	fpwm/PI()*(Eon+Eoff)*Igen2/Inom* Vdc/Vnom	0.5*(Vd0*(Igen/2)/PI()+rd*(Igen/2)^2/4)- Mgeninv*DPFgen*(Vd0*(Igen/2)/8+ 1/3/PI()*rd*(Igen/2)^2)	1/PI()*fpwm*Erec*(0.45*(Igen/2)/Inom+0.55)* Vdc/Vnom	geninvloss = (6*(IGBT cond loss + IGBT sw loss + diode cond loss + diode sw loss)+fixedloss)/1000	Utility inverter power input = Pgout - geninvloss	0.5*(VCEO*(Igrid/2)/PI()+Rdigbt* (Igrid/2)^2/4)+Mgridinv*DPFutilinv* (VCEO*(Igrid/2)/8+1/3/PI()*Rdigbt*(Igrid/2)^2)	fpwm/PI()*(Eon+Eoff)*(Igrid/2) /Inom*Vdc/Vnom	0.5*(Vd0*(Igrid/2)/PI()+rd*(Igrid/2)^2/4)- Mgridinv*DPFgrid*(Vd0*(Igrid/2)/8+ 1/3/PI()*rd*(Igrid/2)^2)	1/PI()*fpwm*Erec*(0.45*(Igrid/2)/Inom+0.55) *Vdc/Vnom	utilinvloss = (6*(IGBT cond loss + IGBT sw loss + diode cond loss + diode sw loss)+fixedloss)/1000	filterloss = (kfilter*Igrid^2)/1000	Total loss = 2*geninvloss+2*utilinvloss+ filterloss	efficiency = (Pgout-total loss)/(Pgout)
	RPM	Pgout	emf	Fgen	DPFgen	Vgen	Igen	Mgeninv					geninvloss						utilinvloss	filterloss		
3	45.8	28	158	21.4	1.00	157	121	0.25	18	40	10	13	3	25	6	10	1	13	3.2	0.0	13.3	53.2%
3.5	53.5	47	184	25.0	1.00	183	171	0.29	26	57	13	14	4	43	10	17	2	13	3.3	0.0	13.8	70.4%
4	61.1	71	210	28.5	0.99	209	227	0.33	36	75	17	14	4	67	16	26	3	13	3.3	0.1	14.5	79.5%
4.5	68.8	101	237	32.1	0.99	236	288	0.37	47	95	21	14	4	97	23	38	4	13	3.5	0.1	15.2	84.9%
5	76.4	139	263	35.7	0.98	263	359	0.41	61	119	25	14	4	135	33	53	5	14	3.6	0.2	16.1	88.4%
5.5	84.0	186	289	39.2	0.98	291	436	0.46	78	144	29	15	5	181	45	71	7	14	3.8	0.4	17.3	90.7%
6	91.7	242	315	42.8	0.97	321	521	0.50	97	172	34	15	5	237	59	93	10	14	4.1	0.8	18.7	92.3%
6.5	99.3	308	342	46.4	0.95	351	614	0.55	119	203	38	16	5	303	77	119	12	14	4.3	1.2	20.4	93.4%
7	107.0	386	368	49.9	0.94	384	715	0.60	145	236	42	16	6	380	99	149	16	15	4.7	2.0	22.6	94.2%
7.5	114.6	476	394	53.5	0.92	418	823	0.66	174	272	46	16	6	470	125	184	20	15	5.1	3.0	25.2	94.7%
8	122.3	578	421	57.1	0.90	456	940	0.72	208	311	50	17	7	572	156	224	24	16	5.5	4.4	28.5	95.1%
8.5	129.9	694	447	60.6	0.88	496	1065	0.78	246	352	54	17	7	687	193	269	29	16	6.0	6.4	32.5	95.3%
9	137.5	825	473	64.2	0.85	541	1197	0.85	289	396	57	18	8	818	237	320	35	17	6.7	9.1	37.5	95.5%
9.5	145.2	970	500	67.7	0.82	589	1335	0.93	337	441	60	19	8	961	288	376	42	18	7.3	12.6	43.5	95.5%
10	152.8	1132	526	71.3	0.79	642	1484	1.01	393	491	62	19	9	1123	349	440	50	19	8.1	17.1	51.0	95.5%
10.5	160.5	1312	552	74.9	0.76	701	1640	1.10	455	542	64	20	9	1303	420	510	59	20	9.1	23.1	60.1	95.4%
11	163.7	1493	563	76.4	0.72	750	1835	1.18	529	607	70	21	10	1483	497	580	68	21	10.0	29.9	70.6	95.3%
11.5-27.5	163.7	1576	563	76.4	0.70	770	1941	1.21	569	642	75	21	11	1565	533	612	72	21	10.4	33.3	75.8	95.2%
8% OS	163.7	1584	563	82.5	0.73	744	1940	1.17	570	642	74	21	11	1573	536	615	73	21	10.5	33.6	76.2	95.2%
14% OS	163.7	1588	563	82.5	0.73	744	1946	1.17	572	643	74	21	11	1577	538	617	73	21	10.5	33.8	76.5	95.2%

Parameters (all inverters)

DC bus voltage (volts)	Vdc = 1100
PWM switching frequency - Hz	fpwm = 3000
IGBT Vceo (fixed portion Vce - volts)	VCEO = 1.5
IGBT dynamic resistance (Ohms)	rdigbt = 9.00E-04
Diode Vd0 (fixed portion Vd - volts)	Vd0 = 1.25
Diode dynamic resistance (Ohms)	rddiode = 3.30E-04

Parameters (all inverters)

IGBT turn-on energy loss (Joules)	Eon = 3.50E-01
IGBT turn-off energy loss (Joules)	Eoff = 3.30E-01
Current for Eon, Eoff (Amps)	Inom = 1200
Voltage for Eon, Eoff (volts)	Vnom = 900
Diode recovery energy loss (Joules - at Inom, Vnom)	Erec = 2.00E-02
Fixed loss per bridge (fans, gate drivers, etc. - watts)	fixedloss = 3000

All calculations based on two parallel inverters, generator and grid side

Other Parameters

Filter loss consant	kfilter = 0.0097
Grid RMS line-line voltage	VgridRMS = 690
Grid inverter displacement PF	DPFgrid = 0.95
Modulation index	Mgridinv = 0.8871

Appendix H

Variable Speed Windfarm Design using Line-Commutated SCR Converters

A UNIQUE VARIABLE-SPEED WINDFARM DESIGN USING LINE-COMMUTATED SCR CONVERTERS

William Erdman
Consultant
850 Greenstone Ct.
Brentwood, CA 94513
(925) 634-9932
Erdmanbill@aol.com

Terry Lettenmaier
Global Energy Concepts, LLC
5729 Lakeview Dr. NE, #100
Kirkland, WA 98033
(425) 822-9008
tlettenmaier@globalenergyconcepts.com

Jamie Chapman
OEM Development Corporation
840 Summer Street
Boston, MA 02127-1533
(617) 464-4708
jccoem@compuserve.com

ABSTRACT: This paper reports on a unique approach to wind plant design using variable-speed wind turbines with SCR line-commutated inverters. The wind plant uses the aggregation of wind turbines to deal with interconnect standards normally required by wind plants. The paper begins with a discussion of interconnect standards including IEEE 519-1992 and the proposed standard IEEE P1547. A discussion of the wind plant configuration including the turbine architecture, collection system impedances, and power factor improvement are all discussed. Early simulation results for a 12-turbine wind plant are provided at the end of the paper.

1 INTRODUCTION

Wind turbine interconnection design in the past has been predicated in part on the need to meet power quality and protective relaying standards at the point of wind turbine coupling. This has been the case whether a single wind turbine has been connected to a utility distribution system or a large number of turbines are connected to a common collection system in a large wind plant, without additional utility customers. The acceptance criteria for wind plant interconnection has typically fallen to the local utility, and the criteria have been the application of power quality and protective relaying at the point of common coupling, i.e., the aggregation of turbines at the interconnecting substation rather than at each turbine. This misalignment of the design and acceptance criteria has gone on for some time, and the authors argue that this has affected the economic performance of wind plants.

In this paper, the authors present a wind plant design that removes the restriction of power quality and protective relaying at the wind turbine, in an appropriate wind plant setting, and argue that this can lead to a lower cost of energy for the wind plant. The wind plant design uses variable-speed wind turbines with synchronous generators, diode bridges, and SCR line-commutated inverters. Thus the turbines are variable speed and take advantage of optimal tip speed ratio and load mitigation typical of variable-speed turbine designs. The aggregation of electrical outputs is then used in a unique interconnecting fashion to eliminate the known SCR line-commutated inverter problems of harmonic injection and non-selectable, non-unity power factor.

The paper begins with a brief review and discussion of existing and developing standards in North America which are often applied to wind plant installation. It is shown how the letter and the intent of the standards are met with the proposed aggregation approach. The paper then moves on to discuss the configuration of the wind plant, discussing three principal elements of its design: a concept of turbine grouping, the use of wind plant impedances to assist in reduction of harmonics, and the strategic location of power factor correction and harmonic filter components within the plant. Early simulation results for a 12-turbine wind plant are provided at the end of the paper.

2 EXISTING AND DEVELOPING INTERCONNECTION STANDARDS

Wind plant power quality requirements in North America are principally governed by the document IEEE 519-1992 entitled *IEEE Recommended Practices and Requirements for Harmonic Control in Electrical Power Systems.* This document has become the defacto standard for wind plant and other distributed resource interconnection and is slowly finding its way into state and utility documents governing interconnection. In addition to 519, a new document is currently being developed which is intended to address the interconnection of all distributed resources including wind turbines, solar, fuel cells, gensets, and storage devices such as batteries and flywheels. This later standard is in draft form and enjoys wide support as the United States moves towards standardizing interconnection rules across many states, regions, and private utilities. The developing standard is known as IEEE P1547/Draft 8 and is entitled *Draft Standard for Interconnecting Distributed Resources with Electric Power Systems.* This document addresses many different aspects of interconnection including power quality and protective relaying. For the most part, power quality requirements in P1547 transfer directly from, and are harmonious with 519.

Figure 1(a) is taken directly from the P1547 and is meant to show the clear distinction between the point of distributed resource connection and the point of common coupling (PCC). P1547 specifies power quality requirements at the PCC. Figure 1(b) is a redrawn version of the figure using terminology more specific to a wind plant setting.

In the work presented in this paper, the authors use the important distinction between point of wind turbine coupling and the PCC as the basis for removing the power quality requirements from the wind turbine itself. Instead, the power quality requirements are enforced at the PCC only. In a wind plant electrical environment where the distribution-level collection system is not shared with other utility customers, the removal of the wind turbine power quality requirement can be used to reduce the cost of energy (COE). This is the premise for the low-cost, variable-speed interconnection approach discussed in this paper.

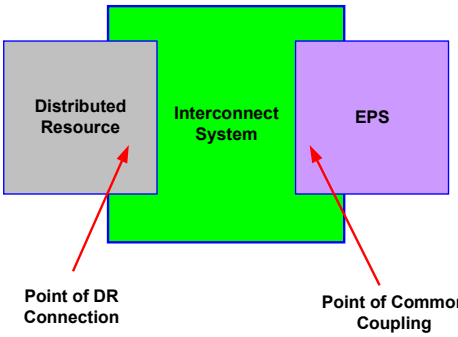

(a)

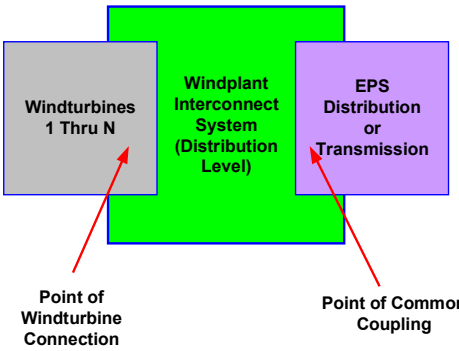

(b)

Figure 1. (a) Figure from P1547 showing point of distributed resource connection and the PCC, (b) redrawn for wind plant study. EPS is Electric Power System.

A summary of the power quality requirements from 519 is provided in Table I for review purposes. The table shows current distortion requirements when connecting to typical distribution-level systems.

Table I. Power Quality Requirements at PCC

IEEE 519-1992 Table 10.3
Current Distortion Limits for General Distribution Systems (120V thru 69000)
Maximum Harmonic Distortion in Percent of I_L
Individual Harmonic Order (Odd Harmonics)

I_{SC}/I_L	<11	11<h<17	17<h<23	23<h<35	35<h	TDD
<20*	4.0	2.0	1.5	0.6	0.3	5.0
20<50	7.0	3.5	2.5	1.0	0.5	8.0
50<100	10.0	4.5	4.0	1.5	0.7	12.0
100<1000	12.0	5.5	5.0	2.0	1.0	15.0
>1000	15.0	7.0	6.0	2.5	1.4	20.0

Even harmonics are limited to 25% of the odd harmonic limits above.

Current distortions that result in DC offset, e.g., half-wave converters, are not allowed.

**All Power generation equipment is limited to these values of current distortion, regardless of actual I_{SC}/I_L.*

I_L is the rated current.

In Table I, TDD is the Total Demand Distortion defined as

$$\text{TDD} = \frac{\sqrt{\sum_{k=1,n} I_k^2}}{I_L}. \qquad (1)$$

where I_L is the rated current of the wind plant.

3 LOW COST WIND PLANT SYSTEM

The wind plant power conversion and collection system discussed in this paper uses the wind plant collection system to filter the wind turbine current harmonics. This low-cost system takes advantage of moving the power quality requirements to the PCC. This system is based on four fundamental design elements:

- a low-cost wind turbine PE architecture using a 6-pulse, line-commutated SCR converter.
- a unique grouping of turbines which provides for a reduction (and in some cases) elimination of low order harmonics using conventional line-commutated SCR inverters,
- inclusion of the wind plant impedances in the system design – this is both out of necessity of line commutation and out of desire as these impedances can be used to reduce current harmonics,
- strategic location (due to system impedances) of power factor correction capacitances and harmonic filters to form a robust "system" filter for reducing non-zero harmonics.

Wind Turbine PE Architecture

The wind turbine architecture assumed in this discussion uses a synchronous generator connected to a passive diode rectifier, a DC current link and a line-commutated SCR inverter back to the utility, as shown in Figure 2. It is assumed that the turbine operates over a 2:1 speed range and the power curve follows a cubic power profile over that speed range. Modifications to these assumptions can be made without seriously altering the discussion or the results.

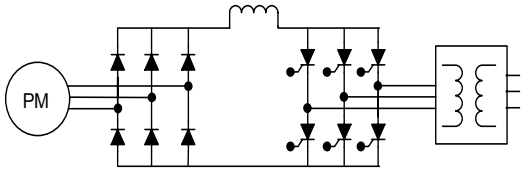

Figure 2. Wind Turbine PE Architecture

The SCR inverter is chosen based on a significant cost advantage over other power conversion approaches and because of the ability to scale this design to medium voltage levels and significantly larger MW ratings of turbines. These advantages are offset by a number of documented problems including the generation of objectionable harmonics and an uncontrolled displacement power factor. In the proposed architecture, these problems are alleviated without adding substantially to the cost of the system.

Turbine Grouping

To alleviate the problem of objectionable low order harmonics, it has been proposed that higher pulse count inverters using the approach of phase multiplication can be implemented, [1], [2], and [3]. Remaining higher order harmonics are effectively removed using traditional filters. While this approach can be effective, the per-turbine cost necessarily rises. The approach suggested in this paper is unique in that it uses the phase multiplication approach, but does so by the grouping of turbines and by applying phase multiplication at the turbine padmount transformers. This has the advantage of reducing (eliminating under certain conditions) low order harmonics without the additional cost of high pulse count inverters and filters at each turbine. Figure 3 shows how turbines could be grouped to provide higher pulse count waveforms while still using low pulse count inverters. The figure is restricted to a maximum 24 pulse waveform although higher pulse counts are feasible.

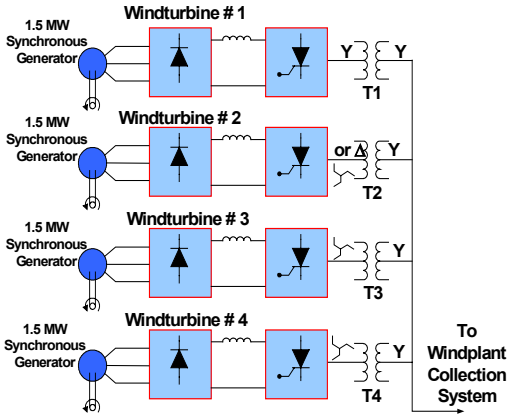

(a)

Group Description	# Turbine Group	T_1	T_2	T_3	T_4
6-Pulse	1	0°	-	-	-
12-Pulse	2	0°	30°	-	-
18-Pulse	3	0°	20°	-20°	-
24-Pulse	4	-15°	0°	15°	30°

(b)

Figure 3. (a) Turbine grouping and phase multiplication at padmount transformers, (b) phase shift requirements of padmount transformers.

A second approach to turbine grouping is shown in Figure 4. This simply builds on the ideas of Figure 3. The configuration is mentioned because it is the configuration used in the simulation studies presented in this paper. The Figure 4 approach accommodates two distinct windings on a six-phase permanent magnet generator. As a first attempt at designing the system filter, this approach is believed to be less demanding than four separate 6-pulse inverters.

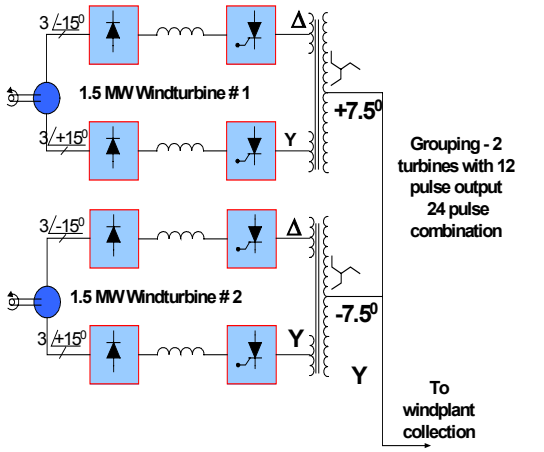

Figure 4. Two-turbine grouping using 12-pulse inverters and split power from 6-phase generator. This architecture is used in the simulation studies.

Use of Wind Plant Impedances

The second element of the wind plant collection system is the inclusion of the system impedances in the design. When forcing the turbine to meet power quality standards at the wind turbine or when force-commutated inverters are applied, the system impedances can often be neglected or do not factor heavily into the design process. As mentioned, with a line-commutated inverter, the system impedances need to be considered out of necessity because this system impedance affects SCR commutation time. This in turn determines the maximum permissible delay angle and by this, the displacement power factor. On the other hand, system impedance can have a small beneficial impact on current harmonics. Typical reduction of current harmonics due to system impedances is presented in Table II, [1].

Table II. Theoretical and Typical Values (in parentheses) of Harmonics in SCR Inverters

Harmonic Component	5^{th}	7^{th}	11^{th}	13^{th}	17^{th}	19^{th}	23^{rd}	25^{th}	THD
6-Pulse	20% (17%)	14% (10%)	9% (4%)	7.5% (3%)	6% (2%)	5% (1%)	4.5% (1%)	4% -	28% (20%)
12-Pulse	0% (2.2%)	0% (1.25%)	9% (7%)	7.5% (4%)	0% (0%)	0% (0%)	4.5% (2.5%)	4% (1.7%)	13% (9%)
24-Pulse	0% (N/A)	0% (N/A)	0% (N/A)	0% (N/A)	0% (N/A)	0% (N/A)	4.5% (N/A)	4% (N/A)	6% (N/A)

Capacitor and Filter Location

The last elements that need to be included in the wind plant collection system are the filters and power factor correction capacitors. These elements are necessary to filter the reduced, but non-zero current harmonics and to control power factor. Since the restriction of power quality has been eliminated at the wind turbine, there is flexibility in locating power factor correction capacitance and harmonic filters, and in so doing, taking advantage of system impedances. For example, these elements can be added at the turbines, at the substation, or anywhere in between.

4 SIMULATION STUDIES

Figure 5 shows a representation of the 12-turbine wind plant used in the simulation studies for which the results are reported in this paper. Turbine grouping is in pairs of turbines. Each turbine has a 12-pulse inverter with either ±7.5° phase shifted primary. This can be accomplished with either a zig-zag wye or extended delta approach. Turbine spacing is 1.5 rotor diameters, there is 200 ft between the padmount transformers and the turbine base and the primary of the padmounts have a 200-ft run at the 13.2 kV level to the collection system. Furthermore, there is a ½ mile length between the first turbine grouping and the substation. Cable sizing is based on underground construction and nationally accepted standards. The impedance of all of the elements including cable runs and transformers is shown in the figure and all impedances use the 69-kV level as a base. A table of the system impedances is provided in Table III.

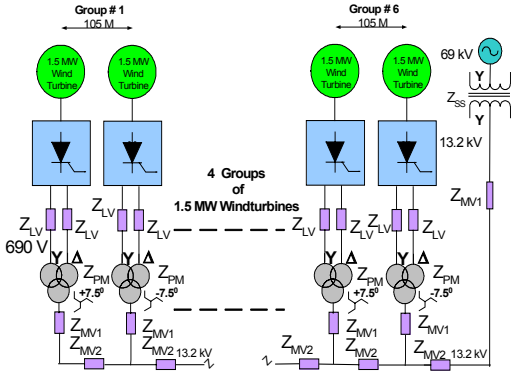

Figure 5. Wind plant layout showing impedances as used in the simulation studies

Table III. Wind Plant Impedance Values with 69 kV as a Base

Impedance	Resistance	Inductance
Zss	1.1 ohms	28 m Henries
Z_{PM}	1.27 ohms	174 m Henries
Z_{LV}	1.4 m ohms	7.15 u Henries
Z_{MV1}	126 m ohms	39.2 u Henries
Z_{MV2}	35 m ohms	36 u Henries
Z_{MV3}	25 m ohms	265 u Henries

To study the wind plant approach described above and the configuration according to Figure 5, a digital simulation model was constructed of the wind plant. The simulation has a full representation of the electrical and electronic system for twelve separate wind turbines. The mechanical system, i.e., turbine inertia and pitch system were approximated by appropriately filtering the random wind speeds applied to each turbine. With this model, many specific cases were run with various wind speed conditions and turbulence intensities.

Two wind speed scenarios are presented in this paper. In the first scenario, the wind plant is operated in region III where all wind speeds are at or above rated speed of 11.5 m/s. In this case, the turbines are all running at nearly the same speed and the inverters are all operating at very near the same delay angle. In this case, the expected cancellation of low order harmonics occurs and the wind plant current waveform is a good approximation to the theoretical ideal 24-pulse waveform. This is an important case because as Table I and Equation 1 above suggest, this is the point at which the power quality is measured against the standard, i.e. the operating current is the rated current. For this region III scenario, four separate cases were run as shown in Figure 6. The first case assumes no wind plant impedances, no filters, and no power factor correction capacitance. The current shown is the substation current at the 69-kV PCC. This case was run to understand the raw current waveform that could be achieved without introducing other factors such as impedance and filtering. The second case is the same as the first except that wind plant impedances are added with a corresponding modest improvement in current harmonics (see Table IV). The third case is the wind plant with impedances and harmonic filtering added at point 1 in Figure 5. Finally, power factor correction is added to the wind plant at the substation and these results are shown in Case 4. This is the most realistic case of the four presented.

A second scenario was run with the wind plant operating in region II where the average wind speeds at the various turbines vary between 7 and 11.5 m/sec (Figure 7). Turbulence is added corresponding to a turbulence intensity of 15% at each turbine. As can be seen, the raw current waveform in Case 1 has a very low harmonic content (see Table V). The second case is the same as the first only with impedances added to the wind plant. The corresponding cases of 3 and 4 from the previous scenario have not been completed as of the writing of this paper.

5 CONCLUSIONS

The interconnection system described in this paper is unique in its approach to dealing with interconnection standards. The principal driver for this system is a significant reduction in wind plant COE which has been shown in other work, but not presented here. The authors have just begun to explore the configuration presented in this paper and acknowledge that a good deal more work and understanding need to be completed before the systems viability can be considered unequivocal. Nonetheless, early results have suggested more promising results than were originally anticipated. The discussion in this paper also suggests that the concept of observing power quality at the PCC can be extended to other power converter configurations such as GTO or IGBT inverters with a resulting reduction in COE.

6 REFERENCES

[1] Dubois, M.R., *Review of Electromechanical Conversion in Wind Turbines*, Report # EPP00R03, Technical University of the Delft, April 2000.

[2] Grauers, A., *Design of Direct Driven Permanent Magnet Generators for Wind Turbines*, Ph.D. Dissertation, Chalmers University of Technology, 1996.

[3] Mohan, N., Robbins, W, Undelands, T., *Power Electronics: Converters, Applications, and Design*, John Wiley, 1989.

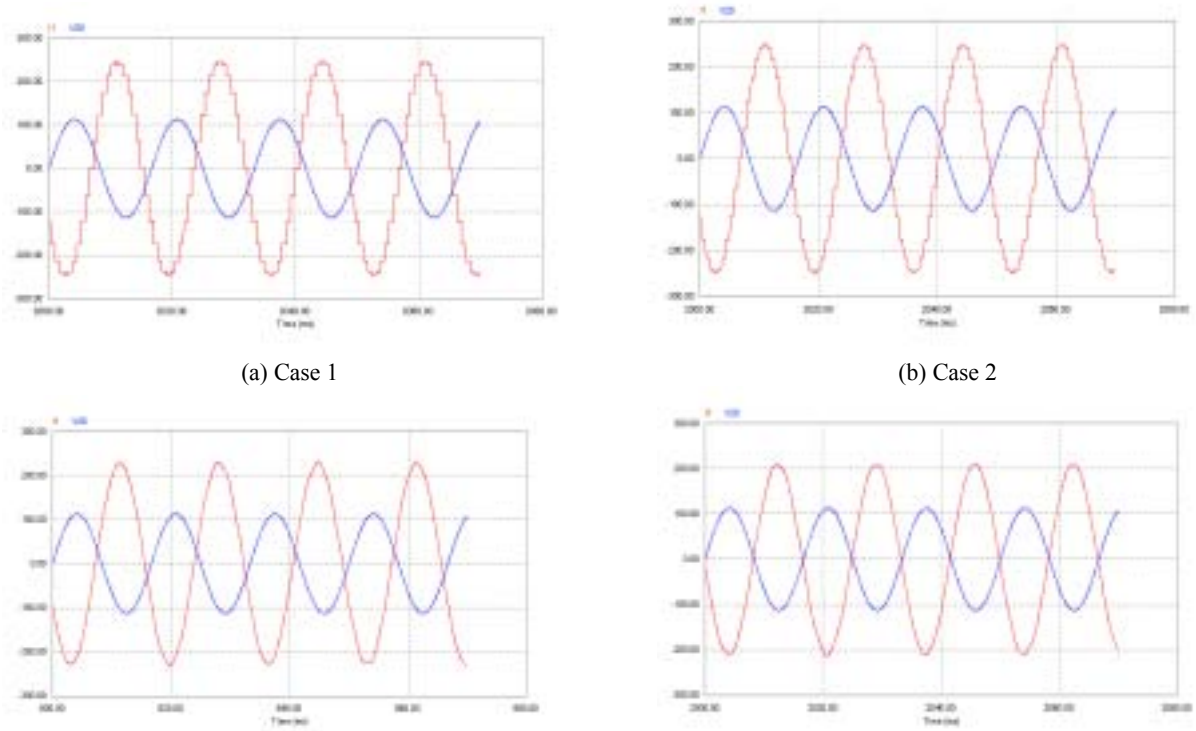

(a) Case 1 (b) Case 2

(c) Case 3 (d) Case 4

Figure 6. Four cases of simulation study discussed in text

Table IV. Summary of Results from Preliminary Wind Plant Simulation: Region III Rated Output

#	***Description***	I_1	I_5	I_7	I_{11}	I_{13}	I_{17}	I_{19}	I_{23}	I_{25}	IDD	TDD
	IEEE 519 Distribution	150	6	6	3	3	2.25	2.25	0.9 (1.8)	0.9 (1.8)	7.5	5%
	IEEE 519 Sub-Transmission & Transmission	150	3	3	1.5	1.5	1.13	1.125	.45 (0.9)	.45 (0.9)	3.75	2.50%
1	Simulation with ideal windplant (no impedances)	172	0.67	0.39	1.04	1.04	0.32	0.27	7	6.8	9.8	6.50%
2	Simulation with non-ideal windplant (real world)	171	0.41	0.37	0.69	0.69	0.21	0.12	6.3	5.5	8.4	5.60%
3	Simulation with non-ideal windplant and passive filter	160	0.78	0.83	0.47	0.47	0.18	0.09	0.001	0	1.37	0.89%
4	Simulation with non-ideal windplant and passive filter and PF correction	148	0.77	0.35	0.36	0.36	0.12	0.02	0	0	1	0.67%

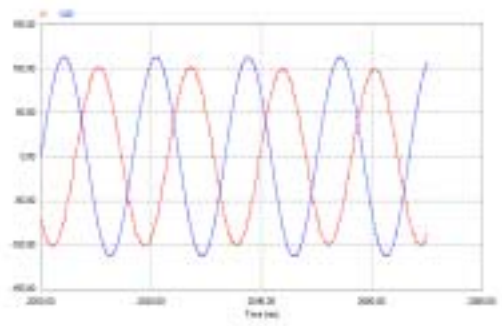

(a) Case 1

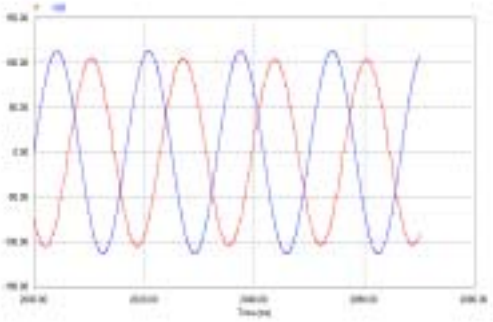

(b) Case 2

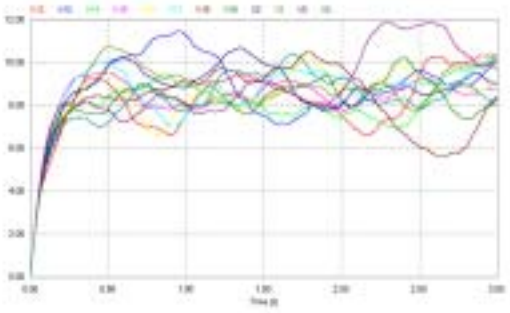

(c) Wind Speeds

Figure 7. Simulation results as discussed in text

Table V. Summary of results from preliminary wind plant simulation: Region II 7-11.5 m/s, TI = 15 %

#	***Description***	I_1	I_5	I_7	I_{11}	I_{13}	I_{17}	I_{19}	I_{23}	I_{25}	IDD	TDD
	IEEE 519 Distribution	150	6	6	3	3	2.25	2.25	0.9 (1.8)	0.9 (1.8)	7.5	5%
	IEEE 519 Sub-Transmission & Transmission	150	3	3	1.5	1.5	1.125	1.125	.45 (0.9)	.45 (0.9)	3.75	2.50%
1	Simulation with ideal windplant (no impedances)	82	0.82	0.61	1.5	1.5	0.12	0.17	2.2	1.8	3.6	2.40%
2	Simulation with non-ideal windplant (real world	97	0.61	0.34	0.8	0.9	0.1	0.09	1.6	1.1	2.3	1.50%

Appendix I

Electrical One-Line Diagrams and Switchgear Estimates

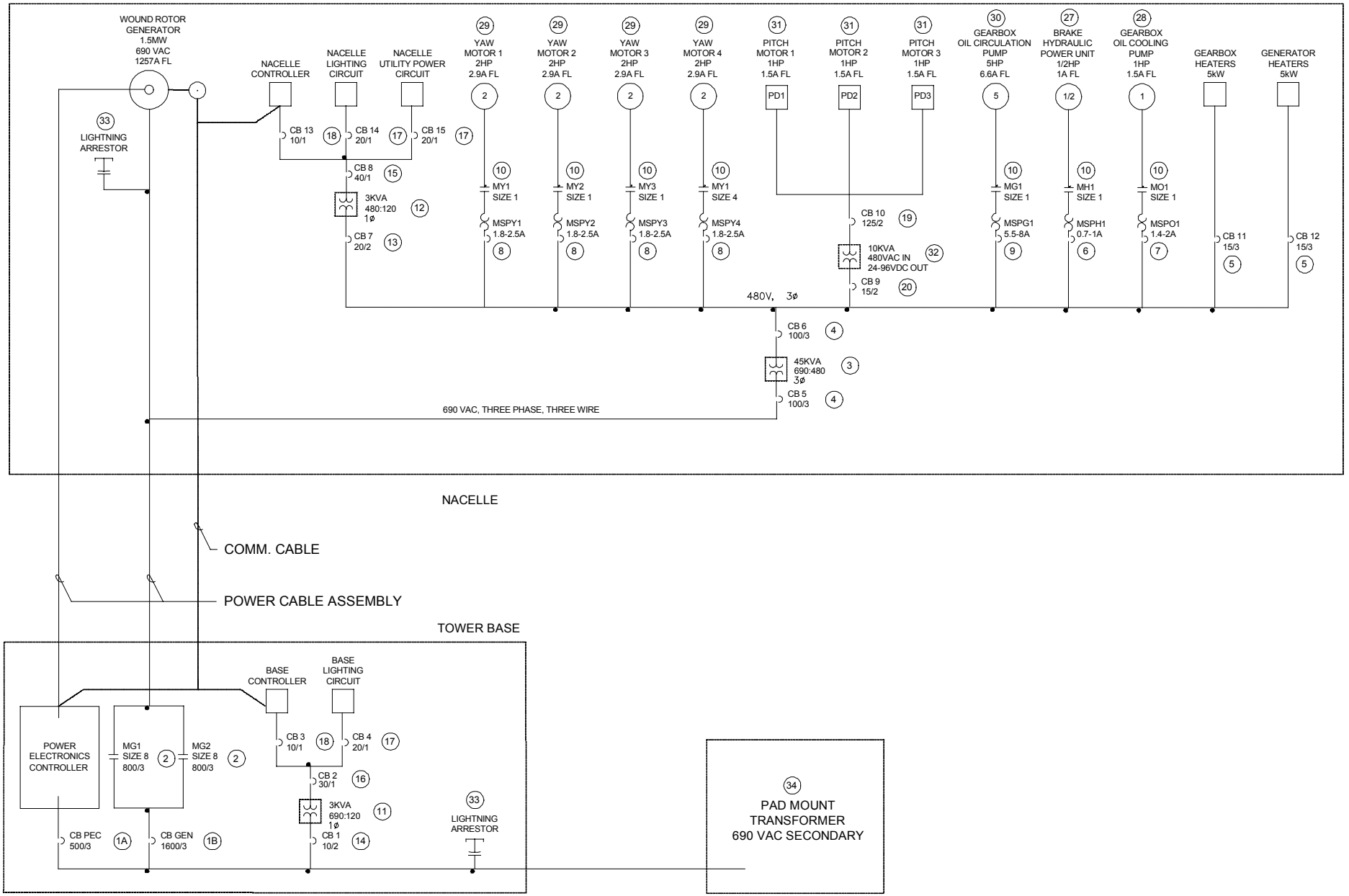

Figure I-1. Baseline Electrical System

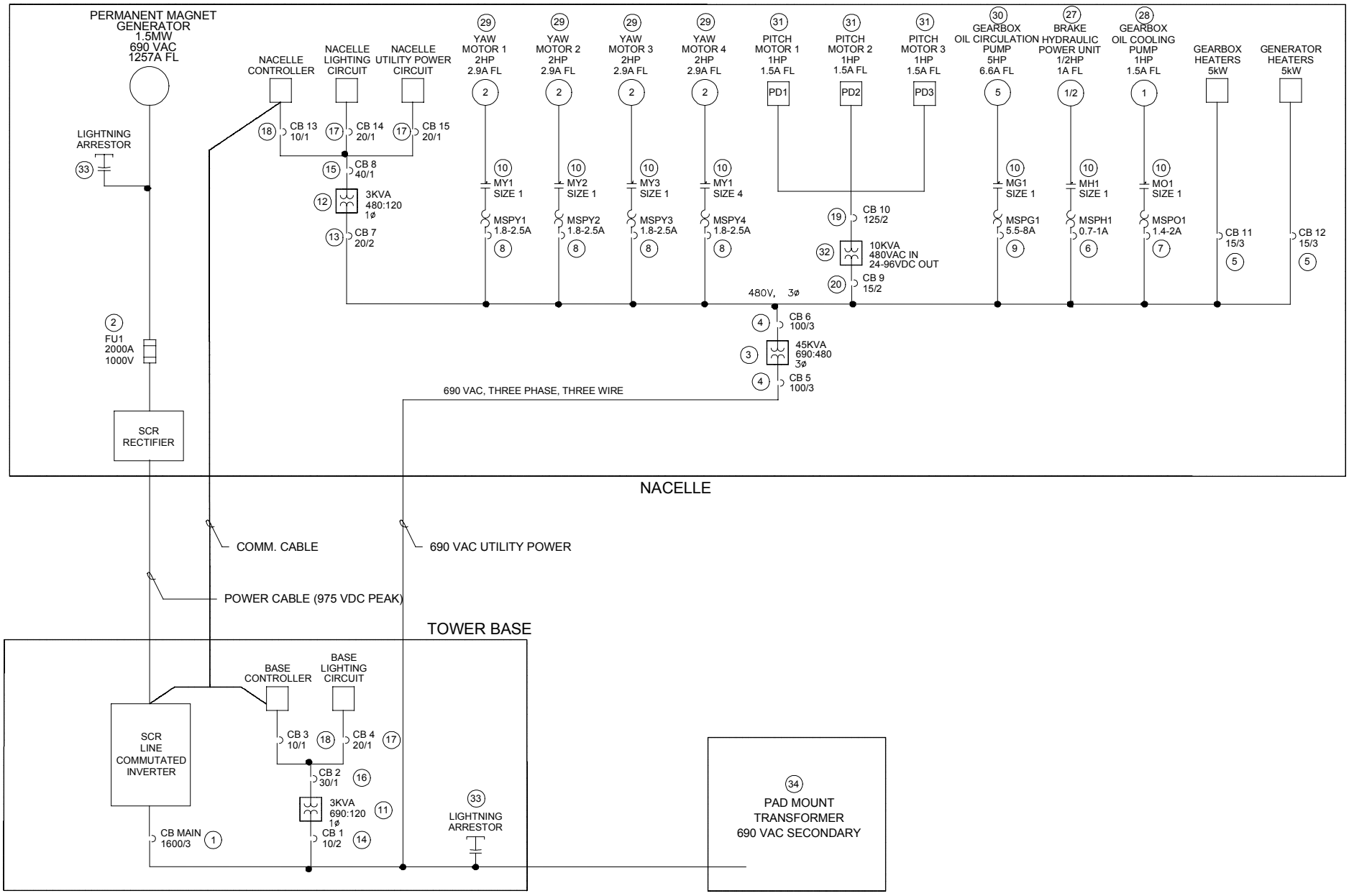

Figure I-2. Electrical System with Single PM Generator and SCR-SCR PE

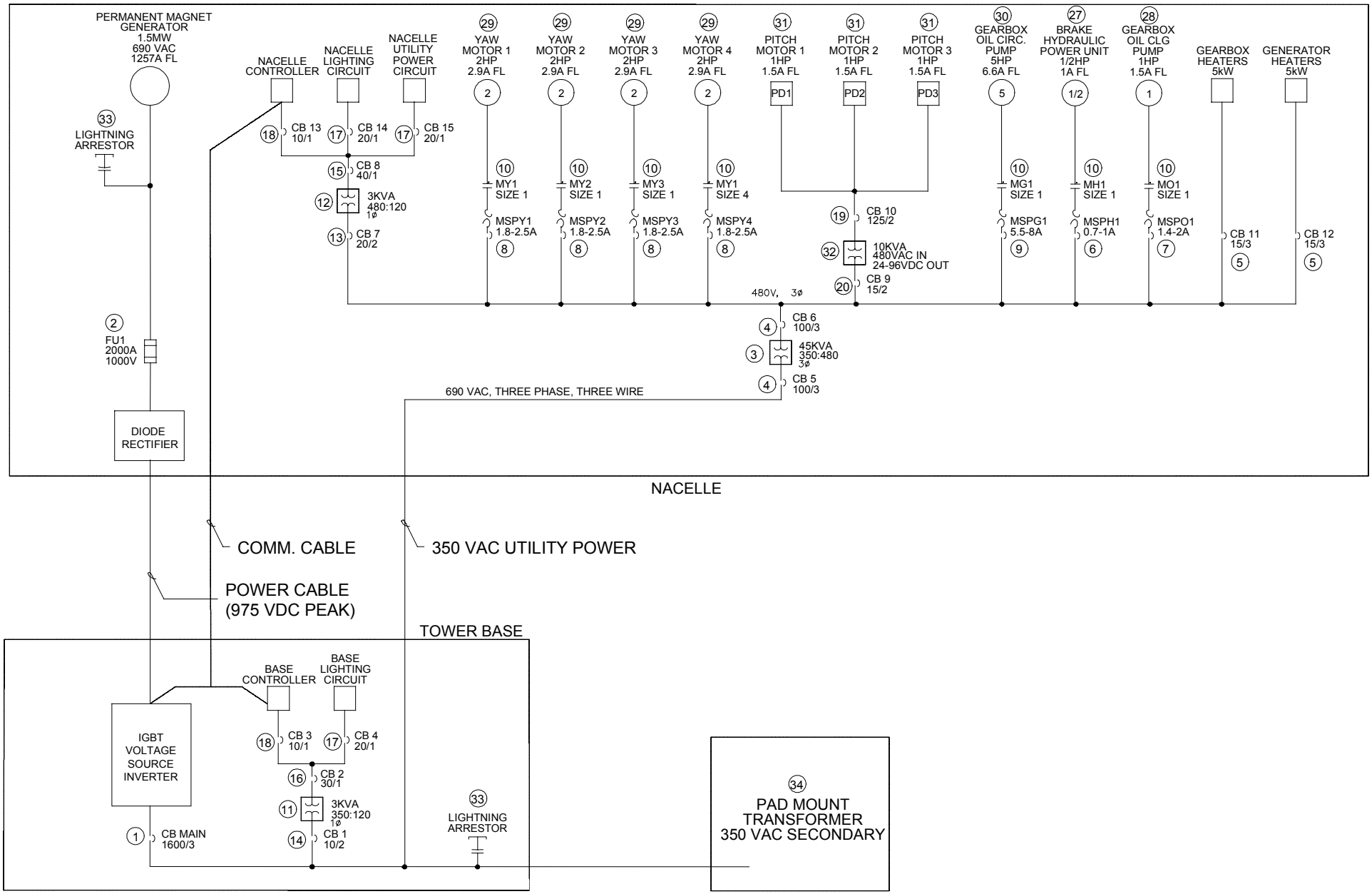

Figure I-3. Electrical System with Single PM Generator and Diode-IGBT PE

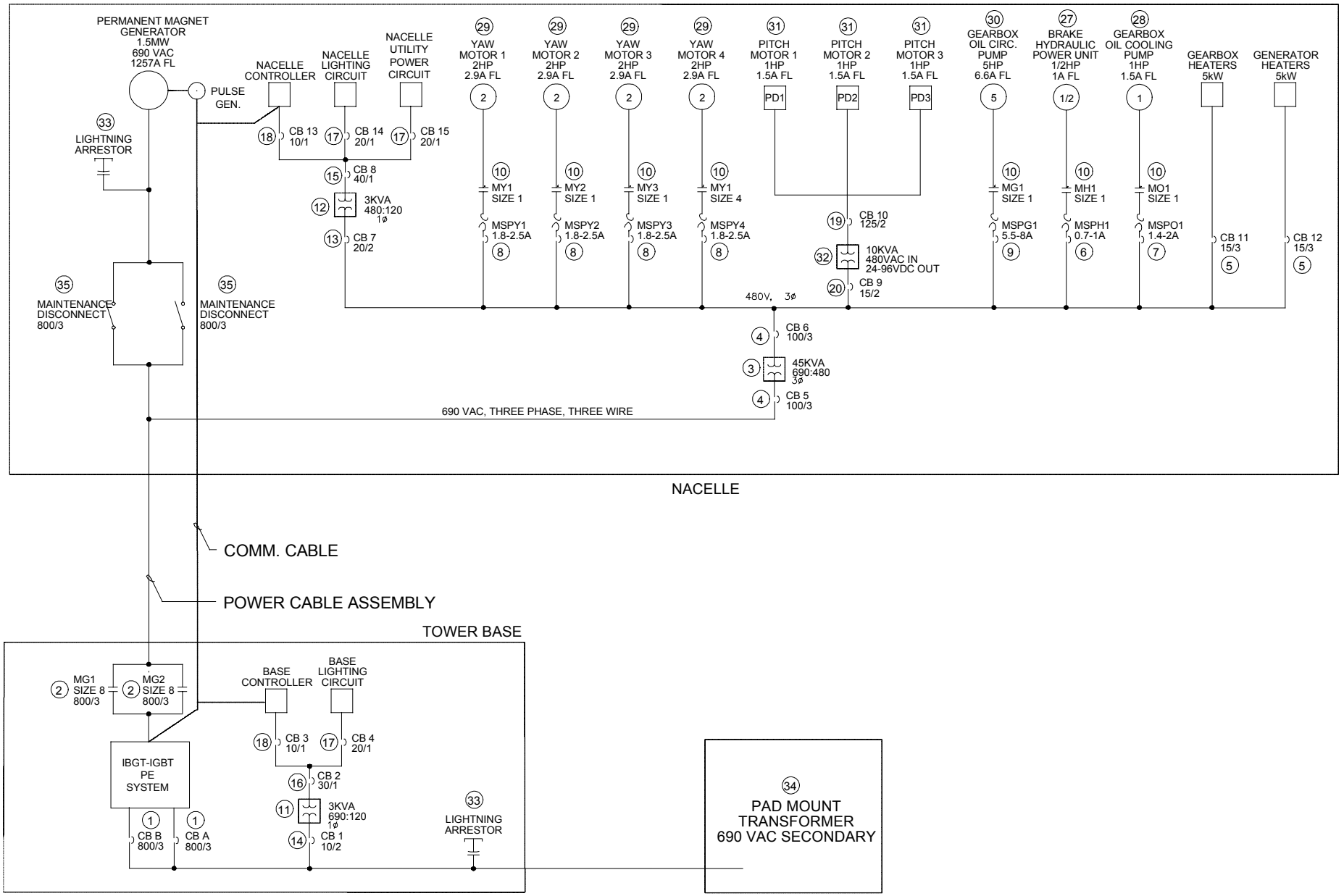

Figure I-4. Electrical System with Single PM Generator and IGBT-IGBT PE

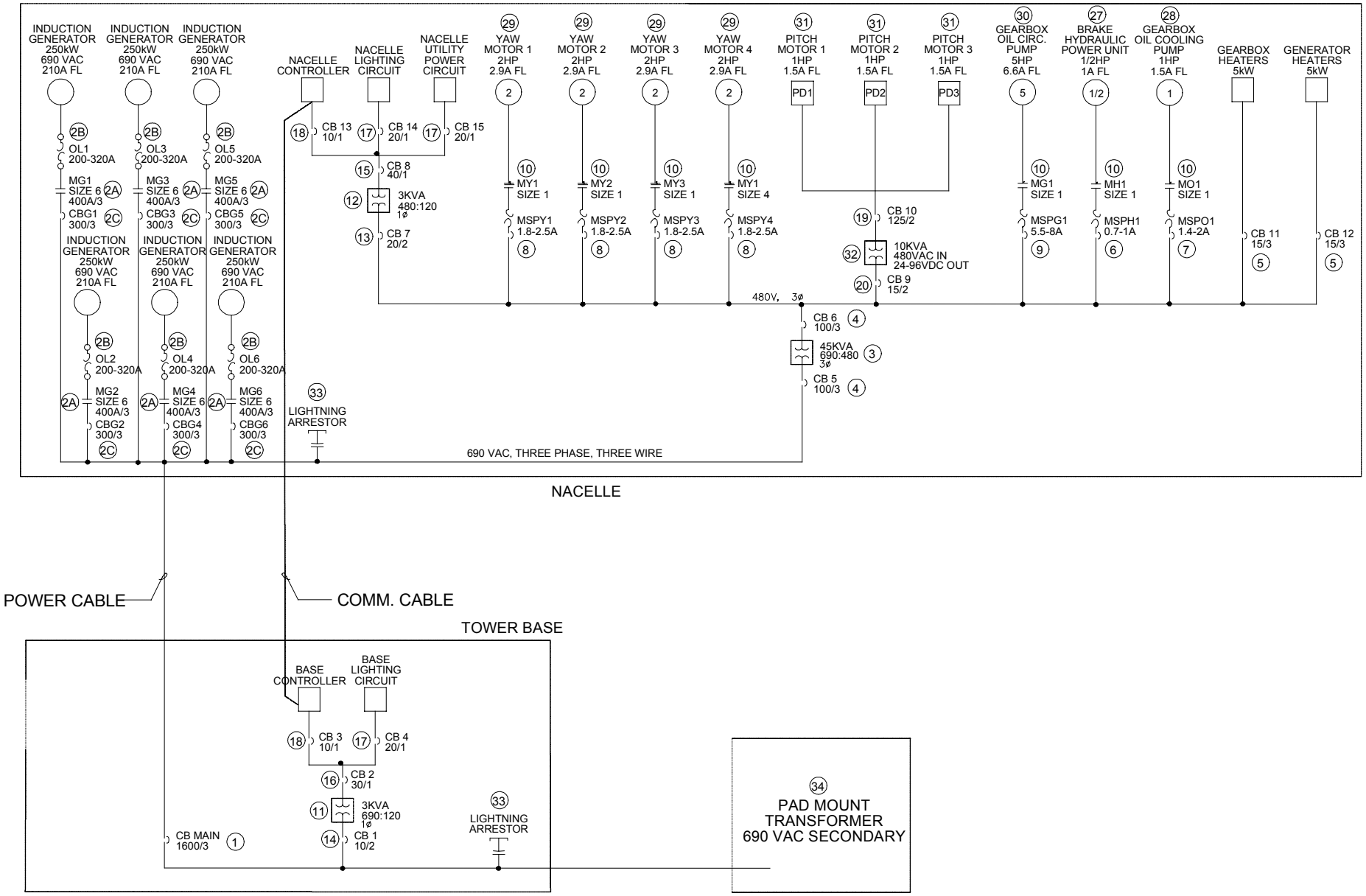

Figure I-5. Multi-Induction Generator Electrical System

Table I-1. Switchgear Costs, Baseline System

Item #	Qty	Description	Mnfr.	Manufacturer Part #	Unit Cost	Extended Cost
	1	Molded Case Circuit Breaker, 500A Trip Unit			$1,027	$1,027
1	1	Molded Case Circuit Breaker, 2000A Frame, 1600A Trip Unit	Siemens	RXD63B160	$4,109	$4,109
2	2	Contactor, 600 Volts, 820 Amps			$1,200	$2,400
	1	Other switchgear - common to all designs				$4,856
		Total				**$12,392**

Table I-2. Switchgear Costs, Single PM Generator and SCR-SCR PE

Item #	Qty	Description	Mnfr.	Manufacturer Part #	Unit Cost	Extended Cost
1	1	Molded Case Circuit Breaker, 2000A Frame, 1600A Trip Unit	Siemens	RXD63B160	$4,109	$4,109
2	1	Fusable disconnect			$1,500	$1,500
	1	Other switchgear - common to all designs				$4,856
		Total				**$10,465**

Table I-3. Switchgear Costs, Single PM Generator and Diode-IGBT PE

Item #	Qty	Description	Mnfr.	Manufacturer Part #	Unit Cost	Extended Cost
1	2	Molded Case Circuit Breaker, 2000A Frame, 1600A Trip Unit	Siemens	RXD63B160	$4,109	$8,218
2	1	Fusable disconnect			$1,500	$1,500
	1	Other switchgear - common to all designs				$4,856
		Total				**$14,574**

Table I-4. Switchgear Costs, Single PM Generator and IGBT-IGBT PE

Item #	Qty	Description	Mnfr.	Manufacturer Part #	Unit Cost	Extended Cost
1	1	Molded Case Circuit Breaker, 2000A Frame, 1600A Trip Unit	Siemens	RXD63B160	$4,109	$4,109
2	1	Fusable disconnect			$1,500	$1,500
	1	Other switchgear - common to all designs				$4,856
		Total				**$10,465**

Table I-5. Switchgear Costs, Multi-Induction Generator

Item #	Qty	Description	Mnfr.	Manufacturer Part #	Unit Cost	Extended Cost
1	1	Molded Case Circuit Breaker, 2000A Frame, 1600A Trip Unit	Siemens	RXD63B160	$4,109	$4,109
2A	6	Contactor, 400HP, 1000 Volts, 400 Amps			$1,000	$6,000
2B	6	Bimetallic Overload Relay, 200-320 Amp, for use w/ 3TF56	Siemens	3UA6600-3D	$407	$2,442
2C	6	Molded Case Circuit Breaker, 400A Frame, 300A, 3-Pole	Siemens	JXD63B300	$834	$5,004
	1	Other switchgear - common to all designs				$4,856
		Total				**$22,411**

Table I-6. Switchgear Costs, Multi-PM Generators (SCR-SCR PE)

Item #	Qty	Description	Mnfr.	Manufacturer Part #	Unit Cost	Extended Cost
1	1	Molded Case Circuit Breaker, 2000A Frame, 1600A Trip Unit	Siemens	RXD63B160	$4,109	$4,109
2	6	Fusable disconnect (6 gens)			$600	$3,600
	1	Other switchgear - common to all designs				$4,856
		Total				**$12,565**

Table I-7. Switchgear Costs, Components Common to all Designs

Other Electrical Switchgear (these components common to all designs)						
Item #	Qty	Description	Mnfr.	Manufacturer Part #	Unit Cost	Extended Cost
3	1	45KVA Transformer, 3-Phase, 690VAC In, 480VAC Out	Acme	T2A795213S	$1,300	$1,300
4	2	Auxiliary Circuit Breaker, 100 Amp, 3-Pole	Siemens	ED63B100L	$110	$220
5	2	Auxiliary Circuit Breaker, 15 Amp, 3-Pole	Siemens	BQ3B015	$28	$56
6	1	Motor Starter Protector, 0.7-1 Amp, 25 Amp Frame	Siemens	3RV1021-0JA10	$38	$38
7	4	Motor Starter Protector, 1.4-2 Amp, 25 Amp Frame	Siemens	3RV1021-1BA10	$38	$151
8	4	Motor Starter Protector, 1.8-2.5Amp, 25 Amp Frame	Siemens	3RV1021-1CA10	$38	$151
9	1	Motor Starter Protector, 5.5-8 Amp, 25 Amp Frame	Siemens	3RV1021-1HA10	$38	$38
10	10	IEC Contactor, 17 Amp, 3-pole, Full Voltage	Siemens	3RT1025-0AK6	$31	$312
11	1	Control Power Transformer, 690VAC Primary, 3KVA	Siemens		$400	$400
12	1	Control Power Transformer, 480VAC Primary, 3KVA	Siemens	MT3000A	$400	$400
13	1	Miniature Circuit Breaker, 20 Amp, 2-Pole	Siemens	5SX2220-8	$19	$19
14	1	Miniature Circuit Breaker, 10 Amp, 2-Pole	Siemens	5SX2210-8	$19	$19
15	1	Miniature Circuit Breaker, 40 Amp, 1-Pole	Siemens	5SX2140-8	$10	$10
16	1	Miniature Circuit Breaker, 30 Amp, 1-Pole	Siemens	5SX2130-7	$10	$10
17	3	Miniature Circuit Breaker, 20 Amp, 1-Pole	Siemens	5SX2120-8	$10	$29
18	2	Miniature Circuit Breaker, 10 Amp, 1-Pole	Siemens	5SX2110-8	$10	$19
19	1	Molded Case Circuit Breaker, 125A Frame, 125A, 2-Pole	Siemens	Q2125	$47	$47
20	1	Molded Case Circuit Breaker, 125A Frame, 15A, 2-Pole	Siemens	Q215	$8	$8
21	2	Enclosure, 48"x36"x12", NEMA 12, with back panel	CEC	37721	$246	$491
22	2	Wall Mounting Bracket, Painted, Set of 4	CEC	37700	$5	$11
23	1	Operating Handle, Rotary Door Mounted, Stainless 4X	Siemens	RHOH4	$16	$16
24	1	Operating Handle, Rotary Breaker Operator, E-Frame	Siemens	RHOEBO	$8	$8
25	1	Breaker Operating Shaft, Rotary Variable Depth	Siemens	RHOSVD	$3	$3
32	1	Pitch Drives Transformer, 480VAC In, 24-96 VDC Out, 10KVA			$800	$800
33	2	Lightning Arrestor			$150	$300
		Total				**$4,856**

Appendix J

O&M Worksheets

Baseline - Unscheduled Maintenance Costs

Component	Spare Cost: x 1.5	Weibull Shape Factor	Average Failures/ Year	MTBE (Years)	MTTR (Hours)	Repair Description	% Spare Cost	# of Crew	Labor/ Event	Mat'l/ Event	Equip/ Event	Total/ Event	Total/ Year
Rotor													
Blades (three)	222,000	3.5	0.001	67	8	Replace	100%	3	1,560	222,000	25,000	248,560	344
Hub	96,000	1.0	0.002	500	16	Replace	100%	3	3,120	96,000	25,000	124,120	241
Pitch mechanisms and bearings	54,000	3.5	0.184	5	12	Repair/replace parts	5%	2	1,560	2,700	-	4,260	784
Drivetrain and Nacelle													
Transmission system													
Gearbox	180,000	3.5	0.011	35	24	Replace	100%	2	3,120	180,000	50,000	233,120	2,591
Mainshaft	30,183	1.0	0.002	476	16	Replace	100%	2	2,080	30,183	50,000	82,263	167
Mainshaft bearing and block	17,550	1.0	0.002	476	16	Replace	100%	2	2,080	17,550	50,000	69,630	142
Elastomeric mounting system	4,095	3.5	0.084	10	8	Replace	100%	2	1,040	4,095	-	5,135	432
Generator isolation mounts	750	3.5	0.084	10	8	Replace	100%	2	1,040	750	-	1,790	150
Support structure	51,150	1.0	0.002	476	8	Repair	20%	2	1,040	10,230	-	11,270	23
Generator cooling system	3,633	3.5	0.184	5	8	Repair/replace parts	2%	2	1,040	73	-	1,113	205
Brake system, hydraulics	7,500	3.5	0.184	5	8	Repair/replace parts	2%	2	1,040	150	-	1,190	219
Coupling	3,573	3.5	0.034	20	8	Repair/replace parts	100%	2	1,040	3,573	-	4,613	157
Nacelle cover	25,983	1.0	0.002	476	8	Repair	10%	2	1,040	2,598	25,000	28,638	58
Generator	90,000	3.5	0.024	25	24	Replace w/rebuilt	50%	3	4,680	45,000	25,000	74,680	1,797
Variable-speed electronics (PE)	92,700	1.0	0.200	5	8	Replace component	5%	1	520	4,635	-	5,155	1,031
0.95-0.95 substation VAR control	-	1.0	0.040	25	4	Replace component	10%	1	260	-	-	260	-
Transformer	33,750	3.5	0.000	100	8	Repair	25%	2	1,040	8,438	1,000	10,478	4
Cable	26,726	3.5	0.011	35	8	Replace portion	20%	2	1,040	5,345	-	6,385	71
Switchgear	18,588	3.5	0.184	5	6	Replace component	10%	2	780	1,859	-	2,639	486
Yaw Drives and Bearings	24,000	3.5	0.084	10	12	Replace drive/bearing	40%	2	1,560	9,600	-	11,160	938
Control and Safety System	10,500	1.0	3.000	0	2	Replace component	5%	1	130	525	-	655	1,965
Tower	276,000	1.0	0.002	476	8	Replace section	50%	2	1,040	138,000	3,000	142,040	289
Foundation	72,000	1.0	0.001	1000	8	Repair	10%	3	1,560	7,200	2,000	10,760	11
Total	**$1,340,681**												**$12,103**
COE													**$0.00250**

MTBE - Mean Time Between Events
MTTR - Mean Time to Repair

Baseline - Scheduled Maintenance

Component	Events/ Year	Interval (Days)	Description	Duration (Hours)	# of Crew	Labor/ Event	Labor Cost/ Year	Mat'l/ Event	Equip/ Event	Total/ Event	Total/ Year
Rotor											
Blades (three)	1	365	Inspect blades, lube pitch brgs	4	2	520	520	50	0	570	570
Hub	1	365	Inspect	1	2	130	130	0	0	130	130
Pitch mechanism (three)	2	183	Check fluid, filters, system	2	2	260	520	50	0	310	620
Drivetrain and Nacelle											
Transmission system											
Gearbox	2	183	Check oil level, filters, inspect gears and brgs	1.25	2	162.5	325	400	0	562.5	1125
Mainshaft	2	183	Inspect	0.25	1	16.25	32.5	0	0	16.25	33
Mainshaft bearing and block (bearing)	2	183	Lube	0.5	1	32.5	65	25	0	57.5	115
Elastomeric mounting system	2	183	Inspect	0.25	1	16.25	32.5	0	0	16.25	33
Generator isolation mounts	2	183	Inspect	0.25	1	16.25	32.5	0	0	16.25	33
Support structure (bedplate)	2	183	Inspect, check pretension	0.5	1	32.5	65	0	0	32.5	65
Generator cooling system	2	183	Check fluid, filters, system	0.5	2	65	130	100	0	165	330
Brake system, hydraulics	2	183	Check fluid, filters, system	0.5	2	65	130	300	0	365	730
Coupling (gem to gearbox)	2	183	Inspect	0.2	1	13	26	0	0	13	26
Nacelle cover	2	183	Inspect	0.5	1	32.5	65	0	0	32.5	65
Generator	2	183	Inspect	1	2	130	260	0	0	130	260
Variable-speed electronics (PE)	2	183	Inspect	1	1	65	130	0	0	65	130
Transformer	2	183	Inspect	0.5	1	32.5	65	0	0	32.5	65
Cable	2	183	Inspect	1	1	65	130	0	0	65	130
Switchgear	2	183	Inspect	0.5	1	32.5	65	0	0	32.5	65
Yaw Drive and Bearing (3)	1	365	Inspect, lubricate	1.5	2	195	195	50	0	245	245
Control and Safety System	2	183	Inspect	1	1	65	130	0	0	65	130
Tower	1	365	Inspect, check pretension	8	2	1040	1040	0	0	1040	1040
Foundation	2	183	Inspect, check pretension	0.5	1	32.5	65	0	0	32.5	65
Total						$3,019	$4,154	$975	$0	$3,994	**$6,004**
COE						$0.00062	$0.00086	$0.00020	$0.00000	$0.00083	**$0.00124**

Baseline - Levelized Replacement Costs

Item	Event Year	Duration (Hours)	# of Crew	Labor	Mat'l	Equip	Total RC (2002 $)	Total PV(n)
Rotor								
Blades (three including pitch bearings)	25	24	3	4,680	44,400	25,000	74,080	16,986
Drivetrain and Nacelle								
Transmission system								
Gearbox - 25 year	25	24	2	3,120	72,000	50,000	125,120	28,689
Yaw Drive and Bearing (3)	25	16	2	2,080	24,000	80,000	106,080	24,324
Total							**$305,280**	**$69,999**
CRF								0.0732
LRC								**$5,124**
LRC-COE								$0.0011

Integrated Baseline - Unscheduled Maintenance Costs

Component	Spare Cost: x 1.5	Weibull Shape Factor	Average Failures/ Year	MTBE (Years)	MTTR (Hours)	Repair Description	% Spare Cost	# of Crew	Labor/ Event	Mat'l/ Event	Equip/ Event	Total/ Event	Total/ Year
Rotor													
Blades (three)	222,000	3.5	0.001	67	8	Replace	100%	3	1,560	222,000	25,000	248,560	344
Hub	96,000	1.0	0.002	500	16	Replace	100%	3	3,120	96,000	25,000	124,120	241
Pitch mechanism (three including bearings)	54,000	3.5	0.184	5	12	Repair/replace parts	5%	2	1,560	2,700	-	4,260	784
Drivetrain and Nacelle													
Transmission system													
Gearbox	179,643	3.5	0.011	35	36	Replace	100%	2	4,680	179,643	50,000	234,323	2,604
Mainshaft (included)	-	1.0	0.002	476	16	Replace	100%	2	2,080	-	50,000	52,080	-
Mainshaft bearing and block	-	1.0	0.002	476	16	Replace	100%	2	2,080	-	50,000	52,080	-
Elastomeric mounting system	-	3.5	0.084	10	8	Replace	100%	2	1,040	-	-	1,040	-
Generator isolation mounts	-	3.5	0.084	10	8	Replace	100%	2	1,040	-	-	1,040	-
Support structure (integrated nacelle)	31,877	1.0	0.002	476	8	Repair	20%	2	1,040	6,375	-	7,415	15
Generator cooling system	4,479	3.5	0.184	5	8	Repair/replace parts	2%	2	1,040	90	-	1,130	208
Brake system, hydraulics	1,956	3.5	0.184	5	8	Repair/replace parts	2%	2	1,040	39	-	1,079	199
Coupling	3,207	3.5	0.034	20	8	Repair/replace parts	100%	2	1,040	3,207	-	4,247	145
Nacelle cover	13,322	1.0	0.002	476	8	Repair	10%	2	1,040	1,332	25,000	27,372	56
Generator	90,000	3.5	0.024	25	24	Replace w/rebuilt	50%	3	4,680	45,000	25,000	74,680	1,797
Variable-speed electronics (PE)	92,700	1.0	0.200	5	8	Replace component	5%	1	520	4,635	-	5,155	1,031
0.95-0.95 substation VAR control	-	1.0	0.040	25	4	Replace component	10%	1	260	-	-	260	-
Transformer	33,750	3.5	0.000	100	8	Repair	25%	2	1,040	8,438	1,000	10,478	4
Cable	26,726	3.5	0.011	35	8	Replace portion	20%	2	1,040	5,345	-	6,385	71
Switchgear	18,588	3.5	0.184	5	6	Replace component	10%	2	780	1,859	-	2,639	486
Yaw Drive (three) and Bearing	24,000	3.5	0.084	10	12	Replace one drive or bearing	40%	2	1,560	9,600	-	11,160	938
Control and Safety System	10,500	1.0	3.000	0	2	Replace component	5%	1	130	525	-	655	1,965
Tower	276,000	1.0	0.002	476	8	Replace section	50%	2	1,040	138,000	3,000	142,040	289
Foundation	72,000	1.0	0.001	1000	8	Repair	10%	3	1,560	7,200	2,000	10,760	11
Total	**$1,250,747**												**$11,185**
COE													**$0.00231**

MTBE - Mean Time Between Events
MTTR - Mean Time to Repair

Integrated Baseline - Scheduled Maintenance

Component	Events/ Year	Interval (Days)	Description	Duration (Hours)	# of Crew	Labor/ Event	Labor Cost/ Year	Mat'l/ Event	Equip/ Event	Total/ Event	Total/ Year
Rotor											
Blades (three)	1	365	Inspect blades, lube pitch brgs	4	2	520	520	50	0	570	570
Hub	1	365	Inspect	1	2	130	130	0	0	130	130
Pitch mechanism (three)	2	183	Check fluid, filters, system	2	2	260	520	50	0	310	620
Drivetrain and Nacelle											
Transmission system											
Gearbox	2	183	Check oil level, filters, inspect gears and brgs	1.25	2	162.5	325	400	0	562.5	1125
Support structure (bedplate)	2	183	Inspect, check pretension	0.5	1	32.5	65	0	0	32.5	65
Generator cooling system	2	183	Check fluid, filters, system	0.5	2	65	130	100	0	165	330
Brake system, hydraulics	2	183	Check fluid, filters, system	0.5	2	65	130	300	0	365	730
Coupling (gem to gearbox)	2	183	Inspect	0.2	1	13	26	0	0	13	26
Nacelle cover	2	183	Inspect	0.5	1	32.5	65	0	0	32.5	65
Generator	2	183	Inspect	1	2	130	260	0	0	130	260
Variable-speed electronics (PE)	2	183	Inspect	1	1	65	130	0	0	65	130
Transformer	2	183	Inspect	0.5	1	32.5	65	0	0	32.5	65
Cable	2	183	Inspect	1	1	65	130	0	0	65	130
Switchgear	2	183	Inspect	0.5	1	32.5	65	0	0	32.5	65
Yaw Drive and Bearing (3)	1	365	Inspect, lubricate	1.5	2	195	195	50	0	245	245
Control and Safety System	2	183	Inspect	1	1	65	130	0	0	65	130
Tower	1	365	Inspect, check pretension	8	2	1040	1040	0	0	1040	1040
Foundation	2	183	Inspect, check pretension	0.5	1	32.5	65	0	0	32.5	65
Total						$2,938	$3,991	$950	$0	$3,888	**$5,791**
COE						$0.00061	$0.00082	$0.00020	$0.00000	$0.00080	**$0.00120**

Integrated Baseline - Levelized Replacement Costs

Item	Event Year	Duration (Hours)	# of Crew	Labor	Mat'l	Equip	Total RC (2002 $)	Total PV(n)
Rotor								
Blades (three including pitch bearings)	25	24	3	4,680	44,400	25,000	74,080	16,986
Drivetrain and Nacelle								
Transmission system								
Gearbox - 25 year	25	36	2	4,680	71,857	50,000	126,537	29,014
Yaw Drive and Bearing (3)	25	16	2	2,080	24,000	80,000	106,080	24,324
Control and Safety System	0	2	1	130	525	-	-	-
Tower	0	8	2	1,040	138,000	3,000	-	-
Foundation	0	8	3	1,560	7,200	2,000	-	-
Total							**$306,697**	**$70,324**
CRF								0.0732
LRC								$5,147.30
LRC-COE								**$0.0011**

Direct Drive - Unscheduled Maintenance Costs

Component	Spare Cost: x 1.5	Weibull Shape Factor	Average Failures/ Year	MTBE (Years)	MTTR (Hours)	Repair Description	% Spare Cost	# of Crew	Labor/ Event	Mat'l/ Event	Equip/ Event	Total/ Event	Total/ Year
Rotor													
Blades (three)	222,000	3.5	0.001	67	8	Replace	100%	3	1,560	222,000	25,000	248,560	344
Hub	96,000	1.0	0.002	500	16	Replace	100%	3	3,120	96,000	25,000	124,120	241
Pitch mechanism (three including bearings)	54,000	3.5	0.184	5	12	Repair/replace parts	5%	2	1,560	2,700	-	4,260	784
Drivetrain and Nacelle													
Transmission system													
Gearbox	-	3.5	0.011	35	24	Replace	100%	2	3,120	-	50,000	53,120	-
Mainshaft	6,414	1.0	0.002	476	16	Replace	100%	2	2,080	6,414	50,000	58,494	119
Mainshaft bearing and block	-	1.0	0.002	476	16	Replace	100%	2	2,080	-	50,000	52,080	-
Elastomeric mounting system	-	3.5	0.084	10	8	Replace	100%	2	1,040	-	-	1,040	-
Generator isolation mounts	-	3.5	0.084	10	8	Replace	100%	2	1,040	-	-	1,040	-
Support structure (integrated nacelle)	76,437	1.0	0.002	476	8	Repair	20%	2	1,040	15,287	-	16,327	33
Generator cooling system	5,039	3.5	0.184	5	8	Repair/replace parts	2%	2	1,040	101	-	1,141	210
Brake system, hydraulics	18,570	3.5	0.184	5	8	Repair/replace parts	2%	2	1,040	371	-	1,411	260
Coupling	-	3.5	0.034	20	8	Repair/replace parts	100%	2	1,040	-	-	1,040	-
Nacelle cover	20,334	1.0	0.002	476	8	Repair	10%	2	1,040	2,033	25,000	28,073	57
Generator	455,996	3.5	0.029	25	48	Replace w/rebuilt	30%	3	9,360	136,799	50,000	196,159	5,663
Variable-speed electronics (PE)	79,679	1.0	0.200	5	8	Replace component	5%	1	520	3,984	-	4,504	901
0.95-0.95 substation VAR control	17,336	1.0	0.040	25	4	Replace component	10%	1	260	1,734	-	1,994	80
Transformer	38,813	3.5	0.000	100	8	Repair	25%	2	1,040	9,703	1,000	11,743	4
Cable	24,069	3.5	0.011	35	8	Replace portion	20%	2	1,040	4,814	-	5,854	65
Switchgear	15,698	3.5	0.184	5	6	Replace component	10%	2	780	1,570	-	2,350	432
Yaw Drive (three) and Bearing	24,000	3.5	0.084	10	12	Replace one drive or bearing	40%	2	1,560	9,600	-	11,160	938
Control and Safety System	10,500	1.0	3.000	0	2	Replace component	5%	1	130	525	-	655	1,965
Tower	276,000	1.0	0.002	476	8	Replace section	50%	2	1,040	138,000	3,000	142,040	289
Foundation	72,000	1.0	0.001	1000	8	Repair	10%	3	1,560	7,200	2,000	10,760	11
Total	**$1,512,882**												**$12,396**
COE													**$0.00248**

MTBE - Mean Time Between Events
MTTR - Mean Time to Repair

Direct Drive - Scheduled Maintenance

Component	Events/ Year	Interval (Days)	Description	Duration (Hours)	# of Crew	Labor/ Event	Labor Cost/ Year	Mat'l/ Event	Equip/ Event	Total/ Event	Total/ Year
Rotor											
Blades (three)	1	365	Inspect blades, lube pitch brgs	4	2	520	520	50	0	570	570
Hub	1	365	Inspect	1	2	130	130	0	0	130	130
Pitch mechanism (three)	2	183	Check fluid, filters, system	2	2	260	520	50	0	310	620
Drivetrain and Nacelle											
Transmission system											
Mainshaft	2	183	Inspect	0.25	1	16.25	32.5	0	0	16.25	32.5
Support structure (bedplate)	2	183	Inspect, check pretension	0.5	1	32.5	65	0	0	32.5	65
Generator cooling system	2	183	Check fluid, filters, system	0.5	2	65	130	100	0	165	330
Brake system, hydraulics	2	183	Check fluid, filters, system	0.5	2	65	130	300	0	365	730
Nacelle cover	2	183	Inspect	0.5	1	32.5	65	0	0	32.5	65
Generator	2	183	Inspect	1	2	130	260	0	0	130	260
Variable-speed electronics (PE)	2	183	Inspect	1	1	65	130	0	0	65	130
0.95-0.95 substation VAR control	2	183	Inspect	1	1	65	130	0	0	65	130
Transformer	2	183	Inspect	0.5	1	32.5	65	0	0	32.5	65
Cable	2	183	Inspect	1	1	65	130	0	0	65	130
Switchgear	2	183	Inspect	0.5	1	32.5	65	0	0	32.5	65
Yaw Drive and Bearing (3)	1	365	Inspect, lubricate	1.5	2	195	195	50	0	245	245
Control and Safety System	2	183	Inspect	1	1	65	130	0	0	65	130
Tower	1	365	Inspect, check pretension	8	2	1040	1040	0	0	1040	1040
Foundation	2	183	Inspect, check pretension	0.5	1	32.5	65	0	0	32.5	65
Total						$2,844	$3,803	$550	$0	$3,394	**$4,803**
COE						$0.00057	$0.00076	$0.00011	$0.00000	$0.00068	**$0.00096**

Direct Drive - Levelized Replacement Costs

Item	Event Year	Duration (Hours)	# of Crew	Labor	Mat'l	Equip	Total RC (2002 $)	Total PV(n)
Rotor								
Blades (three including pitch bearings)	25	24	3	4,680	44,400	25,000	74,080	16,986
Hub	0	16	3	3,120	96,000	25,000	-	-
Pitch mechanism (three) - 20 year	0	16	2	2,080	21,600	-	-	-
Drivetrain and Nacelle								
Generator - 25 year	25	48	3	9,360	91,199	50,000	150,559	34,522
Yaw Drive and Bearing (3)	25	16	2	2,080	24,000	80,000	106,080	24,324
Total							**$330,719**	**$75,832**
CRF								0.0732
LRC								$5,550.46
LRC-COE								**$0.0011**

Single-PM - Unscheduled Maintenance Costs

Component	Spare Cost: x 1.5	Weibull Shape Factor	Average Failures/ Year	MTBE (Years)	MTTR (Hours)	Repair Description	% Spare Cost	# of Crew	Labor/ Event	Mat'l/ Event	Equip/ Event	Total/ Event	Total/ Year
Rotor													
Blades (three)	222,000	3.5	0.001	67	8	Replace	100%	3	1,560	222,000	25,000	248,560	344
Hub	96,000	1.0	0.002	500	16	Replace	100%	3	3,120	96,000	25,000	124,120	241
Pitch mechanism (three including bearings)	54,000	3.5	0.184	5	12	Repair/replace parts	5%	2	1,560	2,700	-	4,260	784
Drivetrain and Nacelle													
Transmission system													
Gearbox	126,654	3.5	0.007	35	36	Replace	100%	2	4,680	126,654	50,000	181,334	1,330
Mainshaft (included)	-	1.0	0.002	476	16	Replace	100%	2	2,080	-	50,000	52,080	-
Mainshaft bearing and block (included)	-	1.0	0.002	476	16	Replace	100%	2	2,080	-	50,000	52,080	-
Elastomeric mounting system	-	3.5	0.084	10	8	Replace	100%	2	1,040	-	-	1,040	-
Generator isolation mounts	-	3.5	0.084	10	8	Replace	100%	2	1,040	-	-	1,040	-
Support structure	30,000	1.0	0.002	476	8	Repair	20%	2	1,040	6,000	-	7,040	14
Generator and gearbox cooling system	6,653	3.5	0.184	5	8	Repair/replace parts	2%	2	1,040	133	-	1,173	216
Brake system, hydraulics	4,769	3.5	0.184	5	8	Repair/replace parts	2%	2	1,040	95	-	1,135	209
Coupling	-	3.5	0.034	20	8	Repair/replace parts	100%	2	1,040	-	-	1,040	-
Nacelle cover	12,288	1.0	0.002	476	8	Repair	10%	2	1,040	1,229	25,000	27,269	55
Generator	89,294	3.5	0.018	25	24	Replace w/rebuilt	50%	3	4,680	44,647	-	49,327	890
Variable-speed electronics (PE)	79,679	1.0	0.200	5	8	Replace component	5%	1	520	3,984	-	4,504	901
0.95-0.95 substation VAR control	17,336	1.0	0.040	25	4	Replace component	10%	1	260	1,734	-	1,994	80
Transformer	38,813	3.5	0.000	100	8	Repair	25%	2	1,040	9,703	1,000	11,743	4
Cable	24,069	3.5	0.011	35	8	Replace portion	20%	2	1,040	4,814	-	5,854	65
Switchgear	15,698	3.5	0.184	5	6	Replace component	10%	2	780	1,570	-	2,350	432
Yaw Drive (three) and Bearing	24,000	3.5	0.084	10	12	Replace one drive or bearing	40%	2	1,560	9,600	-	11,160	938
Control and Safety System	10,500	1.0	3.000	0	2	Replace component	5%	1	130	525	-	655	1,965
Tower	276,000	1.0	0.002	476	8	Replace section	50%	2	1,040	138,000	3,000	142,040	289
Foundation	72,000	1.0	0.001	1000	8	Repair	10%	3	1,560	7,200	2,000	10,760	11
Total	**$1,199,750**												**$8,768**
COE													**$0.00175**

MTBE - Mean Time Between Events
MTTR - Mean Time to Repair

Single-PM - Scheduled Maintenance

Component	Events/ Year	Interval (Days)	Description	Duration (Hours)	# of Crew	Labor/ Event	Labor Cost/ Year	Mat'l/ Event	Equip/ Event	Total/ Event	Total/ Year
Rotor											
Blades (three)	1	365	Inspect blades, lube pitch brgs	4	2	520	520	50	0	570	570
Hub	1	365	Inspect	1	2	130	130	0	0	130	130
Pitch mechanism (three)	2	183	Check fluid, filters, system	2	2	260	520	50	0	310	620
Drivetrain and Nacelle											
Transmission system											
Gearbox	2	183	Check oil level, filters, inspect gears and brgs	1.25	2	162.5	325	400	0	562.5	1125
Support structure (bedplate)	2	183	Inspect, check pretension	0.5	1	32.5	65	0	0	32.5	65
Generator cooling system	2	183	Check fluid, filters, system	0.5	2	65	130	100	0	165	330
Brake system, hydraulics	2	183	Check fluid, filters, system	0.5	2	65	130	300	0	365	730
Nacelle cover	2	183	Inspect	0.5	1	32.5	65	0	0	32.5	65
Generator	2	183	Inspect	1	2	130	260	0	0	130	260
Variable-speed electronics (PE)	2	183	Inspect	1	1	65	130	0	0	65	130
0.95-0.95 substation VAR control	2	183	Inspect	1	1	65	130	0	0	65	130
Transformer	2	183	Inspect	0.5	1	32.5	65	0	0	32.5	65
Cable	2	183	Inspect	1	1	65	130	0	0	65	130
Switchgear	2	183	Inspect	0.5	1	32.5	65	0	0	32.5	65
Yaw Drive and Bearing (3)	1	365	Inspect, lubricate	1.5	2	195	195	50	0	245	245
Control and Safety System	2	183	Inspect	1	1	65	130	0	0	65	130
Tower	1	365	Inspect, check pretension	8	2	1040	1040	0	0	1040	1040
Foundation	2	183	Inspect, check pretension	0.5	1	32.5	65	0	0	32.5	65
Total						$2,990	$4,095	$950	$0	$3,940	**$5,895**
COE						$0.00060	$0.00082	$0.00019	$0.00000	$0.00079	**$0.00118**

Single-PM - Levelized Replacement Costs

Item	Event Year	Duration (Hours)	# of Crew	Labor	Mat'l	Equip	Total RC (2002 $)	Total PV(n)
Rotor								
Blades (three including pitch bearings)	25	24	3	4,680	44,400	25,000	74,080	16,986
Drivetrain and Nacelle								
Transmission system								
Gearbox - 25 year	25	36	2	4,680	50,662	50,000	105,342	24,154
Yaw Drive and Bearing (3)	25	16	2	2,080	24,000	80,000	106,080	24,324
Total							**$285,502**	**$65,464**
CRF								0.0732
LRC								$4,792
LRC-COE								**$0.0010**

Multi-PM - Unscheduled Maintenance Costs

Component	Spare Cost: x 1.5	Weibull Shape Factor	Average Failures/ Year	MTBE (Years)	MTTR (Hours)	Repair Description	% Spare Cost	# of Crew	Labor/ Event	Mat'l/ Event	Equip/ Event	Total/ Event	Total/ Year
Rotor													
Blades (three)	222,000	3.5	0.001	67	8	Replace	100%	3	1,560	222,000	25,000	248,560	344
Hub	96,000	1.0	0.002	500	16	Replace	100%	3	3,120	96,000	25,000	124,120	241
Pitch mechanism (three including bearings)	54,000	3.5	0.184	5	12	Repair/replace parts	5%	2	1,560	2,700	-	4,260	784
Drivetrain and Nacelle													
Transmission system													
Gearbox	79,776	3.5	0.007	35	40	Replace	100%	3	7,800	79,776	50,000	137,576	1,009
Mainshaft	6,816	1.0	0.002	476	16	Replace	100%	3	3,120	6,816	50,000	59,936	122
Mainshaft bearing and block	-	1.0	0.002	476	16	Replace	100%	3	3,120	-	50,000	53,120	-
Elastomeric mounting system	-	3.5	0.084	10	8	Replace	100%	2	1,040	-	-	1,040	-
Generator isolation mounts	-	3.5	0.084	10	8	Replace	100%	2	1,040	-	-	1,040	-
Support structure	28,007	1.0	0.002	476	8	Repair	20%	2	1,040	5,601	-	6,641	14
Generator & gearbox cooling system	8,147	3.5	0.184	5	8	Repair/replace parts	2%	2	1,040	163	-	1,203	221
Brake system, hydraulics	8,397	3.5	0.184	5	8	Repair/replace parts	2%	2	1,040	168	-	1,208	222
Coupling	-	3.5	0.034	20	8	Repair/replace parts	100%	2	1,040	-	-	1,040	-
Nacelle cover	10,949	1.0	0.002	476	8	Repair	10%	2	1,040	1,095	25,000	27,135	55
Generator	116,948	3.5	0.108	25	16	Replace w/rebuilt	13%	3	3,120	14,618	-	17,738	1,920
Variable-speed electronics (PE)	79,679	1.0	0.200	5	8	Replace component	5%	1	520	3,984	-	4,504	901
0.95-0.95 substation VAR control	17,336	1.0	0.040	25	4	Replace component	10%	1	260	1,734	-	1,994	80
Transformer	38,813	3.5	0.000	100	8	Repair	25%	2	1,040	9,703	1,000	11,743	4
Cable	24,069	3.5	0.011	35	8	Replace portion	20%	2	1,040	4,814	-	5,854	65
Switchgear	18,848	3.5	0.184	5	6	Replace component	10%	2	780	1,885	-	2,665	490
Yaw Drive (three) and Bearing	24,000	3.5	0.084	10	12	Replace one drive or bearing	40%	2	1,560	9,600	-	11,160	938
Control and Safety System	10,500	1.0	3.000	0	2	Replace component	5%	1	130	525	-	655	1,965
Tower	276,000	1.0	0.002	476	8	Replace section	50%	2	1,040	138,000	3,000	142,040	289
Foundation	72,000	1.0	0.001	1000	8	Repair	10%	3	1,560	7,200	2,000	10,760	11
Total	**$1,192,281**												**$9,675**
COE													**$0.00194**

MTBE - Mean Time Between Events
MTTR - Mean Time to Repair

Multi-PM - Scheduled Maintenance											
Component	Events/ Year	Interval (Days)	Description	Duration (Hours)	# of Crew	Labor/ Event	Labor Cost/ Year	Mat'l/ Event	Equip/ Event	Total/ Event	Total/ Year
Rotor											
Blades (three)	1	365	Inspect blades, lube pitch brgs	4	2	520	520	50	0	570	570
Hub	1	365	Inspect	1	2	130	130	0	0	130	130
Pitch mechanism (three)	2	183	Check fluid, filters, system	2	2	260	520	50	0	310	620
Drivetrain and Nacelle											
Transmission system											
Gearbox	2	183	Check oil level, filters, inspect gears and brgs	1.25	2	162.5	325	400	0	562.5	1125
Mainshaft	2	183	Inspect	0.25	1	16.25	32.5	0	0	16.25	32.5
Support structure (bedplate)	2	183	Inspect, check pretension	0.5	1	32.5	65	0	0	32.5	65
Generator cooling system	2	183	Check fluid, filters, system	0.5	2	65	130	100	0	165	330
Brake system, hydraulics	2	183	Check fluid, filters, system	0.5	2	65	130	300	0	365	730
Nacelle cover	2	183	Inspect	0.5	1	32.5	65	0	0	32.5	65
Generator	2	183	Inspect	6	2	780	1560	0	0	780	1560
Variable-speed electronics (PE)	2	183	Inspect	1	1	65	130	0	0	65	130
0.95-0.95 substation VAR control	2	183	Inspect	1	1	65	130	0	0	65	130
Transformer	2	183	Inspect	0.5	1	32.5	65	0	0	32.5	65
Cable	2	183	Inspect	1	1	65	130	0	0	65	130
Switchgear	2	183	Inspect	0.5	1	32.5	65	0	0	32.5	65
Yaw Drive and Bearing (3)	1	365	Inspect, lubricate	1.5	2	195	195	50	0	245	245
Control and Safety System	2	183	Inspect	1	1	65	130	0	0	65	130
Tower	1	365	Inspect, check pretension	8	2	1040	1040	0	0	1040	1040
Foundation	2	183	Inspect, check pretension	0.5	1	32.5	65	0	0	32.5	65
Total						$3,656	$5,428	$950	$0	$4,606	**$7,228**
COE						$0.00073	$0.00109	$0.00019	$0.00000	$0.00093	**$0.00145**

Multi-PM - Scheduled Maintenance								
Item	Event Year	Duration (Hours)	# of Crew	Labor	Mat'l	Equip	Total RC (2002 $)	Total PV(n)
Rotor								
Blades (three including pitch bearings)	25	24	3	4,680	44,400	25,000	74,080	16,986
Drivetrain and Nacelle								
Transmission system								
Gearbox - 25 year	25	36	3	7,020	31,910	50,000	88,930	20,391
Yaw Drive and Bearing (3)	25	16	2	2,080	24,000	80,000	106,080	24,324
Total							**$269,090**	**$61,701**
CRF								0.0732
LRC								$4,516.14
LRC-COE								**$0.0009**

Multi-Induction - Unscheduled Maintenance Costs

Component	Spare Cost: x 1.5	Weibull Shape Factor	Average Failures/ Year	MTBE (Years)	MTTR (Hours)	Repair Description	% Spare Cost	# of Crew	Labor/ Event	Mat'l/ Event	Equip/ Event	Total/ Event	Total/ Year
Rotor													
Blades (three)	222,000	3.5	0.001	67	8.0	Replace	100.0%	3	1,560	222,000	25,000	248,560	344
Hub	96,000	1.0	0.002	500	16.0	Replace	100.0%	3	3,120	96,000	25,000	124,120	241
Pitch mechanism (three including bearings)	54,000	3.5	0.184	5	12.0	Repair/replace parts	5.0%	2	1,560	2,700	-	4,260	784
Drivetrain and Nacelle													
Transmission system													
Gearbox	112,841	3.5	0.007	35	40.0	Replace	100.0%	3	7,800	112,841	50,000	170,641	1,252
Mainshaft	6,816	1.0	0.002	476	16.0	Replace	100.0%	3	3,120	6,816	50,000	59,936	122
Mainshaft bearing and block	-	1.0	0.002	476	16.0	Replace	100.0%	3	3,120	-	50,000	53,120	-
Elastomeric mounting system	-	3.5	0.084	10	8.0	Replace	100.0%	2	1,040	-	-	1,040	-
Generator isolation mounts	-	3.5	0.084	10	8.0	Replace	100.0%	2	1,040	-	-	1,040	-
Support structure	16,638	1.0	0.002	476	8.0	Repair	20.0%	2	1,040	3,328	-	4,368	9
Generator cooling system	6,723	3.5	0.184	5	8.0	Repair/replace parts	2.0%	2	1,040	134	-	1,174	216
Brake system, hydraulics	4,145	3.5	0.184	5	8.0	Repair/replace parts	2.0%	2	1,040	83	-	1,123	207
Coupling	2,648	3.5	0.034	20	8.0	Repair/replace parts	100.0%	2	1,040	2,648	-	3,688	126
Nacelle cover	19,641	1.0	0.002	476	8.0	Repair	10.0%	2	1,040	1,964	25,000	28,004	57
Generator	59,948	3.5	0.144	25	16.0	Replace w/rebuilt	9.4%	3	3,120	5,620	-	8,740	1,262
Soft start and PF caps	25,572	1.0	0.200	5	8.0	Replace component	5.0%	1	520	1,279	-	1,799	360
0.95-0.95 substation VAR control	17,336	1.0	0.040	25	4.0	Replace component	10.0%	1	260	1,734	-	1,994	80
Transformer	33,750	3.5	0.000	100	8.0	Repair	25.0%	2	1,040	8,438	1,000	10,478	4
Cable	26,726	3.5	0.011	35	8.0	Replace portion	20.0%	2	1,040	5,345	-	6,385	71
Switchgear	33,617	3.5	0.184	5	6.0	Replace component	10.0%	2	780	3,362	-	4,142	762
Yaw Drive (three) and Bearing	24,000	3.5	0.084	10	12.0	Replace one drive or bearing	40.0%	2	1,560	9,600	-	11,160	938
Control and Safety System	10,500	1.0	3.000	0	2.0	Replace component	5.0%	1	130	525	-	655	1,965
Tower	276,000	1.0	0.002	476	8.0	Replace section	50.0%	2	1,040	138,000	3,000	142,040	289
Foundation	72,000	1.0	0.001	1000	8.0	Repair	10.0%	3	1,560	7,200	2,000	10,760	11
Total	**$1,120,898**												**$9,097**
COE													**$0.00195**

MTBE - Mean Time Between Events
MTTR - Mean Time to Repair

Multi-induction - Scheduled Maintenance											
Component	Events/ Year	Interval (Days)	Description	Duration (Hours)	# of Crew	Labor/ Event	Labor Cost/ Year	Mat'l/ Event	Equip/ Event	Total/ Event	Total/ Year
Rotor											
Blades (three)	1	365	Inspect blades, lube pitch brgs	4	2	520	520	50	0	570	570
Hub	1	365	Inspect	1	2	130	130	0	0	130	130
Pitch mechanism (three)	2	183	Check fluid, filters, system	2	2	260	520	50	0	310	620
Drivetrain and Nacelle											
Transmission system											
Gearbox	2	183	Check oil level, filters, inspect gears and brgs	1.25	2	162.5	325	400	0	562.5	1125
Mainshaft	2	183	Inspect	0.25	1	16.25	32.5	0	0	16.25	32.5
Support structure (bedplate)	2	183	Inspect, check pretension	0.5	1	32.5	65	0	0	32.5	65
Generator cooling system	2	183	Check fluid, filters, system	0.5	2	65	130	100	0	165	330
Brake system, hydraulics	2	183	Check fluid, filters, system	0.5	2	65	130	300	0	365	730
Coupling (gem to gearbox)	2	183	Inspect	0.2	1	13	26	0	0	13	26
Nacelle cover	2	183	Inspect	0.5	1	32.5	65	0	0	32.5	65
Generator	2	183	Inspect	6	2	780	1560	0	0	780	1560
Variable-speed electronics (PE)	2	183	Inspect	1	1	65	130	0	0	65	130
0.95-0.95 substation VAR control	2	183	Inspect	1	1	65	130	0	0	65	130
Transformer	2	183	Inspect	0.5	1	32.5	65	0	0	32.5	65
Cable	2	183	Inspect	1	1	65	130	0	0	65	130
Switchgear	2	183	Inspect	0.5	1	32.5	65	0	0	32.5	65
Yaw Drive and Bearing (3)	1	365	Inspect, lubricate	1.5	2	195	195	50	0	245	245
Control and Safety System	2	183	Inspect	1	1	65	130	0	0	65	130
Tower	1	365	Inspect, check pretension	8	2	1040	1040	0	0	1040	1040
Foundation	2	183	Inspect, check pretension	0.5	1	32.5	65	0	0	32.5	65
Total						$3,669	$5,454	$950	$0	$4,619	**$7,254**
COE						$0.00079	$0.00117	$0.00020	$0.00000	$0.00099	**$0.00156**

Multi-Induction - Scheduled Maintenance								
Item	Event Year	Duration (Hours)	# of Crew	Labor	Mat'l	Equip	Total RC (2002 $)	Total PV(n)
Rotor								
Blades (three including pitch bearings)	25	24	3	4,680	44,400	25,000	74,080	16,986
Hub	0	16	3	3,120	96,000	25,000	-	-
Pitch mechanism (three) - 20 year	0	16	2	2,080	21,600	-	-	-
Drivetrain and Nacelle								
Transmission system								
Gearbox - 25 year	25	36	3	7,020	45,136	50,000	102,156	23,424
Yaw Drive and Bearing (3)	25	16	2	2,080	24,000	80,000	106,080	24,324
Total							**$282,316**	**$64,734**
CRF								0.0732
LRC								$4,738
LRC-COE								**$0.0010**

Appendix K

Kaman Electromagnetics Conceptual Study Report

Drive Train Architecture Study for Wind Turbines

Final Report

June 29, 2001

Re: Subcontract, GEC*/KAC†, dated February 26, 2001

Submitted to
Global Energy Concepts, LLC*
5729 Lakeview Drive, NE, Suite 100
Kirkland, WA 98033
425-822-9008

Prepared by
Kaman Aerospace Corporation†
Electromagnetics Development Center
2 Fox Road
Hudson, MA 01749
978-562-2933

Table of Contents

Drive Train Architecture Study for Wind Turbines, June 29, 2001:

Submitted by:

Kaman Aerospace Corporation
Electromagnetics Development Center
2 Fox Road
Hudson, MA 01749

Prepared by: _____ Date: _____

Approved by:

_____ Date: _____
Name and Title

Revision	Date	Author	Description	Pages

Table of Contents

List of Tables

List of Tables

1. Scope

Kaman Aerospace Corporation (KAC) prepared this report for Global Energy Concepts, LLC(GEC) under the WindPACT Advanced Wind Turbine Drive Train Design contract to the National Renewable Energy Laboratory (NREL). As part of the WindPACT project, scaling studies are being conducted on future turbines and drive train architectures to define preferred technology and advanced concepts that offer great promise for improving performance of wind turbines and decreasing loads and costs. During the first phase of this project, we evaluated preliminary design concepts and sizing studies of innovative drive train architectures and major components to select the most promising candidates.

The scope of this study is to determine the size, weight, and probable costs of the wind turbine drive train's generator and associated power electronics. To assess candidate architectures, we carried out a comparative assessment for a 1.5-MW baseline drive train. The purpose of this report is to evaluate the following specific types of generator candidates:

- **HTLS**: High-torque, low-speed synchronous machines, connected directly to the main shaft (no gearbox), in three variations: (1) axial flux, permanent magnet (PM) excitation; (2) radial flux, PM excitation; and (3) either (1) or (2) with electric field excitation.

- **MTMS**: Medium-torque, medium-speed synchronous machine, driven through a single-stage gearbox in three variations: (1) axial flux, PM excitation; 2) radial flux, PM excitation; and (3) either (1) or (2) with electric field excitation.

1.1 Document Overview

This document consists of the following sections and appendices:

- Section 2: Drive train candidates for wind turbines using synchronous type generators
- Section 3: PM and electrically excited machine candidates
- Section 4: Concept for a PM HTLS generator
- Section 5: Concept for a PM MTMS generator
- Section 6: Thermal trade studies for PM generators
- Section 7: Efficiency, air-gap, and cost studies for PM generators
- Section 8: Power electronics (PE) trade studies
- Section 9: Construction method trade studies
- Appendix I: Cost factors for multi-PM generators operating with a gearbox
- Appendix II: Transportation and handling cost factors

1.2 Background

The analysis objective was to rapidly evaluate the variations of cost and physical size with 1.5-MW drive train configurations to select the most promising generator and PE candidates. The top-level design constraints are included in the initial WindPACT Phase 1 ground rules for evaluating each configuration. In general, the turbine drive train configuration includes gearboxes with single or multiple stages, electrical machines, PE/control systems, and distribution-voltage transformers.

Drive train torque and power input are provided by a variable-speed main shaft (i.e., pitch controlled blades).

We determined the measures of generator system performance based on technical, architectural, and manufacturing concepts. In assessing the various concepts, we focused on technical performance, economics, manufacturability, and logistics factors for wind turbine applications. The preliminary analysis considered the feasibility of integrating components into commercially viable products. The application of advanced technology and engineering or manufacturing concepts that maximize the cost-performance of the total system is expected to result in performance and economic gains.

For this study, we looked at a number of system operating and cost parameters:

- Capital costs
- Energy production performance at various operating points (i.e., system efficiency)
- Ability to manage torque and speed transients (e.g., wind gusts)
- Manufacturability factors such as production tooling, facilities, and costs
- Failure modes and effects on continuous energy production
- Maintenance factors such as repair, field installation, and maintenance
- Technical risk areas
- Development costs (nonrecurring costs for prototyping and preproduction)

1.3 Conclusions and Recommendations

The results of our evaluation of the candidate systems are summarized in the sections that follow.

1.3.1 WindPACT Drive Train Generator Conclusions

- The PM generator is preferred over an electrically excited generator for a 1.5-MW turbine drive train because:
    - It has lower operating costs (less maintenance and higher reliability).
    - It has higher efficiency and volumetric density (size-performance).
    - It is potentially less costly to produce.
    - It has the simplest machine (rotor) design and construction
    - It demands fewer pieces of PE equipment (i.e., no field excitation converter).

- A system of utility power electronics that uses semiconductor switching (e.g., insulated gate bipolar transistor [IGBT]) technology offers performance advantages over grid-commutated inverters (e.g., thyristors) because:
    - It produces higher quality output power (less distortion).
    - Its operation is decoupled (independent) from the power grid.
    - It has better system efficiency resulting from better power factor control.

- The preferred PM generator variant for a 1.5-MW turbine drive train is a radial field topology with an air-gap diameter (machine size) of 2–5 m. This machine has the lowest cost because its construction can be simplified (compared to the axial field alternative)

without a significant penalty in mass and size in this large power class. In addition, these machines fit into conventional sized nacelles and are easy to transport and handle.

- The MTMS version is potentially less expensive than the HTLS version because of its smaller air-gap diameter and mass. The HTLS design's optimum air-gap diameter is 4–5 m compared to 2 m for the MTMS. The HTLS requires greater material/mass to achieve the desired performance. Other considerations include the cooling system alternatives—the HTLS can use either forced air or liquid cooling, but the MTMS requires liquid cooling, which is more expensive.

- PM generator construction concepts for these large machines produce a range of costs and benefits to consider. In general, the benefits of modular construction and assembly of small generator parts (e.g., segmented stators) have the potential for greater economies of scale. They also require less expensive facilities and handling equipment. However, greater material processing costs may partially offset these advantages in the 4- to 7-m air-gap diameter range.

- A direct drive PM generator variation is more realistic than the multistage gearbox type discussed in Section 3. To produce the same overall power output, system performance decreases and costs increase because the generator parasitics are higher. Maintenance and handling gains may be achievable. Other factors such as scalability and economies of size were not considered.

- Estimated cost and performance characteristics for a 1.5-MW PM turbine drive train generator are given in Table 1-1.

- The most difficult development challenges are likely to be uncertainties about production quantities and schedules, which will have a significant impact on product development and investment decisions.

Table 1-1. Estimated Cost and Performance Characteristics for Two Variations of a 1.5-MW PM Generator

	MTMS Radial PM Generator	HTLS Radial PM Generator
Unit production cost, U.S. dollars (USD)	50,000	172,000
Size	Length: 0.66 m Outside diameter (OD): 2.49 m	Length: 1.17 m OD: 4.53 m
Weight	5.8–6.0 tons	19–20 tons
Efficiency	97.15%	97.15%

1.3.2 WindPACT Drive Train Study Recommendations

Kaman's preliminary design concept for the MTMS PM machine described in Sections 4 and 5 of this report should be developed in Phase 2 as the preferred candidate for a 1.5-MW turbine drive train. Development should establish a basic product design for:

- Refined production cost estimates
- Optimal machine performance and sizing characteristics based on cost trades

In addition, significant development challenges and solutions should be identified.

To achieve the desired performance and cost objectives, the power electronics for the Phase 2 machine should be defined based on today's commercially available equipment.

2. Drive Train Candidates—Synchronous Type Generators

In this section, we introduce the types of alternating current (AC) or synchronous generators and associated PE topologies considered as alternatives in this study. The three different types of generator candidates are: electrically excited machines, PM machines, and hybrids (a combination of these two). There are also different configurations or variants for each of these types of directly driven generators. For example, the machine can be a radial-, axial-, or transverse-flux machine design. The path of the magnetic flux is perpendicular to the direction of the rotor shaft in a radial-flux machine and perpendicular to the radial direction of the rotor shaft in an axial-flux machine.

The goal of this work was to describe basic design parameters and architectural similarities and differences that are major factors in producing affordable machines with high torque per unit volume and low losses. Advanced PM machines offer advantages compared to other machine types as described in this section. PM excitation allows the use of a smaller pole pitch than in conventional generators. The efficiency can also be higher in the PM machine than in the conventional machines.

2.1 Synchronous Machine Drive Train Architectures

Generators produce electricity using a process called electromagnetic induction. The voltage, or electromotive force, that a generator produces can be increased by increasing (1) the strength of the magnetic field (number of lines of force), (2) the speed at which it rotates, or (3) the number of windings that cut the magnetic field. Electromagnetism is another important effect to consider. The current produced in a generator also produces a magnetic field that makes it harder to turn. The more electricity produced, the stronger its magnetic field, and the more difficult it is to turn. An AC generator is also called a synchronous generator because it generates a voltage that has a frequency proportional to, or synchronized with, the speed of the rotor.

A synchronous generator has two main parts—an armature and a field structure. The armature contains windings in which the electricity is induced. The (rotating) field structure acts like a magnet and sets up the magnetic lines of force. Electromagnets create the lines of force in electrically excited generators whereas permanent magnets create these lines of force in PM

generators. The coils for the armature and field structure are usually insulated copper wire wound around iron cores, which strengthen the magnetic fields.

The synchronous machines under consideration differ as to how the air-gap field is generated:

- Electrically excited synchronous machines (Figure 2-1a)
- PM machines (Figure 2-1b)
- Hybrids using a combination of permanent magnets and electrical excitation (Figure 2-1c)

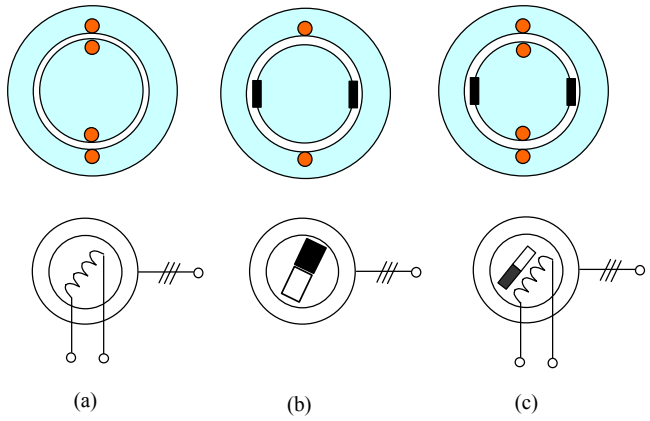

(a) Electrically excited synchronous generator
(b) PM generator
(c) Hybrid (PM + electrically excited) generator

Figure 2-1. Simplified construction of basic synchronous machines

Each type of synchronous machine requires a set of drive train power electronics, as shown in Figure 2-2, to provide variable-speed operation when connected to the power grid.

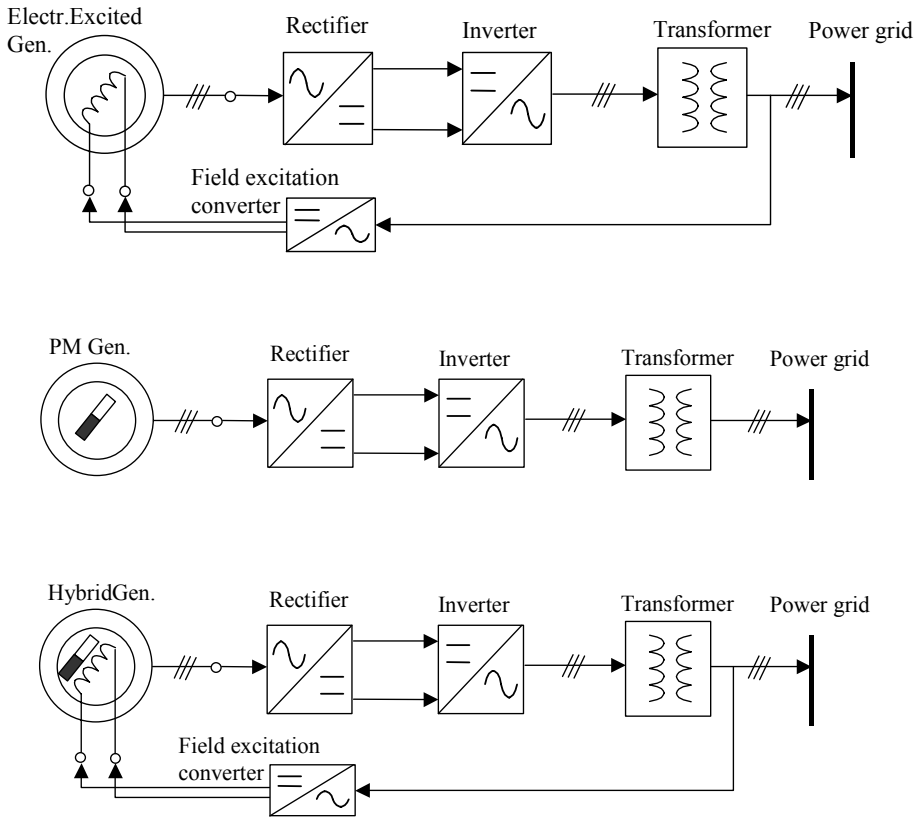

Figure 2-2. Power electronics for variable-speed operation of different synchronous generators

The architectures presented are typical AC-DC-AC (DC is direct current) conversion systems that allow independent frequency and voltage conversion from generated power to grid power. In other words, the DC bus barrier in these architectures allows the turbine to be operated at variable speeds.

Architectures that use synchronous generators (Figure 2-2) are made up of the same major elements:

- Generator
- Rectifier
- Inverter
- Output transformer
- Field excitation converter (not necessary for pure PM generator).

2.2 Synchronous Machine Architectures—Major Differences

Each type of synchronous generator and PE system has inherent advantages and disadvantages that result from differences in construction or from the complexity of the total architecture. The major areas of interest and the inherent differences or challenges for wind turbine applications are summarized below. Table 2-1 summarizes the results for an electrically excited generator drive train. Table 2-2 gives the results for a PM generator drive train. Table 2-3 outlines the results for a hybrid generator drive train.

Table 2-1. Drive Train Based on Electrically Excited Generator

Global Characterization		Positive Consequences	Negative Consequences
Generator-Specific Aspects	Excitation windings on rotor	- Excitation field can be adjusted - Excitation field can be turned off in case of system failure	- I^2R losses on rotor - Complex rotor construction - More mechanical parts in machine design
	Slip rings and brushes to pass the excitation current	None	- Higher maintenance - Decreased reliability - Additional source of losses - Source of hazard (sparks) - Increased operating noise - More mechanical parts in machine design
PE System-Specific Aspects	System requires a field excitation converter	Possible to adjust excitation field to narrow the generated voltage span over the rotor speed range (field weakening)	- Oversized machine design: Possible to use field weakening to narrow the voltage span only to the degree to which the machine magnetics are oversized - Additional power converter needed (low power, however)

Table 2-2. Drive Train Based on PM Generator

Global Characterization		Positive Consequences	Negative Consequences
Generator-Specific Aspects	Magnetic field produced by PM magnets	- Simple rotor construction - Low maintenance - High reliability - High efficiency within the same frame size (because of excitation losses) - High power density - Easy to optimize for low-noise operation	- Fixed magnetic field (i.e., the generated voltage span) cannot be narrowed by excitation field control - Not possible to turn off excitation field in case of system failure; contactor can be used to separate the generator from the power electronics if necessary - Above a temperature of approximately 200°C, high-energy NeBFe magnets have irreversible metallurgical modifications and can become nonmagnetic.*
PE System-Specific Aspects	No need for field excitation converter	One less element in the PE architecture	None

* High-energy magnets (NeBFe) have a Curie temperature of approximately 310°C, which is higher than the 200°C threshold at which metallurgical changes start to occur. Consequently, the temperature limit of NeBFe is determined by metallurgical changes, not the Curie temperature. The recommended maximum operating temperature is typically 150°C. The magnetic field has a reversible temperature coefficient of approximately –1%/°C; i.e., for a 10°C increase of temperature, the field strength decreases by 1%. Or, to think of it another way, for a 10°C lower temperature, the field strength increases by 1%.

Table 2-3. Drive Train Based on a Hybrid Generator

Global Characterization		Positive Consequences	Negative Consequences
Generator-Specific Aspects	Magnetic field partially produced by PM magnets, partially by coils	- Lower rating for excitation coils - Good power density - Possible to electrically adjust field excitation to narrow the voltage span over the rotor speed range	- Complex rotor construction - I^2R losses on rotor - Excitation field cannot be turned off in case of system failure; contactor can be used to separate the generator from the power electronics if necessary - Above a temperature of approximately 200°C, high-energy NeBFe magnets have irreversible metallurgical modifications, can become nonmagnetic.
	Slip rings and brushes for excitation coils	None	- More mechanical parts in machine design - Higher maintenance - Decreased reliability - Additional source of losses - Source of hazard (sparks) - Increased operating noise
PE System-Specific Aspects	Requires a field excitation converter	Possible to adjust excitation field to narrow the generated voltage span over the rotor speed range (field weakening)	- Oversized machine design: possible to use field weakening to narrow the voltage span only to the degree to which the machine magnetic cores are oversized - Additional power converter needed (low power, however)

2.3 Synchronous Machine Architectures—Power Electronics

The power electronics for a wind turbine drive train are composed of:

- The generator PE, which are the power electronics that interface with the generator stator windings
- The utility PE, which are the power electronics that interface with the utility. Note that a transformer is typically used to match the inverter output voltage to the power grid voltage.

Regardless of the generator type/technology, the major elements of the power electronics play the same role in all the drive train architectures presented in Figure 2-2 and described below:

- The output transformer:
  - Matches the inverter voltage to the grid voltage level.
  - Provides electrical isolation of the drive train.

- The utility power electronics (i.e., inverter):
  - Transfer power into the grid (via a voltage matching transformer).
  - Convert DC energy into AC, tracking the grid phase and frequency.

  Note: Self-commutated inverters can also control reversed power flow (from grid to DC bus).

- The generator power electronics (i.e., rectifier):
  - Extract electrical power from generator windings.
  - Convert generated AC power into DC power.

  Note: Self-commutated rectifiers can also control reversed power flow (from DC to generator) for motoring purposes.

- The field excitation converter (used only for electrically excited generators):
  - Excites the field windings.
  - Can adjust the field excitation to narrow the range of generated voltage over the rotor speed range.

Looking at their functionality, one can see which PE components of the drive train are more dependent on generator type. The utility power electronics and the output transformer are less dependent on the generator, and the generator power electronics and the field excitation converter (if a part of the system) are more dependent on the generator. Note that although the generator power electronics are, to some extent, dependent on generator type, the same rectifier topology can be used for all generator types. For instance, a diode-based rectifier can work properly with any of the synchronous generator types (see Figures 2-1 through 2-5). The rectifier choice has more to do with the wave shape of the generated voltage and generator impedance.

The major types of drive train PE candidates are illustrated in the next figures based on the technology used. Figure 2-3 shows the major variants of PE architectures for electrically excited machines using different semiconductor switches. Figure 2-4 depicts the major variants of PM generator PE architectures that use different types of switch devices, and Figure 2-5 displays the major PE architecture variants for hybrid generators.

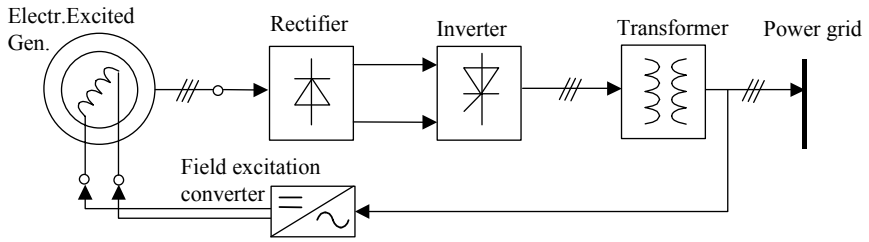

(a) *Diode bridge rectifier + Thyristor inverter*

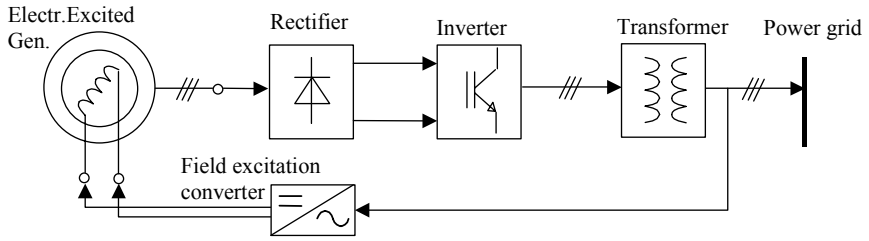

(b) *Diode bridge rectifier + IGBT inverter*

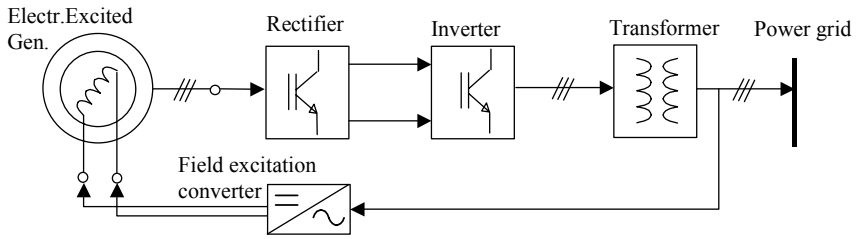

(c) *IGBT switched mode rectifier + IGBT inverter*

Figure 2-3. Electrically excited generator, PE variants by semiconductor switch technologies

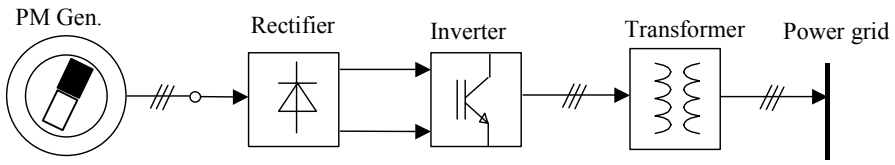

(a) *Diode bridge rectifier, IGBT inverter*

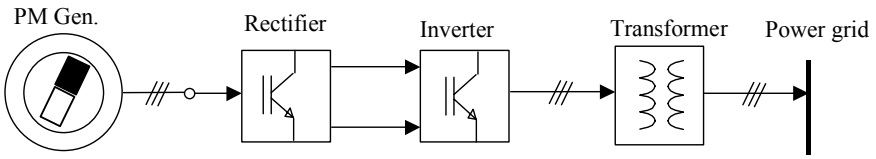

(b) *IGBT switched mode rectifier, IGBT inverter*

Figure 2-4. PM generator, PE variants by different switch technologies

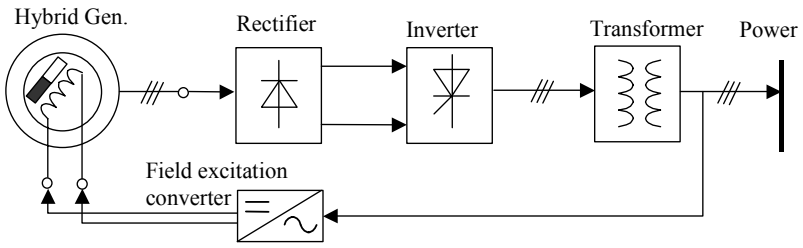

(a) *Diode bridge rectifier + Thyristor inverter*

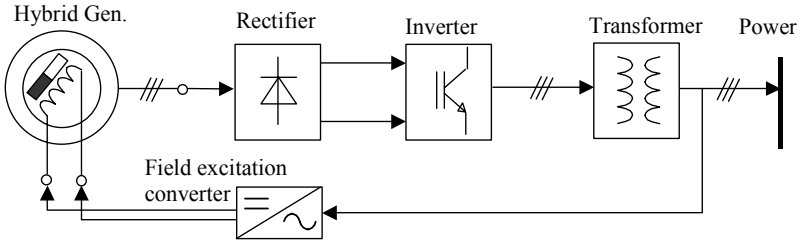

(b) *Diode bridge rectifier + IGBT inverter*

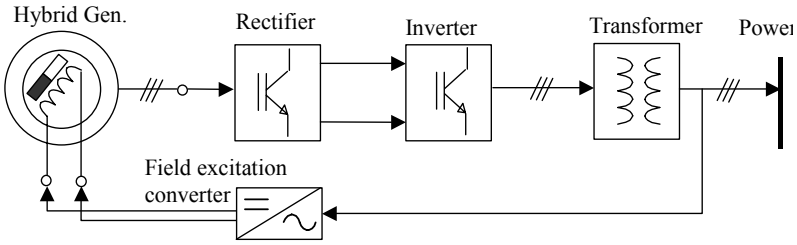

(c) *IGBT switched mode rectifier + IGBT inverter*

Figure 2-5. Hybrid generator, PE variants by different switch technologies

2.4 Overview of the Basic PE Elements

The basic PE elements of the drive train architecture shown in Figure 2-2 (i.e., output transformer, inverter and rectifier) are described below.

The output transformer is a common element that does not depend on the generator technology, and for now it is not the subject of discussion.

Because the utility PE (inverter) is not strictly dependent on the generator technology, the generator type is not considered in this section. The main options for utility PE architectures are
(1) the thyristor-based (grid-commutated) inverter, and
(2) the IGBT-based (self-commutated) inverter.

Tables 2-4 and 2-5 present the major advantages and disadvantages of these utility PE variants.

Table 2-4. Characterization of the Thyristor-Based (Grid-Commutated) Inverter

	Attributes	Rationale/Explanation
Pros	Low-cost method to transmit AC power into the grid	Low-cost semiconductor devices and controls
	Robust power electronics, high current surge capability	High surge capabilities (thyristors)
	Small power dissipation	Low switching and conduction losses
Cons	Provides polluted power (injects high current harmonics into grid)	Grid-dependent switching at low frequency (line frequency)
	Grid-dependent operation; limited functionality	Thyristors turned off, relying on line voltage polarity
	Cannot simultaneously control the reactive power and the active power delivered to grid	Grid-dependent operation and no control over thyristor turn-off
	Requires bulky filters	Notch filters designed to address individual line frequency harmonics (i.e., low and various frequencies)

Table 2-5. Characterization of the IGBT-Based (Self-Commutated) Inverter

	Attributes	Rationale/Explanation
Pros	Clean power (sinusoidal current wave forms) supplied into grid	Wave-form shaping capability because of pulse width modulated (PWM) operation and high switching frequency (kHz range)
	Small size output filters	No low frequency filters required, kHz switching frequency filters only
	Operation not dependent on grid, so functionality increases	IGBT turnoff fully controlled by gate command
	Allows independent control of both reactive and active power delivered to grid (can correct grid power factor)	Operation not grid-dependent
	Good overall power yield resulting from power factor control	Can operate at unity displacement power factor
Cons	Higher complexity (however, proven reliability in power applications)	More sophisticated control
	Higher power dissipation	Higher switching losses
	Limited surge capability	Reduced surge capability (IGBTs)
	Higher initial cost than thyristor inverters (however, proves a better investment in the long run because of increased functionality)	

Note that other semiconductor-based controlled switches, such as Insulated Gate Controlled Thyristors (IGCT) could be considered for inverter implementation.

The rectifier plays a very important role—it extracts maximum electric power from the generator windings. Depending on the rectifier performance, the turbine-rectifier system can be more energy efficient. The main options for generator PE systems are
(1) the diode bridge (uncontrolled) rectifier, and
(2) the IGBT-based (switch mode or boost) rectifier.

Tables 2-6 and 2-7 list the major advantages and disadvantages of these generator PE variants.

Table 2-6. Characterization of Diode Bridge (Uncontrolled) Rectifier

	Attributes	Rationale/Explanation
Pros	Attractive solution in terms of cost, reliability, and overall size	Cheap, robust diodes; no control hardware required
	Minimum complexity and high reliability	No control system necessary
	Does not stress the generator windings with fast changing PWM voltages	No PWM switching
	Reduced power dissipation	Reduced switching and conduction losses
Cons	Limited functionality: - Cannot control/regulate the DC bus voltage - Cannot control the current wave shape into generator windings (i.e., cannot actively control the torque wave shape of the generator shaft and cannot be used to alleviate rotor stability) - Cannot provide reactive power to generator (no power factor control); i.e., it uses the generator kilovolt-ampere only through power factor percentage. - Cannot reverse the power flow from DC bus to generator (say, for example, for motoring purposes)	Uncontrolled operation of diode bridge
	Energy yield dictated/limited by generator power factor	Uncontrolled operation of diode bridge

Table 2-7. Characterization of IGBT-Based (Switch Mode) Rectifier

	Attributes	Rationale/Explanation
Pros	Very good functionality: - Can control power factor at generator at any desired value - Can shape the currents into generator; consequently, can actively control the torque wave shape of the generator shaft and be used to alleviate rotor stability - Can regulate the DC bus voltage at a desired level, independent of rotor speed	Fully controlled switching at high PWM switching frequencies (kHz range)
	Superior energy yield	Can control the power factor
Cons	More complex	Complex control hardware/software
	Higher power dissipation	Higher switching and conduction
	Applies PWM related dv/dt stress on generator windings, although proper winding insulation design not a cost driver in generator design	PWM switching
	Higher initial cost but could be a better long-term investment because of better energy yield	

3. PM and Electrically Excited Machine Variants

This section defines and assesses the figures of merit for electrically excited machines in the wind turbine drive train application. For analysis purposes and so that one system could be compared to another, we developed general utility curves to evaluate parametric performance changes in these variants.

3.1 Basic Aspects of Synchronous Type Machines

Calculation of the operating characteristics of a candidate generator can be simply based on determining how the torque performance is achieved in a particular design scheme. The generator's common design parameters are shear stress, air-gap radius, and air-gap length. Taken together, these parameters define the system performance attributes for a synchronous machine.

The design of electric machines in the speed range of interest for this study (i.e., direct drive and single-stage gearbox wind turbines) is driven by torque.

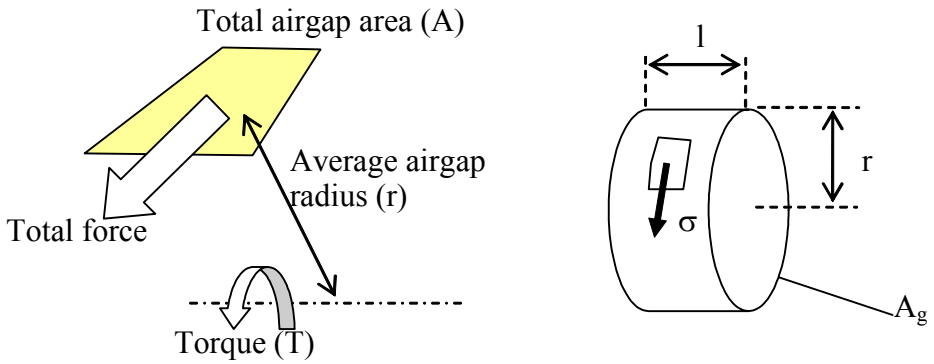

Figure 3-1. Torque design parameters in synchronous generators

As shown in Figure 3-1, torque production is determined by air-gap total area, shear stress, and air-gap average radius where:

- Total air-gap area multiplied by the shear stress gives total motor/generator force.
- Total force multiplied by average air-gap radius gives total torque.

The electromagnetic torque (T) is based on the Lorentz force, which is the interaction between the current (I) passing a conductor of length (l) exposed in a magnetic field (B):

$$F_{Lorentz} = B \cdot I \cdot l \qquad (3\text{-}1)$$

The totality of Lorentz forces multiplied by rotor radius (r) gives the electromagnetic torque:

$$T = (\sum F_{Lorentz}) \cdot r \qquad (3\text{-}2)$$

The torque expression can be also written so that it highlights dependence on the total air-gap area (A_g), the electromagnetic force per unit air-gap area (i.e., shear stress, σ) and the air-gap radius:

$$T = A_g \cdot \sigma \cdot r \qquad (3\text{-}3)$$

A brief discussion on the shear stress (σ) is useful because this parameter has a direct impact on the power density of the machine and its efficiency. Shear stress defined as electromagnetic force (force has tangential direction at rotor circumference) per air-gap unit area is:

$$\sigma = \frac{\sum F_{Lorentz}}{A_g} = \frac{\sum F_{Lorentz}}{2\pi r \cdot l} \qquad (3\text{-}4)$$

where the air-gap area (A_g) has been written for a radial field geometry having: r = air-gap radius and l = air-gap length. Typical values for shear stress could range between 30 and 80 kPa (1 Pa = 1 N/m^2).

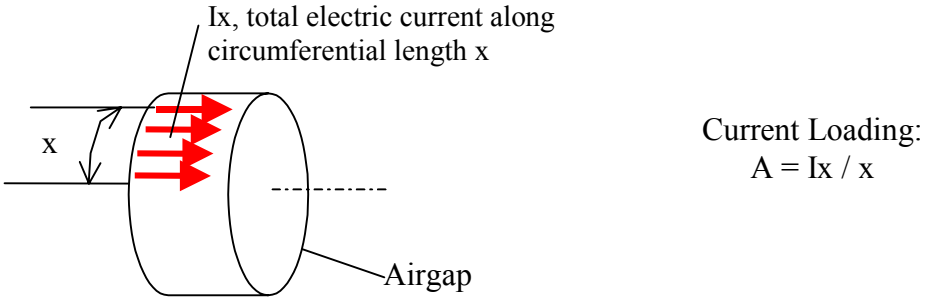

Figure 3-2. Representation of electric current loading (A)

From Equations 3-1 and 3-4, one can see that the shear stress proportionality is:

$$\sigma \sim B \cdot A \qquad (3\text{-}5)$$

where:

B = magnetic flux density [T]
A = current loading [amp/m] (defined in Figure 3-2).

To achieve a maximum utilization of the active part of the machine (i.e., iron, copper, magnets) and thus to reduce the cost of magnetic materials, the shear stress must be maximized. At the same time, the other design factors—such as the losses or the operating temperature—must be kept within the design envelope.

In looking at Equation 3-5, one can see that the shear stress can be increased by:

- Increasing the magnetic flux density (B), that obviously has the limit of iron saturation
- Increasing the current loading, that is limited by the heat transfer from winding to coolant. Higher current loading (A) can be obtained by selecting higher current density (J) in winding copper or deeper slots. Both directions are limited by thermal issues:
    - Because higher current density in copper will exponentially increase the copper losses, better cooling is necessary to keep safe winding temperature.
    - Because the thermal path is longer, deeper slots will make the heat transfer from winding to coolant less effective.

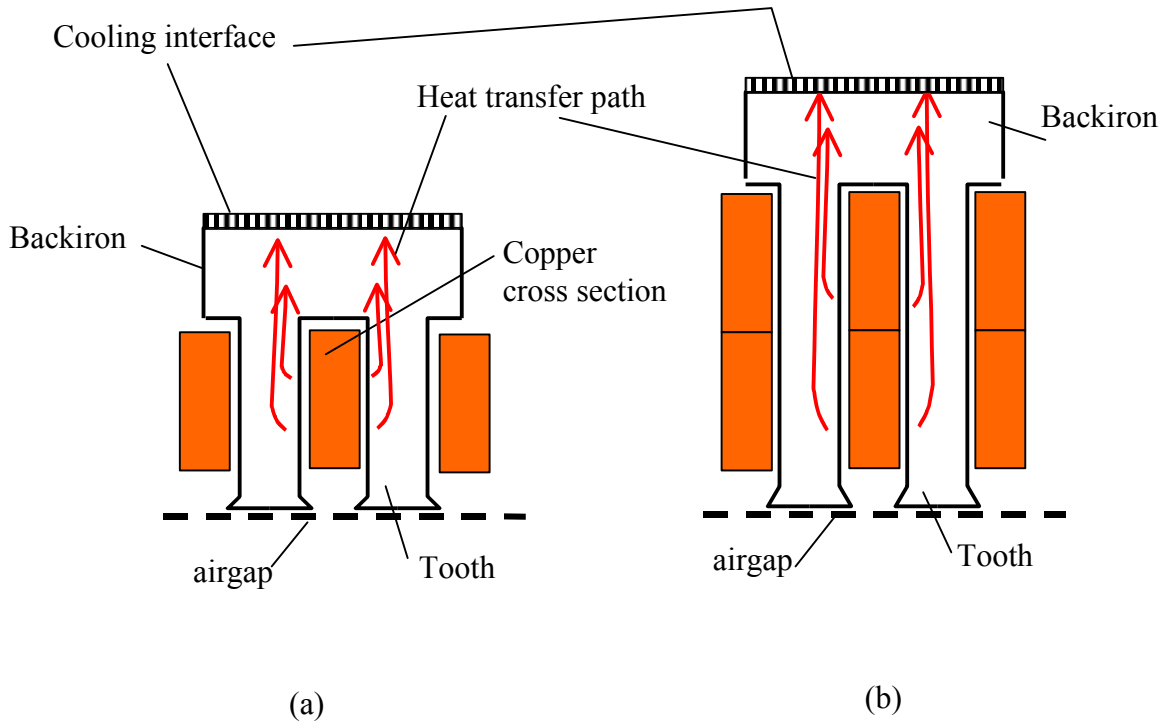

Figure 3-3. Stator slot width parameters

As shown in Figure 3-3, deeper slots increase current loading (and thus the shear stress) for a given current density by accommodating a larger copper section. Alternatively, deeper slots with constant current loading (decreasing current density) lead to lower ohmic losses. The second case is shown in Table 3-1. The longer slots give less effective cooling because the thermal transfer paths are longer. A tradeoff is usually made to select slot depth and current density.

Table 3-1. Comparison of the stator geometries shown in Figure 3-3

	Case (a)	Case (b)
Current loading (amp/m)	A	A (the same)
Copper area (m^2)	S	2x S
Current density (amp/m^2)	J	0.5x J
Ohmic losses (W)	P_{Cu}	0.5x P_{Cu}

Based on the previous aspects we can conclude that:

- Shear stress is limited by the combination of magnetic core saturation and current density in copper and thermal transfer.
- Higher shear stress gives proportionally higher torque density (we will explain this briefly later).
- At a specified current density, higher shear stress gives higher losses (approximately exponential, because of copper losses that depend exponentially on electric current).

- For a specified frame size, there is a trade-off between the torque density and machine losses (i.e., efficiency).

To explain how shear stress impacts machine torque density, we can consider the example of a radial geometry machine. The torque produced by a radial field machine can be expressed as:

$$T = 2\pi r^2 l\sigma \qquad (3\text{-}6)$$

where:

σ = shear stress
r = air-gap radius
l = air-gap length.

As shown in Figure 3-4, the impact of shear stress (σ) on machine power density and losses is

- Torque density is approximately proportional to the shear stress (see Equation 3-7).
- Machine losses tend to be a square function on shear stress (because σ is directly affected by the current density in windings).

Torque density expressed as *torque per occupied volume* (Vol = πr^2 l) is:

$$T/Vol = 2\sigma, \qquad (3\text{-}7)$$

demonstrating that the torque density is directly determined by the shear stress.

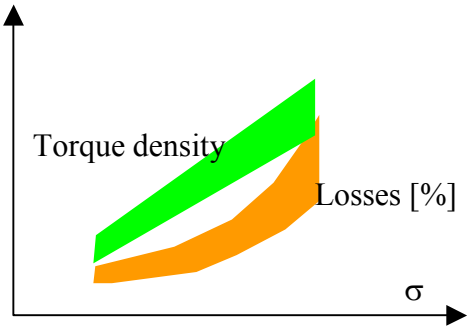

Figure 3-4. Shear stress versus torque density curve

3.2 Radial Field versus Axial Field Construction

To help making this comparison, we will consider the following parameters: the total mass (density) and the manufacturing cost. Taken together, these parameters further define the preferred configuration of a selected synchronous machine candidate.

As an energy converter (mechanical to electric or vice versa) any rotating machine can be built as either radial or axial, as shown in Figure 3-5. The machine part that is actively involved in the energy conversion process is known as the *active part* or the *magnetic part* (e.g., copper, magnetic iron, magnets).

Torque production in the active part of the machine depends on:

- Air-gap area
- Shear stress
- Average radius of the air-gap.

The same active (magnetic) mass of a rotating machine can be distributed so that the magnetic flux linkage crosses the air-gap in radial direction or axial direction, as shown in Figure 3-6.

Figure 3-5. Radial versus axial distribution of the active (magnetic) mass over a 90^{o} segment

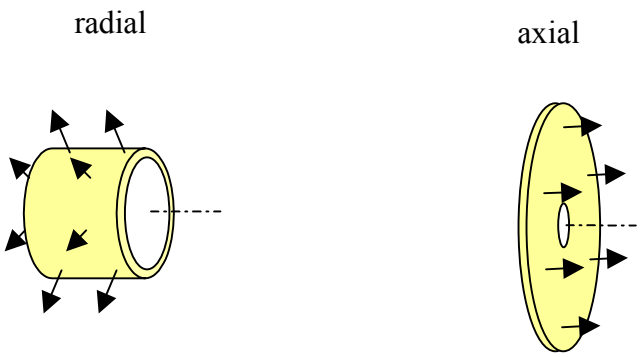

Figure 3-6. Direction of magnetic flux through machine air-gap

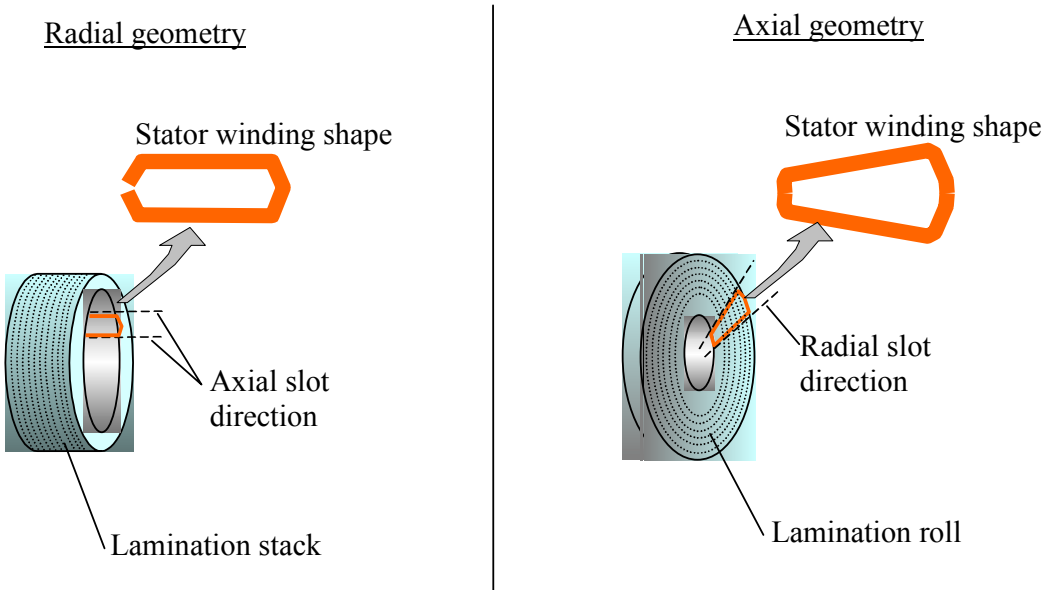

Figure 3-7. Stator construction aspects of radial versus axial field machines

The radial geometry makes use of more standard manufacturing processes and tooling compared to the axial field. These aspects are illustrated in Figure 3-7 and Table 3-2.

Table 3-2. Manufacturing Processes and Tooling—Radial versus Axial Field

	Radial Machine	Axial Machine
Windings	Rectangular shape Conventional manufacturing using automated tooling	Trapezoidal shape Unconventional manufacturing, needs special tooling
Lamination	Stacked lamination Slots in axial direction (can be skewed) Lamination handled as sheets (for large magnetic cores, the number of sheets is high, increasing the handling cost) Longitudinal lamination cut, conventional	Concentric lamination (roll) Slots in radial direction (can be skewed) Lamination handled as rolls (handling is reduced to rolls of magnetic material) Radial lamination cut, less conventional

The comparison in Table 3-2 explains why the axial geometry is more expensive for the same torque and speed design.

The axial geometry is known for its higher torque density compared to the radial geometry, where the *torque density* is defined as generated torque per occupied volume. The key reason is that the rotor inner space is not actually used for torque production. Considering only the active (magnetic) part of the machine, the radial version has more hollow space inside the rotor. Thus, as a first-order

calculation, the ratio between torque and occupied volume is better for an axial field machine (i.e., better torque density is achieved).

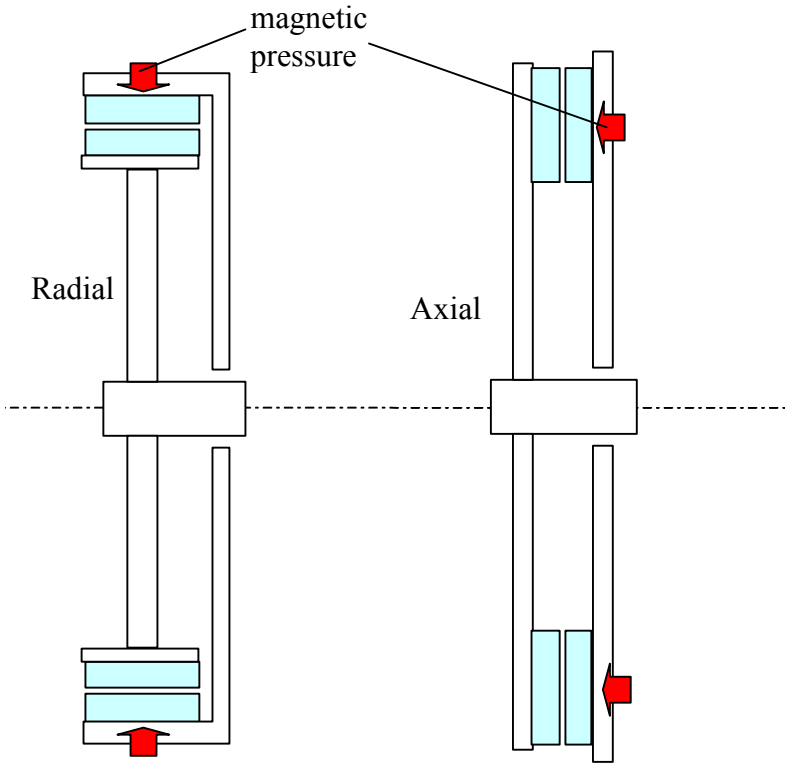

Figure 3-8. The torque density advantage of the axial field machine fades when considering large diameter machines (i.e., diameter is several times larger than the motor length)

For large machines (at the megawatt level) with a large radius (in the order of meters), practical aspects like structural elements and their magnetic pressure loading start to have a significant impact on overall machine volume and weight. As shown in Figure 3-8, the difference between axial and radial geometry in terms of torque density, tends to be less visible.

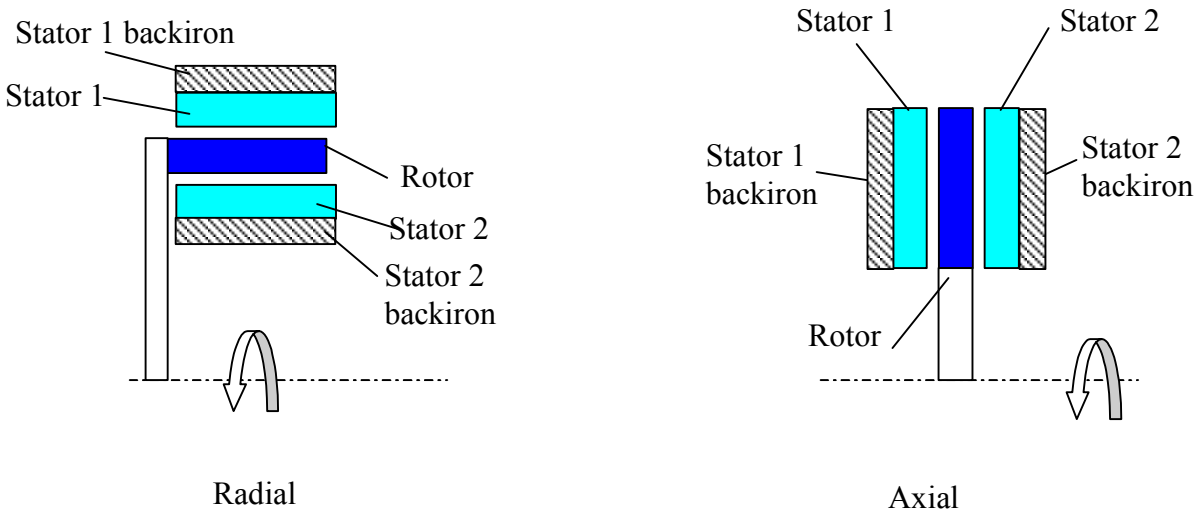

Figure 3-9. Both the axial and radial geometries can be implemented as dual air-gap or, in general, as multi-air-gap.

A dual air-gap arrangement, shown in Figure 3-9, is typically used in axial field machines. It allows:

- Magnetic pressure compensation on rotor disc
- Elimination of backiron on rotor (all backiron is in stationary frame)
- Lower rotor inertia and cooler operation of rotor (less power dissipation into rotating frame).

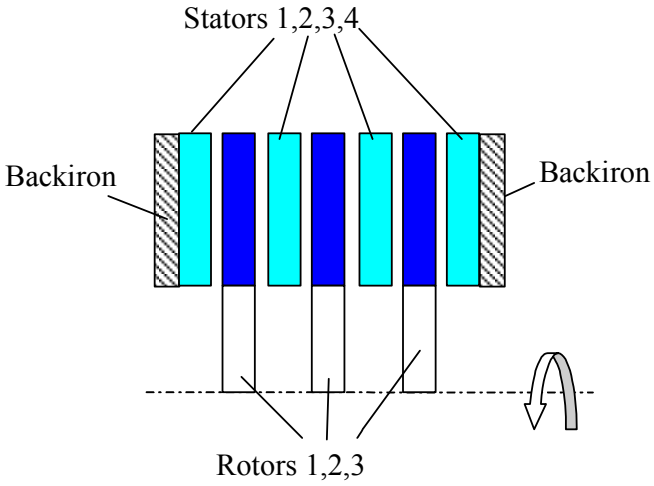

Figure 3-10. "Pancake" construction; practical only for axial field machines

In "pancake" axial construction, shown in Figure 3-10, multiple rotors and stators are stacked axially. The same magnetic field crosses multiple air-gaps, and only at the two ends of the motor, the backiron is necessary to close the magnetic loop.

For this geometry, the total air-gap area (that is responsible for torque) obtained within the overall volume is very large, making the "pancake" axial geometry the most torque-dense configuration.

The major drawbacks of this configuration are related to the practical ways to build it. Although the absence of the backiron in the inner stators leads theoretically to a compact and light architecture, its absence also creates serious difficulties when it comes to inner stator support. Structurally, the stators at both ends have the mechanical support offered by the backiron, but the inner stators do not. These facts lead to complex and expensive motor design, and make this architecture useful only for applications where high torque density is a crucial necessity.

As a consequence of the theoretical and practical aspects discussed so far in this section, we can reach an interim conclusion that the most reasonable candidate geometries are:

- A single air-gap radial flux machine
- A dual air-gap axial field machine.

These two geometries are illustrated in Figure 3-11.

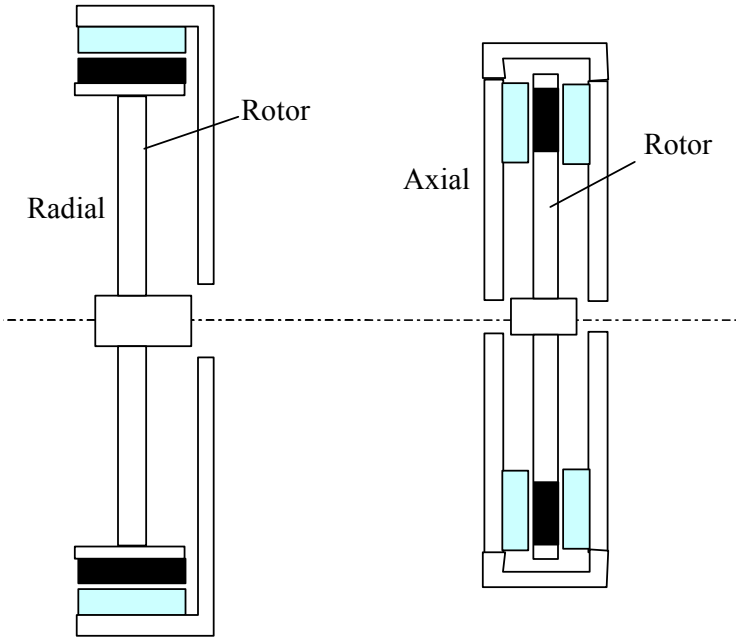

Figure 3-11. Radial single air-gap versus axial dual air-gap geometries

We can compare radial single air-gap geometries and axial dual air-gap geometries in terms of occupied volume. The occupied volumes are calculated from the air-gap length, air-gap area, and active magnetic thickness for each air-gap radius at a given operating torque and shear stress. The relationships between these quantities are described below.

The length of air-gap and the air-gap area can be expressed as functions of the average air-gap radius (r), torque, and shear stress as follows:

Air-gap length of radial single air-gap machine: $l_{rad}(r) = 2T/(\sigma 4\pi r^2)$
Air-gap length of axial dual air-gap machine: $l_{ax}(r) = T/(\sigma 4\pi r^2)$

Air-gap area of radial single air-gap machine: $A_{g\_rad}(r) = T/(\sigma r)$
Air-gap area of axial dual air-gap machine: $A_{g\_ax}(r) = T/(\sigma r)$

The definition of air-gap radius and length for the two machine types is illustrated in Figure 3-12.

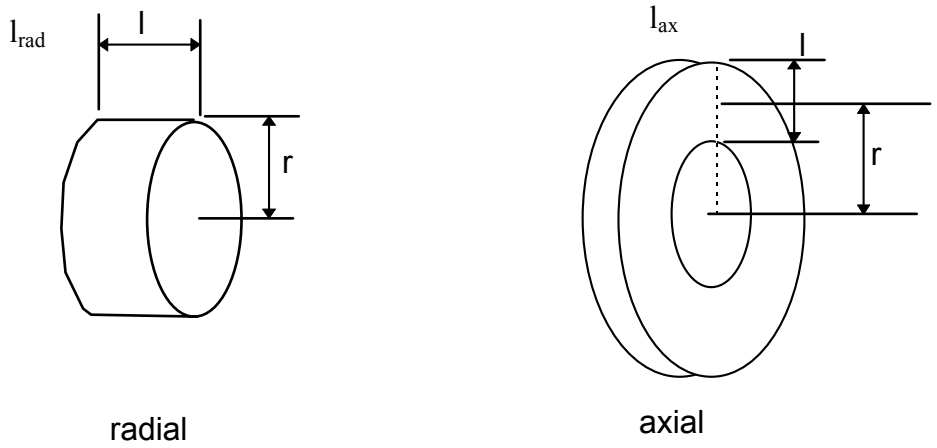

Figure 3-12. Definition of air-gap radius and length of the radial single air-gap and axial dual air- gap machines

From the relations given above, we can see that the air-gap length of the axial dual air-gap machine is 50% of the radial single air-gap machine. This is natural because for the axial dual air-gap machine, the air-gap area is essentially folded in two, achieving half the initial length.

The air-gap areas of both geometries (A_{g_rad} and A_{g_ax}) are equal and have the same dependence on the average air-gap radius r (i.e., D/2). For first-order cost evaluation, this suggests that the cost of the magnetics might be the same for both geometries because the cost is primarily driven by the air-gap area. However, the cost of the axial machine will be higher because the shape and the mechanical arrangement of the magnetic materials are less conventional and therefore more expensive.

Figure 3-13 shows the occupied volume of both geometries for different air-gap diameters. The same results for occupied volume are shown plotted against machine housing diameter in Figure 3-14. The occupied volume determines the torque density of these geometries because the torque density is the ratio of torque per occupied volume. The torque and the shear stress are considered to be the same for both machines and are fixed:

T = 755297 Nm (value specified in the statement of work [SOW])
σ = 68900 Pa

but the air-gap average radius (r) has been varied from 1 to 5 m.

Additional assumptions were

- Thickness of magnetics (air-gap + stator tooth height + stator backiron) = 0.13 m
- Length of winding end turns (in the direction of stator slots) = 0.07 m.

Figure 3-13 shows that the axial geometry occupies less volume for diameters of less than 6 m. The same results are plotted in terms of machine housing diameter in Figure 3-14. It is interesting to note that, in the axial dual air-gap machine, the smaller occupied volume actually originates in the shorter axial length, not the radius.

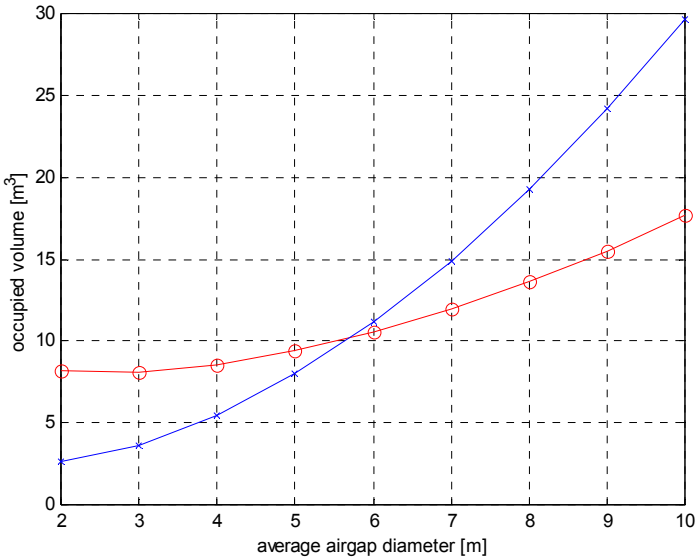

Figure 3-13. Comparison of occupied volumes for 1.62-MW direct drive machine as functions of average air-gap diameter: axial (x) versus radial (o) geometries

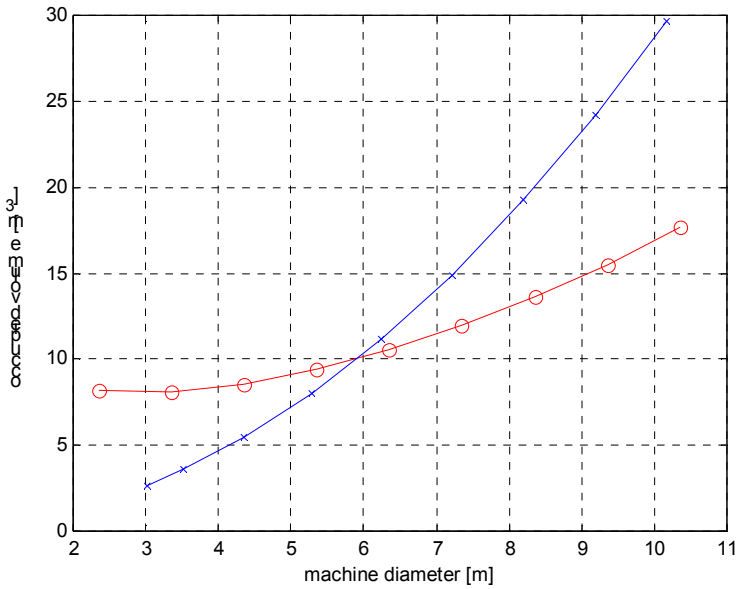

Figure 3-14. Comparison of occupied volumes for 1.62-MW direct drive machine as functions of machine housing diameter: axial (x) versus radial (o) geometries

Table 3-3. Global Characterization of Down Selected Geometries takes into account that these machines have large diameters compared to their length (L/D on the order of 0.1)

	Single Air-gap Radial Flux Machine (SARFM)	Dual Air-gap Axial Field Machine (DAAFM)	Comments
Torque density	Slightly less compared to DAAFM	Slightly higher compared to SARFM	For direct drive machines (with low L/D ratio) the difference is not significant due to impact of support structure geometry. The torque density advantage of the DAAFM fades at larger diameters and at approximately 6-m diameter the SARFM becomes actually more torque-dense.
Design complexity	Simple and modular	Complex	Partitioning of stator core in segments is easily obtained for SARFM but not for DAAFM.
Use of standard parts and/or technologies	Standard windings Stacked laminations	Trapezoidal shaped windings Concentric lamination	The construction of windings and stators of the DAAFM involves more expensive technologies and tooling.
Cost	Less compared to DAAFM	Higher compared to SARFM	The price difference reflects the technologies involved in machining and manufacturing the machine parts.

Whereas the torque density advantage of the dual air-gap axial field machine fades when entering into low-speed, high-torque (HTLS) domain, the price difference does not. Table 3-3 summarizes the comparison of the two machine types. Because all the aspects we have discussed so far point to a higher cost for the axial field geometry, the radial field construction seems to fit the wind turbine applications that are cost sensitive instead of power density demanding. Plus, when the machine diameter is several times larger than the machine length, the torque density of the radial field machine becomes comparable with the axial field machine.

3.3 Single Machine versus Multitude of Machines

In this section, we will compare the baseline approach of a single machine with a multiple machine approach. In the multiple machine approach, smaller machines accumulate a total torque equal to the baseline single machine case. In other words, the smaller machines operate at the same speed as the baseline single machine case.

Note that another way to look at the multiple generator approach is to take into account the geometry of the gearbox and to include into calculation the effects of the gearbox ratio that are dependent on the total radius of the mechanical arrangement gearbox plus generators system. The cost aspects related to this approach are addressed in Appendix I for the generator(s) only and can be merged with gearbox cost formulas for further investigation of an optimum design point at system level: gearbox + generator.

To achieve a fair comparison, we considered the shear stress that primarily drives the power density of the design to be a constant. Because cost will be a part of the comparison (multi-machine versus single machine), it is useful to present first-order parametric cost models.

For cost evaluation, the notion of the *magnetic part* of a machine will be used to designate the totality of elements that contribute to the torque production. The magnetic part of a machine consists of windings, magnetic iron and permanent magnets.

The air-gap area of a machine will roughly determine the mass and the cost of the magnetic part of a machine. The mass of the magnetic part of the machine (*Mmag*) can be expressed as a function of the air-gap area:

$$Mmag = A_g \cdot m_a \tag{3-8}$$

where:

A_g = total air-gap area
m_a = magnetic mass[1] per air-gap unit area (kg/m^2).

In the same manner, the cost of magnetic mass (*Cmag*) of the machine depends on the total air-gap area:

$$Cmag = A_g \cdot c_a \tag{3-9}$$

where:

A_g = total air-gap area,
c_a = cost[2] per air-gap unit area (USD/m^2)

The total cost of the machine includes the nonmagnetic part of the machine (i.e., the stator and rotor support structures, cooling system, and housing).

As shown in Figure 3-15, multiple machines can be built with either equal length to the single machine equivalent, with smaller radius, or with equal radius but shorter length.

[1] Typical values of the magnetic mass per air-gap area could range from 800 to 1500 (kg/m^2) depending on design.
[2] The cost per air-gap area is very sensitive to factors such as production volume, type and grades of materials, and design approach.

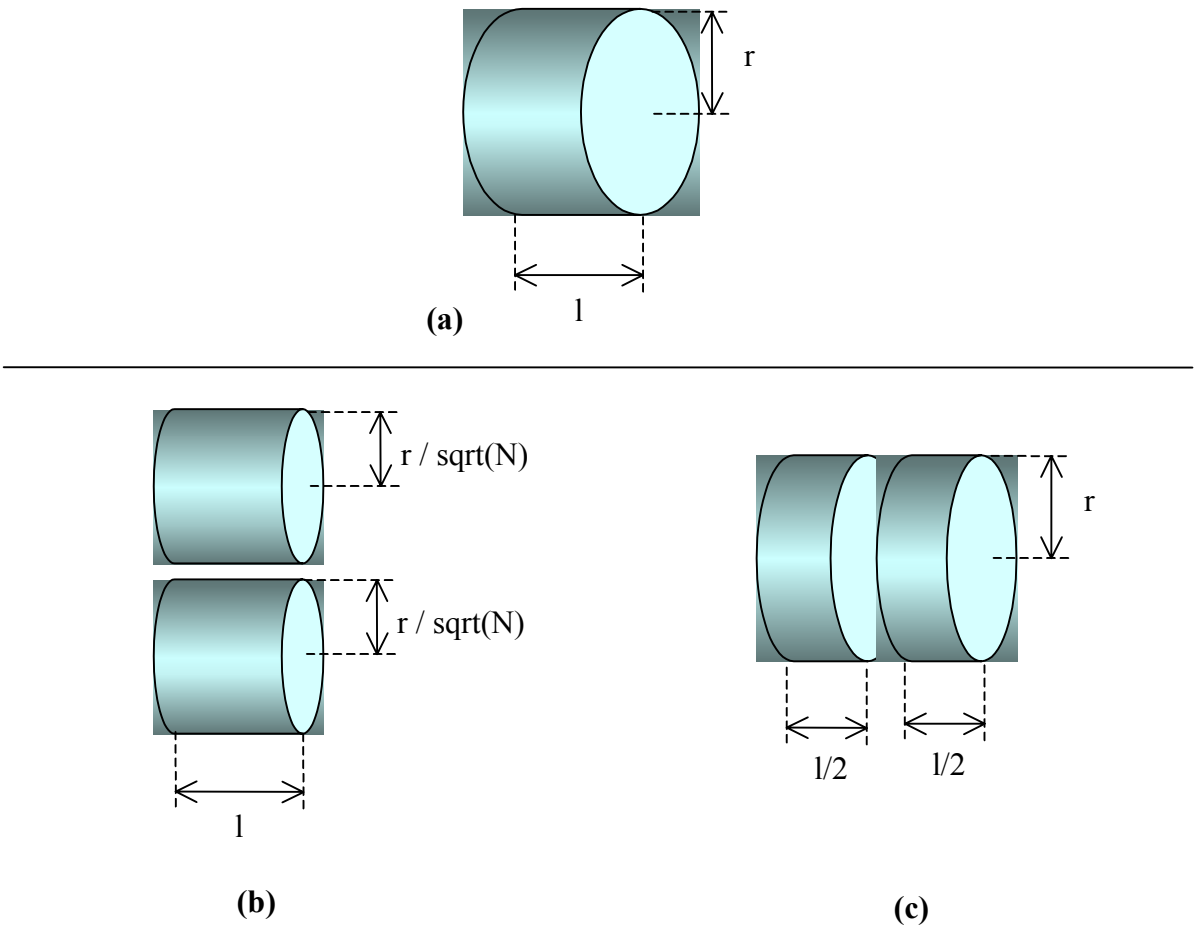

Figure 3-15. Multiple machine versions of the single machine concept having the same speed and total torque as the single machine baseline approach: (a) single machine; (b) N = 2 smaller machines with the same length; and (c) N = 2 smaller machines with same radius

3.3.1 N Machines with the Same Length and Smaller Radius

First consider N machines with the same length and smaller radius. Based on the generic torque expressions

$$T = 2\pi r^2 l\sigma\,, \quad T = N\left[2\pi\left(r_N\right)^2\, l\,\sigma\right], \tag{3-10}$$

the same total torque is obtained if the radius of each individual machine is

$$r_N = \frac{r}{\sqrt{N}} \tag{3-11}$$

- Impact on total magnetic mass:

  The total magnetic mass of the system increases by sqrt(N):

$$Mmag_N = \sqrt{N} \times Mmag_1 \quad (3\text{-}12)$$

where:

$$Mmag_N = N \times 2\pi\left(\frac{r}{\sqrt{N}}\right) l \cdot m_a = \sqrt{N} \times \left(2\pi r l \cdot m_a\right)$$

$$Mmag_1 = \left(2\pi r l \cdot m_a\right) \quad (3\text{-}13)$$

- Impact on machine nonmagnetic parts:

  Globally, a certain degree of redundancy will result for the support structures.

- Impact on total occupied volume:

  At a first-order calculation, the total occupied volume of active parts does not change.

$$Vol_{N(l=ct)} = N\left[\pi\left(r_N\right)^2 l\right] = \pi\left(r\right)^2 l \quad (3\text{-}14)$$

  However, taking into account the inherent redundancy in the nonactive parts of the machines, the total occupied volume will be slightly bigger.

- Impact on electrical and thermal characteristics:

  Not significant

Figure 3-16 shows the impact on costs and economics.

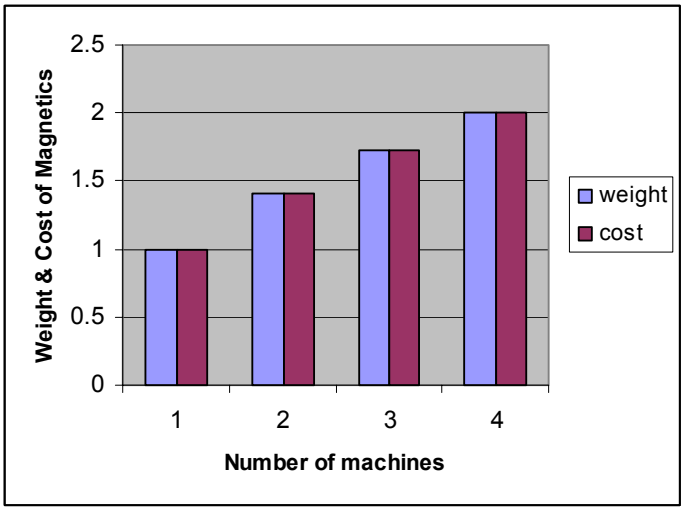

Figure 3-16. Total cost of the magnetic part of the machine increases by sqrt(N)
(because this is proportional with the magnetic mass presented above)

3.3.2 N Machines with the Same Radius and Smaller Length

Based on the generic torque expressions

$$T = 2\pi r^2 l\sigma, \quad T = N\left[2\pi r^2\ l_N\ \sigma\right] \tag{3-15}$$

the same total torque is obtained if the length of each individual machine is

$$l_N = \frac{l}{N} \tag{3-16}$$

- Impact on total magnetic mass:

  The total magnetic mass of the system does not change:

  $$Mmag_N \quad = \quad Mmag_1 \tag{3-17}$$

  where:

  $$Mmag_N = N \quad \times \quad 2\pi r\ l_N \cdot m_a \quad = \quad \left(2\pi rl \cdot m_a\right)$$
  $$Mmag_1 = \left(2\pi rl \cdot m_a\right) \tag{3-18}$$

- Impact on total occupied volume:

  Based on a first-order calculation, the total occupied volume of the active parts does not change. However, taking into account the inherent redundancy in the nonactive parts of the machines, the total occupied volume will be slightly bigger.

- Impact on machine nonmagnetic parts:

  Globally, a certain degree of redundancy will result for the support structures.

- Impact on electrical and thermal characteristics:

  As shown in Figures 3-17 and 3-19, the totality of winding end turns (passive part of winding) will represent a bigger percentage of the system windings. The consequences are:

  - As illustrated in Figure 3-18, in per unit terms the total equivalent reactance will have increased parasitics. This leads to higher leakage inductance and resistance (i.e., lower power factor and higher power dissipation).
  - For liquid-cooled machines, there will be more copper percentage that has weaker thermal coupling to coolant. For air-cooled machines, the opposite tends to be valid.
  - The percentage copper quantity used in the machine will be higher.

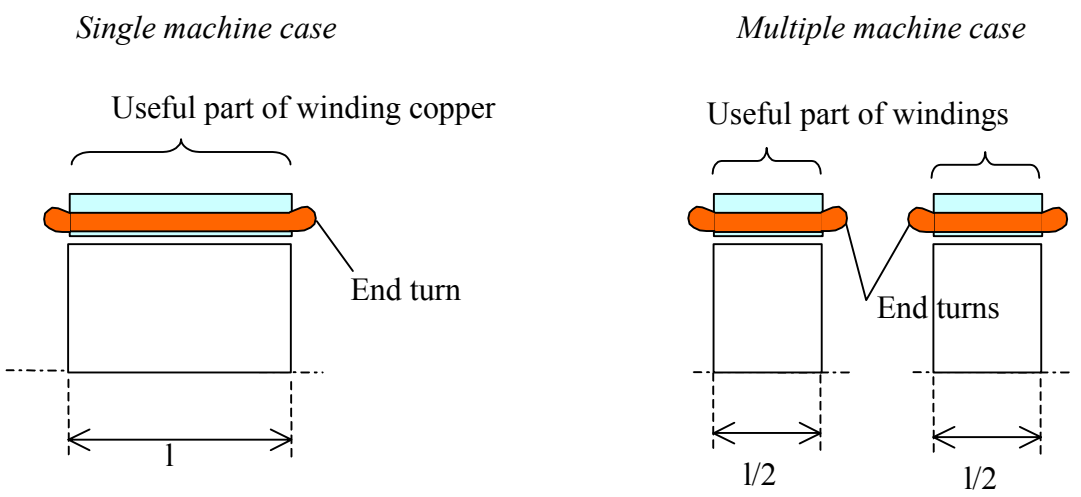

Figure 3-17. In the case of multiple machines, more end turn copper is required

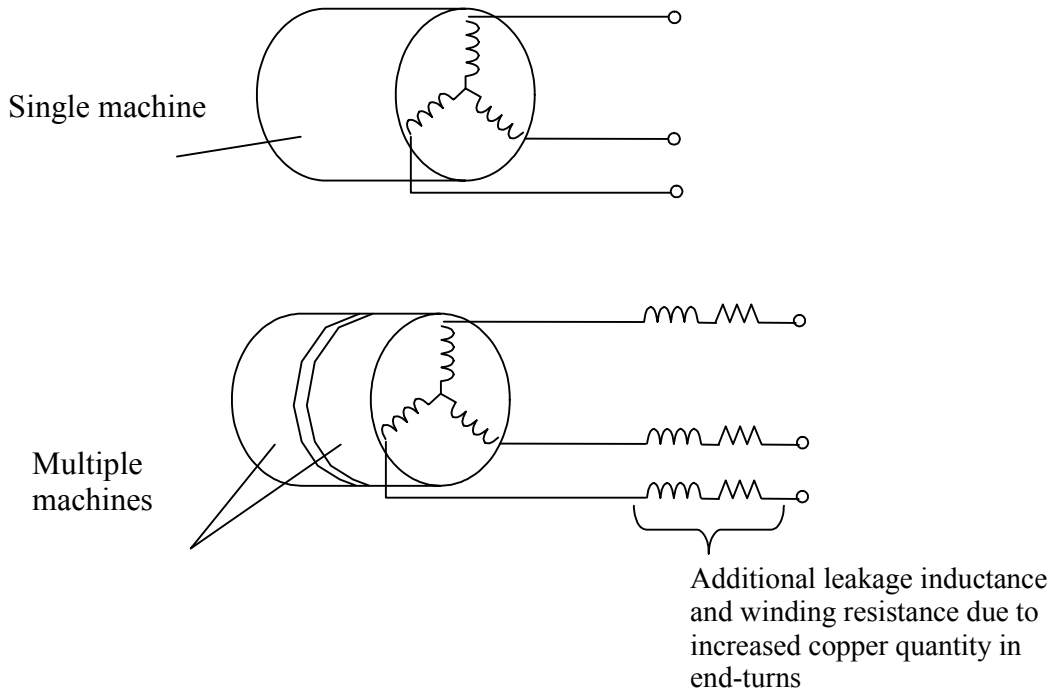

Figure 3-18. For multiple machine approach, total equivalent reactance will have increased parasitics (i.e., lower power factor and higher power dissipation)

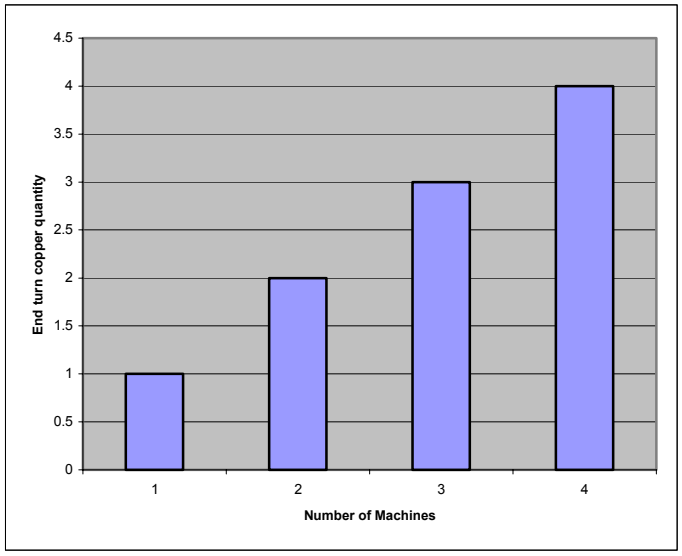

Figure 3-19. End turn copper quantity (unused copper) at system level as function of number of machines totaling the same power level

As shown in Figure 3-19, the copper losses in windings are proportional to the copper quantity, which means that the multiple machine approach has increased copper losses at the system level (i.e., reduced system efficiency). Figure 3-20 assumes 33% copper in the end turns of the baseline one machine case. The two machine case has twice the end turns, giving 33% higher ohmic losses than the one machine case.

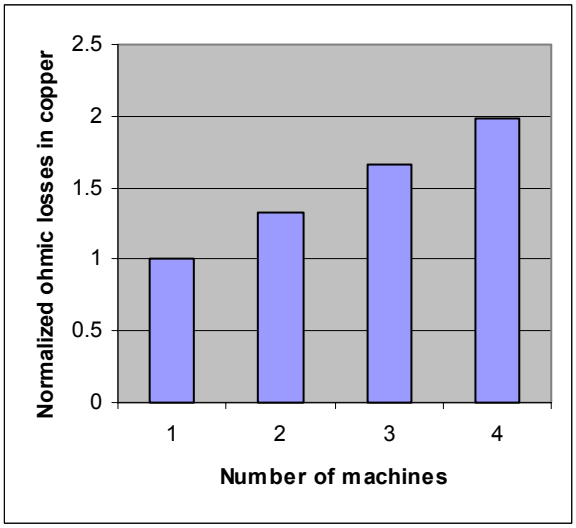

Figure 3-20. Comparison of ohmic losses for generator systems composed of multiple machines

Based on a first-order calculation, the cost of the magnetic mass does not change, since the total magnetic mass does not change. This result is shown in Figure 3-21.

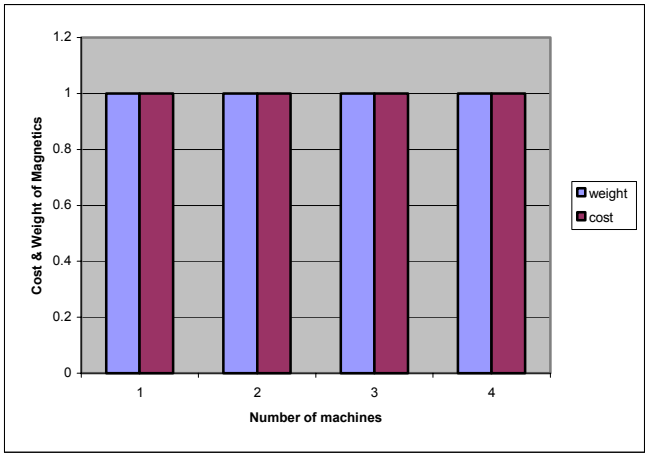

Figure 3-21. Impact on cost/economics

However, various factors could affect the total cost of a multi generator solution:

- Factors driving cost up
  - Existence of redundant elements in support structure
  - More parts, more handling
- Factors driving cost down
  - High volume production
  - Scalability and standardization, i.e., use of the same generator type as a building block to achieve various power levels.

3.3.3 Conclusions

Comparing the single machine and multiple machine approaches, the following conclusions can be made:

- The multiple machine approach based on smaller radius generators is a more expensive solution when the torque sum of all smaller machines equals the torque of the baseline single machine approach (i.e., the torque sum of all small machines equals the torque of the baseline single machine).

- The multiple machine approach based on generators with the same radius and smaller length could be a viable solution to achieve scalability to higher power levels despite slightly reduced generator efficiency.

Another way to look at the multiple generator approach is to include in the calculation the effects of the gearbox ratio that is dependent on the total radius of the mechanical arrangement gearbox plus generators system.

3.4 Form Factor Impact on Machine Design and Cost

Based on the torque expression

$$T = 2\pi r^2 l\sigma\,, \tag{3-19}$$

we can find a family of machines that produce the same torque (at the same speed) but with different aspect ratios.

The fixed parameters are torque (T) and shear stress (σ). The variables are the air-gap radius (r) and length (i) under the constraint to fulfill Equation 3-19. When the radius changes, in order to preserve the same torque, the air-gap length must follow:

$$l = T \,/\, (2\pi r^2\sigma) \tag{3-20}$$

Thus, the air-gap area (A_g) will vary as a function of the radius that has been selected as the input variable:

$$A_g = l \cdot (2\pi r) = \frac{T}{\sigma \cdot r} \tag{3-21}$$

Equation 3-21 indicates that a larger air-gap radius (r) determines smaller air-gap area at the same generated torque. Because the magnetic mass is proportional to the air-gap area, the same specified torque can be achieved with less magnetic mass (and less cost) if the air-gap radius is larger (Figure 3-22).

On the other hand, the mass and the cost of the generator structural parts (rotor and stator support structures) increase as the air-gap diameter increases (Figure 3-23).

These suggest that there is an optimum point where the total cost (i.e., cost of magnetic mass plus cost of structural mass) has a minimum. Numerical results are shown in Sections 4 and 5, which address conceptual design of two PM generators—for a direct drive generator, an optimum diameter would be between 4 and 5 m, but for the MTMS generator the optimum diameter would be approximately 2 m.

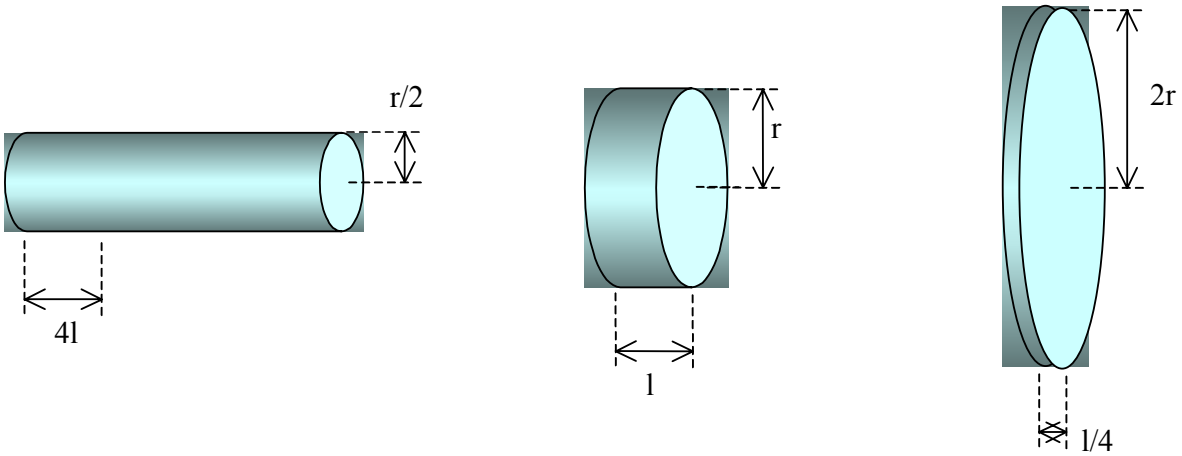

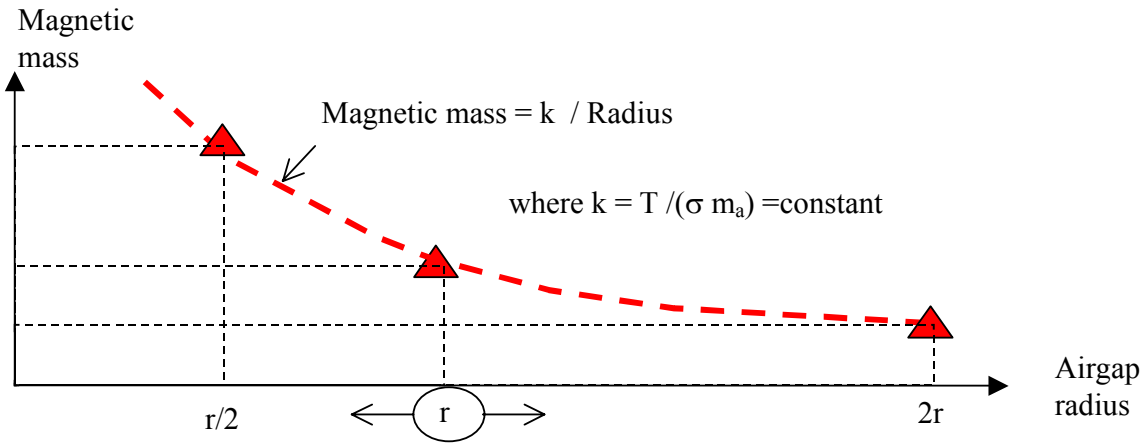

Figure 3-22. Same torque machines with different radius
(the same torque can be achieved with less magnetic mass at larger air-gap radius)

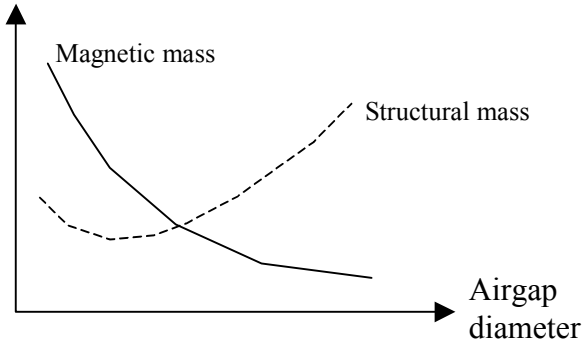

Figure 3-23. Generic variation of magnetic mass and structural mass as function of machine air-gap diameter
(numeric data are shown in Sections 4 and 5)

3.5 PM versus Electrically Excited Machine

The basic difference between PM and electrically excited machines is the way the rotor generates the magnetic flux, as illustrated in Figure 3-24:

- Using DC current in the rotor windings in the case of electrically excited machines
- Using a permanent magnet in the case of PM machines.

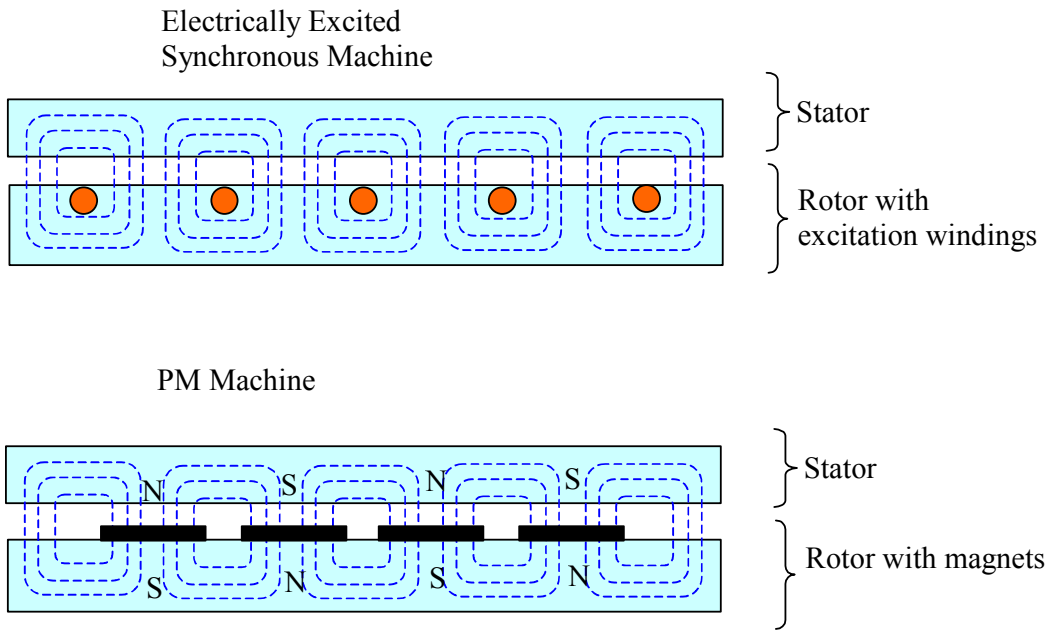

Figure 3-24. Comparison between electrically excited machines and PM machines from a rotor magnetics point of view

The losses in the rotating frame (rotor + magnets) for a PM machine are very low (less than 10% of total machine losses), and they are even lower for low-frequency/low-speed machines. On the other hand, for an electrically excited synchronous machine, the losses in the rotating frame (rotor + excitation winding) account for a much bigger portion of total machine losses (on the order of one-third to one-half).

Thus, at the same power rating and frame size, a PM machine has lower losses compared to the electrically excited machine (a PM machine may have half of the power loss of an electrically excited one).

Reasons for significantly lower losses in a PM machine include:

- The PM machine has negligible excitation losses whereas the electrically excited machine has significant excitation losses. The excitation field in an electrically excited machine is obtained at the expense of passing an electric current through the copper of the excitation winding, whereas in a PM machine the field results from magnets without involving or consuming any electric current.

- The losses in rotor magnetic core are lower in the surface-mounted PM machine. These losses are determined by the stator flux harmonics, which have a much smaller impact on the rotor magnetics because the equivalent stator-to-rotor air-gap is much larger than the mechanical air-gap (l_g). The equivalent air-gap includes also the thickness of the magnets l_m, because the relative permeability of rare earth magnets is close to unity (see Figure 3-25). In other words, because of the magnets' low permeability, the rotor core appears to be at a larger distance from the stator, which significantly reduces the undesired effect of stator flux harmonics into the rotor and leads to very low rotor core losses in a PM machine.

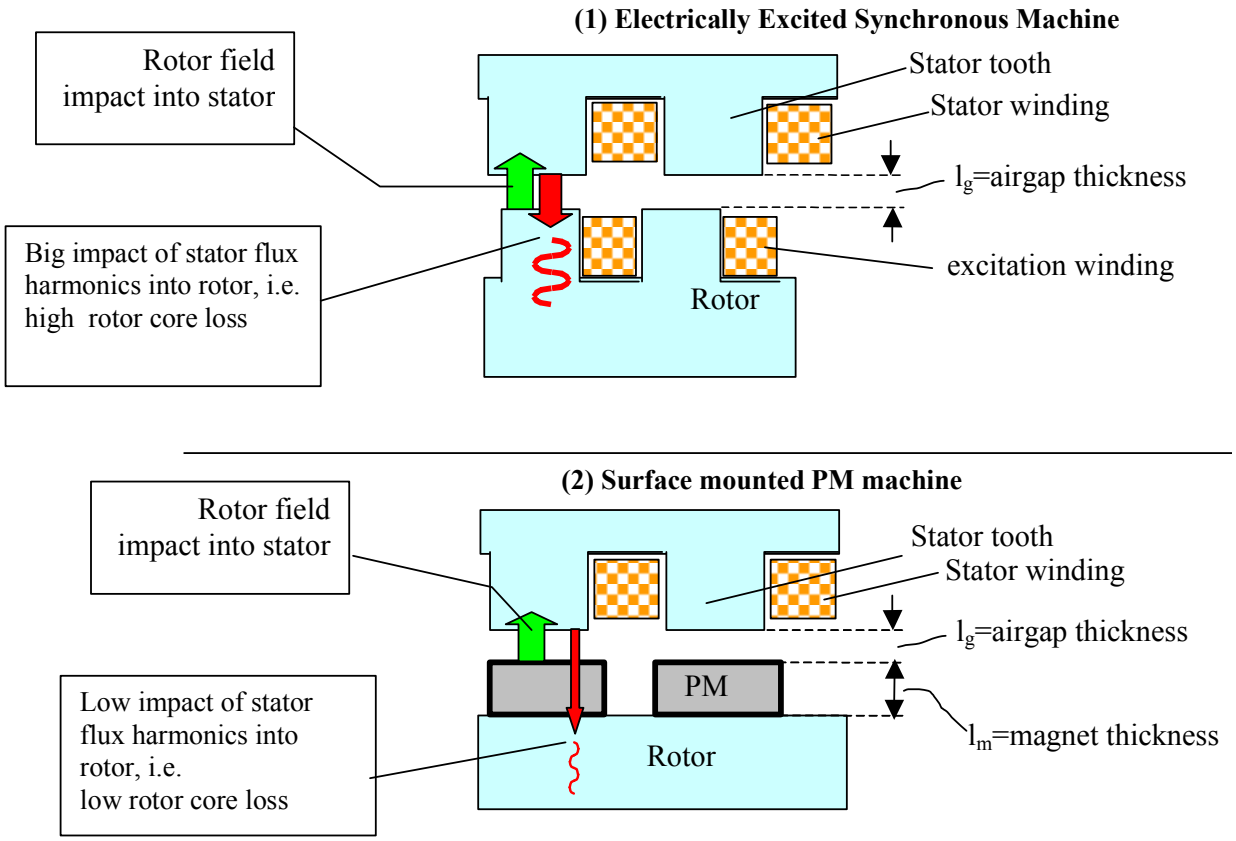

Figure 3-25. Comparison of the undesired impact of stator flux harmonics into rotor core for electrically excited versus surface-mounted PM machine

For an electrically excited machine, the stator flux harmonics (undesired aspect leading to rotor core loss) impact the rotor core via the same air-gap thickness (l_g) through which the rotor flux has an impact on the stator (a desired aspect that leads to torque generation).

For a surface-mounted PM machine, the undesired impact of stator flux harmonics into rotor core is significantly reduced—the stator flux harmonics have an impact on the rotor core via a larger equivalent air-gap (approximate air-gap plus magnet thickness $l_g + l_m$), whereas the rotor flux affects the stator through the air-gap (a desired aspect that leads to torque generation).

Another aspect to address is the pole count. To produce the same air-gap field with the same pole count, a rotor with excitation windings dissipates more power compared to a rotor with PM magnets.

Comparable power dissipation can be achieved in both machines (electrically excited and PM) if the pole count of the electrically excited machine is lowered. However, this leads to increased machine size and weight, as illustrated in Figure 3-26.

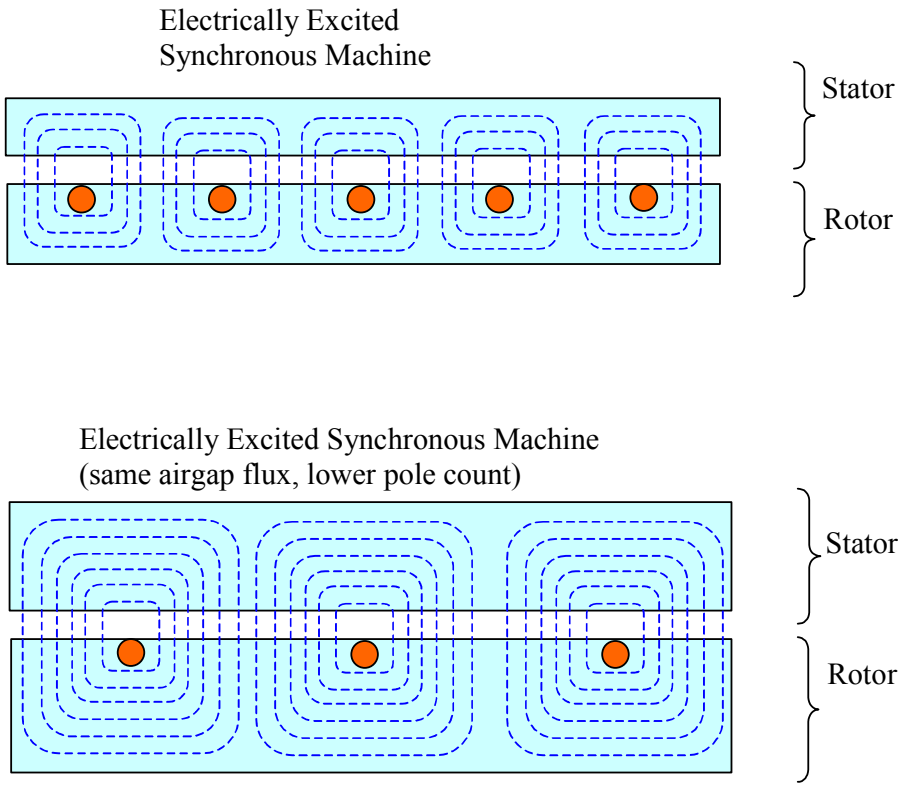

Figure 3-26. Electrically excited machine size for two different pole counts

To reduce rotor losses in an electrically excited machine to a level comparable to the PM machine, lower pole count has to be selected in the electrically excited machine design.

Consequences of lowering the pole count on an electrically excited machine are

- More back iron is needed.
- Because of the thicker back iron, thermal resistance of the machine increases, which makes the heat transfer more difficult.
- Machine size and weight increases and becomes driven by back iron.
- Electrical frequency is lower for the same rotor speed, requiring special attention to PE design (for instance, bulky filters and/or active filtering techniques).
- To achieve the same torque, higher shear stress (i.e., higher currents in stator windings) has to be used. This can lead to two consequences— increased stator losses or having to use more copper.

Table 3-4. Comparison between PM Machines and Electrically Excited Synchronous Machines

	PM Machine	Electrically Excited Synchronous Machine
Losses	Negligible losses in rotating frame (<10% of total losses)	Significant losses in rotating frame (30%–50% of total losses)
Efficiency	Higher efficiency for the same design (same power and frame size)	Lower efficiency (it could have twice the losses of a PM machine for the same design)
Construction	Simple construction; rotor consists of an array of magnets mounted on a rotor spider	More complex rotor construction because of excitation windings and their feeding system (slip rings + brushes, or diode exciter)
Maintenance	Rotor is very low maintenance	Slip rings and brushes are source of hazard (sparks); wear out and require maintenance
Deformation tolerance	Because of the low permeability of magnets, magnetic core is harder to saturate, allowing the use of either less iron or higher current density. Construction less sensitive to manufacturing tolerance	For the same shear stress, the air-gap has to be smaller; i.e., tighter mechanical tolerance required. Magnetic saturation of more concern (more iron or less current density must be used)
Excitation PE	No need for excitation power converter	Needs an extra power converter to feed/control the excitation windings
Excitation adjustment	Excitation field cannot be turned off or varied; contactor could be used to separate the power electronics from generator in case of PE failures	Possible to turn off excitation field in case of system failure. For wind turbines, possible to use field weakening to narrow the generated voltage span (but only to the degree to which the machine magnetics are oversized)
Temperature limits	Maximum magnet operating temperature should be below 150°C (allows a 50°C margin to the 200°C level, at which PM can lose the field)	Rotor operating temperature limited by windings (120°C to 130°C)
Temperature impact on excitation	At 10°C temperature increase, field decreases 1%	At 10°C temperature increase, conductivity of excitation coil decreases by 3.9%; leads to 3.9% decrease in excitation field for the same excitation voltage

4. Concept of Direct Drive PM Generator

4.1 Design Rationale for High-Torque, Low-Speed PM Generator

The input design parameters, according to the SOW, are:

- Input power 1621 kW
- Machine efficiency 97.15%
- Torque at rated power 755297 Nm
- Speed at rated power 20.5 rpm
- Maximum speed 33.3 rpm

At operating speeds that do not raise special structural issues (typically <4000 rpm), the electric machine design is driven basically by torque, given by:

$$T = A_g \cdot \sigma \cdot r \qquad (4\text{-}1)$$

where:

A_g = air-gap area (m^2)
σ = shear stress (N/m^2)
r = air-gap radius (m)

Based on Equation 4-1, Figure 4-1 illustrates how the shear stress and air-gap diameter affects the air-gap area that proportionally drives the cost of the magnetic part.

(a) (b)

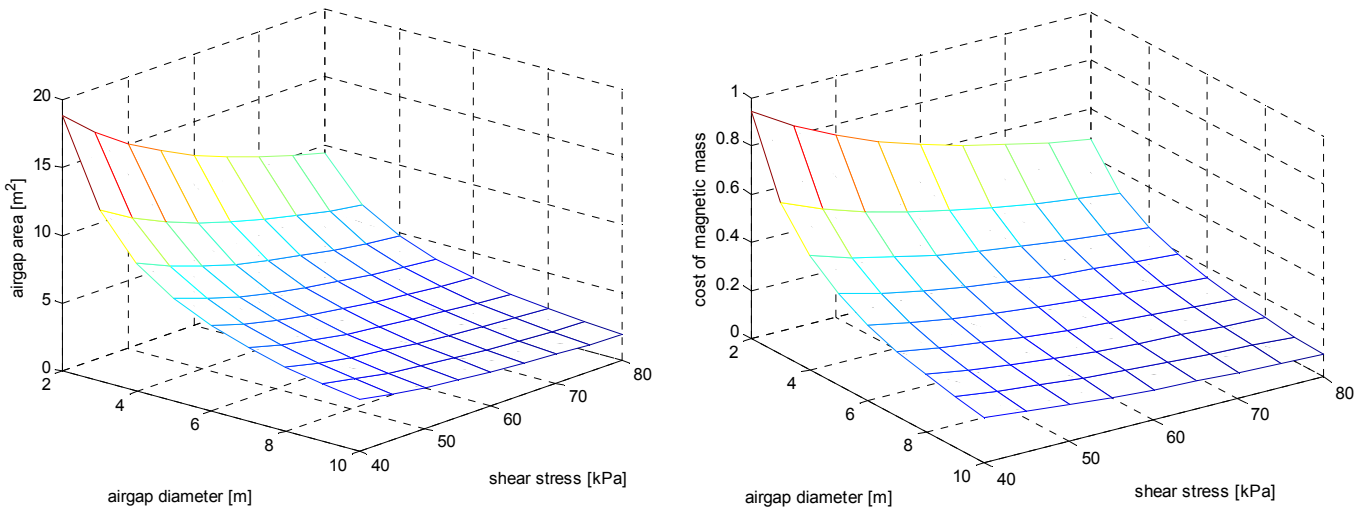

Figure 4-1. Impact of shear stress and air-gap diameter on (a) the size of the air-gap area (and (b) the cost of magnetic mass

Because the cost of the magnetic part is proportional to the air-gap area (A_g) and because this application can be considered cost sensitive, we used a high shear stress (σ) in the design:

σ = 68900 Pa (i.e.,10 psi).

In addition to this shear stress value target, the design also needs to meet the specified efficiency (97.15%), which can be accomplished by using low-current-density copper windings and a larger cross-section area of copper. Note that the bulk of losses in a PM machine are copper losses (ohmic losses), which typically account for approximately 60% to 80% of the total PM machine loss. For this reason, the ohmic losses need special attention when designing for efficiency.

The shear stress value is driven by magnetic induction (B *[T]*), which is determined by the PM grade and the current loading (A [amp/m]):

$$\sigma = kBA \tag{4-2}$$

where k is a constant that depends on the machine geometry and the shape of the magnetic field distribution (sinusoidal or trapezoidal, for example).

Equation 4-2 indicates that, once the magnet selection has been narrowed to a certain grade range, the main knob in designing the shear stress is the current loading (A). The current loading (A) itself is further dependent on the current density (J) in copper and the copper cross-section area (A_{Cu}):

$$A \sim JA_{Cu} \tag{4-3}$$

This leads to a shear stress proportionality of:

$$\sigma \sim B \cdot J \; A_{Cu} \tag{4-4}$$

At the same time, the losses in copper (λ_{Cu}) depend on the current density (J) and the total volume of copper that is proportional to copper area (A_{Cu}):

$$\lambda_{Cu} \sim J^2 \; A_{Cu} \tag{4-5}$$

At this point, we can see from Equations 4-4 and 4-5 that it is possible to obtain desired levels for both shear stress as copper losses by properly calculating the current density (J) and the copper cross-section area (A_{Cu}). Note that the combination of high shear stress with high efficiency drives up the volume of copper and steel that go into the magnetic part but will not affect the volume of the permanent magnets. The limitation is determined by the stator tooth height, which increases when a larger copper area needs to be accommodated within the same unit length on the stator circumference.

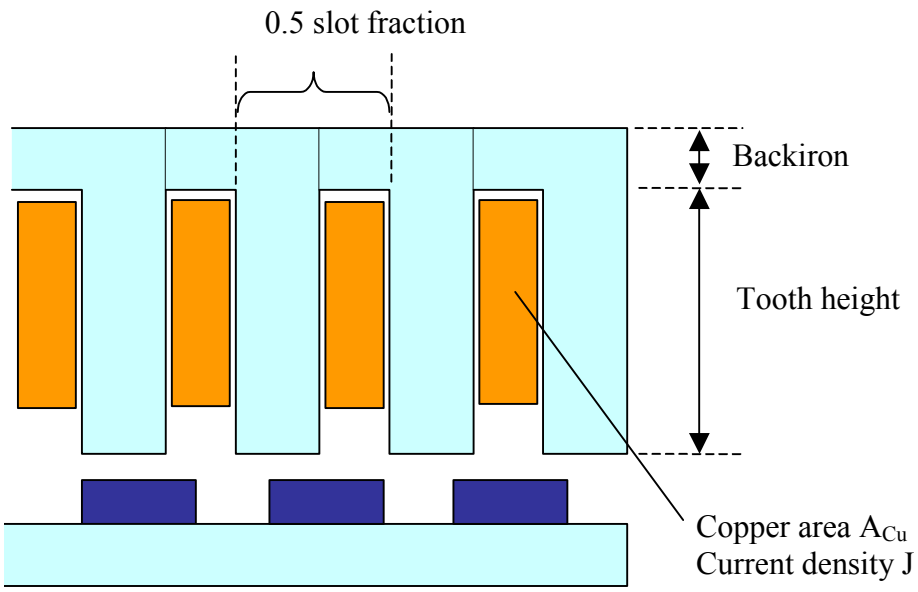

Figure 4-2. Representation of magnetic-mass per unit-air-gap-area

Using the basic requirements of the SOW, we sized a unit-air-gap-area slice of magnetic mass, as represented in Figure 4-2. Next, we wrapped the designed magnetic mass per unit of air-gap area around a family of air-gap surfaces (radial geometry) for air-gap diameters varying from 2 to 10 m.

The resulting magnetic mass per unit air-gap area is on the order of 1400 kg/m^2 consisting of approximately 57% magnetic steel mass, 36% copper mass, and 7% PM mass as shown in Figure 4-3.

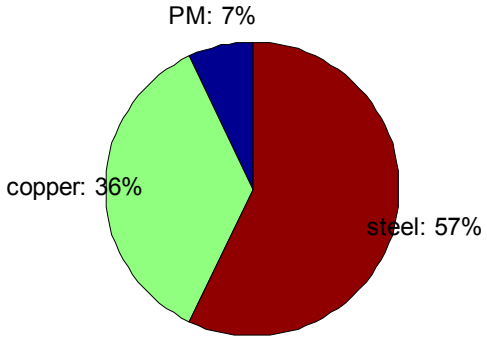

Figure 4-3. Proportion of magnetic part constituents (approximate percentage of magnetic mass)

The cumulated losses in windings (copper), core (steel), and excitation (permanent magnets), as shown in Figure 4-4, represent 2.85% of rated power, meaning that the machine efficiency meets the required 97.15%. Note that no air-friction losses were considered (machine speed is very low at < 33.3 rpm). In addition, no friction losses were considered (the generator has no bearings because its rotating part is installed directly on the main shaft of the turbine).

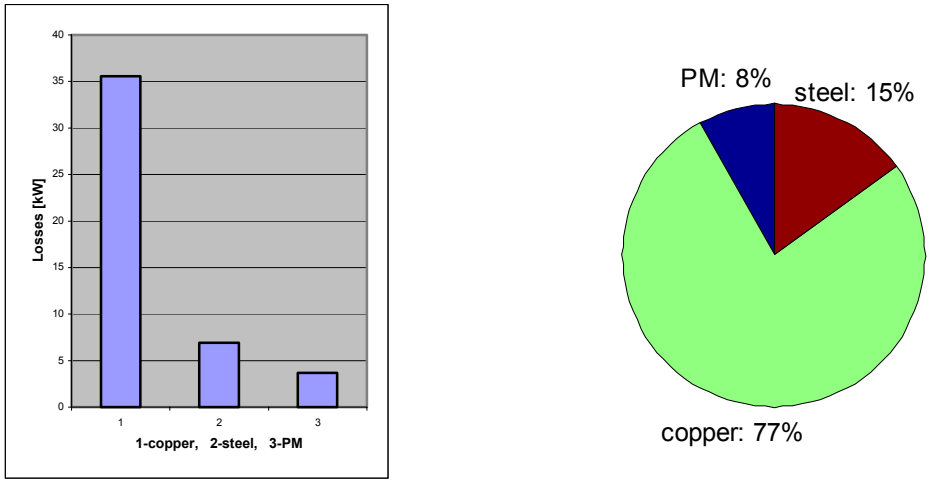

(a) (b)

Figure 4-4. Losses of magnetic-part constituents in (a) kilowatts and (b) as a percentage

The estimated percentage cost breakdown of the steel, permanent magnet, and copper in the assembled machine is illustrated in Figure 4-5. These estimates are for volume production and do not include the costs of prototype design, tooling, set-up or prototype/first-article testing.

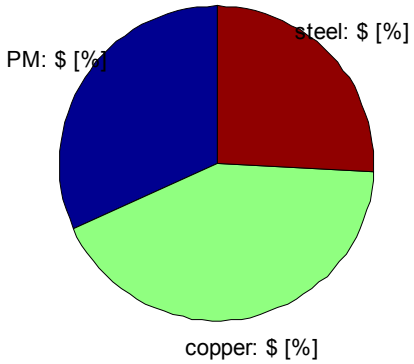

Figure 4-5. Proportion of USD invested into magnetic-part constituents

Figures 4-6 through 4-12 show the effect of generator air-gap diameter on generator length, air-gap area, mass, and the generator cost. All estimates were made by wrapping the designed magnetic mass per unit of air-gap area described above around a family of air-gap surfaces.

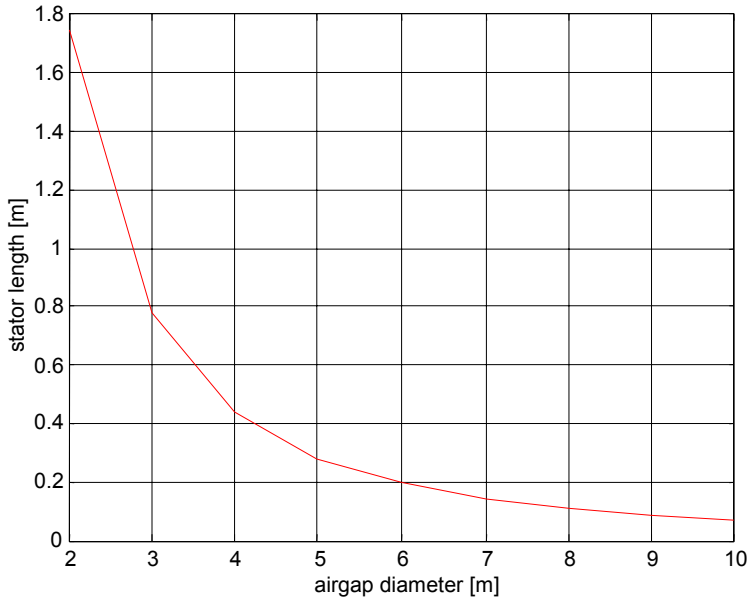

Figure 4-6. Stator length as function of air-gap diameter
(for fixed torque = 755297 Nm and shear stress = 68900 Pa)

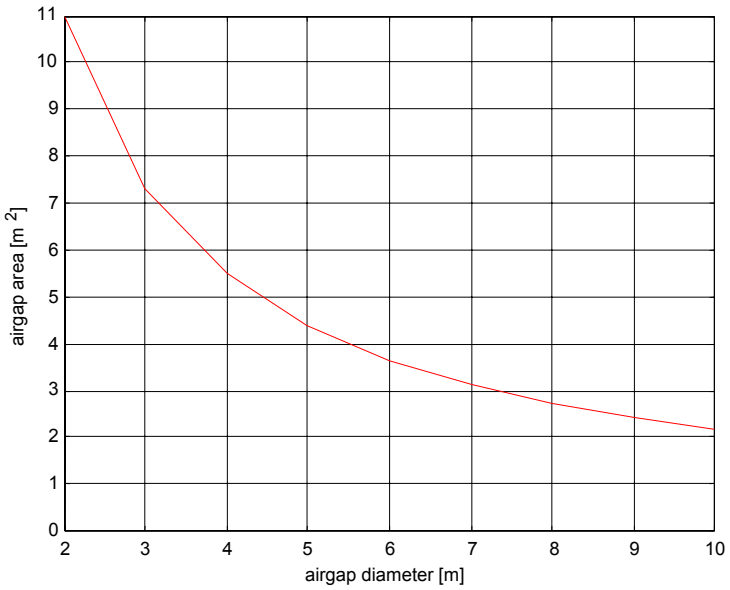

Figure 4-7. Air-gap area as function of air-gap diameter
(for fixed torque = 755297 Nm and shear stress = 68900 Pa)

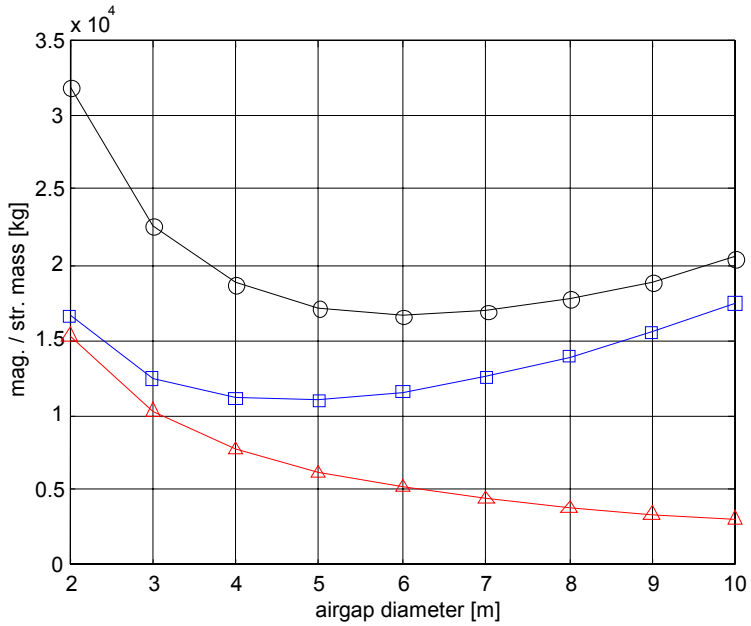

Figure 4-8. Masses as function of air-gap diameter: o-total mass, Δ-magnetic mass, and □-structural mass

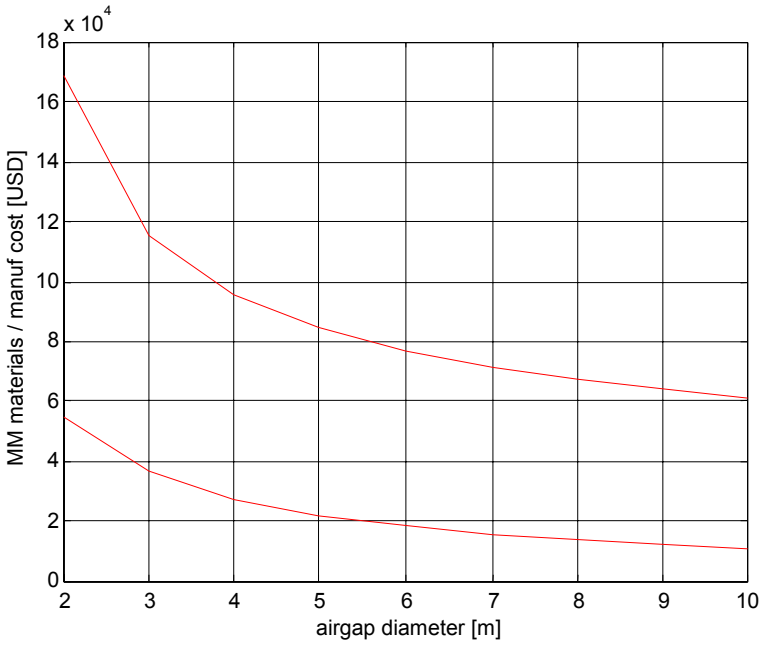

Figure 4-9. Cost of magnetic materials (__) and their integration (- - -) as functions of air-gap diameter for production volume

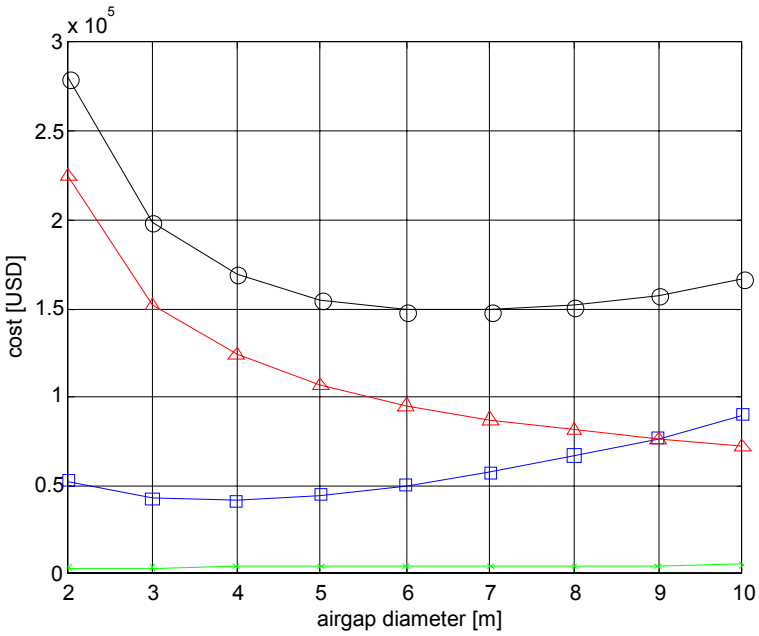

Figure 4-10. Cost based on production volume:
o-total, Δ-magnetics, □-structure, and x-cooling system

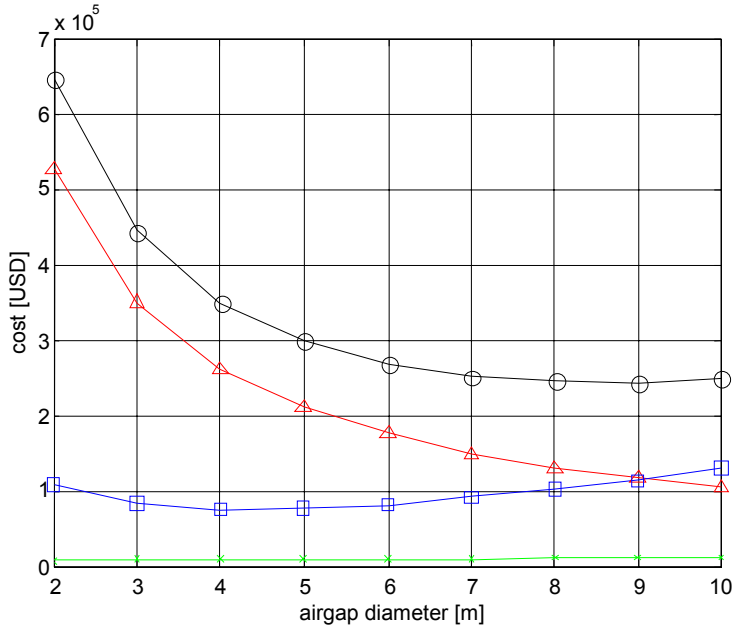

Figure 4-11. Cost of first prototype:
o-total, Δ-magnetics, □-structure, and x-cooling system

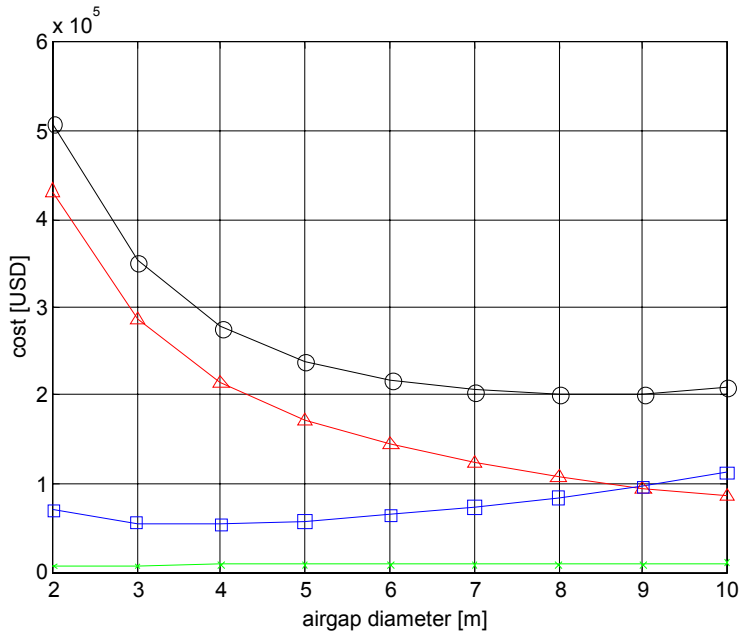

Figure 4-12. Cost based on preproduction volume: o-total, Δ-magnetics, □-structure, and x-cooling system

4.2 Selection of Machine Air-Gap Diameter

Figure 4-10 shows that the total cost curve of the generator has a minimum zone of between 6 and 7 m air-gap diameter. However, other practical aspects can be taken into account, such as:

- Transportation costs (see Appendix II)
- Above a certain size, building the rotor and stator structures as single pieces becomes impractical. Above approximately 5 m diameter, the support structures should be built using a modular approach. Although the modular approach could reduce the cost of transportation, it increases the total cost because more accurate machining of interfaces is necessary and because the generators must be assembled in the field.

Taking into account the transportation factor, the minimum cost zone shifts to the left, with the minimum cost now residing between 5- and 6-m air-gap diameter (Figure 4-13). Thus, the air-gap diameter that could be considered as practical for a direct drive generator is somewhere between 4 and 5 m. We selected the 4-m air-gap diameter as the candidate for the generator because:

- All structural elements can be built as single pieces without having to partition them into sections.
- The form factor of the rotor support structure (L/D = 0.11) is acceptable to allow good mechanical stability, whereas at 5 m the air-gap diameter is L/D = 0.057, which is considered prone to instabilities.
- The 4-m air-gap diameter will guarantee that the overall diameter of the generator, including the housing and all structural parts, will be the below 5.5-6.0 m diameter, which means that the parts can be transported over highways in overwide trucks (with 4–6 m load

width, maximum18 tons load weight, and transportation costs of approximately 4.00 USD per mile).

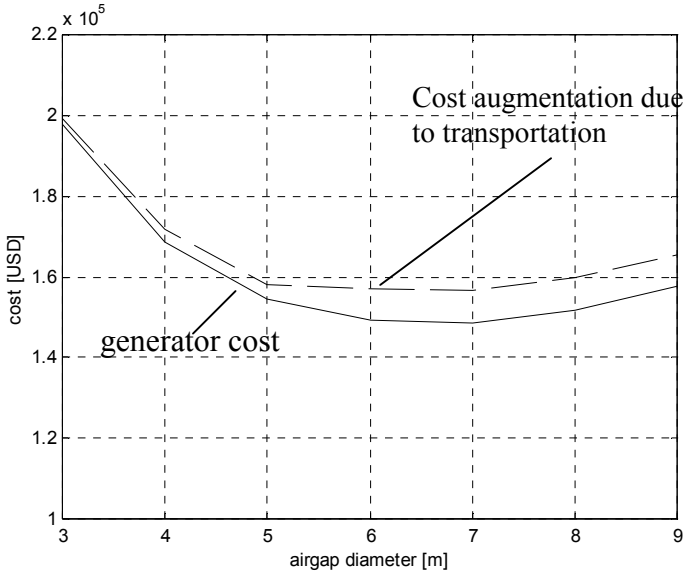

Figure 4-13. Total cost augmentation (dotted line) at large diameters resulting from transportation

4.3 Presentation of Mechanical Drawings—Direct Drive PM Generator

The mechanical drawings showing the conceptual design of the 1621 kW, 4-m air-gap diameter direct drive PM generator are presented in Figures 4-14 through 4-21. The stator is composed of 12 stator segments, with the windings installed onto each segment before it is assembled onto the stator support structure. Stator cooling uses cooling tubes embedded in the outer circumference of the stator laminations. Note that the last two figures (4-20 and 4-21) illustrate the possibility of stacking the stator and rotor assemblies to scale to a higher power (2 ×1.6 MW).

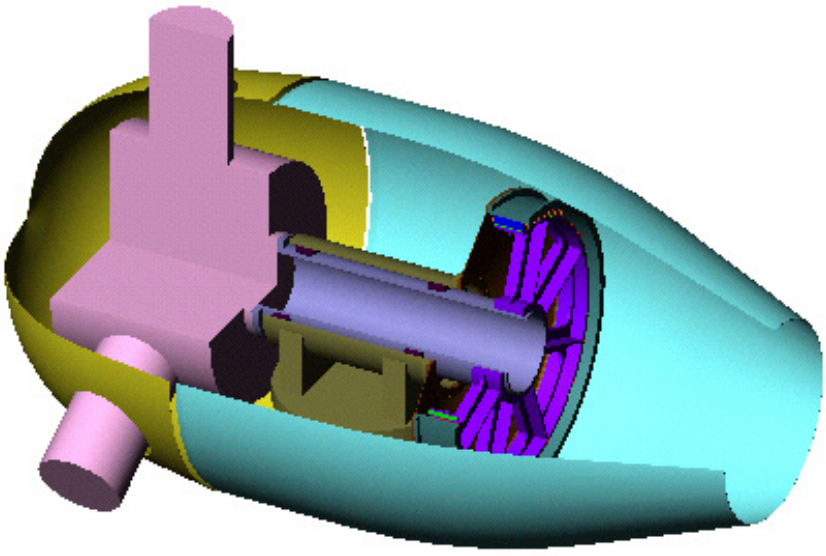

Figure 4-14. Direct drive PM generator (1621-kW, 4-m air-gap diameter)

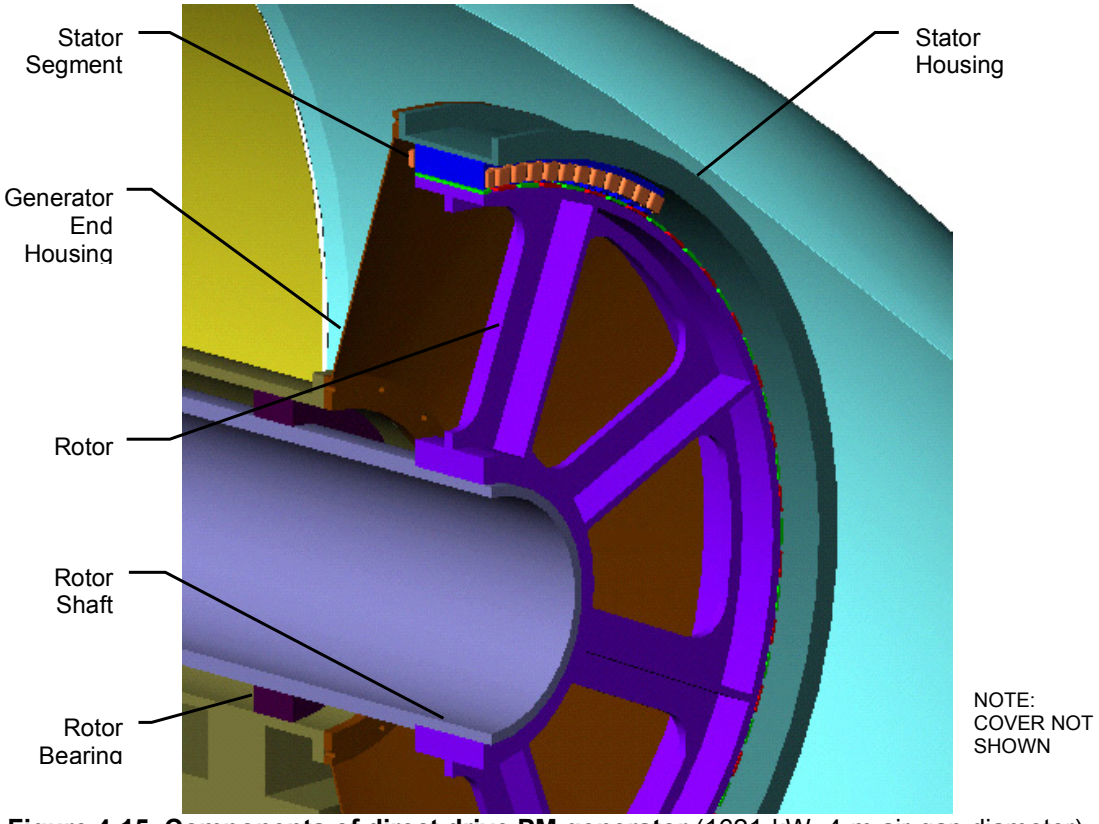

Figure 4-15. Components of direct drive PM generator (1621-kW, 4-m air-gap diameter)

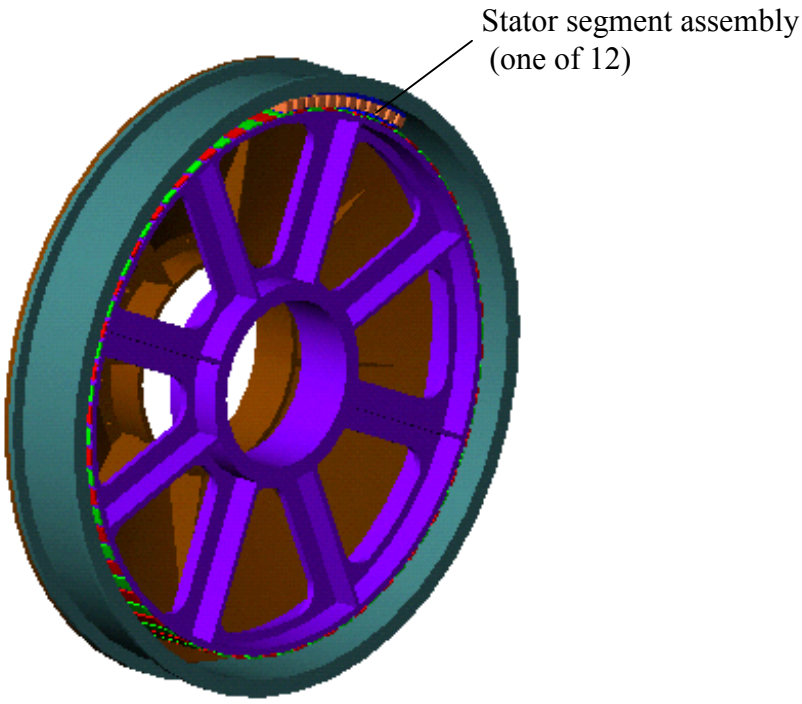

Figure 4-16. Direct drive PM generator (1621-kW, 4-m air-gap diameter)

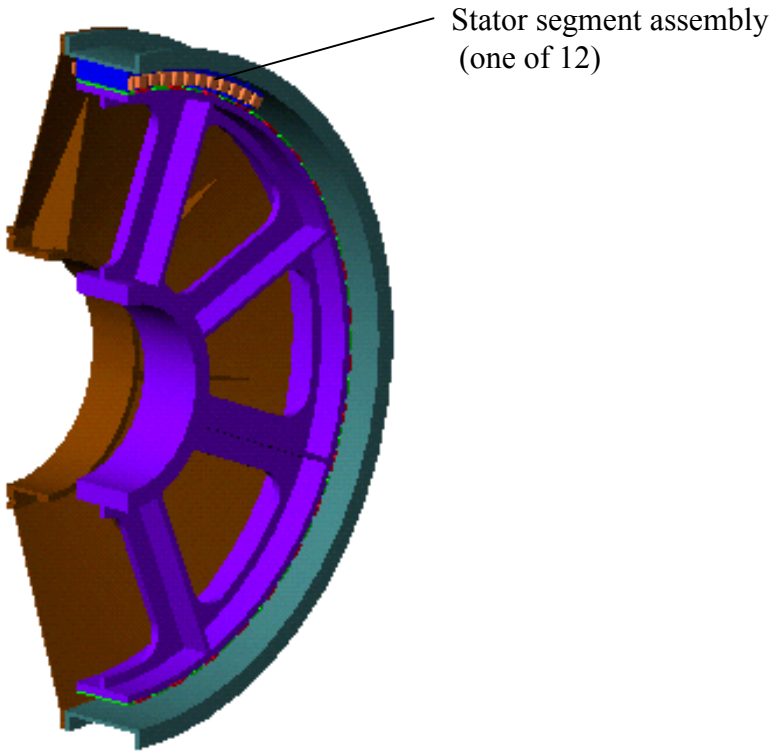

Figure 4-17. Direct drive PM generator (1621-kW, 4-m air-gap diameter)

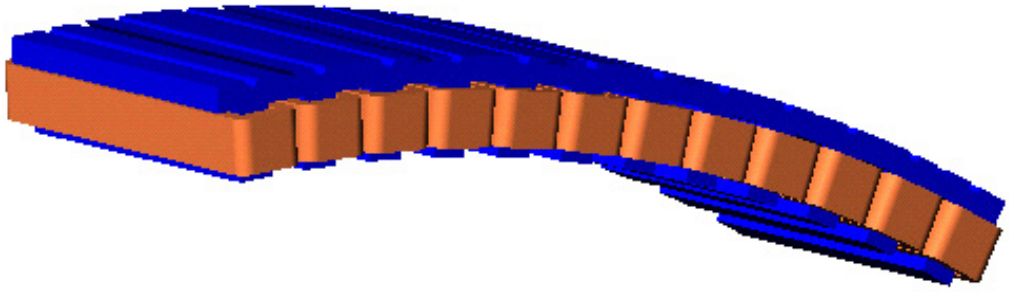

Figure 4-18. Stator segment assembly

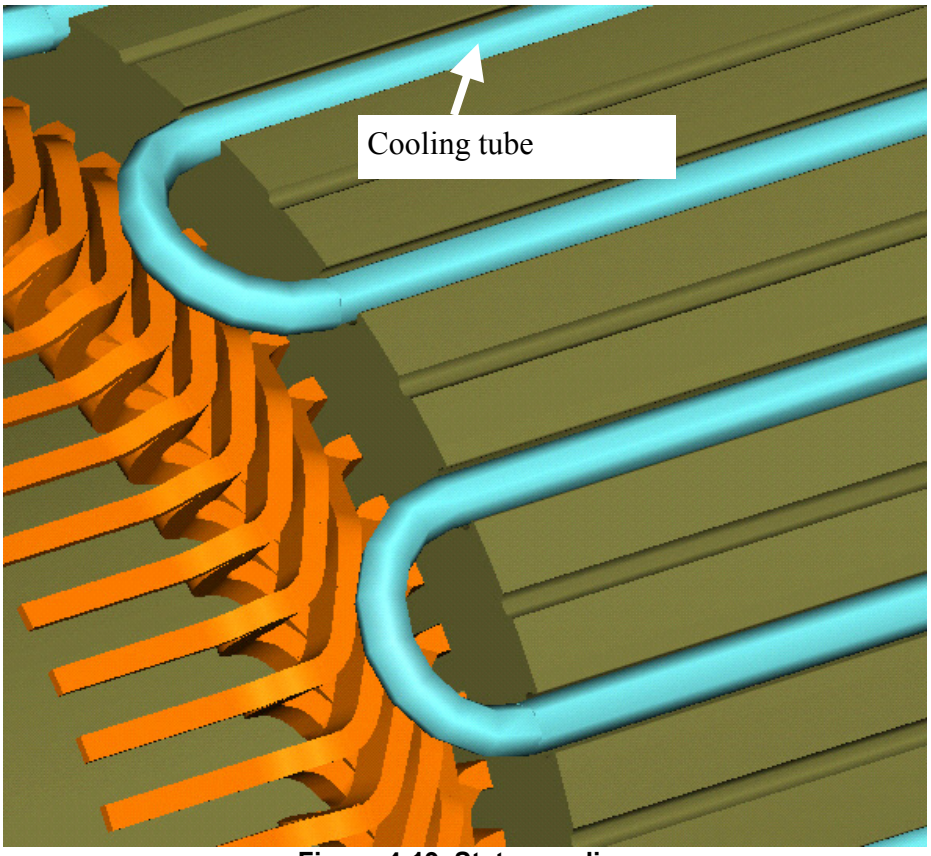

Figure 4-19. Stator cooling

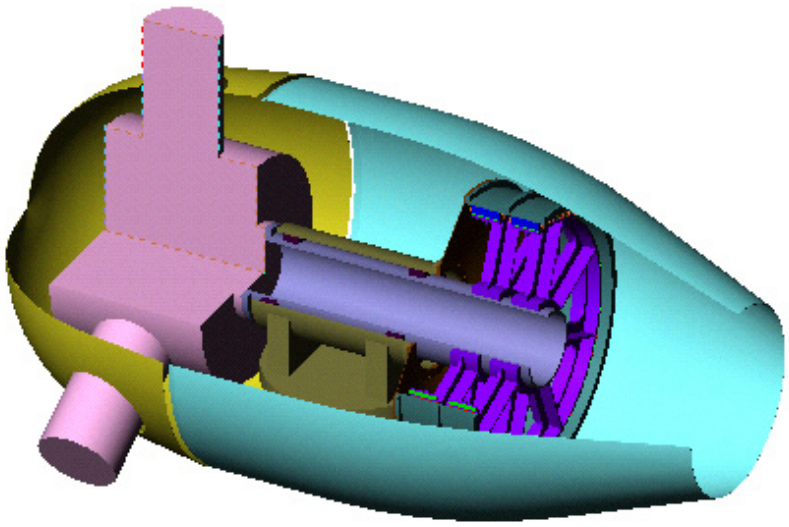

Figure 4-20. Two stacked generators (2 ×1621 kW)

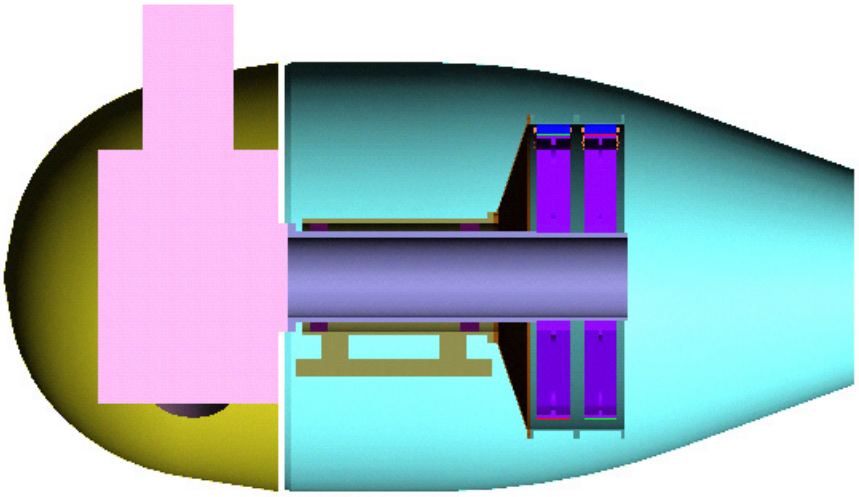

Figure 4-21. Two generators (2 × 1621 kW)

4.4 Presentation of the Cost Models

4.4.1 Cost Model of Generator Magnetic Part

We used the following formula to calculate the cost of the magnetic part (C_{mag}):

$$C_{mag} = C_{PM} M_{PM} + C_{copper} M_{copper} + C_{steel} M_{steel} \quad (4\text{-}6)$$

where:

C_{PM}, C_{copper}, and C_{steel} are the specific costs of the permanent magnet, the copper, and the steel (USD/kg) specified in Table 4-1 for different production volumes

and

M_{PM} , M_{copper}, and M_{steel} are the total mass of the permanent magnet, the copper, and the steel laminations that make up the generator active magnetics, in kilograms. These masses are dependent on the total air-gap-area (A_g), the magnetic mass per air-gap unit area (m_a) and the percentage of PM, copper and steel that constitute the magnetic mass, as follows:

$$\begin{aligned} M_{PM} &= percent_{PM} \cdot m_a A_g \\ M_{copper} &= percent_{copper} \cdot m_a A_g \\ M_{steel} &= percent_{steel} \cdot m_a A_g \end{aligned} \quad (4\text{-}7)$$

The percentages of PM, copper, and steel that go into the magnetic part are shown in Figure 4-3:

$$\begin{aligned} percent_{PM} &= 7\ \% \\ percent_{copper} &= 36\ \% \\ percent_{steel} &= 57\ \% \end{aligned} \quad (4\text{-}8)$$

The magnetic mass per air-gap unit area derived from design is:

$$m_a = 1400\ kg/m^2 \quad (4\text{-}9)$$

The air-gap area A_g can be expressed in terms of parameters as a function of air-gap diameter (D) that was varied from 2 to 10 m in increments of 1 m:

$$A_g = \frac{T}{\sigma D/2} \quad (4\text{-}10)$$

where the torque (T) and shear stress (σ)are:

$$T = 755297\ (Nm) \quad (4\text{-}11)$$

$$\sigma = 68900\ (Pa) \quad (4\text{-}12)$$

4.4.2 Cost Model of the Structural Part

The structural part of the machine is composed of two main parts:

- Rotor support structure
- Stator support structure, which has two parts, the stator main housing and the machine end housing

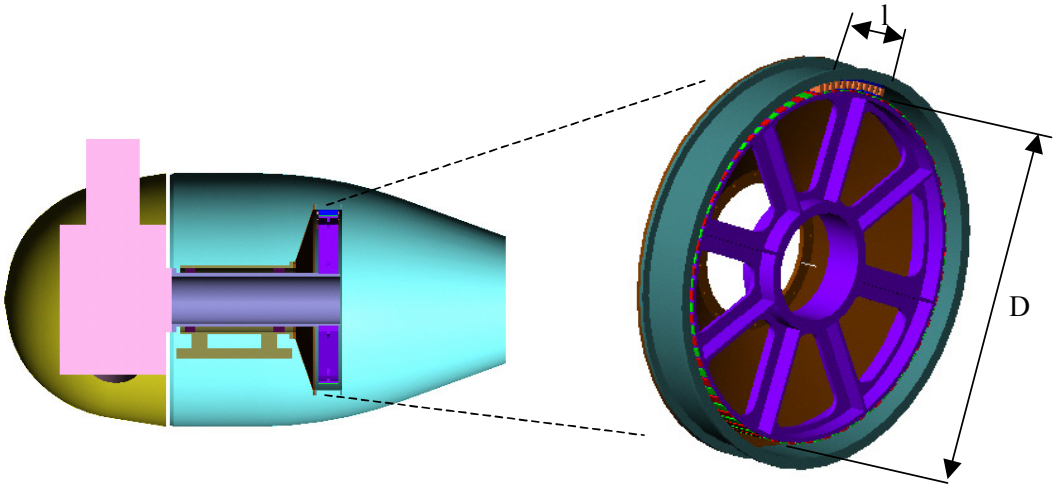

Figure 4-22. Geometry used for support structure mass and cost evaluation

Based on the structure geometry, shown in Figure 4-22, analytic formulas have been derived to express the volume and mass of both. These masses vary as functions of the air-gap diameter as shown in Figure 4-23.

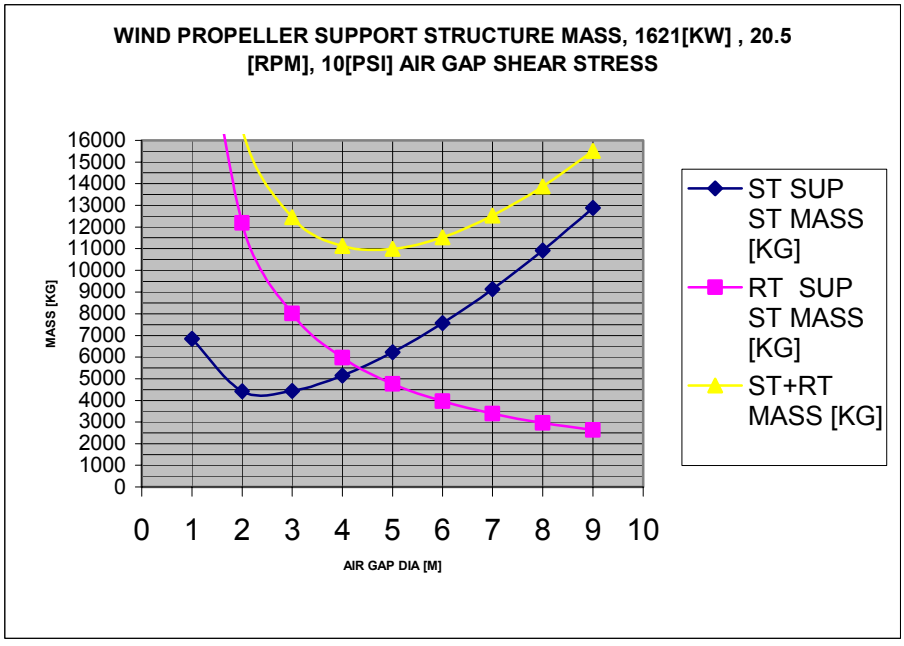

Figure 4-23. Variation of structural masses (rotor and stator) as functions of air-gap diameter

The cost for the support structure is calculated based on:

$$C_{TotStr} = C_{RotStr} M_{RotStr} + C_{RotStr} M_{RotStr} \quad (4\text{-}13)$$

where:

M_{RotStr} and $M_{StatStr}$ are the masses of rotor and stator structures, respectively, in kilograms. and

C_{RotStr} and $C_{StatStr}$ are the specific costs of rotor and stator structures, respectively, in USD/kilogram.

The specific costs for rotor and stator structures depend on several factors:

- Technology involved
- Welding for stator, casting or welding for rotor
- Design approach (modular versus large single piece)

Table 4-2 shows the specific costs we used in this study for the welded stator and the cast rotor.

4.4.3 Cost Model for Cooling System

The machine is liquid-cooled with cooling tubes that are pressed into the stator external circumference, as shown in Figure 4-24.

As illustrated in Figure 4-25, the cost of the generator cooling jacket is a function of air-gap diameter (D) based on the length of the total tube length (L) plus their joints ($\approx \pi \cdot D$).

$$C_{cool} = C_0 (L + 1.5 \cdot \pi \cdot D)$$

where:

- C_0 is the cost of cooling per unit length of tube, in USD/meter
- L is the total length of cooling tubes in the stator. L depends on the total power dissipated in the generator and is independent of air-gap diameter D.
- πD is the approximate total length of the joints.

For the cost estimation of the liquid cooling system, the following parameters have been considered based on machines that Kaman has previously designed:

L = 32 m

C_0 = 78 (USD/meter), production
125 (USD/meter), preproduction
157 (USD/meter), first prototype

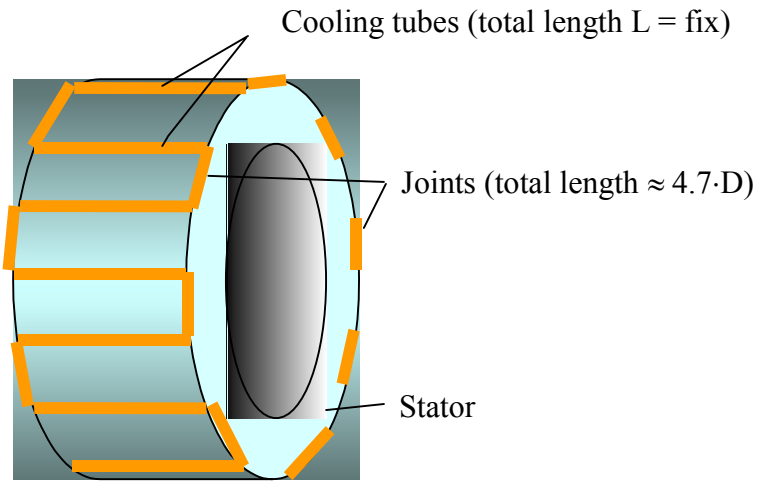

Figure 4-24. Simplified representation of the generator cooling jacket

Table 4-1. Specific Costs for Magnetic Mass Constituents

Costs Related to Magnetic Mass	Production, 130 Units/Year	Pre production, 10 Units	Prototype, First Unit
Copper windings (USD/kilogram)	13	25	30
PM (USD/kilogram)	50	65	70
Magnetic steel lamination (USD/kilogram)	5	13	14
Manufacturing of stator and rotor assembly per air-gap unit area (includes insulation) (USD per square meter)	5,000	10,000	15,000

Table 4-2. Specific Costs for Stator and Rotor Support Structure

Costs Related to Machine Structure	Production, 130 units/year	Preproduction, 10 units	Prototype, First Unit
Welded stator: Material + manufacturing per unit mass (USD/kilogram)	6.5	6.9	7.6
Cast rotor: Material + manufacturing per unit mass (USD/kilogram)	2.9	3.3	6.2

The estimated cooling jacket costs for different air-gap diameters are shown in Figure 4-25.

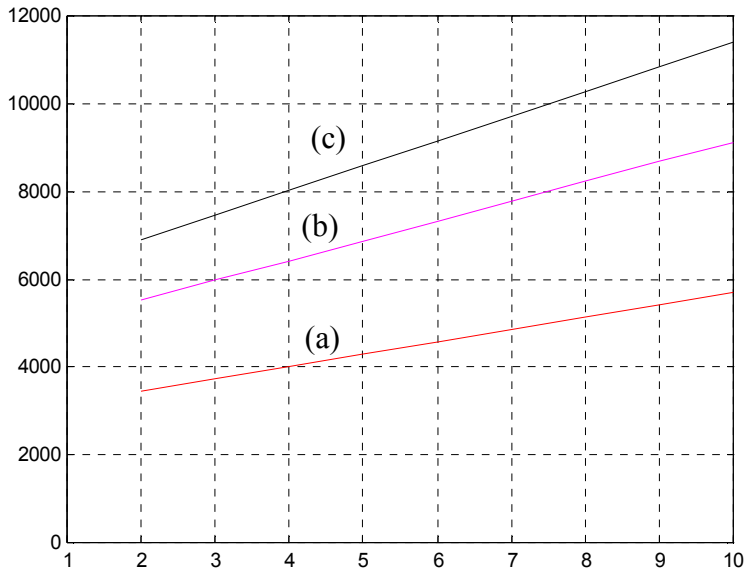

Figure 4-25. Cost of generator cooling jacket as function of air-gap diameter: (a) production, (b) preproduction, and (c) prototype

5. Concept of MTMS PM Generator

5.1 Estimates for MTMS PM Generator

The input design parameters of the Medium Torque Medium Speed (MTMS) machine, according to the SOW, are

- Input power 1589 kW
- Machine efficiency 97.15%
- Torque at rated power 92524 Nm
- Speed at rated power 164 rpm
- Maximum speed 266.4 rpm

For the MTMS PM machine, the magnetic mass per air-gap unit area has been considered to be the same as that of the High-Torque, Low-Speed (HTLS) machine. For this reason the HTLS magnetic mass and cost per air-gap area estimates described in Section 4.1 were used for the MTMS PM machine.

The difference between the MTMS and HTLS machines is the torque—the torque of the MTMS machine is 8 times lower than the HTLS machine. This translates into a different stator length and air-gap area as a function of machine air-gap diameter (i.e., lower values for the same diameter).

Using the lower torque value of the MTMS machine, the estimates made in Section 4.1 for the HTLS machine were repeated. These estimates are shown in Figures 5-1 through 5-6, which are equivalent estimates to those presented in Figures 4-6 through 4-10 for the HTLS machine. Estimates of the effect of air-gap diameter on generator length, air-gap area, mass, and generator cost are included. These estimates were made by wrapping the designed magnetic mass per unit of air-gap area described in Section 4.1 around a family of air-gap surfaces for the MTMS machine.

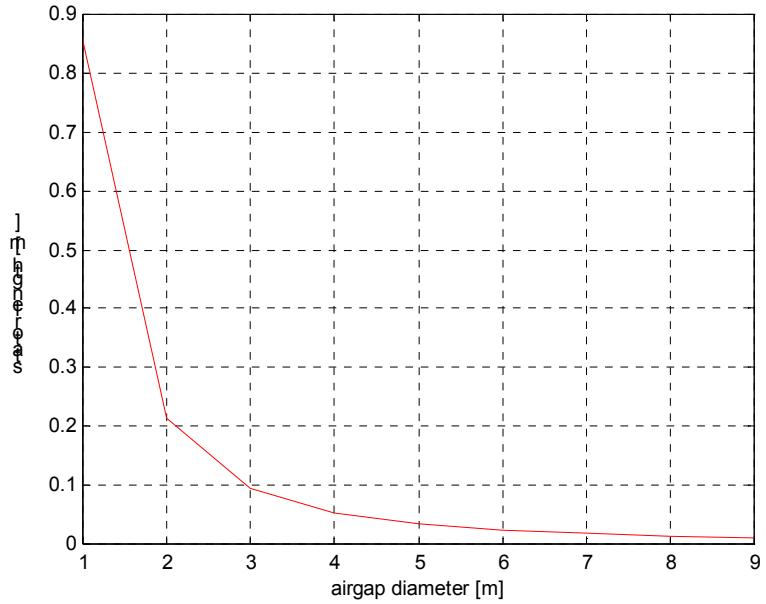

Figure 5-1. Stator length as a function of air-gap diameter
(design case: MTMS, shear stress = 10 psi)

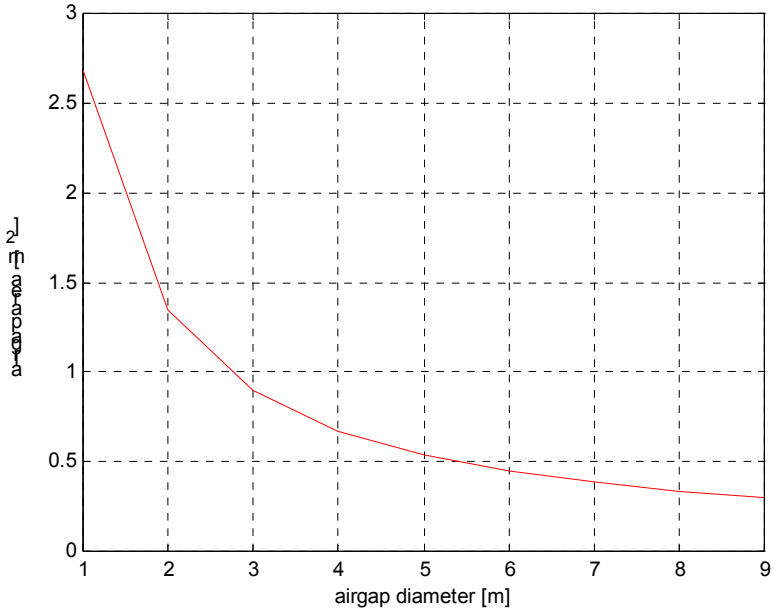

Figure 5-2. Air-gap area as function of air-gap diameter

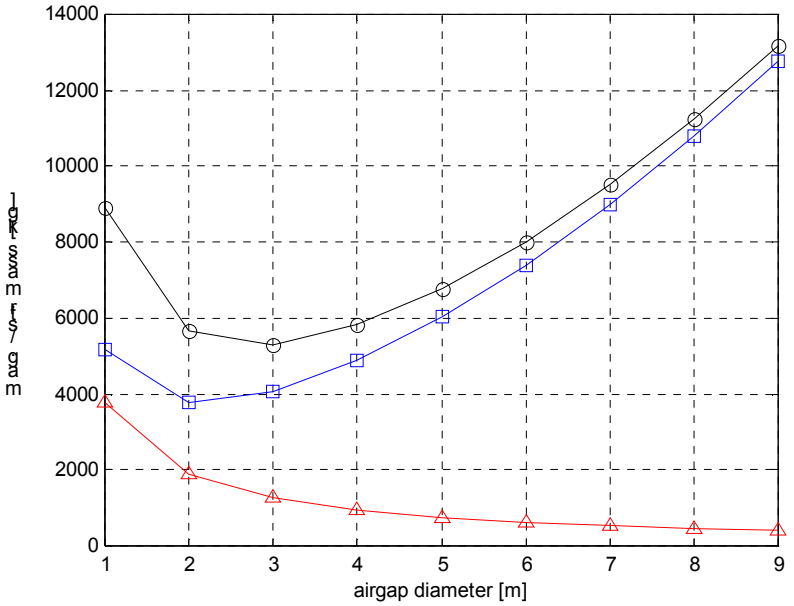

Figure 5-3. Masses as function of air-gap diameter:
o-total mass, Δ-magnetic mass, and □-structural mass

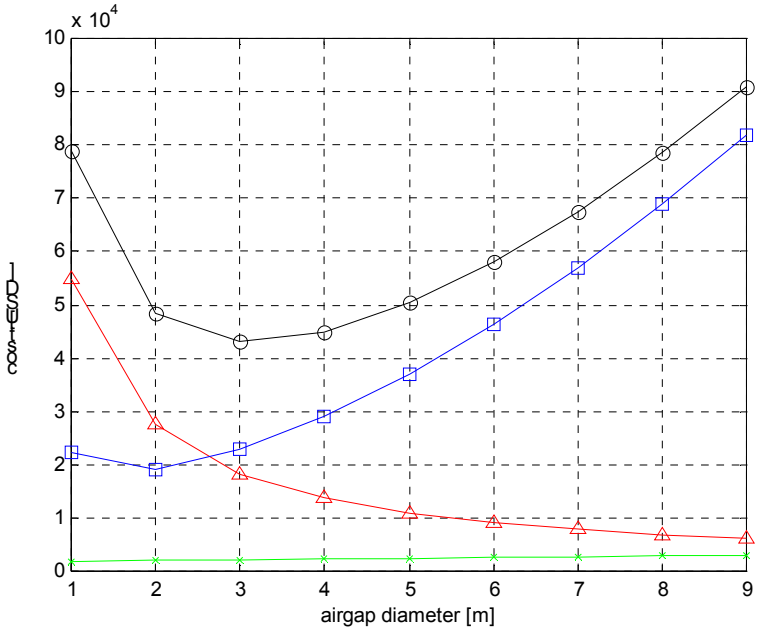

Figure 5-4. Cost based on production volume:
o-total, Δ-magnetics, □-structure (cast rotor), and x-cooling

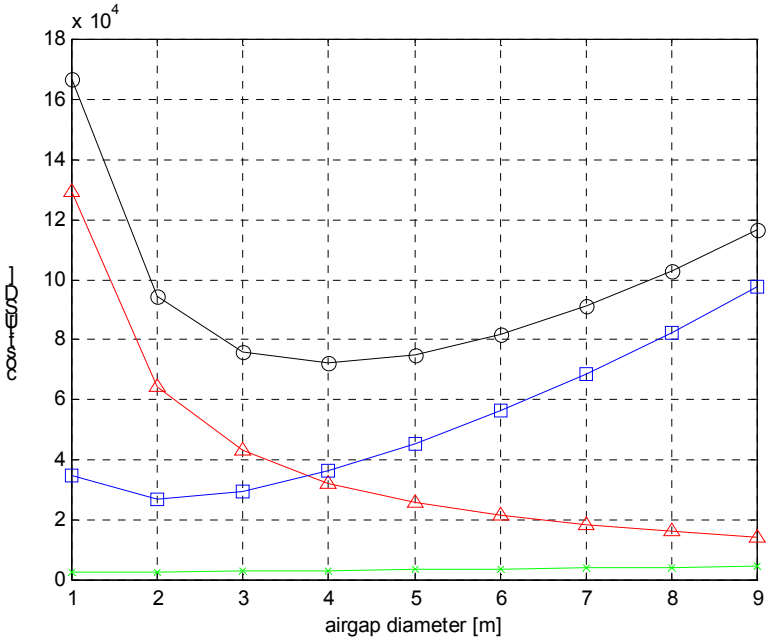

Figure 5-5. Cost of first prototype (cast rotor): o-total, Δ-magnetics, □-structure, and x-cooling

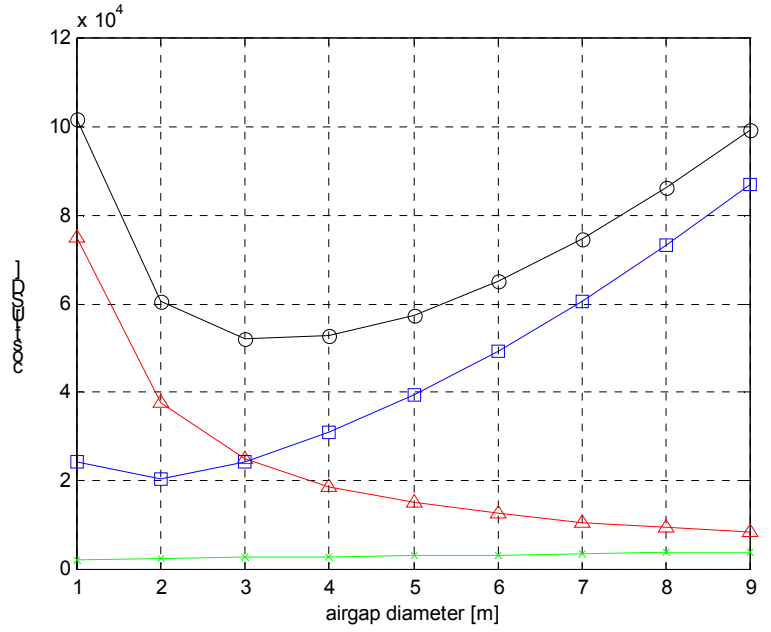

Figure 5-6. Cost based on preproduction volume (cast rotor): o-total, Δ-magnetics, □-structure, and x-cooling

5.2 Selection of MTMS Air-Gap Diameter

The total cost in production mode reaches a minimum at approximately 3-m air-gap diameter. However, at 3-m air-gap diameter, the stator length is only 0.095 m (3.74 in.), which leads to an impractical aspect ratio factor of D/L = 31.57. This factor is prone to stability issues of rotor structure and increased ohmic losses in windings because of a larger percentage of copper in the stator winding end turns.

We have chosen 2 m as a more practical air-gap diameter because:

- The aspect ratio is D/L = 9, which is not extremely big.
- The machine can fit in more conventional types of nacelles.
- The maximum size of machine parts is below 102 in. (2.59 m), which allows standard truck transportation on highways without the need for escort vehicles and special permits.

5.3 Presentation of Mechanical Drawings—MTMS PM Generator

The mechanical drawings showing the conceptual design of the 1621 kW, 2 meter air-gap diameter medium-speed PM generator are presented in Figures 5-7 through 5-11. An 8:1 ratio gearbox is used to drive the generator from the wind turbine rotor. The generator construction is similar to that of the direct drive generator described in Section 4. The stator is composed of 12 stator segments, with the windings installed onto each segment before it is assembled onto the stator support structure. Stator cooling (not shown in figures) uses cooling tubes embedded in the outer circumference of the stator laminations, similar to that used for the direct drive generator.

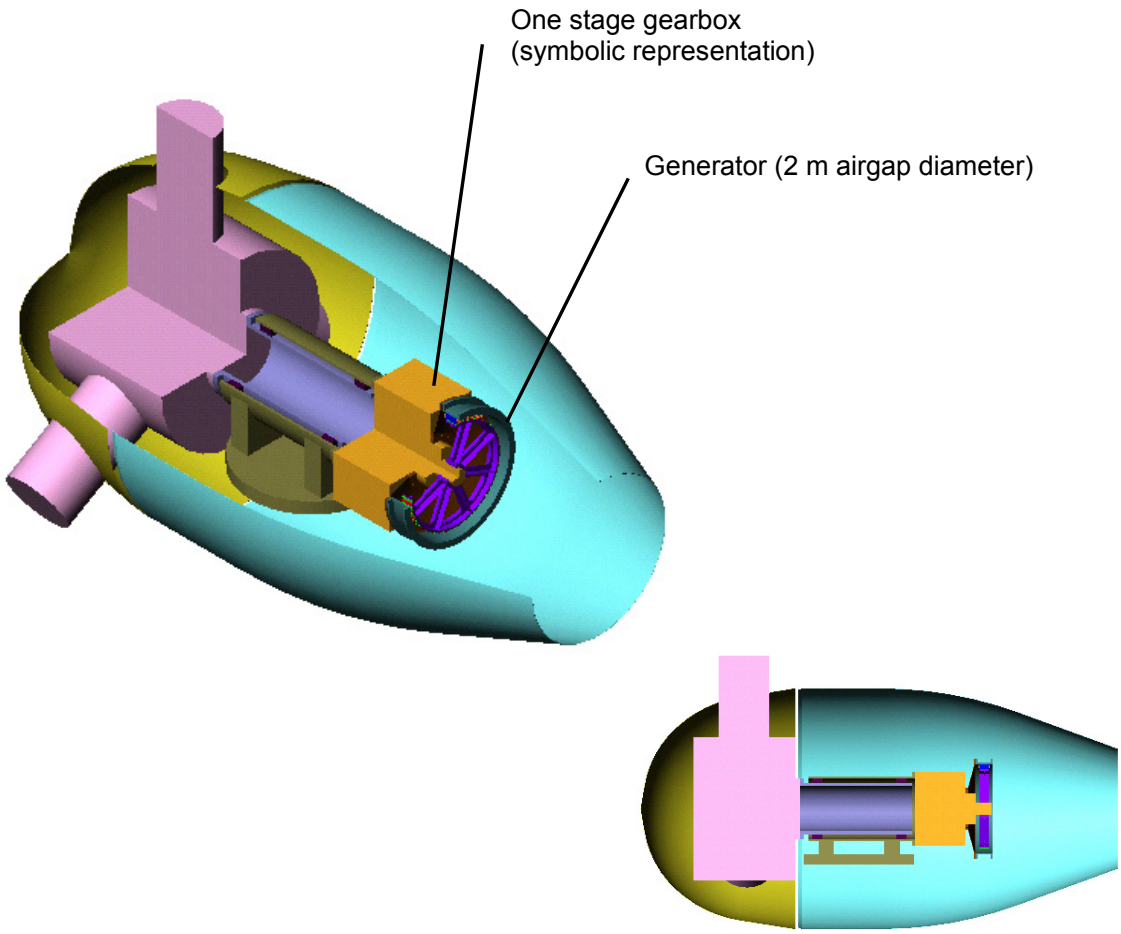

Figure 5-7. MTMS PM generator

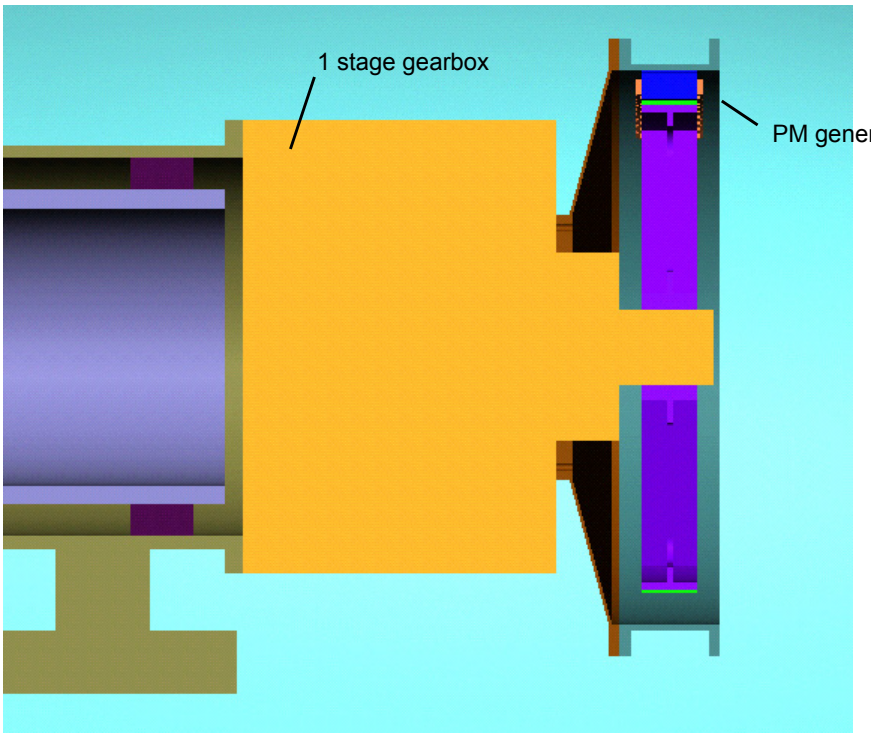

Figure 5-8. MTMS PM generator

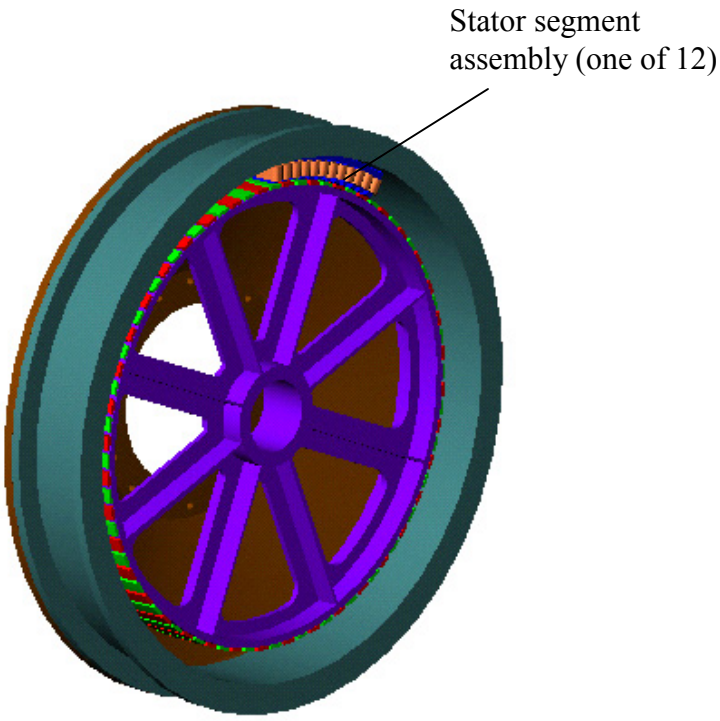

Figure 5-9. MTMS PM generator

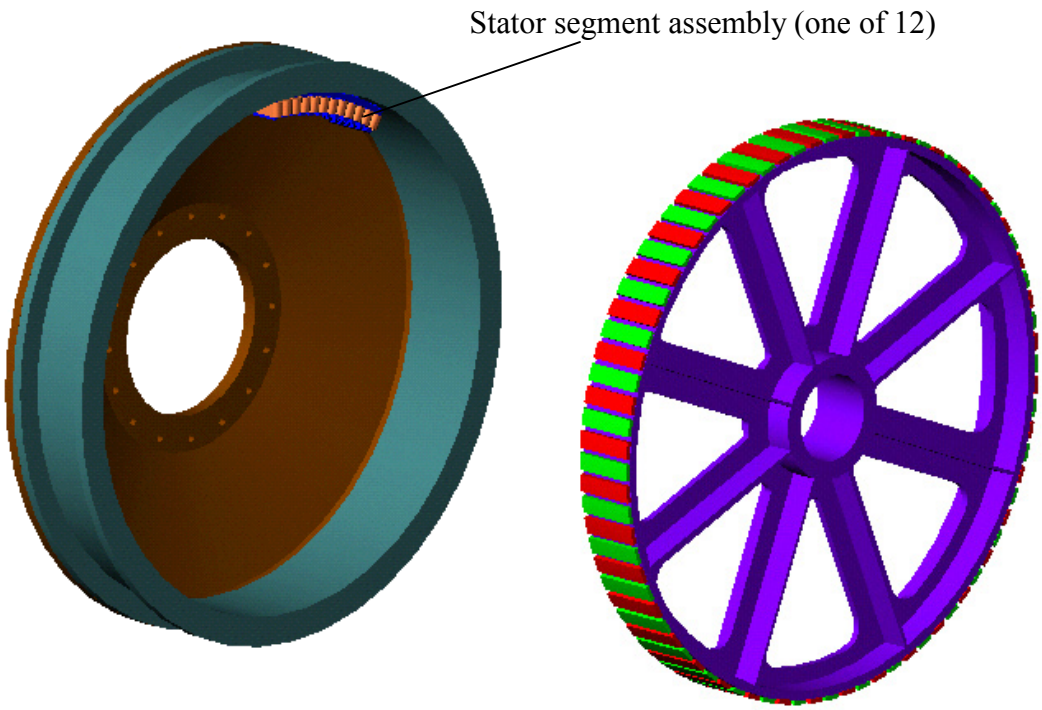

Figure 5-10. MTMS PM generator

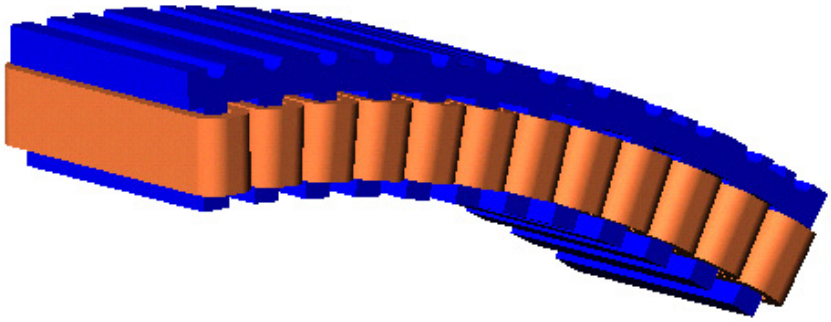

Figure 5-11. Stator segment assembly, MTMS generator

6. Thermal Analysis of PM Generators—Discussion of Cooling Systems

The aim of thermal analysis of the direct drive PM generator was to investigate whether an air-cooling solution might work and what kind of air-cooling option should be used. We did not consider the totally enclosed air-cooling approach because of the large volume of the air-to-air heat exchanger.

6.1 Thermal Analysis of HTLS and MTLS Generators

Figure 6-1 shows a section of the stator that has been thermally analyzed.

The thermal modeling assumptions are (Figure 6-2):

- All losses are located in the stator winding and stator core (this gives a slightly conservative estimate since the rotor losses are accounted into the stator)
- Air temperature in the vicinity of stator housing 50°C
- Air temperature in the vicinity of air-gap 90°C
- Air temperature in the vicinity of winding 95°C
- Heat transfer coefficient, stator housing to air 20 to 1000 W/m^2/°C
- Heat transfer coefficient, air-gap to air 20 W/m^2/°C
- Heat transfer coefficient, winding to air 20 W/m^2/°C

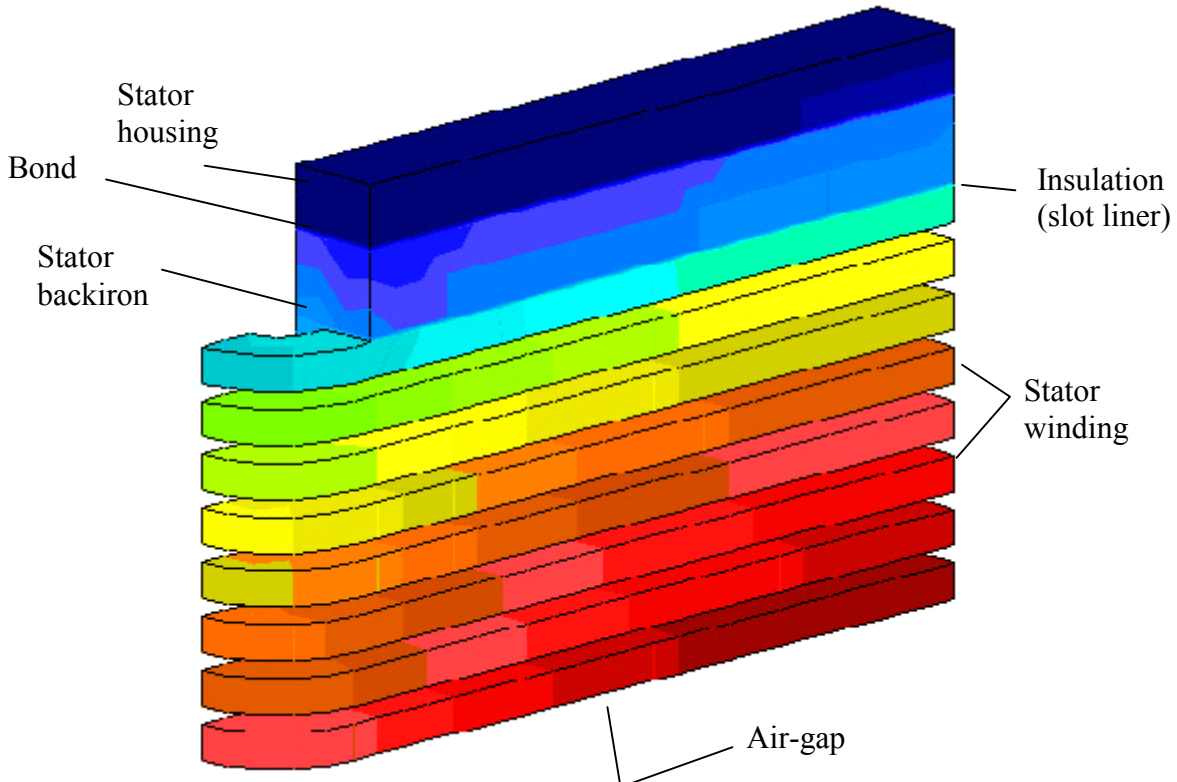

Figure 6-1. Representation of stator "slice" of PM generator considered for thermal analysis
(takes advantage of stator tooth, yoke, and winding symmetries)

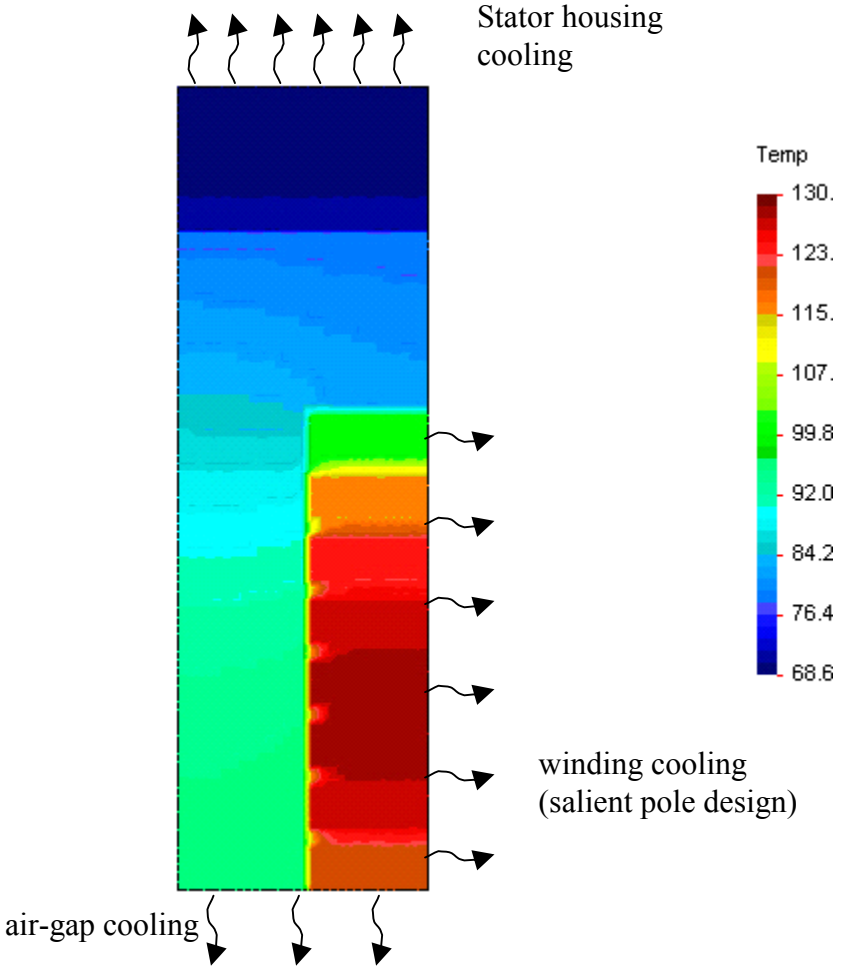

Figure 6-2. FEA model of PM generator considered for thermal analysis with cooling interfaces

We varied the heat transfer coefficient at the stator housing level from 20 to 1000 W/m^2/°C to cover a wide range of cooling options—from a generator housing with a flat surface (no fins), to a housing with fins, then up to liquid-based cooling. Note that the liquid cooling options typically could have a heat transfer coefficient of up to 5000 W/m^2/°C, although here we present results only up to 1000 W/m^2/°C.

The zones marked with A, B and C on Figure 6-3 correspond to different cooling methods:

- Zone A (low values of heat transfer coefficient) is specific to flat surfaces exposed to an airflow in the range of 0 to 10 m/s (convection to forced air cooled).
- Zone B (medium values of heat transfer coefficient) is specific to heat sinks with fins exposed to an airflow of several of 0 to 5 m/s (convection to forced air cooled).
- Zone C (high values of heat transfer coefficient) is specific to liquid cooling systems that can go up to 5000 W/m^2/°C or even higher.

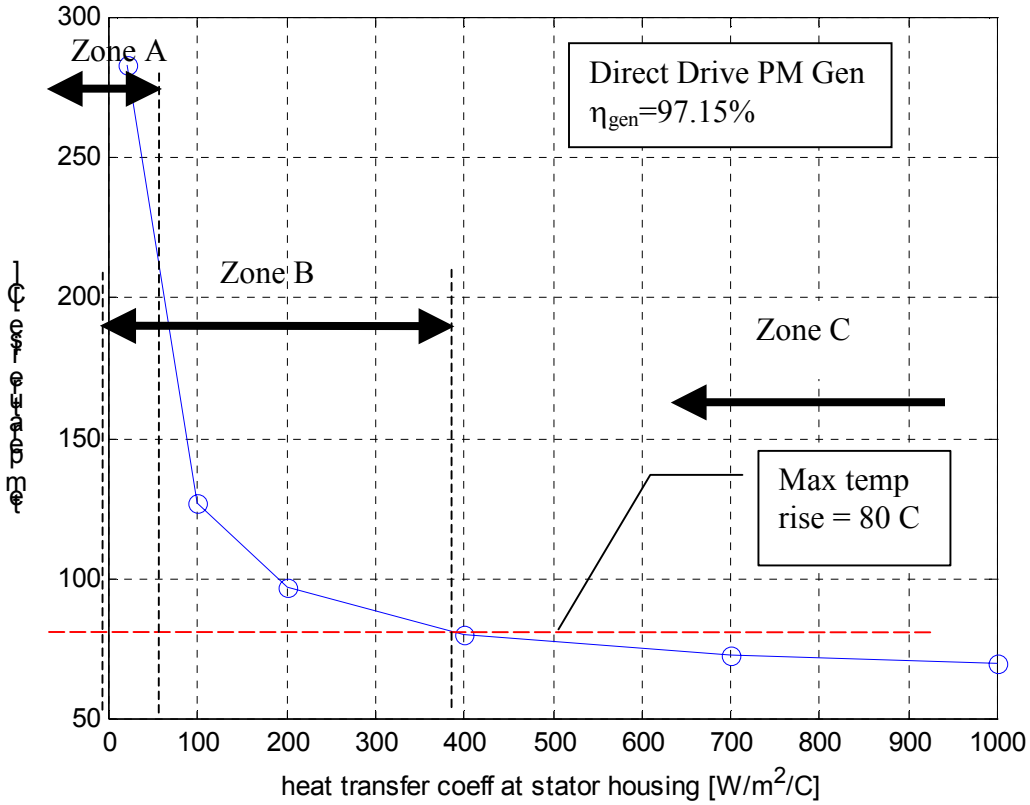

Figure 6-3. Temperature rise of copper windings for direct drive PM generator (good efficiency η_{gen}= 97.15%) at different heat transfer coefficients at stator housing
(i.e., different cooling solutions)

The maximum temperature rise is in the generator windings. Figure 6-3 shows the FEA results for different heat transfer coefficients at the stator housing for the HTLS, direct drive generator at 97.15% efficiency. For a copper temperature of maximum 130°C, at an ambient temperature of 50°C, the maximum temperature rise allowed should be 80°C. Figures 6-4 through 6-9 show the temperature charts for all the points that we used to draw the temperature-rise curve in Figure 6-3.

According to Figure 6-3, the maximum temperature rise of 80°C asks for a heat transfer coefficient at the stator housing of 400 W/m^2/°C or better. This could be achieved by attaching proper aluminum heat sinks (with fins exposed to an airflow of 4 to 5 m/s linear velocity) onto the stator housing.

For the MTMS PM generator, the cooling system must deal with the same dissipated power, but within a smaller volume. The main cooling path, which is via the stator housing, has an area approximately four times smaller than that of the high-torque-medium-speed generator. This indicates that only a liquid cooling solution could be suitable for this case.

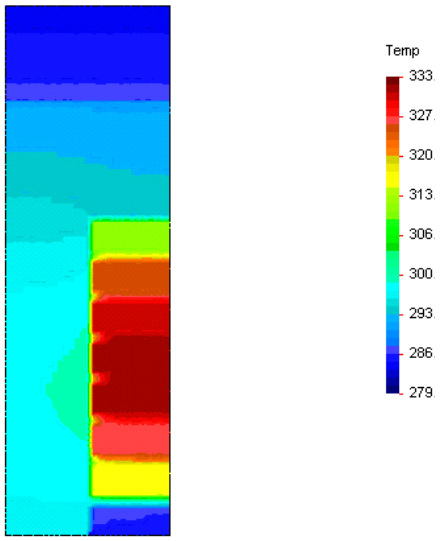

Figure 6-4. Temperature distribution within a stator section of direct drive PM generator: heat transfer coefficient - stator housing to air = 20 W/m^2/°C

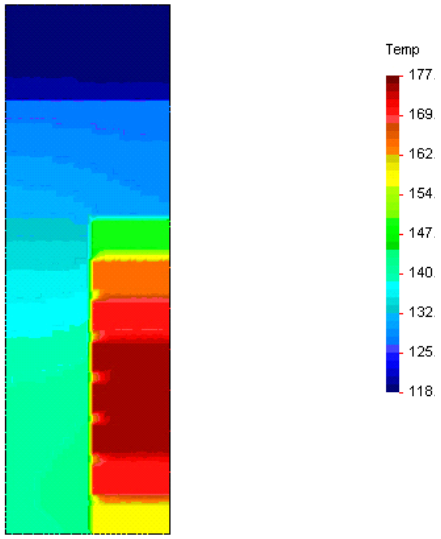

Figure 6-5. Temperature distribution within a stator section of direct drive PM generator: heat transfer coefficient, stator housing to air = 100 W/m^2/°C

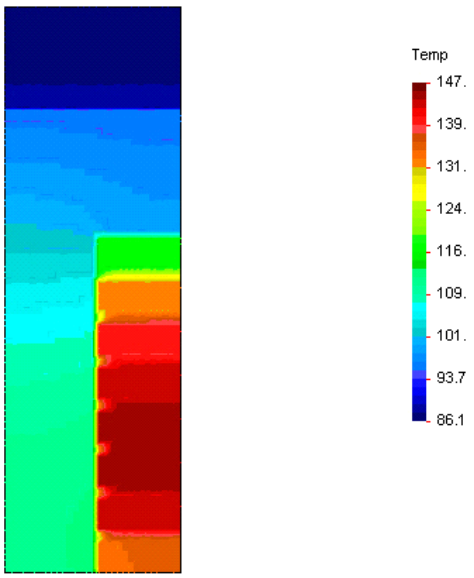

Figure 6-6. Temperature distribution within a stator section of direct drive PM generator: heat transfer coefficient - stator housing to air = 200 W/m^2/°C

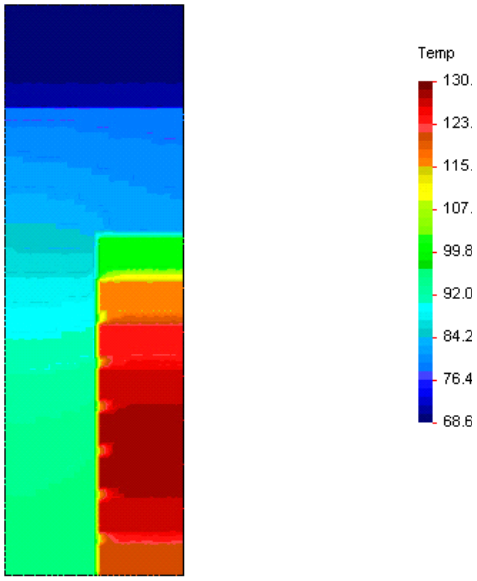

Figure 6-7. Temperature distribution within a stator section of direct drive PM generator: heat transfer coefficient, stator housing to air = 400 W/m^2/°C

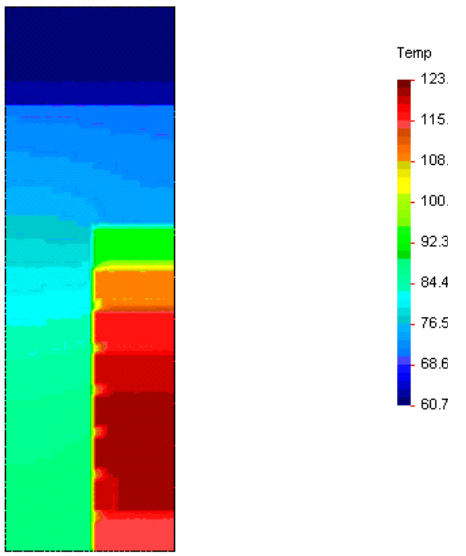

Figure 6-8. Temperature distribution within a stator section of direct drive PM generator: heat transfer coefficient - stator housing to air = 700 W/m^2/°C

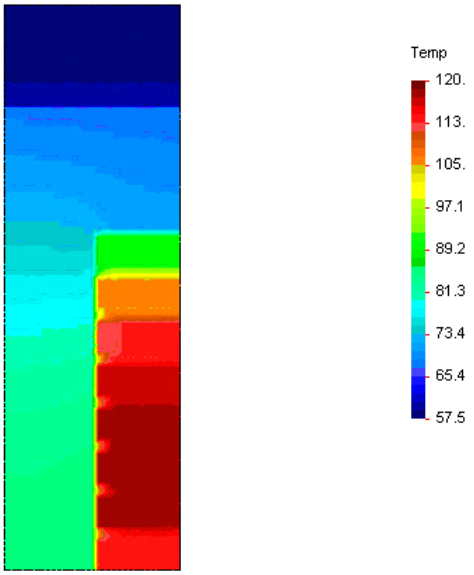

Figure 6-9. Temperature distribution within a stator section of direct drive PM generator: heat transfer coefficient - stator housing to air = 1000 W/m^2/°C

6.2 Cost of Air-Cooling System for the HTLS PM Generator

We investigated the cost of two air-cooling options:

- Extruded aluminum blocks attached to the stator housing OD
- Cast fins onto the stator housing OD

It is important to mention that the cooling effectiveness of the cast fins will be lower, approximately one-half to one-fourth of the aluminum extrusion's one, and therefore the cast fins do not represent a promising option. However, the cost exercise could give more insight into the cost of cooling options.

Table 6-1. Estimated Cost of Air-Cooling System

Volume Cooling Options	Production, USD	Preproduction, USD	Prototype, USD
Aluminum extrusion and thermal interface to stator housing	8,474	9,065	13,040
Cast fins onto stator housing OD	3,000	3,800	12,800
Baseline liquid cooling	4,000		

6.3 Conclusions on Air-Cooling

We drew the following conclusions from our work on air-cooling:

- The direct drive generator (with 97.15% efficiency) could be forced-air-cooled by attaching to the stator housing aluminum heat sinks with fins and ensuring proper air velocity (approximately 4 m/s at stator housing fins and at air-gap and windings).

- The cost of a cooling jacket based on extruded aluminum is significantly more expensive than a liquid cooling solution.

- The cast fins on the stator housing represent a cheaper solution but with questionable cooling effectiveness because the steel has poorer thermal conductivity.

- The MTMS generator requires a liquid cooling solution because the air cooling solutions do not have a high enough heat transfer coefficient, as described in Section 6.1.

7. Impact of Generator Target Efficiency and Air-Gap Thickness on Cost

The generator estimates described in Sections 4 and 5 for the HTLS and MTMS generators, respectively, are based on a full load efficiency target of 97.15% and an air-gap thickness of approximately 6-8 mm. The selection of the target efficiency and the air-gap thickness, both have an effect on the estimated generator cost and these effects are investigated in the following subsections.

7.1 Impact of Target Efficiency on HTLS Generator Unit Cost

As the desired efficiency of the generator increases, the cost and the size of the generator increase as well. Higher efficiency will require a lower current density in the windings because the copper losses account for approximately three-fourths of total machine losses (the magnetic circuit geometry and size have a lower impact on efficiency than copper losses).

We expect, then, that a less efficient generator will be less expensive, although it will need a more effective cooling system (Figure 7-1). The cost reduction is mainly attributed to the need for less magnetic mass, copper, and steel in the machine. We estimated the cost of a family of four direct drive PM generators at different efficiencies. Figure 7-2 shows the results as cost of generator per generated kilowatt of power (USD/kilowatt). These estimates are based on the machine with a 4-m air-gap diameter.

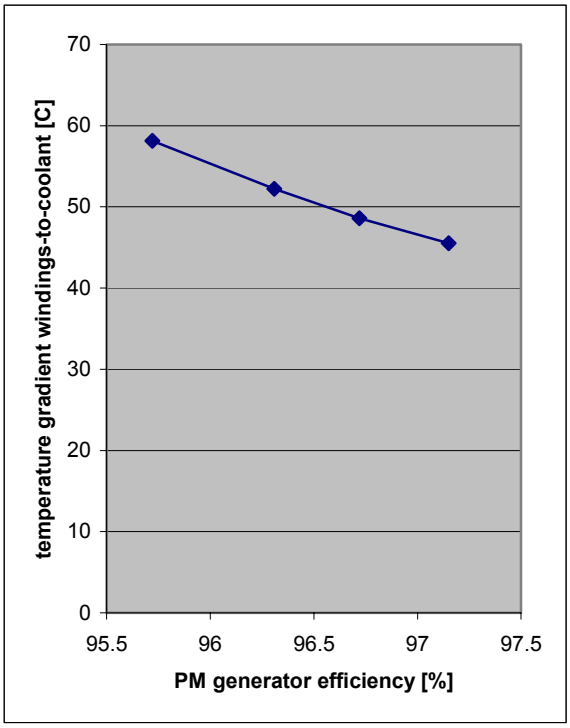

Figure 7-1. Temperature gradient for different generator efficiencies
(4-m air-gap diameter, liquid-cooled direct drive PM generator)

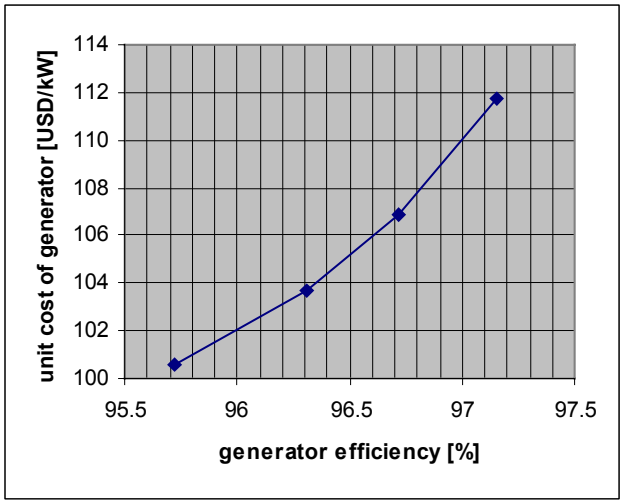

Figure 7-2. Direct drive PM generator cost per generated kilowatt as function of efficiency
(design case: direct drive PM generator)

Note that the lower efficiency version of the generator is less expensive per generated kilowatt. However, for the same generated electric power, the input mechanical power (at generator shaft) has to be higher, a fact that might drive up the cost of the turbine.

For the lower efficiency version of the generator, the cooling system must be more effective because the temperature gradient is higher. Note that the temperature gradient shown in Figure 7-1 takes into account both the differences in energy dissipation and the thermal impedance of the generator. The thermal impedance changes for the different generator designs because different copper and steel quantities are used depending on the target efficiency.

7.2 Impact of Target Efficiency on MTMS Generator Unit Cost

The analysis described in Section 7.1 for the HTLS generator was repeated for the MTMS generator. The results are shown in Figure 7-3, which shows the MTMS generator unit cost for different target efficiencies.

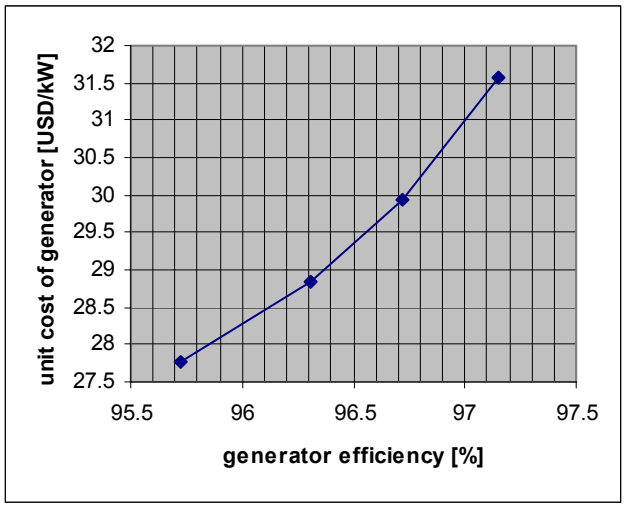

Figure 7-3. Generator cost per generated kilowatt as function of efficiency
(design case: MTMS PM generator)

7.3 Impact of Air-Gap Thickness on the Cost of PM Direct Drive Generator

For a surface-mounted PM machine, the air-gap size is not strictly related to the air-gap diameter as a percentage, as it could be, for instance, in the case of electrically excited machines. The air-gap thickness for a surface-mounted PM machine has to be selected so that it can cover with margin the tolerances in machining the rotor/stator mechanical parts as well as the deformations that result from machine loading and thermal expansion. These deformations decrease the effective air-gap thickness by approximately 2 mm for a 4-m air-gap diameter.

At a first-order evaluation, the air-gap thickness could impact the cost of magnetic mass via the quantity and/or grade of the PM magnets. Assuming that the relative permeability of the magnet is approximately 1, the air-gap flux density (Bg) can be expressed as:

$$Bg = Br\frac{lm}{lm + lg} \tag{7-1}$$

where:

- *Br* is the remaining flux density of the permanent magnet,
- *lm* is the thickness of the magnet,
- *lg* is the thickness of the mechanical air-gap.

For the same magnet (same material and thickness; for example *lm* = 16 mm), a 50% increase of air-gap thickness (for example, from *lg* = 6 mm to *lg* = 9 mm) leads to only a 12% decrease in the air-gap field. To achieve the same value of flux density in the air-gap for increased air-gap thicknesses, we can increase the thickness of the magnets or select higher grade magnets that have a higher remnant field. These approaches can be used separately or combined.

The following shows the cost of magnetic mass for the direct drive PM generator for two cases:

- Figure 7-4 shows the cost versus air-gap diameter for the air-gap thickness dependent on air-gap diameter as shown in Figure 7-6.
- Figure 7-5 shows the cost versus air-gap diameter for constant air-gap thickness (8 mm) for all air-gap diameters.

Conclusions regarding the effect of air-gap thickness on generator design and cost are as follows:

- A larger air-gap increases the cost of the magnetic part of the PM generator for a given air-gap flux density and a fixed loading curve of magnets.
- For a surface-mounted PM machine, because the permeability of the magnets is close to the permeability of the air, the equivalent air-gap for the magnetic circuit is actually larger than the mechanical air-gap (lg).
- For a low-speed PM machine, a 6-mm air-gap can be still considered acceptable up to a 4-m air-gap diameter. At a 4-m air-gap diameter, all cumulated effects of machining tolerance, thermal expansion, and mechanical loading are on the order of 2 mm.

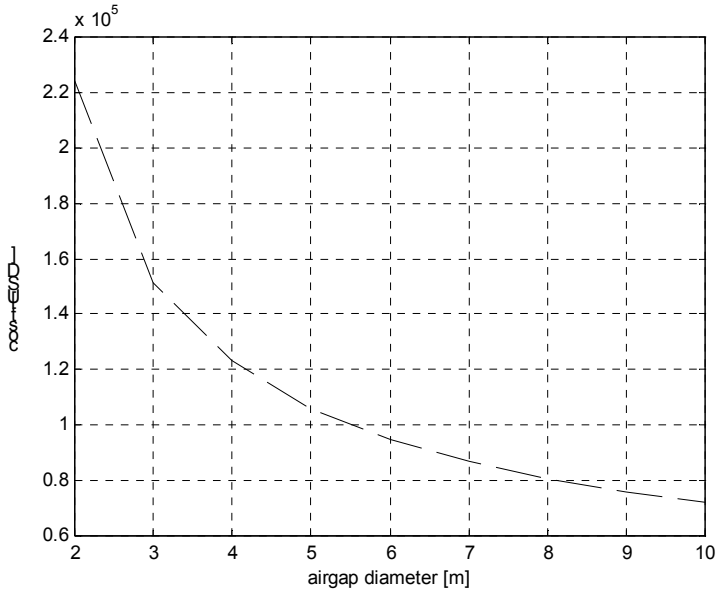

Figure 7-4. Cost of direct drive PM generator magnetics for air-gap thickness dependent on machine air-gap diameter (as shown in Figure 7-6)

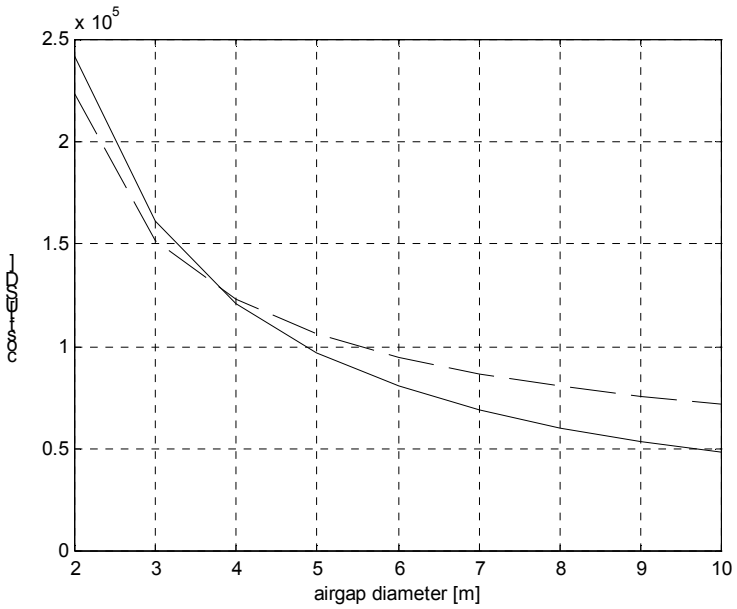

Figure 7-5. Comparison of cost of PM generator magnetics:
Dotted line—air-gap thickness dependent on machine air-gap diameter
Full line—air-gap thickness remaining the same (8 mm) for all diameters

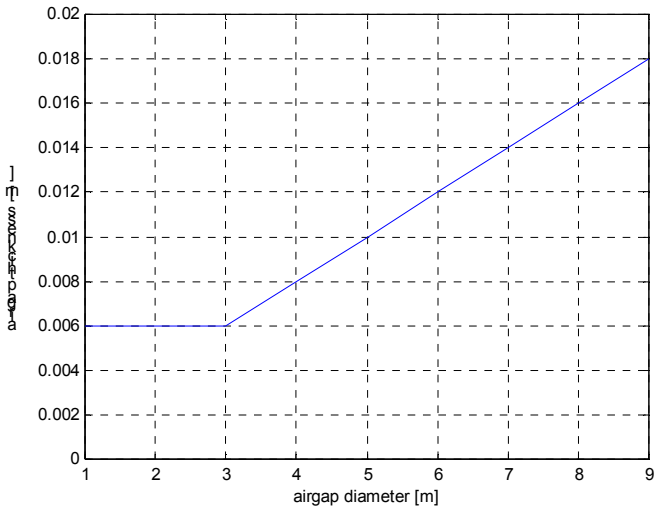

Figure 7-6. Air-gap thickness as function of air-gap diameter used for cost curves in Figures 7-4 and 7-5

8. Comparison of Power Electronics Alternatives

Based on the qualitative assessment of power electronics options for different machine types in Section 2, we made a quantitative comparison of the options available for PM generators. Two categories of power electronics systems were considered for the PM generators, as shown in Figure 8-1. Both of these systems convert the variable frequency AC generator output to DC, then invert the DC back to fixed-frequency AC for interface to the utility grid. The first category uses passive rectification to convert the generator AC to DC, while the second category uses an active IGBT switched mode rectifier for this conversion. The conversion of DC to fixed-frequency AC uses an IGBT switched mode inverter for both categories of systems.

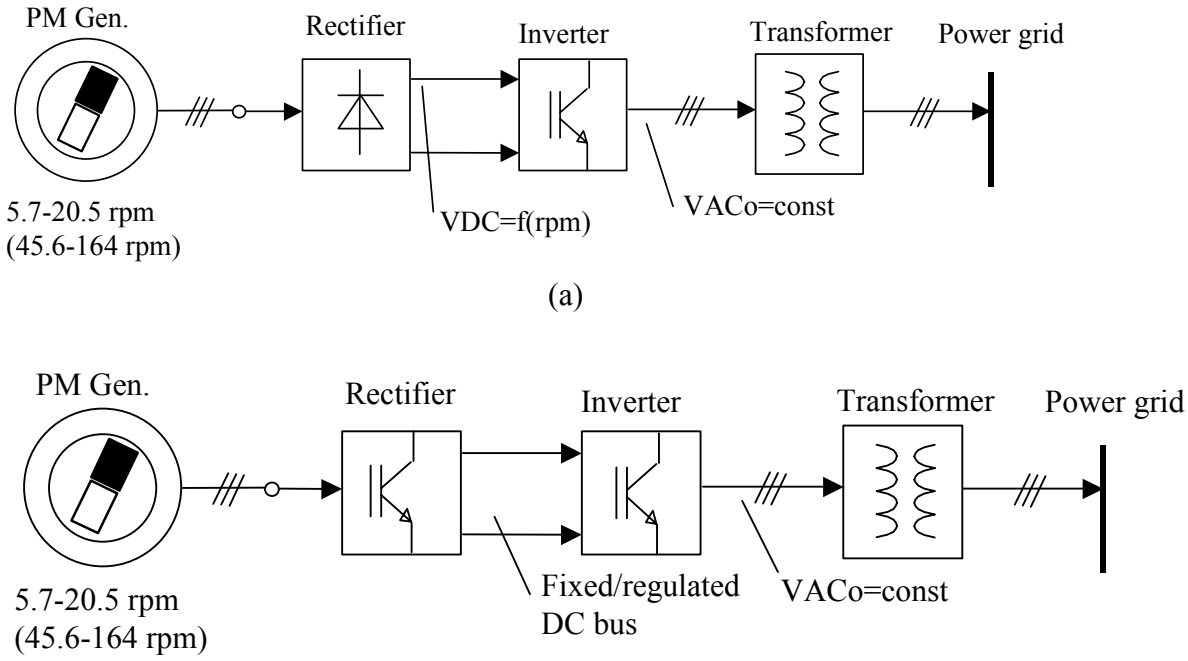

Figure 8-1. Power electronic variants based on different switch technologies for PM generators: (a) diode bridge rectifier and IGBT inverter and (b) IGBT switched mode rectifier and IGBT inverter

The main assumptions used to evaluate each power electronic option are:

- The operating speed range of the PM generator is from 28% to 100% (5.7 to 20.5 rpm or 45.6 to 164 rpm).
- The inverter provides a constant voltage (VACo) at its output regardless of the rotor speed variations (VACo represents the root mean square (rms) line to line value).
- The power delivered to the grid is 1500 kW.
- The efficiency of the three-phase IGBT bridge is 98.5%.
- The efficiency of the three-phase diode bridge is 99.6%.
- Converter pricing based on 60 USD/kVA.

8.1 System using Diode Rectifier and IGBT

The voltage generated by the PM generator is proportional to the rotor speed. Consequently, over the entire speed range, the generator voltage varies from approximately 28% to 100% of its rated value. In the case of the diode bridge rectifier, the rectified DC voltage is approximately proportional to the generator voltage, so the rectified DC voltage will be a function of the rotor rpm as well. Based on a first-order approximation (i.e., where the DC bus voltage is proportional to the rpm), the DC bus voltage will vary from 28% to 100% of its rated value. Note that the DC bus voltage will actually have a narrower variation because of the inductive voltage drop on the generator stator windings (at maximum speed the electric frequency is at its maximum; therefore, the inductive voltage drop is maximum as well).

For this analysis, we assumed that the DC bus voltage has a 1 to 3 variation (at rated rotor rpm the DC bus voltage is 3 times higher than at cut-in rpm).

On the other hand, because the grid voltage is constant (we assume that the transformer voltage ratio is constant), the voltage at inverter output must be constant regardless of the DC bus voltage. Table 8-1 shows first-order approximations of the major PE parameters based on an arbitrary value of the fixed inverter output voltage to the utility grid.

Table 8-1. Variation of Voltages within the AC-DC-AC Topology Based on Diode Rectifier and IGBT Inverter over the Entire Rotor Speed Range

Rotor Speed	AC Generated Voltage (rms line to line)	DC Bus Voltage	Desired Inverter Output Voltage (rms line to line)	Inverter Maximum Output Voltage Capability (rms line to line)[3]
Rated value (100%)	VGmax	VDCmax	VACo	3 * VACo ≈ 0.7 * VDCmax
Cut-in value (28%)	VGmin = 0.28 * VGmax	VDCmin = 0.33 * VDCmax	VACo	VACo ≈ 0.7 * VDCmin

To provide the desired output voltage level (VACo), the inverter input DC voltage must be at least VDCmin ≈ sqrt(2)*VACo, assuming space-vector-PWM control and neglecting the voltage drop on IGBTs in conduction. This condition has to be fulfilled at cut-in speed when the DC bus voltage reaches its minimum value.

We can see that at rated rotor speed, when the system is expected to provide full power to grid, the inverter output voltage is VACo, which represents only 33% of inverter voltage capability.

This means that for this AC-DC-AC topology (diode-rectifier-IGBT-inverter), the inverter kilovolt-ampere rating has to be three times the value actually being used. Consequently, the cost of the power electronics would be approximately three times higher than necessary. Considering a 60 USD/kVA unit cost for power electronics, the total cost of the PE system would be:

3 * 1500 kW * 60 USD/kW = 270,000 USD

[3] The maximum output voltage that an inverter can provide depends on the DC bus voltage and the PWM algorithm. The numerical relationships shown in Table 8-1 assume sinusoidal voltage wave forms with space-vector-PWM, and neglect the voltage drop on IGBTs.

in which two-thirds (180,000 USD) would be wasted on PE oversizing.

Because of the very poor utilization of the PE kilovolt-ampere, the diode-rectifier-IGBT-inverter conversion scheme is not practical for a PM generator with diode rectification.

Note again that this oversizing issue originates in the fact that the turbine is a variable-speed type and the grid voltage has to be constant (whereas the generator voltage is proportional to rotor speed). For a constant-speed turbine, there is no such oversizing issue for the inverter.

8.2 System using IGBT Rectifier and IGBT Inverter

We discussed the advantages of this topology in Section 2, where we pointed out that this topology is the preferred solution when performance and functionality are important. Therefore, we present only the sizing and cost estimate here.

The power ratings of the PE system are illustrated in Figure 8-2. These ratings are based on the assumptions stated at the beginning of this section. The cost estimates below are based on a converter cost of 60 USD/kVA and these power ratings:

Cost of IGBT inverter	≈ 1500 kW * 60 USD/kW	= 90,000 USD
Cost of IGBT rectifier	≈ 1523 kW * 60 USD/kW	= 91,380 USD
Total cost of PE system		= 181,380 USD

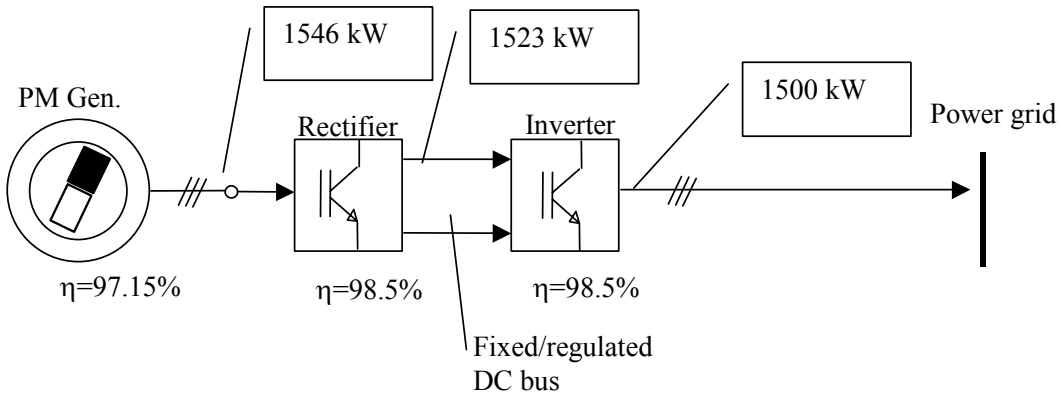

Figure 8-2. Power levels within the IGBT-rectifier-IGBT-inverter topology for 1500-kW output into grid

Note that although, strictly speaking, the inverter and rectifier have different power requirements (1523 kW versus 1546 kW), in practical terms the units are very similar from a hardware point of view. Therefore, we expect that their power rating and cost will be the same.

9. Discussion of Construction Alternatives for the HTLS PM Generator

9.1 Summary of the Baseline Conceptual Design of the HTLS PM Generator

The baseline conceptual design of the HTLS PM generator is based on the following assumptions:

- Modular construction of magnetics (12 stator segments covering the 360 degrees)
- Single-piece cast rotor hub
- Single-piece welded stator housing
- Single-piece welded end housing
- Liquid cooling

The estimated cost of this design, at a 4-m air-gap diameter, is approximately 168,000 USD for production scale. Section 4 contains the details about this cost estimate. We estimated a slightly higher cost of 172,000 USD for the direct drive PM generator with VPI performed on the stator segments before they are assembled onto the stator support structure. This will ensure increased winding protection against the combined effects of moisture and thermal cycling. The estimated cost of the VPI process, including materials, is on the order of 4,000 USD in production mode. Table 9-1 breaks the cost down into major components.

Table 9-1. Cost Breakdown into Major Elements

Major Elements	USD	Lower Level Constituents
Magnetics	123,000	Stator windings, laminations, permanent magnets, bonding, and insulation
Support structure	41,000	Rotor hub/spider, stator housing, and stator end housing
Cooling	4,000	Liquid cooling jacket and thermal interface material
Vacuum pressure impregnation (optional)	4,000	None
Total cost of HTLS PM generator	172,000	None

9.2 Construction Alternative Based on Modular Support Structure

All major components of the support structure have been split into two pieces to facilitate minimum transportation costs using standard trucks (load volume = 2.6 m × 3.7 m × 14 m; see Appendix II for transportation details) for the case of larger diameter generators.

As we can see from Figure 9-1, the cost of the support structure elements is higher for modular construction, primarily because of the additional machining and handling required. Table 9-2 offers a comparison of unit costs (USD per kilogram) for monolithic versus modular construction.

The increased cost of the modular support structure exceeds the savings achieved by transportation; the dotted line in Figure 9-1(b) is higher that the one in Figure 9-1(a). We expect that the actual cost of the modular structure will be even higher because additional work is required to assemble the pieces at the wind farm site.

In conclusion, we can see that:

- For the interval of 4- to 7-m air-gap diameter (where the optimum cost is approximately located), the modular approach for building the support structure elements does not show cost savings.

- The minimum cost of the direct drive generator including transportation dollar figures (Figure 9-1[a]) is reached for the monolithic support structure construction at an air-gap diameter of 5 m. The generator cost in production mode is estimated at approximately 155,000 USD.

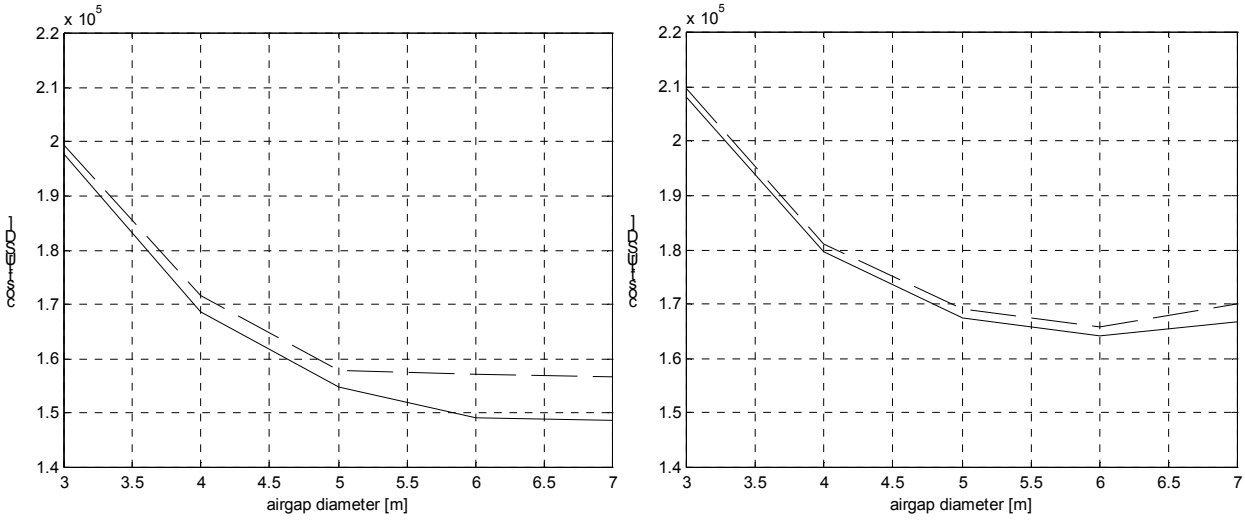

Figure 9-1. Cost of PM generator with transportation cost for (a) monolithic construction of structural elements and (b) modular construction of structural elements

Table 9-2. Unit Cost for Production Mode of the Support Structure Elements, USD per Kilogram

	Cast Iron	Welded Iron
Modular (two pieces) construction of structural elements	3.55	8.26
Monolithic construction of structural elements	2.93	6.03

Acronyms

AC	alternating current
DAAFM	dual air-gap axial field machine
DC	direct current
FEA	finite element analysis
GEC	Global Energy Concepts, LLC
HTLS	high-torque, low-speed
IGBT	insulated gate bipolar transistor
KAC	Kaman Aerospace Corporation
MTMS	medium-torque, medium-speed
NREL	National Renewable Energy Laboratory
OD	outside diameter
PE	power electronics
PM	permanent magnet
PMM	permanent magnet machine
PWM	pulse width modulation
rms	root mean square
SARFM	single air-gap radial flux machine
SOW	statement of work
USD	U.S. dollar(s)
VPI	vacuum pressure impregnation

Appendix I: Cost Factors for Multi-PM Generators Operating with a Gearbox

The following symbols are used in this text:

Table I-1. List of Symbols

P = total power in kilowatts (for example, 1621 kW)
r_N = radius of each generator housing in meters, which according to the geometry in Fig. I-1 depends on the number of generators (N) and outer system radius (R) as follows: $r_N = R * \sin(\pi/N) / [1+\sin(\pi/N)]$
N = number of generators
R = outer radius of gear + generator(s) system
rpm_N = shaft speed of a factional power generator expressed in rpm (multiple generator case)
rpm_1 = shaft speed of the full-power generator (single generator case)

The geometry of the generator arrangement (Figure I-1) enforces a new constraint between the generator dimensions and the number of generators, N, as well as between the generator speed, rpm_N, and N. Note that, in Section 3.3, one dimension (either D or L) and the speed of multiple generators were considered independent on the number of generators, N. Thus, we considered the speed of fractional power generators to be equal to that of the full power generator (i.e., $rpm_N = rpm_1$), which led to the magnetic cost increasing by sqrt(N).

Now, the cost formula (1) has the speed (rpm_N) of the fractional power generators as an additional degree of freedom. This will help the system level optimization (i.e., gear + generator), because the speed rpm_N could be a function of the number of generators, N, gear system outer radius etc., as dictated by the gearbox construction.

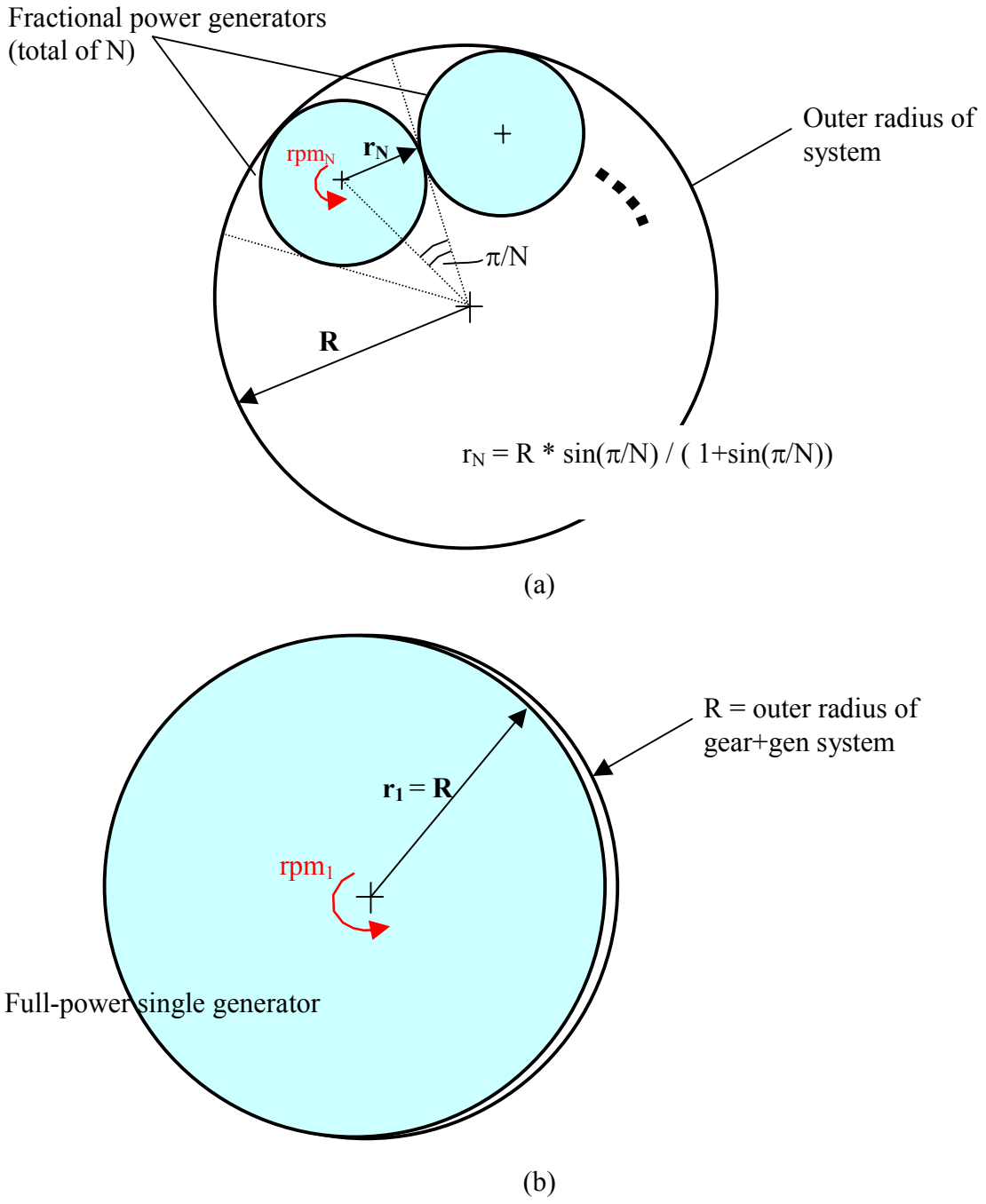

Figure I-1. (a) Arrangement of N fractional power generators on a single side of the gear system and (b) full-power single generator

The cost of the total magnetic mass (for all N generators), expressed in USD in production mode is

$$TotMagCost_N = 3650 * P / (r_N * rpm_N) \quad (1)$$

Note that the index N indicates that the variables depend on the number of generators N.

To give a numeric example,

$$P = 1621 \text{ kW}, r_N = 0.5 \text{ m}, rpm_N = 160 \text{ rpm} \rightarrow TotMagCost_N = 73{,}958 \text{ USD} \quad (2)$$

Note that in Equation 1, the length of the generators L_N does not explicitly appear as a parameter, because L_N is not a free variable. L_N has a value that is uniquely determined by:

$$L_N = \frac{P}{45 \cdot N \cdot rpm_N \cdot r_N^{\,2}} \quad (3)$$

where all symbols are defined in Table I-1.

The total cost of magnetics for multiple generators (Equation 1) has to be used together with the total cost of magnetics for a single generator at full power:

$$TotMagCost_1 = 3650 * P / (R * rpm_1) \quad (4)$$

where R and rpm_1 are defined in Table I-1.

Equation 1 represents a first-order estimation only of the cost of all generator magnetic parts (i.e., magnetic steel laminations, copper windings, and their insulation and magnets). The equation does not include the cost for the support structures for the generator magnetics (i.e., generator housings, shafts, bearings, rotor spiders, and cooling).

The length of fractional-power generators decreases when N increases. This means that placing small generators on both sides of the gearbox will decrease by a factor of 2 the length of the generators that already is decreased by higher N (see Figure I-2). For the same total power, a single generator is more efficient than two generators that have the same diameter but half the length. This suggests that placing generators on both sides of the gearbox is not an attractive solution.

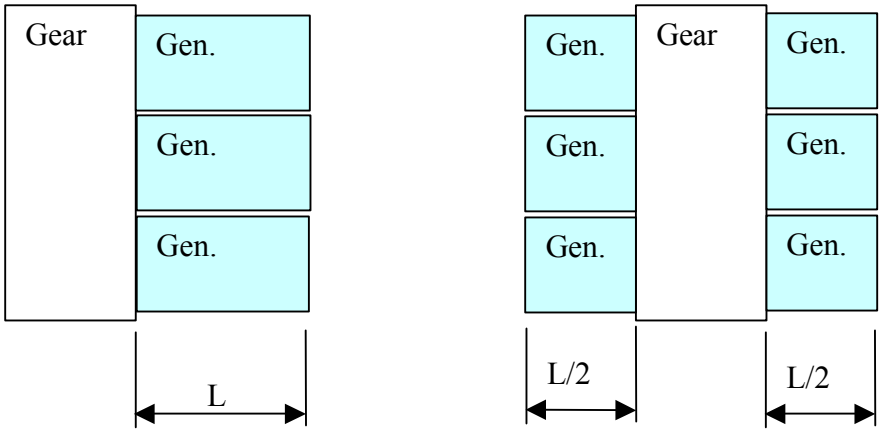

Figure I-2. At the same power level, the total system is more efficient when using generators on the same side of the gearbox

Appendix II: Transportation Costs

II-1. Transportation Costs for Large Numbers of Loads

These costs are approximate and depend on the exact routes traveled and what states the truck must go through, as each state has different requirements. These costs assume that a large number of systems are being installed at one wind farm so many are loads shipped. They also assume that a crane is available to unload at the wind farm.

Note that loads wider than 7.6 m are impractical.

Option 1:
Standard truck, cost approximately 2.00 USD/mile for weights up to 18,000–20,000 kg. Load volume = 2.6 m × 3.7 m × 14 m)

Option 2:
Standard truck, overweight, cost approximately 6.00 USD per mile. Same volumes as option #1 but weights heavier than about 20,000 kg.

Option 3:
Overwide truck, not overweight, cost approximately 4.00 USD per mile. Widths 4-6 m, height less than 3.7 m, weights less than 18,000–20,000 kg.

Option 4:
Extreme overwide truck, not overweight, cost approximately 10.00 USD per mile.
Widths 6–7.6 m, weights less than 18,000–20,000 kg.

II-2. Transportation Cost for One Load

The following costs apply for a 4.88-m wide, overdimensional load that requires special equipment along with permits, escorts and route planning:

Total charge: 16,219 USD

Cost breakdown in USD:

Base rate	4,465.68
Permits	779.00
Overdimensional charge	1,744.00
Escorts	6,965.60
Fuel surcharge	161.80
Route survey	360.00
Air Ride T	647.20
Miscellaneous charges	340.00
NY I-84 Brg	150.00
Fuel surcharge	161.80

Appendix L

Heller-De Julio Report

Heller-De Julio Generator Comparison

Prepared by Heller De Julio Corp.
for
Global Energy Concepts, LLC

September 19, 2002

1. Background and Introduction

Need for Variable-Speed

Until recently, most existing wind generators used fixed-speed induction generators. Over the past 15-20 years of operating experience with wind turbines, it has been found that these fixed-speed machines have several drawbacks:

- The fixed-speed response to wind pulses results in power pulses, which, in turn, cause voltage flicker.

- The wind pulses also result in excessive wear of the speed-increaser gears, which are used to match turbine speed with generator speed.

- In addition, fixed-speed generators are limited in their ability to capture all available wind energy.

These shortcomings can be overcome with the variable-speed generator. The variable-speed generator absorbs the wind energy pulses, smoothing out the power curve to eliminate the voltage flicker and the gear wear, and it can capture more wind energy than fixed-speed machines.

Considering the existing U.S. patent situation for variable-speed wind turbine generators, there may exist a unique significant competitive advantage for the Heller generator. Four U.S. patents for wind turbine generators were issued to Kennetech Windpower. GE Wind Energy (GE) now owns these patents. Two of these are on the power electronic control of the generator and two are on the blade pitch control of torque of the turbine. GE seems to have the rights to variable-speed power electronic control of wind turbine generators through the two power electronic patents, which are very broad. Vestas may have a future problem in the U.S. with the GE patents. Others entering the wind turbine business in the U.S. may have a problem, if they use electronic speed control.

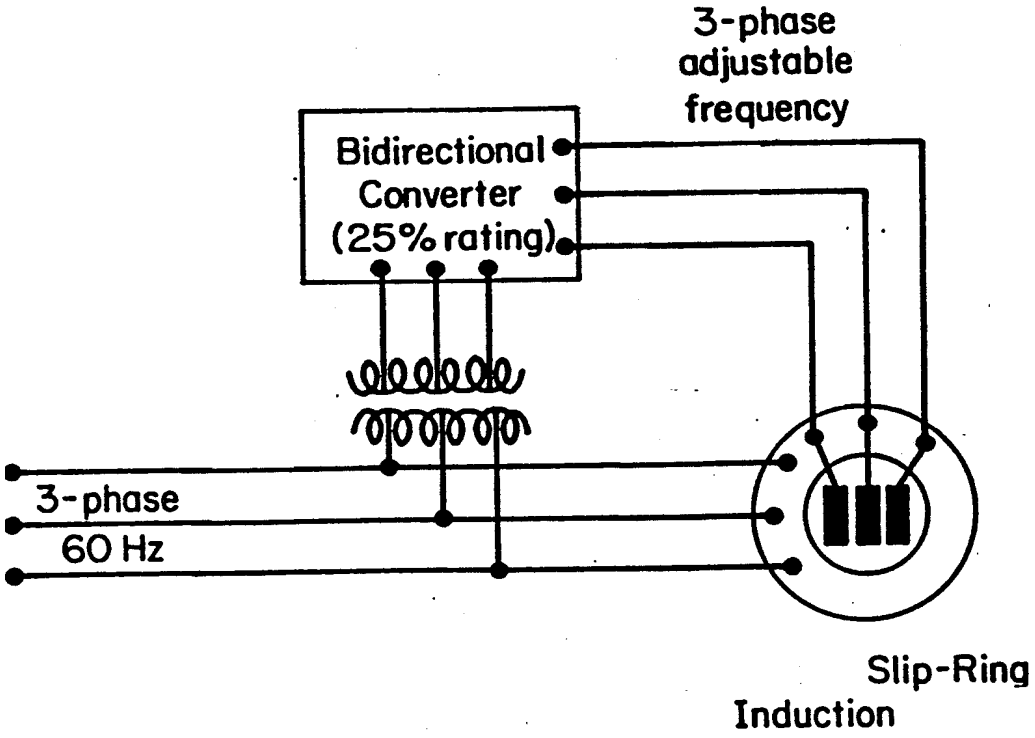

Figure 1
Doubly Fed Generator

How Competing Technologies Achieve Variable Speed

Vestas-American Wind Technologies, Inc., Palm Springs, CA. The Vestas Optislip speed control uses a wound rotor induction generator with electronic chopper in parallel with a resistor in the rotor circuit, all rotating with the rotor. This requires a fiber optic rotor current feedback control to regulate speed over a 10% (1200-1320) rpm range. The resistor and electronics are mounted on the rotor to eliminate the slip rings and carbon brushes associated with the wound rotor machine. The efficiency is the same as that of the Heller-De Julio generator over the same speed range, but the Optislip system requires electronics.

Trace Technologies, Inc., Livermore, CA, also uses the wound rotor induction generator, in this case as a doubly fed generator, Figure 1. Control is by a power electronic rotor current and voltage controller. It offers 800-1450 rpm speed range with a reported overall efficiency of 93%-95% for generator and controller. Trace Technologies has the widest speed range of the current active competing technologies, but the wide

speed range is not totally useful in capturing wind energy. Information provided by GE and NREL shows that most of the wind energy is captured at only moderate speed. At high wind speeds, the turbine blades are feathered to prevent damage to the turbine and the supporting structure. Trace supplies controllers to GE. GE owns the patent rights to the Trace Technologies controller. This system requires carbon brushes and slip rings.

NEG Micon, a major Danish firm, now has an American subsidiary located in Rolling Meadows, IL, and is very active in the wind generation business in the U.S. This company has consistently relied on the fixed-speed squirrel cage induction generator because of its simplicity and reliability and absence of electronic controls. The NEG Micon lack of speed control requires that it use oversized gearboxes to accommodate the power from wind surges. Recent information from NEG Micon indicates they will develop a system probably based on the use of a squirrel cage induction generator and a full-size converter, Figure 2, allowing a speed range of 25%-125%, significantly wider speed range than that of the others.

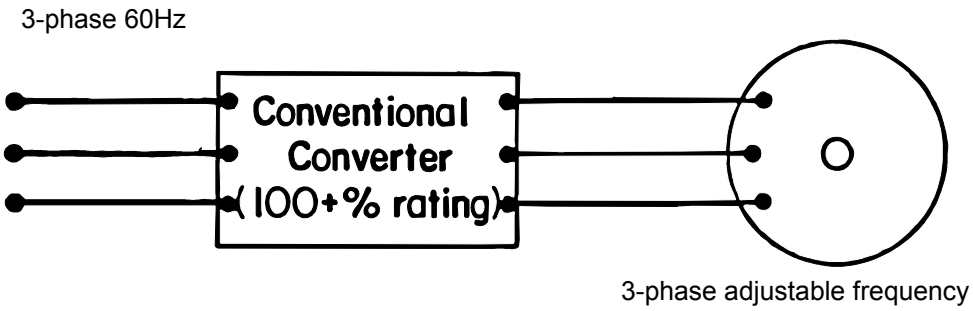

Figure 2
Squirrel Cage Induction Generator with Full-Size Converter

Scope of Work for This Project

Compare technically and economically:
1) 1500 kW Heller generator
2) 1500 kW squirrel cage induction generator with series connected power electronic converter
3) 1500 kW synchronous generator with torque-limiting gearbox (Voith hydraulic coupling and separate gearbox)

Include in the comparison the following information:

- Description
- Selling price
- Train efficiency
- Discuss reliability, maintainability, electrical harmonics, and weight
- Ability to mitigate torque transients, include speed of response, torque range of response relative to the ability of a wind gust to load the drive train.

For the 1500 kW Heller include the following:

- Description, specification, electrical insulation of stator and rotor windings, voltage, number of poles, dimensions, weights, frame, heat removal, overload capability, bearing type, bearing life.
- Description of power train, including output transformer.
- Speed-torque, speed-power characteristics.
- Selling price at the rate of 200 MW per year and 1000 MW per year.
- Loss distribution in generator and passive controls.
- Generator efficiency at 25, 50, 75, and 100% load.
- Generator power factor at 25, 50, 75, and 100% load.
- Manufacturing considerations, including production tooling requirements, facilities and costs.
- Assessment of failure modes and impact on continued energy production performance.
- Maintainability – maintenance requirements and intervals.
- Development cost for brushless version of Heller-De Julio Generator.
- Support facilities required getting to the first prototype.
- Development cost to get to the first prototype.
- Development cost to get to the first three pre-production prototypes.

2. Description of Squirrel Cage Induction Generator with Full-Size Electronic Converter

This system consists of a speed increaser gear, a squirrel cage induction generator, and a full-size power electronic converter, Figure 3. The electronic converter has a rectifier, a DC link and an inverter. The DC link provides a soft connection between the induction generator and the power system. The wind turbine's pitch control provides a turbine speed which, considering the gear ratio, approximates the 1200 rpm speed of the generator. The soft connection of the DC link allows the speed, voltage and frequency of the induction generator to vary with wind speed for wind gusts, maintaining a constant volts per hertz ratio in the generator, which prevents over fluxing the generator magnetic circuit. Two possibilities exist for the electronic converter.

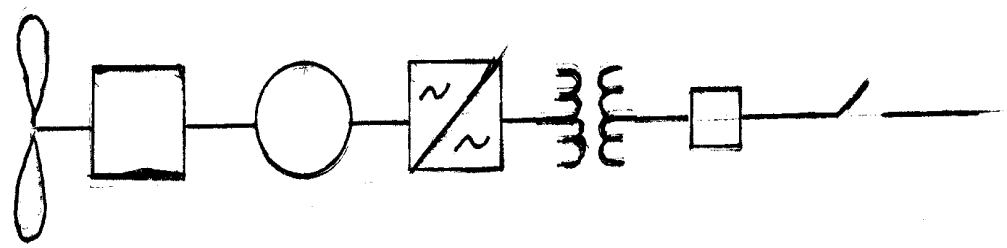

Figure 3
Squirrel Cage Induction Generator System

- A voltage-source system having a rectifier with an active front-end to rectify the AC generator output and frequency to DC. The active front-end allows the varying voltage of the generator as it responds to wind gusts to be rectified to a constant DC bus voltage. The constant voltage DC link voltage is then inverted to 60 Hz and system voltage by the pulse width modified (PWM) inverter. The PWM inverter can provide low current and voltage harmonics to the power system.

- A current-source system with generator output going to a thyristor-controlled rectifier to hold constant DC bus voltage and a gate turn-off thyristor (GTO) inverter with output filter capacitor capable of matching system voltage at 60 Hz. The output filter capacitor can provide an output voltage with low current and voltage harmonics. The induction generator may have shunt capacitors at its terminals to provide reactive amperes for magnetizing current, or it may draw reactive current from the power system.

Reliability

This system has a simple, reliable generator in the nacelle along with the gearbox connecting to the turbine. The electronics need to be mounted in an environmentally secure housing. The electronics could be mounted in the nacelle or in the base of the tower. The system should be quite reliable, with reliability hinging on that of the power electronics. Land-mounted wind turbines with this system should be more reliable than sea-mounted systems because the salt air can have an adverse effect on the electronics.

Power Factor

This system can run at unity power factor, leading or lagging power factor. To minimize the cost of the inverter, it should be designed for unity power factor.

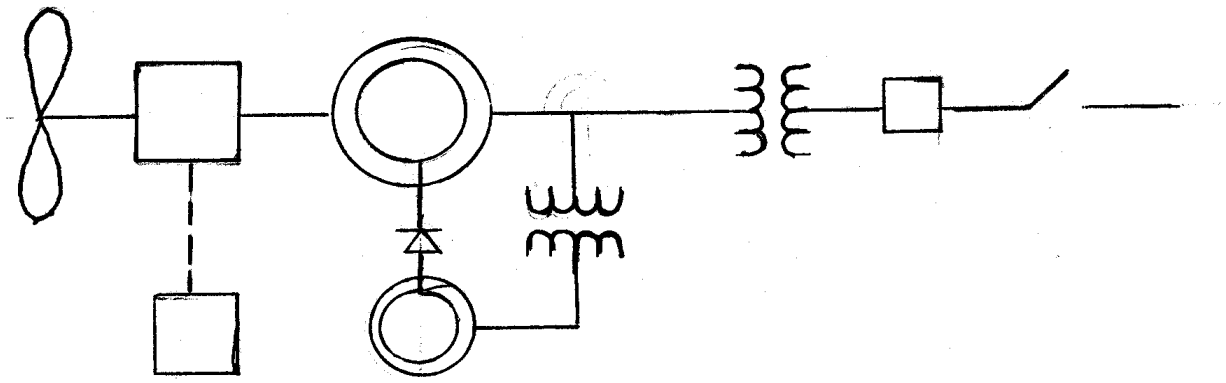

Figure 4
Synchronous Generator with Torque-Limiting Coupling System

Possible U.S. Patent Infringement

The use of power electronics in this system would require addressing the GE patent situation if the system is to be marketed in the U.S.

3. Description of Synchronous Generator with Torque-Limiting Gearbox

This system utilizes a combination speed-increaser gear and hydraulic coupling, with the hydraulic coupling connected to the synchronous generator, Figure 4. In this case, the hydraulic coupling provides the soft connection between the gearbox and the generator. The synchronous generator is synchronized to the power system and operates at exactly 1200 rpm. The wind turbine can operate at a corresponding speed, considering the gear ratio. The hydraulic coupling absorbs the power of the wind gusts, relieving the gears of the extra torque, which can result in gear wear. The generator is a brushless machine, that is, it has no carbon brushes or slip-rings. In place of the carbon brushes and slip rings, it has a shaft-connected exciter alternator with a rotating rectifier. The alternator/rectifier supplies the field winding of the synchronous generator. The field winding of the exciter alternator is supplied from a rectified variable voltage power supply.

Softness to Wind Pulses

The torque-limiting hydraulic coupling type gearbox provides softness in the mechanical system, which will protect the gears from the adverse effects of wind pulses.

Voltage Flicker

The softness in the system provided hydraulic coupling also eliminates any possibility of voltage flicker from wind pulses.

Power Factor

By adjusting the operating value of the field current, the power factor can be adjusted from 0.9 lagging to 0.9 leading or any value in between.

Reliability

The synchronous generator and the torque-limiting coupling have ancillary equipment that can detract from the basic reliability of the generator and fluid coupling. The generator has a shaft-driven alternator exciter, which has rotating diodes with fuses for converting the alternator AC voltage to DC for the generator field winding. The alternator has an electronic rectifier field supply and control for maintaining the correct generator field voltage. The field supply has a circuit breaker. A scoop tube and a hydraulic oil system control the fluid coupling. The hydraulic oil system has a heat exchanger, oil pumps, motors, motor starters and controls.

4. Description of Heller Generator

With no electronics, feedback circuits, hydraulic systems, or excitation systems, the Heller generator, Figure 5, is one of the simplest variable-speed systems available. It is actually a high-slip induction generator with a special passive rotor circuit to allow very good efficiency. The Heller generator trades off some efficiency at high loads for simplicity and reliability with a little loss of overall energy recovery. This concept is important, since some wind turbine owners object to power electronics because the electronics can introduce voltage spikes and electrical harmonics into the power system. Others are concerned about the reliability of power electronics and electronic control systems, particularly in ocean atmospheres that are heavily laden with salt. Also, in third world countries, technicians may not be available to service power electronic controllers. Power electronic systems have been know to cause bearing problems from capacitive transfer of high-frequency current from stator to rotor which flows back through the bearings. The Heller generator is available in a brushless version, which is not possible with some electronic-based systems.

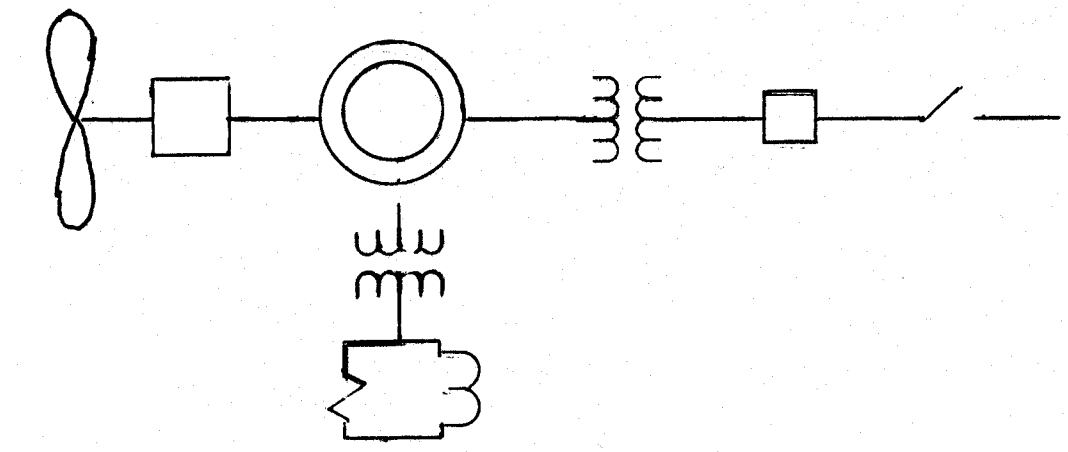

Figure 5
Heller Generator System

The latest wind turbines being applied are in the 50 to 2,000 kW size range, with projections to 5,000 kW and higher in the future. The Heller technology can be used on these machines, and it can be used to retrofit the thousands of fixed-speed machines in existence to extend the life of the gearboxes, increase output, and eliminate voltage flicker.

Basis of the Heller Generator

The Heller generator is a wound rotor induction generator with a resistor and a reactor in parallel in each phase of the rotor circuit, Figure 6. Normally, the resistor-controlled wound rotor generator has relatively poor efficiency. The addition of a reactor in parallel with the resistor significantly changes the efficiency characteristic. Below synchronous speed, the machine is a motor. Starting from synchronous speed as the machine goes into the generate mode operating above synchronous speed, with very low frequency in the rotor winding, the reactor shorts out the resistor and makes a highly efficient generator with about 94%-95% efficiency. As the rotor frequency increases with speed, the reactor becomes less of a short and starts shunting current into the resistor. At about 10% above synchronous speed, the efficiency drops to 90% and drops further with higher speeds and loads. This efficiency characteristic and speed range is suitable for the wind industry. The Heller machine can be classified as a high-slip generator with good efficiency. The power, efficiency and power factor of this machine as obtained from calculations on a 1500 kW standard industrial generator are shown in Figure 7.

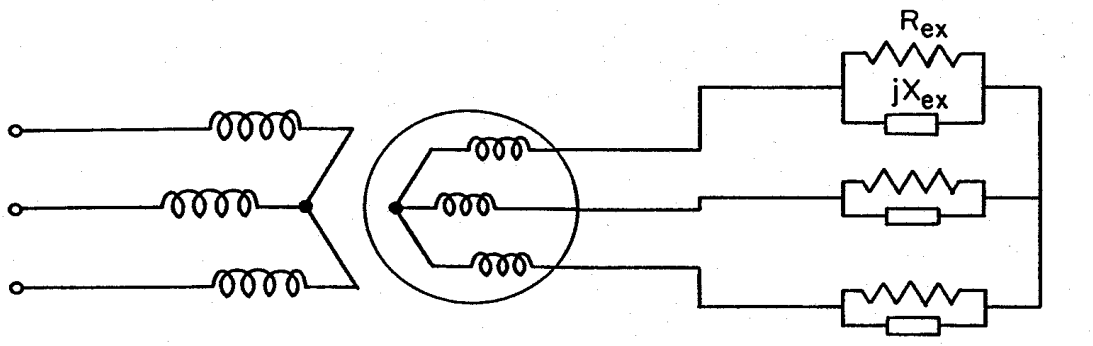

Figure 6
Heller Generator Circuit

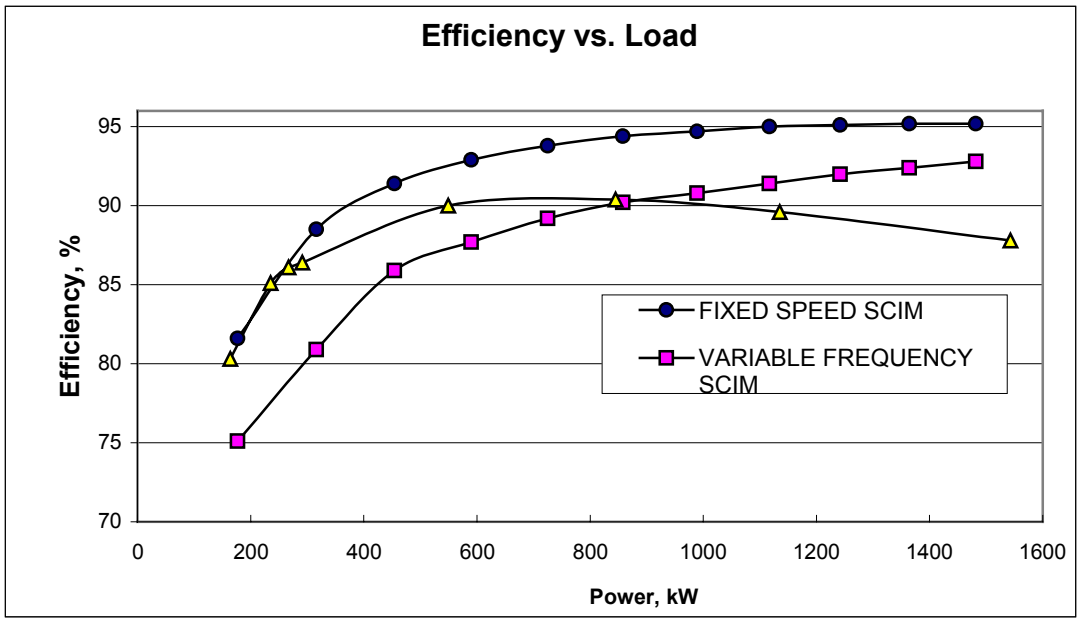

Figure 7
1500 kW Efficiency versus Load Curves
(Heller Generator with 10% speed range)

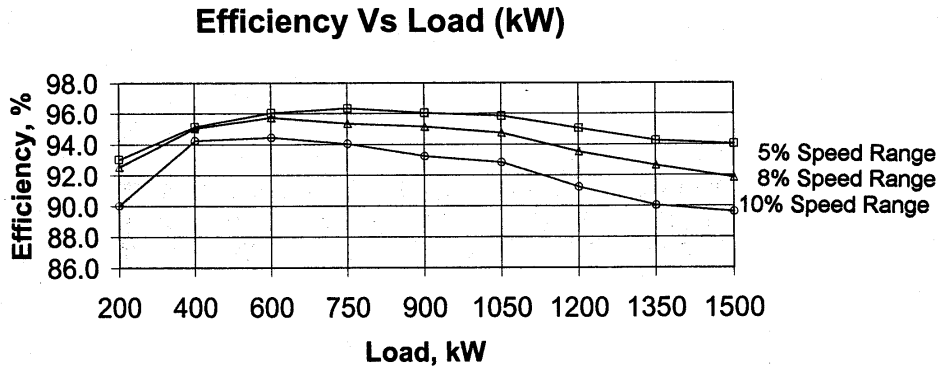

Figure 8
Efficiency Curves for 1500 kW Heller Generator
With 5%, 8%, and 10% Speed Range

Figure 7 shows calculated efficiency versus load characteristics of different 1500 kW drive systems, fixed-speed squirrel cage induction generator (SCIG), variable-speed SCIG with electronic controller, and the high-slip Heller generator with 10% speed range. The efficiency profile of the Heller generator varies with the amount of slip and with base rated efficiency of the wound rotor generator with shorted rotor. For Figure 7, the rated efficiency of the generator was 93.5% with shorted rotor, corresponding to a 104 kW base loss without the resistor/reactor control.

Figure 8 shows the efficiency of the Heller generator for 5%, 8%, and 10% speed range using a 97% efficient wound rotor induction generator which would have a base loss of 46.4 kW. In this case, the selected amount of slip or speed range reduces the efficiency to 96% for 5% speed range, 95% for 8% speed range or 94% for 10% speed range.

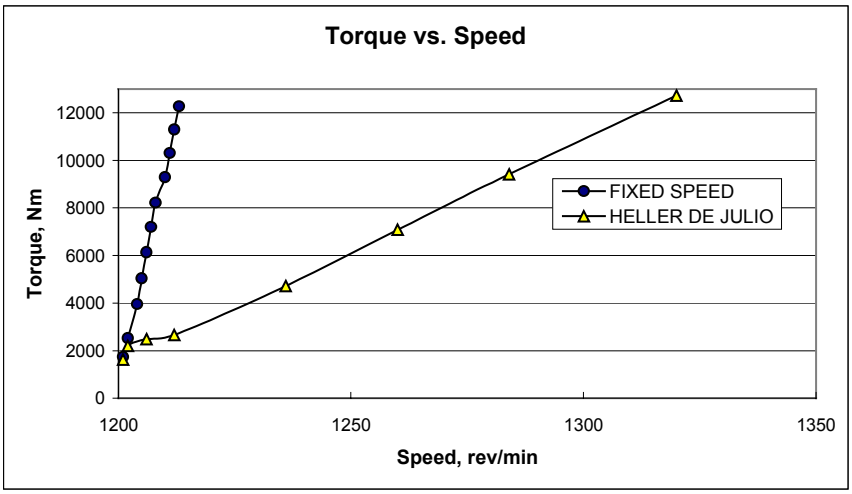

Figure 9
Typical Speed-Torque Curves
1500 kW Heller Generator versus Fixed-Speed Generator

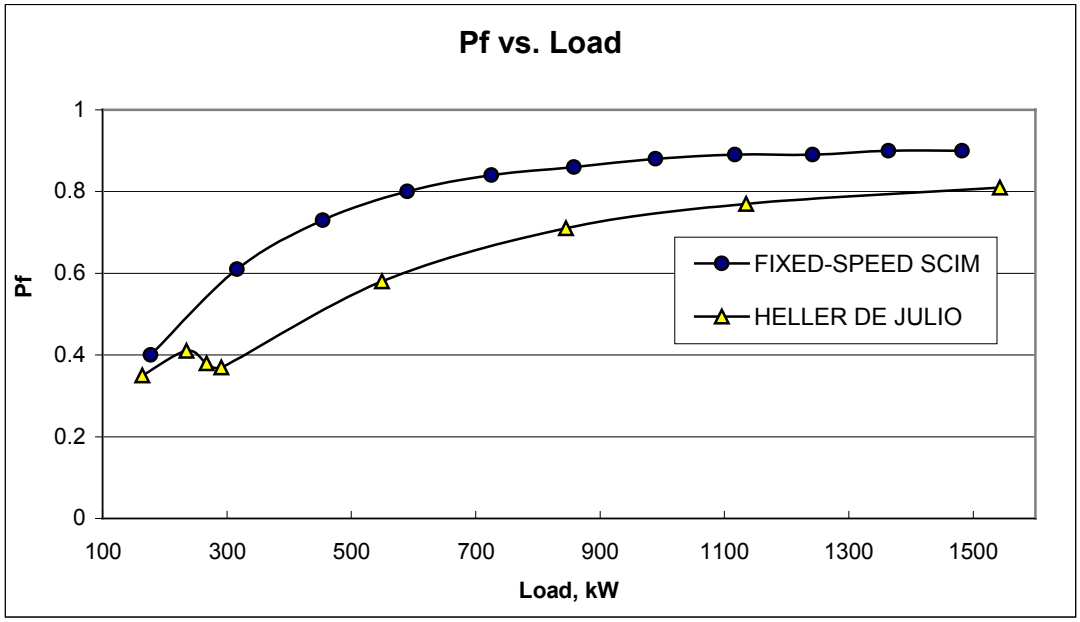

Figure 10
Power Factor versus Load
1500 kW Heller Generator versus Fixed-Speed Generator

Figure 9 shows the typical high-slip speed torque characteristic of the Heller generator as compared to the low-slip characteristic of the fixed-speed induction generator.

Power Factor

Power factor of this system, Figure 10, is that of an induction generator as modified by the effect of the rotor control. Tests show approximately 0.80 to 0.87 lagging power factor, which can be corrected to 0.95 by the addition of power factor correction capacitors. To correct the power factor of the 1500 kW, 2400 volt generator from 0.80 to 0.95 requires 1125 kVAR of power factor correction capacitors which have an estimated cost of $8,100.00.

Loss Distribution

Figure 11 shows the loss distribution of the Heller generator as the rotor resistor I^2R losses increase with increased slip. This distribution is for the 93.5% efficient generator of Figure 7. As can be surmised from Figure 8, the rotor resistor losses increase with the amount of speed range selected, and the overall efficiency is a function of the base generator efficiency and the selected speed range.

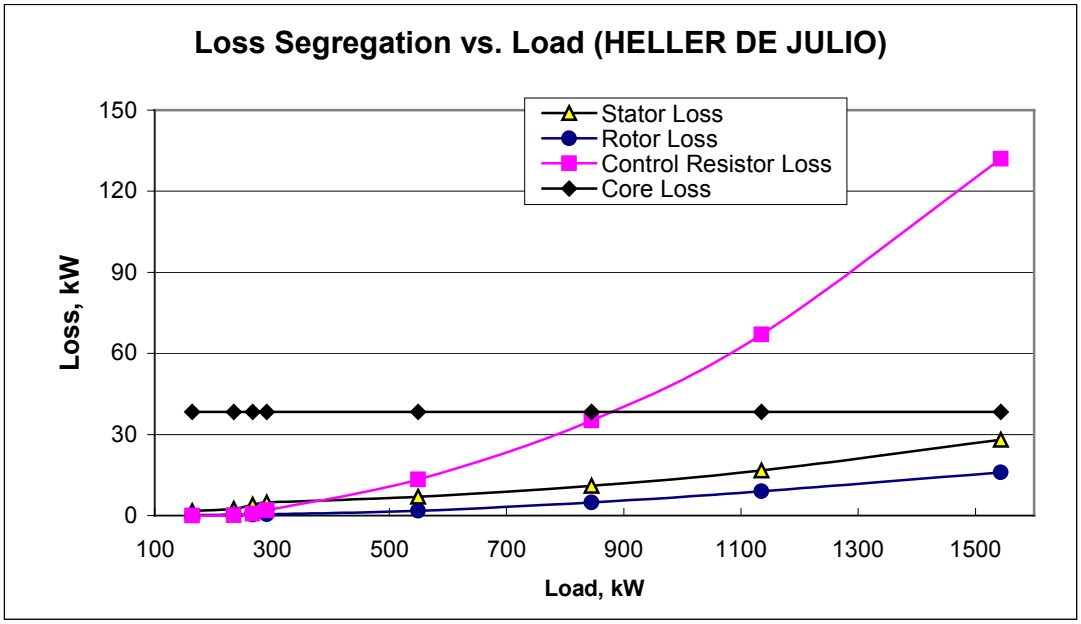

Figure 11
Loss Distribution in 1500 kW Heller Generator

5. Stator Voltage Selection Advantage for Heller Generator and Synchronous Generator

With no electronic control associated with the stator, the voltage rating of the Heller generator (and the synchronous generator option) can be selected to optimize system cost. The squirrel cage generator with full-size converter has a voltage rating of 690 volts to minimize the cost of the electronic converter by utilizing one switching device in series in the rectifier and in the converter. With the Heller generator there are no electronics. Consequently, the Heller generator has a lower weight to power ratio for 500 kW and higher ratings with a stator voltage rating of 2400 volts rather than at 690 volts. This is largely because less material is needed for internal connection rings and busses. Also, much smaller cables are needed for connections between the generator and the transformer and between the generator and the controller for the Heller generator. For the 1500 kW rating, the squirrel gage generator would require three 500 KCMIL cables per phase for these connections. Between the transformer and the generator, the Heller generator would require only one 500 KCMIL cable per phase. For the connection between the generator and the passive control (resistor), the Heller generator would require one number 1/0 cable per phase.

The resistor for the Heller generator rotor control would likely be mounted on top of the nacelle to dissipate the heat loss to the atmosphere. Depending on the arrangement of

the controls and the transformer, there can be a substantial difference in the cost of the electrical cables for the two schemes. A comparison of the cable costs is as follows:

Squirrel Cage Generator, three 500 KCMIL cables per phase in tray
(Generator to converter and converter to transformer).

Cable Cost	
Material, 500 KCMIL/ft	$3.62
Labor, 500 KCMIL/ft	.11
	$3.73
	x9
	$33.57
Cable tray 24” wide x 4” deep	3.63
Cable tray labor	.95
Total cost cable & tray /ft	$38.15

Heller Generator, one 500 KCMIL cable per phase in tray
(Generator to transformer)

Cable Cost	
Material, 500KCMIL/ft	$3.62
Labor/ft	.11
	$3.73
	x3
	$11.19
Cable tray 12” wide x 4” deep	2.60
Cable tray labor	.70
Total cost cable and tray/ft	$14.49

Heller Generator #1-1/0 cable per phase
(Generator to control)

Cable cost	
Material #1/0 cable/ft	$0.75
Labor/ft	.09
	X3
	$2.57
Cable tray 12” wide x 4” deep/ft	2.60
Cable tray labor/ft	.70
Total cost cable and tray/ft	$5.87

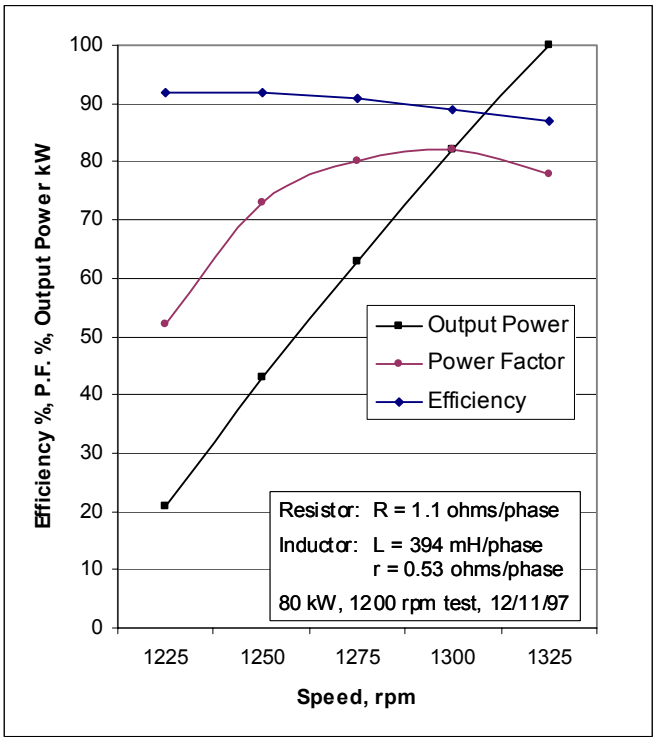

Figure 12
Test Results on 80 kW Heller Generator

6. Future Development Work Proposed for Heller Generator

While the generator can be marketed as it is now, it is desirable to develop this concept into a brushless machine. This is very important as evidenced by the two systems being compared, which are brushless. Many of the electronic control systems in use in wind generators use the wound rotor induction generator as a doubly fed machine or as a slip energy recovery machine.

These require carbon brushes and slip rings that contribute to maintenance and reliability problems. Replacing the brushes and slip rings in the Heller generator with a rotating transformer will eliminate this maintenance and reliability problem. The Corporation owns all three of Mr. Heller's patents relating to the Heller generator plus the two Wallace and Oliver patents. The latest patent covers combining the reactor into the rotating transformer to eliminate the carbon brushes and slip rings. With or without the rotating transformer, the resistor can be located away from the generator to remove the heat it generates. The last patent is U.S. Patent No. 6163137 dated December 19, 2000, "Rotary Induction Machine Having Control of Secondary Winding Impedance." It covers the Heller generator concept with resistor-reactor control including the rotating transformer.

It is possible to further adapt the machine, with one of Mr. Heller's patents, to limit generator output with an added parallel resonant circuit. This would protect the turbine and tower structure during high winds. The self-protecting feature using the added parallel resonance circuit would serve as a backup to the present output limiting turbine features. The "stall" turbine is a fixed-pitch turbine that stalls when the load gets too high and the adjustable-pitch turbine feathers its blades under high wind load conditions.

7. 1500 kW Generator System Costs

For this study the generator costs for each system are shown in Tables 1 through 4. These are equipment costs for an IP-54 enclosure 1500 kW, 6-pole, generator system without installation labor. Prices are based on 690 volt rating for the squirrel cage generator system and 2,400 volts for the synchronous and wound rotor (Heller) generators. Prices are based on 667 units per year. It would appear that the labor cost would be about the same for each system. There is, however, a possible major additional difference in the cost of power cable as is explained later.

Table 1
Costs of 1500 kW Squirrel Cage Generator System

Squirrel Cage/Converter	$/kW	$
Generator $38.00/.746	35.00	52,745
Converter $80.00/.746	107.00	160,500
Gearbox	33.00	49,500
Transformer	10.00	15,000
H.V. Fused Disconnect	10.00	15,000
Total	195.00	292,745

Table 2
Costs of 1500 kW Synchronous Generator System

Synchronous/Fluid Coupling	$/kW	$
Generator $38.00x3.41/.746	151.00	226,710
Gearbox	33.00	49,500
Fluid Drive	57.00	85,000
Contactor	7.00	10,500
Transformer	10.00	15,000
H.V. Fused Disconnect	10.00	15,000
Total	267.00	401,210

Table 3
Costs of 1500 kW Heller Generator

Wound Rotor/Passive Control	$/kW	$
Generator $38.00x1.5/.746	52.00	77,365
Resistor	10.00	15,000
Rotating Transformer	1.00	1,500
P. F. Correction Caps.	5.40	8,100
Contactor	7.00	10,500
Gearbox	33.00	49,500
Transformer	10.00	15,000
H.V. Disconnect	10.00	15,000
Total	128.40	191,965

Table 4
Summary of Comparison Estimated Costs for Generator Systems

1500 kW	Cost $
Squirrel Cage	292,745
Synchronous	401,210
Heller	191,965

How Generator Costs Were Obtained

Per John Rama – Robicon:
1500 kW, 460-volt power converter, voltage-source with active front end:
$80.00/hp for active front end
$70.00/hp for diode front end

$100,000 for 2,000 hp synchronous motor, open drip-proof = $50/hp
$45,000 for induction motor, open, drip-proof = $22.50/hp
This confirms the 2:1 ratio in cost of synchronous over induction

Also per Rama, totally enclosed, fan-cooled (TEFC) carries a 33% cost increase over ODP.

Per Bechtel competitive bids in 1994 for motors 2,000 hp, 1200 rpm, Siemens price is $38.00/hp. This was conformed recently as still valid by Jim Michalec of AEP who has monitored the costs of motors they have recently purchased through competitive bidding.

Prices used in Tables 1, 2, and 3 for generators were prices received from TECO and increased by 10% to cover the profit margin for Heller-DeJulio Corp.

Per Joe Hunter, former V.P. of Engineering of Sterling Electric and of U.S. Electrical Motors:

$33.00/kW for 3-stage gearbox, 2% efficiency loss per stage.

Hunter says a synchronous motor costs 2 times as much as an induction motor and a wound rotor motor costs 1.5 times as much as an induction motor.

Studies done by J.A.O. for the Electric Power Research Institute (EPRI) while at Bechtel: Voith fluid drive cost is $25.00 per hp. Efficiency is 100% when locked to motor speed and declines to 50% at half-speed on a straight-line function. To provide a speed regulating range, the fluid coupling would have to operate at 10% or 15% below locked speed. Fifteen percent would reduce the efficiency from the 100% locked value to 92.5%.

Howard Wille of Voith Transmissions, York, PA, quoted $85,000 for a fluid coupling unit: 17-20/1,200-1,800 rpm, 4,500 pounds, 6 ft wide x 8 ft high, MTBF 200,000 hours. He confirmed on 6-7-01 that the unit did not include a gearbox.

Resistor cost, Post Glover Resistors, 1.0 ohm, 36,000 watts continuous $7,126.
Transformer cost per kVA from John Mousel of Southern California Edison.

400 kVAR, 2400 volt power factor correction capacitor price ($4800.00 list times 0.6 discount) obtained from Commonwealth Sprague, North Adams, MA.

8. Efficiency of Generator Systems

The full load efficiency of the squirrel cage unit would be .95 for the generator times .97 for the converter or .97x.95 = .92 overall. This efficiency would be flat down to half load.

For the synchronous unit: .96 for the generator times .925 for the coupling. .96x.925 = .89. The efficiency of the coupling would drop to 50% at half load, for .96x.5 = .48 overall.

For the Heller unit, the full-load efficiency depends on the percent slip or speed range. For a 10% speed range, efficiency at full load would be .875, but would increase to .91 at half load. With an 8% speed range, full-load efficiency would be .88, increasing to .92 at half load. With a 5% speed range, the full-load efficiency would be .92, increasing to .925 at half load.

All of these values would be reduced by the efficiency of the gearbox of .94 and the transformer of .98.

Table 5
Full Load Efficiency Comparison
1500 kW Generators

	Generator Efficiency	Gearbox Efficiency	Transformer Efficiency	Total Efficiency
Induction	.92	.94	.98	.85
Synchronous	.89	.94	.98	.82
Heller	.88	.94	.98	.81

Table 6
Half Load Efficiency Comparison

	Generator Efficiency	Gearbox Efficiency	Transformer Efficiency	Total Efficiency
Induction	.92	.94	.98	.85
Synchronous	.48	.94	.98	.44
Heller	.92	.94	.98	.85

9. Failure Modes for Wind Turbine Generator Systems

Following is a discussion of failure modes for wind turbine generator systems.

Failure Modes for Electronic Power Converter (EPC) Controlled Systems

Electronic power converters are highly reliable if they are of good quality and if they are applied knowledgeably. Following are some of the considerations in applying this equipment:

EPCs may have inadequate torque capability for the load.

EPCs can trip from events on the power system connected to the EPC:

- Transient overvoltage, sometimes called voltage spikes
- Voltage sags
- Voltage interruptions
- Voltage unbalance

EPCs may experience false trips from electromagnetic interference affecting the signal controlling EPC/generator performance.

Generator windings or bearings can fail from EPC transient voltage effects.

There are solutions to all of these problems. If the solutions are applied in the original installation, the problem does not exist. If the solutions are applied to an existing problem, the problem goes away.

Solutions to quality EPC generator systems:

EPC-Rated Electric Generators

- Design
- Factory testing
- Typical motor failure mechanisms

EPC and Generator Quality of Performance

- EPC rated generators
- Quality EPCs

EPC/Generator Analysis

- Factory testing
- Operating history

Coping with the Quality of Power From the Utility

The quality of power from the utility, while it has been traditionally suitable for residential, commercial and many industrial processes, may not be perfect as far as the EPC/generator system is concerned. Power quality varies with different utilities for a number of valid reasons. Power quality varies by region of the country, by rural versus big city, by heavy industrial load versus residential load, and by other factors.

In regions with a high incidence of thunderstorms, short power interruptions are frequent because of lightning strikes on transmission lines. Regions with high wind may experience interruptions as wind causes wires to touch. Regions with high amounts of tree foliage may experience random interruptions as tree branches contact power lines. Big cities with concentrated power generation have less voltage unbalance than cities served by long untransposed power lines.

High-density residential areas have evening and morning peak loads, but little load from midnight until the morning peak. Industrial areas may have heavy daytime loads, but light nighttime loads. The utility automatically switches capacitors onto electrical lines during heavy load periods to boost voltage. Capacitor switching is accompanied by short time transient overvoltage that may affect EPCs, but nothing else.

Heavy industrial loads may contain significant power electronic load, injecting harmonics into the electrical system that may affect adjustable speed drive (ASD) performance.

In summary, these power quality characteristics, which are repeated below, should not affect EPC/generator system performance, but if not addressed by the EPC/generator system supplier and user, can definitely result in reliability problems for EPC/generator systems:

- Voltage sags or momentary interruptions.
- Transient overvoltage.
- Unbalanced voltage.
- High harmonic content.

Thus, power quality should be defined through discussions with the utility so that there are no surprises.

Power quality problems can be avoided with attention to the specification, and by agreement between the EPC supplier and purchaser, with the following requirements:

- An EPC voltage sag tolerance down to the required voltage level, including zero volts, if necessary, for 30 seconds.

- EPC output transformers of about 5% impedance to prevent the EPC controls from tripping from the high transient overvoltage that accompanies capacitor switching.

- Output transformers help to even-out the voltage unbalance between phases to prevent the occurrence of high currents that can result from the voltage unbalance.

- Output transformers can prevent high 3rd harmonic voltages from reaching the EPC to cause a high current trip.

Coping with the Power Quality of the EPC Inverter Input

This power quality issue on the generator side of the EPC has nothing to do with the power system. The EPC rectifier produces a PWM wave shape consisting of a series of voltage pulses and a sine wave of current that has high frequency harmonics. Each voltage pulse of the inverter output is 1.4 times the system rms voltage, e.g., for a 460 volt system, the EPC output voltage is 644 volts. With the new IGBT EPCs, the rate of change of voltage, or dv/dt transition rise-fall time for a single pulse is .05 to 0.4 microseconds. This is a much higher rate of change of voltage than existed with earlier EPCs and requires an understanding of the effect of this type of voltage on the motor.

At issue are the following:

- Magnetic noise in the generator.
- Overheating of rotor bars in the generator.
- Winding failures in generators.
- Bearing failures in generators.
- Electromagnetic interference, EMI.

Magnetic Noise

Magnetic noise can be a problem if it is loud enough to cause complaints. To correct for this, EPC manufacturers sometimes increase the switching frequency of the voltage of the rectifier to the 12 kHz level. With the switching frequency above the range at which the ear perceives audible noise, there is no noise problem.

Generator Winding Failures

The high switching frequency can cause winding failures in generators, overheating of generator rotor bars, and, in some instances, can cause bearing failures in generators. The winding failure mechanism relates to the combination of high rate-of-rise of voltage characteristic of the rectifier, Figure 3, and the length of cable between the rectifier and the generator. The combination, depending on the dv/dt switching rate and the cable

length, creates a transmission line with low characteristic impedance. When the traveling wave of high rate-of-rise voltage reaches the high characteristic impedance of the generator, the voltage can double and reflect back to the EPC. Doubling the EPC output voltage to 1288 volts on a continuous basis may exceed the voltage capacity of the generator winding insulation, which typically can be 1000 volts.

To prevent generator winding failures, consider the following:

- If high frequency generator magnetic noise is not a problem, as it may not be in many industrial or agricultural applications, keep the switching frequency to the 2.5 to 3 kHz level.

- Use an EPC output line reactor filter to smooth the voltage and current wave shape to prevent the winding problems. A line reactor at the rectifier can be used to slope-off the EPC output voltage to a slower rise time with a reduced peak voltage. A 1000-volt peak with a 10 μs rise time is safe for most generators. This solution can increase the critical cable length between the generator and EPC from 30 feet to 275 feet. The EPC manufacturer should determine the line reactor impedance. Commercially available dv/dt filters consisting of reactors, capacitors and damping resistors are also a possibility to keep motor voltage to 1000 volts or less with a rise time of more than 10 μs.

Bearing Failures

The shaft currents causing bearing failures result from the EPC rectifier frequency being in the 12 kHz or higher region. At this frequency, the common mode voltage of the inverter output, still at the 12 kHz or higher level, excites the generator stator winding and couples to the rotor iron to produce a path to circulate current from stator to rotor through the air gap and back to the stator through the bearings. Since bearing current phenomena is a function of the rectifier switching frequency, the solution is to reduce the switching frequency, insulate the bearing, or provide a grounding brush to drain off the current.

Rotor Winding Overheating

If the generator rotor bars are not designed for the high inverter switching frequency, they may overheat from high frequency eddy currents induced from the stator winding. When purchasing a generator for use with an EPC, the motor manufacturer should concur that the motor is suitable for use with an EPC.

Control of EPC Temperature

EPC electronic components, both power switching devices and control parts, are very sensitive to cooling air temperatures above 40^{o}C. High temperatures can result in failure

of IGBT switching devices and solid-state control components. While high switching rates produce better sine waves, they increase inverter losses. The losses in a switching device, such as an IGBT, consist of two components, a conduction loss and a switching loss. The IGBT, which switches on voltage, has much lower switching losses than earlier bi-polar transistors, but still, if switching an IGBT converter, switching at 12 kHz rather than 3 kHz, larger heat sinks are needed, and there is more heat to remove from the EPC enclosure. These heat losses produced internally by the EPC can add to an already high ambient temperature to cause the EPC to overheat.

Derating, or better cooling or ventilation, may be required to maintain the temperature within the enclosure to 40^{o}C or less. This should be known at the time of purchase so that either a better enclosure, a higher kW rated EPC, or a change to liquid-cooled heat sinks can be obtained. Derating the EPC may be necessary for the following conditions:

- High Ambient Temperature
- High Input Voltage
- High Altitude
- High Carrier Frequency

The source of high ambient temperature can be from locating the EPC in a hot area, or it may be from locating the EPC in an area that is not ventilated, such as in a non-ventilated weather-proof housing.

Table 7
Summary of Application-Related EPC Failure Analysis

PROBLEM	EPC	
SPECIFICATION RELATED	**POSSIBLE CAUSE**	**SOLUTION**
Insufficient Torque	Wrong Torque Spec	Correct Spec
High Output Harmonics	System Voltage Unbalance	Output Transformer Impedance
High Output Harmonics	6-Pulse ASD	12-Pulse ASD
Failure of MOV	Capacitor Switching	Output Transformer
Overvoltage Trip	Capacitor Switching	Output Transformer
Undervoltage Trip	Voltage Sag or Interruption	Power Loss Ride-Thru
Undervoltage Trip	Voltage Sag or Interruption	Run On Power-Up
Generator Winding Failure	High DV/DT, Cable Length	Input Filter
Generator Bearing Failure	High DV/DT, Cable Length	Input Filter
Generator Magnetic Noise	Carrier Freq. in Audible Range	Raise Carrier Freq.
EPC Component Failure	Overheating	Derate EPC
Generator Vibration	Resonant Lateral Vibration	Skip Frequency
Rotor Vibration	Resonant Torsional Vibration	Skip Frequency
Broken Shaft	Resonant Torsional Vibration	Skip Frequency
EPC Trips, No Restart	Loss of Voltage	Run On Power-Up
EPC Trips, No Restart	Voltage Sag	Run On Power-Up
Overload Trip	Voltage Unbalance	Output Transformer

PROBLEM	EPC	
PROCUREMENT PRACTICE RELATED	**POSSIBLE CAUSE**	**SOLUTION**
Poor Quality EPC	Inadequate Specification	Partner with vendors
Poor Quality EPC	Inadequate Specification	Qualify Acceptable Bidders
Poor Quality EPC	Inadequate Specification	Define Expectations
PROBLEM	**EPC**	
MANAGEMENT PRACTICE RELATED	**POSSIBLE CAUSE**	**SOLUTION**
Poor Quality EPC	Procurement Practice	See Above
Poor Quality EPC	Inadequate Staff	EPC Staff Specialist or Consultant

Table 8
Summary of EMI/RFI-Related EPC Failure Analysis

PROBLEM	EPC	
INSTALLATION RELATED	**POSSIBLE CAUSE**	**SOLUTION**
Erratic Operation of EPC	EMI/RFI in EPC Control Input	Control Cable Shielding or Conduit
Erratic Operation of EPC	EMI/RFI in EPC Control Input	Separation of ASD Control and Power Cables
Repetitive Generator Winding Failures	Improper Grounding Scheme for Current-Source Converter	Input Transformer, Proper Grounding
Repetitive Generator Winding Failures	Overload	Set Overload Current Limit

Table 9
Summary of Generator Failure Modes
Squirrel Cage, Synchronous, and Wound Rotor Types

PROBLEM		
STATOR WINDING	**CAUSE**	**SOLUTION**
Stator Winding Failure To Ground	Voltage Puncture	Rewind or Replace
Stator Winding Failure To Ground	Insulation Defect	Rewind or Replace
Stator Winding Failure To Ground	Overheating	Rewind or Replace
Stator Winding Failure To Ground	Single Phase	Rewind or Replace
Stator Winding Failure Turn-to-Turn	Voltage Surge	Rewind or Replace
Overheating	Unbalanced Voltages	Input Filter for EPC
Overheating	Overload	Rewind or Replace
CORE FAILURE	**CAUSE**	**SOLUTION**
	Foreign Material	Repair and Rewind, or Replace
	Burn from Winding Fault	Repair and Rewind, or Replace
	Core Insulation Defect	Repair and Rewind, or Replace
	Rotor-Stator Rub	Repair and Rewind, or Replace
ANTIFRICTION BEARING FAILURE	**CAUSE**	**SOLUTION**
	Inadequate Lubrication	Replace Bearing
	Excessive Side-Thrust	Use roller Bearing
	Exceeded Bearing Life	Replace Bearing
	Shaft Current	Insulate Bearing, or Input filter
	Foreign Material	Replace Bearing
	High Rotor Winding Temp.	Harmonic Filter
	High Vibration	Balance Rotor, or Replace Bearing

10. Reliability Risk Analysis for the Three Systems Being Compared

This analysis assumes there are no application errors for the equipment. It looks at mean time between failures, MTBF, where a failure is defined as loss of function, and mean time to repair, MTTR.

Squirrel Cage Induction Generator with Power Electric Converter

The power electric converter consists of the following components, which are subject to failure:

Voltage Source Converter

Isolation transformer
Rectifier
DC link capacitor
Inverter
Digital control

Current Source Converter

Isolation transformer
Rectifier
DC link inductor
Inverter
Output filter capacitor

Squirrel cage induction generator

Synchronous Generator and Fluid Coupling

Isolation transformer

Synchronous Generator and Excitation System

Gearbox and Fluid Coupling Combination and Hydraulic Controls

Heller Generator

Isolation Transformer

Wound Rotor Generator

Passive Control

The mean time between failure (MTBF) and mean time to repair (MTTR) for these components are as follows according to Reference 1 and other information:

Thyristors and GTOs	Gate Units – GTOs
MTBF 33,000,000 hours	MTBF 1,670,000 hours
MTTR 4 hours	MTTR 4 hours

Solid State Control System – Rectifier
MTBF 100,000 hours
MTTR 4 hours

DC Link Inductor
MTBF 100,000 hours
MTTR 100 hours

Solid State Control System – Inverter
MTBF 200,000 hours
MTTR 4 hours

DC Link Capacitor
MTBF 625,000 hours
MTTR 4 hours

Gate Units – Thyristors
MTBF 33,000,000 hours
MTTR 4 hours

IGBT Modules
MTBF 20,000,000 hours
MTTR 4 hours

Isolation Transformer – Liquid Cooled
MTBF 1,850,000 hours
MTTR 100 hours

Air Cooled
50,000,000 hours
100 hours

Squirrel Cage Induction Generator
MTBF 455,000 hours
MTTR 168 hours

Synchronous Generator
MTBF 250,000 hours
MTTR 168 hours

Fluid Drive
MTBF 455,000 hours
MTTR 168 hours

Automatic Voltage Regulator
MTBF 100,000 hours
MTTR 6 hours

Coupling
MTBF 300,000 hours
MTTR 8 hours

Exciter
MTBF 300,000 hours
MTTR 168 hours

Field Breaker
MTBF 200,000 hours
MTTR 6 hours

Relays
MTBF 200,000 hours
MTTR 6 hours

Feed-Back Controls
MTBF 200,000 hours
MTTR 8 hours

Using the MTBF and MTTR numbers, the financial value of risk of failure can be calculated using the following methodology:

MTBF = mean time between failures
MTTR = mean time to repair
MTTF = MTBF – MTTR = mean time to failure
A = availability = MTTF/MTBF
P = probability = 1.0 – A
C = Consequences of a turbine shut down per day

= $3,600 per day
This is based on annual operation of 182 days, 12 hours per day, 1500 kW operation, and selling power at $0.20/kWh

R = P x C = $ Risk per day
R = P x $3,600 x 182 = P x $655,200 $/year

Risk analysis for the three systems for annual operation of 182 days per year, 12 hours per day, 1500 kW continuous loading, and selling power at $0.20/kWh are shown in Tables 10, 11 and 12.

Table 10
Risk Assessment $/Day
Squirrel Cage Induction Generator

Item	MTBF X103	MTTR X103	MTTF X103	Avail. (A) X10-3	Px10-6	R ($)
Rectifier						
IGBT 1	20,000	4	19,999.996	999.9998	0.7	0.13
IGBT 2	20,000	4	19,999.996	999.9998	0.7	0.13
IGBT 3	20,000	4	19,999.996	999.9998	0.7	0.13
IGBT 4	20,000	4	19,999.996	999.9998	0.7	0.13
IGBT 5	20,000	4	19,999.996	999.9998	0.7	0.13
IGBT 6	20,000	4	19,999.996	999.9998	0.7	0.13
Inverter						
IGBT 1	20,000	4	19,999.996	999.9998	0.7	0.13
IGBT 2	20,000	4	19,999.996	999.9998	0.7	0.13
IGBT 3	20,000	4	19,999.996	999.9998	0.7	0.13
IGBT 4	20,000	4	19,999.996	999.9998	0.7	0.13
IGBT 5	20,000	4	19,999.996	999.9998	0.7	0.13
IGBT 6	20,000	4	19,999.996	999.9998	0.7	0.13
Cooling System	50	4	49.996	999.920	0.08	52.42
Control System	100	4	99.996	999.960	0.04	26.21
DC Link Capacitor	625	4	999.936	999.9936	0.0064	41.93
Feed-Back Controls	100	4	99.996	999.960	0.04	26.21
Coupling	300	8	299.992	999.973	0.027	17.69
Coupling	300	8	299.992	999.973	0.027	17.69
Generator	455	40	454.960	999.012	0.000088	57.66
Gear Box	455	40	454.960	999.012	0.000088	57.66
Transformer	1,850	40	1,849.960	999.978	0.000022	14.41
Main Breaker	526	6	525,960	999.924	0.000076	49.80
Relays	200	4	199.996	999.980	0.00002	13.10
H.V. Disconnect	526	8	525.992	999.985	0.000015	9.83
						312.95

Table 11
Risk Assessment $/Day
Synchronous Generator with Torque-Limiting Coupling

Item	MTBF $X10^3$	MTTR $X10^3$	MTTF $x10^{-3}$	Avail.(A) x10-3	$Px10^{-6}$	R ($)
Generator	250	40	249.960	999.867	0.000133	87.14
Coupling	300	8	299.992	999.973	0.027000	17.69
Coupling	300	8	299.992	999.973	0.027000	17.69
Gear Box	455	40	454.960	999.012	0.000088	57.66
Fluid Coupling	455	40	454.960	999.012	0.000088	57.66
Exciter	300	40	299.960	999.867	0.000133	87.14
Voltage Regulator	100	6	99.994	999.940	0.00006	39.31
Field Breaker	200	6	199.994	999.970	0.00003	19.66
Oil Pump	87	6	86.994	999.993	0.000007	4.59
Oil Pump	87	6	86.994	999.993	0.000007	4.59
Scoop Tube Controls	70	6	69.994	999.914	0.999986	52.35
Motor Starter	200	4	199.996	999.980	0.00002	13.10
Motor Starter	200	4	199.996	999.980	0.00002	13.10
Motor	87	6	86.994	999.993	0.666667	4.59
Motor	87	6	86.994	999.993	0.666667	4.59
Coupling	300	8	299.992	999.973	0.027	17.69
Coupling	300	8	299.992	999.973	0.027	17.69
Heat Exchanger	100	16	99.984	999.840	0.00016	10.48
Transformer	1,850	40	1,849.960	999.978	0.000022	14.41
Main Breaker	526	6	525,960	999.924	0.000076	49.80
Relays	200	4	199.996	999.980	0.00002	13.10
H.V. Disconnect	526	8	525.992	999.985	0.000015	9.83
						614.12

Table 12
Risk Assessment $/Day
Heller Generator

Item	MTBFX10^3	MTTR	MTTF	Avail. (A)	Px10^{-6}	Rx10^{-3} ($)
Generator	455	40	454.960	999.012	0.000088	57.66
Coupling	300	8	299.992	999.973	0.027	17.69
Coupling	300	8	299.992	999.973	0.027	17.69
Gear Box	455	40	454.960	999.012	0.000088	57.66
Resistor	1,850	4	1,849.996	999.998	0.000002	1.31
Reactor (Rotating Transformer)	455	40	454.960	999.012	0.000088	57.66
Transformer	1,850	40	1,849.960	999.978	0.000022	14.41
Main Breaker	526	6	525,960	999.924	0.000076	49.80
Relays	200	4	199.996	999.980	0.00002	13.10
H.V. Disconnect	526	8	525.992	999.985	0.000015	9.83
						296.81

This risk analysis for the three systems was based on annual operation of 182 days per year, 12 hours per day, 1500 kW continuous loading, and selling power at $0.20/kWh. For each of the three generator systems being compared, the following Tables 13, 14, and 15 show the sensitivity of risk for electricity selling price, average annual operating hours, and average annual production rate.

Table 13
Risk Sensitivity to Selling Price, $/Day
182 Days/Year, 1500 kW Avg. Loading

Selling Price, $/kWh	.05	.20	.50	1.00
Squirrel Cage Gen./ Electronic Converter	78.24	312.95	782.00	1,564.75
Synchronous Gen. Torque Coupling	153.53	614.12	2,535.00	3,070.60
Heller Gen. Passive Control	74.20	296.81	742.00	1,484.05

Table 14
Risk Sensitivity to Average Number of Days of Operation per Year, $/Day
$0.20/kWh Selling Price, 1500 kW Avg. Loading

Avg. No, Days/Year	100	150	182
Squirrel Cage Gen./ Electronic Converter	171.95	257.92	312.95
Synchronous Gen. Torque Coupling	337.43	506.14	614.12
Heller Gen. Passive Control	163.08	244.62	296.81

Table 15
Risk Sensitivity to Average Daily Load per Year, $/Day
$0.20/kWh Selling Price, 182 Days/Year Operation

Avg. kW Loading per Year	500	750	1500
Squirrel Cage Gen./ Electronic Converter	104.32	156.48	312.95
Synchronous Gen. Torque Coupling	204.71	307.06	614.12
Heller Gen. Passive Control	98.94	148.41	296.81

Risk Analysis Summarized

From this analysis it can be seen that the squirrel cage induction generator with electronic converter compares well with the Heller generator in terms of reliability. The squirrel cage induction generator is a simple machine and the electronic converter has reliable components. The Heller generator has few parts to fail, which enhances its risk analysis. The synchronous generator with torque-limiting gearbox suffers in this risk analysis because of the complexity of the synchronous generator with its excitation controls and the complexity of the torque-limiting gearbox with its hydraulic controls.

11. Development of Prototype Generator

Following is the strategy upon which the Company's business plan is based. The plan is to develop the company's generator business for wind turbines with a minimum of risk for investors by outsourcing all components. The concept for the Company's business is

to purchase generators in the Far East, manufactured to the Company's specifications. It is anticipated that the generator manufacturer, in the space normally assigned to carbon brushes and slip rings, will install the rotating transformer, Figure 13, which will also serve as the reactor. The generator manufacturer would manufacture the rotating transformer or otherwise acquire it as part of the generator package. Completed generators can be shipped directly to the customer's site and marked up about 10% and still be competitive in price with other wind generator systems. It is anticipated that the Company would need to market the total electrical package associated with a wind turbine installation. This would include generator, passive control system, main circuit breaker, and step-up transformer. Thus, no inventory is needed and no warehousing or manufacturing costs are contemplated.

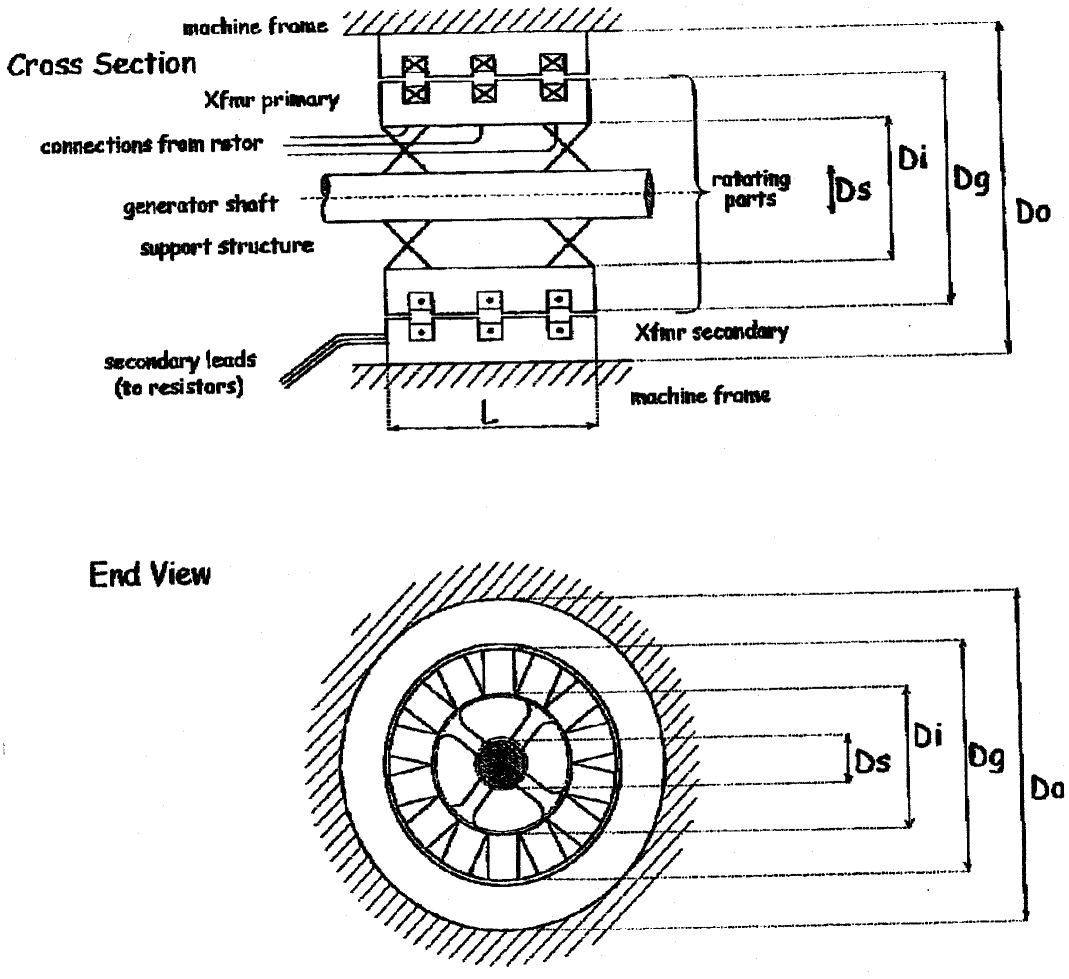

Figure 13
Concept of Rotating Transformer

While the generator can be sold as it is now as a brush-type machine, it is necessary to develop the Heller generator as a brushless machine. Many of the electronic control systems in use in wind generators use the wound rotor induction generator as either a doubly fed machine or as a slip energy recovery machine. Both require carbon brushes and slip rings that contribute to maintenance and reliability problems. The two alternate systems being compared in this study are brushless generators. The squirrel cage induction generator is brushless and the synchronous generator can be configured to be brushless. Replacing the brushes and slip rings in the Heller generator with a rotating transformer will eliminate this maintenance and reliability problem.

To achieve this goal, we propose to work initially with the 80 kW machine located at Oregon State University in Corvallis:

- Rewind the rotor for 960 volts. This would reduce the size of the rotating transformer and the external resistor.
- Develop the rotating transformer.
- Conduct tests of power, torque and efficiency at OSU.

Two other developments are desirable:

- Develop the stand-alone Heller Generator. Based on the technical literature, capacitors can be used to provide excitation to allow the induction generator to be used as a stand-alone generator.
- Develop the self-protecting parallel resonance power-limiting feature.

This work will be done at the Oregon State University under the direction of Dr. Wallace, who has been closely associated with the development to date. He has available the EPRI/DOE test facility and has graduate students for carrying out much of the detailed technical work. This combination provides an efficient, cost effective means of carrying out this development.

Estimated costs for this development work are as follows:

Develop 80 kW generator with rotating transformer $100,000
Modify computer program to include rot. transf. 50,000
$150,000
This work can be completed in 8 months.

Develop stand-alone generator 30,000
Develop parallel resonance power cut-off 50,000
Modify computer model to include design of these features 25,000
Total $105,000

It is estimated that this work can be completed in 6 months.

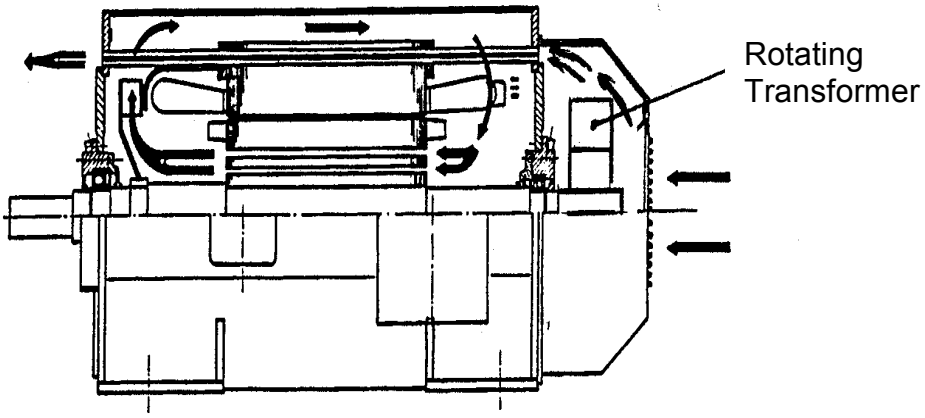

Figure 14
Section of Heller Generator Showing Rotating Transformer

12. Cost to Produce a 1500 kW Prototype and Three Production Models

1. Develop a brushless 80 kW prototype $150,000
2. Develop a brushless 1500 kW prototype
   a. Generator and control $125,000
   b. Engineering 50,000
   Total $175,000

3. Produce three production models $360,000
   a. Engineering 25,000
   Total $385,000

13. References

1. IEEE Standard 500-1984 “IEEE Guide to Collection and Presentation of Electrical, Electronic, Sensing Component, and Mechanical Equipment Reliability Data for Nuclear-Power Generating Stations.

2. P. K. Steimer and A. B. Giesecke. “Increased Availability of Large AC Adjustable Speed Drive Systems.” American Power Conference, Chicago, IL, April 1991.

3. J. A. Oliver, JARSCO Engineering Corp. “Trouble-Shooting Guide for Low Voltage ASD/Motor Systems.” EPRI Report TR-111097 Final Report November 1998.

Appendix – Generator Costs

The prices in the following tables are prices Heller-DeJulio Corporation would charge for generators. These prices are based on information received from their supplier, TECO Motor Company of Taiwan.

Table A-1
Synchronous Generator, 3-Phase, 60 Hz, Foot-Mounted, Type EP-54
Wind Turbine Application
Selling Prices Based on Units per Year

Rating kW	No. Poles	Volt Rating kV	A Qty Per Year	A Price $	B Qty Per Year	B Price $	C Qty Per Year	C Price $
5000	4	2.4	1	408,100	40	363,990	200	354,640
	6	2.4	1	479,490	40	427,790	200	410,080
3000	4	2.4	1	248,050	67	221,980	333	213,070
	6	2.4	1	302,610	67	270,930	333	259,990
1500	4	2.4	1	180,800	133	162,360	667	156,860
	6	2.4	1	260,910	133	234,300	667	226,710
750	4	.69	1	80,060	267	72,875	1333	71,170
	6	.69	1	90,750	267	82,060	1333	80,740

Table A-2
Squirrel Cage Induction Generator, 3-Phase, 60 Hz, Foot-Mounted, Type EP-54
Wind Turbine Application
Selling Prices Based on Units per Year

Rating kW	No. Poles	Volt Rating kV	A Qty Per Year	A Price $	Qty Per Year	B Price $	C Qty Per Year	C Price $
5000	4	2.4	1	190,080	40	178,200	200	173,960
	6	2.4	1	195,700	40	198,990	200	192,940
3000	4	2.4	1	116,160	67	129,010	333	106,865
	6	2.4	1	127,775	67	120,500	333	118,545
1500	4	2.4	1	52,635	133	47,410	667	45,925
	6	2.4	1	60,160	133	54,670	667	52,745
750	4	.69	1	41,580	267	38,610	1333	37,895
	6	.69	1	50,250	267	46,970	1333	46,145
600	4	.69	1	34,100	400	31,515	2000	30,800
	6	.69	1	36,250	400	39,310	2000	33,594
375	4	.69	1	21,120	533	19,910	2667	19,450
	6	.69	1	13,435	533	21,725	2667	21,290
300	4	.69	1	16,225	667	15070	3333	14,740
	6	.69	1	18,810	667	17,390	3333	17,095
250	4	.69	1	14,850	800	13,695	4000	13,365
	6	.69	1	16,280	800	14,960	4000	14,695
150	4	.69	1	17,600	1333	10,650	6667	10,360
	6	.69	1	13,090	1333	11,990	6667	11,605
100	4	.69	1	10,280	2000	9,405	10000	9,075
	6	.69	1	11,550	2000	10,560	10000	10,110
75	4	.69	1	8,745	2667	8,0020	13333	7,865
	6	.69	1	10,175	2667	9.306	13333	8,965

Table A-3
Wound Rotor Induction Generator, 3-Phase, 60 Hz, Foot-Mounted, Type EP-54
Wind Turbine Application
Selling Prices Based on Units per Year

Rating kW	No. Poles	Volt Rating kV	A Qty Per Year	A Price $	B Qty Per Year	B Price $	C Qty Per Year	C Price $
5000	4	2.4	1	222,750	40	200,500	200	193,090
	6	2.4	1	252,450	40	227,205	200	221,670
3000	4	2.4	1	133,650	67	120,340	333	115,830
	6	2.4	1	146,740	67	133,670	333	129,220
1500	4	2.4	1	78,685	133	71,255	667	69,210
	6	2.4	1	88,310	133	79,530	667	77,365
750	4	.69	1	47,915	267	43,615	1333	42,130
	6	.69	1	55,200	267	50,105	1333	48,510
600	4	.69	1	41,910	400	51,205	2000	37,125
	6	.69	1	46,210	400	41,415	2000	40,690
375	4	.69	1	25,740	533	23,165	2667	22,605
	6	.69	1	28,710	533	15,795	2667	25,410
300	4	.69	1	19,965	667	17,985	3333	17,680
	6	.69	1	22,990	667	20,735	3333	20,405
250	4	.69	1	17,875	800	15,730	4000	15,455
	6	.69	1	19,360	800	17,160	4000	17,070
150	4	.69	1	14,520	1333	13,070	6667	17,780
	6	.69	1	10,665	1333	15,070	6667	14,795
100	4	.69	1	12,585	2000	11,460	10000	11,165
	6	.69	1	13,915	2000	12,815	10000	12,485
75	4	.69	1	11,440	2667	10,320	13333	10,065
	6	.69	1	12,575	2667	11,495	13333	11,175

Appendix M

Wind Torque Limited Specifications

WIND TORQUE LIMITED
12 Scotston Ave.
Papanui, Christchurch 5, New Zealand

SPECIFICATION
1500 kW Torque Limiting Gearbox

REV	DATE	DESCRIPTION	PREP	APP
0	8 Feb. 01	Original Issue (Outline for Preliminary Study)	GMH	

Contents

1. INTRODUCTION

The gearbox is to be mounted in a three-bladed, 1500 kW windmill. The main bearings which react the main rotor loads and moments (aerodynamic and gravity) are external to the gearbox.

The gearbox shall incorporate the torque limiting gearbox (TLG) principle, for which patents have been issued in the USA and elsewhere.

1.1 Scope of Supply

The gearbox manufacturer shall supply:

(a) three-stage gearbox with integral keyed high speed shaft (HSS)
(b) brake disc on intermediate speed shaft (ISS) so that braking torque is not dependent on the torque limiting hydraulics
(c) epicyclic final stage to provide TLG capacity and a pinion for the torque limiting reaction pump. This is a radial piston pump, which shall also be supplied and fitted by the gearbox manufacturer
(d) sensors and brackets as described in the following sections
(e) initial fill of oil

1.2 Design Responsibility

The gearbox manufacturer shall be responsible for the detailed design of all the above supply items.

2. PHYSICAL REQUIREMENTS

Mean power transmission	Up to 1,610 kW (mechanical power based on 1500 kWe, 97% generator efficiency, 96% gearbox efficiency)
Input speed	20.5 rpm
Output speed (HSS)	1800 rpm
Ambient temperature range	-15^{o} to 45^{o}C
Working environment	tower top vibration; exposure on front part of case to high winds possibly salt- or sand-bearing
Design life	20 years
Target weight	TBD kg
Noise at full load	80 dBA @ 1.5 m

The general arrangement shall be three stage, with the first stage planetary, second stage parallel. The output of the parallel stage is the ISS (which shall carry the brake disc). The final stage shall be epicyclic, with one of the three members reacted through a parallel gear by a radial piston pump. The output will drive a synchronous generator through a one-way clutch which will be mounted on the generator shaft. The generator is to be rated at 1500 kW(e) and generator efficiency is 97% (electrical power out: mechanical power in). The manufacturer shall estimate the design efficiency of the gearbox as a function of transmitted power. Target efficiency shall be 96% at rated power. Note that a lower achieved efficiency will result in higher input power than the above figure.

Other equipment to be accommodated include:

a) a brake caliper
b) hydraulic equipment for the torque limiting hydraulics
c) various sensors and other minor equipment

3. OPERATIONAL REQUIREMENTS

The gearing shall be designed to BS 436 or equivalent specification. An appropriate application factor, K_a, for the torque limiting gearbox is in the range 1.1 to 1.25 applied to the basic 1,610 kW (750 kNm) rating. This is to allow for occasional minor overloads as indicated in Figure 1.

The total running time of the gearbox over the life of the machine is estimated to be 146,000 hours, of which 39,000 hours will be at rated power.

Mechanical torque will be limited by adjusting the relief valve in the torque limiting circuit to obtain 1,500 kW output from the generator. At rated power the windmill rotor speed will slip relative to the constant 1800 rpm of the generator. (Note: in some applications the windmill will be used for weak grids on offshore islands, etc., where generator speed may vary by ±4%).

The slip of the rotor will be measured by a speed sensor on the torque limiting pump shaft. The slip will be controlled by pitching the blades. A mean slip of 3% will be obtained with variations of ±2%, i.e., the rotor speed will increase to a mean value of 21.1 rpm with excursions between 20.7 and 21.5 rpm. Zero slip shall correspond to zero speed and 3% slip shall correspond to about 75 rpm (estimated) and no more than 90 rpm on the torque limiting pump, which shall be a Poclain MS-18 or similar.

The torque limiting pump shall be capable of turning in either direction under load (positive or negative slip). A one way clutch on the generator shaft will ensure that torque is applied in only one direction, regardless of whether the slip is positive or negative.

The emergency brake on the ISS will apply a torque of 1000 kNm on the low speed shaft (LSS). There are predicted to be 100 such applications over the life of the machine. Generally the braking torque during a normal shut down will be half of that value, applied at a speed of 1.0 rpm on the LSS.

The maximum speed at which the gearbox will be run, with or without the brake applied, will be 33.3[1] rpm at the low-speed shaft, for very short periods only (approximately 1 minute in 20 years).

[1] With a maximum operating speed of 21.5 rpm, we would recommend this be reduced to about 27 rpm (20% above max. operating), which could result in significant economies in this design case.

4. LUBRICATION AND MAINTENANCE REQUIREMENTS

The gearbox shall be splash lubricated with a synthetic oil for long life between oil changes. A filtration system shall be provided comprising:

a) mechanically driven circulating pump
b) 10 micron filter, with clogging alarm
c) oil cooler as required for viscosity control (see below)
d) suction and return lines to the gearbox casing.

In service the filter element will be changed every six months. Oil changes will be made based on the results of annual analysis by the oil supplier. It is expected that the oil life could be up to five years.

Regarding viscosity grade, it is required that the gearbox oil be the same as the oil for the hydraulic system (supplied by others) because of:

a) simplified maintenance requirements
b) the likelihood of mixing due to any leakage from the torque limiting pump into the casing.

To achieve this requirement it is proposed to use an intermediate viscosity grade (for example, ISO 100) with a cooler on the gearbox oil filtration circuit. This cooler will be mounted below the nacelle in the outside airstream. For most applications it can be assumed that the maximum ambient temperature in wind speeds above 10 m/s is 30^{o}C. For any climates where this is not so, a larger cooler or different grade of oil may be necessary.

Based on this assumption, the gearbox manufacturer shall select and advise the following details:

a) cooler type, dimensions and mounting requirements
b) oil viscosity grade
c) design operating temperature

The gearbox manufacturer shall confirm that the use of the same grade of oil for both gearbox and hydraulic system is satisfactory. Note that:

a) the hydraulic power pack will include an oil heater if necessary
b) the gearbox and hydraulic oil systems will not normally mix and will generally run at different temperatures
c) the torque limiting hydraulic circuit will be part of the hydraulic system and will not interface with the gearbox supply except at the ports of the radial piston pump
d) the only mixing between the gearbox and hydraulic oils will occur due to any leakage from the radial piston pump seal. This leakage should be minimal but the gearbox manufacturer shall provide an overflow port – either on the gearbox casing or on the level gauge – to allow leakage oil to return to the hydraulic power pack.

Labyrinth seals shall be provided for the low-, intermediate- and high-speed shafts. Two additional seals shall be provided on the LSS, one for dust exclusion and the other to assist the labyrinth. These must be either easily replaceable or designed for a 20-year life.

5. REQUIRED SENSORS

Electrical sensors are required for low oil level and over-temperature tripping. Provision shall be included for adjustment of the oil level trip setting while the gearbox is running. Alternatively the low oil level sensing may be provided by means of a low pressure switch on the filtration circuit. A sight glass is required for oil level monitoring. This should allow the oil level to be seen from the normal stationary level to 100 mm below this level (for when the gearbox is running).

A speed sensor shall be provided for the torque limiting pump shaft. This shall be a magnetic proximity device mounted so as to sense the teeth on the gear which mates with the torque limiting pump pinion. This shall be set up during gearbox assembly and checked for correct operation during the spin test. Having been tested it shall not be further adjusted or removed prior to shipment.

Two similar speed sensors shall be provided for the LSS. The gearbox manufacturer shall provide brackets, fit the sensors and set them up during the spin test as for the torque limiting pump speed sensor.

All sensors shall be 24 volts dc.

6. MATERIALS

The fatigue loading and life requirements of the gearbox shall be taken into consideration when specifying materials for all drive-train and casing components. Appropriate quality assurance procedures shall be applied to ensure that voids and inclusions in all castings are kept within acceptable sizes.

7. TESTING

The prototype gearbox shall have a 4-hour full-load test at a nominal 1,610 kW. Gear case vibration levels shall be monitored during this test to assess acoustic emission levels. In accordance with ISO 2372, vibration levels shall be less than 7.5 mm/s RMS at any point on the gear case.

Subsequent units shall have a spin test only. The purpose of the tests is to set up the speed sensors, show correct assembly and smooth running of parts. Ultimate strength is covered by calculations and material testing.

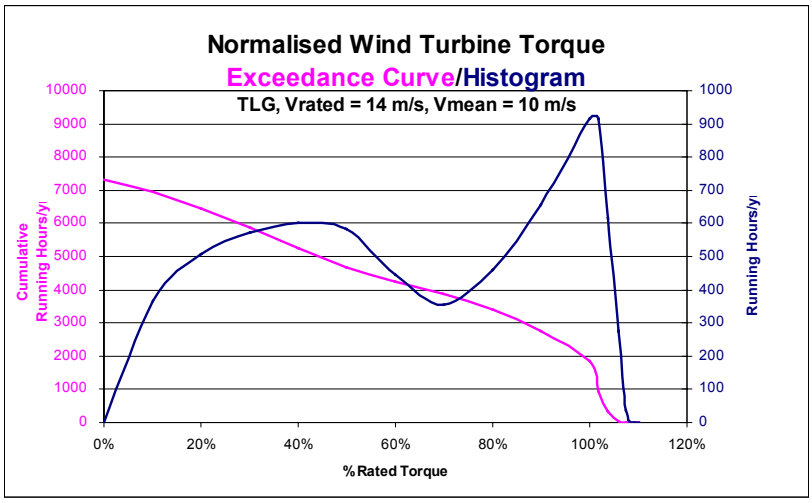

Figure 1 – Variable Torque Duty Specification

WIND TORQUE LIMITED
12 Scotston Ave.
Papanui, Christchurch 5, New Zealand

SPECIFICATION
1500 kW Torque Limiting Hydraulics

REV	DATE	DESCRIPTION	PREP	APP
0	9 Feb. 01	Original Issue (Outline for Preliminary Study)	GMH	

Contents

1. INTRODUCTION

The hydraulic system will be installed within the nacelle of a three-bladed 1500 kW windmill. The system will operate:

a) the yaw motor and brake (supplied by others)
b) the main transmission disc brake caliper (supplied by others)
c) the torque limiting (TL) pump (supplied by others)

These four systems shall operate independently and concurrently. The hydraulic system includes:

a) hydraulic power unit
b) three control modules, one mounted on the power unit and two adjacent to the main gearbox (where the brake caliper and torque limiting pump are mounted)
c) a cooler for the torque limiting circuit
d) pitch actuators, including proportional control valve and electronic controller
e) hoses and interconnecting pipework for the complete system

For this preliminary specification, the scope covers only the control module for the TL pump, the cooler for the TL circuit and associated hoses and interconnecting pipework.

The basic circuit diagram for the TL hydraulics is given in Figure 1. Suppliers should submit alternative circuit diagrams if SD1509 does not suit their conventional configurations.

2. DUTY SPECIFICATIONS

2.1 Torque Limiting Circuit

The torque limiting circuit consists of:

a) a closed circuit which includes a relief valve and has two basic states. In the first (below rated torque) the relief valve is closed, and flow is low and varies depending on torque and flows through a throttle line consisting of a fixed restriction and a variable throttle valve. In the second (torque limiting at rated) the relief valve is open, flow is high and varies independently of torque, which is constant.
b) a cooler to remove the heat which is generated by the relief valve when torque limiting.

These are described further in the following sections.

2.1.1 Closed Circuit

The closed circuit allows flow from the outlet of the pump back to the inlet. The pump will be a Poclain MS-18 unbraked motor/pump or similar. It has a linear relationship between torque and differential pressure (27.8 Nm/bar) and between speed and flow (1747 cm^3/rev).

The relief valve shall be fitted with an auxiliary pressure line to apply pump inlet pressure to the spring chamber (instead of downstream pressure). It shall also be capable of remote pilot operation. The relief valve shall be selected to provide constant pressure control for the full range of flow rates. The pressure drop between the pump outlet and the relief valve, or between the pump inlet and the pressure tapping, shall not exceed 1 bar. Although

sandwich plate valves are preferred, consideration may be given to direct mounting of the relief valve on the pump if necessary to meet this requirement.

When torque limiting, the power input to the pump will be about 45 kW at a speed of 75 rpm. Thus torque will be about 5840 Nm and differential pressure about 210 bar (neglecting mechanical inefficiency). Inlet flow will average 131 l/min and this will vary in proportion to the speed fluctuations on the pump (±50 rpm, i.e ±87 l/min, at most). Because of volumetric inefficiency the outlet flow will be slightly less.

Below rated the only flow will be through the fixed throttle line. This will include:

a) a length of capillary tube or some other constant geometry restriction
b) a variable throttle valve to enable initial set-up of the pump speed slightly below rated.

About 40 l/min shall flow through the fixed throttle line at rated pressure. The supplier shall advise what the design setting of this throttle valve should be.

Parallel to both the relief valve and the fixed throttle line, there shall be a start-up line which shall include a thermostatic valve. This shall open when the upstream oil temperature is below 30^{o}C and close completely when it is above 40^{o}C. The purpose of this line is to prevent high load being applied to the windmill before the torque limiting circuit has warmed up. The design flow shall be 50 l/min at 0^{o}C and 210 bar pressure drop between the pump ports.

Downstream of these three parallel lines there shall be a low pressure filter. This shall incorporate a clogging alarm and bypass. In practice the clogging alarm may be ignored during start-up if it is activated because of low oil temperature.

The circuit will return to the pump inlet via a thermostatic valve which shall be set at 60^{o}C. This valve will control the flow of oil through the cooler.

The supplier shall size all components in the torque limiting circuit in accordance with the above flow requirements. High pressure drops through the filter and thermostatic valve are acceptable and need only be limited by their pressure rating which should be for low pressure duty.

Note that a one-way clutch on the generator shaft will prevent reversal of torque or pump direction.

A positive pressure of at least 4 bar is required on the inlet side of the TL pump. This shall be maintained by a regulator/relief valve from the power unit supply lines. This shall regulate at 4 bar and relieve at 8 bar. The design flow through the regulator/relief valve shall be 30 l/min.

2.1.2 Cooler

The cooler will be mounted below the nacelle in the outside airstream and will not require a fan. The main design parameters of the cooler are as follows:

heat dissipation	45 kW
flow rate	131 l/min
oil temperature	60°C at outlet
air temperature	30°C
wind speed	12 m/s

3. PHYSICAL REQUIREMENTS

3.1 Size

The TL circuit module shall fit within a nominal envelope size of 300 mm high x 200 mm long x 100 mm deep.

3.2 Mounting Arrangement

The TL circuit module shall be mounted on a panel to be fitted on a face inclined at 60° to the horizontal with fixing centres at 150 x 250 mm. The system supplier shall advise what size fasteners are required.

3.3 Hydraulic Hoses and Connections

Hydraulic hoses and connections must be leak-free despite being subject to significant mechanical vibration.

Rigid piping, which shall be welded (including all tees and elbows), shall be used for the main supply and return lines connecting the TL circuit module to the power supply unit. Bulkhead fittings shall be provided for the cooler lines.

3.4 Power and Control Electrical Supply

The electrical power supply will be 480 V, 3 phase, 60 Hz. The control circuit voltage will be 24 Volts dc which will be battery backed up. Screwed electrical connectors shall be oil and waterproof conforming to IP 55, per IEC 60529.

3.5 Corrosion Protection

The cooler, power unit, and all steel components and piping shall be suitably corrosion protected for a 20-year life in an exposed severe coastal environment.

4. OPERATIONAL REQUIREMENTS

4.1 Oil

Regarding viscosity grade, it is required that the hydraulic oil be the same as the lubricating oil for the gearbox (supplied by others) because of:

a) simplified maintenance requirements
b) the likelihood of mixing due to any leakage from the torque limiting pump into the gearbox casing.

To achieve this requirement it is proposed to use an intermediate viscosity grade (for example, ISO 100) with a cooler (supplied by others) for the gearbox oil system. A heater in the power unit will be required to overcome viscosity related problems.

The hydraulic system manufacturer shall confirm that the use of the same grade of oil for both gearbox and hydraulic system is satisfactory. Note that:

a) the gearbox and hydraulic oil systems will not normally mix and will generally run at different temperatures
b) the only mixing between the gearbox and hydraulic oils will occur due to any leakage from the radial piston pump seal. This leakage should be minimal but the gearbox manufacturer will provide an overflow port to allow leakage oil to return to the hydraulic power unit. This shall be integrated into the system return line as shown in Figure 1.

4.2 Valves

The control valves shall preferably be of a sub-plate and sandwich system mounted directly onto the power unit and modules. Provision shall be made for test points in the separate operational circuits as shown in Figure 1. A pressure gauge with a working pressure of 350 bar will be required for the primary circuit. This shall be able to be moved to the various test points.

5. MAINTENANCE REQUIREMENTS

A drain point shall be provided to drain and replace hydraulic oil. Oil filters shall be selected and sited for ease of replacement.

6. OPERATING CONDITIONS

The design ambient air temperature shall be between -15^{o}C and +45^{o}C. The design humidity shall be 100%. The altitude will be from 0 to 2000 m above sea level. Design life shall be 20 years.

7. TESTING

The hydraulic system shall be pressure tested for leak detection and circuit correctness. The circuits shall be pressure tested as follows:

Circuit	Test Pressure
Torque limiting:	
High pressure side	315 bar (4630 psi)
Low pressure side	45 bar (660 psi)

8. DOCUMENTATION

A general arrangement drawing with overall dimensions together with a circuit diagram shall be supplied.

A concise parts list shall be supplied together with a list of recommended spares. An operation and maintenance manual shall be provided. Test certificates shall be supplied.

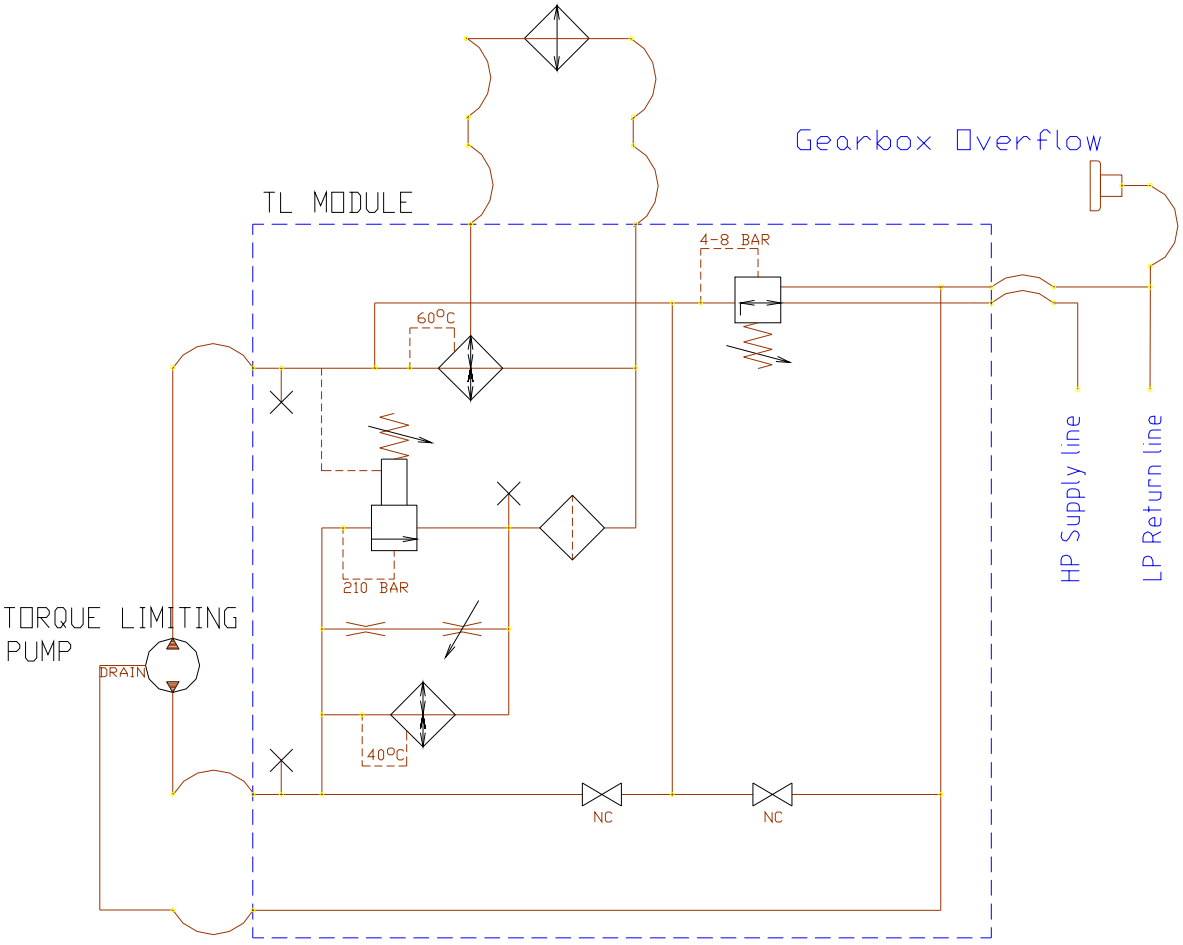

Figure 1 – TL Circuit Diagram

REPORT DOCUMENTATION PAGE

Form Approved
OMB NO. 0704-0188

1. AGENCY USE ONLY (Leave blank)	2. REPORT DATE	3. REPORT TYPE AND DATES COVERED
	August 2003	Subcontractor report: November 1, 2000 – February 28, 2002

4. TITLE AND SUBTITLE
Alternative Design Study Report: WindPACT Advanced Wind Turbine Drive Train Designs Study

5. FUNDING NUMBERS
WER3.1201
YAM-1-30209-01

6. AUTHOR(S)
R. Poore and T. Lettenmaier

7. PERFORMING ORGANIZATION NAME(S) AND ADDRESS(ES)
Global Energy Concepts, LLC
5729 Lakeview Dr. NE, Suite 100
Kirkland, Washington 98033

8. PERFORMING ORGANIZATION REPORT NUMBER

9. SPONSORING/MONITORING AGENCY NAME(S) AND ADDRESS(ES)
National Renewable Energy Laboratory
1617 Cole Blvd.
Golden, CO 80401-3393

10. SPONSORING/MONITORING AGENCY REPORT NUMBER
NREL/SR-500-33196

11. SUPPLEMENTARY NOTES
NREL Technical Monitor: A. Laxson

12a. DISTRIBUTION/AVAILABILITY STATEMENT
National Technical Information Service
U.S. Department of Commerce
5285 Port Royal Road
Springfield, VA 22161

12b. DISTRIBUTION CODE

13. ABSTRACT *(Maximum 200 words)*
This report presents the Phase I results of the National Renewable Energy Laboratory's (NREL's) Wind Partnership for Advanced Component Technologies (WindPACT) Advanced Wind Turbine Drive Train Designs Study. Global Energy Concepts, LLC performed this work under a subcontract with NREL. The purpose of the WindPACT project is to identify technology improvements that will enable the cost of energy (COE) from wind turbines to be reduced. Other parts of the WindPACT project have examined blade and logistics scaling, balance-of-station costs, and rotor design. This study was designed to investigate innovative drive train designs.

14. SUBJECT TERMS
Wind energy; wind turbines; drive train; drive train designs; WindPACT; Global Energy Concepts

15. NUMBER OF PAGES

16. PRICE CODE

17. SECURITY CLASSIFICATION OF REPORT	18. SECURITY CLASSIFICATION OF THIS PAGE	19. SECURITY CLASSIFICATION OF ABSTRACT	20. LIMITATION OF ABSTRACT
Unclassified	Unclassified	Unclassified	UL